# A multi-scale modeling framework to build long-term optimal and secure investments trajectories for power systems in transition

Yacine Alimou

PSL UNIVERSITÉ PARIS

**THÈSE DE DOCTORAT**

**DE L'UNIVERSITÉ PSL**

Préparée à MINES Paris

# *A multi-scale modeling framework to build long-term optimal and secure investments trajectories for power systems in transition*

# Vers une approche multi-échelles dans les exercices de prospective long-terme


Soutenue par

**Yacine ALIMOU**


Le Jeudi 30 Mai 2024

École doctorale n°84

**Sciences et technologies de l'information et de la communication**

Spécialité

**Contrôle, Optimisation, Prospective**

Composition du jury :

| | |
|---|---|
| Philippe DROBINSKI<br>Professeur, École Polytechnique | Président du jury |
| Jean-Charles HOURCADE<br>Professeur, École des Ponts ParisTech | Rapporteur |
| Nadia MAÏZI<br>Professeure, Mines Paris PSL | Directrice de thèse |
| Stephanie BOUCKAERT<br>Directrice de l'unité secteur de la demande, Agence Internationale de l'Energie | Examinatrice |
| Julie SLIWAK<br>Ingénieure Management des Risques, EDF | Examinatrice |
| Edi ASSOUMOU<br>Maître de Recherche, Mines Paris | Examinateur |

MINES PARIS | PSL

**"Mains froides, cœur chaud"**

# Dédication

Je dédie ma thése à la mémoire du Professeur Feu Mahdi ELMANDJRA.

# Remerciements

Tout d'abord, je souhaite remercier l'ensemble des membres du jury qui ont accepté d'évaluer ma thèse. Merci à mes deux rapporteurs, le Professeur Philippe DROBINSKI, pour avoir apporté l'approche multi-échelle développée dans les sciences du climat à l'évaluation de ma thèse, et le Professeur Jean-Charles HOURCADE, pour l'intégration du caractère pratique de la planification et de la vision macro-économique.

Je tiens également à remercier mes examinateurs, Edi ASSOUMOU, Julie SLIWAK et Stephanie BOUCKAERT, pour leurs contributions à l'évaluation technique de mes travaux de thèse.

Je souhaite remercier ma directrice de thèse, la Professeure Nadia MAÏZI, pour son encadrement et ses conseils qui m'ont permis de passer le cap. Je tiens aussi à remercier Jean-Paul MARMORAT pour le temps qu'il m'a consacré afin de suivre mes travaux, en particulier la formulation mathématique.

Je tiens à remercier Gilles GUERASSIMOFF, grâce à qui j'ai pu faire le Mastére specialisé OSE. Je souhaite également remercier Catherine AUGUET-CHADAJ, Amel SAHLI, Sébastien FOLIO et Alice SPASORO pour tous les efforts déployés pour rendre le mastère spécialisé OSE la meilleure année d'études pour chaque étudiant. Merci à Valérie ROY d'avoir fait preuve de patience face à ma procrastination administrative. Merci à tous les chercheurs et doctorants du CMA avec qui j'ai partagé des moments riches d'apprentissage et d'amitié.

Ensuite, je tiens à remercier mes deux encadrants à RTE, Jean-Yves BOURMAUD et Nicolas LHUILLIER, pour leur soutien sans faille, ainsi que pour leurs relectures approfondies de mon manuscrit. Merci, Jean-Yves, pour ta grande connaissance de l'équilibre offre-demande et tes questions toujours pertinentes qui m'ont poussé à robustifier mes recherches. Merci, Nicolas, pour l'efficacité que tu as apportée à la réussite de ma thèse.

Je voudrais également remercier les autres personnes de RTE qui ont permis le bon déroulement de ma thèse. Je pense à Jérôme PIGAT et David GAME pour avoir concrétisé le lancement de mon projet de thèse CIFRE. Je remercie aussi les nombreuses personnes des deux pôles auxquels j'ai appartenu (EODCT, PEPS) avec qui j'ai beaucoup appris. En particulier, je tiens à remercier les doctorants avec qui il me semble avoir grandi et tant appris durant ces années.

# Contents

# List of Figures

# List of Tables

# List of Abbreviations

**AC** Alternating Current

**ACER** Agency for the Cooperation of Energy Regulators

**AEMO** Australian Energy Market Operator

**ANTARES** A New Tool for Adequacy Reporting of Electric Systems

**APS** Announced Pledges Scenario

**BAU** Business As Usual

**BESOM** Brookhaven Energy System Optimization Model

**CCUS** Carbon Capture Utilisation and Storage

**CEP** Clean Energy Package

**CHP** Combined Heat and Power

**CI** Coverage Index

**CMs** Capacity Mechanisms

**CONE** Cost Of New Entry

**CRE** Commission de Régulation de l'Energie: The French National Regulatory Authority

**CSP** Concentrated Solar Power

**DC** Direct Current

**ED** Economic Dispatch

**EENS** Expected Energy Not Served

**EFOM** Energy Flow Optimization Model

**ENSPRESO** ENergy Systems Potential Renewable Energy SOurces

**ENTSOE** European Network of Transmission System Operators

**ERAA** European Resource Adequacy Assessment

**ERCOT** Electric Reliability Council of Texas

**ETSAP** Energy Technology Systems Analysis Program

**EU** European Union

**EUE** Expected Unserved Energy

**EV** Electric Vehicles

**GDP** Gross Domestic Product

**GEP** Generation Expansion Planning

**GHG** Greenhouse Gas

**GVA** Gross Value Added

**HVDC** Voltage Direct Current

**IAMs** Integrated Assessment Models

**IEA** International Energy Agency

**IGCC** Integrated Gasification Combined Cycle

**IRENA** International Renewable Energy Agency

**LCA** Life Cycle Assessments

**LCOE** Levelized Cost Of Energy

**LDC** Load Duration Curve

**LOLD** Loss Of Load Duration

**LOLE** Loss of Load Expectation

**LoLP** Loss of Load Probability

**LP** Linear Programming

**MAF** Mid-term Adequacy Forecast

**MARKAL** MARket ALlocation model

**MCA** Monte Carlo Analysis

**MGA** Modeling to Generate Alternatives

**MIP** Mixed Integer Programming

**MMF** Multi-Scale Framework

**MMFS** Multiscale Modeling and Simulation Framework

**NERC** North American Electric Reliability Corporation

**nRLDC** new Residual Load Duration Curve

**NTC** Net Transfer Capacity

**NZE** Net Zero Emissions

**PRM** Planning Reserve Margin

**PV** solar Photovoltaic

**RES** Reference Energy System

**RLDC** Residual Load Duration Curve

**RM** Reserve Margin

**RO** Robust Optimization

**RoR** Run of River

**RTE** Réseau de Transport d'Electricité

**SA** Stochastic Approximation

**SP** Stochastic Programming

**SRFP** Stochastic Root-Finding Problem

**STEPS** Stated Policies Scenario

**TIMES** The Integrated MARKAL-EFOM System

**TSOs** Transmission System Operators

**VoLL** Value of Lost Load

**VRE** Variable Renewable Energy

**WEO** World Energy Outlook

**WTP** Willingness-To-Pay

# Abstract

As clean energy transitions continue to progress, the role of electricity becomes increasingly central, underscoring the significance of electricity security for society and economies. The acceleration of electrification and renewable energy deployment is evident, yet without well-structured, long-term investment planning, there exists a risk of impeding the momentum of clean energy transitions. From a modeling perspective, conducting technical-economic assessments of potential transition pathways has now become a critical necessity. This approach helps address uncertainties about the future and provides a comprehensive understanding of the ramifications of alternative policy choices. Two fundamental stages in shaping the power sector's transition stand out: long-term energy planning models and operational power system models. Long-term energy planning models are frequently deployed to assist policy-makers in devising cost-effective pathways. These models typically operate at a lower level of temporal, technical, and spatial granularity. On the other hand, operational power system models, responsible for solving the unit-commitment and dispatch problem, focus on the day-to-day operation of a specific power production fleet. They operate at a higher level of technical detail and temporal resolution but do not inherently consider the cost-effectiveness of the overall trajectory. Although both modeling tools are indispensable, they are often employed separately. The primary objective of this thesis is to develop a multi-scale model capable of bridging the long-term scale for planning investments for the transition with the short-term requirements for secure operation. The resulting multi-scale model generates investment trajectories that are operationally feasible, ensuring a secure electricity supply. The security assessment criterion utilized is the Loss Of Load Expectation (LOLE) - a probabilistic generation adequacy metric. Initially, we crafted a bi-directional soft-linking model for a single area, which caters to both single-period and multi-period trajectory planning. Subsequently, we formulated a multi-scale model tailored for a multi-area interconnected power system, powered by a Stochastic Approximation algorithm. This iterative process facilitates the search for solutions that meet predefined adequacy levels, incorporating two update schemes: a decreasing learning rate and a constant learning rate.

The results obtained from applying the bi-directional soft-linking model to the French power system have yielded three noteworthy findings:

1. The power system mix, as determined by the long-term energy planning model, proves to be inadequate.

2. The feedback loop, which relies on capacity credit updates for the peaking reserve

equation within the long-term energy planning model, demonstrates its effectiveness by rectifying the initial solution after only a few iterations.

3. Furthermore, the robustness of the Rolling Horizon algorithm was demonstrated when applying different scenarios (ranging from 60% Variable Renewable Energy (VRE) to 100% uptake by 2050) and changing the look-ahead periods (5 years, 10 years, 15 years, and perfect foresight).

A detailed discussion of our methodology emphasizes the sensitivity of the approach to the estimation of capacity credit values, which has the potential to impact the robustness of the outcomes of the overall soft-linking model.

The multi-scale model was applied to the European power system under two scenarios: Scenario A, representing a future with high VRE uptake, and Scenario B, which additionally aimed for carbon neutrality by 2050. In contrast to the soft-linking model where only a few iterations were conducted, the multi-scale model was run for 500 iterations. A scoring function was developed to assess the model's convergence. The following results were obtained:

1. The power generation adequacy assessments for both scenarios revealed non-compliance with a $LOLE$ limit of 3 hours/year for numerous countries across the planning time frame.

2. All four runs have two distinct phases when the iterations commenced: a transient phase, followed by a steady-state phase, which was typically reached after 100 iterations.

3. The constant learning rate outperformed the decreasing learning rate, rapidly approaching areas near the optimum solution.

4. Additional investments were required to achieve the final adequate solution, with approximately 1% additional annualized cost needed for Scenario A and 6% for Scenario B.

5. A comparative analysis of the scenario performance indicated that Scenario B showed greater score volatility compared to Scenario A.

# Résumé

Alors que les transitions vers un futur décarboné continuent de progresser, le rôle de l'électricité devient de plus en plus central, soulignant l'importance de la sécurité d'approvisionement en électricité pour les sociétés et les économies. L'accélération de l'électrification des usages et du déploiement des énergies renouvelables est évidente, mais sans une planification d'investissement à long terme bien structurée, il existe un risque de freiner l'élan des transitions vers les énergies propres. D'un point de vue de la modélisation, réaliser des évaluations techniques-économiques des trajectoires possible de la transition est devenu une nécessité critique. Cette approche permet de répondre aux incertitudes sur l'avenir et offre une compréhension globale des ramifications des choix politiques alternatifs.

Deux étapes fondamentales de modélisation pour l'aide à la décision de la transition se démarquent : les modèles de planification énergétique à long terme et les modèles opérationnels du système électrique à court-terme. Les exercices de prospective long-terme et les simulations de l'équilibre offre-demande sont deux éléments clefs de la planification à moindre coût du système électrique. Le premier vise à déterminer une trajectoire d'investissements à partir de scénarios exogènes d'évolution du contexte énergétique global. En revanche, le second a pour but principal de diagnostiquer les risques de défaillance possibles, à parc de production donné. Malgré leur évidente proximité, ces exercices sont souvent portés et mis en oeuvre de façon complètement indépendante. Cette approche totalement découplée conduit les prospectivistes à proposer des plans long-terme sans aucune analyse pertinente du risque de défaillance. Symétriquement, les études d'équilibre offre-demande à moyen-terme (cinq à dix ans) sont confrontées aux plus grandes difficultés lorsqu'il s'agit de valider la rentabilité des investissements nécessaires pour "passer la pointe".

L'objectif principal de cette thèse est de développer une approche de modélisation multi-échelle capable de réconcilier l'échelle long-terme propre à la planification optimale et l'échelle court-terme propre à l'opération adéquate. Le modèle multi-échelle résultant génère des trajectoires d'investissement opérationnellement réalisables, garantissant un niveau d'approvisionnement en électricité fiable. Le critère d'évaluation de l'adéquation utilisé est l'espérance de nombre d'heures de défaillance (*Loss of Load Expectation LOLE*) - une mesure probabiliste de l'adéquation de la génération. Initialement, nous avons élaboré un modèle de couplage bidirectionnel pour une seule région, appliqué à une période unique et à l'ensemble de la trajéctoire. Ensuite, nous avons formulé un modèle multi-échelle adapté à un système électrique interconnecté multi-régions, supporté par un algorithme d'approximation stochastique. Ce processus itératif facilite la recherche de solutions (mix de production) répondant

à des niveaux d'adéquation prédéfinis, en incorporant deux schémas de mise à jour : un taux d'apprentissage décroissant et un taux d'apprentissage constant.

Les résultats obtenus en appliquant le modèle de couplage bidirectionnelle au système électrique français ont produit trois conclusions :

- Le mix electrique, tel que déterminé par le modèle de planification énergétique à long terme ne respecte pas le critére d'adéquation reglementaire $LOLE \leq 3heures/an$.
- La boucle de rétroaction, qui repose sur les mises à jour du crédit de capacité pour l'équation de réserve de pointe dans le modèle de planification à long terme, démontre son efficacité en rectifiant la solution initiale après seulement quelques itérations.
- De plus, la robustesse de l'algorithme *Rolling Horizon* a été démontrée lors de l'application de différents scénarios (allant de 60 % d'énergie renouvelable variable à 100 % d'adoption d'ici 2050) et en modifiant les fenetres d'optimisatios (5 ans (myopie), 10 ans, 15 ans, et 25 ans (connaisance parfaite du future)).

Une discussion détaillée de notre méthodologie met l'accent sur la sensibilité de l'approche à l'estimation des valeurs de crédit de capacité, ce qui peut avoir un impact sur la robustesse des résultats du modèle de couplage.

Le modèle multi-échelle a été appliqué au système éléctrique européen selon deux scénarios : le Scénario A, représentant un avenir avec une forte adoption des VRE, et le Scénario B, visant en plus la neutralité carbone d'ici 2050. Contrairement au modèle de couplage où seules quelques itérations ont été effectuées, le modèle multi-échelle a été exécuté pour 500 itérations. Une fonction de scoring a été développée pour évaluer la convergence du modèle. Les résultats suivants ont été obtenus :

1. Les évaluations de l'adéquation de la production d'électricité pour les deux scénarios ont révélé une non-conformité avec une limite LOLE de 3 heures/an pour de nombreux pays au cours de la période de planification.
2. Les quatre exécutions présentent deux phases distinctes lors du démarrage des itérations : une phase transitoire, suivie d'une phase stationnaire, généralement atteinte après 100 itérations.
3. Le taux d'apprentissage constant a surpassé le taux d'apprentissage décroissant, approchant rapidement les zones proches de la solution optimale.
4. Des investissements supplémentaires étaient nécessaires pour obtenir la solution finale adéquate, avec environ 1% de coût annualisé supplémentaire pour le Scénario A et 6% pour le Scénario B.
5. Une analyse comparative des performances des scénarios a indiqué que le Scénario B montrait une plus grande volatilité des scores par rapport au Scénario A.

# Chapter 1

# Introduction

The history of electricity has evolved through several distinct phases over the past decades. It is essential to explore the origins and key developments that have shaped our understanding of electrical energy. In the early stages of human civilization, our ancestors heavily relied on fire to harness light, heat, and facilitate cooking. However, even in those ancient times, the concept of electricity began to emerge as people observed certain fish with the ability to produce electric shocks. Around 2750 B.C., ancient Egyptian texts referred to the electric catfish as the "Thunderer of the Nile," providing evidence of their awareness of this phenomenon. As civilization progressed, early civilizations such as the Greeks, Romans, and Egyptians, possibly influenced by the electric fish, experimented with electricity in medicine, particularly in the treatment of epilepsy. Moving forward to around 500 B.C., the Greek mathematician Thales of Miletus made an important discovery, recognizing static electricity by observing particles of dust being attracted to amber. Despite these early glimpses into the nature of electricity, progress in understanding the subject stagnated between 500 B.C. and 1600. During this period, it remained an intellectual curiosity among thinkers of the time, and the term "electricity" had not yet been coined. It was only later, when scientist William Gilbert introduced the term "electricus" to describe objects that have similar properties to amber, that the modern usage of the word "electricity" emerged. The breakthroughs in the history of electricity occurred during the 18th and 19th centuries when individual scientists conducted experiments that advanced our knowledge significantly. Alessandro Volta, in 1800, invented the first electric battery, known as the voltaic pile. This experiment proved that electricity could be generated not only by animal sources in laboratories but also through chemical reactions that could be controlled and directed in circuits. Following this, in 1821, Michael Faraday made significant contributions to the field by formulating the concept of the electromagnetic field and identifying the laws of electrolysis, which continue to be fundamental in determining the amount of energy required to induce chemical changes. He also pioneered the first electric motor. The late 19th century saw pivotal developments, as Thomas Edison established the world's first coal-fired power station in London in 1882, and later that same year, the Pearl Street Station power plant in New York. This era also marked the "war of the currents," a rivalry between Edison's Direct Current (DC) transmission system and Nikola Tesla's Alternating Current (AC) transmission system. This rivalry spurred

innovations and led to the modern age of electricity, witnessing the widespread implementation of various technologies such as nuclear, hydro-power, renewable energy sources, and advancements in electronics and networks.

Today, the mere act of pressing a switch, button, or knob grants us immediate access to power, showcasing the indispensable role of electricity in modern economies. Its significance goes beyond mere convenience; it underpins critical services, spanning healthcare, banking, transportation, and more. The secure and reliable supply of electricity stands as a cornerstone for the prosperity of societies and is particularly crucial in sustaining the 24/7 digital economy. Amidst the recent challenges posed by the Covid-19 pandemic, the value of electricity has become even more apparent. It plays a vital role in supporting healthcare facilities by operating ventilators and medical equipment, enabling the treatment of numerous patients. Additionally, the continuity of IT services facilitates teleworking and videoconferencing, essential for remote collaboration during these challenging times. Despite currently accounting for only a fifth of total final energy consumption, the share of electricity in the overall energy mix is steadily increasing. Forecasts aligned with the Paris Agreement suggest that electricity could surpass oil as the primary energy source by the year 2040. Furthermore, electricity demand is projected to surge by approximately 50% over the next two decades across all International Energy Agency (IEA) scenarios. This heightened demand is expected to extend beyond traditional applications, as electricity is likely to play a significant role in heating, cooling, and transportation, along with its integration into digitally dependent sectors such as communication, finance, and healthcare. Consequently, effective planning for robust and secure power systems becomes a prerequisite for ensuring the seamless operation of our modern economies. The significance of electricity security now takes precedence on the energy security agenda, which historically revolved around ensuring a stable oil supply, notably in response to the 1973 oil embargo. In their latest World Energy Outlook, the IEA emphasizes the central role of electricity in modern energy security: "Electricity is moving to the heart of modern energy security", reflecting the ongoing transformations within the power sector landscape.

Various factors contribute to this paradigm shift, as the power sector experiences multiple fundamental transformations, adapting to evolving needs and technologies. The demand for electricity is projected to increase by 66% between 2017 and 2040, driven by demographic and economic growth, the electrification of transportation and heating sectors, and the growth of digitalization [1]. Consequently, the share of electricity in total final energy consumption is expected to rise from 19% in 2018 to 24% in 2040 under the Stated Policies Scenario, and potentially reach 31% under the Sustainable Development Scenario [1]. On the supply side, solar photovoltaic (PV) and wind power deployment are anticipated to contribute more than half of the additional electricity generation in 2040 under the Stated Policies Scenario, and nearly all of it under the Sustainable Development Scenario [1]. This transition to a low-carbon power system presents significant opportunities but also introduces new electricity security challenges. Traditional forms of power generation, such as coal, natural gas, nuclear power, and hydro power, offer strong security benefits due to their controllability and the use of rotating synchronous generators that provide "natural" inertia. However,

these thermal power generation technologies are gradually being phased out, particularly in developed countries. While Variable Renewable Energy (VRE) sources are gaining a larger share in the energy mix, concerns have been raised regarding their impact on the power system structure and operation [2–4]. Various studies have documented power system issues associated with VRE generation [5, 6]. One key challenge is its weather-dependent nature (VRE is limited in dispatchability (i.e., the ability to control its output) and has variable seasonal and diurnal (i.e., within-day) patterns of production and uncertainty in its generation forecasts. Additionally, the asynchronous nature of VRE sources, connected to the power grid through power electronic converters/inverters, means they do not contribute to system inertia [7] [1]. As VRE power generation increases, the power system needs to diversify its resource portfolio to effectively manage the challenges associated with VRE operation while maintaining an acceptable level of security. Furthermore, other drivers of the transition are also crucial. Technological innovation, decarbonization goals, and energy efficiency efforts are leading to increased digitalization, including the use of smart grids and smart meters. The decentralization of the power system, facilitated by distributed energy sources such as rooftop solar panels, batteries, and demand-side response devices, has the potential to shift the balance between transmission and distribution grids. These transformations are expected to fundamentally impact the power generation mix and the way the system is planned, governed, regulated, and operated in terms of electricity security. These trends call for the development of a proactive planing for secure power system transition framework. According to the EU project MILESECURE 2050 [8], a secure system evolves over time and achieves an adequate capacity to absorb uncertain events, so that the system is able to continue satisfying the energy service needs of its users. Although the supply of electricity takes places in real time, multiple decisions have to be adopted at different time-scales (from several years for timely investments to seconds before real time to balance supply and demand), by different actors (regulators, investors, system operators, producers and consumers). Assessing the security of electricity supply requires considering its multi-temporal-scale aspects [9]. In the long-term, electricity security mainly involves making timely investments to ensure energy supply aligns with economic developments and environmental goals. In contrast, short-term electricity security focuses on the ability of the power generation mix to promptly respond to sudden disturbances in supply-demand balance. Specifically, reliability, often equated with security of supply, is fundamentally composed of two distinct but related components: adequacy and security [10].

- Adequacy assessment determines whether the power system, utilizing existing and new resources, can meet consumer demand at all times, considering scheduled and reasonably expected unscheduled outages of system elements.

- Security assessment involves evaluating the ability of the electric system to withstand sudden disturbances, such as electric short circuits or unanticipated loss of system elements, given a certain level of risk.

[1] Wind generators can mimic synchronicity through so-called synthetic inertia, drawn from their rotating blades

Consequently, it is important to monitor electricity security to ensure both a secure and clean transition pathways.

From a modeling perspective, technical-economic assessments of possible pathways have become essential to both deal with future uncertainty and clarify the implications of alternate policy choices. Among others, long-term energy planning models and operational power system models are key stages in planning the transition of the power sector. Long-term energy planning models have been applied frequently to help policy makers ensure cost-effective pathways. These models typically use a low level of temporal, technical and spatial detail. In contrast, operational power system models, which solve what is known as the unit-commitment problem, focus on the commitment and dispatch of a given power production fleet. They operate at a high level of detail but do not consider the trajectory cost-effectiveness. Although both modeling tools are equally necessary, they are often employed independently [11].

As VRE deployment increases, one challenge involves the concerns raised over the methodologies and underlying assumptions employed in standard energy system models [12, 13]. In fact, these models were not initially designed to perform capacity expansion in power systems with high shares of VRE. Their modeling was questioned for at least two reasons [2]. First, limited temporal and space granularity is commonly assumed and provides an inadequate basis for capturing the main short-term features of VRE generators. For example, wind and solar in particular have intermittent profiles. Second, omitting the impact of these technologies characteristics on the system flexibility will introduce biases that will favor or disadvantage more flexible investments. As a result, insufficient variability representation in supply or demand as well as operational details could lead to a sub-optimal, or even inadequate, power generation mix [15]. This could create misunderstanding among policymakers and system operators. Both could begin to view power generation portfolios produced by long-term energy planning models as at odds with the secure provision of electricity [11]. Therefore, two contrasting methodologies have been developed to overcome this drawback: a direct integration approach and a model-coupling approach.

The direct integration approach involves either increasing temporal and spatial granularity to improve the representation of VRE variability, or integrating new constraints into the long-term energy planning model to more accurately mimic the effects of some short-term features of the operation [16–19]. A growing body of literature provides significant insights into the impact of directly improving the representation of VRE variability in long-term energy planning models in terms of capacity-mix, dispatch decisions and economics [20–26]. [27] show to what extent increasing temporal granularity impacts the capacity and generation mix produced by long-term energy planning models. To this end, two versions of the Belgian TIMES power system model have been developed (without import/export exchanges), one of which applies 12 time slices per year and the other 8,760 time- slices per year. In both versions, a renewable electricity generation target share of 50% is imposed for 2050. Their analysis reveals a significant impact on the anticipated curtailment and capacity mix. [28]

[2] A more detailed classification of the current challenges in capacity expansion planning and related modeling approaches can be found in [14]

evaluate the effect of the temporal resolution on the dispatch capabilities of an electricity generation planning model. To do so, a new Swiss TIMES electricity model (STEM-E) with an hourly representation of inter-temporal detail is compared to an aggregated model with only two diurnal time slices. The results show significant differences between both models and confirm that the high temporal resolution model offers better insights into the electricity generation schedule [28].

In contrast, model-coupling methodologies are a response to the limitations of using a single model to capture all of the power system's relevant proprieties. [28] recognize that even with a high temporal resolution TIMES framework, they cannot substitute a dispatch model because some features cannot be represented. Hence, closing the gap between short-term operational models and long-term energy planning models requires additional improvements. This research axis is identified by the energy modeling community as more and more important [11]. Terms commonly used to describe the model linkage include "hardlinking" versus "softlinking". These terms are adapted from studies that have linked economic and energy models since the mid-1990s. We use the terms as defined in [29], where softlinking is information transfer controlled by the user, and hardlinking is formal links (the two models overlap partially) whereby information is transferred without any user judgment. This author recapitulates the advantages of hardlinking with the terms "productivity", "uniqueness" and "control", and characterizes the advantages of softlinking with the words "practicality", "transparency" and "learning". A few papers have considered linking approaches in the context of power system planning and operation. One example of power system linked models was reported by [30]. They linked TIMES with PLEXOS for the 2020 Irish power system to analyze the extent to which the temporal resolution and technical constraint of power plants affect investments, as well as dispatch decisions and corresponding costs. Thus, the capacity mix given by TIMES for 2020 was transferred to the unit-commitment model with added degrees of technical detail. The results show that, in the absence of key technical constraints, long-term energy planning models undervalue flexible resources, underestimate wind curtailment, and overestimate the operation of baseload technologies. Recent efforts by the same group involved linking a MONET model (six-region TIMES model of the Italian energy system) to the power systems model PLEXOS_IT (PLEXOS Italian model), with the objective of investigating energy security issues within power systems. Two main outcomes are reported in this study: firstly, an underestimation of the flexibility needs of the Italian system with increasing VRE penetration; secondly, concerns as to whether the Italian energy system can provide adequate guarantees [31].

Before introducing all the chapters of the thesis, it is important to highlight the distinctions between frameworks and models. To accomplish this, it is essential to take a conceptual 'step back' and distinguish between the various levels of theory in science. These levels of theory can be categorized from the most conceptually comprehensive to the most empirically precise as follows: paradigms, frameworks, specific theories, models/archetypes, and cases. Drawing upon the work of Stephan Partelow [32], the following points encapsulate the various levels of a theory:

1. **Paradigms:** "Represent and encompass the large narratives that build and drive

societies and cultures, including science".

2. **Specified theories:** "Specific causal relationships among core variables. Theory is a wide level, ranging from broad sweeping claims to specified interactions, for example with archetypes, which identify".

3. **Frameworks:** "Organize diagnostic, descriptive, and prescriptive inquiry, providing the basic vocabulary of concepts and terms to construct the causal explanations expected of a theory."

4. **Models/archetypes:** "Recurrent patterns among cases in which general regularities that apply to all cases cannot be expected. A detailed context specific explanation of the functional relationships among independent and dependent variables."

5. **Cases:** "Specific empirical observations of unique contexts with identifiable variable relationships and outcomes."

**The primary objective** of this thesis is to develop a comprehensive multi-scale modeling framework that effectively reconciles the long-term scale of investments planning with the short-term scale of a secure operation. This entails ensuring power generation adequacy requirements for power systems decided by long-term energy planning models for interconnected power systems. To achieve this, the thesis adopts an **incremental approach**, wherein a step-by-step methodology is followed. Initially, to manage the complexity of the problem, the research focuses on a single isolated area, specifically France. By following the existing literature, the methodology is presented in a descriptive style. The first phase involves proposing two approaches for ensuring power generation adequacy requirements for a specific target year within the isolated area. Subsequently, these approaches are extended to cover the entire trajectory of the power system. After obtaining results and addressing the limitations of the initial approaches, the research progresses to enhance the complexity of the problem. This involves mathematically formulating the multi-area problem as a multi-scale model. This model accounts for multiple interconnected areas, enabling a more holistic and accurate representation of the power system. Finally, the proposed multi-scale model is applied to the European power system, which stands as one of the world's largest regional interconnected power grids. In the next sections we provide a synthetic overview of each Chapter.

**Chapter 2 and 3** of this thesis provides a vital contextualization essential for comprehending the problem addressed in the research. The chapter encompasses several key aspects, including:

1. An overview of the fundamental changes occurring within the power system landscape. This examination aims to shed light on the evolving dynamics and challenges faced by the transition to a low carbon power system.

2. A comprehensive definition of electricity security and its principal properties. Different outages examples and their relative economic and societal impacts are enumerated. A

special focus is then put on the generation adequacy assessment methodologies and related metrics, and the importance of monitoring the power generation adequacy at different time-scales.

3. Conceptual definitions of power system planning and operation and the need for an integrated approach to transition planning.

4. Introduction to the typologies of energy system models along with an assessment of the state-of-the-art challenges encountered by long-term energy planning models, particularly in the context of the increasing penetration of VRE sources.

5. A clear definition of the research focus, identification of literature gaps, and the main contributions that this thesis aims to make to the existing body of knowledge. This section serves as a roadmap for the subsequent chapters, outlining the specific objectives and research contributions.

No scientific novelty is expected from the Chapter 2 and 3, however it holds significant importance as it lays the groundwork for comprehending the subsequent context, problem and perimeters of the thesis.

In **Chapter 4**, the primary contribution lies in the field of multi-modeling exercises. The core objective of this chapter is to advance the development of a multi-model framework that combines two well-established models for techno-economic power system assessments. Specifically, the energy system model employed is MARKAL/TIMES (referred to as TIMES), while ANTARES-Simulator (referred to as ANTARES) is the probabilistic unit-commitment and dispatch model. The first goal of this contribution is to establish a linkage between TIMES and ANTARES within a one-directional chain model. This connection facilitates the transfer of the power generation mix determined by TIMES for a specific year to the ANTARES input database. For the chosen target year, the second objective centers on examining ANTARES dispatch results and adequacy metrics to provide coherent feedback to TIMES, thereby ensuring an adequate power supply. This undertaking marks the initial step toward planning a cost-effective and reliable power system that adheres to generation adequacy requirements. It's crucial to emphasize that this contribution employs a long-term scenario as a case study to illustrate and elucidate the methodological approach rather than representing precise French power system policies. Detailed analyses of French power system policies are extensively covered in Generation Adequacy reports and other long-term prospective studies [33–36]. The framework developed and proposed is applied to France under an assumption of a "copper plate" scenario, which disregards grid congestions within the French grid. Additionally, it operates on a stand-alone basis, excluding considerations of interconnections with other countries. A notable limitation of this development is the trajectory assessments, as only one targeted year was studied. In the second part of this chapter, a new methodology was developed to take into account the overall planning trajectory. To do so, the soft-linking algorithm developed for only one targeted year was coupled with a Rolling Horizon algorithm to solve the long-term planning model. To achieve this, the soft-linking algorithm, initially designed for a single targeted year, was coupled

with a Rolling Horizon algorithm to include the overall planning time-frame. The algorithm was subsequently tested with various long-term scenarios and distinct configurations of the rolling horizon algorithm to assess its robustness. An analysis of the developed methodology and results reveals its strengths and limitations regarding estimating capacity credits. This motivate the development of the multi-scale model of the next Chapter.

In **Chapter 5**, we propose a formulation of the thesis problem by introducing a novel multi-scale approach. This approach enables us to consider a multi-area interconnected power system for the overall planning trajectory (at once). Building upon the insights gained from the approach developed in Chapter 2 and acknowledging its limitations, the problem under investigation in this thesis is mathematically formulated as a multi-scale problem. The motivation behind this mathematical formulation stems from the need to transition from a descriptive and procedural presentation of the problem to a rigorous mathematical representation. This shift facilitates a clearer understanding of the different scales involved and elucidates how the bridging scale algorithm operates, effectively reconciling the long-term planning scale with the short-term operational scale. The multi-scale model is reinforced by a simulation-based optimization process, employing Stochastic Approximation (SA) algorithm. Using this algorithm, the multi-scale model seeks to find solutions that satisfy power generation adequacy requirements. By integrating multi-scale considerations and simulation-based optimization, this chapter contributes to advancing the analytical methodologies utilized in power system planning and operation.

**Chapter 6** involves the application of the multi-scale model to the European power system model. Firstly, it provides a concise overview of the long-term power system model eTIMES-EU [37], emphasizing its key input data and modeling assumptions. Additionally, the Monte Carlo Modeling assumptions pertaining to the operational power system model ANTARES are presented. In the results section of this chapter, the outcomes of the multi-scale model are showcased for two long-term scenarios developed within this thesis. Scenario A portrays a future with a high uptake of VRE without any constraints on $CO_2$ emissions. On the other hand, Scenario B follows the same assumptions as Scenario A but introduces an additional constraint on $CO_2$ tax, resulting in zero emissions by 2050. At the planning stage, the power generation mix trajectory is analyzed for both scenarios. Subsequently, various techno-economic-environmental measuring points are assessed to validate the multi-scale model's reliability and accuracy. Once the validity of the multi-scale model is established, a power generation adequacy assessment is conducted to determine the extent to which the investment trajectories decided by the long-term energy planning model satisfy adequacy requirements. The stochastic approximation algorithm is employed for both scenarios using two different schemes, one with a decreasing learning rate, and the other with a constant learning rate. Finally, the chapter addresses the robustness and convergence of both scenarios, scrutinizing the model's stability and performance under different conditions. This chapter contributes significantly to the research by applying the developed multi-scale model to a real-world case, the European power system. Through the examination of multiple scenarios, it provides valuable insights into the dynamic interplay between long-term planning, operational considerations, and power generation adequacy in the face of high

VRE penetration and $CO_2$ emission constraints.

**Chapter 7** summarizes the research's findings and key conclusions while providing an outlook for future research.

The thesis reading can be quite overwhelming, and at times, readers may feel a bit disoriented. A significant effort has been made to maintain consistency in the chronological sequence of the "story". However, being human, we may occasionally lose track of our location within the thesis and the questions we are addressing. To mitigate this, the map in Figure 1.1 provides a condensed overview of the structural organization of the various chapters in the thesis.

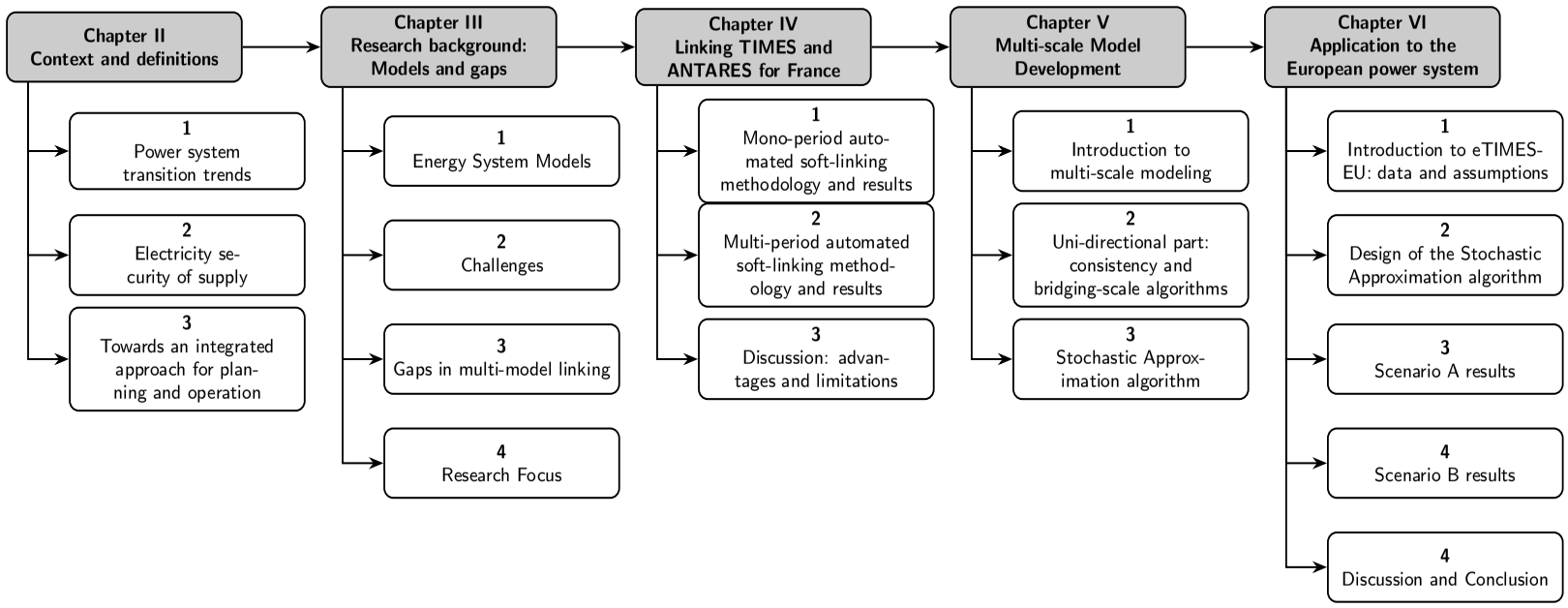


Figure 1.1: Organization of the Different Chapters of the Thesis: A Synthetic Overview

# Chapter 2

# Planning and secure operation of power systems in transition

## Contents

The main purpose of this chapter is to provide the reader with essential ingredients to better understand the transition to a low carbon power system from a planning and operation point of view. After introducing the key transition trends in the electricity sector at a global scale, a particular focus will be placed on the multifaceted notion of electricity security and how it is influenced by present and future trends. Since our work specifically focuses on power generation adequacy and excludes other aspects of electricity security, we will provide a detailed presentation of how power generation adequacy assessment is conducted.

**Résumé en français :**

Le principal objectif de ce chapitre est de fournir au lecteur les éléments essentiels pour mieux comprendre la transition vers un système électrique à faible émission de carbone d'un point de vue de la planification et de l'exploitation. Après avoir introduit les principales tendances de transition dans le secteur de l'électricité à l'échelle mondiale, un accent particulier sera mis sur la notion multidimensionnelle de la sécurité d'approvisionement en éléctricité et sur la manière dont elle est influencée par les tendances actuelles et futures. Étant donné que notre travail se concentre spécifiquement sur l'adéquation de la production d'électricité et exclut d'autres aspects de la sécurité électrique, nous fournirons une présentation détaillée de la manière dont l'évaluation de l'adéquation de la production électrique est menée.

## 2.1 Electricity Mix Trends: Energy Transitions with More Variable Renewable Energy

This section takes a global coverage approach in analyzing the current and future trends that shape the electricity mix, as we aim to develop a non-region specific modeling framework. By adopting this approach, we can capture the broader picture and identify trends that transcend specific geographical boundaries. This global perspective allows us to gain insights into the overall dynamics of the electricity sector. To draw the context we analyse both the electricity demand and supply side. It starts by highlighting recent and future trends in electricity demand. It goes on to examine recent and future trends in electricity supply, noting that the share of variable renewable energy sources are significantly increasing, while thermal sources sees limited growth. The increasing penetration of renewable energy, such as solar and wind, brings about significant challenges in the electricity generation operation and planning. We highlight the importance of the power grid as an enabler of this transition, facilitating the efficient integration of VRE sources and ensuring system security. Finally, this section looks at investments flow to highlight the transition dynamics. When discussing future trends, our analysis draws upon three concurrent scenarios presented in the World Energy Outlook 2022 [38]. The Stated Policies Scenario (STEPS) reflects the current policies in place, while the Announced Pledges Scenario (APS) assumes the successful achievement of all long-term targets and goals within the designated time-frame. Additionally, the Net Zero Emissions (NZE) by 2050 scenario outlines a cost-effective trajectory for achieving emissions neutrality, aligning with the objective of limiting the global average temperature increase to $1.5 \circ C$ by 2100. By considering these scenarios, we aim to provide a basic understanding of the "strong trends" and challenges associated with the transition to a low carbon future power systems.

### 2.1.1 The increasing role of electricity in the decarbonized world

Electricity plays a significant role in economies worldwide as it is central to our modern daily life. Global electricity demand in 2021 reached 24,700 TWh (50 times the French annual consumption), a 6% increase from the previous year due to post-pandemic economic recovery [38]. This represents the highest annual increase rate since 2010, where an average annual increase of 2.6% was observed. Emerging countries drove this recent increase, accounting for approximately three-quarters of the total, with China alone contributing 50% (700 TWh, equivalent to Africa's overall electricity demand). The share of electricity in total final energy consumption is 20%. China, the United States, and Europe account for 60% of global electricity demand, with China leading at 30%, followed by the United States at 16%, and Europe at 14%. Since 2010, advanced economies have experienced a decline of around ten percentage points in their total share, as demand has increased in emerging and developing countries. In the last decade, average electricity demand per capita in advanced countries declined by 0.2% per year, while it increased by 3.5% in emerging and developing economies.

In future scenarios, demand growth to 2030 is projected at 2.4% per year in the STEP scenario, 2.8% in the APS scenario, and 3.5% in the NZE scenario. By 2030, global electricity demand is estimated to reach over 30,600 TWh in the STEP scenario, 31,752 TWh in the APS scenario, and 33,700 TWh in the NZE scenario. The growth is maintained until 2040 before slowing down, reaching 43,700 TWh in the STEP scenario, 54,000 TWh in the APS scenario, and 62,100 TWh in the NZE scenario by 2050. In the STEP scenario, the share of electricity in total final consumption is projected to reach 22% in 2030 and 28% in 2050. In the APS scenario, these shares are expected to be 24% and 40% respectively, and in the NZE scenario, they are estimated to be 28% in 2030 and 50% by 2050. The high increase in electricity demand momentum is evident across all future scenarios.

The buildings and industry sectors are the largest consumers of electricity today, accounting for over 90% of global electricity consumption and 90% of the demand increase in the last decade. In the buildings sector, electricity is mainly consumed by appliances (45% of the total) and space cooling and heating (nearly 30% of the total). In the industry sector, the three main drivers of electricity consumption are electric motors, aluminium smelting, and electric arc furnaces. The demand for space cooling, driven by climate change impact, is expected to be the primary contributor to electricity demand growth in emerging and developing countries in the coming decades. In the STEPS scenario, the increase in global electricity demand due to cooling needs is projected to be 2,800 TWh, while in the APS scenario, due to energy efficiency policies, it is estimated to be 1,400 TWh. Industry accounts for approximately 30% of the total electricity demand increase in the STEPS and APS scenarios by 2030, reflecting the economic growth in emerging and developing economies and transition policies promoting the electrification of industrial processes.

Transport also contributes significantly to future electricity demand growth. Currently, transport accounts for 1.8% of total electricity consumption, with Electric Vehicles (EVs) playing an increasing role. The EV fleet reached 6.6 million in 2021, consuming 100 TWh of electricity annually. Projections indicate that the market share of electric cars reach 25% by 2030 in the STEPS scenario and 35% in the APS scenario. Rail, which has been the largest consumer of electricity in the transport sector, is expected to be surpassed by road transport in the coming years. By 2030, transport electricity demand is estimated to reach 1,169 TWh in the STEPS scenario, 1,570 TWh in the APS scenario, and 2,236 TWh in the NZE scenario.

While energy access is an important sustainable development goal, it constitutes a small portion of the increase in electricity demand. Projections indicate that improving energy efficiency in appliances, motors, buildings, and transportation can reduce electricity demand growth by 10% by 2030 and around 20% by 2050.

### 2.1.2 Growth of Renewable Power Capacity

In the past seven years, annual investments in new renewable power capacity have surpassed the combined investments in fossil fuels and nuclear energy. Over the last decade, renewable capacity has increased by 130%, while other energy sources have only seen a 24% increase. Despite the disruptions caused by the pandemic on global supply chains, approximately 260

GW of renewable generation capacity was added to the grid in 2020, compared to only 50 GW of non-renewable capacity. This record-breaking level of renewable capacity includes 111 GW of wind power and 127 GW of solar PV. In 2021, the total installed renewable capacity worldwide reached 3,064 GW, generating 8,000 TWh of electricity. The share of fossil fuels in electricity generation declined from 65% in 2018 to 62% in 2021, while the share of renewable generation increased from 20% in 2010 to 28% in 2020 [39].

The rapid growth of solar PV installations can be attributed to cost reductions driven by technological innovation, learning curves, policy support, and financial incentives. Utility-scale solar PV projects have experienced an 85% decrease in the global weighted average Levelized Cost Of Energy (LCOE) from 2010 to 2020, dropping from 0.381 USD/kWh to 0.057 USD/kWh. According to data from IRENA [40], recent competitive procurement processes in 2022 resulted in an average price drop of 30% compared to 2020, making it 27% cheaper than coal-fired power plants. The total installed capacity of **solar PV** reached 843 GW, with 133 GW connected to the grid in 2021, of which 57% was located in Asia. Wind power has also experienced significant growth, with a four-fold increase from 2010 to 2020. The total installed **onshore wind** capacity in 2021 reached 769 GW, predominantly driven by Asia with over 358 GW. The cost of onshore wind has decreased by 56%, going from 0.089 USD/kWh to 0.039 USD/kWh. On the other hand, **offshore wind** installations have reached a total capacity of 56 GW in 2021, evenly distributed between Asia and Europe. The global weighted average LCOE for offshore wind has declined by 42%, from 0.162 USD/kWh in 2010 to 0.084 USD/kWh in 2020.

Hydropower currently holds the largest share of renewable installed capacity, reaching nearly 1,230 GW (excluding pumped storage) and accounting for 40% of the total renewable capacity [41]. The year 2013 marked the peak in new hydropower installations with the commissioning of an additional 45 GW. Other renewable technologies such as CSP, bioenergy, geothermal, and ocean technologies have experienced slower growth, with a total installed capacity of 166 GW in 2021. These technologies face barriers such as higher investment costs, limited political and financial support, and a lack of recognition for their flexibility benefits compared to wind and solar power.

Projections for the next 30 years indicate a continuation of the deployment dynamics for renewables, albeit at different rates. In the STEPS scenario, wind and solar PV investments are expected to set new records every year until 2030 and maintain significant annual deployment through to 2050. The share of renewables in total power capacity additions from 2022 to 2050 ranges from 45% to 85%. The APS scenario shows more pronounced deployment of wind and solar, with annual wind capacity increasing from 95 GW in 2021 to 210 GW in 2030 and 270 GW in 2050. Solar PV capacity additions are projected to rise from 151 GW in 2021 to 370 GW in 2030 and 600 GW in 2050. In the NZE scenario, the share of renewables in total generation rapidly increases from 29% in 2021 to over 60% in 2030 and 90% in 2050. Dispatchable hydropower and other renewables also have a significant role in the future power generation mix in all scenarios. Hydropower remains the largest installed capacity until 2030, after which it is surpassed by wind and solar PV. In the APS scenario, other renewables such as bioenergy, geothermal, and Concentrated Solar Power (CSP) ex-

perience faster deployment compared to the STEPS scenario to support the integration of large amounts of wind and solar power. Once again, it is evident that all these scenarios converge toward a future power system with a substantial increase in the share of solar PV and wind in total generation [42, 43].

### 2.1.3 Limited Future Growth for Thermal Dispatchable Sources

The increasing focus on renewable energy systems has brought attention to the need for dispatchable generation. Dispatchable generation has the important capability to adjust power generation based on demand to maintain a balance between supply and demand. While low-carbon dispatchable sources like hydropower and bioenergy are valuable, they face limitations due to factors such as local potential, climatic constraints, and limited resources. In this paragraph, we will specifically discuss thermal dispatchable generation technologies.

**Nuclear** power, the second-largest low carbon electricity source after hydropower, accounted for nearly 10% of global electricity generation, with approximately 2,800 TWh generated in 2020. However, its share has significantly declined from 18% in the late 90s. The growth of nuclear power was highest in the 80s, with 230 GW of new nuclear power plants connected to the grid primarily in Europe and North America, driven by the oil security crisis of the 1970s. The 90s saw a slowdown in new investments with only 25 GW added, largely due to the Three Mile Island and Chernobyl nuclear disasters. However, capacity additions rebounded in the early 2000s, reaching 46 GW in the first decade and 56 GW in the 2010s. In 2020, 6 GW of capacity was added, followed by 5.6 GW in 2021. By 2021, a total capacity of 413 GW with 439 nuclear power reactors was installed and operational in 32 countries. The majority of nuclear capacity, around 70%, is located in advanced economies, but this fleet is aging, with varying average ages across regions. Europe and North America have lost market leadership in recent years to Russia and China. Notably, nuclear power has made a significant contribution to slowing the rise in global $CO_2$ emissions, avoiding nearly 66 Gt of $CO_2$ globally in the past 50 years, resulting in a reduction of nearly 20% in emissions from electricity generation and 6% in overall energy-related emissions [44, 45].

Future projections for nuclear power deployment in the transition depend on decisions regarding the extension of the lifetime of existing reactors and plans to build new units. While some countries do not foresee the need for or reject the importance of nuclear energy, a growing number of countries have announced programs to support new nuclear investments. In Western Europe, several countries continue to express support for nuclear energy and are willing to invest in new nuclear facilities (For example, France plans to extend the lifetime of all reactors and allocate a budget of 50 Euro Billion for the construction of new large reactors, The United Kingdom has committed to expanding their nuclear capacities). Simultaneously, many Western nations are phasing out their reliance on nuclear power (Germany). Additionally, some emerging economies are embarking on the development of nuclear energy programs (China aims to continue its nuclear deployment, targeting approximately 70 GW by 2026. India has initiated the construction of new nuclear reactors). Nuclear power is projected to maintain a 10% share in the global electricity generation in the STEPS scenario. In the NZE scenario, nuclear deployment reaches 24 GW annually, resulting in more than

double the total capacity by mid-century, but its share falls to 8% due to significant growth in electricity demand [42, 43].

**Natural gas** accounted for 23% of global electricity demand in 2021, with an installed capacity of approximately 1,850 GW. The United States has the largest installed capacity of gas-fired turbines with 528 GW, five times more than Russia's second-ranked capacity of 105 GW. From 2010 to 2021, natural gas-fired generation increased by 34%, reaching 6,552 TWh in 2021, driven by rising demand in emerging and developing countries. In the STEPS scenario, gas-fired generation is expected to maintain its 2021 level until 2050. However, in the NZE scenario, it initially increases due to a coal-to-gas shift but then declines by an average of 4% per year by 2030, ultimately reaching 90% lower than 2020 levels by 2040. While power generation from natural gas declines, its capacity remains important for maintaining operational flexibility. To align with NZE Scenario levels, existing gas-fired power plants will need to be coupled with Carbon Capture Utilization and Storage (CCUS) or utilize low carbon fuels like bio-gas or hydrogen or mothballed/dismantled by political decisions.

**Coal** has historically played a significant role in electricity generation, accounting for 65% of global coal consumption and emitting 10.5 Gt of CO2, representing 29% of energy-system carbon emissions. The total coal installed capacity fleet is 2,185 GW, primarily concentrated in emerging and developing countries experiencing rapid electricity demand growth. In 2021, coal-fired power plants accounted for almost half of additional generation, with its share of total electricity generation exceeding 36%. China and India were the main drivers of this growth, with China experiencing a 9% increase (390 TWh) and India a 13% increase (150 TWh) due to post-pandemic electricity demand. Factors such as droughts and higher gas prices led to increased coal generation in the European Union (+20% corresponding to 395 TWh) and the United States (+16% corresponding to 110 TWh). It's worth noting that despite many countries pledging coal retirement at COP26, half of them still saw growth in coal generation in 2021 [46].

Projections indicate that under the STEPS scenario, coal will continue to grow and reach its peak by 2025, driven by the construction of 175 GW of capacity at the beginning of 2022. However, coal-fired generation is expected to decline, representing only 26% of global electricity generation by 2030 and further dropping to 12% by 2050. Developed countries are projected to reduce their coal use in the power sector by 60% between 2021 and 2030, while emerging and developing countries are anticipated to increase their coal use by 3% during the same period.

In the APS scenario, coal experiences a sharp decline from 2025 onward, with its share in electricity generation decreasing to 23% by 2030 and a mere 3% by 2050. In 2030, despite higher electricity demand, there is a significant reduction of nearly 2,100 TWh in coal generation, which marks a substantial deviation from the past decade's trend. In advanced economies, coal generation is projected to decrease by 80% by 2030 and be completely phased out by 2050, with the United States leading the way in terms of the largest reduction. This acceleration of the downward trend has already contributed to a 45% reduction compared to the peak level observed in 2007 in advanced economies. In emerging countries, coal

generation is expected to peak in 2025 under the APS scenario and then decline by 50% by 2040, reflecting China's targets to reduce coal use from 2025 and India's focus on scaling up renewables.

In the NZE scenario, no new coal plants, apart from those already under construction, are commissioned. The share of coal decreases rapidly to 12% by 2030 and ultimately reaches zero by 2040. CCUS retrofits may play a crucial role in achieving a zero-emission future for young coal fleets in emerging and developing countries [42, 43].

**Oil** accounts for a mere 2% of global electricity supply, primarily utilized in remote regions or in close proximity to oil production sites. However, its usage is expected to decrease across all scenarios as power generators increasingly shift towards more cost-effective and environmentally friendly alternatives [42, 43].

### 2.1.4 Multiple phases of VRE integration

The rapid expansion of VRE in electricity generation raises significant questions regarding cost-effective and secure integration. Integration encompasses various aspects such as technical, institutional, policy, and market design adaptations required to ensure reliable and affordable transition pathways. In this context, the term VRE integration specifically refers to wind and solar PV technologies, which play an increasingly prominent role in renewable energy deployment within power systems. The ability to increase the share of renewables in a power system depends on two interconnected factors: the operational characteristics of VRE technologies and the flexibility of the power system they are integrated into. The challenges associated with VRE integration also depend on additional factors, such as the correlation between power demand time series and VRE power generation time series. These challenges are context-specific, varying based on the unique structure of each power system [47].

VRE generators possess five distinctive technical characteristics that differentiate them from traditional dispatchable generators. Firstly, their instantaneous power output relies on the availability of wind and sunlight, causing fluctuations. Secondly, accurately predicting power generation fluctuations beyond a few days in advance is challenging. Thirdly, VRE generators connect to the grid using power converter technology, which means they do not contribute to the stability of power systems. Fourthly, they are modular and often deployed in a distributed manner. Finally, their geographical placement is heavily influenced by resource potential. Despite these general technical similarities, wind and solar technologies exhibit several technical differences [47]. Table 2.1 depicts some five different features.

| Feature | Wind power | Solar PV |
|---|---|---|
| Plant level output variability | Random on sub-seasonal time-scales; | Planetary motion(days, seasons) |
| Output variability when aggregated | Strong geographical smoothing benefit | Smoothing benefits limited by "bell shape" |
| Ramps | Depends on resource, few extreme events | Frequent, deterministic and repetitive steep |
| Technology | Non-synchronous grid connection and mechanical power generation | Non-synchronous grid connection and electronic power generation |
| Capacity factor | 20%-50% | 10%-25% |

Table 2.1: Overview of differences between wind power and solar PV, (source [47])

To understand the different stages of VRE integration, it is crucial to focus on the

concept of flexibility. Power system flexibility, refers "to the ability to cope with variability and uncertainty in generation and demand" [48]. The flexibility of a power system involves the capacity to increase or decrease generation and demand over a range of time-frames - minutes, several hours, seasons- in response to variability. This definition captures the power system's capability to maintain a continuous balance between demand and supply, even in the face of significant fluctuations in generation and consumption caused by various factors. The measure of power system flexibility is typically expressed in terms of different metrics capturing different scale and aspects of it.

Traditional power systems, excluding hydro, have historically relied on non-renewable sources and were designed to handle the variability and uncertainty of electricity demand and conventional power plant supply. Variability in traditional power systems primarily stems from fluctuations in electricity demand, which can vary on an inter-day, weekend, inter-season or inter-year basis. Electricity demand is influenced by various climatic and socio-economic factors, such as weather conditions, seasons, industrial development, energy efficiency awareness, and economic performance (e.g., gross domestic product). On the supply side, base-load units like coal, biomass power plants have limited flexibility due to their reduced cycling capabilities. However, they can generate a steady and substantial amount of energy with low operational costs. Nuclear power is usually presented as poorly-flexible, however, data shows that Nuclear in France is flexible (approximately 40% of the fleet is currently involved in load-following) [49]. In contrast, peaking generators such as gas turbines (open-cycle gas turbines) and internal combustion generators are designed for flexible operation, offering rapid start-up, fast ramping capabilities, and a low minimum generation level. Modern combined-cycle gas turbines and reservoir hydropower plants are considered intermediate generators as they can supply both base and peak loads. Uncertainty in the supply side relates to the operational availability of generation units or the availability of fuel sources. Flexibility in power systems extends beyond the cycling capabilities of dispatchable generators. Other resources play a crucial role in balancing, including energy storage, demand-side management, and response. Interconnection with neighboring power systems and the grid's topology provide flexibility by linking distant flexible resources together, enhancing the system's overall flexibility.

As the share of VRE generation increases in a power system, the complexity of power system operation also increases. To address this, the IEA has developed a framework consisting of six phases that capture the evolving impacts, relevant challenges, and crucial tasks for supporting the growth of VRE. The categorization not only depend on the level of VRE uptake, but also on other technical characteristics of the power system operation [47]. These phases are depicted in the Figure below 2.1.

Before explaining each phase, it is important to define the concept of net load as it plays a crucial role in understanding the operation of the power system at each stage. Net load refers to the electricity demand minus the generation from VRE sources and other non-dispatchable generation resources, such as Run of River (RoR) hydro. Balancing the net load requires a combination of dispatchable thermal power plants, hydro power, interconnections, and energy storage units. The gradual integration of VRE introduces additional variability

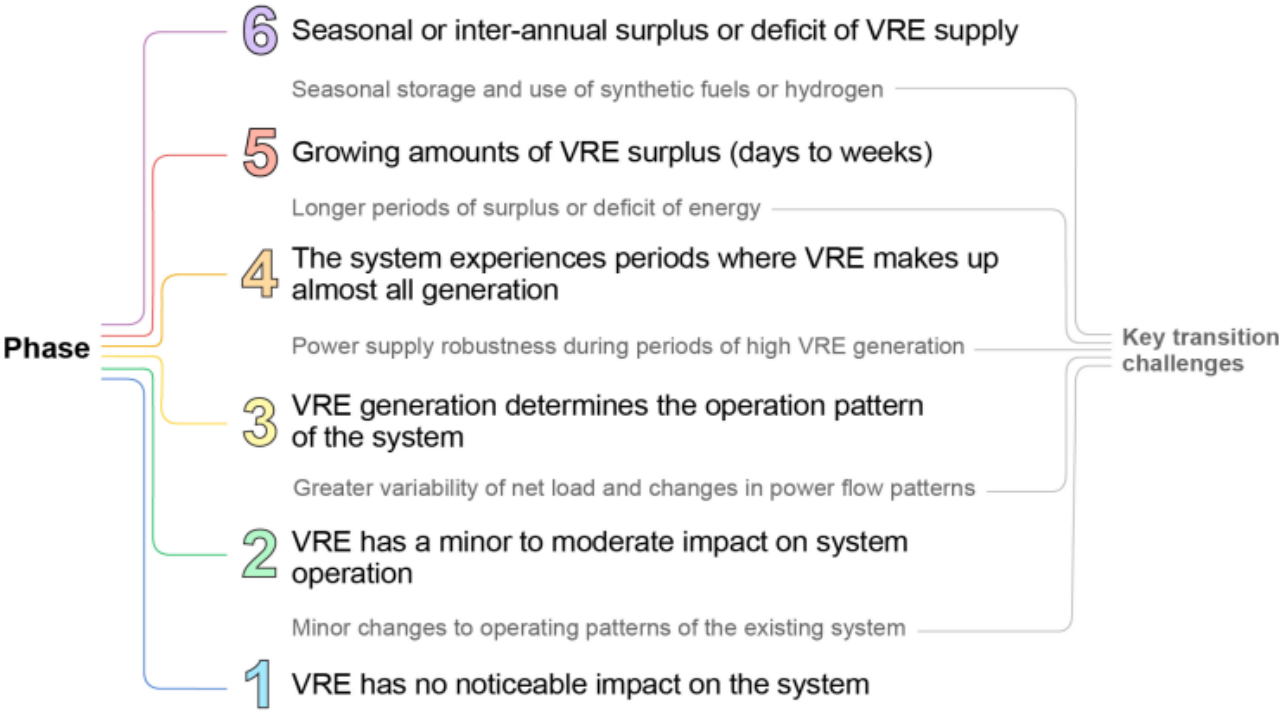


Figure 2.1: Different stages in the integration of renewables in power system (source [50])

and uncertainty to the net load.

**Phase 1** is characterized by a simple system where the capacity of VRE has no noticeable impact. When wind and solar are deployed with a capacity that is marginal in relation to the overall system, their power generation and its variability go unnoticed. In this phase, the net load is approximately equal to the load, but it is essential to ensure the functional connection and output generation of the initial VRE plants. Examples of countries in Phase 1 of VRE integration include Indonesia, South Africa, and Mexico (as of 31 March 2022).

In **Phase 2**, the impact of VRE becomes noticeable. Developing forecasting systems to predict VRE generation becomes crucial at this stage, enabling non-VRE generators to efficiently balance the net load. The operation of the power system becomes more challenging in **Phase 3**, as the impact of VRE generation affects the overall system operation and other power plants. System flexibility becomes crucial in this phase, as the increasing deployment of VRE leads to higher levels of uncertainty and variability in electricity supply. Periods of low net load are observed, requiring more dynamic operation of dispatchable power plants. Flows on the power grid become more variable due to weather influences, which may differ between day and night (with solar dominance). Countries and systems that are in Phase 3 include Germany, Italy, Portugal, Belgium, California and the United Kingdom (as of 31 March 2022).

In **Phase 4**, VRE has the potential to cover all power demand during certain hours. This phase introduces new challenges, particularly concerning the power system's ability to

maintain stable operating conditions immediately following disturbances. Denmark, Ireland and South Australia are considered to be in Phase 4 (as of 31 March 2022). During **Phase 5** of the transition to a high share of VRE generation, a structural surplus of VRE generation occurs. If not addressed, these surpluses could lead to significant curtailment of VRE output, imposing a limit on further expansion. Enhancing flexibility via electrification of other end-use such as heating and transport can overcome this drawback.

In **Phase 6**, a characteristic feature would be the occurrence of structural energy deficit periods, arising from seasonal imbalances between VRE supply and electricity demand. These imbalances could result in multi-day or week-long shortfalls in energy supply, such as extended periods of low wind output. Demand-side response and electricity storage, which provide flexibility over shorter time-frames, may prove insufficient to fill the gap between supply and demand. Therefore, for VRE to become the largest share source of power generation in the system, it may become necessary to convert excess electricity into a chemical form that can be cost-effectively stored at a large scale, such as synthetic natural gas or hydrogen. This would enable long-term energy storage and ensure the continuity of supply.

As the penetration of VRE in electricity systems expands, it becomes imperative to implement structural modifications in the technical, market, regulatory, and institutional frameworks. These changes are necessary to ensure the system's flexibility and guarantee a reliable supply of electricity. A notable example of such proactive measures is the collaboration between, the IEA, and France's transmission system operator, Réseau de Transport d'Electricité (RTE). Commissioned by the French Ministry for the Ecological Transition, they undertook a study to identify the necessary conditions and requirements for assessing the technical feasibility of scenarios characterized by a substantial uptake of renewable energy sources [51].

### 2.1.5 Electricity networks remain a critical enabler of system security: A worldwide perspective

The transmission and distribution networks remain the backbone of the electricity system, as they are essential for maintaining the security of electricity supply, improving system efficiency, and facilitating the integration of VRE resources. Moreover, electricity networks provide flexibility by enabling the sharing of flexible resources across different geographical regions. As the demand for electricity grows and the energy transition accelerates, the development and functioning of electricity networks will be pivotal in determining the economic viability and reliability of the overall electricity system [52].

Globally, the transmission and distribution networks span approximately 80 million kilometers (km) of lines [43]. All the three projections indicate a continuous expansion of the grid in the coming years [1]. For example, in the STEPS, it is estimated that by 2030, around

[1]The BloombergNEF Outlook expect that 152 million kilometers are needed to supply electricity in a net-zero emissions future and avert climate disaster. They used this sentence to capture the attention of the reader: "Imagine it's 2050 and the world has managed to reach net-zero emissions. If you deconstruct the electricity grid and lay it out in a single line, those cables will stretch all the way to the Sun"

13 million km of distribution lines and 1.6 million km of transmission lines will be deployed (14 million km and 1.8 million km, respectively, in the APS) [43]. Looking further ahead, by 2050, an additional 45 million km of distribution lines and 4 million km of transmission lines will be required, representing approximately 80% expansion of the existing grid. This expansion is primarily driven by the growing electricity demand and the need to connect renewable energy sources, which are often located at a greater distance from existing grids. In emerging and developing countries, the demand growth will result in the addition of over 14 million km of new lines by 2030, with China accounting for one-third of this expansion (5.3 million km). Some of these new lines will be large-scale ultra-high voltage transmission links, spanning distances up to 3,300 km, designed to connect solar PV and wind power farms. In advanced economies with well-developed and robust power grids, the focus is more on grid replacement rather than new construction, with a total of 21 million km of lines needing renewal by 2050. This includes 7 million km in the European Union and nearly 8 million km in the United States, which represents two-thirds of the existing networks. While lines, cables, and transformer capacity are the primary components of electricity networks, the integration of renewables necessitates additional investments in digital technologies to monitor and predict electricity flows, enabling more efficient operation of the network.

From an economic standpoint, the STEPS scenario estimates that annual grid investment will increase to USD 550 billion, compared to an average of USD 300 billion per year during the period of 2012-2021. This increase is mainly driven by the growth in electricity demand and the need to adapt the system for higher renewable energy integration. In developed economies, grid investment is projected to reach USD 250 billion annually by 2040, remaining stable and focusing primarily on ensuring grid reliability in a decarbonized power system that requires high flexibility, affordability, and resilience. In emerging markets, grid development expenditures are expected to rise from USD 135 billion to USD 330 billion by 2030, driven by demand growth and efforts to provide electricity access to millions of people. In the more ambitious APS, grid investment increases significantly compared to the STEPS scenario, reaching USD 630 billion by 2040 and USD 830 billion by 2050 [43].

It is important to note that developing large-scale transmission systems can be a time-consuming process, often taking a decade or longer to complete. The planning phase, which involves extensive research and expertise studies, as well as obtaining permits from regulators, can be particularly time-consuming. Additionally, the visual impact of high-voltage power lines often leads to local social opposition. Alternative solutions, such as underground lines, can help address concerns about visual and environmental impacts but may increase project costs. For instance, the construction of a single extra-high voltage aerial line (220 kV or higher) in advanced economies typically takes between 5 and 13 years, while lower-voltage lines require 4 to 7 years, and distribution grid projects take around 4 years. Germany provides an example where only 50% of the 1,655 km of line projects decided in 2009 were operational by 2019. To ensure the reliability of future power systems, long-term vision and planning at the system level are necessary to synchronize supply and network development effectively.

### 2.1.6 Power system investment flow dynamics: A worldwide perspective

Power system investments are crucial for assessing the progress of the energy transition. Global power sector investment experienced a 6% increase in 2022, following a record rebound of 7% in 2021, reaching nearly USD 1 trillion [53]. This growth is primarily driven by investments in renewables, electricity grids, and battery storage, accounting for 80% of the total. Renewables receive the largest share of investments, with over USD 440 billion invested. Solar PV emerged as the leading recipient of power sector investment in 2021, capturing nearly one-quarter of the overall renewable investment. This allocation is evenly split between utility-scale projects and distributed solar PV systems, amounting to USD 100 billion. Investment in fossil fuels amounts to USD 100 billion, with increased spending on natural gas as it replaces the declining trend of coal phase-out. Investment in decarbonized dispatchable generation has remained stable at USD 100 billion in recent years, with a slight rise in nuclear investment and a decline in hydropower. Battery energy storage investments approach USD 20 billion, primarily located in advanced economies and China. Investments in renewables and electricity grids have grown at an average annual rate of USD 50 billion in developed countries and USD 90 billion in China over the past decade, while emerging and developing countries have experienced a more modest increase of only USD 10 billion. Investments in fossil fuel power in emerging countries remain high, comprising 30% of the total, driven by electricity demand growth and the availability of fossil resources. In contrast, developed countries and China have reduced investment in fossil fuel-fired power generation to under 10% of the total. Solar and wind power account for nearly 80% of global investments in renewables. Private sector investment contributes to 60% of renewable investments, and Public finance institutions contribute to 70% of all investments in the power sector.

Across all three scenarios, power system investments continue to rise. In the STEPS, investments are projected to increase by approximately 10% from current levels, reaching an annual investment of USD 1 trillion within the next decade. By 2050, annual investment in the power sector is expected to reach almost USD 1.2 trillion, with 70% of this total allocated to China and developed economies. In the APS, annual investments increase by 30%, reaching USD 1.2 trillion by 2030 and USD 1.8 trillion by 2050. The NZE scenario demonstrates even higher growth, with investments reaching USD 1.7 trillion per year over the next decade. Renewables attract a significant share of investments, averaging USD 480 billion between 2022 and 2030 in the STEPS scenario and reaching USD 630 billion in the APS scenario. Investments in nuclear power increase from USD 30 billion per year to USD 60 billion by 2030 in the STEPS scenario, and USD 80 billion in the APS scenario. On the other hand, investments in fossil fuel-based power plants decrease to USD 50 billion in the STEPS scenario and USD 30 billion in the APS scenario. Investments in electricity grids continue to be the second-largest share after renewables, highlighting their crucial role in supporting a clean and secure energy transition. Battery storage gains momentum as a key driver of power system flexibility, with an annual investment of USD 30 billion projected by 2030.

## 2.2 Introduction to the notion of Electricity security

In the past century, many middle and high-income countries worldwide have successfully achieved a high level of electricity supply security for their economies. The underlying principles that have guided the development of robust electricity security frameworks can be summarized as follows [54, 55]:

- Centralized/Dispatchable: Electricity was predominantly supplied by vertically integrated utilities using large dispatchable thermal and hydro power plants, alongside centralized transmission and distribution networks.
- High Inertia and Stability: Thermal and hydro power plants, with their significant rotating mass for power generation, provided ample inertia. Furthermore, power generators operated autonomously without direct connection to digital networks.
- Central Planning and Operation: Regulatory frameworks designated a single entity responsible for ensuring system reliability and defining electricity tariffs based on marginal pricing [56], ensuring sufficient returns on invested assets.
- Closed Networks with Limited Digital Devices: Networks operated in a closed manner, with a minimal presence of digital devices.

However, the last decade and future trends, as discussed in preceding sections, indicate that the transition to clean power systems will bring about structural changes in the power system landscape. This new power sector paradigm will be shaped by several factors, among others: [54, 55]:

- Rapid Growth of VRE: The increasing deployment of intermittent and variable renewable sources, such as solar and wind power.
- Reduced Role of Conventional Fossil Fuels and Nuclear/Hydropower: Conventional fossil fuel-based power systems are expected to play a smaller role, and nuclear and hydropower contributions may stagnate or decline.
- Increased Device Connectivity: Networks will become more digitalized, open, accommodating a greater number of interconnected devices.
- Changing Climate Patterns: Climate change will introduce shifts in weather patterns, impacting the operation and planning of the power system.

**Our objective is to develop a framework for planning future power system trajectories that meet power generation adequacy requirements, a critical aspect of electricity security**. Before defining power generation adequacy, it is crucial to consider all facets of electricity security. This section provides a detailed examination of electricity supply security, beginning with exploring different types of interruptions that can disrupt

the well functioning of the power system, recognizing their specific relevance to different aspects of electricity security. Key examples of interruptions and their technical, economic, and societal impacts are provided to emphasize the profound consequences of inadequate electricity supply. It then provide a comprehensive definition of the notion of electricity security based on the work of [57]. Then a special focus on the power generation adequacy metrics and analytical assessment is provided.

### 2.2.1 Electricity interruptions: types and historical events

Disruptions in electricity supply have varying societal and economic impacts, depending on their magnitude, affected areas, and duration. The following are the three main categories based on the causes and magnitude of the events:

1. **Cascading blackouts or black system events:** These events typically start with one or more initial failures that trigger a series of increasing line overloads. This chain reaction continues, leading to a cascading failure throughout the system. The process of cascade failures in power systems involves three steps: 1) an initial disruption, 2) a series of line failures and subsequent redistribution of electrical flows, 3) ultimately leading to a comprehensive blackout. These cascade failures initiate when an external disturbance occurs, compelling a redistribution of electrical flows within the network. When a power line experiences an outage, it diminishes the overall capacity of the network. Consequently, this triggers power overloads on the remaining operational lines as the flow of electricity is redistributed in accordance with Kirchhoff's laws. If these overloads are not promptly mitigated, they can lead to additional line failures. This recurring cycle of line outages and flow redistribution, if not effectively controlled, is recognized as a cascade failure. In the broader context, a cascade failure ultimately culminates in a significant blackout event. They are primarily the result of equipment failures, concurrent contingencies [2], or/and insufficient generation capacity at a specific time-scale (ranging from seconds to 15 min). Such events cut off power for all grid-connected customers or a fraction of the customers if some safeguard measure are activated to limit the spatial impact of the blackout [3], except those with backup generation. The social damage caused by these events is dramatic, as they affect vital socio-economic services such as transportation, telecommunication, traffic lights, and food safety.

   One recent example of a blackout is the Hokkaido blackout in Japan in 2018. This blackout, mainly caused by composite factors ("N-3," "N-4"), involved the shutdown of three power plant units and four power transmission lines following a magnitude 6.7 earthquake at 03:08 am on September 6th [58]. To recover from the frequency drop, emergency power transfer was activated using the High Voltage Direct Current

[2]The concurrent contingencies are rare events, example of Tempete 1999 where Cyclone Lothar and Martin caused a major blackout in France

[3]regional blackout in France in 1987

(HVDC) link between Hokkaido and Honshu, but it reached its maximum Net Transfer Capacity. As a result, frequency control failed, leading to the blackout. The blackout affected three million households served by the Hokkaido Electric Company (HEPCO). It took 45 hours to fully restore power supply to the entire area, and consumers were requested to reduce their consumption for two weeks [58].

South Australia experienced a state-wide blackout on the afternoon of September 28, 2016, due to storm damage to the electricity transmission network. The Black System Event Compliance Report conducted by the Australian Energy Regulator -[59] identified two main factors that triggered the blackout: severe weather conditions damaging the transmission and distribution network, followed by reduced wind power generation and a loss of synchronism that caused the Heywood interconnector to fail. While most supplies were restored after 8 hours, the market was suspended for 13 hours. The market suspension had occurred for only two hours since the creation of the National Electricity Market 20 years ago [59]. The table below 2.2 depicts some examples of cascading blackouts and their respective impacts.

| Location | Scale | Duration | Energy Not Supplied | Economic impact |
|---|---|---|---|---|
| Hokkaido, Japan, 2018 Cascade blackout | The Whole interconnected system in Hokkaido affecting 100% of customers, including several vital services | 48 hours | 0.30-9.35% of Hokkaido's annual energy consumption: equivalent to 100 GWh | USD 1.4 billion |
| California, United States 2019 Preventive disconnections: transmission lines shut down to prevent wildfires | 10.7% of PG&E customers including vital services | 3 days | 0.0016% of PG&E annual energy equivalent to 102 GWh | USD 1 billion |
| South Australia, 2016 Cascade outage | State-wide outage | Full blackout for 3 hours. After 7.5 hours over 80% of load was restored. Full reconnection after one day | 0.09% of annual state consumption: equivalent to 100 GWh | USD 271 billion |
| Pakistan, 2021 Tripping of two 500-kV transmission lines | Countrywide | 18 hours | 443 GWh | USD 452 million |

Table 2.2: Cascade outage and black system event interruptions and their impact in duration and energy not supplied. (source [60])

2. **Load-shedding:** is a preventive control action taken to maintain system balance by

curtailing load until the available supply can meet the remaining demand [61]. It is implemented when other measures, such as demand response, emergency supplies, and imports, have been activated but the supply is expected to be insufficient to meet the demand and reserves. Load shedding events are typically short in duration, lasting from minutes to hours, and are targeted at specific segments of consumers while ensuring electricity provision for essential services. Although load shedding may cause interruptions for consumers, it is important to note that the security of supply does not require all consumers to meet their full demand. Load shedding, when properly anticipated, controlled, and limited, is consistent with ensuring the security of supply [62].

Reliability standards worldwide define an acceptable level of load shedding as a measure to maintain the balance between supply and demand. For instance, the Alberta Electric System Operator in Canada applied load shedding in only three events between 2006 and 2013, as specified in their Resource Adequacy Criteria Overview and Historical Performance [63]. These events occurred on July 24, 2006, lasting 106 minutes with an Expected Unserved Energy (EUE)[4] of 465 MWh; July 9, 2012, lasting 180 minutes with an EUE of 303 MWh; and July 2, 2013, lasting 65 minutes with an EUE of 177 MWh. These events resulted in a total duration of 5.9 hours with a non-compliance of energy supply according to reliability standards [63]. Figure 2.2 shows the load shedding events over the period 2006-2013 in Canada.

A proactive measure to prevent load shedding is Ecowatt [5], a voluntary program collaboratively established by RTE in collaboration with ADEME. Originally introduced over a decade ago in Brittany and Provence-Alpes-Côte d'Azur regions in France, which historically faced significant challenges regarding electricity supply security, this initiative has evolved and now extends its benefits nationwide. Its primary objective is to encourage individuals, businesses, and communities to curtail their electricity usage, especially during specific targeted periods when the electricity grid experiences peak demand (typically during the 8-13 and 18-20-hour time slots). According to RTE, this proactive approach is essential to prevent load shedding. Among the recommended eco-friendly practices promoted by Ecowatt are actions such as reducing heating, closing shutters or curtains at night or during absences, lowering both public and private lighting, and delaying the use of energy-intensive electrical appliances.

The table below 2.3 depicts some examples of load-shedding and their respective impacts.

3. **Long periods of electricity rationing:** Long-duration electricity rationing occurs when system operators and governments are forced to limit the level of electricity supply on a planned basis due to insufficient capacity to meet expected demand. These extended rationing events can have harmful impacts on society and the economy.

[4]The Expected Unserved Energy (EUE) is equivalent to the Expected Energy Not Served: two names for the same adequacy metric

[5]https://www.monecowatt.fr/

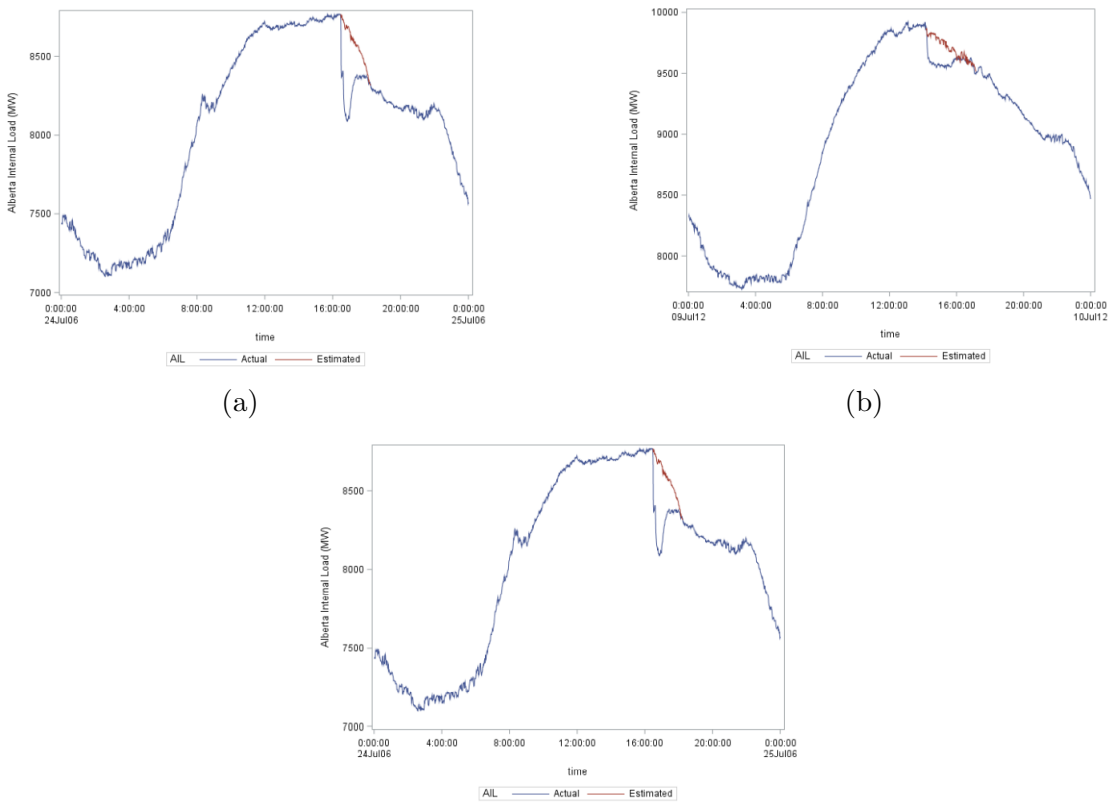


Figure 2.2: The load shedding events over the period 2006-2013 in Canada (source [63])

Several countries have faced electricity rationing. In the UK, in 1974, a major coal miners' dispute led to a state of emergency and daily power outages of up to nine hours, highlighting the importance of coal and electricity to the economy [64, 65]. The Brazilian Energy Crisis in 2001 is another notable example of long-duration electricity rationing. Factors such as delayed investment in generation and drought conditions, given the country's reliance on hydroelectric power, contributed to the crisis [66]. As a response, the government imposed rationing measures on different consumer segments, requiring reductions in electricity consumption of up to 25% for industrial consumers [66]. The crisis had significant negative effects on GDP growth and inflation [66].

Japan experienced electricity rationing following the Great East Japan Earthquake in 2011. Damage to power generation plants and the electricity network led to the activation of an emergency action plan, resulting in a reduction of electricity consumption by up to 27% for large consumers and 11% for households in the Tokyo region [67]. Figure 2.3 illustrates the evolution of electricity demand in affected regions before and after the earthquake, demonstrating the significant reduction in consumption [67]. In many developing countries, electricity demand often exceeds supply, leading to frequent load shedding throughout the day. Nigeria, Pakistan, India, South Africa, Zimbabwe, and

| Location | Scale | Duration | Energy not supplied | Economic impact |
|---|---|---|---|---|
| Alberta, Canda, (events in 2016, 2012, 2013) Short-term load-shedding Exceptional preventive interruptions to avoid cascade blackout | Small area automatically isolated affecting 6.5 % of load, usually not including vital services | 5.9 hours (over three events) | 0.00001% of energy consumption: equivalent to 972 MWh | USD 9.72 million |
| Texas, United States 2021 Short-term load-shedding Exceptional preventive interruptions to avoid cascade blackout | State-wide | 5 days | 1.85 TWh | USD 16.7 billion |

Table 2.3: Load-shedding interruptions and their related impact in duration, energy not supplied and economic impact. (source [60])

Serbia are among the countries grappling with long periods of electricity rationing.

The table below 2.4 depicts some examples of Long periods of electricity rationing and their respective impacts.

### 2.2.2 Electricity security definitions

Together with economic efficiency and environmental compatibility, the security of electricity supply is a fundamental pillar of any energy policy. To comprehend the goals of this thesis, it is important to establish a basic definition of electricity security. The objective is to ensure a reliable supply of electricity at a reasonable cost while managing various threats, such as power plant failures, fuel shortages, operational failures, human errors, or malicious attacks. In general, the European Commission defines electricity security as the power system's capacity to withstand disturbances (events or incidents resulting in abnormal system conditions) or contingencies (failures or outages of system components) with minimum acceptable service disruption. The IEA defines it as "the electricity system's capability to ensure uninterrupted availability of electricity by withstanding and recovering from disturbances and contingencies."

Defining electricity security of supply poses a significant challenge due to its multi-faceted nature and varying interpretations across different contexts. Different authors have conducted a review of its related definitions [69]. For the definitions in this thesis we use the conceptual work conducted by the Joint Research Center (JRC) and Politecnico di Torino University in the context of a PhD thesis titled "Electricity Security: Models and Methods

| Location | Scale | Duration | Energy not supplied | Economic impact |
|---|---|---|---|---|
| South Africa, (since 2007) recurring rolling black-outs | Load-shedding was divided into six stages, each triggered by a specific power shortfall, with each stage resulting in a reduction of 1000 MW in power supply. In 2019, the most severe impact was observed, resulting in a shedding of 30 GWh during the implementation phase. | Since 2014 total duration of load-shedding events amounts to 1 710 hours 2015 saw 852 hours, spanning stages 1 to 3 2019 saw 530 hours, with half of load shed in stages 4 to 6 | 867 GWh (estimated). Of which: 1 325 GWh in 1 352 GWh in 2019 | USD 20 billion |
| Brazil, 2001 Extended period of energy rationing | Country-wide 100% of customers affected either through increased prices or direct rationing | Not known | 7-10% of annual electricity consumption | Not known |

Table 2.4: Extended periods of energy rationing interruptions and their implications in terms of duration and the amount of energy unmet (source: [60])

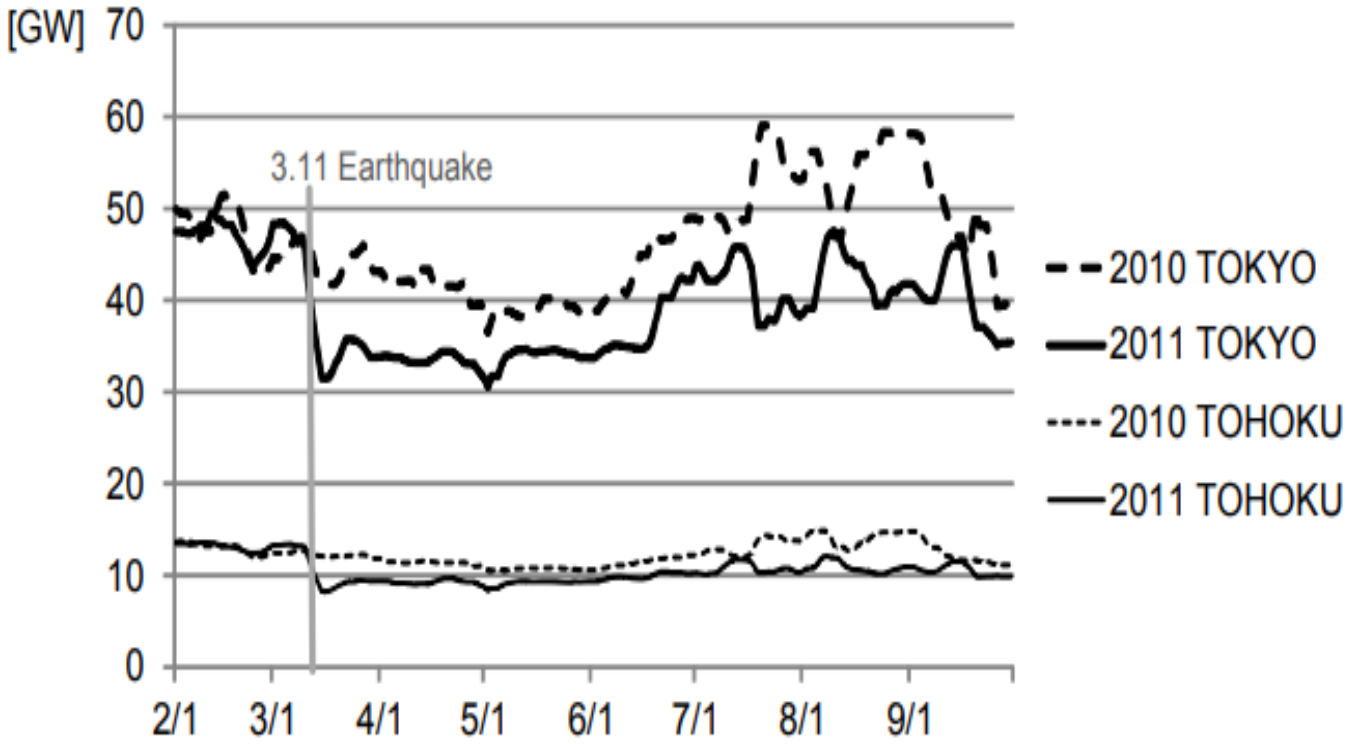


Figure 2.3: Electricity demand evolution during weekdays in the TOKYO and TOHOKU regions before and after the earthquake. (source [68])

for Supporting Policy Decision Making in the European Union" [57]. Electricity security notion encompasses multiple threats, scales, stakeholders, problems, models, approaches, and actions. The mind-map below synthesizes the multi-aspects of the electricity security concept. The author [57] considers the problem of electricity security to have two features: complicated and complex. It is complicated because the electricity grid is often defined as the most intricate human-made machinery governed by non-linear equations. It is complex because multiple actors interact in a system with different scales and layers, and their collective/systemic behavior is challenging to describe using analytical mathematical formulations. The following points enumerate the different aspects of electricity security using the categorization of [57].

1. **A Multi-Threat Problem:** The potential threats that can disrupt the ability of the system to meet the electricity needs of different consumers can be categorized as follows:

    - Natural threats: Caused by non-controllable natural disasters (earthquakes, hurricanes, tsunamis) occurring at various temporal (from seconds to days) and spatial scales (local, national, or continental).
    - Accidental threats: Resulting from component or device failures in the electricity

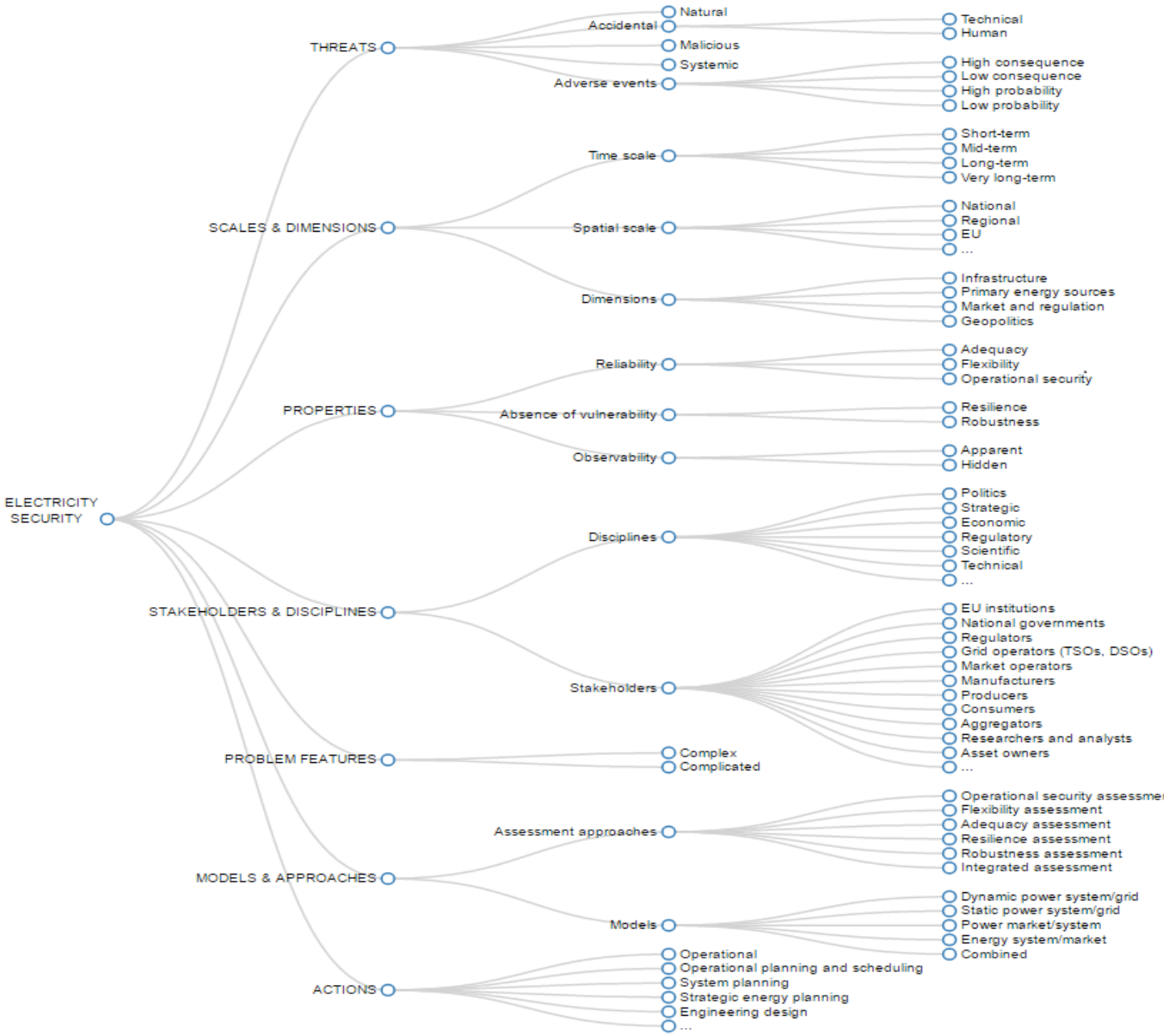


Figure 2.4: Electricity security properties mind map (source [57])

system or human errors, such as operational faults, system equipment failures, or accidents due to human decisions.

- Malicious threats: Deliberate actions aimed at causing damage to the system, such as cyber-attacks, terrorist attacks, criminal group activities, or acts of war.
- Systemic threats: Emerging at the system level due to the structural evolution of the power system, such as integrating more variable energy sources or linking the

power system with other systems like natural gas networks.

2. **A Multi-Temporal Scale Problem:** Studying the security of electricity supply requires considering different time frames. The authors distinguish between four main classes of time frames:

   - Short-term security: Aims to keep the system stable following a perturbation, balance generation and demand, account for their variability, and handle planned and unplanned system component outages. This includes addressing short-term variability and uncertainty of VRE generation, primary and secondary frequency regulation for generation-demand balancing, voltage regulation, and stability issues with high VRE uptake, as well as transmission-distribution system interfacing issues.
   - Mid-term security: Focuses on maintaining the balance between generation and demand, managing market failures, and addressing mid-term variability and uncertainty of VRE generation. This includes tertiary frequency regulation for generation-demand balancing, tertiary voltage regulation, day-ahead and market flexibility, and generation and system flexibility.
   - Long-term security: Pertains to generation and network planning and market design, encompassing the connection of renewable energy resources to the grid, market adequacy, and dealing with demand forecast uncertainties.
   - Very long-term security: Considers the system's evolution over a longer time horizon, accounting for major infrastructure investments, technological changes, and shifts in energy policies.

3. A Multi-Spatial Scale Problem: Electricity security has both local and far-reaching geographical features due to the network's scope, which spans local, national, regional, and international scales.

4. A Multi-Dimension Problem: The dimensions of electricity security represent the physical or virtual corridors through which electricity commodities/services travel to reach end-users. Four main dimensions of electricity can be identified:

   - Infrastructure dimension: Refers to the electricity value chain, including generation, transmission, distribution, and consumption.
   - Source dimension: Relates to the broader energy system that provides primary sources for electricity production or conversion.
   - Regulation and market dimension: Encompasses the set of laws and rules governing electricity operations and transactions.
   - Geopolitical dimension: Concerns the geographical and political spaces where decisions regarding energy infrastructure and resource transportation are made [70].

5. **A Multi-Propriety Problem:** Due to its complexity, electricity security lacks a universally adopted terminology and is interpreted differently depending on the context. However, for clarity, several key building blocks of the security concept can be defined [57]:

    - Adequacy: The ability of the electricity system to supply the aggregate electrical demand within an area under normal operating conditions. Defining what qualifies as normal conditions and understanding how the system copes with other situations is crucial for policy decisions.
    - Flexibility: The capability of the power system to accommodate short- and mid-term variability in generation (e.g., from renewable energy sources) and demand to maintain system balance.
    - Stability: The property of the electricity system to maintain operational equilibrium and recover from disturbances on very short time scales (a few seconds or less). Stability specifically refers to electrical disturbances and a return to equilibrium, while operational security covers broader aspects and may not require a return to equilibrium.
    - Resilience: The mid-term capability of the power system to absorb the effects of a disruption and recover a certain performance level.
    - Robustness: The long-term capability of the power system to cope with external constraints or stresses originating outside the infrastructure dimension.

### 2.2.3 Main actors of Electricity security

Policymakers and planners have long acknowledged the vital importance of assessing power system security in ensuring the smooth operation of the power system. This recognition stems from the understanding that a well-functioning power system is not only essential for economic stability but also plays a crucial role in garnering societal support for the ongoing low-carbon energy transition. Planning and operating the electricity system involve a diverse range of actors and show significant variation both within and between countries. To ensure electricity security of supply across different time-scales, clear delegation of roles and coordination among these actors is of utmost importance. The following institutions play crucial roles in shaping and maintaining electricity security:

**Government:** Governments establish the electricity security policy as defined by law. They utilize legislation and regulation as primary tools to achieve the goals related to electricity security. Ministries responsible for energy and the electricity sector, along with legislators, play significant roles in establishing the fundamental pillars and parameters of electricity security within their jurisdictions. Governments also contribute to emergency preparedness planning in the electricity sector. Risk preparedness plans involve national authorities outlining various types of risks, drawing conclusions from risk assessments, and listing measures taken or planned to mitigate identified risks, as well as measures for emergency preparedness and prevention. In the European Union, for example, European Network of Transmission

System Operators (ENTSOE) defines a methodology that governments apply to ensure effective and efficient risk preparedness [71]. Risk assessments and monitoring reports are typically prepared by Transmission System Operators (TSOs) in most Member States. Generally, risk preparedness plans include:

- Roles, responsibilities, and tasks delegated to various government authorities and bodies.
- Descriptions of electrical crisis scenarios at national and regional levels (if applicable).
- Procedures and measures to be followed in the event of an electrical crisis, including information flow mechanisms between crisis coordinators.
- Summary of market-based measures to be activated during electricity crises.
- Summary of non-market measures to be implemented during electricity crises, specifying necessary conditions and activation procedures.
- Details of communication strategies used to inform the public about electricity crises.
- Emergency preparedness and training tests at different levels.

**Regulators:** Regulation is a form of government intervention that shapes the policies of the electricity security framework. To balance multiple objectives and optimize least-cost service delivery with high quality and reliability, governments delegate this task to an independent institution known as regulators [72]. Electricity regulation aims to find a trade-off between different constraints to achieve policy and social objectives. The complex objectives of power sector regulation can be summarized as follows: design and manage electricity tariffs, maintain system reliability, meet demand growth, and expand electricity access, ensure financial health of utilities, facilitate private investments and protect the interests of poor and vulnerable customers, support technical safety and reliability of the power system, enhance energy security and manage risk. In the context of transitioning to a low-carbon power system, regulators face new challenges. A report highlights four main categories of VRE regulation [72]: enabling the integration of new VRE sources, ensuring the presence of sufficient grid infrastructure, securing short-term supply reliability through flexibility measures, and ensuring long-term supply security through resource adequacy.

**System Operators:** TSOs play a crucial role in maintaining electricity security as they are responsible for the operation of high voltage networks. By construction, TSOs have system-wide visibility at the interface between generation and distribution system operators. Regulators designate TSOs as the balancing authority and assign them the task of monitoring adequacy within different time frames for the regions they cover. Although each power system typically has only one transmission grid, ownership can be divided among various transmission asset owners. In many markets, TSOs perform both system operation and transmission asset operation activities.

In the European Union (EU), the term "system operator" is not used. Instead, the EU defines the "transmission system operator." According to the electricity directive (2003/54/EC), a "transmission system operator" refers to a natural or legal person responsible for operating, maintaining, and, if necessary, developing the transmission system within a specific area. They also oversee the interconnections with other systems and ensure the long-term capability of the system to meet reasonable demands for electricity transmission".

In this thesis, our focus is on three key actors: the government, regulators, and TSOs. These actors are of particular interest due to their roles in defining and ensuring the power generation adequacy requirements. The government and regulators play a vital role in shaping the risk policy related to power generation adequacy. They establish the framework and regulations establish the standards and requirements for ensuring a adequate electricity supply. Their decisions and policies directly impact the long-term planning and operation of the power system and will be considered as an input to our modeling framework. TSOs are responsible for the operation, maintenance, and development of the transmission system. Also, they are responsible for monitoring the security of the operation over different time horizon. While there are other important actors involved in electricity security, such as generation owners and operators, distribution companies, market operators, and consumers, our research consider primarily on the government-regulators, and TSOs.

## 2.3 Generation Adequacy Assessment: Background

### 2.3.1 Outage value assessment: The Value of Lost Load

In order to establish a framework for electricity security, it is essential for policy makers, regulators, and system operators to consider the social and economic consequences of power interruptions during the planning of secure power systems. Quantifying these impacts enables the determination of a reliability level that strikes a balance between the costs of achieving that level (e.g., infrastructure investments) and the costs associated with power interruptions. The economic value of electricity in a given time period is directly linked to the welfare and benefits that consumers derive from its consumption. Unlike most commodities, whose prices reflect consumer valuation, electricity and other goods dependent on collective, capital-intensive infrastructures (e.g., water and waste) have a weaker direct link between price and consumer value. Therefore, in order to properly price reliability and guide decision-making processes, planners require a quantitative metric to assess the economic impact of electricity supply shortages.

A valuable metric for this purpose is the Value of Lost Load (VoLL), which is an economic indicator for power supply security. VoLL represents the cost associated with unserved power and is typically expressed in monetary units per kWh or MWh. More precisely, it reflects society's Willingness-To-Pay (WTP) to avoid a power outage, i.e., the value an average consumer assigns to a shortfall in kWh rather than the cost of that shortfall, or the amount the customer is willing to pay to avoid a minor surplus. Assuming the VoLL can be accurately measured, multiplying it by the energy not supplied during an outage provides an estimate

of the economic impact of the power outage.

The $VoLL$ metric finds application in various areas of study, such as load curtailment contracts and cost-benefit analyses of grid investments. Additionally, it can be utilized to determine an optimal target level for reliability standards in adequacy assessments, which inform decisions regarding necessary capacity expansions. Ideally, the level of supply security should be defined in a manner where the marginal damage costs of interruption, as expressed by $VoLL$, are equivalent to the marginal costs associated with ensuring a reliable electricity supply.

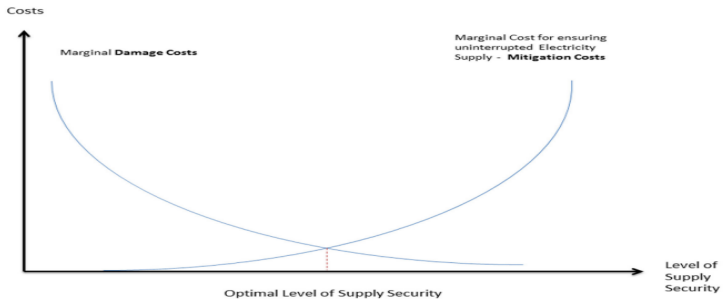


Figure 2.5: Optimum power supply security

Methodologically, three different approaches have been applied in the literature to estimate the VoLL (1) Past outage inference, (2) Survey-based tools, and (3) Proxy/Macroeconomic modeling.

First, some studies utilize data from previous outage events to estimate VoLL. However, the main drawback of this methodology is its case-specific nature, which limits its generalizability.

Second, surveys are conducted to interview individuals or businesses and ask them to estimate their specific VoLL. A commonly used approach in the residential sector is the stated preference methodology, also known as contingent valuation, where participants are asked to estimate their WTP to avoid a hypothetical outage scenario [73]. One key strength of survey-based approaches is their ability to adjust for different interruption characteristics and study a wider heterogeneity of outage experiences. Additionally, these methodologies provide a distribution of VoLL rather than a single point value, as they are administered to different sets of consumers. The relative ease of implementation and the strengths mentioned above have contributed to the popularity of survey-based approaches for estimating VoLL. However, critiques of this approach include potential hypothetical response bias in estimation, difficulty in eliciting true WTP due to budget constraints, the embedding-scope problem (variations in WTP depending on how the good is assessed), and the lack of external validation beyond the context of the study.

The third methodology for estimating VoLL involves linking the value of different goods and services to the underlying electricity consumption that enables their production. One possible approach is to calculate the ratio of the gross economic product of a geographical region (Gross Domestic Product (GDP) or Gross Value Added (GVA)) to the electricity

consumption of consumers in that same region [74]. The main advantage of this approach, compared to survey-based methods, is that it provides an estimate of outage costs based on objective measures. Its simplicity and feasibility stem from the availability of data. This methodology can also be used to provide benchmarks. However, critics argue that the GDP metric does not capture all economic activity in society, leading to an underestimation of the value of electricity. Additionally, this aggregated approach lacks the incorporation of the timing of interruptions.

The economic impact of an interruption is influenced by various factors, such as interruption time, interruption duration, segment of affected consumers, number of impacted consumers, weather conditions during the interruption, current reliability level, and advanced notification of the interruption. These factors collectively contribute to the overall economic consequences resulting from the interruption. The economic cost of an interruption is effectively captured by the VoLL indicator, which quantifies the impact of outages primarily experienced by individual consumers and businesses, especially in the case of short-duration interruptions. It is noteworthy that the VoLL varies significantly across different European countries, ranging from 4,000 euro/MWh in the Czech Republic to nearly 69,000 euro/MWh in the Netherlands. These values are calculated based on the VoLL estimates for various sectors. Figure 2.6 below depicts the different VoLL values for 11 Member States of the European Union, highlighting the wide range and emphasizing the disparities in the perceived value of adequacy among Member States. These differences can be attributed to generic economic characteristics, such as GDP per capita, economic structure, electrification level, or the methodology employed in $VoLL$ calculations.

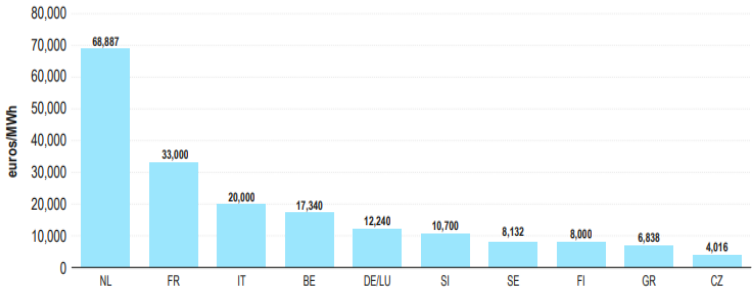


Figure 2.6: VoLL values for 11 Member states of the European Union (source: ACER based on NRA data [75])

### 2.3.2 Metrics and standards used in adequacy assessment

The methodologies used to formulate the metrics and standards employed in electricity adequacy assessments can be categorized into two main approaches.

**Deterministic approaches** estimate the availability of generation at specific time points, typically during winter and summer peak demand periods, under expected faults. These approaches have a fundamental limitation in that they consider only the initial system problems related to specific contingencies by applying a combination of established rules,

expert judgment, and accumulated experience [76]. They fail to capture the variability and uncertainty associated with stochastic variables in the power system. According to the Generation Adequacy Methodologies Report of the European Commission [77], deterministic approaches provide the following system metrics:

- **Reserve Margin (RM):** The most frequently employed deterministic index, which quantifies the surplus capacity available in relation to the projected demand. It is computed by taking the difference between the total available generating capacity and the peak demand, divided by the peak demand.
- **Coverage Index (CI):** The ratio between available generation capacity and peak demand.

Currently, most studies adopt **probabilistic methods** [78]. These approaches estimate the probability that the power system will be unable to meet demand, considering the variabilities and uncertainties associated with energy resources and power demand. Techniques in this field can be broadly categorized into analytical methods and Monte Carlo simulation methods. Analytical techniques describe the system behavior using analytical models and compute the system's risk level through mathematical solutions. These models assume probability distribution functions for different system elements and combine the probabilities and frequencies of these elements using convolution operations to derive adequacy metrics. While efficient for smaller areas, modeling multi-area systems requires a large number of variables and excessive computation time [79]. To overcome these challenges, probabilistic approaches based on Monte Carlo simulation techniques have largely replaced combinatory techniques in studies on interconnected power system adequacy and economic efficiency [80].

Monte Carlo methods, also known as random sampling methods, can be either sequential or non-sequential. The principle behind these methods is to create random samples or snapshots of system elements (generating units, demand) and compute the statistical characteristics of the sample. Non-sequential processes, or time-collapsed models, assess the probability of the margin of available supply over demand by randomly sampling system states without considering chronology. As a result, non-sequential simulation cannot capture time correlations and is unsuitable for modeling unplanned outages or unit start-ups. In contrast, the sequential approach simulates the occurrences of random events over time, recognizing the chronological characteristics of the system and the behavior of its components. For example, the forced outage of a thermal unit plant is typically represented by multiplying the unavailability of equipment during contiguous hours by the length of the outage period [79]. Sequential simulation methods can be used to compute time-related metrics such as the frequency and duration of load loss. Weather conditions significantly impact both demand (thermal sensitivity) and renewable power generation (wind speed and solar radiation), influencing reliability indices. By defining specific sampling rules, weather correlation can be incorporated into power system reliability assessments.

Most probabilistic metrics describe the likelihood and magnitude or frequency of unserved load, considering two main parameters:

- Dimension of load not served: Estimating either the magnitude (amount of energy not supplied) or the frequency (how often periods with unserved load occur).
- Likelihood of unserved load: Estimating an "average" case or explicitly evaluating "tail risks" (high-impact, low-frequency occurrences).

The key metrics utilized in many generation adequacy regulatory frameworks are:

- **Loss of Load Expectation (LOLE):** The expected number of hours per year during which the system will need to shed load.
- **Expected Energy Not Served (EENS):** The expected number of megawatt hours per year during which the system will be unable to supply power.
- **Loss of Load Probability (LoLP):** Similar to LOLE, but expressed as a percentage or without any unit. It represents the probability that the load will exceed the available generation within a certain period of time (e.g., week, month, or year). The LoLP also corresponds to the probability that the Expected Energy Not Served (EENS, see above) occurs at the load peak. For example, if there were one week in a given year in which generation was insufficient, the $LoLP$ calculated on a weekly basis would be equal to a probability of $\frac{1}{52.28}$. The $LoLP$ can also be calculated on an hourly or daily basis.

| Reliability metric | Dimension | Probability |
|---|---|---|
| Reserve margin | Margin of available capacity(% of peak demand ) | None |
| Expected Energy not Served (EENS) | ENS magnitude (MWh) | Average value |
| Loss Of Load Expectation (LOLE) | Frequency of ENS (hour/year) | Average value |
| P95 (95th percentile) | Frequency of ENS (hour/year) | Tail risk, 1/20-year event |
| Loss of Load probability (LOLP) | Frequency of ENS $\in [0, 1]$ | Likelihood of a specific ENS magnitude |

Table 2.5: Different metrics of adequacy (ENS: Energy Not Served)

These metrics play a crucial role in assessing the risk level in the power system and determining whether there is sufficient capacity to meet the expected demand. It is important to note that these adequacy metrics solely measure the adequacy of supply in the system and do not provide predictions regarding the frequency of load shedding or blackouts.

Traditionally, the utility industry has used a $LOLE$ standard of "1 day of shortage in 10 years" (1-in-10 metric) as a standard in generation adequacy studies. By this definition, the adequacy criterion corresponds to an $LOLE$ of 2.4 hours per year. In France, when the French electric utility company (EDF) held a monopoly and was predominantly state-owned, a limit of three hours was considered as an adequacy criterion. Following the 2003 power blackouts in Europe and the USA, as well as Directive 2003/54/EC of the European Parliament and Council of 26 June 2003, which called for common rules in the electricity internal market [81], there were appeals for increased regulation. This led to the adoption of Directive 2005/89/EC of 18 January 2006, which aimed to safeguard the security of electricity supply and infrastructure investment, and required greater government involvement. The

recitals of the Directive emphasize the importance of ensuring an adequate level of generation capacity, maintaining a balance between supply and demand, and establishing appropriate interconnection levels between EU Member States [82]. In France, Article 11 of the Decree of 20 September 2006, as amended on 24 March 2016, outlines the framework, scope, and study periods of Generation Adequacy Reports [83]. This decree sets a high-security target for France, with the LOLE metric not exceeding three hours per year [83] (until July 2022).

However, there is limited standardization of the metrics and standards used in adequacy assessments across different regions. Many countries still rely on reserve margins, while others are transitioning towards adopting probabilistic metrics. At the European level, $LOLE$ is the most commonly employed indicator by Member States. Most countries supplement the information provided by $LOLE$ with other indicators, primarily EENS and measures of capacity excess or deficit of capacity. Member states of the European union illustrate this in the following table 2.6. The following observation pertaining to the values for France should be taken into account: in 2022, the French Energy Regulatory Commission (CRE) revised the security of supply criterion to introduce two distinct thresholds: one based on non-exceptional means (3 hours/year) and another taking into consideration the utilization of exceptional means by the TSO (2 hours/year) [84].

At this stage, it's crucial to emphasize the process of setting reliability standards (RS). In the European context, in accordance with the Electricity Regulation and Regulation (EU) 2019/941 concerning risk preparedness in the electricity sector, the Agency for the Cooperation of Energy Regulators (ACER) has approved the establishment of the LOLE standard using a methodology known as VOLL/CONE/RS, which relies on calculating the VoLL and the Cost of New Entry (CONE). The VOLL represents the value that consumers attribute to an uninterrupted electricity supply, while the CONE represents the cost of adding incremental capacity to the system to reduce the occurrence of demand shortage. The reliability standard aims to strike a balance between the cost of additional capacity and the benefits of minimizing demand shortage.

Estimating the VoLL involves conducting appropriate surveys that capture the preferences of different types of electricity consumers regarding the value they place on uninterrupted power supply during critical time periods. The responses from various consumer groups are then weighted accordingly to calculate a single VOLL value. It is expressed in local currency/MWh. On the other hand, the estimation of CONE relies on techno-economic data related to all feasible resources or reference technologies that can be deployed to mitigate demand shortage. It is expressed in local currency/MW. CONE values are decomposed into two components: fixed $CONE_{fix}$ and variable parts $CONE_{var}$ [9].

Once the VoLL and CONE parameters are determined, the next step involves calculating the target Loss of Load Expectation per reference technology (LOLERT). In its simplest form, LOLERT is the ratio between the CONE associated with the reference technology and

[9]The role of TSOs in this process can be significant. For instance, in France, the TSO conducts the necessary calculations and submits them to the National Regulatory Authority (CRE), which subsequently proposes the reliability standard to the relevant Ministry based on the TSO's analysis.

| Member state | Metric | Target Value | Biding (B)/non-biding (NB) |
|---|---|---|---|
| FR | LOLE | 3 h/y | B |
| | LOLE | 2 h/y | B |
| UK (GB only) | LOLE | 3 /y | B |
| BE | LOLE | 3 h/y | B |
| | LOLE P95 | 20 h/y | B |
| | ENS | 3500 MWh | NB |
| ES | LOLE | 3 h/y | NB |
| | Reserve Margin | 10% | NB |
| IE | LOLE | 8 h/y | B |
| | EUE | 34.5 | |
| Northern IE | LOLE | 4.9 h/y | B |
| | EUE | 33.8 | |
| All-Island | LOLE | 8 h/y | B |
| BG | LOLE | 16h/y | |
| DE | LOLE | 5h/y [6] | NB |
| DK | Outage minutes [7] | 5 minutes | B |
| EE | LOLE | 9h/y | |
| FI | LOLE | 3 h/y | B |
| GR | LOLE | 3h/y | NB |
| ISEM | LOLE | 8h/y | B |
| CY | Reserve Margin [8] | 189 MW | B |
| IT | LOLE | 3h/y | B |
| LT | LOLE | 8h/y | B |
| NL | LOLE | 4 h/y | NB |
| PT | LOLE | 5 h/y | B |
| PL | LOLE | 3h/y | NB |

Table 2.6: National reliability standards applied by EU Member States as of the end of 2019 (ACER Market Monitoring Report 2019) and updated where relevant by more recent ENTSO-E information. Non-listed member states do not have a reliability standard in place.

the VoLL [10]. The reference technologies are then ranked based on their LOLERT values and the additional capacity they can potentially provide. The reliability standard is determined by identifying the target LOLE of the reference technology that is necessary to meet the minimum capacity requirements and achieve the desired adequacy level (see Figure 2.7).

[10] In its elaborated form it is equal to $\frac{CONE_{fixed}}{VoLL - CONE_{var}}$

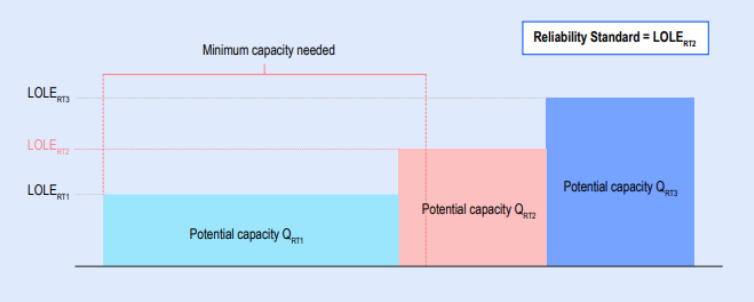


Figure 2.7: How the reliability standard is calculated (source: ACER [75])

### 2.3.3 Monitoring adequacy at multiple time-frames provides significant information

In the real-time scale, system monitoring plays a crucial role in providing system operators with valuable information about the status of system components and operating conditions. This monitoring encompasses various parameters, including voltages, power flows, frequency, component status, and variations in generation and load. Telemetry systems are utilized to collect, monitor, and transmit this data to system operators. By combining monitoring with supervisory control systems, operators are empowered to implement control actions and ensure the smooth operation of the system.

The objective of monitoring adequacy is to assess whether the electricity system can reliably meet the demand within a specific time horizon. This involves evaluating whether there are sufficient power plants, along with other flexible resources such as storage and flexible loads, available to balance the demand. Adequacy analysis considers different time scales, ranging from short-term assessments (e.g., for upcoming seasons like winter or summer) to long-term evaluations. Typically, generation and transmission adequacy are evaluated at a system-wide level. This assessment quantifies the likelihood of the system being unable to meet the entire electricity demand. By quantifying the potential risk of load loss, system operators can take proactive measures to ensure the security of the electricity supply.

Adequacy assessments are an integral part of the monitoring and planning process in large power systems today, ensuring the reliability of the system. Different regions often conduct multiple adequacy assessments, which examine inadequacy risks on various time horizons and employ different methodologies.

For instance, the Electric Reliability Council of Texas (ERCOT) conducts both short-term and long-term adequacy assessments. The short-term assessment focuses on specific seasons (winter and summer), while the long-term assessment evaluates adequacy levels over the next ten years. Likewise, the Australian Energy Market Operator (AEMO) conducts a comprehensive long-term adequacy evaluation called the Statement of Opportunities, which has a ten-year horizon. Additionally, they undertake the Energy Adequacy Assessment Projection, which assesses the security of supply for a shorter two-year period. Additionally, AEMO conducts two ongoing projected Adequacy of System Assessments: one with a one-week horizon published every two years, and another with a two-year horizon published

weekly.

At the European level, the EU's 2009 Third Energy Package establishes the regulatory framework for conducting a Resource Adequacy Assessment. The responsibility of carrying out these assessments falls on ENTSO-E. The following assessments are required:

- European Generation Adequacy Outlook: This assessment is conducted every two years and focuses on the adequacy of generation capacity at the European level.
- Annual Summer and Winter Generation Outlooks: These assessments have a short-term focus and provide insights into generation adequacy during the summer and winter seasons.
- Annual Mid-term Adequacy Forecast (MAF): The MAF is considered as both an EU-wide resource adequacy assessment and a methodology that can be utilized for regional and national assessments. Its purpose is to assist stakeholders and Member States in making informed investment and policy decisions.

It is important to note that these assessments are non-binding, meaning they lack explicit legal implications for national authorities.

In continuation of the progress achieved through the MAF, the European Resource Adequacy Assessment (ERAA) [11] represents a significant advancement in modeling and assessing power generation adequacy within the European context. It is in compliance with The Electricity Regulation 943/2019 and the Risk Preparedness Regulation 941/2019, which were established as part of the Clean Energy Package (CEP). The ERAA operates according to the established methodologies endorsed by The European ACER on October 2, 2020. This positions it as a pivotal instrument for identifying adequacy issues on a European scale and potentially implementing Capacity Mechanisms (CMs). The ERAA encompasses an evaluation of the influence of various system development trends on adequacy, including changes in the generation capacity mix, demand patterns, network developments, and other relevant factors. Key features of these European and national resource adequacy requirements include:

- The inclusion of interconnection between national power systems is a crucial aspect of the resource adequacy assessments. Interconnection enables the transmission of electricity across Member States and provides access to additional resources when national renewable generation falls short. Assessing resource adequacy without considering interconnection would underestimate available resources and potentially lead to unnecessary investments in additional capacity, often based on fossil fuels.
- The ERAA evaluates resource adequacy at both the Union and Member State levels, while national resource adequacy assessments focus on regional resource adequacy. This shift ensures that adequacy assessments consider the power systems of multiple Member States rather than solely focusing on individual countries.

[11] conducted by ENTSOE

- ACER and the Regulatory Assistance Project (RAP) have estimated significant cost savings with a regional or EU-wide approach to resource adequacy, projecting savings of up to EUR 3.5-7 billion (ACER) [85] or even EUR 8 billion (RAP) per year by 2030 [86]. These savings directly benefit consumers.

## 2.4 Towards an integrated approach for power system planning and operation

### 2.4.1 Power system planning components: technico-economic assessments across different scales

Thorough technico-economic assessments of potential pathways are vital for planning the transition to a low carbon power system. These assessments provide essential information and insights into various alternative choices. To ensure cost-effectiveness and the achievement of environmental and policy targets during the transition, both long-term and short-term implications must be considered. The significant report by the International Renewable Energy Agency (IRENA) titled "Planning for a Renewable Future" assists planners in accessing methodologies for evaluating long-term investment trajectories using modeling tools .

The report outlines four standard key stages in the cost-effective transition planning process for power system transformation. These stages are represented in three temporal aspects: the planning time horizon, which indicates the relevant future timeframe for the planning process; the timeframe, which refers to the overall period subject to quantitative technico-economic analysis; and the time resolution, which pertains to the granularity or level of detail of analysis within the time-frame. Figure 2.8 represents the different planning stage and their related temporal proprieties.

1. The first stage, **Generation Expansion Planning (GEP)**, is extensively discussed in academia and among decision makers in the energy sector [87]. GEP addresses the challenge of determining what, when, and how new investments in power generation should be made, as well as when old units should be retired, over a specific planning time horizon. It ensures that the quantity of electricity generated matches the electricity demand throughout the planning horizon, considering load forecasts and various technical, environmental, and political constraints. GEP typically involves a long planning horizon of approximately 20-40 years or more. An extended long-term time horizon is justified due to several reasons [88]:

    - Investment in power plants is costly and has a long-duration lifetime ranging from 25 to 60 years. Therefore, accurate assessment of alternative investment schedules requires a long-term projection.
    - The planning process involves multiple actors, as the construction of a power plant necessitates the reinforcement of transmission and distribution infrastructures.

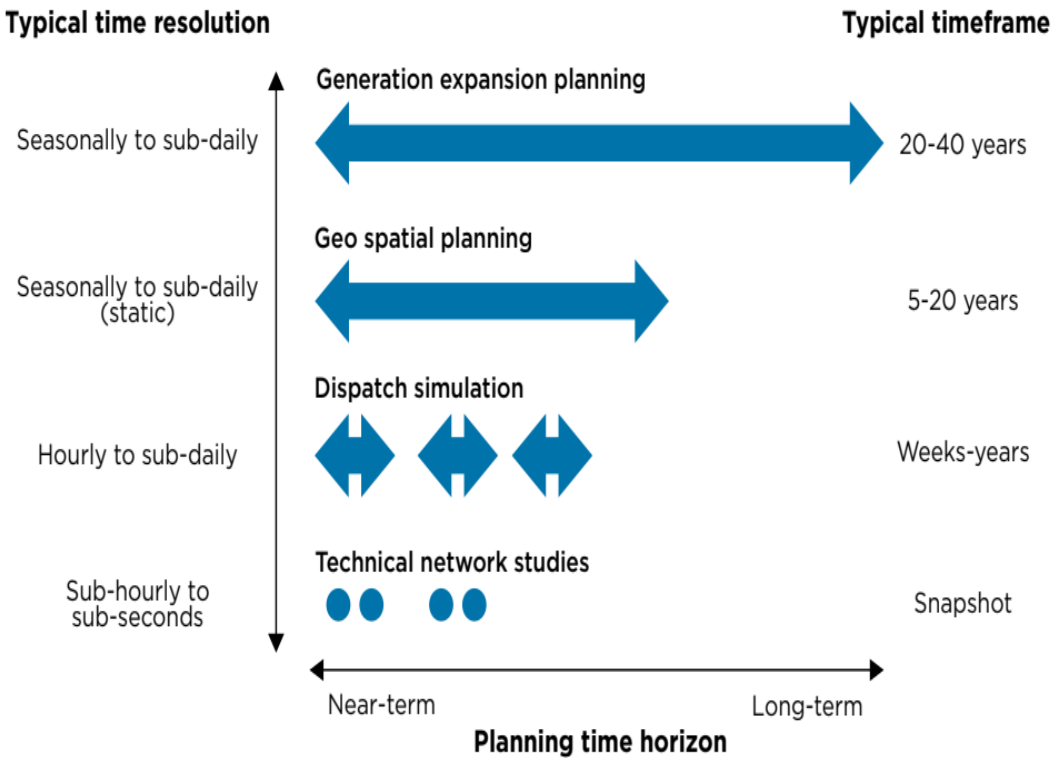


Figure 2.8: Transition planning components and time horizons (source: [5])

- Regulatory approvals, land acquisition, societal acceptance, negotiation of fuel procurement contracts, and infrastructure building often require significant lead times, reducing flexibility in investment decisions.

In making generation expansion planning decisions, operational impacts must also be considered. Power demand have different temporal variability patterns, such as diurnal, weekly, and seasonal variations. Optimal combinations of power plants vary at different times, based on factors such as fuel prices, availability, and technical considerations. Due to the large-scale nature of the problem, detailed system operation (dispatch) modeling is impractical, and reduced-form dispatch approaches with less detailed temporal resolution are employed [89].

The plans generated during the planning process are frequently published as energy or power sector master plans, signifying a political commitment to the power system transition.

2. **Transmission and Geo-spatial Planning**: This planning process is an integral part of the transmission planning conducted by TSOs, regulators, or the TSO-responsible unit within a utility. Transmission (or Geo-spatial) planning refers to the practices and doctrine that define a long-term vision for developing transmission lines, primarily based on reliability and/or economic considerations (weighted and modified objectives).

It identifies the need for transmission network expansion within a 5-20 year timeframe, taking into account factors such as evolving demand, targeted power generation mix, interconnection policies with neighboring networks, and locations of VRE sources, among other constraints. Short to mid-term transmission planning may also be carried out for specific transmission projects.

While specific formats of the transmission planning process may vary from country to country, the general objectives remain consistent. According to Gonen [90], the purpose of transmission system planning is to determine the timing and type of new transmission facilities required to cope with future generating capacity additions and load-flow requirements. Stoll [91] states that transmission planning aims to provide multiple paths between various generation sources and their loads, facilitate power transfers between geographic areas to achieve overall system operating economies, and interconnect the bulk power facilities of individual utilities to enhance system resilience against major disturbances.

Real transmission planning procedures are complex and involve iterative actions by planners to solve the problems identified during their analysis. Transmission need is identified through modeling the flows (determined by power withdrawals and injections) on network models. The transmission grid must comply with three main technical criteria: (1) respecting the physical limits of the lines, known as load flow analysis; (2) ensuring steady-state (static stability) robustness against network outages; and (3) accounting for transient processes during state transitions (dynamic stability). Additionally, the analysis of load flow and stability issues may reveal violations of technical requirements, which can be addressed through various network adjustments such as topological switching or adding new connections. Thus, transmission planning is an iterative process.

A generic transmission planning process is depicted in the Figure 2.9 below, illustrating how scenarios/assumptions mainly influence dispatch models, which produce results that inform technical network analyses. Based on these analyses, the transmission grid is adjusted accordingly. For more detailed information on the process of transmission expansion planning worldwide, readers can refer to a well-documented reference by Madrigal and Stoft [92].

As the share of VRE sources in the power mix continues to grow, the relationship between the cost of expanding transmission lines and the productivity of renewable generation farms becomes a critical consideration in the overall planning process. In systems dominated by thermal generation plants, the significance of geo-spatial analysis is relatively lower since the technico-economic attributes (productivity) of these plants are not location-dependent. In such cases, planning purposes have traditionally relied on expert knowledge that incorporates geographical constraints related to air pollution and water availability. However, in the context of integrating VRE sources, geo-spatial analysis takes on a more complex role. It involves tasks ranging from mapping transmission lines in specific geographical areas to employing advanced geo-spatial

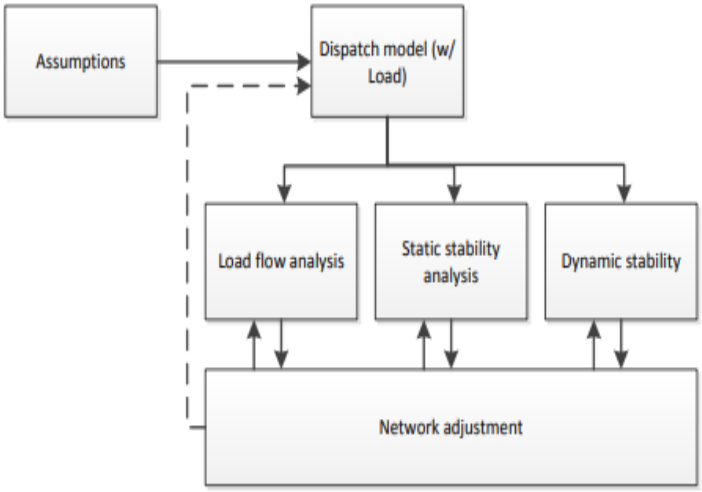


Figure 2.9: Network planning stages (source [92])

planning tools. This expanded analysis is essential to assess the optimal placement and expansion of transmission infrastructure, considering factors such as VRE resource availability, load centers, and potential grid congestion points.

3. **Dispatch planning:** Economic dispatch (ED) lies at the core of efficient power system operation. Its main objective is to optimize the utilization of available power plants, considering various dispatch patterns, maintenance schedules, and potential transmission congestion that may affect their operation. Dispatch planning is conducted within a timeframe ranging from weeks to a few years, during which the power generation mix remains unchanged. It can be applied to both existing power mixes and future targeted power mixes.

   The ED process have two key purposes. Firstly, it ensures the security of power supply. In the short-term, this is achieved by effectively operating the system, while in the long-term, accurate demand forecasting and reserve planning are crucial for maintaining a balance between supply and demand. Secondly, dispatching aims to minimize overall operational costs, taking into account various technical constraints. It can be executed for real-time dispatching, typical daily operations, weekly planning, or even longer-term planning. TSOs utilize dispatch simulation outcomes for operational planning across different time horizons, providing information and alerts to the public and other stakeholders regarding the equilibrium between demand and supply. Power generators use dispatch simulation results for fuel budgeting and maintenance scheduling. Dispatch simulation is increasingly adopted in studies related to the integration of renewable energy sources into the power grid, as recommended by the research community [93].

4. **Technical Network studies:** used for detailed static or dynamic analysis of a system at a point in time, and can be applied either at near-term (e.g. current or 5

years) planning time horizon, or longer-term planning. The main goal of technical network studies is to identify security issues in the grid, such as voltage control and frequency stability. As it was explained before, technical network studies are also used to complement the network planning process. In general, depending on the nature and magnitude of disturbances the stability studies can be classified into two following types: steady state stability and transient stability.

- **Steady-state stability:** This category pertains to a power system's capacity to maintain stability, which means avoiding synchronization loss, when subjected to minor disturbances, such as gradual load changes.
- **Transient stability:** refers to a power system's ability to remain stable during significant disturbances, such as sudden load fluctuations, loss of generation, excitation variations, transmission facility issues, switching operations, and faults.

These planning components are crucial for transitioning to a low-carbon power system, optimizing infrastructure, and ensuring reliable and efficient power system operation. However, it is important to highlight that the planning of a power system transition extends beyond the four stages mentioned earlier, encompassing additional layers. One crucial layer in this planning process is the institutional layer, which includes aspects such as operational rules for renewable integration, market designs, and regulatory frameworks. However, these institutional planning aspects are beyond the scope of this thesis. In this thesis, we specifically concentrate on the two stage GEP and ED, while acknowledging that other stages: transmission planning and technical studies are beyond the scope of our research.

### 2.4.2 A call for an integrated approach for a cost-effective and secure transition planning

Planning for a cost-effective and secure transition in the power system needs to adopt an approach that allows for proactive execution of the planning component, rather than being driven by the "tyranny of the short-term" that triggers investments or addresses immediate problems. A reactive approach is likely to result in delays, insufficient electricity supply, failure to achieve environmental targets, and economic inefficiency.

The IRENA report highlights the need for an integrated approach to techno-economic planning and assessments to ensure short-term robustness [94]. This integrated approach, referred to as "top-down," moves from long-term to short-term planning stages, establishing clear feedback loops within each step. Initially, long-term generation expansion planning establishes future pathways for the evolution of the power generation mix. Based on the investment trajectories established for the power generation mix, network expansion is developed. Subsequently, using the resulting power generation mix and network topology, optimal economic dispatch is carried out to deeply study the operation and assess power generation adequacy requirements. The resulting dispatch is then used to analyze load flows and stability, identifying operational weaknesses and network adjustments. Asami [94] considers such an integrated approach as the key element to ensure a cost-effective and secure

transition, highlighting that the planning stages described earlier are often performed independently. This decoupled practice has the potential to create a range of issues that, if left unaddressed, will undermine the transition of power systems with high shares of renewables.

The following points outline the potential issues with a decoupled planning approach: Decoupling the planning of generation and transmission networks may lead to sub-optimal solutions, resulting in curtailment of renewable generation or rejection of the connection of additional renewable energy into the grid. In a decoupled approach, long-term investment pathways are often presented without any guarantee of compliance with short-term reliability requirements (adequacy, stability). This can create misplaced concerns among policy makers responsible for long-term plans and system operators responsible for the secure operation of the power system. An integrated approach ensures that the essential technical and economic impacts of new investments on the operation are well incorporated in all assessments and policies. The report distinguishes four key functional properties of the planning process for power systems with high uptake of renewables. These properties reflect the key investment implications of VRE deployment on the important functional aspects of an entire power system, namely adequacy, transmission capacity, flexibility, and stability.

The four key planning considerations are as follows:

1. **Planning for adequacy:** Ensuring that the investment trajectory respects the generation adequacy requirements. With high shares of renewables, it is important for power systems to have sufficient supply to cover periods when low amounts of VRE are available, especially in combination with the unavailability of a portion of non-VRE generators. Planning for adequacy is considered the most relevant to long-term investment.

2. **Planning for flexibility:** As the share of VRE supply increases in the overall power generation, the rate, frequency, and amplitude of changes in VRE generation can potentially be significant. Consequently, the variability of the net load (demand minus VRE generation) increases. Flexibility refers to the ability of non-VRE generators to adjust their generation to meet the residual load. This involves investing in an optimal mix of flexible generation and other flexibility measures that complement the highly variable output of VRE. Planning for flexibility is highly pertinent to long-term investments and is inherently intertwined with planning for adequacy.

3. **Planning for transmission capacity:** Insufficient transmission capacity has been a major issue in some countries, leading to delayed connections of VRE generators to the grid or increased VRE curtailment [95, 96]. In general, if VRE resources are far from the network, additional investments in the transmission network will be needed. Considering that investments in generation are more costly than transmission investments, a sequential process that defines the power generation mix first and then expands the transmission network seems logical. Ignoring transmission costs in long-term power generation planning may result in sub-optimal solutions. Planning for transmission capacity is considered highly relevant to long-term investment.

4. **Planning for stability (frequency and voltage response)**: The significant deployment of VRE will affect the system's ability to respond to contingency-driven imbalances in active power (frequency) and reactive power (driven by voltage). Planning future investment trajectories that ensure the ability to return to a state of normal operation following a contingency event is important (ensuring that both frequency and voltage indicators are within acceptable limits). As technical challenges to maintain system stability may arise only with high levels of VRE penetration, this is considered relevant to near-term investments.

In order to facilitate robust decision-making by policy makers, scenarios depicting the long-term evolution of power generation expansion should address the needs for adequacy, flexibility, stability and transmission capacity. Investing in the development of approaches that integrates these three areas is crucial to avoid capital misallocation and suboptimal outcomes. This thesis primarily focuses on planning adequacy, which is the most relevant aspect for long-term investments. It should be noted that a power generation mix that adheres to adequacy requirements also automatically addresses flexibility needs. However, a power generation mix complying with adequacy requirements does not necessarily guarantee an optimal mix of flexible generation. Therefore, flexibility assessment is not included in our work. Additionally, planning for transmission capacity and stability falls outside the scope of this research and will not be addressed.

# Chapter 3

# Models, Challenges, Research Gaps and Thesis Focus

## Contents

In this chapter, the reader will be guided into the modeling part of this thesis, which involves the introduction of energy system models and operational power system models, the two modeling paradigms chosen in this thesis. Four challenges of power system transition modeling, namely (1) resolving time and space, (2) planning while ensuring long-term adequacy requirements (3) including uncertainty (4) societal considerations, will be discussed. Two of these challenges 1 and 2 (and at some point 3 including operational short-term uncertainties for the assessment of power generation adequacy) will be selected as the primary focus of our work. To tackle the selected challenges, the last section will explain in detail the research focus of the thesis.

**Résumé en français:**

Ce chapitre introduit la partie modélisation qui encadre le travail de la thése, en présentant la modélisation des systéme énergetique long-terme et les modèles opérationnels de systèmes électriques, les deux familles de modélisation choisis. Quatre défis de la modélisation de la transition du système électrique seront discutés : (1) résoudre les contraintes propre aux échelles temporelles et spatiales, (2) planifier tout en assurant les exigences d'adéquation à long terme, (3) inclure l'incertitude et (4) prendre en compte les considérations sociétales. Deux de ces défis, à savoir les points 1 et 2 (et dans une certaine mesure 3 en incluant les incertitudes opérationnelles à court terme pour l'évaluation de l'adéquation de la production électrique), seront sélectionnés comme principaux axes de notre travail. Pour relever ces défis sélectionnés, la dernière section expliquera en détail les axes de recherche de la thèse.

## 3.1 Energy System models

According to the Intergovernmental Panel on Climate Change (IPCC) Fifth Assessment Report, an energy system encompasses all components associated with energy production, conversion, delivery, and utilization [97]. Mathematical models called energy system models are developed to accurately represent various energy-related issues, aiding in energy planning and policy impact assessment. To analyze potential pathways for decarbonizing the energy system, energy system planning models are employed. These models offer consistent trajectories for transitioning all energy sectors at national, regional, or global scales over several decades. Numerous long-term planning models have been created. However, choosing an appropriate energy model poses a challenge due to the interplay between policy and technology choices. Techno-economic models, focusing on detailed processes, were initially used in the early 1970s after the 1973 oil crisis to analyze optimal strategies for ensuring energy security. Modern macroeconomic energy models, on the other hand, originated in the late 1950s when energy supply companies and energy administrations had to make decisions about future energy supplies to meet the growing demand in OECD countries.

### 3.1.1 How Future is considered?

A general characteristic of model development is that it involves creating a purposeful and simplified representation of reality [98]. Models are designed to address specific questions and are only applicable to the purpose for which they were developed. The incorrect application of a model can lead to misinterpretations, which is the responsibility of the model users to avoid. Simplification is an inherent aspect of models, as they aim to represent reality in a streamlined manner by simplifying real-world constraints. In addition to this general characteristic, there exist significant differences in features among various modeling approaches.

At this stage, it is essential to emphasize the principal objectives underlying the development of energy system models. Hourcade et al. categorize these objectives into three main purposes that govern the treatment of the future within the model [99]. These three purposes are broadly associated with the domain of Future Studies, which encompasses systematic investigations into potential, likely, and desirable future scenarios.

1. **To predict or forecast the future:** Prediction is primarily based on extrapolation [1] of historical data. Forecasting models are often used for short-term impact assessment when no radical or disruptive events are expected. An important condition for such extrapolation is that critical underlying development parameters remain constant. This approach is rooted in the belief that the future is a logical extension of the past.

2. **To explore the future (exploratory scenario analysis):** Future exploration is conducted through scenario analysis, where contrasting scenarios are compared to a Business As Usual (BAU) reference scenario. The difference between the BAU scenario and extrapolation lies in the fact that the BAU scenario can be conceived without the utilization of extrapolation techniques. A specificity of The BAU scenario is that it portrays a future state with no significant interventions or paradigm shifts within the system. Contrasting scenarios can describe futures that diverge at certain points, such as the adoption or rejection of new technologies, or make assumptions about political constraints, regulations, and system adaptations. According to the IPCC, a scenario is defined as a plausible and often simplified description of how the future may develop [100]. Scenarios are used as means to represent the future, facilitating present actions in light of possible and desirable futures. They are specific representations of the future designed to facilitate consideration of the potential consequences of different events or courses of action [101, 102].

3. **To look back from the future to the present (backcasting or normative):** Backcasting involves envisioning a desirable future and then working backward in time to identify the necessary steps for achieving that future [103]. The major distinguishing characteristic of backcasting analyses is a concern not with what futures are likely to happen, but with how desirable futures can be attained [104]. Backcasting is explicitly normative, focused on problem-solving, and developed to integrate a systemic

[1] Extrapolation extends historical and current trends into the future.

perspective and a long-term view, making it valuable for addressing the high complexity and uncertainty associated with energy planning [105]. Backcasting differs from predictive and exploratory scenarios in terms of the questions they ask and the futures they study. Predictive scenarios study "what will happen," exploratory scenarios study "what can happen," and normative scenarios inquire about "how a certain target can be reached." Traditional forecasting employs predictive scenarios, while backcasting employs a normative approach [106]. Different authors have established step-by-step methodologies for backcasting, with variations in typology [104, 107–109]. These approaches typically involve specifying future targets, describing the present-day system, identifying the target system, describing the pathway to reach the target, and addressing implications, impacts, recommended policies, and strategic pathways. The differences among approaches can be partially attributed to variations in applicability. For example, the Natural Step framework developed by Cook [108] and Herrmann's approach [105] were initially developed for energy utilities and governmental organizations to formulate strategic plans. Anderson's approach focuses on the electricity sector, while the Tyndall and Robinson approaches utilize system analyses.

### 3.1.2 Classification of energy system models

Energy planning and scenario generation have two primary objectives: providing guidance and facilitating constructive discussions on future energy systems, as well as supporting decision-makers in formulating strategies at various scales [110]. Over the past two decades, there has been a significant increase in the number of energy system models, driven by advancements in computational capabilities. Consequently, it becomes crucial to establish a classification framework that delineates the differences and similarities among these models. Numerous classifications of energy system models exist, aiming to assist in the selection of an appropriate model for decision support. A taxonomy based on different attributes to characterize these models holds substantial importance. In the following section, we review taxonomies of energy system models to introduce the models utilized in this thesis.

Grubb et al. (1993) proposed a classification of energy system models, distinguishing between top-down and bottom-up approaches, short-term and long-term analyses, and sectoral coverage [111]. It is important to elucidate the disparities between these two contrasting modeling types.

The terms "top-down" and "bottom-up" referred as shorthand for aggregated and disaggregated models, respectively. In the field of energy planning, top-down models are often referred to as economic models, while bottom-up approaches are associated with engineering models. This nomenclature can be traced back to the historical context wherein earlier energy planning was primarily conducted by economists as part of overall economic planning. However, as energy planning progressed, engineers became involved, incorporating detailed engineering and technological information [112]. The dichotomy of energy system models into top-down and bottom-up approaches stems from competing paradigms.

**Top-down models** are aggregated macroeconomic models that examine the broader economy and incorporate feedback between different markets, triggered by policy-induced

changes in relative prices and incomes. These models typically do not incorporate detailed technological aspects of energy production. Sectors, including energy and non-energy sectors, are represented by production functions, where the output of a specific sector is related to the main factors of production such as capital, labor, and energy. Substitution possibilities are captured through substitution elasticities. However, conventional top-down models cannot account for the involvement of discrete energy technologies and their costs in the future.

On the other hand, **bottom-up models**, often formulated as mathematical programming problems, take an engineering approach and provide detailed descriptions of the technological aspects of the energy system and its potential evolution. Energy demand is treated as an exogenous parameter, and these models analyze how the given energy demand can be balanced in a cost-optimal manner. Bottom-up models are well-suited for analyzing specific changes in technology or command-and-control policies. However, they often fail to account for price distortions, economy-wide interactions, and income effects.

Hourcade et al. (2006) proposed a classification of energy system models based on the differences between top-down and bottom-up approaches [113] and highlighted the importance of hybrid integrated models that combine elements of both approaches. Hybrid models aim to combine the technological explicitness of bottom-up models in representing in detail the reference energy system with the economic richness of top-down models. Various efforts have been made to develop such hybrid models. Van Beek (1996) introduced a synthetic classification that combines the classification frameworks proposed by Grubb (1993) and Hourcade (1996) [99, 111, 114]. This classification is widely recognized as the basis for numerous other works in the field [115–117].

The classification comprises the following dimensions:

1. **Purposes of energy models:** General purposes, as discussed previously, and specific purposes.

2. **Model structure:** Internal assumptions within the model and external assumptions imposed on the model.

3. **Analytical approach:** Distinguishing between top-down and bottom-up approaches, as discussed previously.

4. **Underlying methodology:**

    - Econometric models: Utilize statistical techniques to extrapolate market behavior in the future based on historical data. These models rely on aggregated data to predict the evolution of labor, capital, or other inputs in the short to medium term.
    - Macro-economic models: Focus on the interactions between sectors within the entire economy, utilizing input-output tables to analyze energy-economy linkages.
    - Economic Equilibrium Models: Investigate medium to long-term effects, emphasizing the interrelations between the energy sector and other non-energy sectors of the economy. These models can be partial equilibrium models, which focus on

specific parts of the economy, or general equilibrium models, which aim to achieve equilibrium simultaneously in all markets.

- Optimization Models: Optimize investment decisions in energy endogenously, determining the best strategies based on maximizing or minimizing an objective function while meeting constraints.
- Simulation Models: Reproduce and represent the operation of a given system, simulating the behavior of producers and consumers in response to changes in price and income using differential equations.
- Agent-based models: Represent complex evolving systems where heterogeneous agents interact, giving rise to emergent properties. Interactions and agent responses are governed by behavioral algorithms.
- Others: Additional methodologies beyond the aforementioned categories.

5. **Mathematical approach:**

   - Linear programming (LP): Find the best outcome in a mathematical model with linear relationships, such as maximum profit or lowest cost.
   - Mixed Integer Programming (MIP): Incorporate integer variables into the optimization problem, expanding the scope of optimization possibilities, including decisions represented by yes/no or 0/1 choices.
   - Dynamic programming: Determine an optimal growth path by breaking down the problem into subproblems and calculating optimal solutions for each subproblem.

6. **Geographical coverage:** Indicates the spatial level at which the model is designed, ranging from global to regional, national, local, or project-specific.

7. **Sectoral coverage:** Models may focus on a single sector or include multiple sectors. Single-sectoral models provide information on a particular sector, while multi-sectoral models consider interactions between the modeled sectors.

8. **Time horizon:** The time horizon determines the structure and objectives of the energy system models. While there is no standard definition, Grubb et al. (1993) suggest that periods of 5 years or less are considered short-term, 3 to 15 years are medium-term, and 10 years or more are long-term. Different time scales correspond to varying behaviors of economic, social, and environmental processes.

9. **Data requirements:** Energy system models heavily rely on data, which can be quantitative or qualitative, monetary, and aggregated or disaggregated, depending on the specific model.

Van Beek's synthetic classification provides a comprehensive framework for understanding and categorizing energy system models, facilitating further research and analysis in the field. Based on this classification, Tomaschek (2013) [118] further developed the classification

by Van Beek and presented it in a circular structure in his Ph.D. dissertation. The circular classification, depicted in Figure 3.1, highlights the main features of an energy system model in the outer circle. It is evident that certain features are more commonly employed than others. Of utmost significance is the analytical approach, which allows for the distinction between top-down and bottom-up models. The underlying methodology further distinguishes between general equilibrium, partial equilibrium, optimization, and simulation models. The mathematical methodology is more specific, encompassing techniques such as linear programming, mixed integer programming, and dynamic programming. Additionally, other characteristics play a role in describing the model structure, including geographical and sectoral coverage, time horizon, and time-step granularity. For the purpose of our thesis, we consider that the circular taxonomy presented is adequate in presenting the models of the thesis (see section 3.4.3).

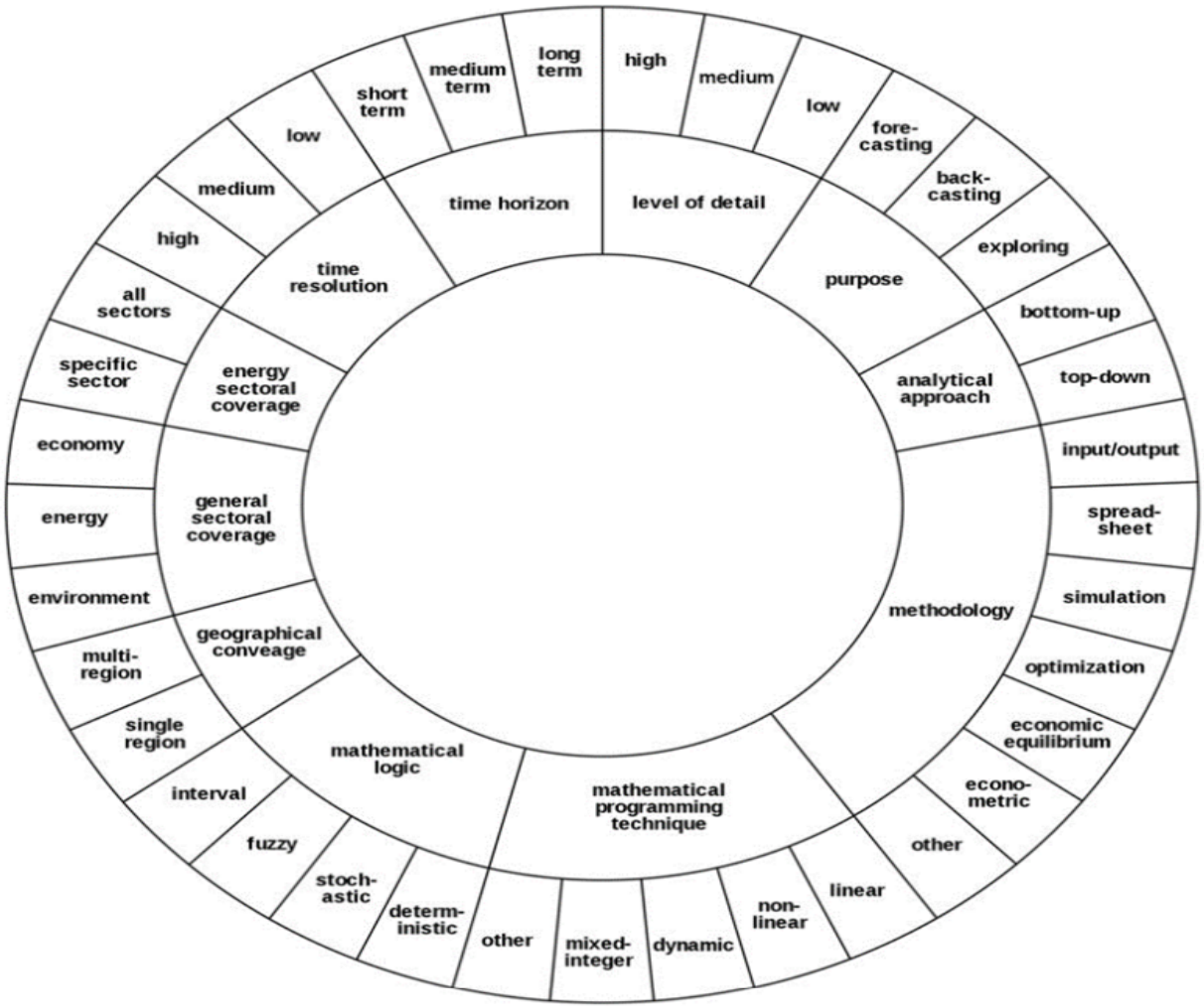


Figure 3.1: Classification of energy system model based on 11 features (source [118])

### 3.1.3 Different Classes of Models for Different Goals

Pfenninger et al. (2014) classify energy system models into four distinct categories: 1) energy system optimization models, 2) energy system simulation models, 3) power systems and electricity market models, and 4) qualitative and mixed-methods scenarios. Additionally, Ponclet categorizes long-term energy system planning models based on two primary criteria: scope and methodology. The scope criterion pertains to the model's coverage in terms of sectors, geographical regions, and timeframes, while the methodology criterion refers to the approach used to generate transition pathways.

- **Integrated Assessment Models (IAMs):** IAMs integrate knowledge from different domains into a single model [117]. They are used to address long-term interdisciplinary issues at a global scope, focusing on generating useful insights for decision-makers, even in the presence of large uncertainties. IAMs consider not only the global energy system but also incorporate macroeconomic interactions, demographics, resource availability, and non-energy greenhouse gas (GHG) emissions. They have been successfully applied in support of climate policy. Hedenus et al. [119] provide a critical assessment of Energy-economy-climate models and highlight common types of questions addressed by IAMs, including the cost of climate stabilization, feasibility of reaching climate targets, burden sharing and timing of mitigation and adaptation options, role of technologies in a climate-constrained future, and scenario exploration. Readers who want to learn about the limitations of this type of model can refer to [120]. Well-known examples of IAMs include MESSAGE, IMAGE, GCAM, POLES, REMIND, and TEAM.

- **Energy-Economy Models:** These models examine the mutual interaction between the energy system and the overall economic system. The goal of energy-economy models is to measure the economy-level response to changes in the energy system, such as policy interventions or technological advancements. The geographical scope of energy-economy models varies, while the time horizon typically ranges from 20 to 100 years. Examples of energy-economy models include NEMS, US-REGEN, MESSAGE-MACRO, and TIMES-MACRO.

- **Energy-system planning models:** These models focus on the entire energy system at a specific spatial scale over a time horizon spanning multiple decades. In contrast to energy-economy models, the interrelation between the energy system and other economic sectors is not endogenously incorporated. Energy-system planning models consider inter-sectoral, inter-temporal, and inter-regional relationships within the energy system. Most energy-system planning models are based on the concept of the Reference Energy System (RES), which captures all the activities involved in the entire energy chain, incorporating technical properties. This approach allows for the representation of existing and future technologies, enabling economic and environmental impact analysis of different technological deployment pathways. The RES approach, initially developed by Hoffman and Wood [121], has paved the way for the development of a new tradition in energy system modeling. Notably, it benefits from its ability to be

adequate representation for optimization techniques to analyze alternative system configurations using potential candidate technologies and energy resources, given a set of end-use demands. An example of an early application of the RES approach using linear programming is the Brookhaven Energy System Optimization Model (BESOM) model, designed to examine inter-fuel substitution and associated costs in the context of resource availability constraints [122]. Initially, it was used as a static model analyzing a snapshot of the system at a particular future point in time. Subsequently, multi-period or dynamic models emerged based on the development of BESOM. Market Allocation Model (MARKAL) developed by the Energy Technology Systems Analysis Program (ETSAP) and Energy Flow Optimization Model (EFOM) developed in the 1970s are early dynamic energy planning models formulated as a sequence of expanded linear programming problems representing the energy systems for each time step. Prominent energy system planning models like PRIMES and TIMES (a combination of MARKAL and EFOM models) have been widely applied to explore future energy system scenarios across the world.

- **Power system planning models:** These models focus specifically on the electrical power sector, encompassing electricity generation and transmission. Their objective is to determine an optimal strategy for the long-term expansion of the power generation, transmission, and sometimes distribution systems to meet forecasted load demands within a set of technical, environmental, economic, and political constraints [123]. Power system planning models typically do not endogenously account for linkages with other energy sectors such as gas, heating, or transport, but may incorporate them as exogenous parameters (e.g., electricity consumption of combined heat and power units or the demand level of the heat sector). Given the importance of power system transition in decarbonization efforts, extensive development of power system planning models has taken place. Well-known examples include ReEDs, LIMES, Switch, and the Resource Planning Model.

### 3.1.4 Main features of long-term energy system planning models

In subsequent paragraph we highlight the three main features of energy system models: temporal resolution, spatial coverage and sectoral coverage. It is important to emphasize that the choice of the level of refinement on a given feature is the result of a compromise with what is done on the other two features.

**Temporal resolution and investment strategy** When examining long-term energy system planning models, an important feature to consider is the time horizon. These models can be categorized into static and dynamic (or trajectory) approaches [124]. The static approach focuses on the configuration of an energy system at a specific point in time, while trajectory models analyze the evolution of the energy system over a longer temporal horizon. The main difference lies in how the transition from one period to another is endogenously modeled. Trajectory models consider the inter-temporal relationship, while static models

focus solely on a target period without considering the path leading up to that point in time.

Another significant feature is the temporal resolution. Long-term energy system planning models incorporate two temporal stages. The first stage represents the evolution of investment decisions. The planning time-frame, spanning from the base year to the time horizon, is divided into periods typically lasting 3 or 5 years. This subdivision into periods reduces computational effort and is sufficient for infrastructure planning, given the long lifetimes and planning horizons. Each period within the time-frame is represented by a representative year or simulation year for which calculations are performed. The results obtained for the representative year are then replicated for the other years within the corresponding period.

The second stage involves representing the operation of the energy system, accounting for inter-annual variability in supply and demand. This is achieved by dividing each simulation year into different time steps, where energy supply needs to meet energy demand. Then, the concept of time-slices becomes important. A time-slice is a stylized temporal representation of a given year and is defined as the number of time-step subdivisions within a simulation year [125]. Long-term energy system models offer flexibility in defining time-slices to capture various components of variability, including seasonal, weekly, and daily patterns. The definition and number of time-slices influence both the number of operational constraints and decision variables. Therefore, the temporal resolution can impact investment decisions since the captured variability of energy demand and supply differs depending on the time-slice definition and number.

During the early stages of long-term energy system model development, only a small number of time-slices were considered. Typically, national and regional models used 12 time-slices (4 seasonal and 3 diurnal: day, night, peak). The relatively limited number of time-slices (ranging from 1 to 32) can be attributed to two main reasons: 1) to reduce computational time and 2) historically, the energy system relied predominantly on thermal generation, as far as their capacity factors are concerned, base load thermal units (nuclear, coal) are much less affected by weather intermittency than peak units. The Figure 3.2 below depicts a decomposition of the simulation year into 32 time-slices.

Another important aspect related to the temporal scale is the investment strategy employed by bottom-up models. This can be categorized as either a myopic or perfect foresight approach, which is closely tied to the optimization technique used to solve the problem. In the myopic approach, investments are solely based on techno-economic data from the current period. This approach assumes that decision-makers make investment decisions without considering future changes in the energy system. On the other hand, the perfect foresight approach assumes that decision-makers have complete knowledge of the evolution of the energy system throughout the planning time-frame. This includes information on cost trends, variations in consumption, technical characteristics over time, and future decommissioning of existing plants. Models employing the perfect foresight approach are considered intertemporal models. The myopic approach is a sequential process where the results of each prior sub-problem are fed into the next optimization sub-problem. These models are also referred to as recursive models. It is important to note that the final solution obtained for

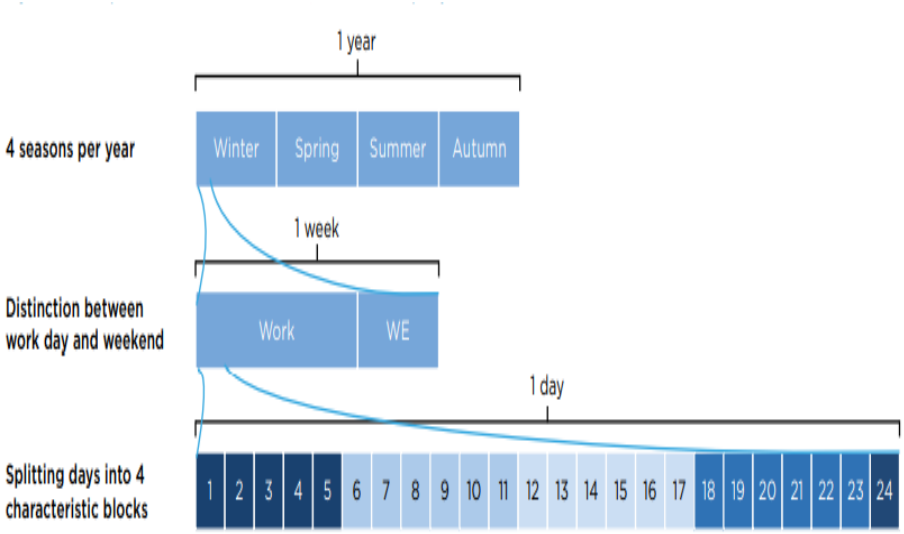


Figure 3.2: Example of time-slice definitions (32 time slices per year) (source: [5])

a given period using the myopic approach may be sub-optimal when compared to a solution derived with complete knowledge of the future. However, the myopic approach can be seen as a realistic representation of decision-making processes, as real-world decision-makers often lack knowledge of the future when making policies.

The **geographical coverage** in long-term energy models varies significantly, ranging from local regions to global coverage. It can be divided into two approaches: single-node and multi-node. The choice of geographical coverage depends on the specific focus of the analysis. A single-node model represents an energy system that does not account for the trade or transport of energy carriers with other regions. However, it may consider exogenous trade with the Rest of the World. The appropriate regional coverage depends on the specific objectives of the analysis. A smaller coverage provides more detailed information about a specific area but requires less computational effort compared to a larger coverage. Furthermore, a single region can be further divided into several sub-regions to incorporate local details and model trade flows of different commodities, such as biomass, gas, oil, and electricity.

**Sectoral coverage** As discussed in the previous section, long-term energy system planning models can focus on a specific sector of the energy system or incorporate multiple sectors. It is important to distinguish between different commodities, such as electricity, biomass, natural gas, and oil, as well as the demand sectors, including buildings, industry, and transport. Wider sectoral coverage offers the advantage of capturing the interaction and competition among energy supply, production, and demand technologies. This means that the end-use sectors can adapt in response to dynamics in the electricity sector. For example, when there is an expansion of electricity generation capacity that lowers the price of electricity,

more buildings may opt for electric heating. Without a multi-sectoral coverage, it would be challenging to capture such interdependencies. Studies often refer to this interlinkage as the connection between the electricity, heating, industry, and transport sectors. More recent developments also include the integration of the natural gas sector and hydrogen.

### 3.1.5 Positioning with respect to the operational power system models

As the name suggests, the main distinction between long-term planning models and operational power system models lies in the consideration of power generation investment. In other words, operational power system models take the power generation mix fleet and the power grid as inputs, without considering new investments. Conversely, power system planning models take into account investments in new generation and transmission capacities to achieve a balance between supply and demand.

Operational power system models are capable of modeling complex and highly detailed technical and economic aspects related to power system operation. They primarily operate on a short-term temporal scale, ranging from milliseconds to an entire year. These models are sensitive to technical details and are predominantly bottom-up engineering models that provide a detailed description of the system. They are primarily used in decision support for reliable power system operation, such as power flow analysis, power plant dispatch, or scheduling maintenance for individual power plants. In his thesis, Profumo [57] differentiates between three operational power system models used in electricity security assessments. This classification is based on the time horizon, temporal granularity, and the domains of the electricity system they focus on. Here, we provide a brief overview of the different classes without going into details, but we place special emphasis on unit commitment and economic dispatch models as they are used in generation adequacy assessments. For those interested in delving deeper into the Dynamic power system and Static power system models, more details can be found in [57].

- Dynamic power system/grid models: These models provide a highly detailed short-term description of the power system, grid, and protection components. They assess the power system's ability to recover from disturbances (e.g., faults, loss of generation, transmission lines, or load) and restore normal operation. This class of models includes rotor angle stability models, voltage stability models, and frequency stability models.

- Static power system/grid models: These models offer detailed representations of the power grid, component by component. They operate over a time horizon of one or several years, using a temporal resolution that depends largely on the model (e.g., power flow, topological, or graph-based).

- Power market/system models: These models typically represent the demand-supply balance and may use simplified assumptions to describe the grid topology (e.g., single node or multiple nodes). The typical time horizon is up to one year (or several

years) with an hourly temporal granularity. This class of models includes production cost models (unit commitment, economic dispatch models, hydro-thermal coordination models...)

In this thesis, we exclude dynamic and static models from our scope, as our primary objective is not centered around planning for system stability. Instead, our focus is solely on Power Market models, particularly the unit-commitment and economic dispatch models.

Unit commitment models are considered techno-economic models that serve the purpose of determining the scheduling, which involves decisions regarding the on/off status of power plants. This constitutes a highly intricate and challenging optimization problem due to the vast number of potential combinations of on/off states for all generating units. Additionally, non-convexities, such as startup costs, further complicate the model. For each time step, ranging from minutes to hours, the unit commitment model optimally determines which power plant units should be activated to meet the demand while adhering to various technical constraints, including ramping constraints and unit availability.

Conversely, economic dispatch models, when provided with a dispatch schedule, ascertain the power output of each generator to meet the demand while simultaneously minimizing the total operational cost and adhering to network constraints. The solution derived from unit commitment and economic dispatch models must conform to technical constraints at both the system and unit levels. System-level constraints include considerations like transmission constraints and reserve requirements, while unit-level constraints encompass factors such as minimum operating levels, restricted ramping rates, and minimum up and down times. Furthermore, achieving an optimal solution requires the incorporation of elements such as start-up costs, spillage costs, and the VoLL into the model.

## 3.2 Challenges of Bottom-up Energy System Modeling

Like any modeling community, bottom-up energy system models face various challenges. Numerous authors have dedicated their work to identifying these challenges. One notable study by Pfenninger, titled "Energy systems modeling for twenty-first-century energy challenges," examines four main challenges: (1) resolution in time and space, (2) balancing uncertainty and transparency, (3) integrating the increasing complexity of the energy sector, and (4) integrating social behavioral economics. Before delving into key challenges of energy system models, it is important to note that a shared consensus on major challenges exists across a large number of reviews.

Helisto et al. [14] present a list of eight challenges associated with planning and operating energy systems in the context of a high share of VREs. These challenges include temporal representation, unit commitment, spatial representation and power flow, short-term uncertainty, power system stability, capacity adequacy, energy system integration, and long-term uncertainty. As seen, the list of challenges is similar but also adds specific challenges related to the operation of the power system, such as stability and adequacy.

In a review on challenges and the state of the art of energy system modeling, Fodstad et al. [126] find that out of nine existing reviews, all nine suggest time and space as a challenge,

six suggest uncertainty, five suggest the multi-energy challenge, five suggest energy behavior and transitions, and six suggest transparency. A successful transition to a low-carbon energy future requires energy system modeling to encompass the dependencies and integration of different energy carriers evolving in various temporal and spatial scales. For example, electricity operation is balanced at lower temporal scales, while natural gas transport can be represented with lower temporal resolution. Uncertainty is a significant challenge as the future development of supply and demand remains uncertain. Factors influencing the evolution of demand and supply are difficult to capture in long-term forecasts, offering only an approximate vision. Therefore, modeling uncertainty regarding key model parameters is crucial for deriving robust long-term investment decisions. Additionally, it is important to consider the societal aspects of the transition, as it will impact society as a whole. When planning the future energy system, incorporating social aspects and behavioral elements such as acceptability becomes important. While transparency is also important, it is a common challenge across different scientific communities and will not be discussed in detail here. In the following paragraph, we will address four main challenges.

### 3.2.1 Challenge 1: Temporal and Spatial Scale

Several trends in power system development challenge the standard use of temporal and spatial resolution within long-term energy system planning models.

Temporal resolution has been a subject of discussion in various works. The choice of "best" temporal resolution (in terms of the necessary trade-off between granularity to accurately represent operation and computational time) has gained increased attention with the development of renewable energy sources. The introduction of vre, storage, flexibility options, and demand-side management requires a higher level of temporal detail. For example, Haydt [127] studied the importance of temporal granularity and techno-economic details on the outcomes of bottom-up long-term energy system models. They compared three methods to capture the variability of demand and supply: the integral method with only a few time slices, the semi-dynamic method with an intermediate number of selected time slices using a representative day's approach, and the dynamic method using 8,760 time slices. They emphasized that high temporal resolution is important for obtaining accurate model insights and that temporal resolution is more critical than techno-economic detail. Similarly, Ponclet et al. [27] demonstrated the impact of different temporal resolutions and techno-economic details on the final results of three different bottom-up long-term energy system models of the Belgian electricity system. They also showed that methods such as the representative day's method for choosing time slice structures can provide high-quality solutions compared to an hourly approach. Prina et al. [128] propose a classification of time resolution into three categories based on the number of time slices and selection approach:

- Low: 1-32 time slices
- Medium: 36-288 time slices
- High: 8,760 time slices (hours of the year)

Pina et al. [26] used a long-term energy system planning model (TIMES) with 288 time slices to demonstrate the differences in terms of investment and operation compared to a classical 12 time-slice approach. Correlation and chronology are also important to capture. Correlation is crucial for capturing the mutual evolution of load, wind speed, and solar irradiation. Chronology is necessary to consider when assessing the flexibility needs resulting from the variability of load and renewable generation. Neglecting chronology strongly impacts the results of long-term energy system planning models, as demonstrated by Nweke et al. [15].

Space is another significant challenge in energy system models. Energy and space have strong interactions, and this interaction has been highlighted for several decades. Nijkamp [129] identified five issues related to the interaction between energy and space, including the impact of changes in the energy sector on the spatial distribution of energy, assessing regional economic and technological variations, exploring different pathways, investigating regional economic and environmental interdependencies, and evaluating the distributional impacts of energy. However, with the increasing share of renewable energy, the spatial dimension becomes more relevant. The potential and generation productivity of VREs depend strongly on geographical location. Furthermore, the aggregation of generation across different locations smooths out their variability. Spatial resolution increases when multiple nodes are used to represent the system under study. A weak spatial resolution is characterized by a single node. Although our work does not focus on increasing the spatial resolution, we provide a brief review of the need to enhance spatial resolution in national-scale energy system optimization models.

It is common practice to use political and administrative divisions within energy system models, but modelers often mention the spatial resolution briefly without explicit justification for their choice. This choice is driven by the models' purpose of providing policy advice at those spatial levels. Many energy system models, such as JRC-EU-TIMES and METIS, used by the European Commission, as well as different versions of the open-source model framework OSeMOSYS for various regions, utilize countries or groups of countries as spatial units. While the practice of using political and administrative divisions in energy system modeling is widespread, modelers often provide only a brief description of their spatial resolution without explicit justification. However, this has not prevented energy system modelers from studying the impact of spatial resolution on model outcomes. Krishnan and Cole [130] used the ReEDS model, an electricity system capacity expansion model for the USA, with three different spatial resolutions: 134 balancing areas, state-level (48), and North American Electric Reliability Corporation (NERC) region level (13), to evaluate how the spatial aggregation of renewable energy sources affects the share of wind and solar PV. Their results show that spatial aggregation (moving from 134 nodes to 13 nodes) impacts the competitiveness of renewable resources, potentially leading to sub-optimal investments in capacity, with solar being less deployed compared to wind when aggregated.

Increasing spatial and temporal resolution alone is not always sufficient to capture all the operational features of the power system with higher renewable energy integration. Techno-economic detail is also crucial. Specifically, the operation of individual power plants is con-

strained by various factors, including maximum and minimum generation levels, ramping limits, minimum uptimes and downtimes, and costs associated with start-up and shut-down. Additionally, start-ups and ramping limits cannot be accurately modeled without considering short-term temporal chronology. These technical constraints faced by individual power plants, along with detailed system constraints aimed at ensuring reliability, are typically not considered in long-term energy planning models. As discussed in the previous section, this level of detail is usually reserved for operational power system models such as unit commitment and economic dispatch models. Concerns have been raised regarding the impact of neglecting technical constraints on the solutions provided by long-term energy system planning models.

In their article on the impact of technical detail on the power planning problem, Ponclet et al. [131] concluded that neglecting unit commitment constraints has been shown in various studies to have a highly significant effect on capacity mix, generation mix, carbon emissions, and cost projections.

### 3.2.2 Challenge 2: Generation Adequacy awareness

One of the key factors that long-term models must take into account is the availability of sufficient capacity to ensure system adequacy. Currently, utilities and regulatory bodies typically measure resource adequacy using the planning reserve margin. Various calculations and definitions of the planning reserve margin exist, but simply speaking, it represents the ratio of available capacity to expected peak demand, expressed as a percentage value over 100%. For example, a system with 100 GW of available capacity and an 80 GW peak demand would have a planning reserve margin of 20% [2]. Traditional reserve margin calculations focus solely on peak demand and do not account for each generator's contribution to meeting the load during periods of high LOLP. However, more sophisticated calculation methodologies are developed and take into account uncertainty and variability of different technologies into the calculation of the reserve margins. For example, in France, the utilization of an anticipation strategy by the system operator RTE for evaluating the necessary reserves and existing margins has proven effective in efficiently operating the grid, especially as the share of VRE has been on the rise. Introducing a novel tool known as MAUI, the system operator has automated the real-time calculation of required reserves and available margins over different time horizons [**book**].

For a robust assessment of generation adequacy, probabilistic simulations that consider the loss of load expectation (LOLE) metric, as mentioned earlier, are preferred. These simulations take into account forced and planned outages of thermal power generation units, as well as wind and solar availability during periods of highest LOLP. Milligan and Porter (2008) demonstrated a disconnect between planning reserve margin and LOLE, showing that the planning reserve margin required to maintain a LOLE level of 3 hours/year varies nonlinearly when assuming different forced outage rates for thermal power plants. Despite the importance of reserve margin in ensuring adequacy, Cole estimates that modelers often

[2]Typically, reserve margin values range from 10% to 25%.

pay less attention to this sensitive input compared to other techno-economic factors such as fuel prices, costs, demand growth, power plant retirements, and policies.

As a commonly employed method, a peaking-reserve constraint is introduced to enforce a planning reserve, stipulating that the cumulative installed firm capacity must equal or exceed the projected demand augmented by a predefined buffer, referred to as the Planning Reserve Margin (PRM). Prominent examples of planning models that incorporate these reserve margins include TIMES [132], ReEDS [133], and RPM [134]. While this approach offers simplicity, it necessitates an ex-ante evaluation of the impact of model simplification on adequacy issues, ultimately influencing the appropriate magnitude of the PRM. On an intuitive level, it is evident that a lower level of PRM can result in inadequacies within the generation system, while an higher level of PRM may lead to unnecessary capacity requirements.

Most models reported in the literature use **historical** PRM as a lower bound for the total installed capacity above peak demand that must be maintained in the model. This approach, adopted across different models, provides a transparent and computationally tractable constraint within long-term planning models. However, it faces two primary difficulties when representing resource adequacy. The first challenge is related to estimating the contribution of VRE resources in meeting peak demand, also known as capacity value or capacity credit. The second challenge is determining the level of resource adequacy required in the future.

To address the first challenge, various methodologies have been developed to estimate the contribution of VRE generators to resource adequacy. Long-term energy planning models typically use external high-resolution data, such as hourly wind and solar data, to estimate VRE capacity value and incorporate it into the optimization problem to ensure that the investment solutions respect the reserve margin. While methodologies have been developed to estimate the contribution of VRE to resource adequacy, it is not possible to conclusively prove that systems will meet the adequacy requirements anticipated by reserve margins [135]. Although significant research has been conducted on VRE contributions, less attention has been given to estimating the appropriate reserve margin for future power systems. Most long-term planning models are used to analyze different pathways of the power system, including radical changes such as carbon neutrality and electrification. Even scenarios considered as Business as Usual involve an increase in the share of renewable energy. Thus, the future power system may be substantially different from the current system. Consequently, models using historical or current planning reserve margins cannot guarantee that these metrics will be sufficient for the future power system. Readers who want to have further details on this challenge can be referred to work carried out by Tim Mertens which investigated in details the impact of the reserve constraint on the adequacy of the resulted power generation mix of the long-term energy planning models [136].

### 3.2.3 Challenge 3: Uncertainty

In his article [137], Pfenninger identified uncertainty as the second among four primary challenges. Drawing from the work of Kiureghian [138], he distinguished between two fundamental types of uncertainty pertinent to modeling: epistemic and aleatory uncertainty. The

choice of how to model uncertainty in a specific model lies within the modeler strategy: it is considered epistemic if the modeler thinks that acquiring more and higher-quality data or improving the model itself can reduce uncertainty. In contrast, it is categorized as aleatory if uncertainty cannot be further diminished. While addressing epistemic uncertainty requires enhancing the quality and accuracy of data and refining the modeling assumptions, formal methodologies exist to tackle aleatory uncertainty.

Long-term policy analysis conducted using energy system models necessitates decision-making under conditions of profound uncertainty. As per Lempert, this profound uncertainty can be characterized by three main aspects:

1. The absence of consensus regarding the most appropriate conceptual models for describing the interrelationships among the key driving forces that will shape the long-term future.

2. The lack of a probability distribution to describe the uncertainty associated with the key variables and parameters utilized in these conceptual models.

3. The challenge of determining how to assess the desirability of alternative outcomes, as they directly impact policy decisions.

Numerous energy system models have employed scenario analysis with a limited number of potential cases. This **deterministic** approach has played a pivotal role in offering valuable policy insights for future pathways by exploring a range of narrative-based "what-if" scenarios. It has been widely utilized in informing policies aimed at achieving cost-effective pathways. Usher and Strachan (2012) have argued that deterministic methodologies are ill-suited for addressing complex and multifaceted problems characterized by inherent uncertainties [139]. Trutnevyte et al. (2016) have underscored that simplistic deterministic modeling approaches often fall short in capturing the dynamic nature of real-world developments within the energy system [140]. Morgan and Keith have posited that scenarios featuring intricate narratives tend to underestimate the range of potential outcomes, potentially introducing cognitive biases that make these scenarios appear more probable and plausible than they truly are [141].

Modeling uncertainty is a key challenge for energy System models if robust outcomes are expected to derive reliable pathways for the transition. A systematic review on the approaches to uncertainty assessment in Energy System Optimization models distinguish between four main approaches [142]. Before reviewing those methodologies, the author categorize two uncertainty categories: parametric uncertainties and structural uncertainties. The parametric uncertainties arise due to the lack of knwoledge about empirical values associated with model parameters, and structural uncertainties refer to uncertainties in the model equations defining the model structure. An example of the first category is uncertainty of the evolution of the commodity prices in the future. An example of the second category include for example the modeling structure that ignore the manner in which non-economic considerations factor into energy decisions.

1. **Monte Carlo Analysis (MCA)**: In comparison to scenario and sensitivity analysis, MCA offers a systematic approach to address parametric uncertainties. The fundamental concept involves propagating uncertainties by simultaneously perturbing multiple uncertain input parameters, which are represented by probability distributions. This process involves several steps:

   (a) Define probability distributions for multiple exogenous stochastic variables.

   (b) Generate a random sample of values.

   (c) Incorporate the generated sample into the models and compute the resulting outcomes.

   (d) Repeat this procedure N times to obtain N model outcomes.

   (e) Assess sets of outputs using statistical techniques.

   A systematic review identified that nine studies utilized MCA for uncertainty analysis. The most recent study employed probabilistic assessment to explore 4000 decarbonization pathways using ETSAP-TIAM with MCAThe random variables subject to probability distributions include:

   (a) Capital costs of solar PV, wind turbines, and other technologies.

   (b) Potential of biomass, solar PV, wind, oil and gas, and $CO_2$ storage.

   (c) Social discount rate.

   (d) Energy service demand drivers.

   (e) Gross Domestic Product.

   (f) Population.

   (g) Elasticity of Energy Service Demands to their drivers and price.

   (h) Emissions from land-use change.

   (i) Climate sensitivity.

   By sampling these key parameters, uncertainty estimates are derived over time for various model outcomes, including temperature change, greenhouse gas emissions and concentrations, energy technology investments, energy commodities, energy system costs, and marginal greenhouse gas emission abatement costs. The findings can be summarized in several key points: 1) Delaying action to achieve the $2°C$ target incurs costs similar to taking immediate action for the $1.5°C$ target. 2) Demand electrification is projected to be higher in 2050 compared to the present in 100% of Monte Carlo samples. 3) Hydrogen is employed in 99% of the model runs to meet the $1.5°C$ target.

2. **Stochastic Programming (SP)**: Monte Carlo Analysis (MCA) assumes equal likelihood for each scenario, resulting in outcomes that fail to identify the optimal course of action. Furthermore, it assumes perfect foresight, wherein all uncertainties are revealed at the present time. This "learn now, then act" approach diverges from reality

because decision-makers often face uncertainties that become apparent only after taking action. In contrast, SP offers a singular course of action that accommodates future uncertainties.

SP stands out as the predominant technique for addressing uncertainty within energy system models. This method addresses multiple unresolved future uncertainties and determines optimal strategies by striking a balance between the consequences of various potential paths. Among the most widely utilized and studied stochastic programming models are bi-level programs. In these models, the decision-maker initiates action in the first stage, after which a random event influences the outcome of the initial decision. Subsequently, a recourse decision can be made in the second stage to mitigate any adverse effects resulting from the initial choice. The optimal solution from such models consists of the best immediate actions alongside a collection of recourse decisions (equal to the number of possible outcomes).

This approach has seen extensive application, especially after its integration into an improved version of MARKAL [143] and MESSAGE [144] in the 1990s, and later within the TIMES model [145]. Moreover, uncertainty has been incorporated into the TIAM modeling framework using a AP approach. This was done to evaluate the impact of climate change on the economic assessment of long-term energy policies [146], assess the role of CCUS in climate mitigation [147], and analyze climate stabilization strategies, considering the effects of climate sensitivity uncertainties in the long term [148].

In addition to its practical applications, quantitative metrics like the Expected Value of Perfect Information (EVPI) and the Value of the Stochastic Solution (VSS) are occasionally employed to gauge the significance of flexibility in providing robust hedging options against uncertainty. For instance, [149] leverages EVPI to evaluate the costs associated with uncertainties in fossil fuel prices, while [150] utilizes VSS to quantify the expenses incurred by disregarding uncertainty in Greenhouse Gas (GHG) reduction policy. It is important to note that this methodology faces challenges, primarily stemming from its computational demands. The scenario-based structure of this approach results in a substantial increase in memory requirements as the number of considered scenarios grows. However, these issues can be partially mitigated through the application of decomposition techniques and parallel computing.

3. **Robust Optimization (RO):** When the computational cost is higher when adopting stochastic program, robust optimization represent a cheaper alternative. The reduction in computational time is due to the less requirements of uncertainty information. Only the range of variation is needed for each uncertain parameter and no probability distribution is required. Readers who wants to learn more on the application of this methodology for energy system models can refer to [142].

4. **Modeling to Generate Alternatives (MGA):** The methodologies discussed earlier primarily address parametric uncertainties within energy system models. However, the energy system modeling community has stressed the need for a more profound focus on

structural uncertainties in these models, as highlighted in the reference by Hunter et al. [151]. One straightforward approach to mitigate structural uncertainties is either developing more complex models to accurately represent the system under study or comparing the outcomes of different model structures. Alternatively, confronting the model outcomes with expert reviews is another avenue. Nevertheless, it's important to note that increasing model complexity does not entirely eliminate structural uncertainties, particularly when energy system modeling aims to represent a complex system under a multitude of uncertainties. In such cases, exploring near-optimal solutions may be a more suitable approach, especially when unmodeled considerations, such as unforeseen risks, are not considered in the scenario design.

Energy system models offer a powerful means to investigate alternative energy system configurations under conditions of deep uncertainty using an optimization technique known as MGA. This approach involves relaxing the optimal solution and instead utilizes a modified formulation of the problem to explore the near-optimal solution space, seeking solutions that differ in the decision space. DeCarolis [152] pioneered the application of this methodology in the context of investigating alternative energy scenarios within the USA's power system and transport sector. The MGA was executed in four runs with varying slack values representing energy cost deviations of 1%, 2%, 3%, 5%, and 10%. In these MGA runs, the decision variables of interest were the energy outputs of various technologies. Comparisons were made between the outcomes of the MGA scenarios, a reference base scenario, and a carbon-constrained scenario. This comparative analysis revealed a diverse array of deployed technologies, with the diversity increasing as the slack value grew. Notably, technologies such as Integrated Gasification Combined Cycle (IGCC), biomass, and wind power exhibited significantly higher levels of penetration within the MGA scenarios.

### 3.2.4 Challenge 4: Societal considerations

While the energy system is described as an "integrated set of technical and economic activities operating within a complex societal framework," it is noticeable that energy system models primarily concentrate on techno-economic aspects and do not adequately incorporate social dimensions. There is a widespread consensus in the research community that non-technical factors play crucial roles as drivers and constraints in energy transition, exerting diverse influences on the dynamics of the transition process. As an illustrative example of how societal considerations impact the drivers of the energy system transition, citizens assume a dual role within the power system landscape [153]. On one hand, they can proactively contribute to the advancement of the energy transition by generating their own energy or by participating in demand flexibility initiatives. Conversely, the presence of public resistance to renewable energy installations or network development can impede the progress toward a low-carbon power system [154]. Neglecting to account for these social dimensions in energy system modeling may lead to suboptimal policy decisions. Therefore, it is imperative to reassess techno-economic modeling methodologies with the explicit goal of accurately

addressing the societal aspects of the energy transition within their frameworks [155]. This necessitates the inclusion of various societal stakeholders, recognition of socio-political dynamics, and acknowledgment of the continuous interplay between society and technology. Such an approach promises to yield a more robust and realistic examination of future energy system trajectories [156]. Societal considerations are not considered in this thesis, but will be discussed in the conclusion chapter.

In their paper titled "Modeling social aspects of the energy transition: What is the current representation of social factors in energy models?," Krumm et al. outline five significant social and behavioral factors that hold relevance for socio-technical transitions and, therefore, should be incorporated into energy system models:

1. **Behavior and Lifestyle:** This factor pertains to the behaviors of all actors within the energy value chain and how these behaviors influence the dynamics and pathways of energy transitions. It encompasses material and non-material needs, values, norms, and preferences. Changes in consumer behavior and values can significantly impact demand projections and, consequently, the required expansion of the supply side.

2. **Heterogeneity of Actors:** As the energy transition evolves, various actors come into play. This aspect is closely linked to the concept of agency and "heterogeneity across and within societies."

3. **Public Acceptance and Opposition:** This factor deals with the influence of public acceptance (defined as a favorable or positive response to proposed or existing technologies or socio-technical systems by members of a given social unit [157]) and opposition on the deployment pace of infrastructure required for the transition. Three dimensions are distinguished here: i) socio-political acceptance, which relates to the general public's acceptance of energy transition policies; ii) community acceptance, referring to the approval of local communities regarding targeted policies; and iii) market acceptance, which involves the market's response to innovations.

4. **Public Participation and Ownership:** This factor involves public participation in a bidirectional manner, allowing individuals to influence the transition process and actively engage in local transition initiatives.

5. **Transformation Dynamics:** This aspect encompasses transformation dynamics at different system levels and scales. It includes considerations such as the speed of transformation, path dependencies, and the quality of different system states.

## 3.3 Multi-model linking approach development

This section describes the focus of the thesis in relation to the previously discussed context and methodologies. It discusses the research gap in multi-model approaches and summarizes the main scientific contributions of the thesis.

### 3.3.1 The need of developing multi-model approaches

Based on the challenges that energy system modeling faces in the transition to a low-carbon power system, this thesis closely focuses on the temporal resolution and technical detail required to effectively model power system operations. The thesis also addresses some short-term uncertainties at the operational level needed for the assessment of power generation adequacy. Both the spatial resolution, long-term uncertainties and societal challenges are not considered in this thesis. One solution to tackle these challenges is the use of model coupling approaches, which provide multidimensional views that can address the energy transition more comprehensively than a single model. In the following paragraphs, we provide an overview of the linking multiple models approach and then focus on the efforts made in the power system domain and the research gaps in the existing literature relevant to our thesis.

The transition towards a low-carbon future energy system is inherently complex, and up to this point, no single model has been able to comprehensively address all the challenges associated with modeling this transition. To overcome the challenges faced by energy system planning models, efforts have been made to link different model classes, allowing for insights into the energy system and improved representation of various dimensions [158]. Model coupling, or linking, can be achieved by feeding the outcomes of one model into another model via a systematic protocol, iterative feedback between models, or by integrating models to run as a single unit [159]. However, the categorization of linking approaches lacks consistency across the literature. In our work, we adopt the categorization proposed by Helgesen and Tomasgard [159], which classifies linking into three categories: soft-linking, hard-linking, and integrated models. Soft-linking refers to user-controlled information exchange between models, hard-linking involves formal computer-led data transfers with shared code, and integrated models combine models to handle data as one. Reviewing various linking exercises across energy system models, Miguel Chang [158] observed that soft-linking is the most commonly used approach, followed by hard-linking and integrated models. This is mainly due to the fact that hard-linking and integration require more model development and present challenges in computational complexity and data consistency. These challenges are especially pronounced when the linked models have heterogeneous data assumptions, formulations, and outputs. Previous studies have utilized model linking to expand scenario analyses by coupling energy system models with Life Cycle Assessments (LCA) [160], behavioral models [161], energy demand models [162], economic models [163], and operational power system models [27, 164–166].

A conceptual research gap identified by Chang [167] in purpose-driven coupling of energy system models is that most existing studies focus only on proposing technical blueprints for their multi-model frameworks or providing specific case studies. This results in a lack of a general perspective on model coupling that explains the modeling paradigms and dimensions of coupling. To address this research gap, Chang [167] presents a conceptual framework in which the necessity of coupling exercises can be understood. He distinguishes between linking energy system models with different paradigms and linking energy system models with other knowledge domains.

1. **Linking with different paradigms:** he outlines that two predominant paradigms in

energy system modeling are simulation and optimization. Coupling these paradigms can complement the features found across energy system models. A simulation model aims to replicate the operation of an energy system using heuristics and rules, while an optimization model formulates the energy system as an optimization problem, seeking an optimal solution while respecting constraints. Simulation models are associated with predictive scenario planning, exploring possible future outcomes under a set of assumptions, while optimization models are related to normative scenario planning, providing prescriptive solutions to reach an optimal criterion [168]. Linking these two approaches can enhance the outcomes generated by a single energy system model, allowing for a wider exploration of the solution space. This can provide energy planners with robust and consistent scenario design frameworks.

2. **Linking with other knowledge domains:** Chang highlights its desirability but notes that developing a universally comprehensive framework is impossible. Therefore, purpose-driven model coupling is necessary to address specific questions about the energy transition.

In this thesis, the purpose of developing a multi-model approach is to ensure that future investment trajectories derived from long-term energy planning models meet the power generation adequacy requirements. In the following paragraphs, we discuss the literature on the multi-model approach specifically applied to the power system. Two classes of models commonly used in the coupling approach are long-term energy planning models and operational power system models. We provide a brief overview of the differences between these models.

Long-term energy system models are generally employed to derive investment trajectories and enhance our understanding of decarbonization. However, they face challenges in adequately representing the detailed structure of the power system in terms of technologies (rather than units) and incorporating short-term operational variations associated with the high penetration of VRE sources. According to Collins et al. [169], long-term energy system planning models with simplified power system representations suffer from significant limitations in accurately capturing the characteristics of VRE sources and can yield misleading results regarding operational requirements.

On the other hand, operational power system models are well-suited for representing the day-to-day operation of the power system but lack the ability to track vintage investments in installed capacities and possess long-term perfect foresight necessary for deriving transition trajectories. From a technical standpoint, as discussed in previous sections, long-term energy planning models and operational power system models differ in scope and resolution across three key dimensions: temporal, spatial, and technological. Operational power system models use higher temporal resolution to capture supply and demand variability compared to energy system models. This allows for the incorporation of detailed technical and economic characteristics such as ramping capabilities, start-up costs, and minimum up and down times. Operational power system models typically represent individual power plants or clusters, while energy system models focus on operational aspects based on specific technology categories. In addition to resolution differences, the explicit modeling of short-term uncertainties is of primary importance. Operational power system models, such as Monte Carlo

simulations, are at the forefront of modeling operational short-term uncertainties. In contrast, deterministic approaches are more common in long-term energy system models. The use of Monte Carlo simulations or stochastic programming for unit commitment problems enables the evaluation of flexibility requirements and accurate assessment of power generation adequacy. By linking both models, we can harness their complementary strengths to address specific challenges related to the integration of higher levels of renewable energy into the power system.

Different approaches have been developed in recent years to address the temporal resolution gap discussed in the challenges section between long-term energy models. In the literature, these linking approaches are classified as either uni-directional or bi-directional linkage, using the terminology proposed by Seljom et al. [170]. In both configurations, the long-term energy planning model is the "master" model, while the operational power system model is the "slave" model.

### 3.3.2 Uni-directional soft-linking approach

In the uni-directional linkage configuration, a set of decision variables from the energy system model is used as input for the operational power system model. An early example of uni-directional linkage is presented in Deane et al. [30], where TIMES is linked with PLEXOS to analyze the impact of temporal resolution and technical constraints of power plants on investments, dispatch decisions, and associated costs for the Irish power system in 2020. The capacity mix provided by TIMES for 2020 is transferred to the unit-commitment model, which includes additional technical details such as ramping, start-up costs, and minimum up time that are not incorporated in the Irish TIMES model. The findings demonstrate that the Irish energy system model provides reliable power system operation. However, when essential technical constraints are not considered, long-term energy planning models tend to undervalue flexible resources, underestimate wind curtailment, and overestimate the utilization of baseload technologies. In a related study conducted by the same research group, they developed a link between the MONET model (a six-region TIMES model representing the Italian energy system) and the PLEXOS-IT power systems model. The primary objective was to investigate energy security aspects within power systems. This research yielded two significant insights. Firstly, it highlighted an underestimation of the flexibility requirements in the Italian system as variable renewable energy penetration increases. Secondly, it raised concerns regarding the Italian energy system's ability to ensure sufficient supply for adequacy.

Incorporating the OSeMOSYS modeling framework for long-term planning, Welsch et al. [171] compare the multi-model approach (TIMES-PLEXOS linking as in [30]) for the Irish case with different extended versions of OSeMOSYS for the target years 2020 and 2050. These versions include OSeMosys Simple, which uses the core code of OSeMOSYS, OSeMosys 70% Wind, which ensures a maximum wind penetration of 70% using external hourly data analysis, and OSeMosys Enhanced, which incorporates external wind data analysis alongside constraints on minimum stable generation, reserve contribution, and operating reserve. The results demonstrate that without extending the temporal resolution, the enhanced OSeMOSYS model converges to results (in terms of investment) of the coupled model

TIMES-PLEXOS, with a decrease from 21.4% (OSeMosys Simple) to 5%. Additionally, when variability is ignored (OSeMosys Simple), power system investments in 2050 are underestimated by 14.3%. The study concludes that energy policies derived from many long-term models can lead to an underestimation of investments (and consequently the cost of meeting long-term emission reduction targets), highlighting the importance of using a multi-model soft-linking approach.

The uni-directional soft-linking methodology developed by Deane et al. [30] is also applied to the MARKAL-NL-UU long-term energy planning model, coupled with the REPOWERS operational power system model for the Netherlands in 2030 and 2050 [172]. The goal is to analyze the economic viability of power plants under four contrasting scenarios. The findings reveal that the revenues of power plants will be significantly impacted by the increasing share of variable renewable energy generation, discouraging investors from investing in generation capacity to support power system adequacy. these studies focus on a national spatial scale.

An important contribution was made by Collins et al. [173] in 2017, where the geographical coverage was expanded from national to European level. The study links the PRIMES energy system model, used to inform EU energy and climate policy, with the PLEXOS model to enhance and validate electricity generation for the target year 2030. Three aspects are analyzed: 1) variable renewable electricity curtailment, 2) level of interconnector congestion, and 3) wholesale electricity prices. The highly detailed operational results provided by the PLEXOS models, compared to PRIMES outcomes, reveal: 1) an overestimation of variable renewable generation by 2.4%, 2) isolated member states experiencing an excess of curtailment of 11%, 3) an average interconnector congestion of 24%, and 4) a decrease in wholesale electricity prices. Additionally, low capacity factors for natural gas-fired power plants may potentially impact their economic viability.

Another European-level linking work involving multi-area modeling includes the coupling of JRC-EU-TIMES (a long-term multi sectoral planning model) and Dispa-SET (a unit commitment and optimal dispatch model covering multiple energy sectors) [166]. The objective is to perform a highly detailed large-scale multi-sector unit commitment and power dispatch model to: 1) provide a detailed operational analysis of sector-coupling options and their mutual contribution to flexibility, and 2) explore system adequacy, GHG emissions and operational costs. The results highlight that the transport sector is the largest contributor to flexibility in terms of renewable curtailment, load shedding, and congestion in interconnectors. The cumulative flexibility contribution of individual sectors presents the optimal solution concerning system adequacy, GHG emissions, and operational costs.

Other contributions in the uni-directional soft-linking of long-term energy system planning models with operational power system models include Deane et al. [174], which identifies the best temporal resolution and technical constraint modeling in TIMES models, and Quoilin et al. [175], which employs stochastic coupling between JRC-EU-TIMES and the Dispa-SET model.

### 3.3.3 Bi-directional soft-linking approach

The use of bidirectional linkage, although less developed than uni-directional linkage, is used to respond to specific purposes. While uni-directional linkage is commonly employed to gain insights into power system analysis and assess its robustness, bidirectional linkage is driven by specific objectives. The information transfer from the operational power system to the energy system model strongly depends on the modeling goals. In the following section, we present six studies that utilize bidirectional linkage. Two of these studies employ IAMs instead of energy planning system models and will be discussed in the next paragraph.

The first study, conducted in 2007 before the well-known work on uni-directional linking [30], links the PERSEUS energy system model for the German electricity sector (excluding end-use sectors such as buildings, transport, and industry) with the operational power system AEOLIUS [176]. Both models share the same exogenous electricity consumption. The linkage procedure involves transferring the power generation mix obtained from the energy system model to the power market model. Based on the performance of this power generation mix using the operational power system, additional constraints are added to the energy system model to represent the relationship between intermittent and flexible capacity. Unfortunately, this article lacks sufficient details on the linking methodology and does not explicitly discuss the additional constraints or the convergence criterion.

The second study, dating back to 2009, employs the TIMES-Norway energy system model with the EMPS operational power system model [170]. In the long-term energy system planning model, the electricity sector is represented by a set of exogenous prices (7 internal regions, each with an electricity price), with endogenous electricity consumption and no new investments in power generation capacities allowed. The linkage is based on transferring electricity consumption from TIMES-Norway to the inputs of EMPS. The endogenous electricity prices provided by the power market model are then feedback to TIMES-Norway. The feedback loop iteration between the two models continues until successive iterations in electricity prices from the power market model and electricity consumption in the energy system model show minimal differences. Seljom et al. [170] note in their literature review of bi-directional linking approaches that the convergence of the previous study is measured using the same parameters exchanged between the models.

The third study involves linking the TIMES energy system model, representing only the power system of Portugal, with the EnergyPLAN operational power system model. Once again, the procedure entails using the power generation mix of TIMES as an input to the power market model. The feedback from EnergyPLAN to TIMES is achieved by setting an upper binding constraint on the maximum renewable capacity based on EnergyPLAN outcomes. The convergence of the feedback loop is determined by the criterion that the generation of intermittent renewable capacity in EnergyPLAN reaches 90% of its corresponding energy in TIMES.

In 2020, Seljom et al. [170] attempted to address the gaps in previous studies by using long-term energy planning models that cover all supply and demand sectors of the energy system, not just electricity. They proposed a transparent linking methodology with a clear definition of convergence criteria. The linkage is demonstrated using TIMES-Norway (with-

out representation of neighboring power systems) with the EMPS operational power system model at the European level. The purpose of the linking is to design a modeling framework that improves the representation of hydropower generation and electricity trade between Norway and external electricity markets in the energy system model. The linking strategy involves TIMES-Norway providing electricity demand, generation capacity mix, and transmission capacity of Norway to the power market model EMPS. The outcomes of EMPS in terms of electricity trade prices and hydropower operation are then fed back to TIMES-Norway. The feedback loop is stopped when the difference between the hydropower income derived from both models satisfies a convergence criterion. The linkage is applied only for two distinct periods of the planning horizon: 2030 and 2050, and for the five internal regions represented in TIMES-Norway. Convergence is tested for four instances (two scenarios for each period). The first scenario assumes that the power generation mix structure and consumption outside Norway remain the same as in 2015. The second scenario assumes a highly decarbonized energy system in 2030 and 2050 following the Highways2050 prospective scenarios. The linking strategy failed to converge under the second scenario in 2050. The authors attribute this result to significant differences in electricity prices generated by the two models under a very high share of intermittent generation. Other studies that have employed IAM models in their bidirectional linking are Brinkerink et al. [177] and Gong et al. [178].

### 3.3.4 Limits of linking approaches

At this stage, we highlight the first weakness associated with the unidirectional linkage approach, which fails to capitalize on the insights gained from the operational power system. In this configuration, the operational power system is solely used to evaluate the performance of the power system derived from long-term energy system models without improving the quality of the results. In the context of power generation adequacy compliance, which is our primary goal, a unidirectional approach is unsuitable as it does not capture whether investments should be modified based on the highly detailed modeling used in the operational power system.

We also emphasize four other gaps that were not adequately addressed in the aforementioned studies when assessing adequacy. Firstly, we believe that power generation adequacy can only be assessed using a probabilistic approach that accounts for multiple contingencies affecting generation adequacy levels. Additionally, the term "generation adequacy" mentioned in previous contributions is often used without referring to compliance with generation adequacy requirements set by public authorities.

Secondly, focusing only on specific periods does not guarantee compliance with power generation adequacy in the preceding or subsequent periods. Considering the trajectory evolution of investments and, consequently, power generation adequacy is of primary importance. Neglecting this aspect can lead to inconsistencies in the required investments. It is important to note, that in 2021, Thomas Hegarty addressed this gap by developing a bi-directional linkage between OSeMOSYS and ANTARES [179], taking into account the overall trajectory rather than just a single period. His work will be elaborated upon in the

following chapter to discuss the methodology developed in this thesis.

From a system perspective, assessing the adequacy of a power system connected to other systems via interconnections cannot be achieved solely through single-area modeling or reliance on exogenous data for imports and exports based on historical information. Thus, it is crucial to consider the potential evolution of the power mix structure in neighboring countries.

Regarding the reviewed bi-directional linking studies, we believe that the linking strategy, which involves linking two models with different spatial coverage, can introduce distortions in the results due to changes in optimization problems. For instance, Seljom et al. [170] linked TIMES-Norway with a European power system, while Gong et al. [178] linked a global energy model with a single-area power system model. In our case, maintaining consistency of spatial coverage in both models is of primary importance, particularly for interconnected power systems.

We also highlight that, to the best of our knowledge, only two studies have discussed the question of convergence with different definitions and approaches. It is expected to have different convergence criteria as the linking is purpose-driven. Seljom et al. [180] employ a set of endogenous decision variables in both models to assess convergence, while Gong et al. [178] employ a mapping of the Lagrangians from two optimization problems with distinct time resolutions, resulting in a comprehensive convergence of both decision variables and shadow prices within the model.

To summarize, in order to address the gap -identified at the beginning of the PhD- in the existing literature concerning the fulfillment of power generation adequacy requirements in the power system planning process, the following aspects are of significant importance.

- **Gap 1:** Develop a comprehensive and well-defined multi-model linking framework employing a bi-directional approach, accompanied by a clearly defined convergence criterion.
- **Gap 2:** Incorporate long-term generation adequacy requirements using a probabilistic approach in the planning process.
- **Gap 3:** Consider the overall temporal investment trajectory when assessing long-term generation adequacy.
- **Gap 4:** Examine long-term generation adequacy requirements beyond national borders, accounting for interconnections.

## 3.4 Focus of this thesis

### 3.4.1 Research axes of the thesis

This thesis focuses on modeling the transition of power systems towards a low carbon future, assessing long-term generation adequacy, and integrating long-term energy system planning

models with operational power system models. The main objective is to develop a multi-scale approach that bridges long-term planning with short-term secure operation. The outcome of this approach is a framework that enables the derivation of long-term investment trajectories respecting predefined generation adequacy requirements, specifically expressed in terms of the $LOLE$ metric.

The thesis follows an incremental methodology, exploring three main aspects. Initially, the focus is on a single-area system, specifically France, with a single target year. The methodology employed in this axis involves model linkage with bi-directional feedback loops. The second aspect addresses the notion of trajectory and the temporal inter-dependence of investments in the power system's generation mix, while employing a Rolling Horizon approach. Based on these two developments and their results and limitations, an integrated multi-scale approach is formulated and applied to the European multi-area interconnected system, focusing on the planning trajectory from 2020 to 2050. Figure 3.3 illustrates the three research axes, with one contribution in each quadrant. The axes are numbered clockwise from the lower-left quadrant.

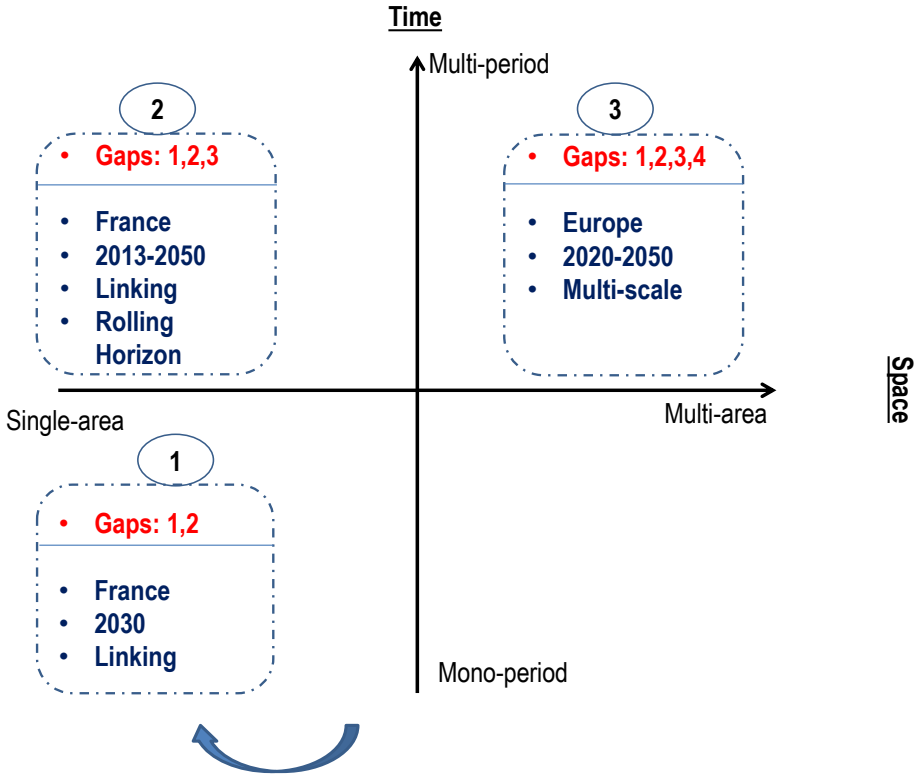


Figure 3.3: Research axes of the thesis decomposed of three main axes

The common objective of the three research axes is to ensure long-term power generation adequacy for future power systems. As depicted in Figure 3.3, the first axis employs a multi-model linking approach, focusing on the power generation mix and its adequacy for the

French power system in the year 2030. A bidirectional linking approach with clearly defined convergence criteria is applied to ensure that the power generation mix derived for 2030 satisfies the generation adequacy requirements set by the French public authorities. However, at this stage, the inter-temporal dependencies of investments in the power generation mix (and their impact on generation adequacy) are not considered (Gap 3).

To address this gap, a new approach combining the linking approach with a Rolling Horizon approach is developed to incorporate the dynamics of investments, including new investments, retirements, and prolongations, in the assessment of overall power generation adequacy within the planning trajectory. This framework is applied to the French power system (without interconnection) for the time frame 2013-2050. The outcomes of these two applications, which will be discussed in detail in the subsequent chapters, motivate the formulation of a new multi-scale approach that mathematically represents an integrated model capable of ensuring power generation adequacy for multi-area interconnected power generation mixes.

We believe that this abstraction, moving from a model linking approach to a more general multi-scale approach, allows for a transition from a descriptive methodology to a more generic one. We examine the convergence characteristics of a Stochastic Approximation (SA) algorithm when applied to our simulations for assessing the adequacy of long-term power generation mixes. Although we are unable to provide a mathematical proof demonstrating the fulfilment of all the assumptions required for asymptotic convergence offered by stochastic approximation algorithms, our focus is on achieving finite convergence. To accomplish this, we construct a score metric that enables us to evaluate convergence within a finite number of iterations.

### 3.4.2 Choice of the modeling scope in this thesis

First and foremost, our modeling scope is limited to the power system. While bottom-up energy system planning models are suitable for capturing the interactions among different energy sectors, in this thesis, we concentrate solely on modeling the power system. These models provide system-level optimal decisions and do not incorporate the behavior of individual investors, operators, and other actors. They enable the assessment of the impact of energy and environmental policies and guide decision-makers in designing future pathways that optimize socio-economic factors. They allow for the consideration of inter-temporal dependencies to derive investment trajectories that minimize total actualized costs while satisfying a range of technical, economic, and environmental constraints. Within our modeling scope, the environmental constraints primarily relate to carbon dioxide emissions. Our modeling of long-term investment trajectories is limited to deterministic models, without considering short-term or long-term uncertainties.

However, to assess security of supply, particularly power generation adequacy, a high level of technical and temporal detail is required. This level of detail, as previously highlighted, is typically reserved for operational unit commitment and economic dispatch models. The framework for power generation adequacy assessment used in our work follows the methodology employed by the French Transmission System Operator (TSO) (as well as other European

countries), which is based on a probabilistic simulation approach. This approach, when applied to a system (whether a single area or multi-area interconnected system), considers the key stochastic contingencies that have the potential to threaten security of supply. These contingencies include:

- Outdoor temperatures, which result in thermal sensitivity of the load due to heating in winter and cooling in summer.
- Wind and solar PV production.
- Unscheduled outages of thermal power generation units and relevant HVDC interconnectors, maintenance schedules.
- Hydro conditions, encompassing normal, dry, and wet conditions.
- Main correlations between different contingencies.

These contingencies define different future states, also known as Monte Carlo years, which are simulated by the hourly operational power system. The definition of Monte Carlo years represents the initial step in the adequacy assessment. To ensure convergence of adequacy metrics, a sufficient number of Monte Carlo years is required. Practical exercises conducted by the TSOs estimate that an amount of 400-1000 Monte Carlo years is adequate to achieve convergence. The second step in the adequacy methodology involves simulating power dispatch for each Monte Carlo year and identifying structural shortage periods—periods during which electricity production on the market is lower than electricity demand. Based on these structural shortage periods, generation adequacy metrics are computed, providing information about the level of adequacy.

### 3.4.3 The models of the thesis: TIMES and ANTARES

In this thesis, two models were employed to address the research objectives and explore the underlying problematic. Firstly, TIMES was chosen as the long-term power system planning model. This model generator was used to find optimal long-term trajectory investments for the power system in transitions. Secondly, ANTARES was chosen as the operational power system used for the dispatch and generation adequacy assessment [181].

**The long-term power system planning model: TIMES** TIMES is a bottom-up modeling framework, providing a detailed techno-economic description offer resources, energy carriers, conversion technologies and energy demand from a social welfare perspective. It is used for medium to long-term planning and analysis at a global, regional or local scales. The model minimizes the total discounted cost of the energy system to meet the exogenous demand over the planning time-frame.

In this thesis we use two instances of TIMES models. TIMES-FR for France and eTIMES-EU for the European power system. In order to not repeat the description given for energy system models. We classify both models using the taxonomy of Van Beek [114]. Specific details of each model will be given in the next chapters.

| Characteristic | TIMES-FR | e-TIMES-EU |
|---|---|---|
| Purpose | Exploring with scenarios | Exploring with scenarios |
| Analytical approach | bottom-up | bottom-up |
| Methodology | Optimization | Optimization |
| Mathematical programming technique | mixed integer | linear |
| Mathematical logic | Deterministic | Deterministic |
| Geographical coverage | single region | multi-region (29 regions) |
| General sectoral coverage | Energy | Energy |
| Energy sectoral coverage | Power system | Power system |
| Time-resolution | Medium (84 time-slices) | Medium (64 time-slices) |
| Time-horizon | 2050 | 2050 |

Table 3.1: Classification of long-term power system planning models of the thesis

**The operational power system: ANTARES** The ANTARES-Simulator, a software developed by RTE, is an open-source tool for analyzing large interconnected power grids in the context of short-term and long-term studies. This tool has been designed to address three aspects 1) generation/load balance studies (generation adequacy); 2) economic assessment of generation projects; 3) economic assessment of transmission projects. It employs a sequential Monte Carlo simulation approach and offers a time resolution of one hour over a span of one year. Notably, ANTARES is widely recognized as a reference market model and has been utilized in various national assessments and studies conducted by entities such as RTE, ELIA, and ENTSO-E. ENTSO-E, in particular, relies on the ANTARES model for key studies, including the MAF, the ERAA, and the assessment associated with the 10-year network development plan published biennially. Functionally, ANTARES operates as an operational power system model, enabling the calculation of optimal unit-commitment and generation dispatch strategies based on economic considerations. It strives to minimize generation costs while adhering to the technical constraints imposed by each individual generation unit. The resulting price, known as the marginal cost of the system, represents the cost of adding an additional megawatt of consumption to the system node. In other words, the marginal system cost corresponds to the dual value of the demand-supply balance constraint in the optimization problem

ANTARES is a sophisticated unit commitment and economic dispatch model that employs optimization techniques to determine the most cost-effective dispatch combination of power generation units and HVDC interconnectors to meet the electricity demand. The decision-making process relies on the supply merit order, which prioritizes power sources based on their marginal costs, and the demand curve of each bidding zone. For each bidding zone and hour, the model calculates the intersection of the demand curve with the supply curve, determined by the marginal costs of each generation unit. On the supply side, the optimization problem includes decision variables related to dispatchable generation (including thermal and hydro generation modeled as reservoirs) and storage technologies (such as batteries and pumped-storage plants). The model also considers interconnection flows be-

tween bidding regions, represented either by Net Transfer Capacity (NTC) or the Flow-based approach, as crucial decision variables. Non-dispatchable power generation, such as Run of River hydro, decentralized thermal production, wind, and solar PV, are taken into account as input time-series. Consequently, the model defines the dispatch based on the net load, which is the load minus the aggregated non-dispatchable generation.

ANTARES utilizes a Monte Carlo approach to simulate a year by solving weekly optimization problems (52 sub-problem) for the system under study. This process yields for each Monte Carlo year an hourly dispatch schedule for the power generation mix given as an input (installed capacities) throughout the year, accounting for generation, storage, market response capacities, and interconnection flows. Several crucial modeling assumptions must be taken into account:

1. Market simulations assume that market clearing occur hourly.

2. The optimization objective seeks an optimal solution that minimizes the overall cost of generation, encompassing both unsupplied energy and unserved energy within the simulated system.

3. Perfect one week foresight is assumed for renewable generation, consumption, and unit availability, known one week in advance through ex-ante draws. Consequently, storage, hydro reservoirs, and thermal dispatch are optimized with this foresight. However, real-world scenarios involve planned outages and unforeseen outages that necessitate system coverage.

4. The model assumes a perfect market without market power or bidding strategies, simplifying the scope of the model [3].

5. Pumped storage units, batteries, and market response are dispatched and activated with the objective of minimizing the system's operational cost. In reality, their utilization may differ, serving to balance specific loads within smaller zones or responding to other signals. The modeling approach assumes that economic dispatch of these technologies is primarily driven by price signals.

6. Prices calculated within the model rely on marginal cost/activation of each unit/technology.

These modeling assumptions should be taken into account to properly interpret the results obtained from the ANTARES simulation.

[3] In the general version of the ANTARES model, it is possible to incorporate market bids prices as an alternative to bidding with marginal prices.

# Chapter 4

# A bi-directional soft-linking methodology based on capacity-credit updates of the peaking reserve constraint: results and limitations

## Contents

In this chapter two main contributions are conducted, bellow a brief presentation of each one. The first contribution was published in Applied Energy revue in an article entitled "Assessing the security of electricity supply through multi-scale modeling: The TIMES-ANTARES linking approach" [182].

1. **Ensuring power generation adequacy for a single target year:**

   Long-term energy scenario planning models and dispatch simulations represent two crucial stages in the methodology for achieving a cost-effective transition to a low-carbon power system. Despite their equal significance, these stages are often carried out independently, potentially leading to future investment decisions based solely on long-term energy planning models without ensuring an adequate electricity supply. To address this challenge, the primary objective of this research axis was to develop a comprehensive methodological framework utilizing a multi-model approach to meet long-term adequacy requirements. An automated soft-linking model was employed to sequentially perform the following tasks:

   - **Plan Optimal Power Generation Mix:** The framework initially plans the optimal power generation mix to meet anticipated future electricity demand levels, subject to various constraints. This is achieved through the TIMES framework.
   - **Assess Adequacy:** The adequacy of the generated power generation mix is then assessed under different climatic and operational scenarios in the future. This assessment is carried out using the probabilistic operational open-source model ANTARES.
   - **Implement Iterative Feedback Loop:** An iterative feedback loop is implemented based on the estimated capacity of various generation technologies to support peak demand (referred to as capacity credit) for the peaking-reserve constraint. This ensures that the total firm capacity aligns with the electricity supply criterion.

   This methodological approach was applied to a case study involving power generation planning in France for the period 2013-2050, with a specific focus on the year 2030 as the linking target year. The results demonstrate that relying solely on TIMES for power generation planning in 2030 result in an inadequate supply. Conversely, the activation of iterative feedback loops considering capacity-credit exogenous parameters has the potential to simultaneously ensure the economic efficiency of the mix and meet the electricity supply security criterion set by French public authorities ($LOLE \leq 3hours/year$).

2. **Ensuring power generation adequacy for the whole planning time-frame:**

   This contribution introduces a novel approach referred to as the "Linking & Rolling" algorithm, designed to optimize long-term expansion strategies for power systems while adhering to short-term power generation adequacy requirements for the whole trajectory. In contrast to the linking approach developed in previous research, which focused on fulfilling one-year generation adequacy requirements, this contribution integrates linking models with the rolling horizon optimization method. This integration ensures the fulfillment of generation adequacy requirements across the entire planning timeframe. This method empowers planners to decide optimal and reliable expansion pathways while exploring the impact of different look-ahead periods. In essence, it enables them to identify economic objectives that effectively balance short-term and long-term advantages. Our primary contribution is the extension of the linking approach to cover the entire planning trajectory, achieved through the application of the Rolling Horizon technique. To evaluate the effectiveness of this methodology, we applied it to the context of the French power system transition, targeting a 60% renewable energy uptake by the year 2050. Additionally, we considered scenarios involving 80% and 100% VRE uptake. Our findings indicate that the results underscore the robustness of our proposed methodology in addressing trajectory adequacy.

**Résumé en français :**

Dans ce chapitre, deux principales contributions sont réalisées, ci-dessous une brève présentation de chacune d'entre elles. La première contribution a été publiée dans la revue Applied Energy dans un article intitulé *"Assessing the security of electricity supply through multi-scale modeling: The TIMES-ANTARES linking approach"* [182].

1. **Assurer l'adéquation de la production électrique pour une seule période :**

   Les modèles de planification des systémes énergétiques à long terme et les simulations de dispatch représentent deux étapes cruciales dans la méthodologie visant à réaliser une transition rentable vers un système électrique à faible émission de carbone. Malgré leur importance égale, ces étapes sont souvent réalisées de manière indépendante, ce qui peut potentiellement conduire à des décisions d'investissement futures sans garantit d'un approvisionnement électrique adéquat. Pour relever ce défi, l'objectif principal de cet axe de recherche était de développer un cadre méthodologique complet utilisant une approche multi-modèles pour répondre aux exigences d'adéquation à long terme. Un modèle de couplage bi-directionnelle a été utilisé pour :

   - **Planification optimale du mix de production électrique :** Le modéle de couplage planifie initialement le mix de production électrique optimal pour répondre aux niveaux anticipés de demande d'électricité future, sous réserve de diverses contraintes. Cela est réalisé grâce au modéle TIMES.
   - **Évaluation de l'adéquation :** L'adéquation du mix de production d'électricité décidé est ensuite évaluée pour un ensemble de scénarios climatiques et opérationnels futurs. Cette évaluation est réalisée à l'aide du modèle opérationnel probabiliste open-source ANTARES.
   - **Mise en œuvre d'une boucle de rétroaction itérative :** Une boucle de rétroaction itérative est mise en œuvre en fonction de la capacité estimée des différentes technologies de production pour satisfaire la pointe (appelée crédit de capacité). Ces parametres agit sur l'équation dite de réserve du modéle TIMES.

   Cette approche méthodologique a été appliquée à une étude de cas portant sur la planification de la production électrique en France pour la période 2013-2050, avec un accent particulier sur l'année 2030 en tant qu'année de couplage. Les résultats démontrent que TIMES décide un mix de production qui ne respecte pas le critére d'adéquation. En revanche, l'activation de boucles de rétroaction itératives considérant les paramètres exogènes du crédit de capacité a le potentiel de garantir simultanément l'efficacité économique du mix et de répondre au critère de sécurité de l'approvisionnement électrique défini par les autorités publiques françaises ($LOLE \leq 3heures/an$).

2. **Assurer l'adéquation de la production électrique pour l'ensemble de la trajectoire de planification :**

Cette contribution présente une nouvelle approche appelée *"Linking & Rolling"*, conçue pour optimiser les stratégies d'expansion à long terme des systèmes électriques tout en respectant les exigences d'adéquation de la production électrique à court terme pour l'ensemble de la trajectoire. Contrairement à l'approche de couplage développée dans l'axe de recherche antérieure, qui se concentrait sur la satisfaction des exigences d'adéquation de la production électrique d'une seule période, cette contribution intègre le modélde de couplage bidirectionnelle avec la méthode d'optimisation de l'horizon glissant. Cette intégration garantit la satisfaction des exigences d'adéquation de la production électrique sur l'ensemble de la période de planification. Cette méthode permet aux planificateurs de décider des trajectoires d'expansion optimales et fiables tout en explorant l'impact de différentes fenetre d'optimisation (de la myopie à la connaissance parfaite du future). Cette méthode permet d'identifier des objectifs économiques qui équilibrent efficacement les avantages à court et à long terme. Notre contribution principale est l'extension de l'approche de couplage pour couvrir l'ensemble de la trajectoire de planification, réalisée grâce à l'application de la technique de l'horizon glissant. Pour évaluer l'efficacité de cette méthodologie, nous l'avons appliquée au contexte de la transition du système électrique français, en visant une part de 60% d'énergies renouvelables d'ici l'année 2050. De plus, nous avons envisagé des scénarios à 80% et à 100% d'ENR. Nos résultats mettent en évidence la robustesse de notre méthodologie proposée pour planifier une trajéctoire adéquate.

## 4.1 Ensuring Adequate Power Generation for a Single Period

This next section outlines the methodology developed to integrate TIMES with ANTARES. The primary steps to achieve this objective include:

- **Planning a Cost-Effective Power Generation Mix:** This step involves determining an optimal power generation mix to meet future electricity demand targets, taking into account various constraints that represent energy and environmental policies.
- **Assessing Generation Adequacy:** A probabilistic approach is employed to evaluate generation adequacy. This assessment provides technical and economic insights into power system operation under various realization scenarios.
- **Establishing Iterative Feedback Loops:** Feedback loops are established between both models. These loops use the electricity security of supply criterion set by public authorities as a yardstick to ensure adequate power supply.

### 4.1.1 Methodology: Short model description

Below is a brief description of the two models constituent structures.

**Energy system model: TIMES-FR**

Long-term energy planning models specific to the French power system are formulated within the TIMES framework. The TIMES model generator overseen by the ETSAP under the IEA [183], is employed for this purpose. The term "model generator" implies that while the mathematical structure remains consistent, various model instances are generated based on input data provided by the modelers. TIMES frameworks have gained widespread adoption, with approximately 250 institutions across 100 countries utilizing them to devise energy systems at local, national, and multi-regional scales [184].

Technically, TIMES is a bottom-up (technology-rich) and cost-optimization modeling framework. The objective function of TIMES is to minimize over the considered horizon the total discounted energy system cost in its standard version and maximize societal welfare (consumer-producer surplus) in its elastic demand version [132]. The full mathematical linear programming structure in the TIMES model generator is presented in [185]. The scope of the model is usually applied to the analysis of the entire energy sector, but may also represent detailed individual subsectors, such as the power system. In addition, the model can be used to analyze environmental energy policies, which can be represented thanks to its explicit representation of technologies and fuels in all sectors.

At the core of TIMES is a so-called RES that represents an energy system with all of its interrelations and dependencies. The most convenient way of expressing the RES is through a network diagram that depicts all possible flows connecting primary resources, conversion technologies, and end-use demand through different energy commodities. Building the reference energy system therefore requires four types of exogenous data: energy service demands, primary resource potentials, a policy setting, and a description of energy technologies. For the runs reported here, the RES is adapted from the TIMES-FR-ELC (hereafter TIMES-FR) power system model developed by [34] (see Figure 1).

TIMES incorporates multiple nested levels of time granularity within its framework. The timeframe defines the specific period in the future for conducting planning analyses and is further divided into time periods. Each time period consists of several years, with each year within a given period considered identical and represented by a milestone year. It's essential to note that investment decisions are exclusively computed during milestone years. Figure 4.1 shows that the overall time horizon extends to 2050, while the timeframe spans from 2013 to 2050. The second level of granularity involves the temporal divisions within a year. TIMES offers the flexibility to introduce additional dynamics into either supply or demand by segmenting the year into various temporal segments of differing durations, often referred to as time slices. To effectively model seasonal dynamics, TIMES-FR further subdivides each annual period into seven seasonal periods. These encompass six monthly periods, along with one that simulates a potential week characterized by cold weather (high demand and no wind or solar power generation). Subsequently, each seasonal period is further divided into two typical days, which serve to represent several similar days while distinguishing between working days and weekends (weekly divisions). Finally, each typical day is partitioned into six hourly periods (daily divisions), with two time slices allocated to the nighttime, two for the morning, one for the afternoon, and one corresponding to peak demand at 7 pm.

A comprehensive exposition of the primary categories of TIMES-FR constraints can be

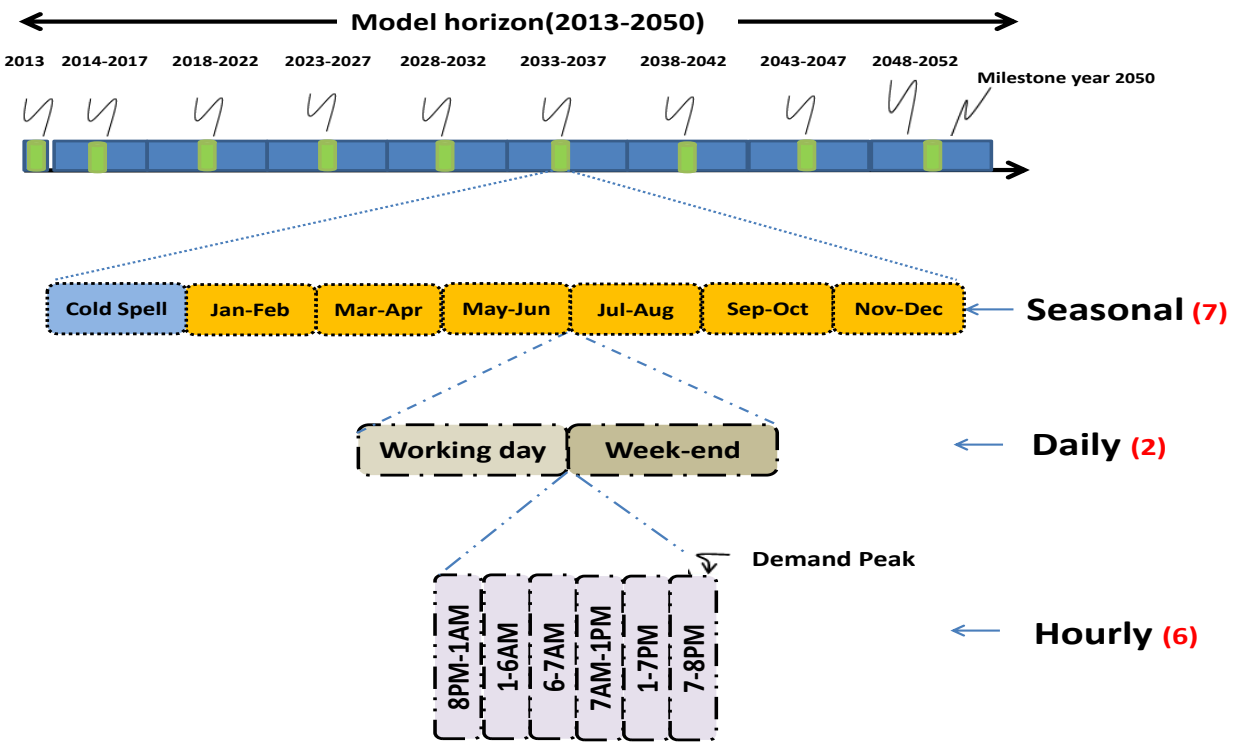


Figure 4.1: Temporal depiction tree in TIMES-FR. The first stage is dedicated to investment and the three others to the operation.

found in extensive detail in the references [34, 185]. Recognizing the paramount significance of maintaining an ample supply of firm capacity to ensure the system's adequacy, an essential constraint, termed the peaking reserve constraint, is introduced in Equation 4.1. This equation stipulates that all installed capacity units responsible for generating electricity during the peak time slice must surpass peak demand by a specific percentage, determined by the peak reserve factor. This calculation takes into consideration the actual contribution of each technology in meeting peak demand, referred to as capacity credits.

- The capacity credit describes the share of a technology's capacity available in the peak time-slice to cover the peak electricity load. Due to intermittency, VRE has much lower capacity credit levels than conventional energy sources, such as nuclear or natural gas.
- The peak reserve factor (28% in TIMES-FR) is chosen to respond to uncertainty regarding supply (unplanned equipment) and demand (excess high peak demand).

$$\forall t \in T, \sum_{i \in Tech} cc_{i,t} * Cap_{i,t} > (1 + 0.28) * D^{peak} \tag{4.1}$$

Where

- $cc_{i,t}$ (never higher than 1) and $Cap_{i,t}$ are respectively the capacity credit and installed capacity of technology $i$ in period $t$.

- $D^{peak}$ is the peak demand occurring in period $t$.

Please note that this constraint exclusively addresses the sizing of capacity and does not impose any limitations on the involvement of technologies in fulfilling demand during any of the time periods. Key model outputs encompass:

- The resulting investment requirements (capacity) and costs over the planning timeframe,
- energy flow by fuel,
- and pollutant emissions.

**Power system model: ANTARES-FR**

The unit commitment model employed is ANTARES, an open-source stochastic power system model developed by RTE, the French power grid system operator. ANTARES is designed to simulate the equilibrium between supply and demand across interconnected systems. This model is routinely utilized in European projects and national assessments, as evidenced by its inclusion in various reports and initiatives, such as the RTE French Generation Adequacy reports [**tyn**, 186, 187], PLEF adequacy study [188], TwenTies project [**europe**], e-Highway2050 project [**MID**], ENTSOE-MAF TYNDP [189], OSMOSE project [190], and ERAA [191].

The paper by [192] provides a comprehensive overview of ANTARES' architectural framework. The mathematical problem formulation for this power system analysis software is detailed in [193]. ANTARES is designed to address hydro/thermal scheduling and dispatching with a focus on the following key specifications:

- Network representation is based on nodes and edges, where each node corresponds to a specific market zone, and edges symbolize potentially aggregated transmission lines.
- The software conducts sequential simulations over a year, with hourly time resolution.
- It relies on 8,760-hour time series data, encompassing load profiles, available capacity for thermal power plants, wind and solar power generation outputs, etc., derived from either historical/forecast time series or stochastically generated time series by ANTARES.
- For hydroelectric power generation, the model supports water values as well built-in heuristics to deal with water management strategies at both monthly and annual scales.
- Commercial exchange capacities between nodes are considered, using the concept of maximum fixed commercial capacity known as Net Transfer Capacity (NTC). It's important to note that in this study, only one node is modeled, treating France as a single "isolated" system.
- ANTARES operates under the assumption of a perfect market, without accounting for market power or bidding strategies.

- Optimization is performed within a weekly perfect foresight timeframe.
- Additional constraints are applied to the links flow.

The primary simulation process employed by ANTARES is summarized in Figure 4.2. This simulation framework can be decomposed into two interconnected modeling components:

1. **Monte Carlo Scenario:** The first component involves the creation of Monte Carlo scenarios related to critical input variables. This phase entails generating a set of Monte Carlo years that represent potential future scenarios based on technical and meteorological parameters. These parameters encompass factors like thermal fleet availability, hydro inflow, wind and solar power generation, as well as load profiles. The scenario builder ensures the utilization of diverse data sources, ranging from pre-existing time series to entirely stochastic data generated by dedicated algorithms [194].
2. **Simulator:** The second component focuses on optimizing the hydro/thermal dispatch for each Monte Carlo scenarios, operating under the assumption of perfect market conditions. The optimization problem is formulated as follows for each Monte Carlo year within the preliminary sample: Minimize the overall generation cost of the interconnected power system throughout the year, while respecting the following constraints:
    - Ensure that each available thermal power plant operates within its specified minimum and maximum power output limits, and satisfies the minimum downtime and uptime requirements.
    - Manage the monthly availability of hydro (reservoir) energy.
    - Abide by the maximum interconnection capacities between different areas or zones.

ANTARES simulations take into account key events that could put security of supply at risk:

- The temperature sensitivity of power demand (cold spells can lead to higher peak demand);
- The unavailability risk of the thermal power fleet (reduction in available capacity);
- Variations in water flow (flexibility impact);
- Variable renewable generation (variable and unpredictable).

To achieve this goal, the probabilistic simulations incorporate a reference framework for climatic variables, encompassing 200 scenarios calculated in collaboration between Météo France (the French Meteorological Office) and RTE (as elaborated in the data and assumptions next section). The assessment of power system adequacy, relying on probabilistic risk

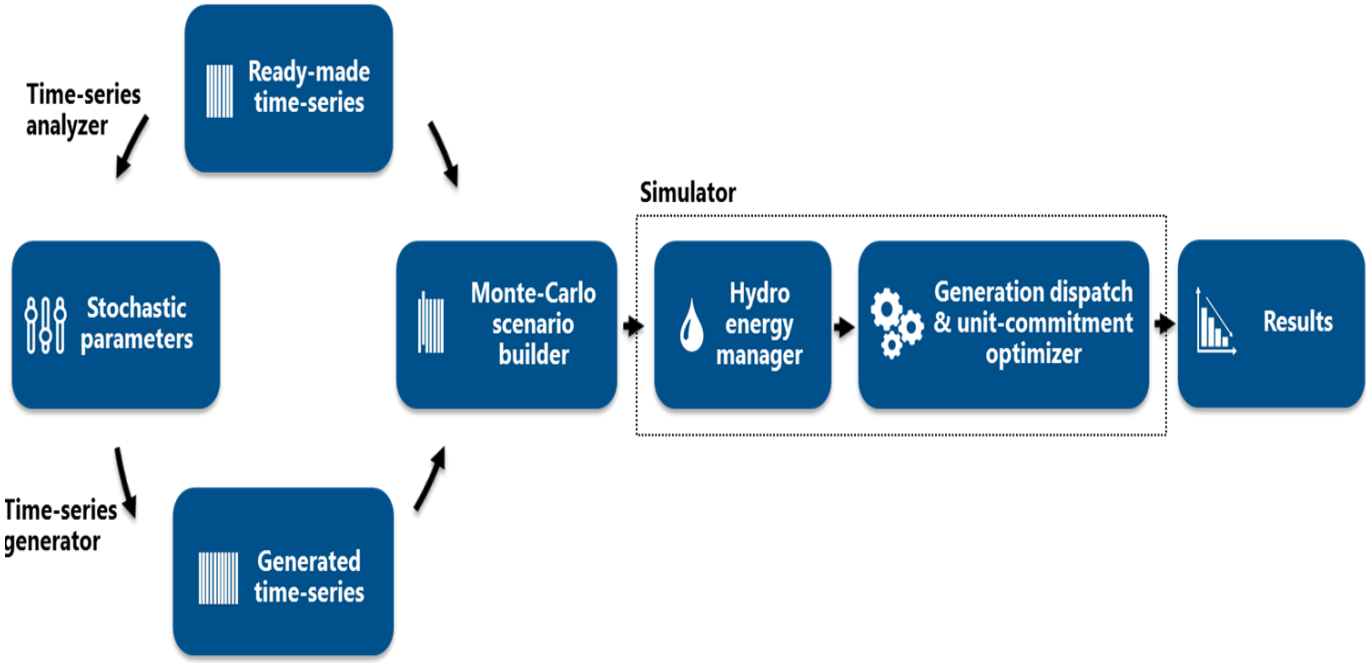


Figure 4.2: ANTARES simulation scheme. The time-series analyzer learns from historical data, the time-series generator draws new samples according to selected statistical laws.

analysis, necessitates the simulation of a substantial number of future states to address adequacy metric convergence challenges. In other words, the quantity of future states to be simulated must ensure the convergence of adequacy metrics while maintaining a desired level of accuracy, as discussed in previous studies [188, 195]. The required convergence for the indicator stipulated by regulations, typically the $LOLE$ metric, anywhere from 200 to 1,000 Monte Carlo years are necessary. This implies that all 200 climatic years must be simulated, each coupled with varying thermal power fleet availabilities and hydrological conditions, which differ across each of the simulated future states. Following the completion of the Monte Carlo simulations, the model's outcomes provide a wide array of indicators that can be determined for further analysis and assessment:

- Dispatch indicators (generation per fuel/technology, imports/exports).
- Adequacy indicators ($LOLE$, $EENS$);
- Economic indicators (operational costs, spillage costs and unsupplied energy costs);
- Sustainability indicators (emissions, renewables shares);

### 4.1.2 Modeling framework proposed: an automated soft-linking approach

The framework, as depicted in Figure 4.3, provides an illustration of the connection between TIMES and ANTARES through an automated soft-linking tool, a process divided into two primary components: the coupling part and the feedback part. The initial stage, the coupling part, focuses on establishing a connection between TIMES and ANTARES as distinct modeling tools. Subsequently, the feedback part is designed to address generation adequacy concerns. In this manner, TIMES is employed to optimize investments in new generation capacity within a time frame spanning from 2013 to 2050. The resultant power generation mix for a specific year (2030) is then transmitted to ANTARES, where detailed hydro/thermal dispatch decisions are made at an hourly resolution, considering a multitude of stochastic scenarios representing weather and operational uncertainties. Following the computation of results by ANTARES, the primary objective of the feedback loop is to ensure the adequacy of the generation mix. However, establishing this feedback with the long-term energy planning model is not a straightforward process and necessitates an iterative approach. In practical terms, the stopping criterion for the feedback loop is defined as an upper bound of 3 hours/year for the $LOLE$.

**Coupling part**: the following two steps are built to align ANTARES inputs with TIMES outputs:

- Global Input Database and TIMES Initialization: Since TIMES and ANTARES are utilized to model the same power system reality, there is an intersection in their input data. Before initiating the feedback loop, the initial step in the linking process involves identifying the disparities and commonalities between these two modeling approaches. The following three steps, as explained in detail by [196], are applied in this soft-linking approach:
  - Identifying Basic Differences Between the Models: In the process of identifying differences between the models, various aspects are considered, such as reconciling deterministic versus stochastic model paradigms, representing technology, and addressing differences in hourly or time-slice temporal resolution.
  - Identifying Overlaps: This step entails determining clear mappings of overlaps since both models describe the same power system. For instance, the principal overlap lies in the representation of the power generation mix.
  - Identifying and Deciding Upon Common Exogenous Variables: Assumptions related to exogenous inputs are defined through scenarios, and standardizing common inputs between the two models is crucial. Typical common inputs in both models include electricity demand, PV and wind capacity factors, as well as technical and economic characteristics of power plants. ANTARES, being probabilistic, describes electricity demand and VRE capacity factors using multiple time series to simulate multiple years. In contrast, TIMES-FR is used in its deterministic version, representing only one year. Consequently, it was determined to employ

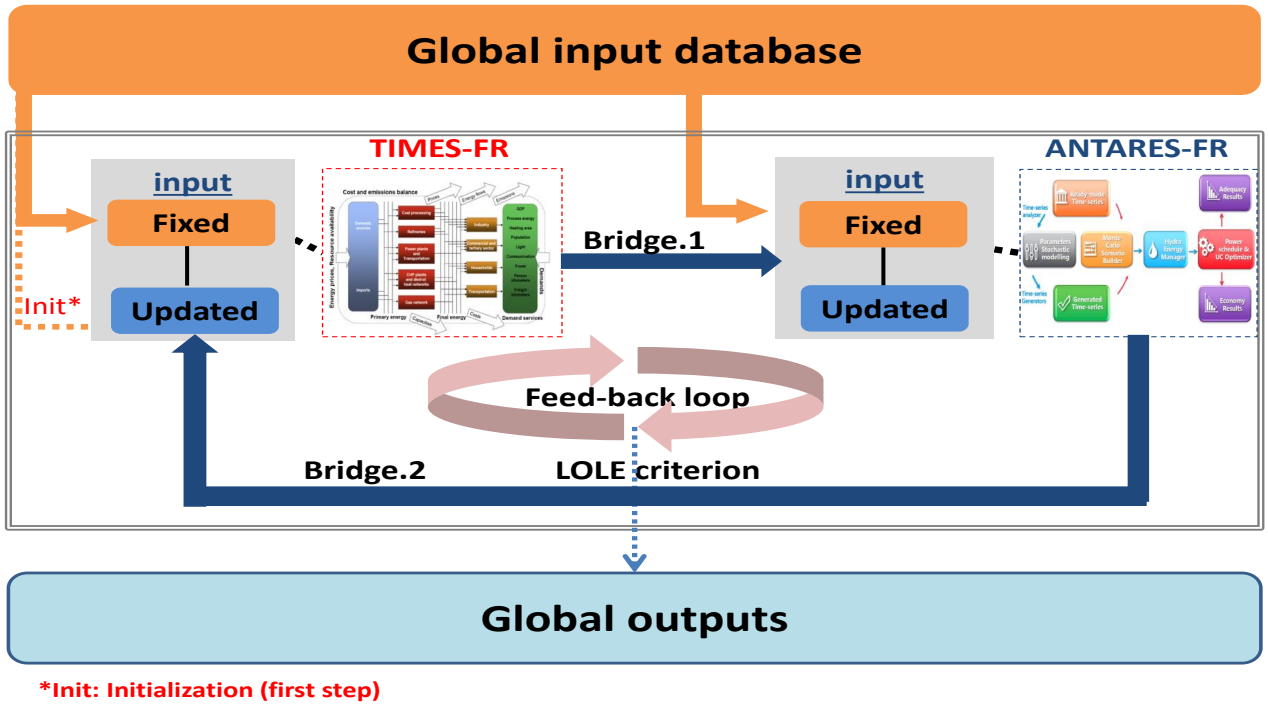


Figure 4.3: Schematic overview of the TIMES-ANTARES linking model. The uninterrupted line describes the information flow interactions, and the dashed line indicates the initialization step which is considered as the start of the linking process. The first step of the iteration is a TIMES solution. ANTARES is then run with a TIMES solution for a target year, and operates a Monte Carlo dispatch. The iteration ends as soon as the *LOLE* criterion is achieved. The global outputs are the power generation mix obtained and the insights offered by the linking model.

the ANTARES median scenario [1] as the input for TIMES. In this manner, the orange block labeled "global input data" encompasses key input data required for TIMES and ANTARES, serving as the starting point for the linking exercise.

Once this input consistency is established, the initial step is to execute the TIMES model for the entire planning period.

- Bridge.1: This step is the linchpin of the linking model. It begins with the extraction of the power generation mix for a specific year of interest based on the TIMES solution. Subsequently, ANTARES is employed with this targeted mix as input to simulate the supply/demand equilibrium within the power system, considering a range of operational and climatic conditions. It is imperative to emphasize that, within ANTARES,

[1] The median scenario is determined as the time-series that is near to the median time-series calculated over all scenarios. The nearest time-series is determined using a metric called Nash–Sutcliffe metric

the stochastic nature of VRE, power demand, hydro generation, and thermal power plant availability is addressed by incorporating a substantial number of annual scenario conditions through Monte Carlo simulations. Each conceivable future state corresponds to an alternative realization, which is generated using forecasted meteorological data. These realizations are composed of annual time-series data, offering hourly resolution and utilizing RTE data [83].

**Feedback part**: This part is designed to assess the power system generation adequacy.

- Bridge.2 and feedback loops: After running ANTARES, the outputs are analyzed in terms of the difference between: dispatch decisions, annual expected power generation, and finally the adequacy of the power system. Two things can happen:

  1. If the outputs show that the legal adequacy criterion is not met ($LOLE \geq 3hours/year$), then some parameters will need to be updated in the long-term optimization model;
  2. If the outputs show that the legal adequacy criterion is met, then the process ends.

One integral aspect of this framework involves the feedback loop from ANTARES to TIMES. The adopted approach revolves around assessing whether the generation portfolio determined by TIMES can meet the 3-hour limit requirement. The objective is to guarantee an adequate amount of firm capacity, which refers to capacity that can reliably meet the load at all times, particularly during peak demand periods. Several strategies can be considered to achieve this goal. Taking inspiration from the IRENA report on planning for a Renewable Future, which underscores the significance of integrating exogenous capacity credit into long-term energy planning to ensure the expansion of the system maintains an adequate level of firm capacity [11], the focus was placed on capacity credits. Specifically, by assigning capacity credit values to different types of power plants, including VRE, the TIMES model can provide adequate expansion of the power generation capacity mix. In the TIMES-FR model, capacity credit is integrated as an exogenous parameter within the peaking reserve constraint (see Equation 4.1).

A growing body of literature has made significant strides in providing more accurate representations of the capacity credit associated with VRE sources within long-term energy planning models, employing various approaches to estimate it [197–201]. These studies universally acknowledge that the level of capacity credit depends on several key parameters, including the average capacity factor, its day-to-day variability, and the desired security of supply level. In our work, we introduce a novel methodology inspired by the IEA approach to estimate the capacity credit value while considering the outputs generated by ANTARES. In the projections made using the World Energy Model, VRE capacity credit is computed as the difference between peak demand and peak residual demand, expressed as a percentage of the installed capacity of variable renewables [202]. Consequently, the capacity credit is assessed concerning ANTARES outputs, as outlined in Equation 4.2.

$$cc_i = median_{s \in Scenario} \frac{(LDC^s(t_{peak}) - RLDC_i^s(t'_{peak}))}{Capacity_i} \tag{4.2}$$

Where

- $LDC$ is the Load Duration Curve defined as a curve representing the relationship between load and time. On this curve, the load values are plotted in descending order of magnitude, with the highest load positioned at the left end, followed by progressively lower loads as one moves towards the right, and the lowest loads situated at the far right end.
- $RLDC_i$ is the Residual Load Duration Curve defined as the curve between the net load (equal to the load minus the generation of the technology $i$) plotted in the order of decreasing magnitude
- $Capacity_i$ is the installed capacity of a technology $i$.
- $t_{peak}$ is the peak hour of the $LDC$.
- $t'_{peak}$ is the peak hour of the $RLDC_i$.
- $Scenario$ is the set of ANTARES Monte Carlo scenarios indexed by scenario $s$.

The bi-directional data exchange between the two models is set up as follows:

- TIMES mainly provides the generation portfolio;
- For a specific year, ANTARES assesses the generation adequacy criterion and provides capacity credit iteratively over available technologies.

### 4.1.3 Methodology: Data assumptions and simulation strategy

The aim of this section is to explain how major data transfers were carried out from one model to the other and the simulation variants hypothesis.

**Electricity demand and renewables capacity factor datasets**

Climatic conditions wield a substantial influence over both renewable generation and power demand, making weather events a critical determinant of power system operation and adequacy. Consequently, it is important to consider the range of climatic conditions that will affect both renewable generation and power demand. Furthermore, wind, solar radiation, temperature and precipitation are mutually correlated. For instance, during extremely cold periods, wind energy production often diminishes while consumption surges while there is a significant increase in consumption due to the thermo-sensitivity of load.

Given these considerations, we integrated a database that includes 200 meteorological time series datasets, covering parameters such as wind speed, solar radiation, and temperature. These datasets were intentionally crafted to represent diverse potential states for

the focal year of interest, which in this context is 2030. In this section, we develop the methodology employed to successfully harmonize TIMES and ANTARES with respect to modeling power demand and renewables capacity factors, with a specific focus on wind and solar. Importantly, we ensure that the inherent mutual correlations among these variables are retained throughout this process.

In our study, we assume the average long-term evolution of future electricity demand, regardless of specific climatic conditions, over the period from 2013 to 2030. This assumption is based on the projections outlined in the "High Consumption" scenario of the Generation Adequacy Report [33]. According to this scenario, the anticipated rise in demand will primarily result from substantial electrification of end-use sectors and concerted energy efficiency measures. Furthermore, we consider a stable, flat evolution for the period spanning from 2030 to 2050.

The power demand time-series are calculated using an analytical approach and stacking model (ORPHEE [2], developed by RTE), considering the three following phases:

- Forecasting the annual energy demand;
- Forecasting the power demand, applied to an hourly reference profile for temperature;
- Adding the temperature sensitivity effect for end-uses sensitive to weather conditions using two hundred annual reference temperature series produced by Météo-France.

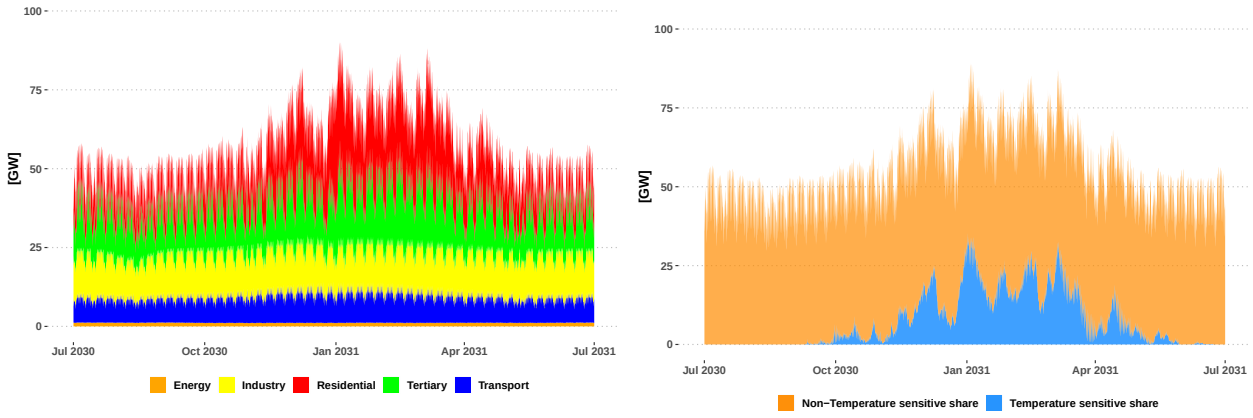


(a) Load time-series breakdown by sector of activity

(b) Temperature sensitivity of load curve

Figure 4.4: Power load curve of the median climatic scenario: (a) represents the 2030 load curve breakdown by sector of activity and (b) the temperature sensitivity.

The first phase involved forecasting the annual total electricity demand, which required aggregating power demand across various sectors of activity (residential, tertiary, industry, energy, transport, and agriculture). Each sector was further divided into specific end-uses.

[2]The model is not open-source; instead, it is an in-house proprietary tool.

Once the total annual demand was projected, an hourly normalized load curve profile was constructed for each end-use, assuming reference temperatures (normal conditions).

In the final phase, temperature sensitivity was applied to end-uses affected by weather conditions, such as heating and air conditioning. This step utilized the 200 temperature time series forecasts from the meteorological database. The demand forecasts for each end-use were then aggregated to generate the total load curve scenario inputs, resulting in 200 hourly time series for ANTARES. Figure 4.4a illustrates the shape of the median scenario load curve categorized by sectors of activity, while Figure 4.4b displays the temperature-sensitive portion of the same load curve. Notably, high consumption occurred during winter, primarily due to seasonal electric heating in residential and tertiary sectors. Additionally, the transport, industry, and energy sectors experienced minimal seasonal and daily fluctuations. For a more comprehensive analysis of French electricity consumption, please refer to the Generation Adequacy Report [33].

Within the TIMES models, the annual electricity demand for 2030 was computed for each sector by aggregating the corresponding end-use demand levels from the ANTARES median load scenario. The hourly profile was further aggregated to assign energy demand levels to each time slice. This assignment technique ensured that both models yielded the same total energy consumption. The results in terms of duration load curve representation between ANTARES (with hourly resolution) and TIMES (with 84 time slice resolutions) are depicted in Figure 4.5. Notably, the inclusion of a set of time slices representing a cold week in January-February facilitated the capture of load peaks. In terms of load curve representation, the methodology used for assigning load values to time slices provided a reasonably accurate approximation of the complete load duration curve, particularly concerning the peak load ($R^2 = 80\%$). To summarize, Table 4.1 compiles and compares the characteristics of the energy demand data used in both models.

Table 4.1: TIMES and ANTARES demand profiles assumption comparison

| Demand | TIMES | ANTARES |
|---|---|---|
| Power demand | Seven end-use sector electricity demands [MWh] | Total load consumption [MW] |
| Time-horizon | Planning period 2013-2050 | 2030 |
| Temporal resolution | Annual demand level, aggregated into 84 time slices | Hourly time series (8,760 hours) |
| Input Scenario | Median climatic scenario | 200 climatic scenarios |

In terms of renewables, the capacity factors for onshore and offshore wind turbines, as well as solar PV panels, are derived from 200 forecast climatic scenario datasets provided by RTE. ANTARES utilized 200 hourly capacity factor forecasts to account for the uncertainty of wind and solar conditions. Our objective was to replicate the observed mutual correlations among climatic variables, including temperature, wind, and solar radiation. To achieve this condition, a straightforward approach was adopted: the capacity factor time series were derived from the same weather scenario used for the demand time series. Once again, the median climatic scenario was chosen to serve as the availability factor input for 2030 in TIMES. This availability factor was incorporated into TIMES at a time slice level through an averaging process applied to the hourly capacity factor profile. As a result, the

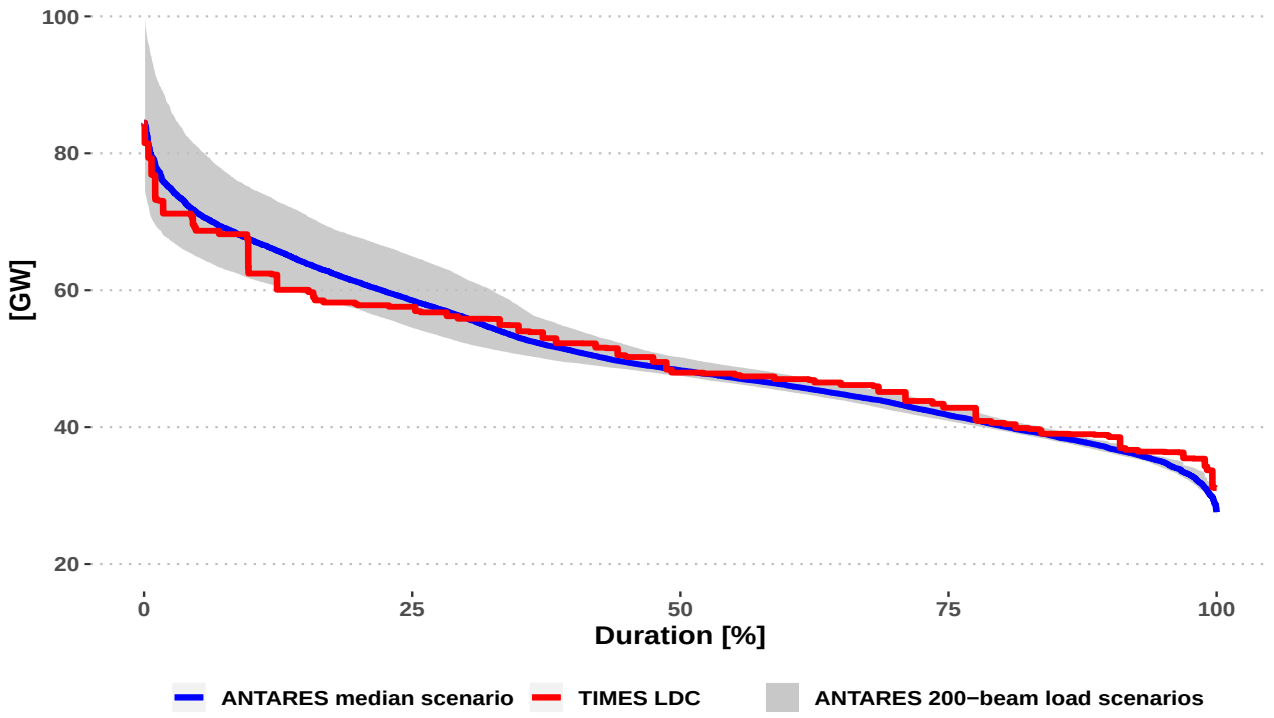


Figure 4.5: TIMES LDC estimation (red line) based on ANTARES median scenario (blue line). The gray area represents the min-max load scenarios.

representation of the onshore wind capacity factor duration curve showed limited accuracy due to its high variability. Conversely, the repeated Gaussian shape of solar radiation enabled a more adequate approximation of PV capacity factors. Table 4.2 provides a summary and comparison of VRE representation in both models.

Table 4.2: TIMES and ANTARES wind and solar capacity factor input comparison

| VRE | TIMES | ANTARES |
|---|---|---|
| Capacity factor | Capacity factor [%] | Available capacity (Installed Capacity*Capacity factor) [MW] |
| Temporal resolution | Yearly aggregated 84 capacity factor time slices | Hourly production time series |
| Scenario simulated | Median scenario (number $\frac{178}{200}$) | 200 climatic scenarios |

**Fuel costs and thermal marginal costs**

In the TIMES model, fuel costs for fossil resources such as gas, coal, and uranium spanning the period from 2013 to 2050 are determined based on projections from the New Policies Scenario as outlined in the World Energy Outlook (WEO). Conversely, in ANTARES, marginal costs for thermal units are calculated, assuming fixed Operation and Maintenance (O&M) costs, a carbon tax, and fuel price. Notably, start-up costs are not factored into the computations within the ANTARES model.

**Power generation technologies**

The technical representation of the power system in the TIMES model includes 30 existing technologies that are currently operational, alongside 89 new technologies that have the potential to be deployed in the future. When modeling the existing power fleet within the French electricity system, individual units are considered, or they are grouped into several processes based on technology and fuel. Additionally, over the period from 2013 to 2050, a range of new electricity generation technologies becomes available in nine milestone years. To ensure a consistent technological representation across both models, the TIMES linear formulation is modified to incorporate a lumpy investment option, accommodating the granularity of unit-level investments. This adjustment facilitates a common representation of technologies in both models. A comprehensive list of the technologies modeled in TIMES-FR, along with their associated economic and operational characteristics, including cost and price assumptions, can be found in recent works.

Table 4.3 depicts the thermal power plants differences between TIMES and ANTARES. Within ANTARES, the thermal power plants are grouped into clusters that have similar generation characteristics. For each cluster, several technical and economic characteristics are taken into account:

- The number of units and nominal capacities, defining the installed capacities: based on TIMES decisions (new capacity investment and residual capacity);
- The cost, including marginal cost [Euro/MWh]: based on fuel price assumptions and technical-environmental technology assumptions.
- The operational constraints for minimum stable power [MW], and minimum up-and-down duration [Hours]: based on data from the IRENA report [11].
- Planned and forced outage generation rates and average duration based on RTE data [%].

Table 4.3: TIMES and ANTARES thermal power plants comparison

| Characteristic | TIMES | ANTARES |
|---|---|---|
| Thermal | Technology level (existing power fleet)<br>Unit-by-unit level (new investment) | Unit by Unit or Clusters |
| Technical detail | Min. stable generation (MW)<br>Max. generation (MW),<br>(no equivalent)<br>(no equivalent)<br>Availability factors (%) | Min. stable generation (MW)<br>Max. generation (MW),<br>Min. up and down times (hours)<br>Planned and forced outage rates and average duration (%)<br>average duration (%) |
| Economic data | (no equivalent)<br><br>No equivalent (endogenous) | Startup cost<br>No-load cost<br>Marginal cost = Market bid |

For hydro power generation, three categories of hydro plants are used: Run-of-river (RoR) plants; storage plants that possess a reservoir to postpone the use of water; and pumped-storage stations (PSP).

### 4.1.4 Methodology: Simulation strategy

Before examining the simulation strategy adopted, it's important for readers to note that this study models the French power system without considering cross-border exchanges with neighboring countries. The TIMES-FR model has been calibrated for the base year 2013, replicating the historical energy system in France as reported by RTE data. Cross-border exchanges with the rest of the world are only considered for this base year. The primary focus of this work is on the year 2030, which serves as the target year for our linking model.

In previous instances, TIMES-FR has been used to conduct various scenario analyses for the French power system. However, the main objective of this paper is to apply the linking methodology rather than extensively exploring the policy implications for the French power generation mix. Consequently, a long-term scenario, characterized by a 60% uptake of VRE in power generation, has been selected as a case study. This scenario adheres to specific constraints, including [34]:

- Constraint on nuclear power production, reflecting the French Energy Transition Act, which foresees reducing the nuclear power production share from 75% to 50% by 2025 .
- Constraint on the French power system's CO2 emissions to below 2012 levels (39 Mt) for each period.
- Constraint on VRE penetration assuming legal objectives for 2020 and 2030 while attaining 60% in generation by 2050.

Based on these constraints, two simulation variants were implemented in the ANTARES model to gain insights into power system operation and adequacy. These variants aim to assess the sensitivity of the power generation mix determined by TIMES to a subset of pertinent variables affecting power system operation:

- **Sensitivity to Climatic Events:** This involves simulating 200 future climatic years representing the conditions in 2030. It doesn't take into account thermal plant technical constraints or hydro energy conditions. This test evaluates the adequacy of the power system derived from TIMES when subjected to climatic variability.
- **Sensitivity to Climatic Events and Operational Impacts:** This combines the climatic impact with thermal power fleet operation constraints (including technical details and unavailability) and different hydro conditions (wet, normal, or dry). This results in simulating 1,000 future states, akin to Monte Carlo years. This test assesses the impact of critical operational constraints on power system adequacy.

Detailed outcomes from these two simulation variants are extensively discussed in the Results section.

The first part involves a comparison and analysis of the dispatch schedule results generated by both models. This analysis is based on the first ANTARES variant, utilizing data from 200 Monte-Carlo years and focusing on the median scenario dispatch results. The second part focuses on evaluating shortages in the median scenario to determine whether ANTARES, when provided with the same input scenario as TIMES, identifies any potential problems related to power shortages. The third part centers on assessing the generation adequacy across 1,000 Monte-Carlo years and examining the impact of the iterative feedback loop on the power generation mix structure and associated costs.

All simulations were undertaken on an HP Intel core i5 laptop equipped with 2.40GHz processors. The longest TIMES simulation, comprising only one iteration, took approximately 20 minutes. On the other hand, the longest ANTARES simulation, which was the second simulation variant, had a runtime of around 30 minutes for a single iteration. The linking model was entirely managed through various packages developed using the R programming language, and its execution time was less than 1 minute.

### 4.1.5 Results: Generation capacity mix and dispatch schedule

In linking long-term energy planning models with the operational power system (Bridge.1 in Figure 4), the goal is to translate the generation portfolio projections decided by TIMES into detailed, cluster-by-cluster power system model inputs. The long-term energy planning model TIMES is designed to function on a technology detail level, which means that it does not respect the same power generator representation as ANTARES (see data and assumption section). To enhance the alignment between TIMES' outputs and ANTARES' inputs, we developed a capacity generation transfer routine. To illustrate the operation of the first bridge, let's consider the example of the nuclear power fleet (a similar process was conducted for other thermal power technologies). Figure 4.6 shows the optimum capacity mix decided by TIMES for 2013-2050 following a 60% VRE scenario. On the right side of the figure, investments in new power plants are detailed on a unit-by-unit basis, with the "lumpy" mode activated in TIMES. Consequently, new investments are grouped into the same characteristic clusters and subsequently transferred directly to ANTARES. However, since the remaining capacity of the existing stock and retrofit is presented on a technology basis, the residual nuclear fleet needs to be divided into three standardized technical clusters. This division is accomplished using a MILP program, which determines the allocation of units to each cluster.

- The 900 MW cluster;
- The 1,300 MW cluster;
- 1,400 MW or N4 cluster

In this paragraph we analyse the underlying impact of the temporal representation on generation scheduling from both models (hourly for ANTARES, by time slice for TIMES). To achieve this, we employ the first simulation variant, which simulates 200 potential climatic

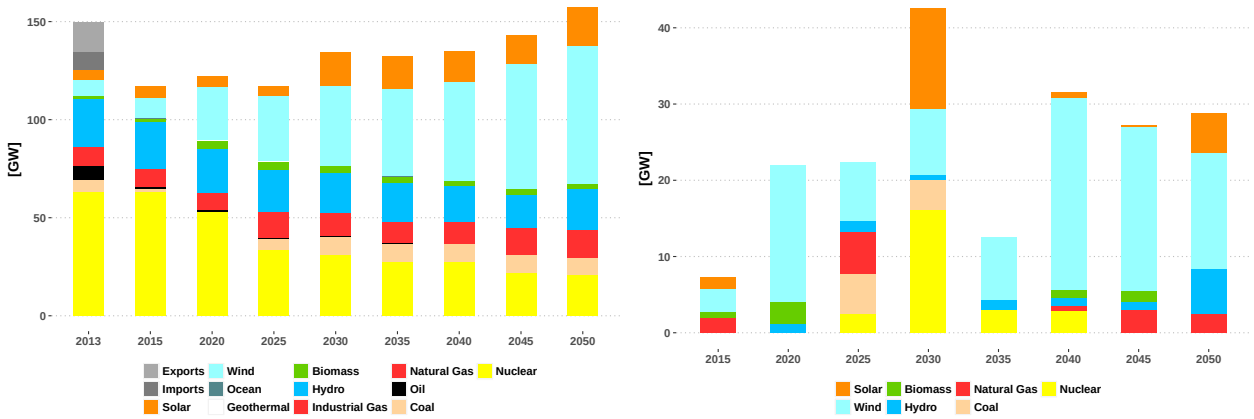


(a) Total installed capacities over the planning time-frame

(b) New installed capacities over the planning time-frame

Figure 4.6: TIMES power generation mix over the period 2013-2050. (a) Total installed capacity and (b) the new installed capacity

scenarios for 2030. It's important to note that we use the median scenario as input for TIMES to ensure a consistent comparison between the models.

Firstly, we focus on the outputs related to the production stack and how both models approximate the residual load curves. Secondly, we quantify a global comparison indicator, namely annual power generation. This indicator helps us assess the differences between the model outputs and explicitly evaluate the quality of our linking exercise. An initial observation reveals that despite having an identical power generation mix in both models, differences in dispatch schedules are noticeable (see Figure 4.7). The primary reason for these differences in model results lies in how they approximate the residual load. Residual load is defined as the load remaining after deducting non-dispatchable generation. One crucial distinction between the models in approximating the Residual Load Duration Curve (RLDC) is their approach to renewable generation. TIMES has the capability to curtail renewable generation, whereas ANTARES generates all available renewable generation without curtailment.

Figure 4.7 provides a visual representation of the Load Duration Curve (LDC) and RLDC model approximations, while Figure 4.8 illustrates the dispatchable schedule derived from ANTARES (Figure 4.8a) and TIMES (Figure 4.8b). By definition, the energy below the RLDC is provided by dispatchable sources of generation (or load-shedding in extreme situations). The empty white area between the LDC and RLDC represents the contribution of wind and solar generation.

This graphical representation shows two dependent patterns:

- **Temporal Resolution Impact:** The use of 84 time slices within the TIMES model has the effect of reducing the high variability seen in wind and solar capacity factors. As a result, the ANTARES hourly capacity factor profile is simplified into a piece-wise curve within TIMES. Consequently, this leads to an overestimation of the residual load

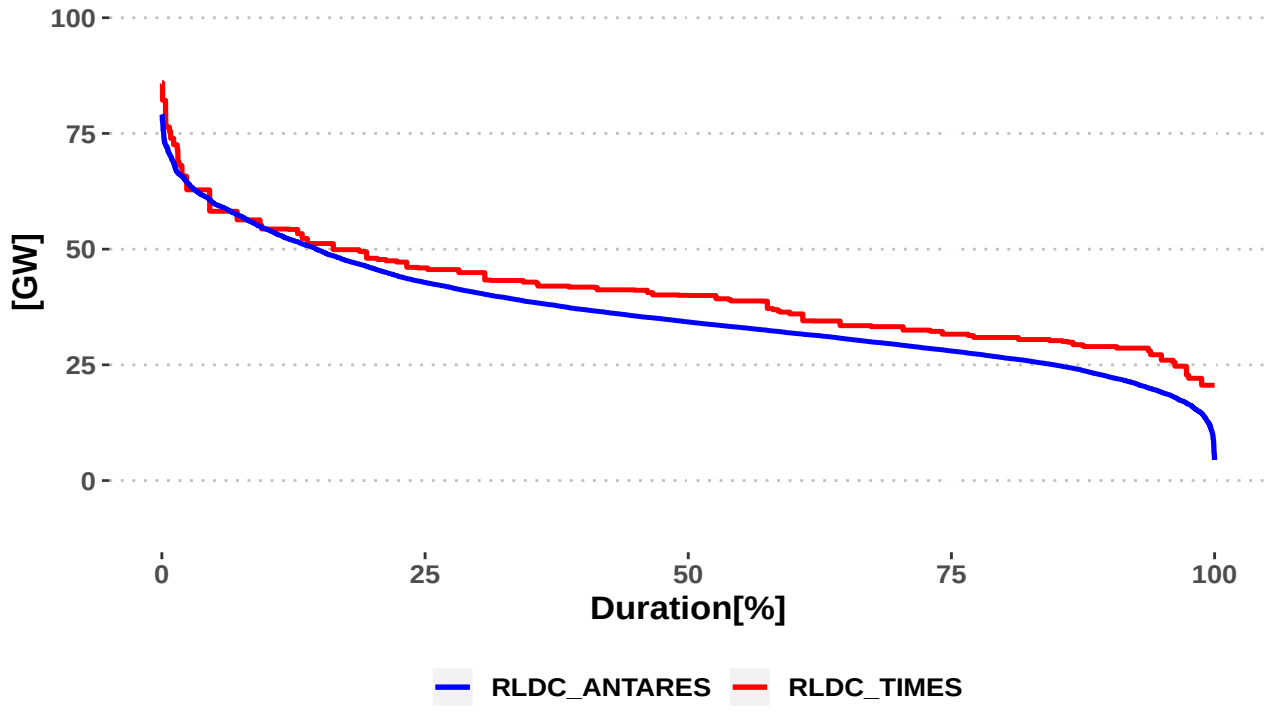


Figure 4.7: The Residual Load Duration Curve comparison between TIMES and ANTARES median scenario (2030).

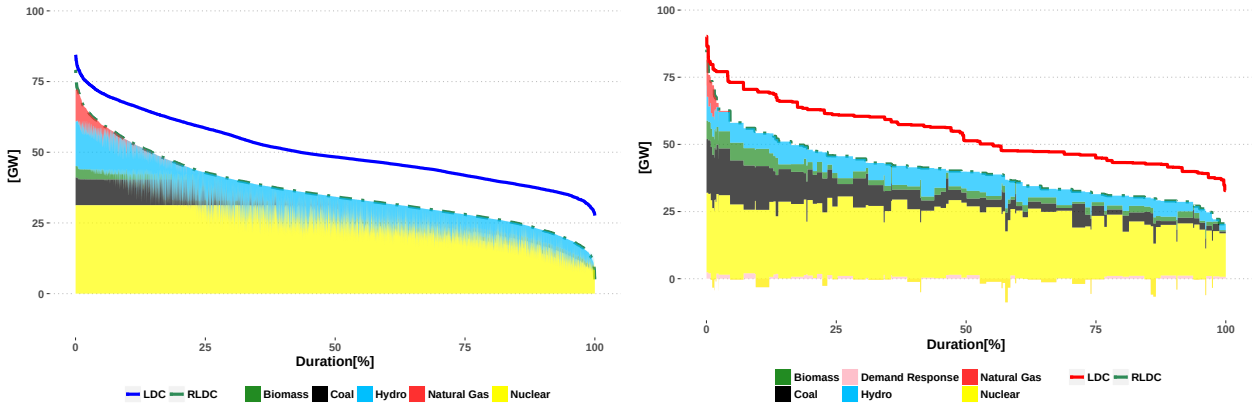


(a) ANTARES production stack

(b) TIMES production stack

Figure 4.8: 2030, production stack comparison between TIMES and ANTARES. (a) ANTARES hourly production stack for the median scenario and (b) the TIMES 84 time-slice production stack.

duration curve when compared to ANTARES, as depicted in Figure 4.7.

- **Thermal Power Plant Flexibility:** Within the TIMES model, thermal power plant flexibility is somewhat overestimated due to the omission of certain technical constraints. Notably, factors such as ramping limits, minimum uptimes, and downtimes are not accounted for in TIMES, whereas they are considered within the ANTARES model. This overestimation of flexibility tends to result in the over-utilization of mid-merit load power plants.

As a result of these factors, differences in annual energy generation can be observed across various technologies. Figure 4.9 provides a comparative view of the annual power generation for each installed technology in the year 2030, as computed by the TIMES model (shown in red) and the corresponding ANTARES model (shown in blue). Minimal differences are evident for both non-dispatchable generation technologies, especially wind and solar, as well as nuclear. These differences can be attributed to various factors, including the economic merit order, which prioritizes renewables and nuclear. However, noticeable disparities emerge in the case of mid-merit power plants, such as coal and biomass. Consequently, TIMES indicates an approximate surplus of 26 TWh in total annual power generation compared to ANTARES. The primary reason for this disparity in hydro power generation is that ANTARES utilizes the entire available hydro energy stock, whereas TIMES retains the option to not fully exploit the upper bound of this resource.

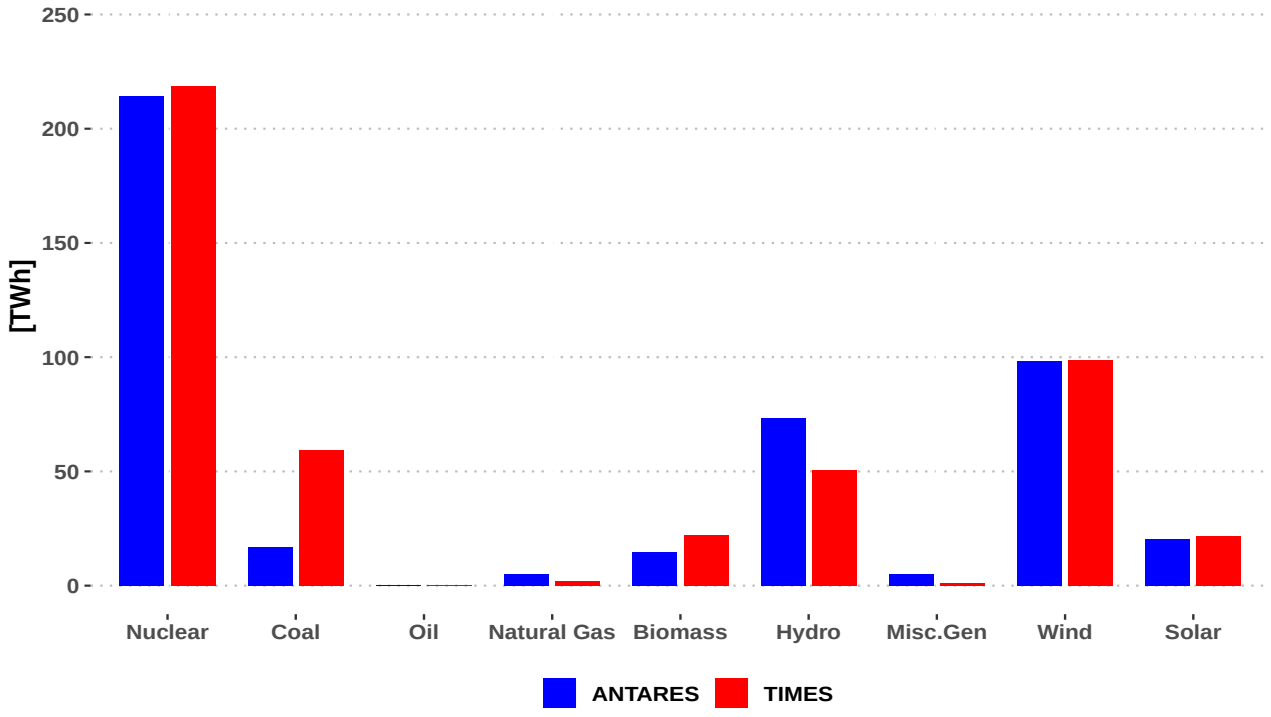


Figure 4.9: 2030, Annual power generation comparison by technology (x axis) and by model (red: TIMES and blue: ANTARES).

Combining these results, it can be concluded that TIMES, due to its limited capture of residual demand variation and omission of thermal power plant flexibility constraints, tends to overestimate the utilization of mid-merit order load technologies when compared to an hourly dispatch approach. These findings align with the observations in the study by [203], emphasizing the significance of incorporating renewable energy variability into long-term energy planning models.

### 4.1.6 Results: Shortfall risk analysis

The objective of analyzing the supply-demand balance of the power generation mix determined by TIMES is to assess its adequacy in power generation. In this regard, the first simulation set is utilized to characterize potential shortfalls in the power generation mix. Initially, the median scenario, serving as a reference point, is examined to understand how the use of an hourly unit commitment model affects the adequacy of the power generation mix established by TIMES. Subsequently, the 200 scenarios are employed to calculate the $LOLE$ adequacy metrics.

Regarding the various adequacy metrics detailed in the previous chapter, the primary metric used to evaluate the adequacy of power generation in the median scenario is expressed mainly in terms of the Loss of Load Duration ($LOLD$). Figure 4.10 illustrates the hours of loss of load for the median scenario, revealing that the input scenario used in TIMES results in 16 hours of loss of load. Notably, the periods of unmet demand occur primarily during the winter months, particularly in the January-February period. Of these critical situations, 56% transpire around 7 pm, coinciding with peak demand, while the remaining 46% occur during the morning peak. The durations of these shortfall hours vary, ranging from one hour to nearly three hours.

Secondly, the occurrences of shortfalls result from a combination of factors. The specific hours at which structural shortages are identified can be pinpointed using the RLDC. Figure 4.10 provides an overview of how electricity demand is met by available generation resources throughout the year. The graph reveals that structural generation shortfalls primarily coincide with the peak of the RLDC, meaning that cold spells exacerbate these shortfall situations. The introduction of intermittent renewable energy sources has a notable impact on the shape of this residual curve, which must be addressed by dispatchable technologies. Non-intermittent renewable energy sources such as run-of-river and Combined Heat and Power (CHP) also play a role, although to a lesser extent. However, even if all dispatchable generation technologies operate at their maximum capacity to meet the peak residual load, the supply falls short. In conclusion, a combination of high demand levels and low renewable power outputs can significantly affect the adequacy of the power system projected for 2030 by TIMES.

To comprehensively evaluate the overall impact of climatic conditions on adequacy, we rely on the ANTARES outcomes derived from 200 different scenarios. The primary criterion for assessment is based on the loss of load expectation ($LOLE$), expressed in hours. This $LOLE$ distribution is computed by analyzing load losses observed across 200 Monte Carlo years (Figure 4.11). Consequently, the ANTARES simulations yield a $LOLE$ value of 36.19

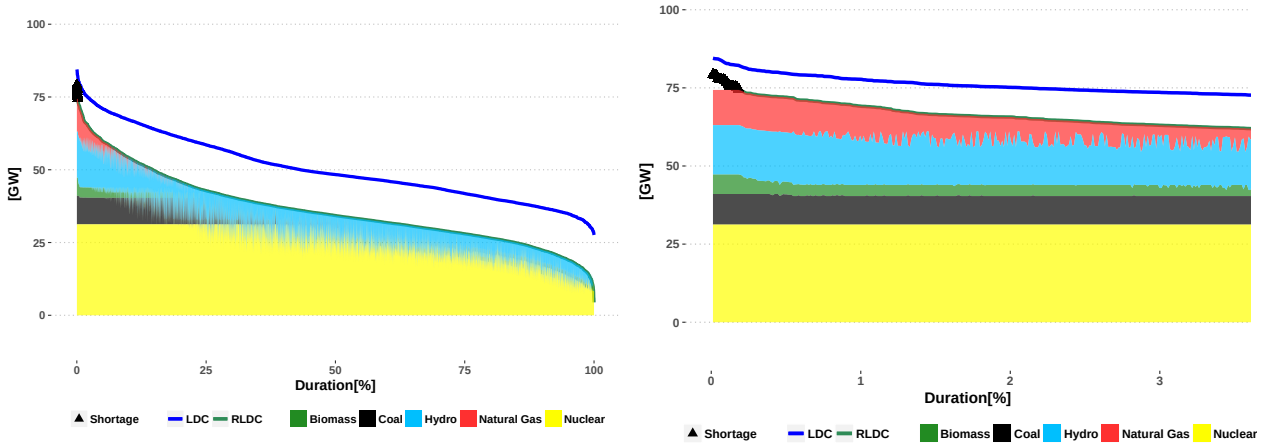


(a) (b)

Figure 4.10: The shortage hours of the ANTARES median scenario. (a) shows the position of shortage hours at the entire RLDC (16 hours), and (b) represents a zoom on the RLDC peak

hours, which exceeds the stipulated three-hour limit. A statistical examination of the loss of load duration reveals that nearly 10% (equivalent to 1 in 10) of the 200 climatic scenarios extend beyond 100 hours, with a maximum duration of 395 hours.

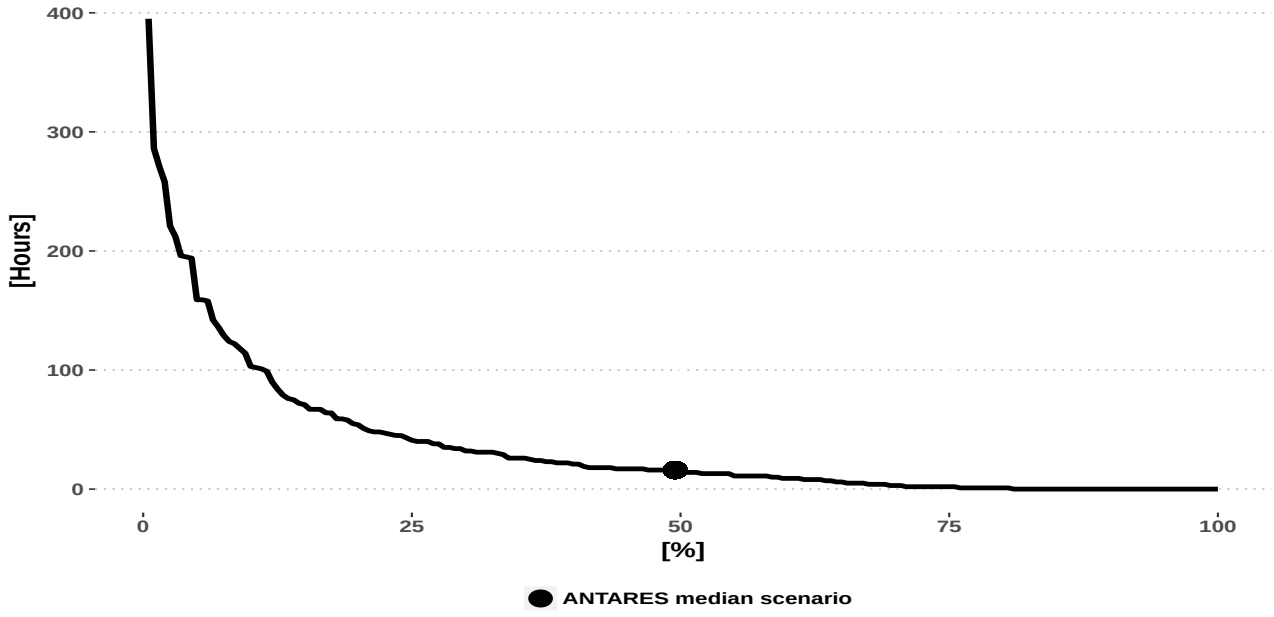


Figure 4.11: Loss of Load duration curve for the first simulation variant (200 scenarios simulated in ANTARES)

In summary, the adequacy assessment conducted above underscores that the 2030 capacity mix formulated by TIMES falls short of meeting adequacy requirements. Firstly, when subjected to evaluation under various climatic conditions, representing 200 scenarios encompassing load and renewable power output variations, the loss of load expectation criterion is not satisfied, with a value of 36 hours per year. Secondly, the results for the second set of scenarios (presented below in 4.1.7) indicate a LOLE level of 79 hours per year. These findings emphasize both the substantial impact of incorporating technical details in adequacy assessments and the absolute necessity of assessing the power generation approach of the power generation mix determined by TIMES to verify its compliance.

### 4.1.7 Results: Feedback loop impact on adequacy and cost evaluation

The feedback loop between ANTARES and TIMES is predicated on the concept of a power plant's capacity credit, which serves as a metric for gauging its contribution to peak demand. To illustrate this method, we conducted an analysis on the second set of simulations involving 1,000 Monte Carlo years. In this section, we scrutinize the adjustments in solutions (output models) that occur during the iterative feedback loop between both models. We evaluate these adjustments in terms of the resulting power generation mix, adequacy, and a qualitative assessment of costs.

The first iteration (Iteration.1) primarily focuses on renewables capacity credit, while the second iteration (Iteration.2) primarily addresses hydro capacity credit, and the final iteration (Iteration.3) for the thermal power fleet. It's important to note that the sequence order of these iterations holds significance, as the power generation mix undergoes changes from one iteration to the next, thereby altering the capacity credit of all technologies involved. The challenge with thermal capacity credit lies in the potential for unplanned outages and ramping constraints to impact their ability to meet peak demand. Additionally, the variability in available hydro energy (ranging from wet to dry conditions) could reduce the fraction of its rated capacity.

Consequently, using the outcomes generated by ANTARES, capacity values are computed for each simulated scenario, and the median value across all scenarios is selected. Table 4.4 provides an overview of the evolution of the median capacity credit values across the activated iterations. Solar technologies are assigned a capacity credit of zero since, in the considered scenario in France, peak demand occurs during winter evenings. In the case of wind, the TIMES initialization step (Iteration 0) assumes a capacity credit of 22% for wind, a value provided by the TIMES-FR modeler. However, based on the load and renewables capacity factor conditions for 2030, the median value is adjusted to 15% (Iteration.1). In the second iteration, the capacity credit for hydro is estimated using a methodology akin to that of renewables. The results reveal that run-of-river hydro contributes 50% of its installed capacity, while reservoirs achieve a 75% level (Iteration.2). The final three iterations pertain to estimating the capacity credit for thermal clusters as represented in ANTARES. With the introduction of technical constraints and the possibility of unplanned outages, the

capacity credit for the thermal power fleet demonstrates a reduction from 100% to 60%. The same capacity credit value was assigned to all thermal technologies since ANTARES results indicate that all clusters have a relatively similar value.

Table 4.4: Capacity credit values estimation over the iterative feedback loop (the red color indicates the main value change in each iteration).

| Steps | Iteration.0 | Iteration.1 | Iteration.2 | Iteration.3 | Iteration.3.1 | Iteration.3.2 | Iteration.3.3 |
|---|---|---|---|---|---|---|---|
| Solar | 0 | 0 | 0 | 0 | 0 | 0 | 0 |
| Wind | 22%% | 15% | 15% | 15% | 15% | 15% | 15% |
| Run of River | 100% | 100% | 50% | 50% | 50% | 50% | 50% |
| Hydro | 100% | 100% | 75% | 75% | 75% | 75% | 75% |
| Thermal | 100% | 100% | 100% | 92% | 85% | 75% | 60% |

Once the capacity credit values have been determined, the next step involves running the TIMES model again, incorporating the updated values. Figure 4.12 illustrates the impact of iteratively updating the capacity credit values on the loss-of-load distribution calculated by ANTARES (Figure 4.12a) and the least-cost power generation mix determined by TIMES (Figure 4.12b). Following the described procedure, only seven iterations (or three iterations for the first simulation variant) were necessary to establish a power generation mix with sufficient capacity to meet the adequacy criterion. Two important observations emerge: the first iteration significantly reduces the $LOLE$ indicator, while the final iterations, which affect the thermal power fleet, has a more limited impact, resulting in a reduction of 1-4 hours in $LOLE$. Additionally, the feedback loops primarily impact the peaking-reserve constraint, which predominantly governs behavior during peak time-slice. Conversely, mid-merit power plants (such as biomass) increase their share over iterations. This shift occurs because the peaking reserve constraint functions as an investment constraint rather than an operational one; it ensures excess capacity but does not restrict the contribution of each technology to meeting power demand in any time period. As a result, feedback loops don't merely add peak generation to the existing mix; instead, they substantially alter the mix structure by adjusting the capacities of all power plants.

From an economic perspective, any enhancements in system adequacy entail additional costs. To illustrate this effect, two costs are analyzed here:

1. **Discounted Total Cost by TIMES:** This cost includes investment costs, variable costs, and fixed costs spanning the period from 2013 to 2050. Figure 4.13a displays the evolution of this cost over the different iterations.

2. **Overall Cost in ANTARES:** This cost includes operating costs and fictional costs related to unsupplied energy and spilled energy for the year 2030 only, and it is presented in Figure 4.13b.

Figure 4.13 reveals that the total cost calculated by TIMES increases over iterations, while the overall cost shown by ANTARES decreases. This pattern arises due to the correlation between a power system's investment cost and its adequacy: with each iteration,

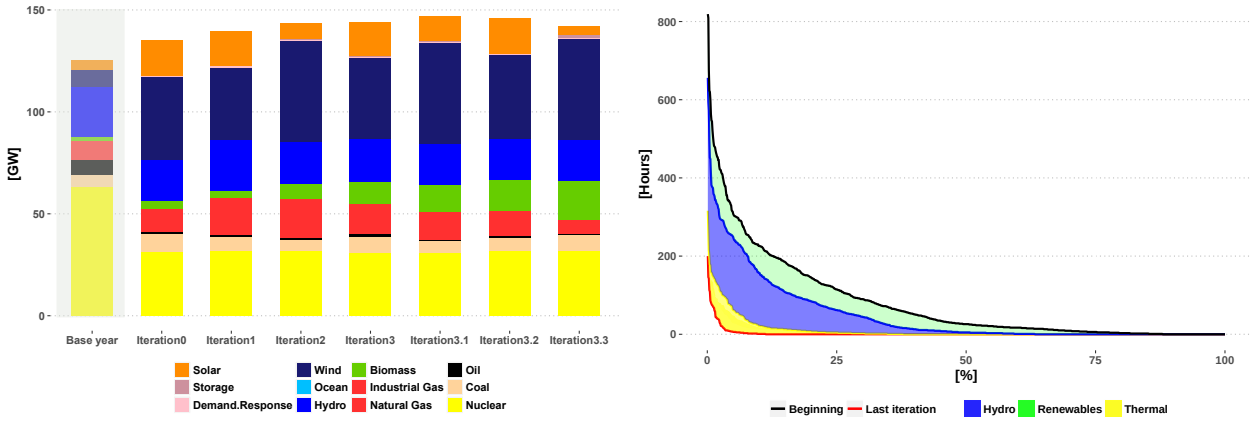


(a) (b)

Figure 4.12: The impact of the feedback loop on the power generation mix and adequacy. (a) represents the power generation mix evolution over iterations and (b) the loss of load duration curve over iterations.

TIMES invests more to reduce the amount of unsupplied energy perceived by ANTARES, subsequently lowering the overall cost of the system in the next iteration of ANTARES. Upon completing the loop, the overall cost calculated by ANTARES has been reduced by 55%, transitioning from an average of 79 hours of LOLE to less than 3 hours per year. Finally, Figure 4.13 illustrates that the costs of the French energy system increase by 28% over iterations compared to the initial decision to meet the 2030 adequacy criterion, primarily driven by increased investments. The initial iterations, which reduce the LOLE from over 75 hours to around 10 hours, have a very limited impact on the increase in investment costs. Conversely, the later iterations indicate that eliminating the last few hours (3-4 hours) of inadequacy requires approximately half of the total increase in investments. In this case study, improving adequacy to meet official criteria incurs additional costs that are not insignificant in relation to the total investment, warranting careful consideration.

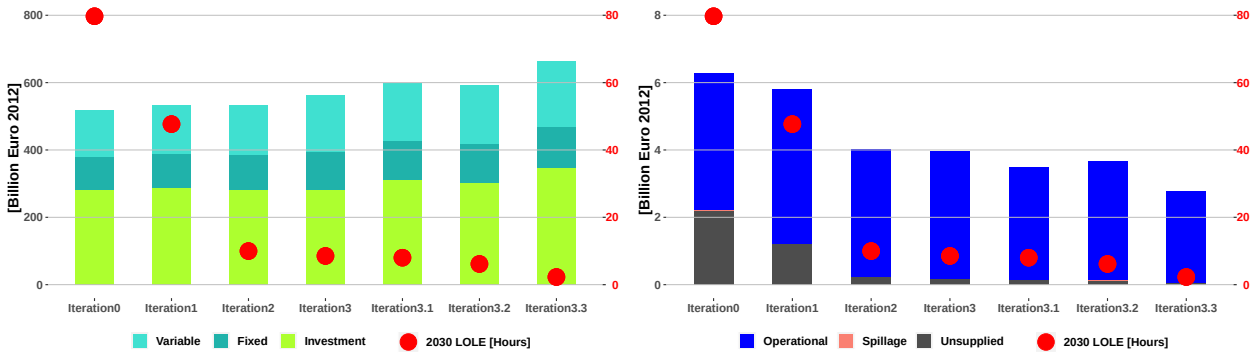


(a) (b)

Figure 4.13: The impact of the feedback loop on the power system costs (derived from TIMES). (a) is the total discounted cost (using a discount rate of 8%) over the planning period over iterations and (b) is the overall operational costs for 2030 over iterations (derived from ANTARES as the sum of operating costs and fictional costs (for unsupplied energy and spilled energy)).

## 4.2 Ensuring the adequacy of the overall trajectory

### 4.2.1 Short Introduction

Two primary categories emerge in planning problems: static and dynamic. Static planning is geared toward identifying an optimal system state for a single forthcoming time period. This category aims to determine the necessary investments to construct an optimal system within the specified future time frame, without considering the timing of these investments. On the other hand, dynamic planning addresses situations where multiple time periods are considered, requiring the identification of an optimal dependent-sequence of investments spanning the entire planning horizon.

While investment planning in the power system can assume either a static or dynamic form, the escalating intricacies of transitioning to a low-carbon power system have propelled dynamic planning to the forefront, offering enhanced adaptability, flexibility, and foresight into the investment strategy. The ever-evolving landscape of power systems transformation introduces a host of complexities demanding meticulous investigation during the planning phase. The concept of "transition" within this context inherently pertains to dynamic changes from one state to another, necessitating the consideration of temporal evolution to effectively monitor progress while attaining the desired objectives.

However, a notable challenge in the recent developed model-coupling framework lies in the concept of trajectory. The crux of this difficulty emerges from the fact that long-term power system planning models entail multi-period optimization issues, whereas operational power systems are rooted in single-period optimization problems. This section introduces a methodology aimed at bridging the multi-period TIMES power system planning model with the probabilistic single-period operational problem ANTARES. The overarching objective

centers around finding a cost-effective investment trajectory that adheres to the 3-hour Loss of Load Expectation limit for each period. To achieve this goal, we implement a bidirectional linking approach combined with a rolling horizon algorithm.

The subsequent sections of this research axis are structured as follows: Section 2 provides an in-depth exploration of the developed framework. Section 3 offers insights into the French case study, encompassing outcomes for a scenario featuring a 60% VRE share by 2050. Furthermore, we present an analysis of the methodology's robustness concerning the optimization parameters of the rolling horizon algorithm. Section 4 provides a synthesis of findings.

### 4.2.2 Main features of a Rolling horizon approach: a utility power generation planner example

#### Key concepts

In the subsequent paragraph, we draw upon the instance of a utility power generation planner to expound upon the rolling horizon approach. This illustration is based on the study by [204]. Our choice of this work as an illustrative example stems from its relative simplicity.

Generation planners undertake the task of formulating optimal power generation mix expansion strategies that minimize the aggregate system cost while satisfying technical, economic, and environmental constraints. The decisions involved in expansion planning inherently involve complex trade-offs. When determining the technology to invest in - be it peaking, intermediate, base load, or renewable - planners are tasked with striking a balance between technical viability, economic expenses, and environmental constraints. The application of optimization techniques facilitates the automated assessment of these trade-offs, resulting in a solution that effectively harmonizes distinct competing constraints. Temporal considerations also assume a pivotal role in these trade-off evaluations, in the sense that the complexity arises from the fact that the optimal solution is contingent upon the time horizon linked to financial objectives. The decision-maker must decide whether the objective is to minimize costs in the upcoming year, a decade, or even three decades ahead.

Examining the various available strategies to tackle a dynamic problem proves insightful. In the following discourse, we adopt the term "policy" as used in dynamic programming, referring to any approach employed to determine an action based on a state. This concept encompasses different algorithmic strategies, each suited to different problems with distinct computational requirements. In his book on Approximate Dynamic Programming, Warren B. Powell classified the array of policies into four categories [205]. For our study, two categories hold particular significance:

- Myopic Policies: These represent the most straightforward policies. They optimize the objective function in the present, without explicitly considering forecasted data or accounting for future decisions.

- Lookahead Policies: These policies make decisions in the present by explicitly optimizing over a defined horizon while taking into account data from the future.

Among these, myopic policies constitute the simplest class as they do not utilize any forecasted future information or endeavor to model forthcoming decisions. In fact, myopic policies find widespread application in expansion planning problems. Approaches that optimize the system on a year-by-year basis, considering each year in isolation, fall under myopic policies. During the optimization year, no insight into future data is available. Such year-by-year optimizations often tend to favor the deployment of peaking units — units characterized by low capital costs but high fuel expenses.

Lookahead policies make a decision now by solving the problem over some horizon. The information about the future can be revealed partially or completely. In power system planning, K. D. Le describes two kind of optimization that could be classified as lookahead policies [204].

- **Year-by-Year Optimization with Static Look-Ahead:** This approach entails optimizing the system on a year-by-year basis while employing a static estimation of the future. A common assumption for this static projection is that power generation plants maintain a constant capacity factor throughout the look-ahead period. This technique can capture some vital information for making generation planning decisions, such as cost escalation rates. However, it still fails to incorporate dynamic system characteristics, such as load growth or changes in the generation mix, into the decision-making process.

- **Global or Perfect-Foresight Optimization:** Here, the system undergoes optimization over the entire planning period, which typically spans 20 to 30 years. The expansion plan is selected to minimize the present value of total system costs over this planning duration. Global optimization programs typically favor the selection of large base load units, characterized by high capital costs but low operating expenses. This approach may impose short-term costs on the system to achieve long-term benefits.

Solving the optimization problem over an extensive time horizon can be computationally demanding. To mitigate the rapid growth in problem complexity, a natural approach involves approximating the problem through decomposition into multiple sub-problems with shorter horizons. Imagine being at a time period $t$ and having the capability to optimally solve the problem over the interval $[t, t + H]$ with a given small horizon $H$. Let's denote $x_t$ as the optimal decision executed during period $t$. The process is then repeated for optimization within the time-frame $[t + 1, t + 1 + H]$. In this context, the optimization logic essentially "rolls" the horizon one time period ahead. This technique is also recognized as the "receding horizon procedure" in operations research and "model predictive control" in the field of control theory. For our generation planner, this approach provides several advantages:

1. The method offers flexibility: the rolling-horizon technique can implement any of the three optimization approaches described earlier [3], simply by appropriately defining two crucial parameters: the length of the dynamic look-ahead period and the length of the static look-ahead period .

[3] Assuming that we do not encounter a numerical limit.

2. The method can achieve dynamic optimization using intermediate look-ahead periods. By employing intermediate look-ahead periods, such as five or ten years into the future, the planner can devise expansion strategies that:

    - Achieve reasonably favorable long-term benefits without incurring significant short-term penalties.
    - Are less susceptible to inaccuracies in long-range data forecasts.

3. The method enables planners to conduct sensitivity and robustness analyses concerning the proposed expansion plans for different horizons. This analysis empowers planners to recommend financial objectives that effectively balance short-term and long-term benefits.

**Problem statement**

Consider the dynamic expansion problem for a hypothetical power system represented by the capacity and load characteristics illustrated in Figure 4.14. Assume that the planning time-frame begins in year 1 and extends twenty years into the future. Three curves can be distinguished:

- Curve A: Projects the peak power load for the planning time-frame.
- Curve B: Depicts the additional capacity needed to meet reliability requirements.
- Curve C: Illustrates the evolution of actual installed capacity, accounting for the retirement of old power plants and the implementation of decisions made before the planning time-frame.

It can be observed from Figure 4.14 that the studied system possesses ample installed capacity (existing + committed generation) until year 10. Commencing from year 11, the system requires new additional capacity to meet the rising demand. Importantly, this required additional capacity must be implemented prior to year 11 due to the lead-time needed for the construction of power plants.

**Algorithm**

The steps needed to implement a Rolling Horizon Method is shown in the following flowchart.

1. The initial step involves the selection of the two key parameters:

    - $H_D$: This denotes the length of the dynamic look-ahead period. During this period, the optimization problem include all temporal changes in the system's characteristics, including load growth, capacity retirement and installation, shifts in unit dispatch, and the maturation of new units.

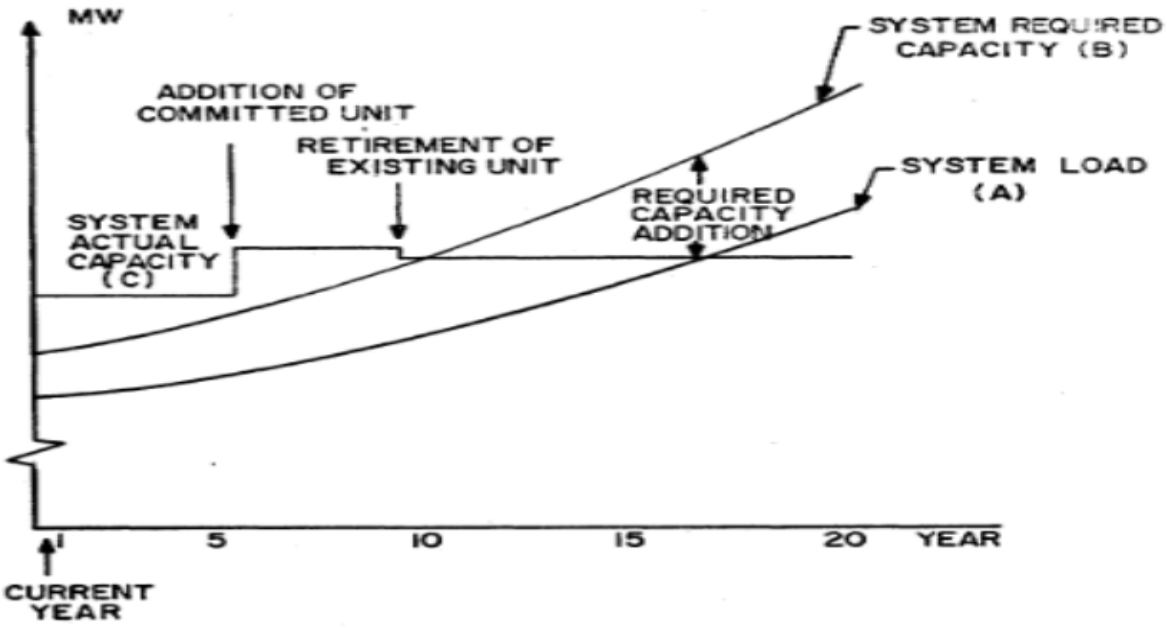


Figure 4.14: Load and Capacity requirements for the next 20 years (from [204])

- $H_S$: This signifies the length of the static look-ahead period. In the first year of the static look-ahead period, a snapshot of the system is taken. The operational attributes of the system are assumed to remain constant throughout this static look-ahead period, although costs are permitted to escalate.

Figure 4.15 illustrates the dynamic and static look-ahead periods for the initial planning horizon. The dynamic look-ahead period spans from year 1 to year 6, encompassing the explicit consideration of changes in system characteristics within the optimization problem. Subsequently, from year 7 to year 14, the static look-ahead period ensues, during which the system's attributes are assumed to remain unchanged ("frozen").

2. Once these two parameters are defined, the Rolling Horizon method solves $P$ N-year optimization subproblems, where $P$ represents the number of years in the planning time-frame.

$$N = \begin{cases} L_d \text{ if } L_s = 0 \\ L_D + 1 \text{ if } L_s \geq 1 \end{cases}$$

3. Begin the first rolling horizon sequence: $I = 1$

4. Solve an $N$-year optimization problem that minimizes the total system cost over the time-frame period $[I, I + N - 1]$

5. Save the investment decisions for installed capacities for the year $I$

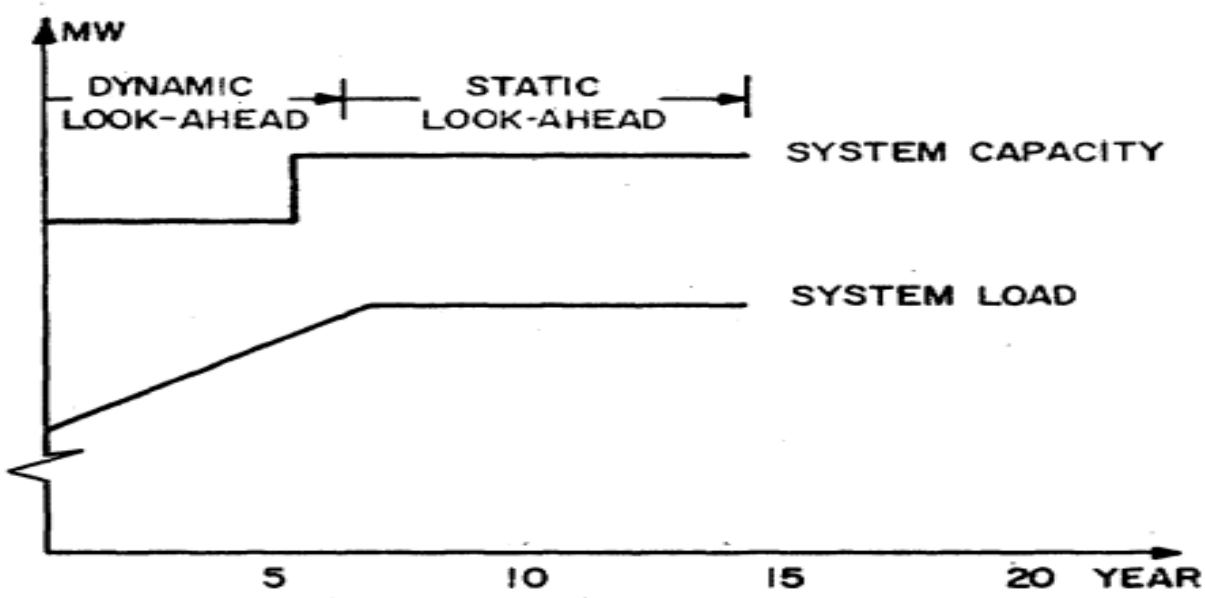


Figure 4.15: Look-ahead Periods (dynamic and static) for the first planning sequence period (source: [204])

6. If the end of the horizon is reached, exit. Otherwise, continue to the next rolling horizon sequence by setting $I = I + 1$.

**Results of a numerical example**

They investigate a test system designed to resemble a typical power company in the Texas-Oklahoma Region in 1980, referred to as Utility E. This utility begins with an initial total system capacity of 8500 MW, distributed among 33 dispatchable units, and a peak load of 7,000 MW. The peak load is projected to increase by 3% annually. To meet required reliability standards, the power company must maintain a 15% reserve margin. According to Table 4.5, Utility E has a significant portion of its capacity derived from natural gas power plants (53%), followed by coal (19%), nuclear (19%), and oil (9%). Utility E exhibits an over-reliance on peak load technologies and a shortage of base load technologies. The case of Utility E is compelling from a power generation planning standpoint, as it illustrates a sub-optimal power generation mix.

In this exemplary study, the potential new investments encompass four potential options: 50 MW combustion turbines, 200 MW, 400 MW, and 600 MW coal units. Employing the Rolling Horizon optimization technique, the authors try to answer this questions:

- Optimal Generation Expansion Plan: What constitutes the most effective strategy for expanding generation capacity to rectify the prevailing suboptimal power generation mix?

Table 4.5: Characteristics of the power company in 1980

| Quantity | Unit Size [MW] | Technology | Forced Outage [%] | Scheduled Outage [%] |
|---|---|---|---|---|
| 2 | 800 | Nuclear,Steam | 15 | 9.6 |
| 3 | 600 | Gas,Fossil | 7 | 5.8 |
| 11 | 200 | Gas,Fossil | 7 | 5.8 |
| 2 | 600 | Coal,Fossil | 21 | 7.7 |
| 1 | 400 | Coal,Fossil | 13 | 7.7 |
| 10 | 50 | Gas,Turbines | 24 | 3.8 |
| 2 | 400 | Oil,Fossil | 13 | 7.7 |

- Deployment Dynamics of Baseload Capacity: If it is advised to introduce additional baseload capacity, how does its implementation evolve over the course of the planning time-frame?

- Optimal Unit Size for Future Additions: What size of units should be optimally selected for future additions to the power generation mix?

To address these questions, the authors employed five distinct expansion plans, aligned with varying dynamic look-ahead lengths of one, three, four, and 20 years, along with a zero static look-ahead length. The outcomes of their investigation are as follows:

- The authors emphasize the significance of utility financial objectives, whether short-term or long-term, in determining an optimal expansion strategy. Under a short-term horizon, the economics lean towards integrating smaller peaking power plants, whereas a longer look-ahead planning horizon favors larger baseload power plant additions. For Utility E, the optimization yields the following solutions:
  - Short-term (1-year look-ahead): 17 units of 50 MW combustion turbines, 6 units of 200 MW coal plants, and 6 units of 600 MW coal plants.
  - Long-term (20-year look-ahead): 1 unit of 50 MW combustion turbine, 1 unit of 200 MW coal plant, and 9 units of 600 MW coal plants.

- An observed 3.9% reduction in total system revenue requirements, corresponding to 711 million dollars, is achieved when extending the look-ahead period from 1 year to 20 years.

- The increase in the look-ahead period results in higher margins for baseload power plants. A longer look-ahead is more responsive to potential future reliability changes, prompting the construction of new capacity before operational necessity arises.

- The utilization of a long look-ahead period incurs a short-term cost penalty for the system. For instance, between 1986 and 1993, the 10-year look-ahead plan costs more than the 1-year look-ahead plan.

- The previously mentioned 3.9% savings can be attributed as follows:
  - 48% from transitioning from a 1-year to a 2-year look-ahead period.
  - 25% from moving between 2-year and 3-year look-ahead periods.
  - 5% from shifting between 3-year and 4-year look-ahead periods.
  - 22% from extending the look-ahead from 4 years to 20 years.
- The authors suggest utilizing intermediate look-ahead periods to mitigate the impact of unstable economic conditions when critical input data, such as demand growth and cost escalation, are challenging to forecast. This approach, they argue, makes the optimal plan less vulnerable to errors in forecast data.

### 4.2.3 Methodology: Combining the bi-directional linking and Rolling horizon technique to assess the trajectory adequacy

It is clear that the methodology developed in the first section assess only the power generation adequacy of a predetermined target year. The aim of this section is to explain the methodology that we have developed in order to assess the whole trajectory using both decomposition techniques:

- The bidirectional linking methodology: to asses power generation adequacy of future power generation mix. In fact a reliability-constrained planning problem is a large-scale, mixed-integer optimization problem. The incorporation of reliability constraints into long-term energy planning models requires an additional variables decision for a large number of realizations (this decisions grows combinatorially with the number of generating units in the system) [8]. A decomposition technique is then needed to split the large problem into a series of sub-models.
- Rolling horizon methodology: This technique involves constructing an appropriate trajectory by breaking it down into different sequences. The same methodology applied in the previous example is followed here, assuming varying look-ahead periods and a static period of zero years.

#### The feed-back loop algorithm

To present the methodology in a synthetic manner and to facilitate the description of the algorithms we rephrase the feedback loop introduced in the first section using the language of optimization problems. Similar to our previous approach, we utilize the TIMES framework for investment planning. Our objective is to identify optimal expansion strategies that minimize the overall discounted system cost while satisfying political, economic, and environmental constraints. The optimization problem within the $[TIMES]$ context, focusing on a single region, can be represented by the following simplified model:

$$\begin{aligned} \underset{X,Y}{\text{minimize}} \quad & \sum_{t\in T, ts\in TS} (1+\alpha)^{y_{ref}-t}(I(X_t)+O(Y_{t,ts})) \\ \text{subject to} \quad & AX_t > a, \forall t \in T, \\ & BY_{t,ts} > b, \forall (t,ts) \in T * S \end{aligned} \tag{4.3}$$

The variables and parameters are as follows: $\alpha$ represents the discount rate, $T$ denotes the set of periods within the planning time-frame, $TS$ stands for the set of inter-annual time slices that represent supply and demand variability, $X_t$ represents the vector of investment decision variables for each time period $t$, and $Y_{(t,ts)}$ symbolizes the vector of operational decision variables for time period $t$ and time slice $ts$. The term $I(X_t)$ corresponds to the investment cost, while $O(Y_{(t,ts)})$ pertains to the operational cost. The constraints $AX_t \geq a$ (investment), $BY_{(t,ts)} \geq b$ (operation) encompasses all the investments and operational constraints inherent to the TIMES framework. Such constraints could include limitations on the deployment rate

of installed capacity for a particular technology, emission restrictions, minimum renewable energy share in the mix, and more.

An investment path, denoted as $\Pi = \{X_t\}_{t \in T}$, is essentially a sequence of investment decision vectors for each period within the planning horizon. However, using only time slices to account for supply and demand variation might not be accurately enough to truly capture real-world operations. The operational aspects of the problem are often much more intricate than what the $[TIMES]$ model assumes. Many essential details are often omitted, such as hourly resolution, uncertainty, unit commitment considerations, thermal and hydro operational constraints, and more. Consequently, there might be a need to employ a probabilistic unit commitment optimization model to better simulate the operational dynamics of the power system.

Furthermore, after obtaining an investment decision solution $\underline{X_t}$ for a particular year $t$, the $[ANTARES]$ problem, developed by RTE, comes into play. This problem aims to determine the optimal hydro-thermal power dispatch for each hour of the year in order to meet customer demand while minimizing the overall cost. The principal cost factors include transmission expenses, hydro and thermal operational costs, costs associated with unsupplied energy, and spillage energy costs. The formulation of $[ANTARES][\underline{X_t}]$ can be expressed as follows:

$$\begin{array}{ll} \underset{y|mc}{\text{minimize}} & \sum_{h \in H} O'(y^{mc}_{t,h}) \\ \text{subject to} & Cy^{mc}_{t,h} > c, \forall h \in H \end{array} \tag{4.4}$$

In the provided equation, $y_{t,h}$ represents the decision variables for hourly operational unit commitment. The constraint $Cy_{t,h} \geq c$ encompasses all the operational constraints of $[ANTARES]$. Conducting studies related to generation adequacy or transmission projects involves formulating and solving a series of weekly operation problems, each spanning a week for each Monte Carlo year. This general optimization problem is denoted as $[ANTARES]^m_t c$ (hereafter simply $[ANTARES]_t$ ), where $t$ signifies the period of interest, and $mc$ represents an index covering all Monte Carlo years.

Following the methodology developed earlier, Algorithm 1 elucidates the detailed steps necessary for constructing a reliable power system for a given period $t$. Initially, the $[TIMES]$ (master) problem is solved, yielding the vector of installed capacities for the period $t$, denoted as $\underline{X_t}$. With the obtained solution $\underline{X_t}$, the operation sub-problem $[ANTARES][\underline{X_t}]$ is executed for 1,000 possible Monte Carlo realizations of the period $t$. Subsequently, an assessment is conducted to ascertain if the 3-hour $LOLE$ limit has been exceeded. If the solution is infeasible, a new sizing constraint is generated within the $[TIMES]$ framework:

$$\sum_{i \in Technology} cc_{i,t} * X_{i,t} \geq (1 + r) * D^{peak}_t \tag{4.5}$$

The capacity credit of each technology, denoted as $cc_{i,t}$, is estimated based on the hourly dispatch determined by the $[ANTARES][\underline{X_t}]$ operation. Here, $X_{i,t}$ signifies the installed

capacity of technology $i$ at period $t$, and $D_t^{peak}$ represents the demand during the peak time-slice of period $t$. The equation explicitly embodies the reliability constraint as it guarantees that the installed capacity is adequate to meet the demand during the peak time slice. This determination takes into account the capacity credit of each supply technology and a peak reserve factor, denoted as $r$ (set at 28% in our study), which necessitates the installation of excess capacity. This iterative procedure is applied to all technologies until the condition $LOLE \leq 3h/year$ is met.

**Algorithm 1:** TIMES-ANTARES feed-back loop algorithm to ensure the power generation adequacy of the year $t$

**Input:** The power generation mix $\underline{X_t}$ decided by [**TIMES**] for a specific target year $t$

**Output:** The power generation mix $\underline{X_t}$ decided by [**TIMES**] for a specific target year $t$ respecting the LOLE criterion : $LOLE \leq 3hours/year$

**Data:** The ANTARES Monte Carlo operational scenarios

Solve $[ANTARES][\underline{X_t}]$ /* Solve the ANTARES problem corresponding to the $\underline{X_t}$ power generation mix for 1000 Monte Carlo year representing the target year $t$ */

$LOLE \leftarrow \sum_{mc \in MC} \frac{LOLD_{mc}}{|MC|}$

**if** $LOLE \geq 3hours$ **then**

  **for** $i \in Technologies$ **do**

    $cc_{i,t}^{ANTARES} = \underset{mc \in MC}{\text{median}}\{\frac{LDC_t^{mc}(h^{'}=1) - RLDC_{i,t}^{mc}(h^{'}=1)}{\underline{\mathbf{X_{i,t}}}}\}$

    **if** $cc_{i,y}^{TIMES} \geq cc_{i,y}^{ANTARES}$ **then**

      $cc_{i,y}^{TIMES} \leftarrow cc_{i,y}^{ANTARES}$ update the capacity credit of technology $i$ within [**TIMES**]

      Solve the updated [**TIMES**] using CPLEX

    **else**

      Change the median value to a lower percentile /* This decreasing change in the estimator of $cc_i$ allows to install more capacities */

Algorithm 1 outlines the iterative steps necessary to formulate a power generation mix for a specific period $t$ that adheres to power generation adequacy requirements. In essence, for each iteration, a tentative solution is derived from the TIMES master problem and forwarded to the slave problem. The ANTARES sub-problem operates the hourly dispatch of the power generation mix $\underline{X_t}$ and assesses its conformity with the $LOLE$ criterion. If necessary, it furnishes a new constraint to enhance the representation of reliability in the master problem. This procedure is reiterated sequentially for all technologies until an appropriate solution that offers minimal total cost is achieved.

**Rolling Horizon algorithms**

As elucidated in the preceding section, the objective of the rolling horizon method is to iteratively solve the problem at regular intervals, incorporating additional insights from proximate subsequent periods. Initially, we present the algorithm that implements the Rolling Horizon method to solve a multi-period $[TIMES]$ optimization problem. Let $t_0^s$ signify the commencement time period of sub-problem $s$. Let $M^s$ represent the number of time periods encompassed within sub-problem $s$. Notably, $M^s$ corresponds to the look-ahead period mentioned earlier, where the static look-ahead period is conventionally considered to be zero. Each approximated sub-problem is denoted as **[TIMES(s)]**. In each approximated sub-problem, the investment decision variables $X_t$ and operational decision variables $Y_{t,ts}$ are activated for $t_0^s \leq t \leq t_0^s + M^s$ and "frozen" for $t \geq t_0^s + M^s$. Upon resolving a sub-problem, the values of decision variables for $t \leq t_0^s + M^s$ are set. This process continues until all sub-problems are solved, thereby concluding the procedure.

**Algorithm 2:** TIMES Rolling-horizon algorithm without overlap

**Input:** A sequence of minimization problems **[TIMES(s)]**
**Output:** An investment trajectory $\Pi = \{\underline{X_t}\}_{t \in T}$, solution of **[TIMES]** over the overall planning time-frame T
**Data:** TIMES parameters

```
t_0^s, s ← 1, M^s, terminate ← false
while terminate = false do
    Activate (X_t, Y_{t,ts}) t_0^s ≤ t ≤ t_0^s + M^s
    Solve the approximate sub-problem [TIMES(s)] using CPLEX
    t_0^s ← t_0^s + M^s
    s ← s + 1
    Set the values of decision variable (X_t, Y_{t,ts}) for t ≤ t_0^s
    if t_0 ≥ |T| then
        terminate ← true
```

In each iteration, Algorithm 2 implements the plan for the $M^s$ periods within the planning window $[t_0^s, t_0^s + M^s]$ and subsequently shifts by assigning the new starting period $t_0^s$ as the final period of the current planning window. Following this approach would essentially mean conducting a solution procedure every $M^s$ periods. Nonetheless, in real-world scenarios, this operational principle would be impractical for several reasons. First, several exogenous parameters crucial for optimization, like demand growth, capacity factor evolution, and costs, are inherently uncertain. The accuracy of estimating these uncertain parameters improves over time. Additionally, disruptive innovations such as the emergence of new technologies and unforeseen process advancements can render expansion plans obsolete. Consequently, real-world planning involves overlaps. This implies that after implementing a plan for periods $t_0^s, ..., t_0^s + M^s$ (spanning $\Delta T \geq 1$ periods), a new plan is formulated for the periods $t_0^s + \Delta T, ..., t_0^s + M^s + \Delta T$. In essence, the power generation mix for the periods $t_0^s + \Delta T, ..., t_0^s + M^s$

undergoes a re-planning process. Notably, if $\Delta T \leq \frac{M^s}{2}$, certain periods are revised more than once. The only adjustment in the algorithm without overlap is initializing $t_0^s$ as $t_0^s + \Delta T$.

**Trajectory adequacy: Combination of Rolling Horizon and Linking approaches**

To construct a reliable trajectory, we introduce a new optimization approach known as the Rolling Horizon Method. Our methodology combines the linking approach, which ensures the adequacy of a specific target year (as detailed in Algorithm 1), with the Rolling Horizon approach, which is used to build the trajectory.

This approach decompose the planning problem $[TIMES]$ into several sub-problems. Let $t_0^s$ denote the initial time period of sub-problem $s$, and $M^s$ represent the number of time periods encompassed by sub-problem $s$. Each approximated sub-problem is designated as $[TIMES(s)]$. The solution to each approximated sub-problem entails setting the decision variables that are active for $t_0^s \leq t \leq t_0^s + M^s$, and keeping those for $t \geq t_0^s + M^s$ frozen. Upon resolving a sub-problem, Algorithm 1 is applied to all milestone years falling within the active periods. Subsequently, this process is reiterated, moving to the next sequence of the rolling horizon by updating the initial time period as $t_0^s = t_0^s + M^s - \Delta T$. Through this iterative process, more future information becomes available. If the overlap years between both cycles prove to be adequate, the investments made by TIMES are then established at $t = t_{overlap}$. The procedure concludes once all sub-problems have been addressed. One might wonder why we assess adequacy in two consecutive sequences before finalizing the investment decisions. The reason lies in the inter-temporal interdependencies inherent in power generation adequacy. The adequacy of a given year $t$ is significantly influenced by the investments made in the preceding year $t-1$, which in turn will impact the adequacy of the subsequent years. This 2 sequence assessment approach recognizes that the decisions made in one period reverberate and have cascading effects on the power system's adequacy across multiple time periods. Results not presented here indicate that when no overlapping years are used, the algorithm may show trap period. A trap period, in this context, refers to a situation where the adequacy assessment of the trap year cannot be achieved through the feedback loop iterations because all the available potential has been utilized.

**Algorithm 3:** Trajectory Adequacy algorithm (with an overlap period)

**Input:** A sequence of minimization problems [**TIMES(s)**]
**Output:** A Π path solution of [**TIMES**] respecting Adequacy requirements
**Data:** TIMES data, ANTARES data

$t_0^s$, $s \leftarrow 1$, $M^s$, $\Delta T$,$Years \leftarrow \{\}$ ,$terminate \leftarrow$ **False**, $LOLE \leftarrow 0$
**while** $terminate = false$ **do**
  **Cycle1:** Activate ($X_t$,$Y_{t,ts}$) for $t_0^s \leq t \leq t_0^s + M^s$
  Froze ($X_t$,$Y_{t,ts}$) for $t \geq t_0^s + M^s$
  Solve the approximate sub-problem [**TIMES(s)**] using CPLEX
  $Years_1 \leftarrow$ Milestone($[t_0^s, t_0^s + M_s]$) /* Extract the Milestone years belonging to the RH-active period */
  **for** $t \in Years_1$ **do**
    **Call:** Algorithm 1 for period $t$/* Call the feed-back loop TIMES-ANTARES algorithm in order to ensure the adequacy of the year $t$ */
  $t_0^s \leftarrow t_0^s + M^s - \Delta T$
  **if** $t_0 \geq |T|$ **then**
    $terminate \leftarrow$ **true**
  $s \leftarrow s + 1$
  **Cycle2:** /* reveal more future data information */
  Activate ($X_t$,$Y_{t,ts}$) for $t_0^s \leq t \leq t_0^s + M^s$
  Froze ($X_t$,$Y_{t,ts}$) for $t \geq t_0^s + M^s$
  Solve the approximate sub-problem [**TIMES(s)**] using CPLEX
  $Years_2 \leftarrow$ Milestone($[t_0^s, t_0^s + M_s]$) /* Extract the Milestone years belonging to the RH-active period */
  **for** $t \in Years_2$ **do**
    **Call:** Algorithm 1 /* Call the feed-back loop TIMES-ANTARES algorithm in order to ensure the adequacy of the year $y$ */
  $t_{overlap} = Y_1 \cap Y_2$
  **if** *Adequacy of* $t_{overlap}$ *is ensured in Cycle1 & Cycle2* **then**
    Fixing the values of TIMES variable ($X_t$,$Y_{t,ts}$) for $t_{overlap}$
  **if** $t_0 \geq |T|$ **then**
    $terminate \leftarrow$ **true**
  $s \leftarrow s + 1$

### 4.2.4 A 60% Renewable uptake scenario: configuration with dynamic look-ahead of 15 years and an overlap of 5 years

The presented framework is applied to a case study focusing on the transition of the French power system. We select a scenario that embodies a constraint on nuclear power production, in line with the French Energy Transition Act's objective to decrease the nuclear power share from 75% to 50% by 2025. Additionally, we enforce limitations on the power system's CO2 emissions for each milestone year between 2013 and 2050, ensuring they remain below the 2012 levels (39 Mt). Lastly, we establish a trajectory that transitions the power system from a 40% variable renewable energy (VRE) share in 2040 to a 60% VRE share by 2050.

**Results of the feed-back loop applied to the 2013-2030 planning period:** In the first sequence of the Rolling Horizon algorithm, implemented with a 15-year look-ahead and a 5-year overlap, the active planning window covers the years 2013 to 2030. The assessment of power generation adequacy commences in the year 2030 (as depicted in Figure 4.16). The application of the automated soft-linking model, based on the feedback loop outlined in Algorithm 1, is directed towards the target year 2030. Notable differences from the previous section's exercise (when the model is run for the whole planning time-frame) are summarized below:

- In the earlier section, the TIMES model was solved for the entire trajectory spanning from 2013 to 2050, with the power generation mix for the year 2030 being derived. In this section, the TIMES optimization process is solely conducted within the active planning window (2013-2030).
- If necessary, the capacity credit values' updates during the iterative feedback process are only implemented within the active planning window. Conversely, in the previous section, the capacity credit acquired in 2030 was updated across all periods of the trajectory.

The findings reveal that initially, TIMES suggests a power generation mix with an associated $LOLE$ of 62 h/year (compared to a $LOLE$ of 73 h/year in the preceding section). Upon the application of Algorithm 1, three iterations were necessary to find an adequate power generation mix. The evolution of the power generation mix during the iterative process is illustrated in Figure 4.16b. By the third iteration, the power generation mix determined by TIMES have an acceptable $LOLE$. The updates affecting capacity credits are detailed in Table 4.6. Evidently, wind capacity credit remains constant. Nonetheless, a marked shift in the capacity credit values for hydro (both dam and run-of-river) is observable due to substantial change in the resulting power generation mix. Consequently, the capacity credit value for thermal power generation mix reaches 92%, given the substantial reduction in hydro's capacity credit values. By the end of the feedback loop process, the combination of capacity credit values (and consequently the number of iterations) required to achieve an adequate power generation mix for 2030 differs from the configuration in the previous section.

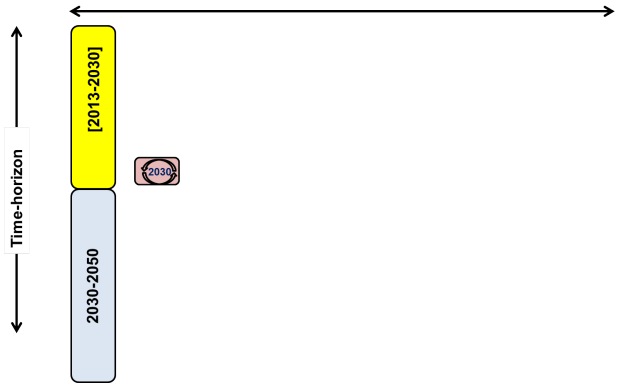


(a) The planning time-frame decomposed on a look-ahead period (in yellow) and a frozen period (in blue)

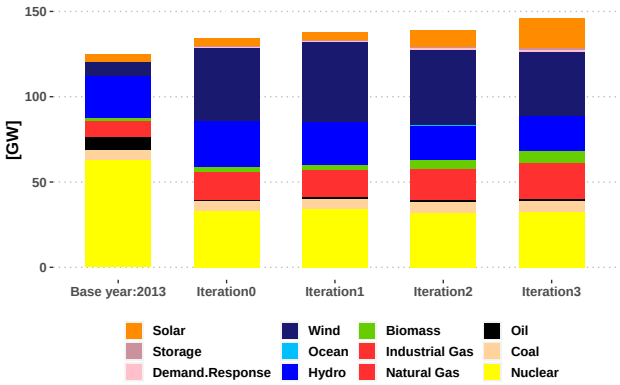


(b) The evolution of the 2030 power generation mix over the feed-back loop process

Figure 4.16: The first sequence of the Rolling Horizon algorithm with a look-ahead period of 15 years (left) and the feed-back impact on the power generation mix of 2030 (the first target year)

Table 4.6: Capacity credit values estimation over the iterative feedback loop (the red color indicates the main value change in each iteration).

| Steps | Iteration.0 | Iteration.1 | Iteration.2 | Iteration.3 |
|---|---|---|---|---|
| Solar | 0% | 0% | 0% | 0% |
| Wind | 40%-28% | 14% | 14% | 14% |
| Run of River | 100% | 100% | 50% | 50% |
| Hydro | 100% | 100% | 44% | 44% |
| Thermal | 100% | 100% | 100% | 92% |

Figure 4.17 depicts the impact of feed-back process on the total system cost derived from TIMES for the planning time-frame 2013-2030 and the overall operational cost derived from ANTARES for 2030. From an economic point of view the 28% increase in the actualized total system cost observed in the results of the section before are not yet valid. Only 3% of increase in the total system cost from the initial TIMES solution to the iteration 3 is reported. However, approximately the same decrease amount in the overall operational cost computed by ANTARES is observed, as the number of shortage hours in 2030 is roughly the same. This decrease in the number of iterations and also in the underestimation of the total actualized system cost comparing with the results obtained before can be explained as follows:

- The end of horizon bias: the combined capacity credit used to find an adequate power generation mix for the year 2030 was implemented throughout the entire trajectory in the exercise outlined in Section 2. Consequently, due to this capacity credit signal, the power generation mix of all periods after 2030 have increased their investments.

This increase in investment over the trajectory is included in the 28% increase of the actualized total cost. However, with an active planning window of only 2013-2030 the capacity credit update was only applied to the active period. The 3% additional investment, represent the net additional cost to ensure 2030 power generation adequacy. So the 28% reported before is a value impacted by the active planning time-frame and doesn't present the real additional investment to ensure only 2030 adequacy.

- The sensitivity of the technological capacity credit values to the overall power generation mix structure. It is obvious that the planning time-frame impacts the resulted power generation mix. This lead to different possible combination of capacity credit resulted from the application of the feed-back loop of Algorithm 1.

In summary, the interaction of these factors leads to the nuanced variations between the current and previous results, ultimately underscoring the sensitivity of the developed methodology to the planning horizon and how capacity credits are updated within the long-term energy planning model.

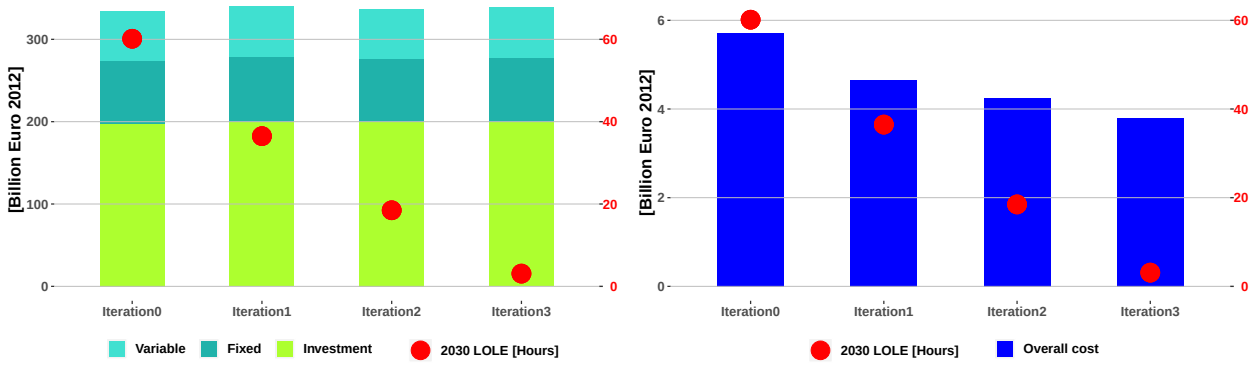


(a) The evolution over the feed-back iterations of the total system cost for the planning time-frame 2013-2030 derived from TIMES

(b) The evolution over the feed-back loop iteration of the overall operational cost derived from ANTARES

Figure 4.17: The impact of the feed-back loop process on the TIMES total system cost (left) and ANTARES overall operation cost (right) for 2030

**Results of the whole trajectory** For the sake of clarity, we provide the outcomes of Algorithm 3 applied to our specific case study in Figure 4.18. In this depiction, the active planning window spans 10 years with a 5-year overlap. Notably, the graph underscores that overlap years are exclusively set if their adequacy is successfully met in both cycles. The optimization problem sequences [TIMES(s)] ($s \in 1:4$) are depicted in yellow. In the instance of the initial overlap period in 2030, the initial trial solution yields an LOLE of $62h/year$. It takes three iterations to establish a power generation mix for the year 2030 that adheres to the adequacy requirements. In the next step, we freeze all investments preceding the overlap

year and reveal additional insights about the future interval [2025, 2040]. This enables the re-planning of the power generation mix for 2030. As this revised mix satisfies adequacy standards in both the first and second cycles, its power generation mix is established in the third cycle. The algorithms iterate through the entire trajectory until achieving a power generation mix that meets the adequacy requirements for each individual period. 2 iterations where needed in 2045 to achieve adequacy.

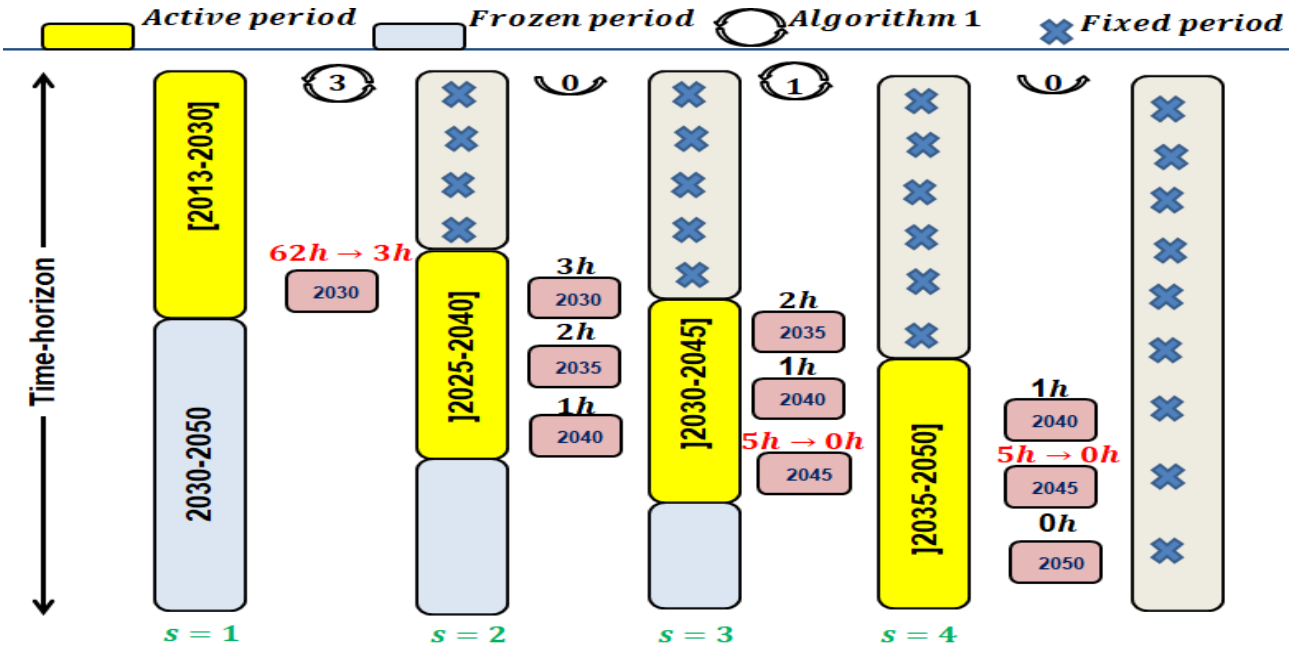


Figure 4.18: A graphical illustration of the application of Algorithm 3 with a 10 year look-ahead and 5 years overlap.

Figure 4.19 illustrates the total additional investments required to attain adequacy. Two specific periods, 2030 and 2045, reveal insufficient supply. In the case of 2030, Algorithm 1 introduces around 14 GW of investments, resulting in a decrease of LOLE from 63h/year to 3h/year. Conversely, for 2045, 2 GW is necessary to meet the targeted adequacy level. From an economic perspective, Figure 4.20 showcases the total system cost as computed from TIMES. Unlike the 28% supplementary cost needed solely to achieve the 2030 LOLE threshold (depicted by the red dots) as reported in the first section (see section 4.1), the Linking & Rolling Horizon approach appears to offer more cost-effective solutions. Nearly 4% additional investments are necessary to ensure adequacy in 2030, and 2% for 2045.

At the end of the rolling horizon algorithm coupled with the feed-back loop algorithm, TIMES decides a multi-period power generation mix that respect adequacy requirements over the entire horizon. Figure 4.21a depicts the total installed capacity of each period of the trajectory, while Figure 4.21b represents only the new investments decided by TIMES to satisfy both the 60% VRE uptake scenario and the power generation adequacy requirements.

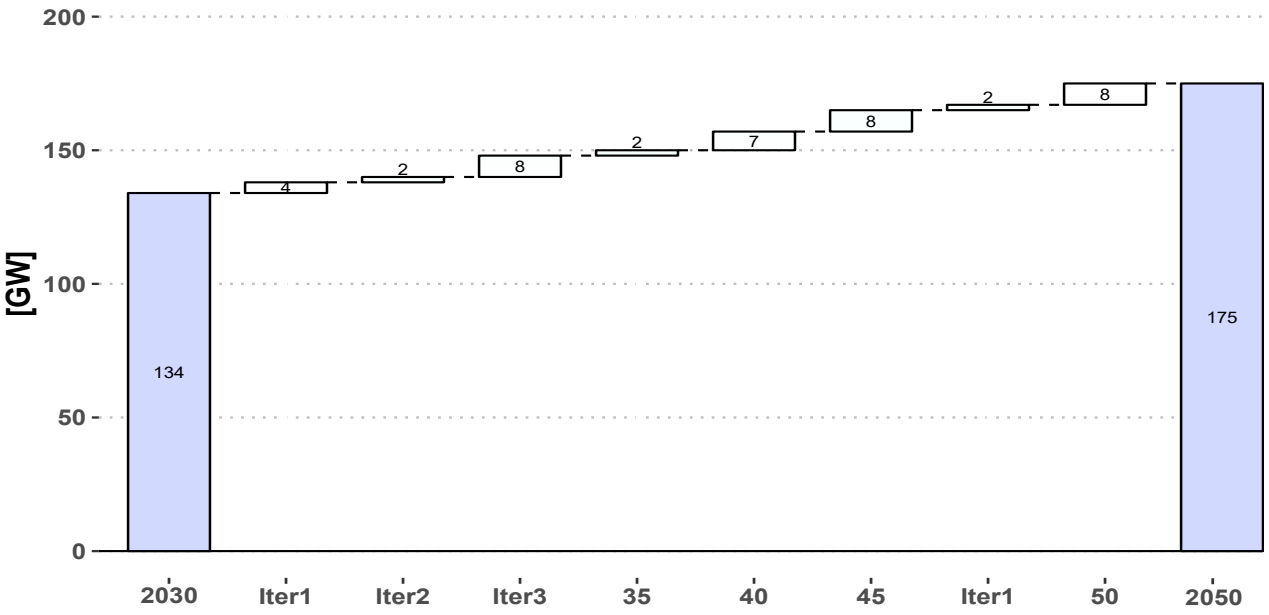


Figure 4.19: The breakdown of the total new installed capacities over the planning time-frame based on the rolling horizon sequences

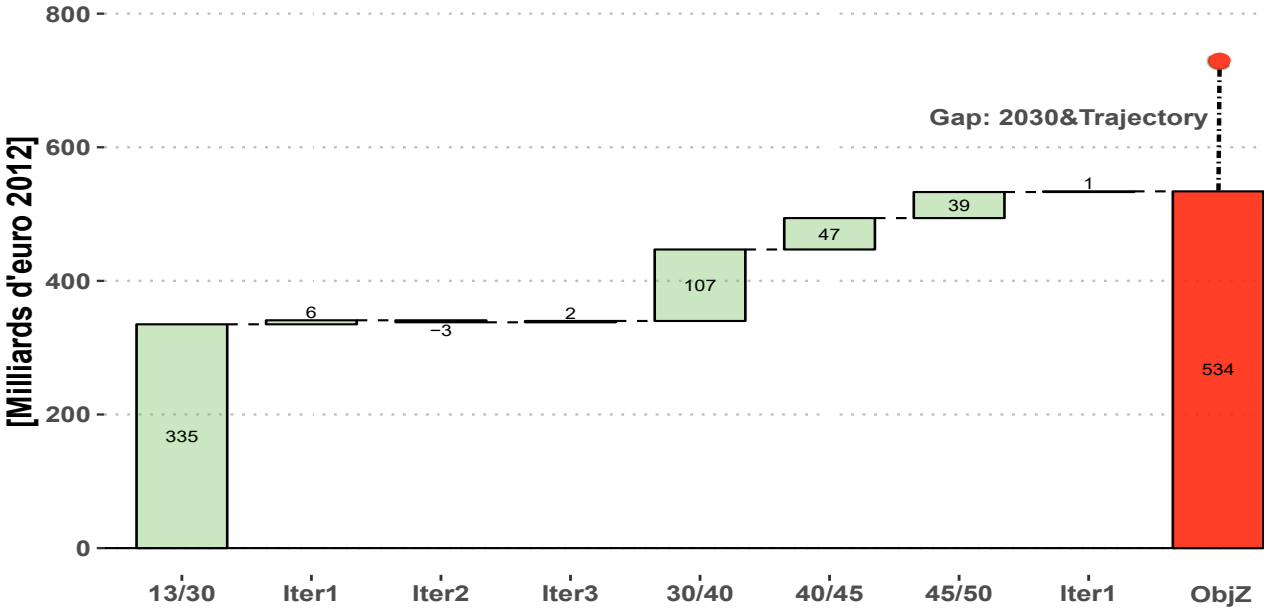


Figure 4.20: The total system cost breakdown over the planning-time frame based on the Rolling horizon sequences and a comparison with the total system cost when only 2030 was studied (see section 1)

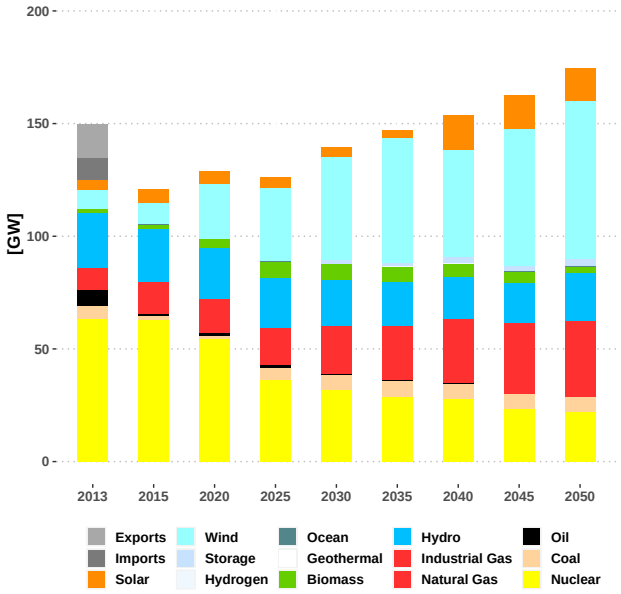


(a) Total installed capacities over the planning-time frame

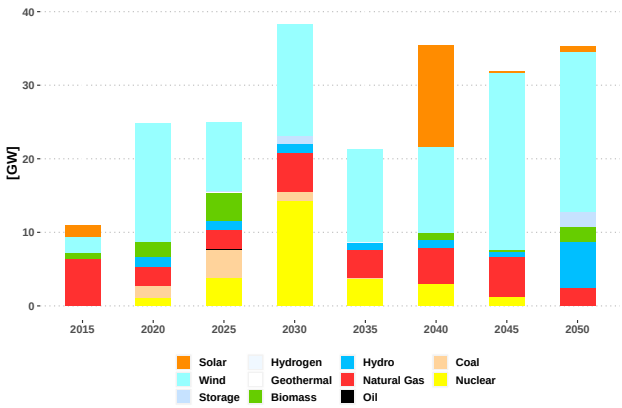


(b) New installed capacities over the planning time-frame

Figure 4.21: The resulted power generation mix trajectory for the 60% VRE uptake scenario (left) and the new installed capacities (right): look-ahead of 15 years and an overlap of 5 years

### 4.2.5 A 60% Renewable uptake scenario: Robustness regarding rolling horizon parameters

The rolling horizon technique's results depends on the chosen lengths of the look-ahead periods and the length of the overlap. This section presents the outcomes of six potential configurations of Algorithm 3. In a perfect foresight scenario, the planner possesses precise knowledge regarding future demand and supply developments, rendering the solution a global optimum. In contrast, a myopic foresight relies solely on the given demand and supply information for the decision period (typically five years). We further examine four additional rolling horizon configurations employing look-ahead periods of 10, 15, 20, and 25 years, each integrated with a 5-year overlap. The aim is to evaluate the investment dynamics and the sensitivity of optimality within our proposed methodology.

To provide a visual illustration, we compare the differences in new investments between a reduced foresight approach with a 15-year look-ahead and a perfect foresight configuration. Figure 4.22 showcases this distinction across the trajectory. Since both configurations share the same active period for the first sequence, no disparities are evident during the time span $[2013, 2025]$. However, distinctions start becoming apparent from 2030 onward. The magnitude of these differences is relatively minor, constituting at most 2.6% of the total installed capacity by 2050. For instance, in a perfect foresight configuration, natural gas

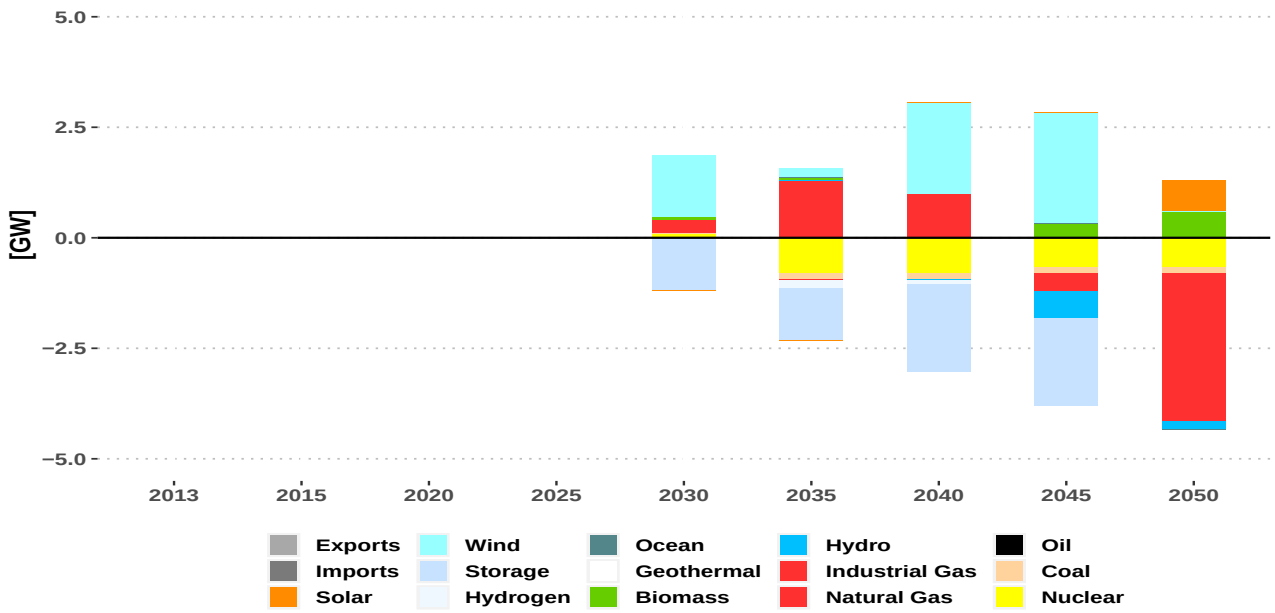


Figure 4.22: Additional new investments difference between the perfect foresight the reduced foresight with a 15-year look-ahead

investments exhibit a continuous distribution, while in a reduced foresight setting, a peak of investment occurs in 2050. These differences are difficult to analyze and merit careful examination as they emerge from a balance of various optimization constraints. In contrast to the example demonstrated in the methodology section – which indicated the preference for installing base-load power plants with extended look-ahead periods – drawing similar conclusions within a complex scenario involving constraints on renewable integration becomes challenging. The essential takeaway from this illustration is that the dynamics of investments undergo transformations as the length of the look-ahead period changes. In the subsequent section, we elucidate these shifts in investment dynamics by comparing the total investments, excluding technological changes.

From an economic standpoint, Figure 4.23a illustrates the total system cost of the adequate TIMES solution achieved through Algorithm 3. Notably, the myopic configuration displays an anomalous total cost primarily driven by operational expenses. In fact, instead of producing an infeasible solution, TIMES resorts to hypothetical costly imports to maintain a balance between demand and supply. The evolution of new investments for the myopic configuration is depicted in Figure 4.24. This behavior is rooted in the fact that under a myopic optimization strategy, TIMES refrains from investing between 2035 and 2045. However, come 2050, TIMES makes a substantial 50 GW investment. Yet, due to various constraints within the TIMES framework, a deployment rate cap of 50 GW per period triggers expensive imports. Relaxing this constraint (with a new run) to permit necessary additional investments aligns the total system cost across the planning horizon. Regarding the rolling horizon configurations, the cost analysis, as presented in Figure 4.23b, presents marginal

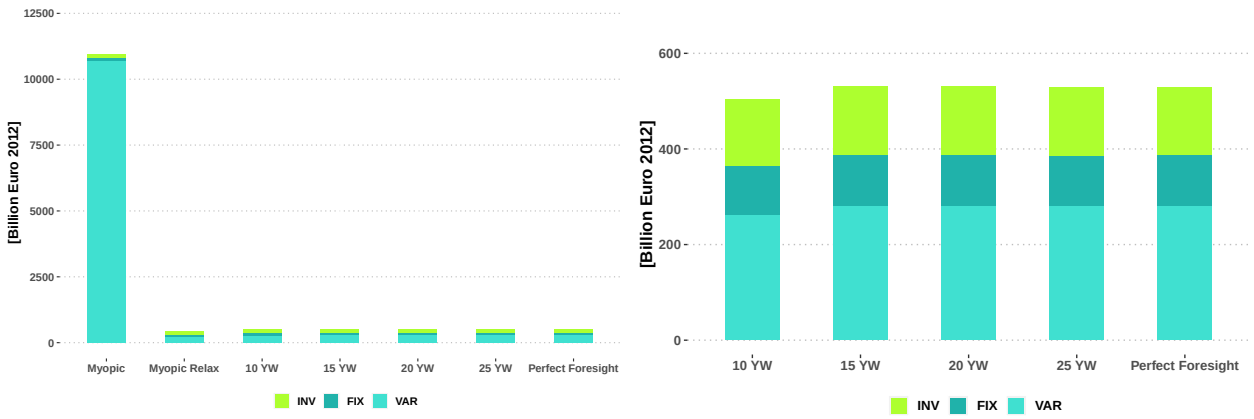


(a) TIMES total system cost for each configuration breakdown into investment, variable and fixed part.

(b) A closer examination of alternative configurations excluding the myopic configuration.

Figure 4.23: Total system breakdown into investment, variable and fixed costs over the planning time-frame for each rolling horizon configuration

disparities between configurations with a look-ahead duration of 10 years, 15 years, 20 years, or 25 years. Only a minor 5% divergence is observed between the 10-year configuration and the others. In comparison to a perfect foresight approach, no discernible cost savings are apparent. In essence, from an economic perspective, revealing future data into supply and demand dynamics over the subsequent 15 years is analogous to revealing information for the entire planning timeframe.

For each configuration, it becomes evident that the dynamics of investment will undergo changes. This is demonstrated in Figure 4.25, which showcases the cumulative new investments for various configurations. Two key observations can be drawn. Firstly, both the Myopic and Myopic Relaxed configurations show a 15-year plateau spanning from 2030 to 2045, followed by a surge in new investments in 2050. In addition, a 5-year plateau is evident in the configuration with a 10-year look-ahead. Conversely, the configurations employing 15 years, 20 years, and 25 years of look-ahead display the same patterns of new investment dynamics as the perfect foresight configuration. From an economic perspective [4], revealing only 15 years of future data suffices to reproduce the same outcomes as a perfect foresight optimization configuration. However, employing look-ahead periods of less than 15 years may result in a phenomenon we called "investment lethargy."

[4] using the same discount rate over all configurations

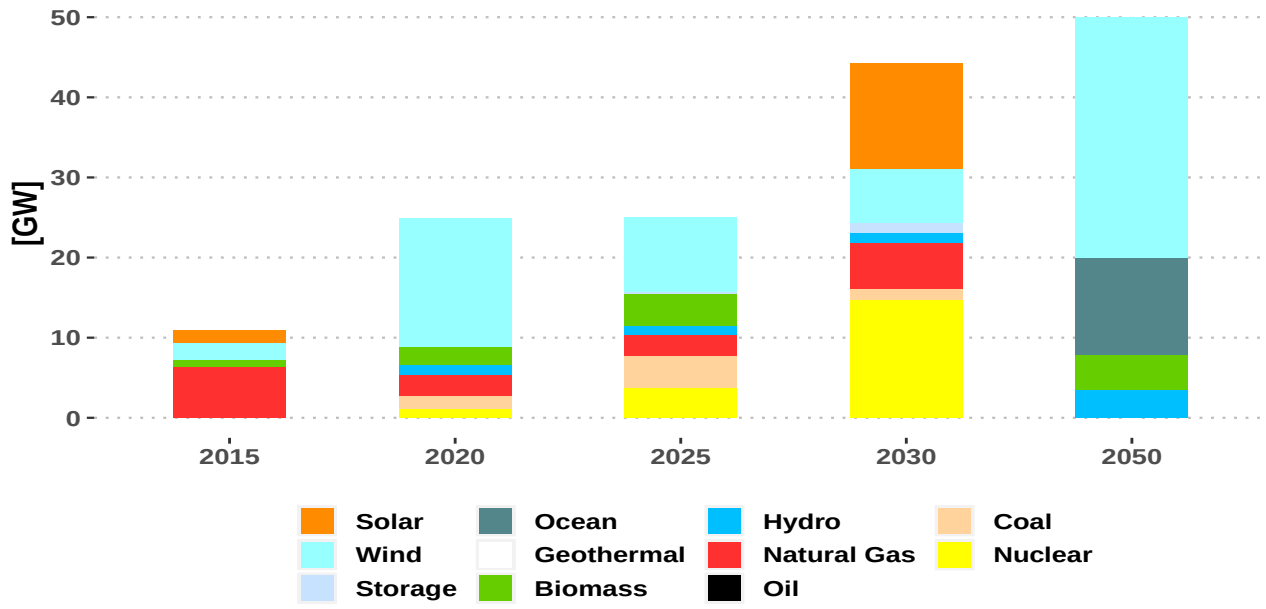


Figure 4.24: New investments for the myopic configuration and the upper bound constraint of 50 GW/year on the deployment rate


(a) The trajectory of the cumulative new installed capacities for the different rolling horizon configurations

(b) The trajectory of the total installed capacity for the different rolling horizon configurations

Figure 4.25: Investment deployment dynamics comparison between different rolling horizon configurations

### 4.2.6 Application to other scenarios: 80% and 100% VRE uptake, remarks and methodological issues

**80% VRE uptake scenario** In this section, we present key findings obtained by applying the methodology to an alternative long-term scenario. In the scenario with an 80% VRE

uptake, the capacity credit values were updated simultaneously for all technologies [5]. Notably, when this approach was employed, only a single iteration was necessary to achieve the desired adequacy. The resulting capacity credit values were as follows: 15% for wind, 48% for Run Of River, 21% for hydro reservoir, and 85% for thermal power plants. As discussed in Section 2, the order in which capacity credit values are updated can influence the outcomes. Employing the same Rolling Horizon configuration with a look-ahead period length of 15 years and an overlap of 5 years, the 80% VRE scenario shows an inadequacy in supply only for the year 2030. This contrasts with the 60% VRE scenario, where two inadequate periods were identified: 2030 and 2045.

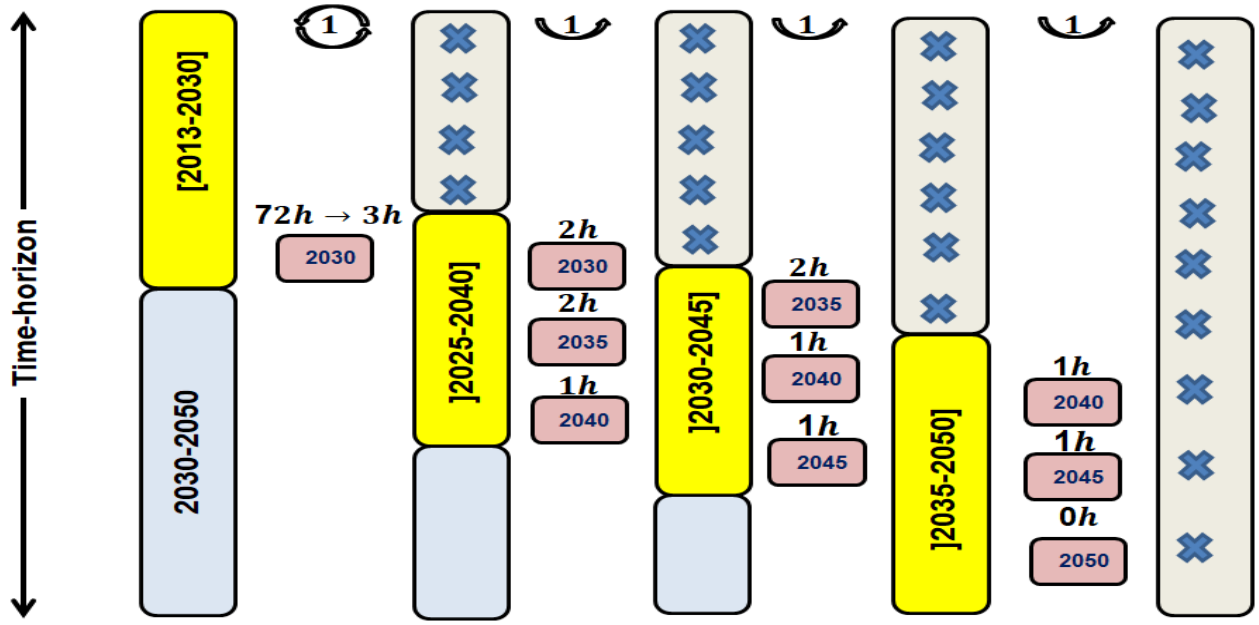


Figure 4.26: A graphical illustration of the application of Algorithm 3 with a 15-year look-ahead and 5 years overlap.

The power generation mix resulting from the 80% VRE uptake scenario while satisfying power generation adequacy requirements is illustrated in Figure 4.27a. In the year 2050, which marks the end of the horizon period, an additional investment of 26 GW is required to transition from a 60% VRE uptake to an 80% VRE uptake. This increase is primarily driven by investments in wind and solar power generation. From an economic perspective, the single iteration required to establish an adequate power generation mix for 2030 results in a gain of 2 billion Euros. This constitutes 0.5% of the total actualized cost for the period spanning from 2013 to 2030. This reduction in the total system cost while maintaining adequacy requirements demonstrates that the reserve capacity constraints do not necessarily lead to more investments, but rather prompt an adjustment in the mix's structure based on the

[5]This choice is made to illustrate the feed-back loop's sensitivity to the sequence of capacity credit updates.

capacity credit values. For the entire trajectory, the 80% VRE scenario incurs a cost that is 7% higher compared to the 60% scenario, as shown in Figure 4.27b.

From an operational perspective, transitioning from a 60% VRE uptake to an 80% VRE uptake presents new operational challenges. Figure 4.28 illustrates the 2050 hourly power generation stack in terms of a residual load duration curve (RLDC) for both scenarios. The positive portion of the RLDC represents the demand that must be met by dispatchable generation technologies. Several observations can be made from this figure:

1. **Changed Dispatch Profile:** The RLDC comparison reveals that the number of full-load hours, where dispatchable generation is required at its maximum capacity, is reduced. Without variable renewables, a significant portion of the load is balanced by base load power plants that provide all necessary generation. However, with the presence of variable renewables, dispatchable power plants need to frequently ramp up and down to accommodate the variability of renewable sources.

2. **Capacity Credit vs. Penetration:** It is evident from the figure that a substantial amount of renewable generation leads to a relatively small capacity credit. The upper-left point of the RLDC approaches the upper-left point of the load duration curve (LDC) represented by the blue line. This means that only a fraction of variable renewable generation can be reliably depended upon during peak hours. Thus, a sufficient number of dispatchable power plants are required to balance the demand during these times.

3. **Negative Residual Load Hours:** The RLDC presentation also highlights the hours of the year during which the residual load is negative. Negative residual load hours indicate periods when the generation from wind and solar sources exceeds the power demand. During such hours, thermal power plants may still contribute due to technical ramping constraints. However, without export capacity or energy storage solutions, this overproduction must be curtailed, as it cannot be utilized to satisfy load. The number of hours per year with negative residual load increases significantly from 2% for the 60% VRE scenario to 20% for the 80% VRE scenario.

It's also important to consider spillage, defined as hours during which power generation exceeds power demand. These hours can occur due to overproduction from non-dispatchable technologies or when thermal power generation operates at a level beyond what's needed.

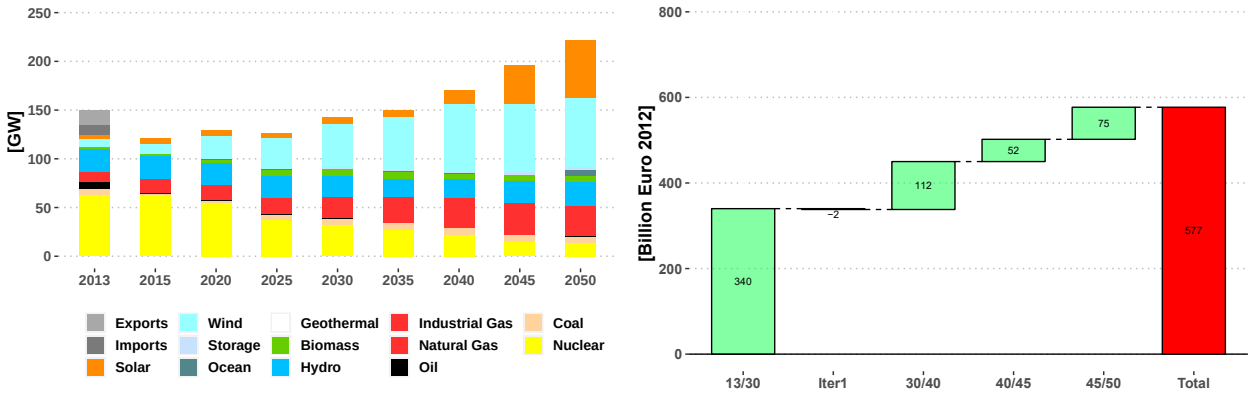


(a) The evolution of the power generation mix following the 80% VRE uptake scenario over the planning time-frame

(b) The breakdown of the total system cost over the planning time-frame based on the rolling horizon sequences

Figure 4.27: The power generation mix evolution following the 80% VRE uptake scenario over the planning time-frame and the corresponding total system cost breakdown

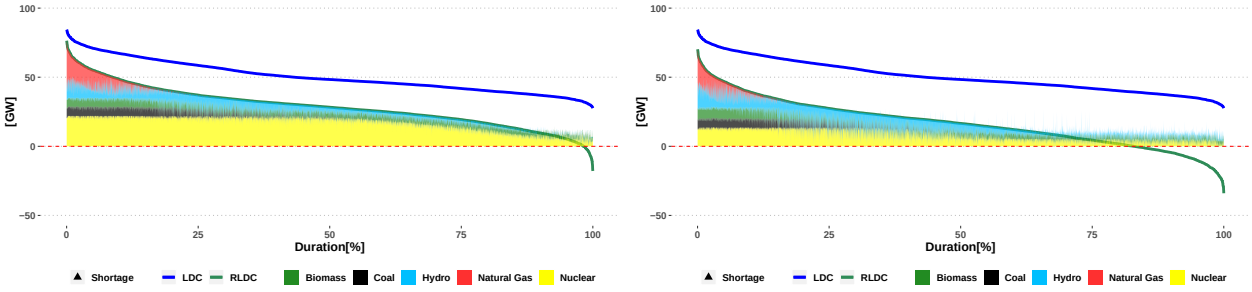


(a) 2050, RLDC power generation stack following 60% VRE uptake scenario

(b) 2050 RLDC power generation stack following 80% VRE uptake scenario

Figure 4.28: The RLDC representation for the hourly dispatch decided in 2050 for the 60% VRE scenario (left) and 80% VRE scenario (right)

**100% VRE uptake scenario: methodological limitations** In the scenario of 100% VRE uptake, a minimum constraint is imposed on the annual total renewable energy production, set at 63% in 2040 and 100% in 2050. This scenario holds methodological significance in comparing the operational behavior of both the TIMES and ANTARES models based on the given power generation mix. For this scenario, a rolling horizon configuration with a look-ahead period of 15 years and an overlap of 5 years is employed. This scenario is used to illustrate a limit in the developing methodology regarding a scenario with 100% VRE uptake. This limitation is illustrated through two important aspects: the first one is the use of residual thermal fossil-based power plants in the operation within ANTARES and it's related impact on costs and adequacy. Secondly, the respect or not of the constraint of 100% VRE uptake within ANTARES.

Utilizing the same deployment rate constraints as in the other scenarios, the 100% VRE uptake scenario proves to be infeasible. The total system cost over the look-ahead period is depicted in Figure 4.29a, indicating that infeasibility becomes apparent in the period 2045-2050. This infeasibility is attributed to the deployment constraint, which restricts investments to not exceed 50 GW in each period.

Figure 4.29 presents the new investments determined for each period. It is evident that for the period 2040-2050, the deployment constraint on total investments becomes saturated. The high total system cost in this scenario primarily results from operational expenses, driven by the importation of expensive electricity (50 TWh, equivalent to 10% of total consumption).

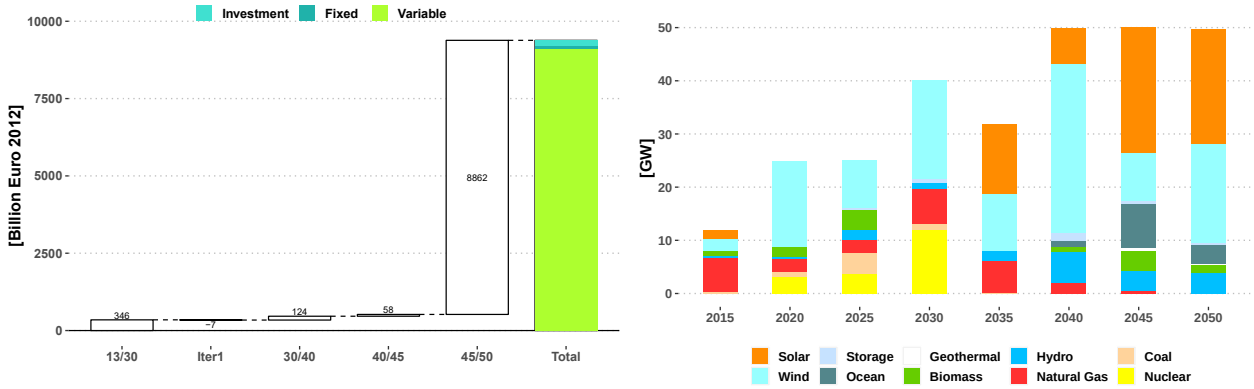


(a) Breakdown of the total system cost over active look-ahead periods

(b) New installed capacities trajectory

Figure 4.29: The breakdown of the total system cost over the look-ahead periods for the 100 % VRE uptake scenario (left) and the corresponding new investments needed to achieve scenario targets (right)

In 2050, the power generation mix determined by TIMES can be operated differently based on whether we permit the use of existing thermal power generation plants. When no thermal production is permitted in 2050 to satisfy 100% VRE uptake, TIMES relies solely on biomass, hydro, and renewable sources. To illustrate this, two potential options are compared using ANTARES. The Figure 4.30 below contrasts TIMES and ANTARES (across 1,000 Monte Carlo years) in terms of annual production for each technology. It is evident from both figures that, for both options, TIMES generates zero TWh from nuclear, coal, and natural gas. ANTARES follows the same pattern when the thermal power plant fleet (excluding biomass) is removed from the power generation mix. However, when the residual thermal power plant fleet is allowed to participate in 2050's operation, the power generation from these technologies is no longer zero. For instance, Figure 4.31 showcases the 2050 production stack of the median Monte Carlo year for the two options. When the residual thermal power plant fleet is disallowed from participating in the balance, around 28% of the time experiences insufficient supply, marked by shortage hours in black.

Hence, the $LOLE$ value in a simulation that excludes the utilization of the thermal

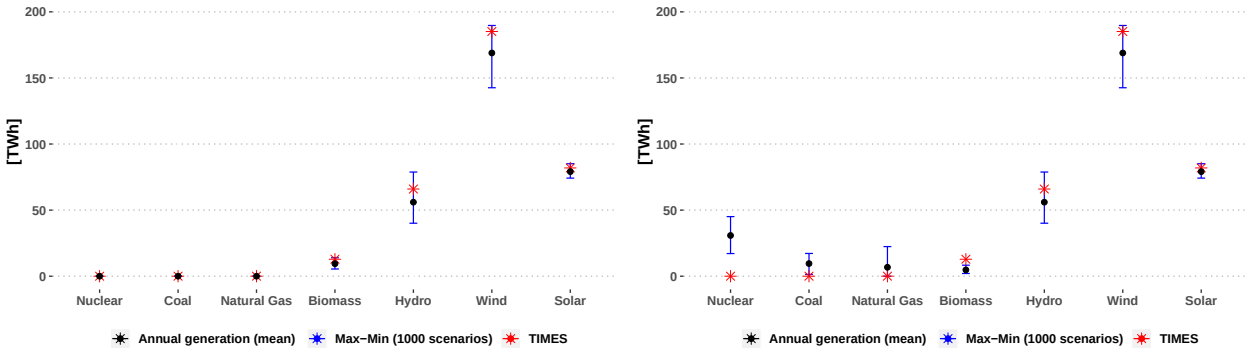


(a) Without the participation of the residual thermal power plant fleet

(b) With the participation of the residual thermal power plant fleet

Figure 4.30: 2050, annual power generation by technology comparison between TIMES and ANTARES when thermal stock is allowed to participate in ANTARES generation (left) and when it's not allowed (right)

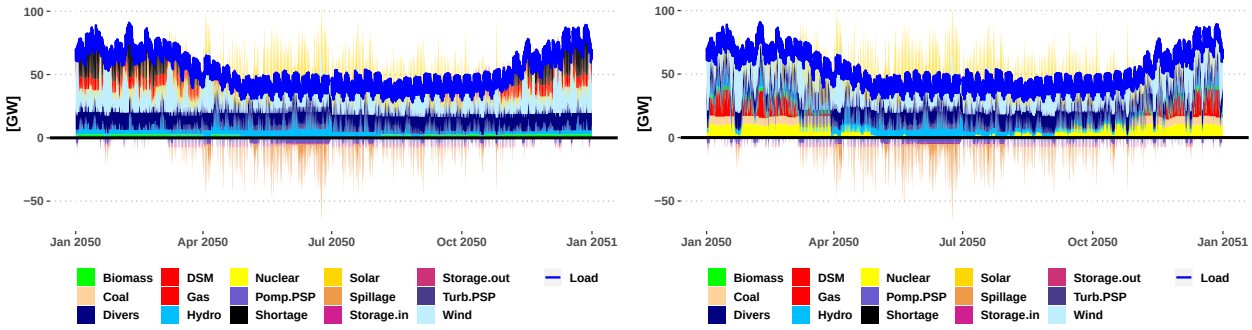


(a) Without the participation of the thermal stock

(b) With the participation of the thermal stock

Figure 4.31: 2050, annual power generation by technology comparison between TIMES and ANTARES when thermal stock is allowed to participate in ANTARES generation (left) and when it's not allowed (right)

power plant stock reaches 1,000 hours/year, whereas it reduces to only 1 h/year when the residual thermal power plant stock is permitted to contribute to the supply-demand balance. The appeal of "fictitious costly imported" electricity, noted in TIMES costs, is mirrored in ANTARES when comparing the overall operational costs of the two distinct simulations. In particular, Figure 4.32 illustrates the significant difference in operational costs between the two scenarios (simulation 1: with the participation of the thermal power plant stock, and simulation 2: without). The overall operational cost rises dramatically by a factor of 100 when the thermal power plants are prohibited from generating. This increase is predominantly driven by the shortage costs. Both models accurately capture the inadequate supply situation towards the end of the horizon when the residual thermal power plant fleet is not allowed from generating.

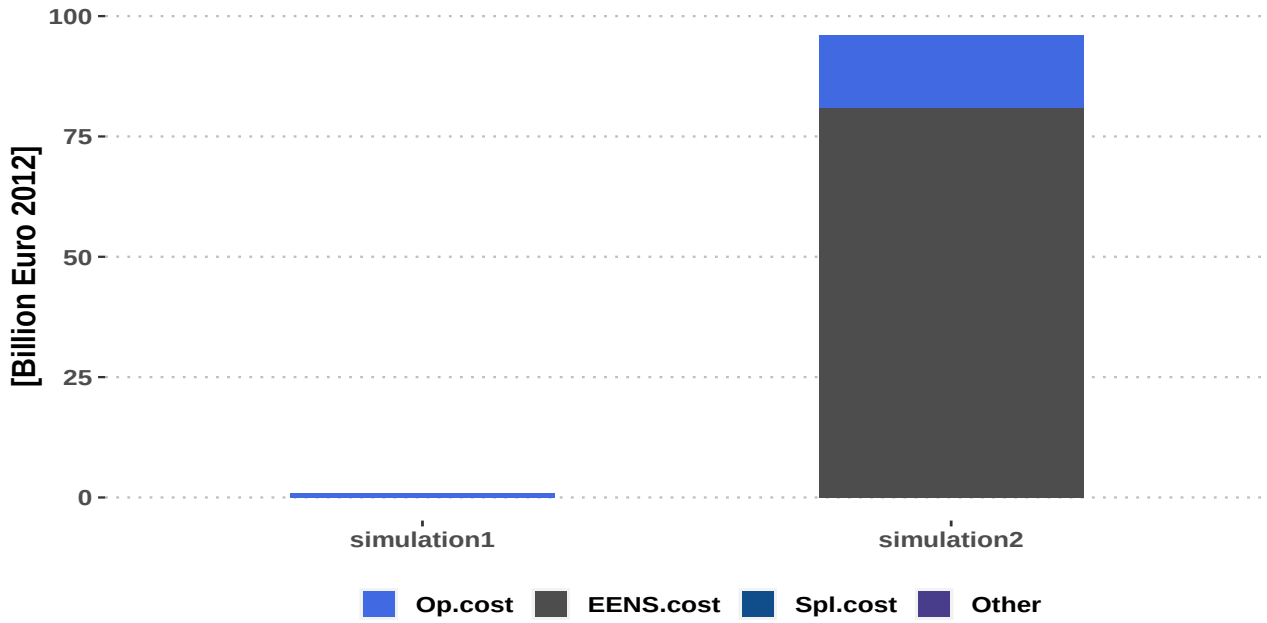


Figure 4.32: 2050, overall operational cost derived from TIMES for two simulations (with and without thermal fossil-based power plants).

To demonstrate the adherence of VRE uptake constraints from TIMES to ANTARES, we calculate the VRE uptake for each Monte Carlo year and every period. The presented figure displays the VRE uptake duration curve for the 1,000 Monte Carlo years simulated across the horizon. The blue portion of the curve indicates scenarios that adhere to the TIMES limits, while the red region represents scenarios that violate the TIMES limits. In 2035, around 95% of Monte Carlo years respect the 50% VRE uptake constraint. For the 2040 period, approximately 80% of Monte Carlo years conform to the 63% VRE uptake constraint set by TIMES. The trend continues in 2045, where around 95% of Monte Carlo years observe the 80% VRE uptake TIMES constraint. However, by 2050, only 50% of the Monte Carlo years adhere to the 100% VRE uptake constraint, while the other 50% of scenarios involve the utilization of the thermal power plant stock during operation. Notably, the utilization of the thermal power plant stock in the operation accounts for at most 10% of the total generation.

It is evident that until 2045, ANTARES effectively respects the VRE uptake limits established by TIMES, even without additional constraints integrated into its optimization problem. However, in 2050, if the power generation mix prescribed by TIMES is directly transferred to ANTARES without supplementary constraints, the estimation of power generation adequacy would be inaccurate, given that 50% of Monte Carlo years do not conform to this constraint.

In conclusion, our results highlight that applying the developed Rolling Horizon algorithm to a scenario with 100% VRE uptake requires additional reconciliation of constraints, particularly concerning the participation of thermal fossil-based power generation within the

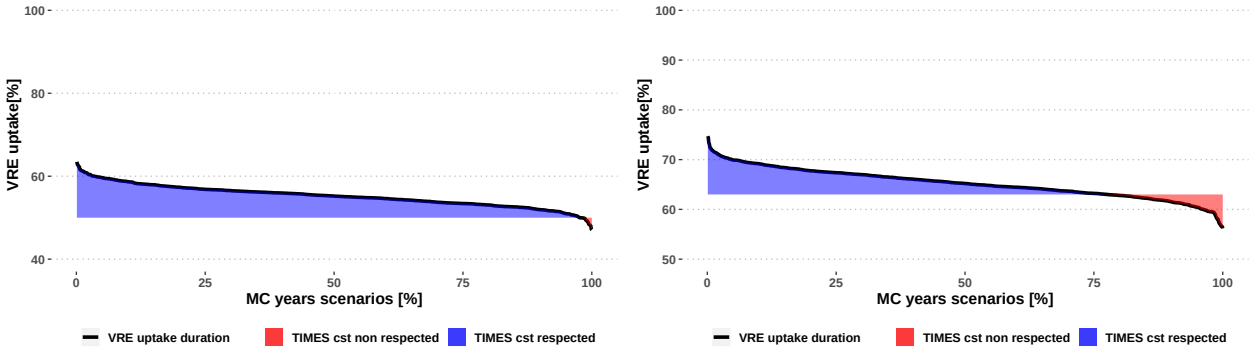


(a) 2035: 50% VRE uptake limit




(b) 2040: 63% VRE uptake limit

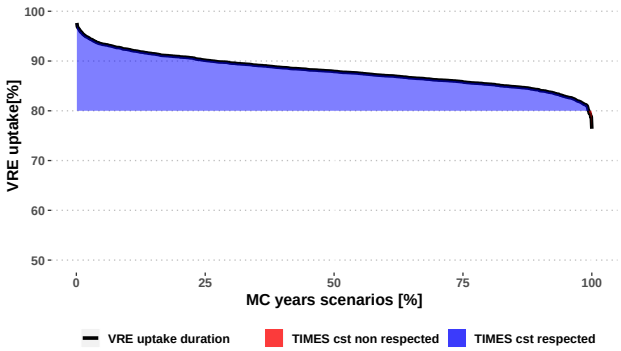


(c) 2045: 80 % VRE uptake limit

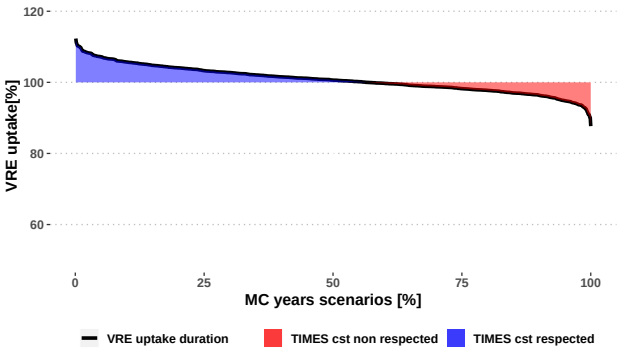


(d) 2050: 100 % VRE uptake limit

Figure 4.33: 2050, annual power generation by technology comparison between TIMES and ANTARES when thermal stock is allowed to participate in ANTARES generation (left) and when it's not allowed (right)

ANTARES model. This finding underscores the importance of harmonizing constraints between different models when transferring power generation mixes to ensure consistency in power system adequacy assessments. This will be considered in the next chapter.

## 4.3 Discussion

Modelers have explored the development of a new generation of model-linking approaches to deal with the power sector transition. The advantages of this methodology compared to a single integrated model are twofold: First, it is more flexible, since it leaves the constituent models intact for independent runs, thus making further model development easier. Second, the linking approach contains both the pathway cost-effectiveness foundation of long-term energy planning models and the operational richness of power system models. This chapter contributes to fill the gap 1 and 2 thanks to its careful focus on generation adequacy risk assessment. Thus, our only key question is, "Do long-term energy planning model (TIMES)

outcomes match power systems generation adequacy requirements?"

In this spirit, the purpose of the first section was to address electricity security of supply in the long-term power system planning process. State-of-the-art system adequacy assessment is probabilistic by nature. Grid operators around the world have been using probabilistic tools for decades. By ensuring input-output data consistency, we developed a rigorous methodology for linking a long-term energy planning model (TIMES power system model) with a probabilistic operational power system (ANTARES). For a specific target year, in our model we established an iterative feedback loop with a stopping criterion representing three-hour annual loss-of-load expectation to ensure an adequate power generation mix. Furthermore, most previous studies have highlighted the regrettable lack of consistent long-term energy demand forecasts, as well as capacity factor forecast data sources. As for all models, the quality of our results is conditioned by the quality of the input data. However, our databases benefit from the expertise of the power grid operator (RTE) regarding long-term forecasting studies. Readers who want to form their own opinion about the quality of the data used are referred to the French generation adequacy report for 2017 [83].

One of the key questions concerning the bidirectional linkage (feed-back loop process) between a long-term energy system and a short-term operational model approach is whether the convergence is guaranteed by the feedback loop strategy. At this level, it is important to clearly define two possible definitions of convergence which depend mainly on the goal of the linkage.

- The convergence criterion is based on an endogenous variable in both models.
- The convergence criterion is based on a metric that is external to both models.

An example of the former definition can be found in the study [170], which proposes a novel bidirectional linkage between a TIMES-Norway energy system model and an EMPS power market model to improve the modeling of hydropower generation and external electricity markets in the TIMES-Norway model. As the Norwegian power system is hydropower-dominated, the chosen convergence criterion is the income difference of hydropower producers, which is endogenous in both models. The feedback strategy, meanwhile, uses electricity trade prices and operational hydropower constraints from EMPS as an input to TIMES-Norway. However, our particular focus is the power generation adequacy assessed by the Loss of Load Expectation metric, which is external to both models in the sens that no constraint related to the $LOLE$ is incorporated in both model. Thereby our convergence definition belongs to the second category.

Taking this for granted, our proposed feed-back loop strategy is based on the peaking-reserve constraint using capacity credit value updates. Two possible extreme outcomes could be considered:

- Capacity credit values are over-estimated (for example, 100% for all technologies): the power generation as derived from TIMES has insufficient supply and therefore adequacy is not guaranteed.

- Capacity credit values are under-estimated (for example 10% for all technologies): the power generation as derived from TIMES has sufficient supply and therefore adequacy is guaranteed.

Our approach aimed to provide capacity credit values that neither overestimate nor underestimate, as it calculates the median value across all Monte Carlo years. In fact, using ANTARES operational dispatch decisions to estimate the capacity credit values results in a "real" approximation of the contribution of each investment in the overall adequacy. Two simulation variants have been tested, and the number of iterations was 3 for the variant with 200 operational scenarios and 7 iterations for the variant with 1,000 operational scenarios. However, at the present stage of research, the authors have decided to not discuss in further detail the mathematical proof of convergence for the TIMES-ANTARES feed-back loop.

However, the methodology used for capacity credit estimation has its drawbacks, as highlighted in the research conducted by Thomas Hegary as part of the OSMOSE project [179]. The approach employed in our feedback loop, which utilizes capacity credit estimation based on Equation 4.2 and Equation 4.1, underwent thorough testing in Thomas Hegarty's thesis, with a particular emphasis on its application to the Germany node. After careful investigations, Hegarty identified several limitations in the previously used approach, which can be summarized as follows:

- **Inadequate Investment Pathway:** The feedback technique fails to consistently generate an appropriate investment pathway, as it cannot effectively distinguish between situations of under-investment and over-investment. This may lead to positive feedback loops as the iterative process advances. Additionally, increased investment does not necessarily lead to a reduction in $LOLE$ levels, making the technique insufficient for achieving adequate solutions. Furthermore, in studies optimizing investment for a target year rather than a pathway, the structural issues of this feedback technique may not become apparent.

- **Capacity Credit Gap:** The capacity credit values as expressed in Equation 4.2 show a disparity between intuitive expectations and their actual representation. While they provide a rough estimate of how extensively a technology is utilized to satisfy peak net load, the primary interest lies in determining a technology's potential to meet peak net load when required, which this formulation does not fully capture.

- **Equivalency Issues:** For VRE sources, the notions of capacity credit and potential to meet peak net load are equivalent. However, this equivalence breaks down for dispatchable generation. In scenarios where peak electricity demand coincides with significant VRE generation, it is unreasonable to expect the availability of peaking generation. Consequently, the maximum value calculation tends to result in inaccuracies.

- **Bounding Limitations:** Equation 4.2's failure to bound capacity credit values within the $[0, 1]$ interval often leads to negative capacity credit values for storage assets. This misrepresentation obscures these technologies' actual contributions to peak net load.

Moreover, the equation implies that if a technology had no installed capacity in a particular soft-linked year during iteration $i$, it will possess no capacity credit value in iteration $i+1$. This limitation impedes the valuation of its ability to contribute to the reserve margin.

Thomas Heggarty ultimately concludes that, due to the structural issues described, the feedback technique is unsuitable for its intended purpose, leading to its exclusion from multi-node case studies [179]. Nevertheless, the fundamental concept of the feedback technique retains significant value. In his thesis, Hegarty introduces a new methodology for computing capacity credit, ensuring that these values are aligned with their intended purpose. Its goal was to develop a method that is not only applicable to variable renewable energy (VRE) sources but also to dispatchable generation, energy storage, and interconnections.

$$cci_{r,t,y} = median_{wy \in WeatherYear}(mean_{hnl \in HighNetLoad}(\frac{Production_{r,t,y,wy,h}}{Capacity_{r,t,y}})) \tag{4.6}$$

Where: $wy$ : Monte Carlo years and $hnl$ the set of 100 hours where net load is highest.

The same principle applies for interconnectors: each link is assigned a pair of capacity credit values, based on the mean flow during the 100 hours of highest net load in each of the two connected regions. Note that this may lead to a negative value.

$$tradecci_{r,rr,f,y} = median_{wy \in WeatherYear}(mean_{hnl \in HighNetLoad}(\frac{InterconnectorFlow_{r,rr,f,y,wy,h}}{Capacity_{r,rr,f,y}})) \tag{4.7}$$

Despite Heggarty's efforts to find a precise formulation for capacity credit estimation using the top 100 hours of highest net load, it is important to note that capacity credit estimation, as shown in an important study on the sensitivity of the capacity credit to the estimation methodology [206], offers various methods, each providing different estimations. In this report funded by the US. Department of Energy, the Solar America initiative aimed to assess different methods for valuating photovoltaic PV capacity. Various methodologies were devised, resulting in divergent outcomes. Here are some of the key methodologies commonly used for capacity credit estimation.

- **Effective Load Carrying Capability (ELCC):** The Effective Load Carrying Capability (ELCC) of a power plant quantifies its capacity to augment the total generation capacity within a specific local grid, without increasing the probability of load loss. The ELCC is determined by evaluating the Loss of Load Probability (LOLP) for two resources. The first resource is the actual resource with its output varying over time, while the second resource is an "equivalent" resource with a constant output. The details of how to calculate the $ELCC$ are presented in the report [206].

- **Load Duration Magnitude Capacity (LDMC):** The LDMC parameter is a metric defined as the average photovoltaic (PV) output for all loads exceeding a specific LDMC threshold. This threshold is determined as the peak load ($L$) of the utility

grid multiplied by a factor of $(1-p)$, where $p$ represents the PV penetration fraction. The PV penetration fraction, denoted as $\frac{X}{L}$, characterizes the ratio of installed PV capacity ($X$) to the grid's peak load ($L$). The LDMC parameter, provides a direct measure of the impact of PV penetration on the grid.

- **Load Duration Time-based Capacity (LDTC):** This metric, termed $LDTC$, shares similarities with the $LDMC$, albeit with a distinction in how penetration ($p'$) is defined. Penetration is defined temporally rather than based on size: $LDTC$ threshold = nth ranked load. Here, the value of $n$ is determined by the specified penetration level: $n = p'N$ Where '$N$' represents the total count of load data points in the load duration curve. For example, in the case of an annual dataset comprising hourly loads ($N = 8760$), a 10% penetration level would establish the threshold at the 876th highest hourly load.

- **Solar-Load-Control-Based Capacity (SLC):** SLC quantifies the additional guaranteed load reduction achievable with PV deployment when demand response is available. It is expressed as a ratio of load reduction achieved with PV and load control to load reduction without PV: $SLC = \frac{X-Y}{X}$. '$Y$' signifies the extent of load reduction attainable without PV but with the same cumulative load control measures needed to ensure a load reduction equivalent to '$X$' when PV is present.

- **Minimum-Buffer-Energy-Storage-based Capacity (MBESC):** MBESC calculates the minimum energy storage needed to ensure that PV-plus-storage meets loads above a specified threshold. It assesses effective capacity based on peak load reduction achieved with storage but without PV. Essentially, it addresses the question of how much additional guaranteed load reduction can be achieved by deploying PV in combination with a certain amount of dispatchable storage available to a grid or substation operator.

  With a PV penetration represented as $p = \frac{X}{L}$, the Minimum Buffer Energy Storage (MBES) is the minimum quantity of energy storage required to ensure that a PV-plus-storage system can meet all loads surpassing the threshold determined by the LDMC metric. To determine the effective capacity derived from MBES, the process involves initially calculating the peak load reduction $Y'$, which is achieved using a storage system of the same capacity as the MBES but without PV. The MBESC is subsequently defined as: $MBESC = \frac{X-Y'}{X}$

- **Demand-Time Interval Matching (DTIM):** This method examines the worst-case output of the PV system by subtracting the PV system output from the load (in TEPs case this is done over 10 second time intervals) and the capacity value is based on the worst-case difference between the load duration curve over the dispatch sampling interval.

- **Time/Season Windows (TSW):** The TSW method calculates capacity credits for specific time intervals, including hours, months, and seasons. Variations of this method,

such as the ERCOT method and the MAPP method, determine capacity credits by considering peak demand periods and median capacity values.

There are at least two different approaches to the calculation. The ERCOT method specifies a peak demand time frame, for example, May to October from 10 AM to 6 PM, and defines capacity as the minimum output likely to occur with a certain probability, denoted as $\alpha$ (in the case of ERCOT-wind, $\alpha = 8$). Meanwhile, the MAPP method employs a median capacity value over a four-hour window within each month.

- **Capacity Factor (CF):** The capacity factor quantifies a power plant's average output relative to its installed capacity. However, it does not consider load served or grid penetration.

This study conducted a comprehensive analysis of these methodologies and underscored their sensitivity to capacity credit valuation. Among the methods assessed, three emerged as more favorable for capacity credit valuation: Effective Load Carrying Capacity, Solar Load Control, and Minimum Buffer Energy Storage (grouped due to similarities). This investigation identified geography and time sampling as two primary factors influencing the estimation results. In our multi-model methodology, the incorporation of the feedback loop into capacity credit estimation significantly impacts the model's outcomes. Applying different methodologies within our multi-model framework yields diverse results. Therefore, in the forthcoming chapter, we endeavor to develop a novel methodology characterized by reduced sensitivity to parameter estimation.

## 4.4 Conclusion

This chapter introduces a linking model approach aimed at evaluating the long-term security of electricity supply. One of the primary motivations behind this approach was to address concerns regarding whether the methodologies and assumptions used in traditional long-term energy planning models are suitable for capturing the short-term aspects of future decarbonized power systems. By concurrently considering models at different scales, this proposed linking methodology combines the long-term cost-effectiveness of the TIMES model with the detailed temporal resolution, technical specificity, and probabilistic aspects of the ANTARES model.

The initial linkage's (first section) objective is to build a long-term power generation mix for a specified period that adheres to generation adequacy requirements. As a case study, the methodology developed in the first section was applied to power generation planning for France, focusing on the 2013-2050 timeframe and aiming to achieve a 60% renewable power generation uptake by 2050. For practical reasons, the adequacy assessment was conducted only for 2030 (with 40% VRE uptake), positioned midway between the starting point and the planning horizon.

Several key conclusions have emerged from this initial contribution:

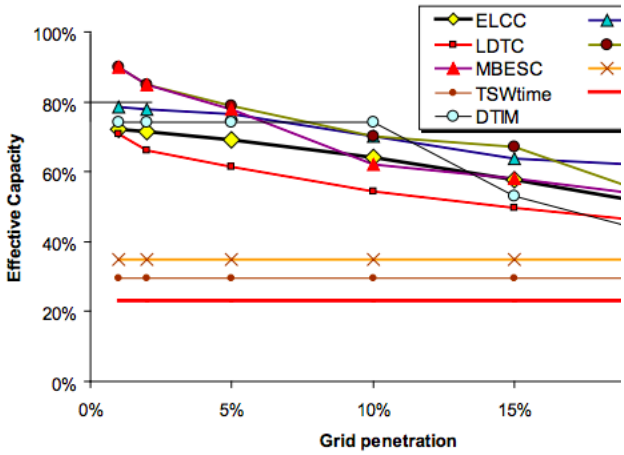


(a)

Figure 4.34: Comparing all capacity credit metrics for Nevada Power as a function of the amount of PV on the grid from 1% of peak ( 55 MW) up to 20% of peak ( 1,100 MW)

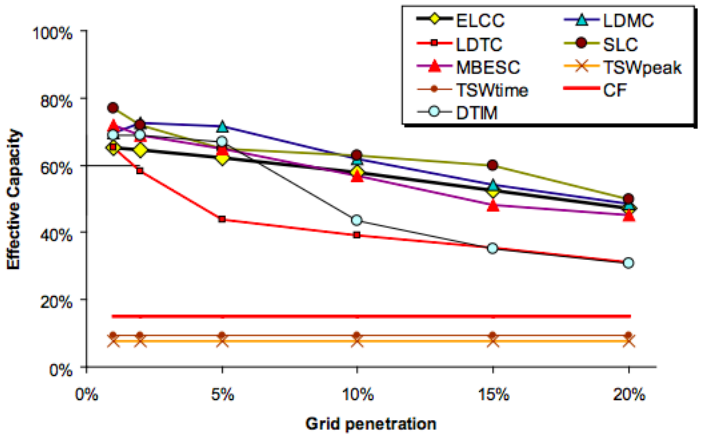


(a)

Figure 4.35: Comparing all capacity credit metrics for Rochester Gas and Electric as a function of the amount of PV on the grid from 1% of peak ( 16 MW) up to 20% of peak ( 320 MW).

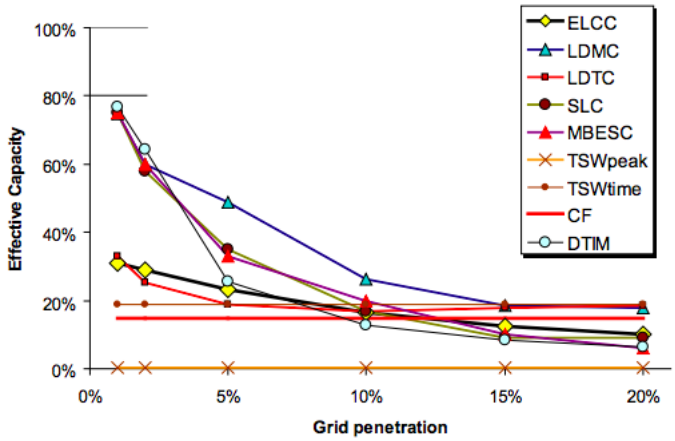


(a)

Figure 4.36: : Comparing all capacity credit metrics for Portland General as a function of the amount of PV on the grid from 1% of peak ( 35 MW) up to 20% of peak ( 700 MW).

Figure 4.37: The capacity credit comparison of three different utilities and different methodology for the estimation of capacity credit values (source: [206])

- Dispatch results from both models exhibit significant differences, primarily attributed to the underestimation of VRE and load variability, resulting in an overestimation of the residual load duration curve observed by TIMES.

- The capacity mix derived from TIMES for 2030 does not effectively meet the electricity security of supply requirements set by French public authorities ($LOLE \leq 3h/year$).
- Implementing feedback loop between ANTARES and TIMES, based on capacity credit estimation, has the potential to ensure adequate firm capacity to meet demand. Seven iterations were required to converge to the 3 hours/year LOLE criterion.
- Operationally, the ANTARES adequacy outcomes indicate that the 2030 LOLE decreases from 79 hours to 3 hours, with Expected Energy Not Served decreasing from 442 GWh to 10 GWh.
- From a planning perspective, the TIMES economic outcomes underestimate the total discounted cost (including investment costs for new investments and retrofits, fixed and variable annual costs) by 28%, primarily due to investment shares.
- A significant takeaway from this section is the importance of paying careful attention to long-term electricity security of supply, as it may be underestimated by standard long-term energy system planning models.

The second section's primary objective was to develop a new methodology for planning a cost-effective transition strategy and ensuring long-term power generation adequacy throughout the trajectory. To achieve this, a combination of two methodologies was proposed. The feedback loop based on capacity credit estimation methodology ensures adequacy for a given period, while the rolling horizon optimization algorithm builds a trajectory that meets generation adequacy requirements. The following results were obtained:

The Rolling & Linking algorithm successfully identified an investment trajectory compliant with adequacy requirements for a scenario with a 60% VRE uptake, a 15-year look-ahead period, and a 5-year overlap. Various configurations for the 60% VRE uptake scenario yielded suitable solutions. Sensitivity analysis, particularly concerning the look-ahead period, revealed different investment dynamics across configurations, with 5-year and 10-year look-ahead periods exhibiting plateaus lasting 10 and 15 years, respectively, with no investments made. Economically, with the considered discount rate, disclosing data for the next 15 years was found to be equivalent to perfect foresight for the total actualized cost. Transitioning from a 60% VRE scenario to an 80% VRE scenario in 2050 revealed distinct phenomena in the RLDC, including modified dispatch profiles, reduced capacity credit for renewables, and an increase in the number of negative residual load hours. In a scenario targeting 100% VRE uptake, the objective cannot be met as a substantial residual fossil thermal power fleet turns out to be indispensable for the power generation mix to remain adequate (resulting in a LOLE of 1 hour/year). However, when this fleet is excluded from operation, the LOLE increases to 1000 hours/year. Consequently, the scenario with 100% VRE uptake necessitates additional constraint reconciliation between the long-term energy planning model and the operational power system model.

# Chapter 5

# A new multi-scale framework to build secure and optimal investment trajectories for multi-area power systems

## Contents

The preceding exercises carried out hold significant importance in comprehending the underlying challenges associated with the development of multi-model approaches. By applying the developed methodologies to France, we were able to gain a thorough understanding of model behaviors and streamline the complexity of the algorithms that support the linkage. Due to the limitations outlined in the previous chapter, in the following section, we further refine the problem formulation addressed in this thesis. Instead of employing a descriptive style typically found in most studies utilizing a linking approach, we present the problem as an integrated mathematical multi-scale problem. To accomplish this, we initially furnish a detailed analysis of the various scales and interactions involved in the problem, followed by the formulation of the integrated mathematical model that encapsulates these complexities. The mathematical formulation is based on a unified representation of the underling optimization problem. The bridging scale algorithms needed for the multi-scale model are detailed. Assessing consistency and the validity of the multi-scale model is also given. To ensure the power generation adequacy requirement for the investments trajectories we apply the simulation-based optimization via stochastic approximation algorithms which is a powerful approach that combines simulation modeling and optimization techniques to solve complex problems. This approach is especially valuable when it is not feasible to analytically evaluate the objective function, which involves minimizing the disparity between the LOLE metric and the desired adequacy value, and can only be estimated through multiple simulations. By utilizing stochastic approximation algorithms, which rely on a sequence of random samples, this methodology iteratively improves the solution by adapting the decision variables based on feedback obtained from simulations. The simulations in this context arise from the integrated multi-scale model. The motivation behind developing such a sophisticated algorithm is to enable an "intelligence" -in the sense that is independent from the subjective judgment [1] of the modeler- that facilitates the interaction between long-term and short-term

[1] As opposed to the sensitivity of the preceding methodology to the capacity credit estimation approach

scales within the multi-scale model when exploring the solution space. The development of this multi-scale model eliminates two important drawbacks of soft-linking models: they are time and labor consuming and need the human intervention at each iteration, so convergence may not be tested stringently. Current state-of-art articles have reported convergence in few iterations cycles. Our contribution at this level is therefore to utilize the developed multi-scale model supported by a simulation based optimization algorithm to check we are able to reach convergence.

In this chapter we give first an introduction of the multi-scale modeling, its related methodologies and the vocabulary used for the development and design of multi-scale framework. Secondly, we identify and formulate our problem: planning secure future power systems as a multi-scale problem. The theoretical and computational frameworks are developed. The conclusive result of this chapter is a multi-scale framework bridging the long-term scale of system planning and the short-term scale of a secure operation.

**Résumé en français :**

Les exercices précédents revêtent une importance significative pour la compréhension des défis sous-jacents associés au développement d'approches multi-modèles. En appliquant les méthodologies développées à la France, nous avons pu acquérir une compréhension approfondie des comportements des modèles et rationaliser la complexité des algorithmes qui soutiennent le couplage. En raison des limitations énoncées dans le chapitre précédent, dans la section suivante, nous affinons davantage la formulation du problème abordé dans cette thèse. Au lieu d'adopter un style descriptif généralement présent dans la plupart des études utilisant une approche de couplage, nous présentons le problème sous la forme d'un problème mathématique intégré à plusieurs échelles. Pour ce faire, nous commençons par une analyse détaillée des différentes échelles et interactions impliquées dans le problème, suivie de la formulation du modèle mathématique intégré. La formulation mathématique repose sur une représentation unifiée du problème d'optimisation sous-jacent sous forme matricielle. Les algorithmes d'échelle de liaison nécessaires pour le modèle multi-échelle sont détaillés. L'évaluation de la cohérence et de la validité du modèle multi-échelle est également abordée. Pour garantir l'exigence d'adéquation de la production électrique pour les trajectoires d'investissement, nous appliquons l'optimisation par simulation via des algorithmes d'approximation stochastique, une approche puissante qui combine la modélisation par simulation et les techniques d'optimisation pour résoudre des problèmes complexes. Cette approche est particulièrement interessante lorsqu'il n'est pas possible d'évaluer analytiquement la fonction objective, qui consiste à minimiser l'écart entre la métrique $LOLE$ et la valeur d'adéquation souhaitée, et qui ne peut être estimée que par de multiples simulations. En utilisant des algorithmes d'approximation stochastique, qui reposent sur une séquence d'échantillons aléatoires, cette méthodologie améliore itérativement la solution en adaptant les variables de décision en fonction des retours obtenus des simulations. Les simulations dans ce contexte proviennent du modèle multi-échelle intégré. La motivation derrière le développement d'un tel algorithme sophistiqué est de permettre une "intelligence" - au sens où elle est indépendante du jugement subjectif [2] du modélisateur - qui

[2]Contrairement à la sensibilité de la méthodologie précédente à l'approche d'estimation du crédit de

facilite l'interaction entre les échelles à long et court terme dans le modèle multi-échelle lors de l'exploration de l'espace des solutions. Le développement de ce modèle multi-échelle élimine deux inconvénients importants des modèles de couplage : ils sont chronophages et nécessitent l'intervention humaine à chaque itération, de sorte que la convergence peut ne pas être testée rigoureusement. Les contributions scientifiques actuels ont rapporté une convergence en quelques d'itération. Notre contribution à ce niveau est donc d'utiliser le modèle multi-échelle développé, soutenu par un algorithme d'optimisation basé sur la simulation, pour vérifier que nous sommes en mesure d'atteindre la convergence.

Dans ce chapitre, nous donnons d'abord une introduction à la modélisation multi-échelle, à ses méthodologies connexes et au vocabulaire utilisé pour le développement et la conception du cadre multi-échelle. Ensuite, nous identifions et formulons notre problème : planifier des systèmes électriques futurs sécurisés comme un problème multi-échelle. Les cadres théoriques et computationnels sont développés. Le résultat concluant de ce chapitre est un cadre multi-échelle qui relie l'échelle de planification à long terme du système et l'échelle de l'opération sécurisée à court terme.

capacité du modèleur

## 5.1 Introduction to the multi-scale modeling

Whether explicitly recognized or not, many real-life phenomena and complex systems involve interactions across different temporal and spatial scales. Our concept of time is organized into hourly, daily, monthly, and yearly intervals due to the multi-scale dynamics of our solar system. Similarly, our societies are structured hierarchically across different geographical levels, ranging from towns to cities, countries, and continents. In the domain of modeling, the Fourier Transform is a crucial tool to decompose spatial and temporal functions, such as signals and geometrical shapes, into various spatial and temporal scales. In physics, the behaviors of materials, such as deformation, stress and strain, corrosion failure, and wave propagation, are defined by the characteristics of nuclei and electrons at the microscale. As the study of complex systems, like physical, biological, energy, and chemical systems, becomes increasingly important, the concept of multi-scale modeling has emerged. Multi-scale modeling offers a new scientific approach to investigate and understand these complex systems. It diverges significantly from traditional modeling approaches that focus solely on one scale. Instead, multi-scale modeling takes into account the interactions and interdependencies that exist across different scales, leading to a more comprehensive and accurate representation of real-life phenomena and complex systems.

In various disciplines, such as complex fluids, materials science, applied mathematics, numerical analysis, and biomedical research, significant efforts have been made to develop multi-scale modeling, as evident in numerous publications [207–210]. Notably, in the past 22 years, Google Scholar has indexed 24,000 review articles containing the term "multiscale" in the title, seven times more than the previous decade (3,290 articles in the period 2000-2010). This surge in interest reflects the growing attention of diverse science and engineering communities towards multi-scale modeling [211].

Certain fields, particularly those involving multi-physics, have benefitted from centuries of theory development, and their governing equations have paved the way for multi-scale modeling theories [209, 212]. For instance, in materials science, the field theory that combines quantum and continuum scales enables the study of polymer materials, where the macro-scale behavior relevant for technological applications is highly influenced by microscopic interactions between atoms [213]. Earth system science also leverages multi-scale modeling to understand interactions among different components, such as the ocean, atmosphere, land, and cryosphere, across a wide range of spatio-temporal scales [214]. Clouds, being the largest source of uncertainty in climate models, have been extensively studied using multi-scale modeling frameworks to represent realistic 3D clouds and cloud systems over varying spatial coverage. The Multi-Scale Framework (MMF) model developed by NASA is a significant advancement in comprehending cloud and precipitation behavior across different scales, encompassing cloud microphysical processes to large-scale circulations [215].

However, in certain fields like energy systems and socio-economic domains, multi-scale modeling is still relatively nascent. In a position paper about multi-scale modeling, Alfons Hoekstra emphasized that genuine synergy among scientific communities is a crucial driver for its success, as it inherently requires a multidisciplinary approach [208]. He also highlighted a significant challenge in multi-scale modeling, namely the lack of standardization

in terminology, formal mathematical approaches, and model validations among researchers, making it difficult to reach a consensus on the best practices for developing, sharing, and communicating about multi-scale models. In the following subsections, we propose a definition of the term "multi-scale" and identify the essential components for the development of a multi-scale modeling framework.

### 5.1.1 What is multi-scale modeling?

Before defining the multi-scale modeling, it is essential to address a fundamental question: what is a scale? The term "scale" is interpreted differently across various communities and among scientists. According to the dictionary, scale is an ordered system of numbering or indexing used as a reference standard for measurement, wherein each number corresponds to some physical quantity. However, this definition is incomplete as it excludes non-physical quantities. Clark offers a more comprehensive and generic definition in his analysis of the concept of scale and human dimensions of global change. He uses the term "scale" to encompass the spatial, temporal, quantitative, or analytical dimensions employed by scientists to measure and study objects and processes [216]. This definition allows for the inclusion of more abstract scales, such as monetary and material flow in economic models.

Moreover, Clark notes that the terms "level" and "scale" are often used interchangeably. He defines "levels" as units of analysis located at the same position on a specific scale. In the spatial domain, the most well-known scales are nano, micro, meso, and macro, referring to phenomena of tiny, small, medium, and large sizes, respectively. Similarly, in the temporal domain, short, medium, and long-term are the most relevant levels of scale.

The term "multi-scale modeling" is defined differently in various literature sources [217, 218]. For our specific context, a definition that aligns well is provided by Growen: "Multiscale modeling is a divide-and-conquer paradigm in which multiscale models are built as assemblies of individual unit processes, often also referred to as at-scale models, operating at distinct spatial or temporal scales" [219, 220]. Despite the diversity of definitions, they all share a common understanding that a multi-scale model can be formulated as a compilation of coupled single-scale sub-models. In the context of optimization methods, the decomposition/coordination modeling approach can be seen as a multi-scale approach. This approach is applied to systems where conventional optimization algorithms are not directly applicable due to complexity arising from three main aspects: **Spatial Aspect:** Involves a large number of variables, interconnected subsystems, and heterogeneity. **Temporal Aspect:** Encompasses different time scales and discontinuities in behavior. **Informational Aspect:** Involves multiple decision-makers with different information and objectives. The decomposition phase entails formulating smaller subproblems from an optimization perspective. The coordination phase, on the other hand, focuses on implementing an information exchange process between these subproblems to ensure the successful resolution of the original, complex problem.

### 5.1.2 Multi-scale modeling methods classification

Different classes of multi-scale models have been developed, with many of them originating from the domain of multi-physics multi-scale problems [218]. These multi-scale models can be categorized into two main classes: hierarchical methods and concurrent methods.

- **Hierarchical coupling method:** Also known as sequential (serial or message passing or implicit) methods, this approach links a series of numerical models in which the inputs of the coarse-scale models use the output of the fine-scale models and vice versa. This approach is computationally efficient, as each constituent model performs well to represent its corresponding scale. It is suited for multi-scale problems in which the scales under study are decoupled or weakly coupled.

- **Concurrent coupling method:** This approach consists of building a single combined model considering all the different scales involved in the problem. This is done by incorporating what are known as handshaking procedures that enable the fine-scale models to communicate directly and instantly (not only at the end input/output) with the coarse-scale models and vice versa. Concurrent coupling methods are also called parallel or explicit methods. They are suited for multi-scale problems in which the scales under study are strongly coupled, meaning that the behavior at a given scale depends on what happens in other scales.

Another new wave of multi-scale modeling methodologies exploring recent advances in artificial intelligence has emerged. In a systematic review of multi-scale modeling, the recent two approaches described above are named Multiscale modeling 1.0 and a new era of multi-scale modeling based on machine learning and high-performance computing labeled 2.0 has emerged. By integrating machine learning with multi-scale modeling, modelers can leverage the potential of both and develop efficient frameworks to model complex systems [221–223]. In their review article in Nature, Mark Alber demonstrates that machine learning and multi-scale modeling can be naturally integrated to build robust predictive models that incorporate the underlying physics to solve ill-posed problems and explore massive design spaces [224]. On one hand, machine learning offers valuable tools for enhancing training data, mitigating overfitting, addressing ill-posed problems, constructing surrogate models, and quantifying uncertainty. These capabilities are instrumental in exploring extensive design spaces and uncovering correlations. On the other hand, multi-scale modeling integrates the underlying physics to identify relevant features, explore their interaction, elucidate mechanisms, bridge scales, and understand the emergence of function, with the ultimate goal of predicting system dynamics and identifying causality. Multi-scale modeling and machine learning interact on the parameter level by constraining parameter search space, estimating parameter values, and carrying out sensitivity analysis, and on the system level by exploring the underlying physics and determining system dynamics.

### 5.1.3 Steps to build and implement a multi-scale model

Different attempts to build a generic framework for multi-scale modeling have been conducted in recent years. These developments have been driven by the need for a unified multi-scale theory not tied to a specific field, which would enable better communication among different groups of researchers. To our knowledge, only a few authors have shown interest in such a problem, and two of them caught our attention for their formalism of a "multi-scale theory" independent of the field of application.

The first one is an ontological [3] conceptualization of multi-scale modeling. Aidon Yang and Wolfgang Marquard chose to build their work upon a general conceptualization of the system notion, from which the notions of interest in multi-scale modeling are derived. Based on this conceptual foundation, definitions of multi-scale model structure and classification are then derived [225]. In contrast to existing work, which is mainly inductive - meaning that the general understanding of multi-scale modeling is mainly obtained by generalizing existing applications - this work seems to be deductive. The authors recognize that even with the high level of abstraction used in the formalism, their contribution should not be considered a universally valid classification of multi-scale modeling. Readers interested in a systemic point of view for multi-scale modeling will find interesting definitions and classifications. For our work, we are more interested in "engineering and generic" frameworks that offer a deeper understanding of how multi-scale models could be developed.

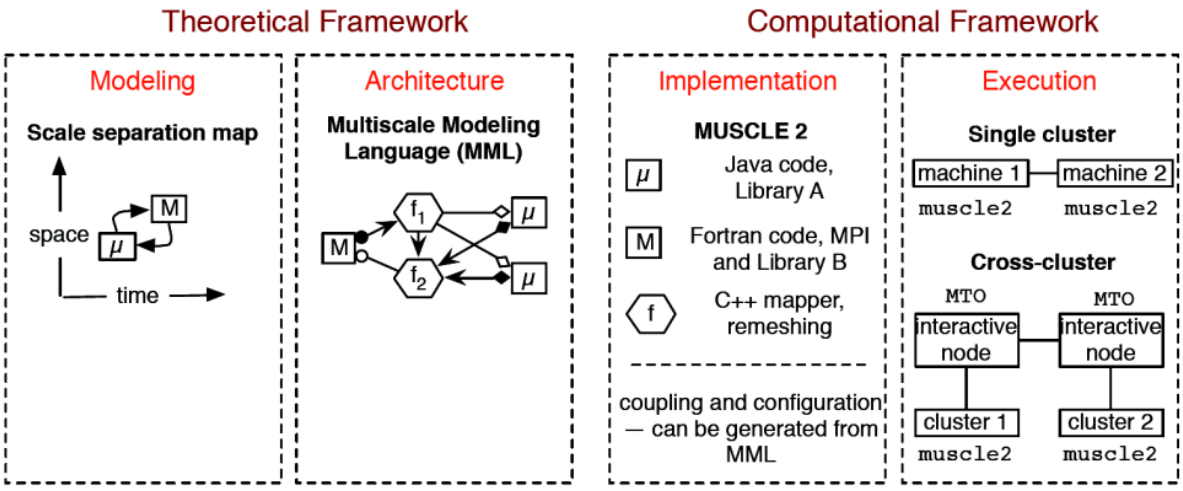


Figure 5.1: The sequence of steps required to create and execute a multiscale application within the Multiscale Modeling and Simulation Framework (MMSF). (credit: [226])

One interesting research supported by the MAPPER project [227] proposed a framework to design, implement, and execute multi-scale models. Named the MMFS, the authors

[3] In the field of computer science, ontology aims to provide a clear and detailed definition of a conceptual framework representing a specific subject area or domain of discussion.

formalize a generic multi-stepped (from design to execution) process to build multi-scale models [226]. Figure 5.1 depicts all the necessary steps proposed by the authors to build the multi-scale model. Based on their formalism, the first step consists of identifying the relevant scales and the relevant processes (and hence the constituent sub-models) involved in the problem. After that, the authors proposed a Multiscale Modeling Language describing the architecture of the multiscale model. It is based on graphical representation and an XML language to help multiscale developers establish the set of scales and their related sub-models, their coupling, the type of coupling, and information transfer type and rate (input/output data exchange).

The second step concerns the implementation of each sub-model or the reuse of existing ones, as well as the implementation of the scale bridging techniques. Existing models will require some additional changes to enable their coupling with other models, while bridging scale techniques will need to be implemented specifically to support the coupled models. The bridging scale method implementation is constituted of three constructs: plain conduits, filters, and mappers. Plain conduits are simply channels to transfer information, whereas filters modify the information exchanged according to the scales of the submodels they are connected to. Mappers allow combining inputs from different conduits and producing multiple outputs. Their multi-scale formalism and framework have been interestingly applied to various applications from different disciplines of science and engineering.

### 5.1.4 Important challenges in multi-scale modeling

The development of a solid foundation for multi-scale modeling is facing multiple challenges that must receive considerable attention during the development of a multi-scale model. Various authors have discussed the challenges they are facing in their respective disciplines [228, 229]. Despite the differences in application, most authors share the same challenges regarding the use of multi-scale modeling. Here is a brief summary of some challenges associated with multi-scale modeling gathered from three important articles:

1. Models construction at different scales and calibration: The construction of sub-models is a crucial step in multi-scale modeling. Determining the appropriate level of complexity for each sub-model to accurately describe the processes under study requires careful consideration. Before proceeding with coupling, a precise understanding of each sub-model is essential. This includes the mathematical formulation, underlying assumptions, and required data, which will help define the model's capabilities and limitations. To achieve this, multi-scale model developers must be well-informed about the specific modeling challenges associated with each problem. Once the construction and understanding of sub-models are achieved, the next challenge is to choose or estimate appropriate parameters and initial values, a process known as model calibration. Data plays a vital role in providing exogenous parameters and initial values for calibration. Iterative procedures are often employed to obtain well-calibrated models that accurately represent the problems under study.

2. Numerical Implementation and Solution: Multi-scale models are analytically intractable

and need to be solved numerically. Modelers seek efficient, stable, and accurate numerical solutions for these complex models. The coupling of multiple models across different scales involves numerically estimated parameters, which can lead to numerical instabilities in the final solution. Careful consideration must be given to the numerical implementation choices, such as choosing appropriate numerical schemes for models with differential equations and selecting suitable solvers and algorithms for models involving optimization problems.

3. Consistency and Error Propagation Analysis: The coupling of different sub-models through scale-bridging techniques can introduce errors, especially at the interfaces where data is exchanged. Error propagation occurs when errors from one model affect the results of another model. This can lead to numerical instabilities in the multi-scale model. Assessing error propagation is essential but can be challenging, especially for numerically solved models. Different works on error analysis and consistency of multi-scale models have been conducted, but the analysis seems to be highly dependent on the field of application. Using uncertainty quantification and sensitivity analysis techniques may help assess error propagation in multi-scale models.

4. Model Validation: Once the multi-scale model is built and numerically functional, validation becomes crucial. Modelers often validate their models by comparing the model results with experimental data or observations. Qualitative and quantitative comparisons can be used to validate the multi-scale model's outcomes. However, there is an ongoing challenge on how to validate multi-scale models effectively. One approach could involve developing a set of metrics and corresponding thresholds. Each metric would indicate how well the multi-scale model reproduces the process under study. The model is considered valid if the metrics fall within the defined thresholds (upper or lower bounds).

In the next sections, we present the theoretical framework of the multi-scale model. We start by providing a concise formulation of the two sub-models used. Despite their distinct formulations, both sub-models share the same optimization paradigm. This commonality allows us to formulate the constituent problems in a unified manner, leading to a mathematical representation of the multi-scale model. For simplicity, we divide the overall multi-scale model into two parts: the uni-directional and bi-directional models.

The uni-directional multi-scale model is designed to transfer investment trajectories determined by [**TIMES**] to [**ANTARES**], while ensuring data consistency at various levels. On the other hand, the bi-directional multi-scale model is developed to meet power generation adequacy requirements by exchanging data between [**ANTARES**] and [**TIMES**]. Throughout each stage, several bridging scale algorithms and methods have been developed to facilitate the seamless integration of the sub-models and ensure effective information exchange.

## 5.2 Problem statement as a multi-scale problem

### 5.2.1 Multi-scale problem statement and formulation

In this section, we approach the thesis problem as a multi-scale problem, utilizing the vocabulary and methodologies discussed in the previous section. The technical background and relevant state-of-the-art information required to comprehend the problem were extensively covered in the second and third chapters. Our objective in the following paragraphs is to present a mathematical formulation of the problem under study and to outline the essential steps for constructing the multi-scale model.

Firstly, we formulate the specific question to be answered: **In the context of transitioning to a low-carbon power system, how can we determine optimal long-term investment trajectories that ensure short-term operational security?** Each term in the question holds significance, and the multi-scale problem we are tackling arises from the interplay between long-term planning and short-term operational requirements. The context of the transition to low-carbon power systems sets the planning horizon for the long-term. IWe define operational security solely in terms of power generation adequacy, excluding considerations of stability and other technical aspects. Though not explicitly stated, the spatial scale is implicitly defined by the power system topology, either multi-area or single-area. For this work, we focus on country-level scales for both planning and operational stages, rendering our multi-scale problem a temporal one.

Secondly, as mentioned in the previous section, we need to create a "scale separation map" to visualize the different scales and processes involved. The scale separation map is a powerful tool that defines ranges (represented as rectangles) of the various scales that must be addressed to solve the problem at hand. It becomes evident that to fully resolve our problem, we need to consider a broad temporal domain, spanning from seconds for operational aspects to decades for planning. However, the advantage of multi-scale modeling lies in its ability to "divide" the domain and retain only the relevant parts. In this work, our split strategy

involves focusing on operational aspects at an **hourly temporal scale**, which is essential for power generation adequacy studies, and adopting a **multi-annual scale** (coupled with a coarser temporal scale representing operational variability) for long-term planning. Figure 5.2 bellow depicts the different scales for the power system operation and planning.

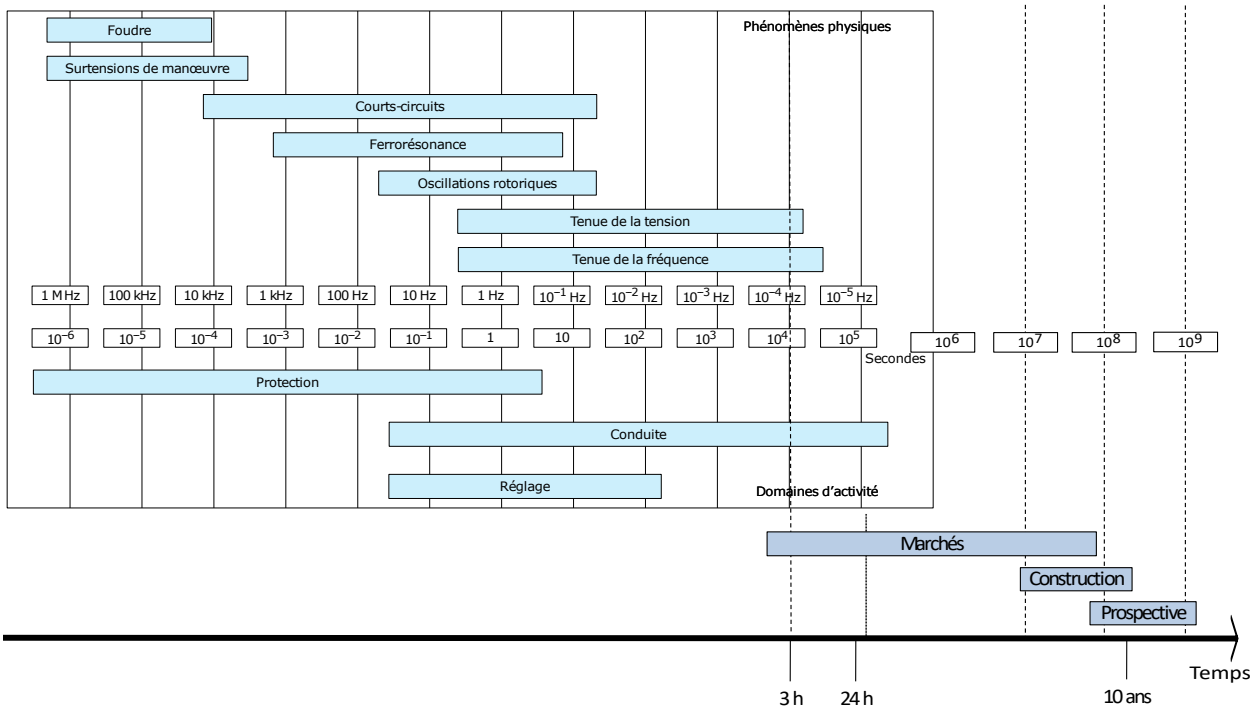


Figure 5.2: The scale separation map illustrating the process of "scale splitting": the multi-scale domain is decomposed into several "single-scale"

Once the scale separation map is precisely defined, the selection of sub-models for each reduced range of scales becomes crucial. In addressing complex issues related to power system planning and operation, numerical modeling has emerged as a prominent approach. Different modeling methodologies have been developed to handle the relevant problems at each temporal scale. These methodologies fall into two classes: long-term energy system planning models and short-term operational power system models. The former, employing an optimization framework, encompasses studies concerning the power system's evolution over the long term (20-100 years ahead). The latter, based on optimization and simulation frameworks, focuses on the technical, economic, and environmental aspects of power system operation. For our research, we have chosen the TIMES framework for the long-term planning component and the ANTARES simulator for the short-term operational component (as elaborated in Chapter 3). The coupling between these models, denoted as [**TIMES**]↔[**ANTARES**], will be elaborated in detail in the theoretical framework section.

In this chapter, we adopt an efficient hierarchical approach to multi-scale modeling. The two models, [**TIMES**] and [**ANTARES**], interact in a two-way manner, exchanging data without sharing any part of their problem formulations. This approach ensures the models

maintain their autonomy and independence while effectively interacting to address the multi-scale problem at hand. Finally, the formulation of the multi-scale problem is as follows: Given a specific long-term transition scenario $s$, the objective is to find an optimal investment trajectory $\Pi_{inv}^{TIMES,s}$ determined by [**TIMES**] that satisfies the power generation adequacy requirements assessed by [**ANTARES**]. The key adequacy metric used is the $LOLE$ (see Chapter 2 for the definition). Mathematically, for a long-term transition scenario $s$, a time-frame $T$ (e.g., 2016-2050) decomposed into $n$ milestone-periods, and a set of regions $R$, the goal is to find a reliable capacity investments trajectory $\Pi_{inv}^{TIMES,s}$ that satisfies Equation 5.1.

$$\Pi_{inv}^{TIMES,s} = \{X_t^s = \cup_{r \in R} X_{r,t}^s | LOLE_{r,t}^s < \zeta_{r,t}\}_{t \in T} \tag{5.1}$$

Here, $X_{r,t}^s$ refers to the power generation mix (i.e., installed capacities) determined for the transition scenario $s$ in a specific region $r$ at period $t$, and $X_t^s$ represents the overall power generation mix across all regions. $LOLE_{r,t}^s$ denotes the Loss of Load Expectation metric for region $r$ and period $t$, and $\zeta_{r,t}$ represents the adequacy requirement limit. For the sake of notation simplicity, we omit the $s$ index in the notation for $X$, $LOLE$, and $\zeta$.

### 5.2.2 The long-term energy system planning model: The TIMES optimization problem

The optimization problem in the [**TIMES**] model is defined using abstract variables and mathematical equations. These variables and equations are created using sets and parameter values that represent the characteristics of an energy system for each unique region within the model. The primary objective is to find the optimal combination of technologies in each time period that can meet the customer demand while minimizing the total cost. The optimization problem utilizes linear programming techniques, and Equation 5.2 presents a simplified form of the objective function for an inelastic and deterministic TIMES model.

**Main decision variables:** TIMES have nearly 26 variable decisions, only the main important decision variables for the modeling of the power system are presented here.
Process related: For a process $p$, three main decision variables are important: newly installed capacities (*ncap* in [GW]), total installed capacities (*capt* in [GW]), and the level of its activity (*act* in [PJ]). It is possible to add a vintage option for process. This option enables the assignment of technical attributes to the time when the capacity was initially installed, rather than the current time period, denoted as $t$. Process are not vintaged in a default setting.
Commodity related: For a commodity $c$, the imported or exported quantities (*trade* in [PJ]), or the quantities extracted from mining or the potential for renewables.
Flow oriented: flow of a commodity $c$ in or out of a process $p$ ($flow$ in [PJ]).
Storage related: flow of a commodity $c$ in ($in$) or out ($out$) of a storage process.

**Objective function:** The major cost components in [**TIMES**] include investment costs, costs for sunk material during construction time, variable costs, fixed operating and maintenance costs, surveillance costs, decommissioning costs, taxes, subsidies, recuperation of sunk material, and salvage value. The objective function parameters encompass cost documentation of investments made before the first model year, technical and economic lifetimes, investment and decommissioning lead-times, and general and technology-specific discount rates. The equilibrium computed over the study horizon ensures the maximization of both the supplier's and consumer's surplus, making total cost minimization equivalent to total net surplus maximization. It is important to note that the salvage value is considered a payback from the investment and is therefore defined as negative.

$$\min_{r,y} NPV = \sum_{r\in R}\sum_{t\in T}(1+\alpha(r))^{t_{ref}-t} * \begin{cases} INVCOST(r,t) + INVTAXSUB(r,t) + INVDECM(r,t) + \\ INVXCOST(r,t) + FIXTAXSUB(r,t) + SURVCOST(r,t) + \\ VARCOST(r,t) + VARTAXSUB(r,t) + ELASTCOST(r,t) - \\ LATEREVENUES(r,t) \end{cases} - SALVAGE(t,t_{ref}) \tag{5.2}$$

$INVCOST$ represents the portion of the cost objective for year $t$ and region $r$ that corresponds to investments occurring in the year the investment is decided and/or during its installation lead-time. Within TIMES, four investment cases are implemented to represent the flow of payments and revenues ([230]). These cases differentiate between small and large projects and consider the project's technical life and when the investment occurs. For

detailed algorithms implemented in each case, readers can refer to [230]. $INVTAXSUB$ represents the portion of the cost objective function for year $t$ and region $r$ that corresponds to investment taxes and subsidies. It is assumed that taxes/subsidies on investments occur at the same time as the investment. $INVDECOM$ represents the portion of the cost objective function that corresponds to capital costs linked to the decommissioning of a process. It is important to highlight that decommissioning occurs at the end of the process's life and may also be delayed by a user-defined lag period. The corresponding costs follow the same rules as those for investment costs. $FIXCOST$ represents the portion of the cost objective function that corresponds to fixed annual costs. These expenses are considered to be incurred in the same year that the facility becomes operational. The term $FIXTAXSUB$ pertains to taxes and subsidies associated with fixed annual expenses. $VARCOST$ represents the portion of the cost objective function that corresponds to variable annual costs. These costs are computed assuming that each activity has a constant activity cost over a given period $t$. $VARTAXSUB$ represents variable annual taxes and subsidies. $ELASTCOST$ represents the portion of the cost objective function that corresponds to the cost incurred when demands are reduced by price elasticity. $LATERREVENUES$ represent the segment of the objective function responsible for delayed revenues resulting from recycling materials from decommissioned processes that take place beyond the end-of-horizon period. $SALVAGE$ signifies the segment of the cost objective function that pertains to the residual value of investments and other non-recurring expenses. This value is discounted to the base year denoted as $tref$.

**Constraint:**

**Transfer capacity constraint** This equation sums the investments (*ncap*) that have been initiated in the current and prior periods and are still in effect in the current period and past investments being made before the beginning of the model horizon and either assigns it to the capacity variable *cap* or applies directly lower or upper capacity bounds to it.

$$\forall r \in R, \forall t \in T, \forall p \in P,$$
$$capt(r,t,p) = resid(r,t,p) + \sum_{(t-t_0)\leq t'} ncap(r,t',p) \tag{5.3}$$

- $resid(t,t,p)$: is the residual existing capacity stock of process $p$ still available in the period $t$. Its value is determined by the installed capacity in the base year (before the first period in the time-frame) and its life-time and the profile of its evolution given by the modeler.
- $capt(r,t,p)$: total installed capacity of the process $p$ ([PJ/year] for the energy process and in [GW] for power generation plants).
- $t_0 = life(r,t',p)$ the technical lifetime
- $(t - t_0 \leq t^{'})$ a condition ensuring to account only new investments on process still available at the period $t'$
- $ncap(r,t',p)$: new installed capacity of the process $p$ at period $t'$

**Activity-flow constraint** The activity-flow constraint establishes a relationship between the activity variable ($act$) and the fundamental flows associated with a process. These primary flows are user-defined for each specific process $p$.

$$\begin{gathered} \forall r \in R, \forall v \in V, \forall t \in T, \forall p \in P, \forall s \in S \\ act(r,v,t,p,s) = \sum_{c \in PCG} \frac{flow(r,v,t,p,s,c)}{actflo(r,v,p,c)} \end{gathered} \tag{5.4}$$

- $V$: the set of vintage year.
- $S$: the set of time-slices.
- $act(r,v,t,p,ts)$: the level of a activity of the process $p$ at the time-slice $ts$ in [PJ].
- $PCG$: The primary commodity group defining the input and and output commodities of the process $p$.
- $flow(r,v,t,p,ts,c)$: the quantity of a consumed or produced commodity of the process $p$.
- $actflo(r,v,p,c)$: conversion factor equal to the flow unit per activity unit (usually equal to 1).

**Capacity-activity constraint** The capacity-activity equation relates the activity of a process to its capacity in period $t$. The availability of the existing capacity during a particular time period $t$ and time-slice $ts$ is determined by the availability factor.

$$\begin{gathered} \forall r \in R, \forall v \in V, \forall t \in T, \forall p \in P, \forall s \in S \\ act(r,v,t,p,s) \leq af(r,v,t,p,s) cap2act(r,p) fr(r,s) cap(r,v,t,p) \end{gathered} \tag{5.5}$$

- $af(r,v,t,p,s)$: availability factor of the process $p$
- $cap2act$: conversion factor between the capacity unit and activity unit. For an activity in PJ and a capacity in GW, the conversion factor is equal to 31,536.
- $fr(r,s)$: the duration fraction of the time-slice $ts$ in the year.
- $cap(r,v,t,p)$: installed capacity of the process $p$ at period $t$.

**Commodity balance constraint:** This equation ensures that, for each time period and time-slice, the total procurement of a commodity matches its total disposition. Commodity procurement can occur through various means, such as imports, production via technologies (activity and capacity-based), or release during the retirement of certain investments. Similarly, commodities can be disposed of in various ways, including exports, consumption by technologies (activity or capacity-based), consumption by demand, or being "sunk" at the time of process investment. The default condition for the balance constraint of an energy carrier and emissions is set to $\geq$, allowing procurement to exceed disposition if necessary. This

flexibility helps prevent infeasibilities that may arise from inflexible processes with multiple inputs or outputs.

$$\forall r \in R, \forall v \in V, \forall t \in T, \forall c \in C, \forall s \in S$$

$$\eta(r,t,c,s)\Big(\sum_{p\in P, c\in OUT(p)} (flow(r,v,t,p,c,s) + stg_{eff}(r,v,p)sout(r,v,t,p,c,s)$$

$$+ \sum_{p\in P, c\in IMP(p)} trade(r,t,p,c,s,"imp") + \sum_{p\in P} release(r,t,p,c)ncap(r,t,p,c)\Big)$$

$$\geq \sum_{p\in P, c\in IN(p)} (flow(r,v,t,p,c,s) + sin(r,v,t,p,c,s))$$

$$+ \sum_{p,c\in EXP(p)} trade(r,v,t,p,c,s,"exp") + \sum_{p\in P} sink(r,t,p,c)ncap(r,t,p,c) + fr(r,s,c)dm(c,t) \tag{5.6}$$

- $IN(p)/OUT(p)$ the set of input and output commodities of the process $p$
- $EXP(p)/IMP(p)$: set of imported or exported commodities through process $p$;
- $\eta(r,t,c,ts)$: the efficiency of transportation of the commodity $c$ through the system, for example the efficiency of the transportation and transmission of electricity.
- $stg_{eff}(r,v,p)$: efficiency of the storage process $p$;
- $sout(r,v,t,p,c,ts)$: the quantity of commodity $c$ discharged by the storage process $p$
- $sin(r,v,t,p,c,ts)$: the quantity of commodity $c$ charged by the storage process $p$
- $trade(r,t,p,c,ts,"imp"/"exp")$: quantity of commodity $c$ imported or exported by the region $r$ through the exchange process $p$
- $release(r,t,p,c)$: The quantity of commodity $c$ per unit of capacity released when a process $p$ is decommissioned.
- $release(r,t,p,c)$: Amount of commodity $c$ per unit of capacity needed during the construction of a process (important parameter to represent the needed quantity of a material or energy for the construction of a process).
- $fr(r,s,c) \in [0,1]$: Fraction of the consumed or produced quantity of the commodity $c$ occurring in times-slice $s$ (for a commodity without time-slice definition $fr(r,s,c) = 1$)
- $dm(c,t)$: commodity demand projection at the period $t$.

**Demand balance constraint:** The constraint to satisfy the demand of a given commodity $c$ is the same as the commodity balance equation. This constraint ensures that at each period $t$ and time-slice $s$ the production of the commodity $c$ must be greater or equal than the demand.

**All constraints description:** Table 5.1 describe all the constraints available in the [**TIMES**] model.

| Constraint | Description |
|---|---|
| $EQ(l)_{ACTBND}$ | Bound on the activity of a process |
| $EQE_{ACTEFF}$ | Equality relationship that defines the activity efficiency of a process |
| $EQ_{ACTFLO}$ | Equality relationship that defines the activity of a process in terms of its flow variables |
| $EQ_{ACTPL}$ | Defines the efficiency deterioration of a process at partial loads |
| $EQ_{ACTRAMP}$ | Defines bounds on the ramping of process activity, in proportion to its online capacity, in either direction (LO/UP) |
| $EQL_{ACTUPC}$ | Sets a lower limit on the successive on-line / off-line hours of capacity |
| $EQE_{ACTUPS}$ | Expresses that the change in process on-line capacity between successive time-slices must be equal to the capacity started-up–shut-down |
| $EQL_{ACTUPS}$ | Expresses that the sum of process started-up capacity over a cycle must be at least equal to the max. amount of capacity put off-line in the cycle |
| $EQ(l)_{ASHAR}$ | Establishes advanced share constraints between process flows |
| $EQ(l)_{BLND}$ | Special blending constraints used to specify the composition of refined oil products |
| $EQ_{BNDCST}$ | Establishes a variable representing the cumulative amount of process costs, taxes and/or subsidies over a time interval, for defining a bound |
| $EQ(l)_{BNDNET}$ | Bound on the net amount (production minus consumption) of a commodity |
| $EQ(l)_{BNDPRD}$ | Bound on the total production of a commodity |
| $EQ(l)_{CAFLAC}$ | Relates the flows in the primary group of a process to its available capacity; may be rigid (=) or flexible ($\leq$) |
| $EQ(l)_{CAPACT}$ | Relates the activity of a process to its available capacity; may be rigid (=) or flexible ($\leq$,$\geq$) |
| $EQL_{CAPFLO}$ | Relates a flow not in the primary group of a process to its available capacity; only an upper bound for the flow $\leq$ is supported |
| $EQ_{CAPLOAD}$ | Relates the activity of a process to its available on-line capacity in each timeslice; only for processes with flexible availability ($\leq$,$\geq$) |
| $EQ(l)_{CPT}$ | Calculates the current capacity of a process in terms of all past and current investments in that process |
| $EQ(l)_{COMBAL}$ | Balance equation of a commodity |
| $EQE_{COMPRD}$ | Definition of the total production of a commodity |
| $EQ_{CUMFLO}$ | Bound on the cumulative flow or activity of a process over a time interval |
| $EQ_{CUMNET}$ | Bound on the cumulative production of a commodity over a time interval |
| $EQ_{CUMPRD}$ | Bound on the cumulative net quantity of a commodity over a time interval |
| $EQ_{CUMRET}$ | Establishes a variable representing the cumulative amount of retired capacity of a process |
| $EQ_{DSCNCAP}$ | These two constraints ensure that some investments may only be made in certain discrete sizes |
| $EQ_{DSCRET}$ | Ensures that early capacity retirements may only be made in multiples of a certain discrete block size |
| $EQ(l)_{FLOBND}$ | Bound on the sum over a commodity group, of the commodity flows of a process |
| $EQ(l)_{FLOFR}$ | Relationship between a flow in one timeslice and the annual flow, for a given process |
| $EQ(l)_{FLMRK}$ | Expresses for a given commodity that the amount produced/consumed by a process is tied to the total amount produced/consumed of that commodity |
| $EQ_{IRE}$ | Expresses that imports of a commodity by region r must be equal to all exports by other regions to region |
| $EQ_{IREBND}$ | Bound on exchange of a commodity between two regions |
| $EQ_{XBND}$ | Bound on total exchanges of a commodity by one region |
| $EQ(l)_{INSHR}$ | For a given process, expresses that the inflow of a commodity is tied to the total inflows of all commodities in a certain group |
| $EQ(l)_{OUTSHR}$ | For a given process, expresses that the outflow of a commodity is tied to the total outflows of all commodities in a certain group |
| $EQ_{PEAK}$ | Expresses that capacity available must exceed demand of a selected commodity in any time slice by a certain margin |
| $EQ_{PTRANS}$ | Establishes an equality relationship between (groups of) inputs and certain (groups of) outputs of a process |
| $EQL_{SCAP}$ | Bounds the amount of capacity salvaged if early retirements are active. |
| $EQ_{STGAUX}$ | Establishes an equality relationship between storage main flows or activity and an auxiliary storage flow |
| $EQ_{STGIPS}$ | Ensures the storage of a commodity between two time periods |
| $EQ_{STGTSS}$ | Ensures the storage of a commodity between two timeslices |
| $EQ(l)_{STGIN}$ | Bounds the input into a storage process |
| $EQ(l)_{STGOUT}$ | Bounds the output of a storage process |
| $EQ_{STSBAL}$ | Defines balances between timeslice levels in a general timeslice storage |
| $EQ(l)_{UCRTP}$ | Defines a dynamic bound on the growth / decay in the installed capacity, new capacity or activity of a process over successive periods |
| $UC_{SLH}$ | User defined constraints that have a user defined constant RHS timeslice-dynamic |
| $UC$ | User defined constraints that involve only a single region rand period $t$ but both timeslice sand the preceding timeslice $s$–$rs_stg(r,s)$ |
| $UC_{d,t,t+1}$ | User defined constraints that involve both period t and the succeeding period $t+1$ |
| $UC_{d,t,t-1}$ | User defined constraints that involve both period t and the preceding period $t$–1 |

Table 5.1: Description of [**TIMES**] constraints

### 5.2.3 The short-term operational model: The ANTARES optimization problem

The ANTARES problem [**ANTARES**], can be defined on a graph involving up to a few hundreds of region-sized nodes, tied together by edges whose characteristics summarize those of the underlying power grid. The ultimate goal is to determine the optimum hydro/thermal power dispatch in each hour of the year that will satisfy the customer demand at a minimum possible total cost. The major cost components included in [**ANTARES**] are the cost related to transmission, hydro, thermal, unsupplied energy and spillage. The sets, input parameters and decision variables are summarized in Table 5.2.

| Symbol | Description |
|---|---|
| **Grid** | |
| $k \in K$ | optimization periods (weeks) over which [**ANTARES**] are defined |
| $t \in T$ | individual time steps of any optimization period k (hours of the week) |
| $G(N, L)$ | undirected graph of the power system |
| $n \in N$ | vertices of G, N is an ordered set |
| $l \in L$ | edges of G |
| $A$ | incidence matrix of G (dimension $N * L$) |
| $g$ | spaning tree of G |
| $C_g$ | cycle matrix associated with g (dimension $L * (L + 1 - N)$) |
| $L_n^+ \subset L$ | set of edges whose n is the upstream vertex |
| $L_n^- \subset L$ | set of edges whose n is the upstream vertex |
| $u_l \in N$ | vertex upstream from l ($l \in L_{u_l}^+$) |
| $d_l \in N$ | vertex downstream from l ($l \in L_{d_l}^-$) |
| $u \cdot v$ | inner product of vector u and v |
| $u_\uparrow^o \in \mathbb{R}^{Size}$ | vector resulting from the permutation on $u \in \mathbb{R}^{Size}$ : $u_{\uparrow_i}^o = u_{(i+o)mod(Size)}$ |
| **Thermal Units** | |
| $\theta \in \Theta_n$ | thermal clusters (sets of identical units) installed in $n$ |
| $\Theta$ | set of all thermal clusters of the power system $\Theta = \cup_{n \in N} \Theta_n$ |
| $\bar{P}_\theta \in \mathbb{R}_+^T$ | maximum power output from cluster $\theta$ (depends on units availability) |
| $\underline{\mathrm{P}}_\theta \in \mathbb{R}_+^T$ | minimal power output demanded from cluster $\theta$ (units availability allowing) |
| $\chi_\theta \in \mathbb{R}^T$ | running unit in $\theta$: cost proportional to the output (reference conditions) |
| $\sigma_\theta^+$ | start up cost of a single unit in cluster $\theta$ |
| $\sigma_\theta^+$ | shutting down cost of a single unit in cluster $\theta$ |
| $\tau_\theta^+$ | running unit $\theta$: cost independent from output level (a.k.a NoLoadHeatCost) |
| $l_\theta$ | unit in $\theta$: minimum stable power output when running |
| $u_\theta$ | unit in $\theta$: maximum net power output when running |
| $\Delta_\theta^+ \in 1 : \lvert T \rvert$ | unit in $\theta$: minimum on time when running |
| $\Delta_\theta^- \in 1 : \lvert T \rvert$ | unit in $\theta$: minimum off time when not tuning |
| $\Delta_\theta = \max(\Delta_\theta^+, \Delta_\theta^-)$ | duration above which both state changes are allowed |
| $M_\theta \in \mathbb{N}^T$ | number of running units in cluster $\theta$ |
| $\bar{M}_\theta \in \mathbb{N}^T$ | maximum number of running units in cluster $\theta$ |
| $\underline{\mathrm{M}}_\theta \in \mathbb{N}^T$ | minimum number of running units in cluster $\theta$ |
| $M_\theta^+ \in \mathbb{N}^T$ | number of units changing from off state to on state in cluster $\theta$ |
| $M_\theta^- \in \mathbb{N}^T$ | number of units changing from on state to off state in cluster $\theta$ |
| $M_\theta^{--} \in \mathbb{N}^T$ | number of units changing from state on to state outage in cluster $\theta$ |
| **Reservoir-Hydro units** | |
| $\lambda \in \Lambda_n$ | reservoirs connected to node $n$ |
| $\bar{W}_\lambda \in \mathbb{R}_+$ | nominal maximum energy output from $\lambda$ throughout the optimization period |
| $\underline{\mathrm{W}}_\lambda \in \mathbb{T}_+$ | nominal minimum energy output from $\lambda$ throughout the optimization period |
| $\bar{H}_\lambda \in \mathbb{R}_+^T$ | maximum power output from reservoir $\lambda (\sum_{t \in T} \bar{H}_{\lambda_t} \geq \underline{\mathrm{W}}_\lambda)$ |
| $\underline{\mathrm{H}}_\lambda \in \mathbb{R}_+^T$ | maximum power output from reservoir $\lambda (\sum_{t \in T} \underline{\mathrm{H}}_{\lambda_t} \geq \bar{W}_\lambda)$ |
| $H_\lambda \in \mathbb{R}_+^T$ | nominal power output from reservoir $\lambda$ |
| $\rho_\lambda \in \mathbb{R}_+^T$ | the highest possible ratio between the peak output power and the daily average output power. $(1 \leq \rho_\lambda \leq 24)$ |
| $\epsilon_\lambda \in \mathbb{R}_+^T$ | water value (shadow price) of power outputs from reservoir $\lambda$ |
| **Demand, unsupplied and spilled energy** | |
| $D_n \in \mathbb{R}^T$ | net power demand expressed in node n (demand -(wind + solar + must run generation)) |
| $\gamma_n^+ \in \mathbb{R}_+^T$ | normative unsupplied energy in node n corresponding to the Value of Load Loss (VoLL) |
| $G_n^+ \in \mathbb{R}_+^T$ | unsupplied power in the nominal state |
| $\gamma_n^- \in \in \mathbb{R}_+^T$ | normative spilled energy in node n corresponding to the Value of wasted energy |
| $G_n^- \in \mathbb{R}_+^T$ | spilled power in the nominal state |

Table 5.2: Description of the ANTARES sets, parameters and decision variable

The [**ANTARES**] can be formulated as follows [193].

$$\underset{M_\theta \in ArgMin(\Omega_{Unitcom})}{\text{minimize}} \quad \Omega_{DISPATCH} = \begin{cases} \Omega_{transmission} = \sum_{l\in L}(\gamma_l^+ \cdot F_l^+ + \gamma_l^- \cdot F_l^-)+ \\ \Omega_{hydro} = \sum_{n\in N}\sum_{\lambda\in\Lambda_n} \epsilon_\lambda \cdot H_\lambda + \\ \Omega_{thermal} = \sum_{n\in N}\sum_{\theta\in\Theta_n}(\chi_\theta \cdot P_\theta + \\ \sigma_\theta^+ \cdot M_\theta^+ + \sigma_\theta^- \cdot M_\theta^- + \tau_\theta \cdot M_\theta)+ \\ \Omega_{unsupplied} = \sum_{n\in N} \gamma_n^+ \cdot G_n^+ + \\ \Omega_{spillage} = \sum_{n\in N} \gamma_n^- \cdot G_n^- \end{cases} \tag{5.7a}$$

$$\text{subject to} \quad \sum_{l\in L_n^+} F_l - \sum_{l\in L_n^-} F_l = (G_n^+ + \sum_{\lambda\in\Lambda} H_\lambda + \sum_{\theta\in\Theta_n} P_\theta) - (G_n^- + D_n), \tag{5.7b}$$

$$G_n^+ \leq \max(O, D_n), \tag{5.7c}$$

$$G_n^- \leq -\min(O, D_n) + \sum_{\lambda\in\Lambda_n} H_\lambda + \sum_{\theta\in\Theta_n} P_\theta, \tag{5.7d}$$

$$F_l^+ \leq C_l^+, \tag{5.7e}$$

$$F_l^- \leq C_l^-, \tag{5.7f}$$

$$F_l = F_l^+ + F_l^-, \tag{5.7g}$$

$$\underline{\mathrm{W}}_\lambda \leq \sum_{t\in T} H_{\lambda_t} \leq \bar{W}_\lambda, \tag{5.7h}$$

$$\underline{\mathrm{H}}_\lambda \leq H_\lambda \leq \bar{H}_\lambda, \tag{5.7i}$$

$$\max_{t\in(24k+1:24k+24)} H_{\lambda_t} \leq \rho_\lambda \sum_{t\in(24k+1:24k+24)} H_{\lambda_t}, \tag{5.7j}$$

$$\underline{\mathrm{P}}_\theta \leq P_\theta \leq \bar{P}_\theta, \tag{5.7k}$$

$$\underline{\mathrm{M}}_\theta \leq M_\theta \leq \bar{M}_\theta, \tag{5.7l}$$

$$l_\theta M_\theta \leq P_\theta \leq u_\theta M_\theta, \tag{5.7m}$$

$$M_{\theta_t} = M_{\theta_{t-1}} + M_{\theta_t}^+ - M_{\theta_t}^-, \tag{5.7n}$$

$$M_{\theta_t}^{--} \leq M_{\theta_t}^-, \tag{5.7o}$$

$$M_{\theta_t}^{--} \leq \max(0, \bar{M}_{\theta_{t-1}} - \bar{M}_{\theta_t}), \tag{5.7p}$$

$$M_{\theta_t} \geq \sum_{k=t+1-\Delta_\theta^+}^{k=t} (M_{\theta_k}^+ - M_{\theta_k}^{--}), \tag{5.7q}$$

$$M_{\theta_t} - \bar{M}_{\theta_{t-\Delta_\theta^-}} \geq \sum_{k=t+1-\Delta_\theta^-}^{k=t} \max(0, \bar{M}_{\theta_k} - \bar{M}_{\theta_{k-1}}) - \sum_{k=t+1-\Delta_\theta^-}^{k=t} M_{\theta_k}^- \tag{5.7r}$$

**Objective function:** The model minimizes the overall system operation cost, considering all proportional and non-proportional generation expenses, alongside transmission fees and external costs like the expense associated with energy not supplied (generation shortage) or, conversely, the cost of spilled energy (generation excess).

**Constraints:** The model is subject to different constraints representing the participation of all power system components to the supply/demand balance. Equation 5.7b is the first Kirchhoff's law representing the hourly balance between generation and demand. The unsupplied power on each grid node is bounded by the excess positive demand (equation 5.7c). Similarly, the excess electricity generation that spills over on each node is capped by the total generation capacity of that node, including both must-run and dispatchable power sources (as specified in equation 5.7d). Flows are bounded by the sum of initial capacity (equations 5.7e 5.7f 5.7e). Three constraints are specified for the hydro-reservoir power. Equation 5.7h set a bound on the energy produced throughout the optimization period. Equation 5.7i set a bound on the called power. Equation 5.7j set bounds on the intra-daily power modulations. The remaining constraints pertain to thermal power generation (Equation 5.7m). The number of running units is bounded (Equation 5.7l). Power output remains within limits set by minimum stable power and maximum capacity thresholds (Equation 5.7m). Minimum running and not-running durations constraints are expressed in equations (Equations 5.7o, 5.7p,5.7q,5.7r).

### 5.2.4 Models uniform formulation: A matrix representation

As seen in previous sections, both models have different optimization formulations. To build a mathematical formulation of the developed multi-scale framework, a unified formulation based on matrix representation is used. This uniform formulation has the advantage of providing a common presentation for both models, thereby facilitating the development of the multi-scale model.

Table 5.3 presents all the essential sets, parameters, and main decision variables required for the development of the new multi-scale framework.

| Symbol | Description |
|---|---|
| **Sets** | |
| $R$ | Set of internal regions indexed by $r$ (region) |
| $T$ | Set of representative years (middle years) for the model periods within the planning time-frame indexed by $t$ (time). $y_{ref}$ is the base year |
| $S$ | Set of all time-slices (define the sub-annual divisions of a period) representing the variability in supply and demand, indexed by $ts$ (time-slice). |
| $H$ | Set of hours within a year equal to $[\![1, 8760]\!]$ indexed by $h$ (hours) |
| $MC$ | Set of Monte Carlo possible realization of a given period $t$ used for Monte Carlo Simulations, indexed by $mc$(a Monte Carlo year) |
| $P$ | Processes in TIMES model, indexed by $p$ |
| $C$ | Commodities in TIMES model, indexed by $c$. This set is further divided into natural supplied commodities $C_{supply}$ and produced commodities $C_{prod}$. |
| **Parameters** | |
| $\alpha$ | The discount rate used in the cost minimization of [**TIMES**] |
| $I$ | [**TIMES**] costs related to investments |
| $O$ | [**TIMES**] costs related to operation |
| $O'$ | [**ANTARES**] costs related to operation |
| $A$ | [**TIMES**] investments coefficients |
| $a$ | [**TIMES**] investments bounds |
| $B$ | [**TIMES**] operation coefficients |
| $b$ | [**TIMES**] operation bounds |
| $C$ | [**ANTARES**] operation coefficients |
| $c$ | [**ANTARES**] operation bounds |
| **Decision Variables** | |
| Investments related | |
| $X_{r,t}$ | [**TIMES**] Decision variables related to installed capacities occurring in region $r$ and period $t$. |
| Operation oriented | |
| $Y_{r,t,ts}$ | [**TIMES**] Decision variables related to the operational level at time-slice $ts$, period $t$, and region $r$. |
| $y_{r,t,h,mc}$ | [**ANTARES**] Decision variables related to the operational level (dispatch) at hour $h$, period $t$, and region $r$. |

Table 5.3: The main sets, parameters, and decision variables required for the multi-scale model development

The [**TIMES**] optimization model can be formulated as follows.

$$\begin{aligned} \underset{X,Y}{\text{minimize}} \quad & \sum_{r\in R}\sum_{t\in T, ts\in TS}(1+\alpha)^{y_{ref}-t}(I(X_{r,t})+O(Y_{r,t,ts})) \\ \text{subject to} \quad & AX_{r,t} > a, \forall (r,t) \in R*T, \\ & BY_{r,t,ts} > b, \forall (r,t,ts) \in R*T*S \end{aligned} \tag{5.8}$$

**Objective function:** To simplify the total system cost, it can be divided into two main components: the investment part represented by the decision variable $X_{r,t}$ (installed capacities in [GW]), quantified by the linear function $I(X_{r,t})$; and the operational part represented by the decision variable $Y_{r,t,ts}$ (generation of energy commodities in [PJ]), quantified by the linear function $O(Y_{r,t,ts})$. The objective function includes various parameters, such as the cost documentation of investments made before the first model year, technical and economic lifetime of assets, investment and decommissioning lead-times, general and technology-specific discount rates denoted by $\alpha$.

**Constraints:** The minimization problem is subject to a series of constraints, described in Table 5.1. For simplicity and to suit the purpose of our work, the set of constraints can be divided into two main classes. The first class includes constraints on investments, denoted by $AX_{r,t} \geq a$ (e.g., maximum installed capacity of a technology). The second class includes operational constraints, denoted by $BY_{r,t,ts} > b$ (e.g., emission constraints, minimum share of renewables in the energy mix, etc.). A third class that is not presented is constraints that link investments decision variables to operational decision variables summarized in the following formula: $EX_{r,t} + FY_{r,t,ts} \geq g$. However for simplicity of our formulation we omit this set of constraint as it can be expressed in the right hand side of the first two classes. Each scenario $s$ is defined by a combination of specific user-defined investment and operational constraints.

**Main outputs:** The important result of this problem is the investment trajectory, denoted as $\Pi_{inv}^{TIMES,s} = \{\underline{X_t} = \cup_{r\in R}\underline{X_{r,t}}\}_{t\in T}$, where the underline symbol represents the optimal investment solution [4]. Another output is the operational trajectory, denoted as $\Pi_{op}^{TIMES,s} = \{\underline{Y_t} = \cup_{r\in R, ts\in S}\underline{Y_{r,t,ts}}\}_{t\in T}$.

As ANTARES is an operational power system model (without investment decision variables), the operated power generation mix is given as an input. Based on the investments made in a certain period, the [**ANTARES**][$\underline{X_t}$] refers to the multi-regional unit-commitment model for the period $t$, given the power generation $\underline{X_t}$ decided by [**TIMES**]. It can be formulated as follows:

$$\begin{aligned} \underset{y|mc}{\text{minimize}} \quad & \sum_{r\in R}\sum_{h\in H} O'(y_{r,t,h,mc}) \\ \text{subject to} \quad & Cy_{r,t,h,mc} > c, \forall (r,h) \in R*H \end{aligned} \tag{5.9}$$

[4] In an optimization problem, an optimal solution is typically denoted as $x^*$, with the asterisk symbol representing an upper bound. However, since we will be using the right side of the variable to specify distinct decisions, we have employed the underscore symbol instead.

**Objective function:** For each Monte Carlo year $mc$, the sum of the five cost components presented and detailed in the previous section could be summarized as a linear function $O'$ related to hourly dispatch decision variables $y_{r,t,h,mc}$.

**Constraints:** The set of operations constraints presented and detailed in the previous section are summarized in the matrix constraint $Cy_{r,t,h,mc} > c$.

**Main output:** The important output is the hourly operational dispatch decisions for a single period $t$ $\Pi_{op,t} = \{\underline{y_t} = \cup_{r \in R, mc \in MC} \underline{y_{r,t,h,mc}}\}$, while under-line symbol refers to the optimal dispatch solution. The trajectory version will be discussed in the next section.

## 5.3 The Uni-directional part of the multi-scale model

The master problem is represented by [**TIMES**], while the slave problem is represented by [**ANTARES**]. The development of the multi-scale model involves two main steps: uni-directional and bi-directional coupling. In the uni-directional coupling step, the results of the master problem are passed to the slave model. This step aims to accurately represent the operation of the master power system using fine temporal scales, detailed technical representations, and probabilistic simulations. The bi-directional coupling step, on the other hand, focuses on ensuring the generation adequacy requirements. It involves passing the results of the slave problem back to the master problem.

The flowchart for the uni-directional multi-scale coupling is presented in Figure 5.3. The constituent optimization problems are presented in the two nodes, and the main results passed are the investment trajectory decisions $\Pi_{inv}^{TIMES,s}$ from [**TIMES**] to [**ANTARES**]. Consistency of input parameters between both models is ensured through the two dashed lines $O \longrightarrow O'$ and $(C, c') \longrightarrow (B, b)$.

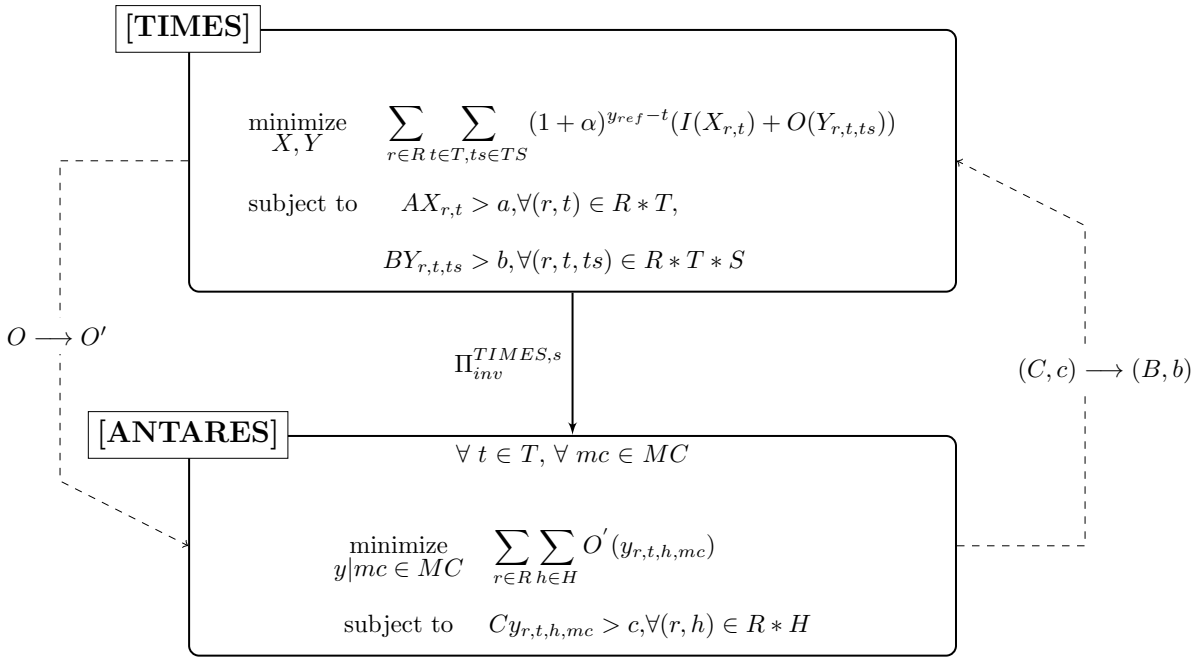


Figure 5.3: Flowchart of the main interactions between models. Dashed lines represent the primary bridging scale operations to ensure consistency between the two constituent optimization problems. Once the consistency of overlaps is established, [**TIMES**] is solved. The solid line indicates that the trajectory investment solution decided by [**TIMES**] is fed to [**ANTARES**], thereby creating an ANTARES model for each period $t$ of the planning time-frame.

In the development of a hierarchical multi-scale framework, resolving the consistency of overlaps between quantities (parameters, sets, or decision variables) in both models is a

crucial challenge. To address this issue, the first step is to conduct a map of overlaps. This involves classifying the system based on supply technologies and demand, which allows us to identify overlaps in each system component. For each overlap quantity, a specific method is employed to ensure harmonization, ensuring that both models share the same common information. To illustrate the process of ensuring common inputs between models, we use a matrix presentation, and the two columns below depict the consistency.

**[TIMES]**

**Decision variables:**

$$\mathbf{X}_{r,t} = \begin{bmatrix} X_{r,t}^{Ren} & X_{r,t}^{Thr} & X_{r,t}^{Hyd} & X_{r,t}^{Str} & X_{r,t}^{Ire} & \left[\tilde{X}_{r,t}\right] \end{bmatrix}^t$$

$$\mathbf{Y}_{r,t,ts} = \begin{bmatrix} Y_{r,t,ts}^{Ren} & Y_{r,t,ts}^{Thr} & Y_{r,t,ts}^{Hyd} & Y_{r,t,ts}^{Str} & Y_{r,t,ts}^{Ire} & Y_{r,t,ts}^{Flx} & \left[\tilde{Y}_{r,t,ts}\right] \end{bmatrix}^t$$

**Objective function:**

$$\mathbf{I} = \begin{bmatrix} I_1 & I_2 & \dots & I_n \end{bmatrix}$$

$$\mathbf{O} = \begin{bmatrix} O_1 & O_2 & \dots & O_p \end{bmatrix}$$

**Constraints:**

$$\mathbf{A} = \begin{bmatrix} A_{i,j} \end{bmatrix}$$

$$\mathbf{a} = \begin{bmatrix} a_j \end{bmatrix}^t$$

$$\mathbf{B} = \left(\begin{array}{cccccc|c} \left[Ren\right] & 0 & 0 & 0 & 0 & 0 & \\ 0 & \left[Thr\right] & 0 & 0 & 0 & 0 & \\ 0 & 0 & \left[Hyd\right] & 0 & 0 & 0 & \\ 0 & 0 & 0 & \left[Str\right] & 0 & 0 & 0 \\ 0 & 0 & 0 & 0 & \left[Ire\right] & 0 & \\ \left[Ren\right] & \left[Thr\right] & \left[Hyd\right] & \left[Str\right] & \left[Ire\right] & \left[Flx\right] & \\ \hline \multicolumn{6}{c|}{\tilde{\mathbf{B_1}}} & \tilde{\mathbf{B_2}} \end{array}\right)$$

$$\mathbf{b} = \begin{bmatrix} ren & thr & hyd & str & ire & d & \tilde{b} \end{bmatrix}^t$$

**Output of interest:**

$$\underline{\mathbf{X}}_{r,t} = \begin{bmatrix} \underline{X_{r,t}^{Ren}} & \underline{X_{r,t}^{Thr}} & \underline{X_{r,t}^{Hyd}} & \underline{X_{r,t}^{Str}} & \underline{X_{r,t}^{Ire}} & \left[\underline{\tilde{X}_{r,t}}\right] \end{bmatrix}^t$$

$$\underline{\mathbf{Y}}_{r,t,ts} = \begin{bmatrix} \underline{Y_{r,t,ts}^{Ren}} & \underline{Y_{r,t,ts}^{Thr}} & \underline{Y_{r,t,ts}^{Hyd}} & \underline{Y_{r,t,ts}^{Str}} & \underline{Y_{r,t,ts}^{Ire}} & \underline{Y_{r,t,ts}^{Flx}} & \left[\underline{\tilde{Y}_{r,t,ts}}\right] \end{bmatrix}^t$$

$\forall t \in T$ **[ANTARES]**$[\underline{\mathbf{X}_{r,t}}]$

**Input and Decision variables:**

$$\begin{bmatrix} \underline{X_{r,t}^{Ren}} & \underline{X_{r,t}^{Thr}} & \underline{X_{r,t}^{Hyd}} & \underline{X_{r,t}^{Str}} & \underline{X_{r,t}^{Ire}} \end{bmatrix}^t = Input$$

$$\mathbf{y}_{r,t,h} = \begin{bmatrix} y_{r,t,h,mc}^{Ren} & y_{r,t,h,mc}^{Thr} & y_{r,t,h,mc}^{Hyd} & y_{r,t,h,mc}^{Str} & y_{r,t,h,mc}^{Ire} \\ & y_{r,t,h,mc}^{Flx} & y_{r,t,h,mc}^{Spil} & y_{r,t,h,mc}^{Unsup} & \end{bmatrix}^t$$

**Objective function:**

$$\mathbf{I} = \begin{bmatrix} 0 \end{bmatrix}$$

$$\mathbf{O'} = \begin{bmatrix} F(O_1) & O_2' & \dots & O_k' \end{bmatrix}$$

**Constraints:**

$$\mathbf{A} = \begin{bmatrix} 0 \end{bmatrix}$$

$$\mathbf{a} = \begin{bmatrix} 0 \end{bmatrix}^t$$

$$\mathbf{C} = \left(\begin{array}{ccccccc|c} \left[Ren'\right] & 0 & 0 & 0 & 0 & 0 & 0 & \\ 0 & \left[Thr'\right] & 0 & 0 & 0 & 0 & 0 & \\ 0 & 0 & \left[Hyd'\right] & 0 & 0 & 0 & 0 & \\ 0 & 0 & 0 & \left[Str'\right] & 0 & 0 & 0 & 0 \\ 0 & 0 & 0 & 0 & \left[Ire'\right] & 0 & 0 & \\ \left[Ren'\right] & \left[Thr'\right] & \left[Hyd'\right] & \left[Str'\right] & \left[Ire'\right] & \left[Flx'\right] & \left[1\right] & \\ \hline \multicolumn{7}{c|}{0} & \tilde{\mathbf{0}} \end{array}\right)$$

$$\mathbf{c} = \begin{bmatrix} ren' & thr' & hyd' & str' & ire' & d' \end{bmatrix}^t$$

**Output of interest:**

$$\underline{\mathbf{y}}_{r,t,h} = \begin{bmatrix} \underline{y_{r,t,h,mc}^{Ren}} & \underline{y_{r,t,h,mc}^{Thr}} & \underline{y_{r,t,h,mc}^{Hyd}} & \underline{y_{r,t,h,mc}^{Str}} & \underline{y_{r,t,h,mc}^{Ire}} \\ & \underline{y_{r,t,h,mc}^{Flx}} & \underline{y_{r,t,h,mc}^{Spil}} & \underline{y_{r,t,h,mc}^{Unsup}} & \end{bmatrix}^t$$

As [**TIMES**] is an energy system model, it includes the interaction of the power system with other systems, such as commodity supply. On the other hand, [**ANTARES**] focuses solely on the power system's supply and demand. To develop a multi-scale approach between both models, [**TIMES**] problem is divided into two main components: one for the supply/demand of the power system and another for the representation of other sectors. This division allows for a more focused and efficient coupling between the two models.

**Decision variables:**

The investment variables $\mathbf{X}r, t$ are split into two main components. The first component represents investments related to the power system supply, including renewable, thermal power generation, hydraulic, storage, and interconnections. The second component represents investments that could be made outside the power system supply, such as investments in $CO_2$ storage facilities. In [**ANTARES**], there is no equivalent for $\mathbf{X}r, t$, as investments are not allowed in this model. However, [**ANTARES**] is fed with the power system decided by [**TIMES**] for the period $t$.

The operational variables $\mathbf{Y}_{r,t,ts}$, which represent the level of activity at the time-slice $ts$, have the same classification as in [**TIMES**], with the addition of a new demand-technology representing the demand flexibility ($F$ index) within the supply-demand power system component. The variables $\tilde{Y}_{r,t,ts}$ encompass other activity levels outside the power system supply.

**Objective functions:**

$I$ represents all [**TIMES**] investment-related costs, and $O$ represents all operational-related costs. The first component $O_1$ encompasses the power generation variable costs, while $O_2, \ldots, O_p$ represent the operational costs of the remaining components. The equivalent operational cost in [**ANTARES**] is denoted as $O'$, which includes a power generation costs component $F(O_1)$ and other costs $O_2, \ldots, O_p$ (non-proportional generation costs, such as start-up costs, and external costs, such as spilled and shortage costs).

**Constraints:**

The investment constraints $AX_{r,t} > a$ have no equivalent in [**ANTARES**]. However, for the operational constraints, both models must share the same representations (with different scales and technical details) for the power system. That is why the coefficient matrix $B$ and the right-hand side $b$ are split into a power system component and other components, which are indexed by a tilde character. The only component that interests us for the multi-scale model is the power system sub-matrix, which is further split into different technologies (diagonal terms) and an overall power system term (last line term). The matrices $[Ren]$, $[Thr]$, $[Hyd]$, $[Str]$, $[Ire]$, and $[Flx]$ are respectively the coefficient matrices for renewable, thermal, hydraulic, storage, interconnections, and demand flexibility in [**TIMES**]. The same notation is applied for the coefficient matrices in [**ANTARES**] with an index $'$. Additionally, the same notation is applied for the left and right-hand-side coefficient matrices, with $d$ and $d'$ referring respectively to the demand in [**TIMES**] and [**ANTARES**]. The following paragraphs will detail the algorithm applied at each system component to make the consistency between both models.

### 5.3.1 System representation and Investments reconciliation

The system representation for a given region within [**TIMES**] is based on the RES representation. If the [**TIMES**] model consist of several internal regions its called a multi-regional model. In the context of multi-area interconnected power system modeling, an internal region typically corresponds to a specific country. Each of the internal regions is represented by its one and unique RES depicting the particularities of the system. In order to model the commodities exchanges between regions, an inter-regional exchange process connecting specific regions is added. There are two modeling options to choose from: bilateral trade, which involves trade between two regions, and multilateral trade, which encompasses trade between several supply and demand regions. The bi-lateral trades occurs between determined pairs of regions through the inter-regional exchange process. This is done, by defining the two pair-wise connections (regions, flow directions and traded commodities). Exchange process capacity (Net Transfer Capacity for electricity) and related costs (investments costs and operational costs) are the main important parameters. For the development of our methodology only bi-lateral trade is considered. [**ANTARES**] is based on a grid topology (graph) described with areas and links. The Algorithm 6 below shows how the ANTARES empty grid (without supply) is created based on TIMES presentation. First of all, for each internal-region a node (a country) is created. To create the links between nodes for a given period $t$, the [**ANTARES**] solution regarding installed interconnections $\underline{X_{r,t}^{Ire}}$ is needed.

**Algorithm 4:** Create the [**ANTARES**] multi-regional power grid topology for a given period $t$

**Input:** Set $R$ of TIMES inter-regions
$\underline{X_{r,t}^{IRE}}$: the [**TIMES**] interconnections installed capacities solutions for region $r$ and period $t$
**Output:** The [**ANTARES**] grid topology

```
for r ∈ R do
    Create an empty area-node for the region r
    L_r ⟶ Extract regions sharing an interconnection with r form X_{r,t}^{Ire}
    for l ∈ L_r do
        Create a link between r and and l
        Affect the NTC (direct r to l, and indirect l to r) between r and l based on
         X_{r,t}^{Ire} solution
```

### 5.3.2 Temporal scales bridging: multi-period vs mono-period investment scales, time-slice vs hourly operational scales reconciliation

At this point, it is important to highlight the different temporal scales dealt with in both models. Figure 5.4 depicts the various temporal scales used in the two constituent models.

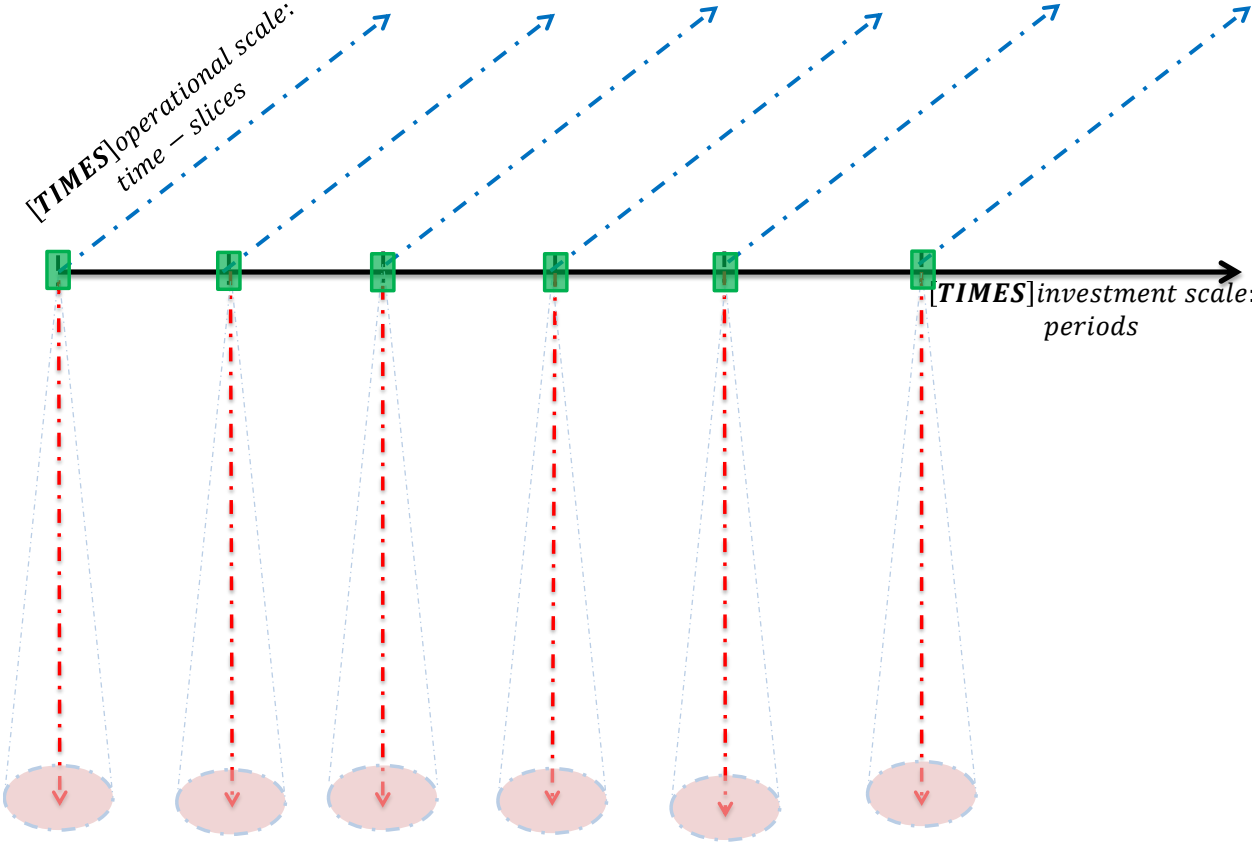


Figure 5.4: Schematic graph showing the different temporal scales evolved in the two constituent models. The black line represents the scale of investments, decomposed into several representative investment years (in green) within TIMES. The blue dashed line represents the TIMES operational scale, based on the time-slices convention, to represent the variability in either supply or demand. The red line represents the hourly time-scale used within ANTARES. The red dashed cone represents the different possible operational realizations of a given period used for Monte Carlo simulations.

While [**TIMES**] is a multi-period optimization problem, [**ANTARES**] is a mono-period optimization problem. To incorporate the entire trajectory of investments into [**ANTARES**], an [**ANTARES**] model is created for each milestone-period of the trajectory (green tiles).

Therefore, the trajectory version of ANTARES can be formulated as a concatenation of the different milestone-periods of the trajectory: [**ANTARES**]=$\cup_{t\in T}$[**ANTARES**][$\underline{X_t^{ps}}$].

The operation of the power system is represented by two operational time-scales with different time resolutions.

- The time-slice scale (dashed blue line) represents the temporal operational scale used in [**TIMES**]. It allows for the subdivision of a year into multiple periods to capture inter-annual variability. Modelers can choose to create time-slices representing seasons, quarters, months, weeks, or even days. These time-slices may also account for differences between weekdays and weekends or various periods within a day. The sum of hours across all time-slices must equal the total number of hours in a nominal year. (typically 8760 hours).

- The chronological hourly scale (dashed red line) represents the temporal operational scale used in [**ANTARES**] to represent the power system operation. It divides the year into 8760 hours, allowing for a detailed representation of the system's hourly operation.

The multi-scale model resulting from the coupling of [**TIMES**] and [**ANTARES**] must handle the differences between temporal scales. The aggregation law is a crucial operation that facilitates the bridging between the time-slice and hourly temporal scales. This law allows for the transformation from the fine scale (hourly) to the coarse scale (time-slice). The algorithm 6 below provides a detailed explanation of the aggregation operations for a given operational quantity $w$.

**Algorithm 5:** Aggregation of the quantity $w$ from hourly ($L$) to time-slice ($l$)

**Input:** An hourly chronological time-series of the quantity $w$:
$L_h = (L_1, L_2, \ldots, L_{8760})$
A time-slice set $S$ represented by $k$ time-slices $S = (ts_1, ts_2, \ldots, ts_k)$
**Output:** A time-slice aggregation $l_{ts} = (l_{ts_1}, l_{ts_1}, \ldots, l_{ts_k})$

```
for ts ∈ S do
    H_ts ⟵ Hours(ts) /* extract the hours belonging to the time-slice ts */
    if w is an energy quantity then
        l_ts ⟵ Σ_{h∈H_ts} L_h /* If the quantity w have an energy dimensional unity
            (production or consumption) */
    else
        l_ts ⟵ mean_{h∈H_ts} L_h /* for example capacity factor. Other operators: min,
            max, median could also be used */
```

Algorithm 6 distinguishes between two cases based on the nature of quantity $w$. If the operational quantity $w$ is an energy-related quantity, such as demand or generation, the aggregation operator used is summation. This means that the algorithm aggregates the total

energy consumed or produced within the corresponding time-slice hours. On the other hand, if the quantity $w$ is non-energy related, such as the capacity factor of wind, the aggregation operator used is the mean (or median, min, max). This operator computes a representative value of the non-energy quantity $w$ at a given time-slice $ts$, based on the statistical mean, median, minimum, or maximum value, depending on the choice made.

### 5.3.3 Uncertainty scale bridging: Monte Carlo simulations vs Deterministic settings

For [**ANTARES**], a Monte Carlo Simulation methodology is used to account for uncertainty in the future possible operational parameters. This step is crucial in building the [**ANTARES**] model for a given period $t$. The Monte Carlo years are used to cover the uncertainty related to the thermal power generation fleet, including technical failures, as well as the impact of weather conditions on renewable generation, hydro generation, and demand profiles due to thermo-sensitivity effects. For a given period $t$ and region $r$, each Monte Carlo year is a combination of the following factors:

- **Climate conditions** for temperature, wind, sun and precipitation. This data is used to create time series of renewable capacity factors, hydro generation and consumption (by taking into account the 'thermosensitivity' effect). The correlation between climate variables is maintained both in terms of geography and time. This means that the climatic data for a particular variable (such as wind, solar, hydroelectric, or load) for a specific year is consistently paired with data from the same climatic year for all other variables.

- Random samples of **thermal power plant availability** is drawn by the model by considering input parameters of planed and fortuitous outage rates and length of unavailability. This resulted in different time series for the availability of the thermal power plants (available capacity).

A time series of the thermal power plant availabilities is associated to a 'climate year' (a combination of wind, solar, hydro generation and load) to constitute a "Monte Carlo year". This process is used to create $N = card(MC)$ Monte Carlo years for the simulation. Each Monte Carlo year represents a potential state of the power system, accounting for various uncertainties. Figure 5.5 bellow recall how Monte Carlo years are constructed.

Based on the input data from the $N = N_{climatic} * N_{thermal}$ Monte Carlo years, one year is selected as the chosen year to provide inputs to [**TIMES**]. At this stage, the modeler has the flexibility to select a specific year, and a reasonable choice could be the median Monte Carlo year. From an operational standpoint, the selected year will serve as a reference year for comparing the dispatch decisions of both models. It will also be used to assess the performance and quality of the developed multi-scale model. The selected Monte Carlo year is denoted as $mc_{TIMES}$.

The number $N$ of Monte Carlo years plays a crucial role in the power generation adequacy assessment. It is essential to carefully define the number of Monte Carlo years to ensure

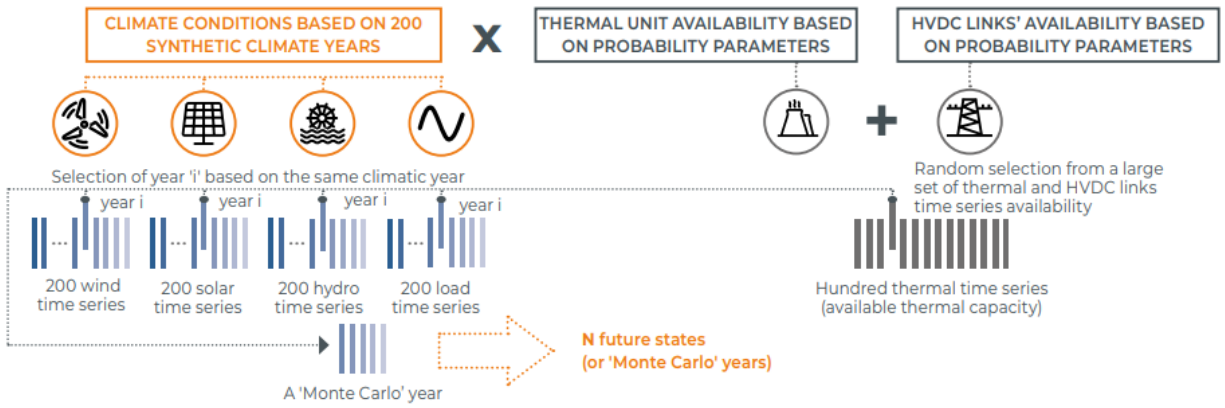


Figure 5.5: Generation of a Monte Carlo year based on different parameters

robust estimations of the metrics. In this case, the metrics of interest are the Loss of Load Expectation ($LOLE$) and the Expected Energy Not Served ($EENS$). To estimate an acceptable value for $N$, a convergence check based on the coefficient of variation for these metrics is performed. For the Expected Energy Not Served ($EENS$), $EENS_N$ is calculated as the mean of the energy not served over the $N$ simulated years using Equation 5.10. The coefficient of variation is then computed using Equation 5.11, where $Var[EENS_N] = \frac{Var[ENS]}{N}$. The convergence criterion is defined in Equation 5.12, where $\epsilon$ is the convergence threshold set to 0.001. The convergence check allows for determining the minimum number of Monte Carlo years required to achieve a satisfactory level of accuracy for the power generation adequacy assessment.

$$EENS_N = \frac{\sum_{i\ in 1:N} ENS_i}{N} \tag{5.10}$$

$$\alpha_N = \frac{\sqrt{Var[EENS_N]}}{EENS_N} \tag{5.11}$$

$$\frac{|\alpha_N - \alpha_{N-1}|}{\alpha_{N-1}} < \epsilon \tag{5.12}$$

### 5.3.4 Objective function reconciliation $O \longrightarrow O'$

The main common component between both models for the objective function is the proportional operating costs related to dispatchable thermal power generation. For each existing technology or potential new invested technology, [**TIMES**] utilizes variable costs and fixed operating and maintenance costs in its optimization. The main operation involves computing the variable operational cost of [**ANTARES**] based on [**TIMES**] operational costs. This computation is carried out by Algorithm 4 below. Algorithm 4 demonstrates how the corresponding variable cost in [**ANTARES**] is computed for a given [**TIMES**] process $p$. As a result, the sub-matrix $O_1$ for [**TIMES**] contains all defined processes (existing and potential processes). However, the [**ANTARES**] sub-matrix $O'_1$ contains only the supply processes chosen by [**TIMES**] to participate in the power system. The other components in $O'$ consist of non-proportional operational costs (start-up costs) and external costs (spilled energy cost and unsupplied energy cost). The shortage costs are not considered in TIMES because the optimization logic will determine sufficient investments to satisfy the demand. The spillage cost is not considered, as TIMES only satisfies the demand level. Therefore, no reconciliation is needed for these costs.

In fact, unlike the ANTARES model, which considers individual power plants, TIMES operates at a technology-type level. Hence, in its standard version, TIMES does not explicitly take into account the technical load-following constraints of individual power plants and the associated cycling costs (start-up costs). Additionally, TIMES does not consider the cost of unsupplied energy because the main goal of its objective function is to find necessary investments to cover the entire demand. However, to avoid infeasible solutions, modelers can add fictitious imports that are costly (equivalent to the unsupplied energy cost) to satisfy the supply-demand balance. The values of non-proportional and external costs used in ANTARES will be provided in detail in the application chapter.

**Algorithm 6:** Proportional operating cost reconciliation: $O_1 \longrightarrow O_1' = F(O_1)$

**Input:** [**TIMES**] operational cost of a process $p$ consuming a fuel $f$:

- $process.eff$: Electric net efficiency of process $p$ [%]
- $fuel.price$: Fuel price of $f$ [Euro/MWh]
- $fuel.emission$: Fuel $CO_2$ emission factor of $f$ [tCO2/MWh]
- $process.varom$: Variable costs associated with the activity of $p$ [Euro/MWh]
- $co2.tax$: $CO_2$ tax [Euro/tCO2]

**Output:** $m$: [**ANTARES**] marginal operating cost of the process $p$ [€/MWh]

$emission.factor = \frac{fuel.emission}{process.eff * 1000}$ /* Compute the emission factor, which measures the quantity of CO2 emitted when burning a given quantity of fuel */

$process.varom = process.varom * 3.6$ /* render it to [€/MWh] */

$fuel.factor = \frac{fuel.price}{process.eff}$ /* compute fuel factor */

$m = process.varom + emission.factor * co2.tax + fuel.factor$ /* The function $F$ allowing to pass from $O_1$ to $O_1'$ */

### 5.3.5 Constraints reconciliation $\mathbf{BY_{r,t,ts} > b \longrightarrow Cy_{r,t,h,mc} > c}$

The reconciliation of constraints is of paramount importance in ensuring the consistency of the developed multi-scale model. In the following paragraphs, we introduce the main operations and bridging scale algorithms required to reconcile both models. It is essential to note that all the reconciliation algorithms presented in this section are intended for one specific region $r$ and period $t$. To construct the multi-regional reconciliation, replication of these algorithms for all constituent regions is necessary.

**Wind and Solar generation:** $Ren' \longrightarrow Ren$

Within [**ANTARES**], wind and solar generation are considered non-dispatchable and are given priority in the merit order. They are subtracted from the load to obtain the residual load, along with other non-dispatchable generation. Then [**ANTARES**] determines the optimal hydro/thermal dispatch and interconnection flows to satisfy the resulting residual load. In other words, in [**ANTARES**], the renewable dispatch decision variables $y^{Ren}_{r,t,h,mc}$ are known beforehand and considered as fixed values in the optimization.

On the other hand, within [**TIMES**], wind and solar also take precedence in the merit order. However, their level of operation (activity) is governed by an equation that relates the activity to their available capacity, i.e., $Y^{Ren}_{r,t,ts} < af^{Ren}_{r,t,ts} * X^{Ren}_{r,t}$. The availability factor $af$, which has a time-slice resolution within [**TIMES**], serves as the primary common input between the two models. The following two algorithms 2 and 1 demonstrate how to construct the generation time-series in [**ANTARES**] and compute the wind and solar availability factor for [**TIMES**].

**Algorithm 7:** Computation of the [**ANTARES**] renewable power generation based on [**TIMES**] installed capacities

**Input:** $\underline{X_{r,t}^{Ren}}$ the wind (or solar) installed capacity decided by [**TIMES**] for a region $r$ and period $t$ [MW]

**Data:** $cf_{mci\in 1:N}$: $N_{climatic}^{Renewable}$ renewable hourly capacity factor times-series for a period $t$ and a region $r$ [%]

**Output:** $y_{r,t,h,mc}^{Ren,input}$: $N_{climatic}^{Renewable}$ hourly power generation times-series for a period $t$ and a region $r$ [MWh]

1 **for** $mc \in 1 : N_{climatic}^{Renewable}$ **do**

2 $\quad y_{r,t,h,mc}^{Ren,input} \longleftarrow cf_{mc} * \underline{X_{r,t}^{Ren}}$ /* multiply the TIMES installed capacity with the capacity factor of the Monte Carlo $mc$ */

**Algorithm 8:** Computation of the [**TIMES**] renewable availability factor input

**Input:** $mc_{TIMES}$: the Monte Carlo year selected to feed TIMES input data

**Data:** $cf_{mci\in 1:N_{climatic}^{Renewable}}$: $N_{climatic}^{Renewable}$ renewable hourly capacity factor times-series for a period $t$ and a region $r$ [%]

**Output:** $af_{r,t,ts}^{Ren}$: the renewable availability factor with time-slice resolution for the period $t$ and region $r$ [%]

1 $af_{r,t,ts} \longrightarrow$ **Call** the aggregation Algorithm **??** to be applied to $cf_{mc_{TIMES}}$

**Thermal generation**

In [**ANTARES**], the thermal fleet is constructed using the decided thermal installed capacities $\underline{X_{r,t}^{Thr}}$ for each region-node and period $t$ as provided by [**TIMES**]. The representation of the thermal power plant fleet in [**ANTARES**] is based on a classification of technologies, similar to the one used in the process definitions of [**TIMES**]. This classification distinguishes mainly between nuclear, coal, lignite, biomass, natural gas, and other fuels. However, it is important to note that there exists a main difference between the two models in the way they represent the thermal power plant fleet.

- [**ANTARES**]: In this model, the given thermal fleet is divided into clusters, where each cluster signifies either an individual power plant or a cluster of power plants that share similar attributes or characteristics. For each cluster, specific technical and economic parameters necessary for unit commitment and dispatch calculations are taken into account.

- [**TIMES**] Linear Version: In this version of [**TIMES**], the installed capacities for a given process are represented as real positive values, allowing fractional capacities.

- [**TIMES**] Lumpy Investment Version: In this version, a rule is enforced where certain installed capacities are allowed only in multiples of a given size, achieved by introducing

integer variables. This means that capacities are constrained to be discrete and not continuous.

- To address this difference between [**ANTARES**] and the two versions of [**TIMES**], two possible solutions can be proposed: If the lumpy investment version is activated in [**TIMES**], then the clustering approach is available in [**ANTARES**]. This means that when a new investment is made in [**TIMES**], it will be clustered into known implementable nominal capacities. For example, a new investment of 1500 MW will be clustered into 3 units of 500 MW.

- If the linear version of [**TIMES**] is used (without lumpy investments), then [**ANTARES**] will directly use the installed capacities provided by [**TIMES**] without clustering.

For each cluster (or process) in [**ANTARES**], specific technical and economic parameters are taken into account for unit commitment and dispatch calculations. These parameters include:

- The number of units, nominal capacities, and capacity modulation (if any) defining the installed capacities for each hour.

- The cost parameters, including variable costs (which may vary within the year) and start-up costs (details on how these costs are computed based on [**TIMES**] data are available in the objective function reconciliation).

- Parameters related to the availability of units, such as forced outage rate and duration, planned outage rate and duration, and the minimum and maximum planned outage amounts for each day.

- Technical constraints, such as minimum stable power, partial must-run requirements, and minimum up and down durations. These technical constraints are not considered in the standard version of the TIMES model we used in the development of our multi-scale model. However, TIMES can include dispatching and unit commitment features within its optimization problem [231].

Both [**TIMES**] and [**ANTARES**] share the same installed capacities, which are used as inputs to generate different time-series of thermal available capacities. However, there are certain parameters related to the availability of thermal power plants that are only considered in the [**ANTARES**] model. These parameters include the forced outage rate and duration, the planned outage rate and duration, and the technical constraints such as minimum stable power, partial must-run requirements, and minimum up and down durations.

**Hydro generation: Run of River**

Run of River (RoR) power generation is non-dispatchable, and its generation depends solely on the hydrological inflows. RoR comes first in the merit order, along with wind and solar power. The RoR power generation is subtracted from the load to obtain the residual load. Similar algorithms used for wind and solar are applied to compute the RoR power generation.

To generate the input RoR power generation time-series in [**ANTARES**], the installed RoR capacities $\underline{X_{r,t}^{RoR}}$ (where $\underline{X_{r,t}^{Hydro}} = [\underline{X_{r,t}^{RoR}}, \underline{X_{r,t}^{Stor}}, \underline{X_{r,t}^{PSP}}]$) and capacity factors time-series are used. The time-slice RoR availability parameter in [**TIMES**] is computed based on the hourly capacity factors time-series corresponding to the Monte Carlo year $mc_{TIMES}$. Algorithms 2 and 1 detail the needed operations for RoR technology.

**Algorithm 9:** Computation of the [**ANTARES**] RoR generation based on [**TIMES**] installed capacities

**Input:** $\underline{X_{r,t}^{RoR}}$ the RoR installed capacity decided by [**TIMES**] for a region $r$ and period $t$ [MW]

**Data:** $cf_{i\ i\in 1:N_{climatic}^{RoR}}^{RoR}$: $N_{climatic}^{RoR}$ RoR capacity factor times-series for a period $t$ and a region $r$ [%]

**Output:** $y_{r,t,h,mc}^{RoR,input}$: $N_{climatic}^{RoR}$ hourly RoR power generation times-series for a period $t$ and a region $r$ [MWh]

1 **for** $i \in 1 : N_{climatic}^{Renewable}$ **do**

2 $\quad y_{r,t,h,mc}^{RoR,input} \longleftarrow cf_i^{RoR} * \underline{X_{r,t}^{RoR}}$ `/* multiply the TIMES installed capacity with the capacity factor of the RoR climatic year` $i$ `*/`

**Algorithm 10:** Computation of the [**TIMES**] RoR availability factor input

**Input:** $mc_{TIMES}$: the Monte Carlo year selected to feed TIMES input data

**Data:** $cf_{i\ i\in 1:N_{climatic}^{RoR}}$: $N_{climatic}^{RoR}$ renewable hourly capacity factor times-series for a period $t$ and a region $r$ [%]

**Output:** $af_{r,t,ts}^{RoR}$: the renewable availability factor with time-slice resolution for the period $t$ and region $r$ [%]

1 $af_{r,t,ts} \longrightarrow$ **Call** the aggregation Algorithm 6 to be applied to $cf_{mc_{TIMES}}$

**Hydro generation: Storage plants**

In ANTARES, hydro storage possesses a reservoir to postpone the use of water and its power generation depends on inflows and economic data. The annual or monthly inflows are split into weekly amounts of energy. This breakdown follows a heuristic based on:

- Residual demand pattern: calculated from load, renewable generation and must-run generation.
- Hydro management parameters: defines whether the storage should be explicitly modeled or not and parameters defining how residual load is weighted for energy dispatching from year to months and from month to weeks.
- Reservoir rule curves: to define minimal and maximal curves in order to constrain the dispatching of hydro energy and to define the maximal power variation with the variation of the reservoir level.

The reservoir generation for all countries is managed using the "reservoir management heuristic" implemented in ANTARES. This heuristic dynamically adjusts reservoir generation on an annual basis, taking into account both the annual inflows and the net load (which is the load minus the non-dispatchable generation). The heuristic allocates more hydro energy to months and weeks with higher net load, while ensuring that the overall annual energy requirements are met. Subsequently, the allocated weekly energy is further optimized by ANTARES within the specific hours of the week to achieve an efficient utilization of hydro resources.

Three inputs are needed:

- Maximal turbining capacity (result of TIMES).
- Daily inflows time-series and the reservoir capacity.
- Hydro management parameters.

In order to reconcile the ANTARES representation with TIMES, a constraint on operation is added to constraint the TIMES model with the ANTARES inflows $Y_{r,t,ts}^{Hydro.Stor} \leq MaxFlow_{r,t,ts}$. The algorithm bellow describes the computation of the maximum allowed generation.

**Algorithm 11:** Computation of the upper bound on the hydro storage power generation in [TIMES]

**Input:** $mc_{TIMES}$: the Monte Carlo year selected to feed TIMES input data
**Data:** $SP_{ii\in 1:N_{climatic}^{Stor}}$ : $N_{climatic}^{Stor}$ ready-made daily natural inflows time-series considered to be storable into a reservoir for later use [MWh]
**Output:** $MaxFlow_{r,t,ts}^{RoR}$: maximum hydro storage power generation for a region $r$, period $t$ and time-slice $ts$ [MWh]
1 $MaxFlow_{r,t,ts} \longrightarrow$ **Call** the aggregation **??** to be applied to $SP_{mc_{TIMES}}$

**Hydro generation: Pumped-storage plant**

Pumped-storage plants (PSP) operate based on economic data and play a crucial role in the power system. These plants have the capability to pump water during low-demand periods, store it in reservoirs, and later release it to generate electricity during high-demand periods. In the context of the multi-scale framework, ANTARES optimizes the operation of PSP in conjunction with other dispatchable units, ensuring that the total energy stored (accounting for the roundtrip efficiency of the PSP) equals the total energy generated during the week.

The modeling of PSP in ANTARES is modeled as follows: It is represented within the model using a conceptual node named $00\_PSP\_STO$, which is virtually connected to all other nodes through a fictitious link. To account for PSP generation capacity, a fictitious generator named *z_psp_gen* is added to each individual node, and its capacity corresponds to the PSP generation capacity at that node.

The capacity of the fictitious link between the real node and the fictitious node is set to match the PSP storage capacity (pumping capacity) of the respective node. However, the

capacity of the link is set to zero in the opposite direction (from the fictitious node to the real node). This modeling approach allows the representation and optimization of Closed PSP generation, ensuring efficient utilization of pumped storage for managing energy production and consumption over weekly periods. Figure 5.6 bellow illustrates the modeling of the PSP using multiple nodes.

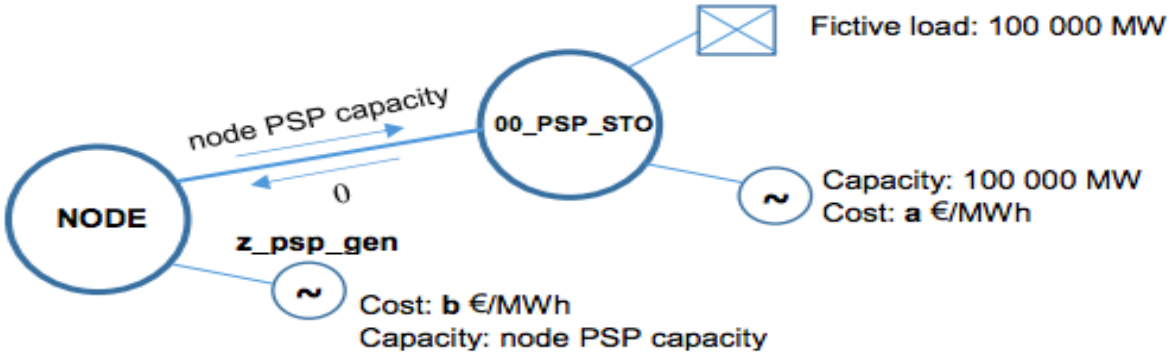


Figure 5.6: Illustration of the modeling of PSP within ANTARES (source [232]). During the optimization process, it becomes cost-effective to store energy during hour $H1$ and generate on hour $H2$ if $(marginalCost_{H1} - b > geq\frac{(marginalCost_{H1}-a)}{efficinecy}$. This means that generation costs can be chosen such that $b = \frac{a}{efficiency}$)

A weekly binding constraint is implemented to ensure that all energy stored within a week is returned to the system during the same time period, accounting for a 75% efficiency ratio:

$\sum 0.75 * flow(NODE \rightarrow 00\_PSP\_STO) - z\_psp\_gen = 0$

To enforce reservoir capacity constraints, two additional fictitious generators ($z\_NODE\_psp\_1$ and $z\_NODE\_psp\_2$) are introduced in a fictitious node named $00\_xtra$ which is not connected to any real node. These generators represent the reservoir levels and are linked through hourly binding constraints:

$\forall h \in H z\_NODE\_psp\_1(h) = z\_NODE\_psp\_2(h)$

$$z\_NODE\_psp\_1(H+1) = z\_NODE\_psp\_2(H) + flow(NODE \rightarrow 00\_PSP\_STO) - z\_psp\_gen * \frac{1}{0.75}$$

To maintain continuity between different weeks of the year, a third binding constraint ensures that the reservoir level is equal to 50% of its capacity at the beginning and end of each optimization period (i.e., the week).

**Storage**

Grid batteries use the exact same modelling as PSP with an efficiency ratio of approximately 90% and daily (instead of weekly) cycle (and hence a daily binding constraint).

**Interconnections**

Interconnection reconciliation have been discussed in the section related to the system reconciliation. For reminder, the interconnections decided by [**TIMES**] optimization model are used to create link between the nodes representing each regions. For each link, the direct

and indirect transfer capacity is the Net Transfer Capacity installed by [**TIMES**].

**Demand and flexibility** $d \longrightarrow D$

Among others, demand is important as it is the main driver of the optimization for both models. Two important parameters are to be supplied to [**TIMES**] optimization problem: the annual projection of the demand for each demand-commodity and the commodity fraction representing how the annual demand is allocated at each time-slice. In[**TIMES**] different electricity demand commodities could be presented. However for [**ANTARES**] only one aggregated electricity demand is presented. To reconcile both demand presentation, the following data will be necessary for each region.

- Trajectory evolution of all the electricity demand-commodities for each period of the planning time-frame.
- Hourly power demand time-series of all the electricity demand-commodities.

It is clear that based on this data, the [**ANTARES**] demand $d$ is the sum of all the electricity demand commodities represented in [**TIMES**]. However, the TIMES demand is constructed based on ANTARES demand $d$. Algorithm bellow show how to construct the right left hand side $D$ based on its counterpart $d$.

**Algorithm 12:** Construction of [**TIMES**] **demand based on** [**ANTARES**] **data for a region** $r$ **and**

**Input:** $mc_{TIMES}$: the Monte Carlo year selected to feed TIMES input data

**Data:** $\{d_{c,i}\}_{i \in 1:N^{Demand}_{climatic}, c \in C_{elec}}$: $N^{Demand}_{climatic}$ ready-made hourly power demand for the electricity demand commodity $c$, region $r$ and period $t$ in [MW]

**Output:**

- $D_c$: [**TIMES**] annual demand
- $cfr_{r,t,c,ts}$: the demand commodity fraction for each time-slice $ts$

$D_c \longleftarrow \sum_{h \in H} d_{c,mc_{TIMES}}$ /* Compute the annual demand based on the hourly time-series */

**for** $ts$ *in* $S$ **do**

  $H_{ts} \longleftarrow Hours(ts)$ /* extract the hours belonging to the time-slice $ts$ */

  $cfr_{r,t,c,ts} \longleftarrow \frac{\sum_{h_i n H_{ts}} d_{c,mc_{TIMES}}}{D_c}$ /* Compute the commodity fraction of the demand commodity at each time-slice $ts$ */

Demand can also be flexible and optimally allocated. For example the EV charging demand. In line with the prevailing car usage patterns, the EV charging is assumed to follow a daily cycle. A specific percentage of the daily EV load profile (for example 6% ) can be optimally allocated by [**ANTARES**]. This allocation is accomplished using a fictitious node with a loss-of-load cost (VOLL) of 0 Euro, which ensures that the daily flow on the link corresponds to the optimized load value. The charging capacity is reduced by 2/3 between 9

am and 6 pm on working days to account for a lower rate of vehicle connection to charging stations during working hours.

## 5.4 Validation and assessment of the uni-directional part of the multi-scale model quality

This section aims to validate the uni-directional multi-scale linking model by conducting a comparison at various measuring points. A measuring point refers to a shared output (decision variable) of both [**TIMES**] and [**ANTARES**]. To achieve this, diverse metrics are devised, encompassing technical, economic, and environmental aspects. Furthermore, the assessment is conducted across different temporal and spatial scales to comprehensively evaluate the model's quality and performance. This rigorous evaluation of the model's performance is a crucial step in the development of the entire multi-scale framework. It serves as a valuable tool to identify any potential issues in the modeling assumptions or implementation, allowing the modeler to make necessary adjustments and enhance the model's accuracy.

### 5.4.1 Metric of performance assessment

As evident from the preceding sections, both models involve operational decisions. The primary outputs of the uni-directional multi-scale linking model are the operational trajectories $\Pi_{op}^{ANTARES,s}$ determined by [**ANTARES**] and $\Pi_{op}^{TIMES,s}$ determined by [**TIMES**]. These operational decisions serve as crucial indicators to analyze the operational behavior of the corresponding power system. The significance of certain solution outcomes may vary based on the specific analysis conducted. As our focus is primarily on the operational aspect, we consider highly detailed [**ANTARES**] outcomes as the reference solution against which [**TIMES**] operational decisions will be compared.

**Monte Carlo year of comparison**

In order to ensure the consistency of the comparison metrics, we select the Monte Carlo year for comparison to be the same year used to feed [**TIMES**] inputs. This choice is straightforward since both models will encounter the same operational constraints, albeit at different scales (ANTARES: highly detailed, TIMES: aggregated). Subsequently, only the dispatch decisions of $mc_{TIMES}$ are utilized to calculate the following technical, economical, and environmental quantities. It is crucial to emphasize that these metrics are computed for each period $t$ within the planning time-frame.

**Technical: energy generation mix**

is based on the total annual generation by technology class divided by the sum of the power generation of all installed technologies.

$$E_{tech}^{TIMES} = \frac{\sum_{ts \in S} Y_{r,t,ts}^{tech}}{\sum_{tech \in TECH} \sum ts \in SY_{r,t,ts}}$$

$$E_{tech}^{ANTARES} = \frac{\sum_{h \in H} y_{r,t,h,mc}^{tech}}{\sum_{tech \in TECH} \sum h \in SY_{r,t,ts}}$$

The mean absolute difference between TIMES and ANTARES provides a scalar comparison metric.

$$\Delta E^{mix} = mean_{tech \in Tech} | E^{TIMES}_{tech} - E^{ANTARES}_{tehc} |$$

**Economical: Electricity marginal cost** in ANTARES, electricity marginal cost is the dual value of the load-supply balance constraint. For each hour $h$ of the period $t$ a marginal value is obtained. In TIMES the electricity marginal cost is the dual value of the electricity commodity balance constraint. For each time-slice $ts$, a marginal value is obtained. However, within TIMES, three electricity commodities are presented: high, medium and low voltage. To compute the electricity marginal cost metric only dual values from the high voltage electricity commodity is used.

**Economical: Annual total operational cost**

Annual total operational cost is the objective function value for the [**ANTARES**] optimization and include operating cost (proportional and non-proportional costs) + unsupplied cost+ spilled cost. The corresponding cost in [**TIMES**] are variable annual costs equal to the portion of the objective function cost for a year $t$ and period $r$. Variable costs are proportional to the activity of process. To make the difference with ANTARES costs feasible, only the power system process are taken into account, other activity process are not included. $\Delta C^{total}_{op}$ is the operational cost metric for a given period $t$ and a region $r$.

$$\Delta C^{total}_{op} = \frac{AC^{TIMES}_{op} - C^{ANTARES}_{op}}{C^{ANTARES}_{op}}$$

**Environmental: Carbon dioxide emissions:** Carbon dioxide ($CO_2$) emissions are computed for the whole power system for a given region $r$ and period $t$. The main driver of the $CO_2$ emissions are mainly the thermal power generation plants. A scalar percent difference is computed in the same manner as the total annual operational cost.

**Thresholds of performance**

After computing the performance metrics, the modeler needs to establish the thresholds that define acceptable levels of quality for the developed uni-directional multi-scale model. The primary focus is on the technical metrics, as the economical and environmental metrics are secondary and may highlight issues in the reconciliation of economical and environmental inputs.

In our developed multi-scale model, we will utilize a threshold solely for the technical metric to assess the quality. A maximum threshold of 20% for deviations in the total energy mix is considered acceptable performance. Should values surpass this threshold, two potential solutions can be considered: Revisit the implementation of the bridging algorithms and modeling assumptions to improve the accuracy of the multi-scale model. or Implement a bi-directional coupling between [**TIMES**] and [**ANTARES**], allowing for iterative improvements and feedback between the two models to achieve better consistency.

- Reconciliation problem: the modeler must verify whether the implementation of the uni-directional multi-scale model is accurate.

- If the verification shows no implementation problem, increase the number of the time-slices. This option seems to be the major driver of the difference of operational decision between models. An increase in the number of time-slice will consequently decrease the differences.

## 5.5 The bi-directional part of the multi-scale model

Once the performance assessment confirms the validity of the developed uni-directional multi-scale linking model, the primary objective of the bi-directional multi-scale model is to ensure power generation adequacy requirements. To achieve this goal, three key steps are crucial:

1. **Adequacy Metrics Computation:** The first step involves computing adequacy metrics such as Loss of Load Expectation ($LOLE$) for each region $r$ and period $t$, based on the operational trajectory $\Pi_{op}^{ANTARES,s}$ obtained from [**ANTARES**]. Other adequacy metrics like Expected Energy Not Served ($EENS$) may also be calculated.

2. **Adequacy Assessment:** Next, the multi-regional adequacy requirement targets need to be defined and established for each region $r$ and period $t$, as the adequacy criterion can evolve throughout the trajectory

3. **Feedback Equation Development:** If the adequacy criterion is not met, an adequacy-equation must be formulated and integrated as a constraint-equation within the [**TIMES**] model.

4. **Feedback Algorithm Implementation:** Once the equation is developed, a feedback control strategy is required to ensure convergence towards the desired adequacy requirement targets.

By completing these four steps, the bi-directional multi-scale model can effectively address power generation adequacy requirements. The following subsections details each step.

### 5.5.1 Adequacy metric computation

The key adequacy metric is the Loss of Load Expectation ($LOLE$). It is defined as the average number of hours per year when the available generation and imports are not enough to cover the load of a region. $LOLE$ describes the duration of a loss of load event but not the severity nor the frequency. Despite these deficiencies, it is the most widely used probabilistic adequacy standard, used in generation adequacy planning studies. It is important to highlight that $LOLE$ is an external metric to the [**ANTARES**] optimization problem (not a decision variable). The algorithm shows how this adequacy metric is computed based on the Monte Carlo operational dispatch decisions.

**Algorithm 13:** Computation of the adequacy metric $LOLE_{r,t}$ for a given period $r$ and period $t$

**Input:** $\Pi_{op}^{ANTARES,s}$ the operational trajectory decided by [**ANTARES**]
**Output:** $LOLE_{r,t}$: the Loss of Load Expectation metric for a given period $r$ and period $t$

**for** $mc \in MC$ **do**
  $G^{+}_{r,t,h,mc} \longleftarrow$ **Extract** unsupplied power variable decision for region $r$ and period $t$ from $\Pi_{op}^{ANTARES,s}$
  $LOSS_{r,t,h,mc} \longleftarrow \begin{cases} 1 if G^{+}_{r,t,h,mc} \geq 0 \\ 0 otherwise \end{cases}$
  $LOLD_{r,t,mc} \longleftarrow \sum_{h \in H} LOSS_{r,t,h,mc}$
$LOLE_{r,t} \longleftarrow \frac{1}{card(MC)} \sum_{mc \in MC} LOLD_{r,t,mc}$

### 5.5.2 Adequacy assessment

Once the calculation of the adequacy metric has been conducted, defining the adequacy requirement targets in a multi-area power system becomes a challenging task for two reasons. Firstly, the adequacy assessment is a national and sensitive issue, and there may be a lack of publicly available information regarding its establishment. Secondly, different metrics and targets could be used within a multi-area power system, such as the European power system, which adds complexity to the process.

Secondly, as our multi-scale model is intended to be a tool for supporting future decision-making, questioning or re-defining the actual criteria and corresponding targets is also an important step in prospective studies. However, in our methodological work, neither the re-definition nor questioning of the adequacy limit criterion is out of scope. We focus on the most widely used adequacy metric, which is the $LOLE$. For each region $r$ and period $t$, a target of $\zeta_{r,t}$ is set as the adequacy limit criterion [5]. Hence, the goal of the bi-directional multi-scale model is to ensure the adequacy of the investment trajectory decided for a given long-term transition scenario $s$. The output of the multi-scale model is an investment trajectory $\Pi_{inv}^{TIMES,s}$ that satisfies equation 5.13.

$$\Pi_{inv}^{TIMES,s} = \{X_t = \cup_{r \in R} X_{r,t} | \forall r \in R, \forall t \in T, LOLE_{r,t} < \zeta_{r,t}[h/year]\}_{t \in T} \tag{5.13}$$

.

[5] The methodology we have developed (see next section) can support any risk metric expressed as the expectation of a stochastic variable, such as the EENS.

### 5.5.3 Which feed-back equation?: a new adequacy proxy constraint equation

The core step in the development of the feedback between the short-term operational power system model and the long-term energy system model is the determination of which operational information should be utilized and how it will be transferred. Given that, the primary objective of the developed multi-scale model is to ensure power generation adequacy requirements, an adequacy-proxy constraint equation is formulated. The rationale behind this equation is to address the possibility that the minimization of the total actualized cost under the initial investment and operational constraints of TIMES might not always result in an adequate power system. In regions where there is a risk of not meeting adequacy requirements, a reinforcement of the initial constraint becomes necessary to ensure generation adequacy.

This reinforcement is achieved through the introduction of a new equation within the TIMES framework, known as the adequacy proxy constraint equation. The decision variables of this equation are the investment installed capacities, and the coefficients are quantities that are computed based on the outcomes from the operation of the [**ANTARES**] model. The adequacy proxy constraint equation serves as a means to incorporate operational information from the short-term power system model into the long-term energy system model, allowing for a more robust and reliable assessment of power generation adequacy.

The proposed feedback from [**ANTARES**] to [**TIMES**] is centered around the two trajectories, $\Pi_{inv}^{TIMES,s}$ and $\Pi_{op}^{ANTARES,s}$, which are determined by both models. The objective is to reinforce the [**TIMES**] optimization problem with supplementary constraints that reflect how the initial investment assets (installed capacities) have been dispatched to meet the electricity demand. Such information is inherently embedded in the operational trajectory $\Pi_{op}^{ANTARES,s}$.

The feedback process involves utilizing the operational decisions obtained from [**ANTARES**] to adjust the long-term investment decisions made by [**TIMES**]. These adjustments are carried out through the introduction of an adequacy-proxy constraint equation, which influences the investment installed capacities in [**TIMES**] based on the operational outcomes of [**ANTARES**].

$$\underline{y_{r,t,h,mc}^{Ren}} + \underline{y_{r,t,h,mc}^{Thr}} + \underline{y_{r,t,h,mc}^{Hyd}} + \underline{y_{r,t,h,mc}^{Str}} + \underline{y_{r,t,h,mc}^{Flx}} + \underline{y_{r,t,h,mc}^{Ire}} = D_{r,t,h,mc} + \underline{y_{r,t,h,mc}^{Spil}} - \underline{y_{r,t,h,mc}^{Unsup}} \quad (5.14)$$

As we seek to obtain reliable investments that respect power generation adequacy requirements, the idea of the adequacy proxy constraint is to rewrite equation 5.14 with the introduction of [**TIMES**] investment decision variables. To do this the effective participation coefficient for a given technology is calculated based on initial models solutions as $ep_{r,t,h,mc}^{tech} = \frac{\underline{y_{r,t,h,mc}^{tech}}}{\underline{X_{r,t}^{tech}}}$. Hence the additional adequacy proxy constraint is written as.

$$\sum_{tech \in Tech} ep_{r,t,h,mc} X_{r,t}^{tech} \geq D_{r,t,h,mc} + \underline{y_{r,t,h,mc}^{Spil}}(-\underline{y_{r,t,h,mc}^{Unsup}} = 0) \quad (5.15)$$

This equation is a proxy of adequacy as the unsupplied power is well included and the need of additional investment is taken into account. Also the temporal synchronization between supply and demand is kept. However, two main problems are still in the selection of "adequate" situation that capture different operational situations of a given power generation mix $X_{r,t}$. The first one is the huge amount of information resulting from Monte Carlo simulations (for each region $8760 * card(MC)$ equation could be written). And the second one is the selection method. To address the first problem, we propose a new compact object that synthesizes Monte Carlo dispatch decisions. Searching through the space of chronological hourly dispatch for all Monte Carlo Years can be challenging, as the only order available is the temporal timeline, and no operational order is in place. Therefore, the aim of the compact object is to sort all the hourly dispatch results from the Monte Carlo simulation using an operational order described in the next paragraph. For the second problem, a new flexible temporal-dimension (in addition to the investment and operational dimensions: $T$ and $TS$ ) representing adequacy is added within [**TIMES**] model.

The goal of the compact object is to put some order into the Monte Carlo chronological hourly dispatch decisions encompassed within $\Pi_{op}^{ANTARES,s}$. This order is done by the mean of the inverse of the cumulative distribution function of the **new residual demand**. The new residual load is computed as demand subtracted from all technologies except thermal power generation (see Equation 5.16).

$$D_{r,t,h,mc}^{residual} = D_{r,t,h,mc} + \underline{y_{r,t,h,mc}^{Spil}} - \underline{y_{r,t,h,mc}^{Unsup}} - \underline{y_{r,t,h,mc}^{Ren}} - \underline{y_{r,t,h,mc}^{Hyd}} - \underline{y_{r,t,h,mc}^{Str}} - \underline{y_{r,t,h,mc}^{Flx}} - \underline{y_{r,t,h,mc}^{Ire}} \quad (5.16)$$

The compact object is called the new Residual Load Duration Curve ($nRLDC$), which is nothing than quantile function. The $nRLDC$ specifies the value of the residual demand such that the probability of the residual demand being less than or equal to that value equals the given probability. For a given region $r$ and period $t$ regional $nRLDC$ is a map from $[0,1] \to \mathbb{R}$ :

$$nRLDC_{r,t} : [0,1] \to \mathbb{R}$$
$$\theta \mapsto d_\theta \text{ such that } \mathbb{P}(D_{r,t,h,mc}^{residual} \leq d_\theta) = \theta.$$

The $nRLDC_{r,t}$ is a decreasing function. At $\theta = 0$, the operation of the power system is more constrained with lower margin at disposal. However at $\theta = 1$, the operation is less constrained with higher margin (or higher spillage) at disposal. Instead of generating $8760 * card(MC)$ constraints, which will be computationally consuming the new temporal-scale is used to sample the $nRLDC_{r,t}$ into only predefined number of constraints. The new temporal-scale represents the adequacy scale within the long-term planning model [**TIMES**]. Its flexibility is that the modeler can choose the number $k$ of samples (constraints) he wants to generate, and also the region $r$ and period $t$ to which this adequacy scale must be added. Let $tsa$ denotes the new temporal scale of adequacy and $k$ the number of samples: $tsa =$ **Sample(theta)** $= (\theta_1, \theta_2, \ldots, \theta_k)$. The sample function used in our work is simple: it uses the same definitions as the time-slice scale to cover the whole year and take the highest value of $nRLDC$ within each time-slice. So the number of sample $k$ is equal to the number of time-slices. Algorithm 4 bellow shows how to derive adequacy temporal scale $tsa$.

**Algorithm 14:** Construction of the adequacy temporal scale $tsa$ for $\theta \in [0,1]$

**Input:** $nRLDC_{r,t}$: the new Residual Load Duration Curve for region $r$ and period $t$

**Output:** $(\theta_1, \theta_2, \ldots, \theta_k)$: $k = card(S)$ positions samples of the $nRLDC_{r,t}$

**for** $j \in 1:k$ **do**

  $\Theta_{ts_j} \longleftarrow$ **Extract** $\theta$ positions belonging to the time-slice $ts_j$ /* Extract all the $\theta$ positions belonging to the time-slice $ts$, the number of positions is equal to $8760 * card(MC) * length(ts_j)$ */

  $\theta_{ts_j} \longleftarrow$ **Which.max**$(nRLDC_{r,t}(\Theta_{ts_j}))$ /* Affect the sample position $\theta_{ts_j}$ to the $nRLDC$ peak position */

$(\theta_1, \theta_2, \ldots, \theta_k) \longleftarrow$ **Sort** $\{\theta_{ts_j}\}_{j=1:k}$ by a decreasing order based on $nRLDC$ values.

The 4 uses all the available $\theta$ positions in $[0,1]$ to generate a sample. For the development of the feed-back control wee need a variant of this algorithm which use another input position $\theta_n$ to generate a sample only for $\theta \geq \theta_n$. Algorithm 4 bellow is the extension of the previous algorithm with a $\theta_n$ filter position.

**Algorithm 15:** Construction of the adequacy temporal scale $tsa$ for $\theta \in [\theta^n_{r,t}, 1]$

**Input:**

- $nRLDC_{r,t}$: the new Residual Load Duration Curve for region $r$ and period $t$
- $\theta^n_{r,t}$: a given filter position $\theta^n_{r,t} \in [0,1]$ for region $r$ and period $t$

**Output:** $(\theta_1, \theta_2, \ldots, \theta_k)$: $k = card(S)$ positions samples of the $nRLDC_{r,t}$

**for** $j \in 1:k$ **do**

  $\Theta_{ts_j} \longleftarrow$ **Extract** $\theta \in [\theta^n_{r,t}, 1]$ positions belonging to the time-slice $ts_j$ /* Extract all the $\theta$ positions belonging to the time-slice ts, the number of positions is equal to $length([\theta^n_{r,t}, 1]) * card(MC) * length(ts_j)$ */

  $\theta_{ts_j} \longleftarrow$ **Which.max**$(nRLDC_{r,t}(\Theta_{ts_j}))$ /* Affect the sample position $\theta_{ts_j}$ to the $newRLDC$ peak position */

$(\theta_1 = \theta^n_{r,t}, \theta_2, \ldots, \theta_k) \longleftarrow$ **Sort** $\{\theta_{ts_j}\}_{j=1:k}$ by a decreasing order based on $newRLDC$ values. /* It is clear that as we choose the maximum value of the $nRLDC$ for each $\Theta_{ts_j}$, the first position will be the same as the filter position $\theta^n_{r,t}$. Consequently $\theta_1 = \theta^n_{r,t}$ */

Given a filter position $\theta^n_{r,t}$, the Algorithm 4 construct a position sample of the $nRLDC$. Each component $\{\theta_j\}_{j=1:k}$ have its corresponding hour $h \in [1:8760]$ and a Monte Carlo year $mc \in MC$ denoted $h_{\theta_j} = (h, mc)$. The adequacy proxy constraint will be activated only for

risky [6] period and regions $(R_{risky}, T_{risky})$.

$$\forall h_{\theta_j} \in tsa, \forall (r,t) \in (R_{risky}, T_{risky}) \sum_{tech \in Tech} ep_{r,t,h_{\theta_j}} X^{tech}_{r,t} \geq D_{r,t,h_{\theta_j}} + \underline{y^{Spil}_{r,t,h_{\theta_j}}} - \underline{y^{Unsup}_{r,t,h_{\theta_j}}} \quad (5.17)$$

For the [**TIMES**] optimization problem, the set of adequacy proxy constraints expressed in Equation 5.17 is formulated as a new set of equations $D^{\theta^n_{r,t}} X_{r,t} > d^{\theta^n_{r,t}}$

### 5.5.4 Which feed-back control strategy: an introduction to Stochastic Approximation

First of all, in this paragraph, we elucidate the rationale behind the feedback control strategy. If the constraint set $DX_{r,t} > r$ is generated without any restriction on $\theta$, the highest value of unsupplied power will be considered (at $\theta = 0$). This could lead [**TIMES**] to readjust its initial solution and decide on a power generation mix that risks being oversized (with no shortages at all). However, if the sampling process is conducted with $\theta \geq \theta_{filter}$, the level of the highest unsupplied power will be reduced compared to the unfiltered case. The objective is to determine the appropriate filter position $\theta^*_{r,t}$, at which the sampling process should start, to trigger a $LOLE$ of $\zeta_{r,t}$. In other words, we are searching for an adequate filter position $\theta^*_{r,t}$ for which $LOLE_{r,t}(\theta^*_{r,t}) = \zeta_{r,t}$ holds for all $(r,t) \in (R_{risky}, T_{risky})$.

In the iterative process, the only variable is the filter position $\theta_{r,t}$, while the $nRLDC$ object is kept constant. Maintaining the $nRLDC$ constant during iterations is logical because we aim to determine how the initial constraints of [**TIMES**] model need to be reinforced to ensure adequate power generation. This process allows us to identify the optimal filter position that achieves the desired adequacy levels while balancing the trade-off between power supply adequacy and system capacity. In other words, we are searching for a specific point in the space of all possible realizations simulated by the Monte Carlo Scenarios that corresponds to the targeted $LOLE$ level. This point represents the optimal sizing hour that ensures the desired adequacy level for power generation.

The problem described in the first paragraph corresponds to a Stochastic Root-Finding Problem (SRFP). The goal of an SRFP is to find the unique root $\theta^*$ of the equation $M(\theta^*) = \zeta$, where $M : D \subset \mathbb{R}^q \longrightarrow \mathbb{R}^q$, and
$M(\theta) = [M_1(\theta_1, \theta_2, \ldots, \theta_q), \ldots, M_q(\theta_1, \theta_2, \ldots, \theta_q)]$. In contrast to deterministic root-finding problems where the function $M$ is known, SRFPs deal with cases where $M(\theta)$ can only be estimated using a consistent estimator $\bar{y}$ for any given value of $\theta$. These types of problems arise in controlling stochastic systems through numerical simulations: $\zeta$ represents the desired system target, $\theta$ is the value of a control variable, $M(\theta)$ denotes the corresponding system performance, and $\bar{y}(\theta)$ is the estimated performance obtained from a user-provided Monte Carlo simulation procedure. SRFPs can be formulated as simulation-based optimization problems, aiming to find local minima. The formulation is provided below:

**Stochastic Root Finding Problem**
**Given:**

[6] Risky in the sens that the $LOLE$ criterion is not satisfied

1. A constant vector $\zeta \in \mathbb{R}^q$

2. An oracle (computer procedure) capable of generating for each $\theta \in D \subset \mathbb{R}^q$ an estimate $\bar{y}(\theta)$ of $M(\theta)$

**Find:** the unique root $\theta^*$ satisfying $M(\theta^*) = \zeta$ using only the estimator $\bar{y}(\theta)$ and assuming that one such $\theta^*$ solution exists.

There are two classes of algorithms to solve SRFP: prospective and retrospective. A prospective algorithm explores the set of feasible solutions $\theta$ to find the root $\theta^*$, much like a miner prospecting for valuable resources in a chosen area. A classical prospective algorithm is Stochastic Approximation (SA), introduced in 1951 by Herbert Robbins and Sutton Monro [233]. On the other hand, a retrospective algorithm looks at the past. It generates a sample-path approximation to the real stochastic problem and then solves a sequence of deterministic root-finding problems [234]. The first mention of this algorithm in the context of optimization was by Healy, Schruben, and Shapiro in 1991. In our work, we focus solely on the SA algorithm to solve SRFP.

The recursion used in the stochastic approximation algorithm is a "Newton-like" iteration designed for solving SRFP. It involves substituting the estimator $\bar{y}$ for $M$ and incorporating a carefully chosen learning rate sequence $\alpha_n$ with the goal of nullifying the impact of randomness:

$$\theta_{n+1} = \theta_n + \alpha_n(\zeta - \bar{y}(\theta_n)) \tag{5.18}$$

While the recursion in 5.18 is simple, different works have been conducted to respond to the following two questions:

- What conditions on the structure of the function $M$, the estimator $\bar{y}$, and the learning rate $\alpha_n$ ensure that the recursion of equation 5.18 converges to the root of $M$?

- What is the rate of convergence, and what choice of the learning rate $\alpha_n$ could lead to a fast rate of convergence?

In the process of addressing these questions, various variants of algorithms have been developed, collectively referred to as Stochastic Approximation (SA) methods. The primary distinctions between these algorithms lie in the selection of the sequence $\alpha_n$, which aims to strike a balance between efficiency, computation time, and convergence rate. Below, we present basic SA algorithms. The theoretical properties of SA algorithms are beyond the scope of this introduction; readers interested in further details can refer to survey articles on the subject [235].

In understanding the recursion in equation 5.18, it is useful to re-write it as the sum of a "deterministic" part and a "stochastic part":

$$\theta_{n+1} = \theta_n + \alpha_n(\zeta - M(\theta_n)) + \alpha_n(M(\theta_n) - \bar{y}(\theta_n)) \tag{5.19}$$

This decomposition emulates the deterministic Newton's recursion, with $\theta_n$ being a random variable, hence the use of quotes around "deterministic." For the recursion to converge in

a specific sense, two main assumptions must be established: (i) assumptions on the structure of the function $M$ analogous to those in the deterministic root-finding algorithm, and (ii) assumptions on the estimator $\bar{y}$ and the learning rate $\alpha_n$ to neutralize the stochastic component. Robinson and Monro proved the convergence of iterates in one dimension [233], while Blum presented a proof for convergence in multiple dimensions [236]. The following theorems present their results.

**Theorem.1 (Convergence of SA method in one dimension, $q = 1$).** Assume the following

1. Suppose that there exists a $C_1$ such that

$$\forall\theta \qquad \mathbb{P}\{|\bar{y}(\theta)| \leq C_1\} = 1 \tag{5.20}$$

2. Suppose further that $M$ satisfies the following conditions. There exists a real number $\zeta$ and a $\eta \geq 0$ such that

$$M(\theta) \leq \alpha - \theta \text{ for } \theta \geq \zeta \text{ and } M(\theta) \geq \alpha + \eta \text{ for } \theta \geq \zeta \tag{5.21}$$

3. and there exist $C_2$ and $C_3$ such that $\frac{C_2}{n} \leq \alpha_n \leq \frac{C_3}{n}$ for $n \geq 0$. Then if $\theta_0$ is of finite variance,

$$E[(\theta_n - \zeta)^2] \longrightarrow 0 \text{ when } n \longrightarrow \infty \tag{5.22}$$

This implies of course the convergence of $\theta_n$ to $\zeta$ in probability. The assumption 1, imposes that $\bar{y}$ is bounded with probability one. Assumption 2 ensures that there is at most one root, and Assumption 3 ensure that the iterates are positive and bounded. Robbins and Monro also proved the following result.

**Theorem.2 (Convergence of SA method in one dimension, $q = 1$).** Assume the following

1. If Assumption 2 is replaced by the following conditions: $M$ is non-decreasing and the first derivative of $M$ at $\zeta$ exists and positive then the conclusion of Theorem.1 remains valid

From the perspective of a practitioner focused on the method's applications, these two theorems are generally sufficient. However, from a more mathematical viewpoint, questions about the convergence of $\theta_n$ with probability 1 are of interest. The first theorem addressing convergence with probability 1 was introduced by J. R. Blum [236]. Blum further relaxed the assumptions of Robinson-Monro, requiring that the variance of $\bar{y}$ be uniformly bounded over $\theta$, and that the function $M$ be bounded by a linear function of $\theta$.

**Theorem 3 (Convergence of SA method in multiple dimensions, $q \geq 2$)**: For the case of multiple dimensions assume the following.

1.

$$\sum_{n=0}^{\infty} \alpha_n = \infty \tag{5.23}$$

2.

$$\sum_{n=0}^{\infty} \alpha_n^2 \leq \infty \tag{5.24}$$

3. There exists a positive-valued function $f$ with unique minimum at $\zeta$, and having continuous first and second partial derivatives such that

   - $sup_{\epsilon \leq \theta - \zeta} \nabla(\theta)^T M(\theta) < 0$ for all $\epsilon > 0$, where $\nabla(\theta)$ is the column vector of the first partial derivatives of the function $f$ at $\theta_n$ and
   - $E[G(\theta)^T H(\theta) G(\theta)] \leq \infty$ where $H(\theta)$ is the matrix of second partial derivatives of the function $f$ at $\theta$

   Then the iterates $\theta_n$ converge to $\zeta$

## 5.6 The overall multi-scale model: Definition and design of the $LOLE$-Stochastic Root Finding Problem Algorithm

Figure 5.7 depicts all the necessary steps needed in the design of the LOLE-SRFP algorithm. The ultimate goal of this algorithm is to find a combination of $\theta^*$ positions representing the roots of the $LOLE(\theta^*) = \zeta$.

**Oracle: The oracle capable of computing long-term adequacy metric at a given position $\theta^n$**

The Oracle is nothing than the multi-scale model developed before. It allows for a given position $\theta^n = \{\theta^n_{r,t}\}_{r \in R, t \in T}$ (at iteration $n$) to generate a new reinforced [**TIMES**] model with the additional set of adequacy-proxy constraint $D^{\theta^n_{r,t}} X_{r,t} > d^{\theta^n_{r,t}}$ for risky regions. The reinforced [**TIMES**] model is generated and solved and the trajectory investments $\Pi^{TIMES,s}_{inv,n}$ is obtained (notice that an index $n$ is added to $\Pi$ to illustrate the iteration process). The uni-directional multi-scale model allowing to create the short-term operational model [**ANTARES**] based on $\Pi^{TIMES,s}_{inv,n}$ is used while ensuring the optimizations models consistencies with ($O \longleftarrow O'$ and $(C, c) \longrightarrow (B, b)$ operations decided in details in previous sections). After [**ANTARES**] is run, and based on its trajectory operation $\Pi^{TIMES,s}_{inv,n}$, the unbiased estimation of $LOLE$ function at position $\theta^n$ is computed.

**The Stochastic Root Finding Problem Applied to $LOLE$ function**
**Given:**

1. The Oracle capable of generating for each filter position $\theta = (\theta_1, \ldots, \theta_q)$ an estimate $\bar{y}(\theta) = [\bar{y_1}(\theta), \ldots, \bar{y_q}(\theta)]$ of $LOLE(\theta)$: $[0,1]^q \longrightarrow \mathbb{R}^q$. $q$ is the number of the risky couple (region,period).

2. A constant vector of adequacy targets $\zeta = (\zeta_1, \ldots, \zeta_q) \in \mathbb{R}^{+q}$, representing the target $LOLE$ level.

**Find:** the root $\theta^*$ satisfying $LOLE(\theta^*) = \zeta$ using only the estimator $\bar{y}(\theta)$ assuming that such root exists.

The SRFP applied to the multi-regional $LOLE$ function is to solve $q$ equations with $q$ unknowns. For each component $q = (r,t)\ \forall (r,t) \in (R_{risky}, T_{risky})$.

$$\begin{aligned} LOLE_1(\theta_1, \theta_2, ..., \theta_q) &= \zeta_1 \\ LOLE_2(\theta_1, \theta_2, ..., \theta_q) &= \zeta_2 \\ &\vdots \\ LOLE_q(\theta_1, \theta_2, ..., \theta_q) &= \zeta_q \end{aligned}$$

To solve this problem, we consider the projected form of the equation 5.18, where $\Pi_{[0,1]}(x)$ denotes the closest point in $[0,1]$ from $x$, that is $\Pi_{[0,1]}(x) := argmin_{x' \in [0,1]} \|x' - x\|$ ($[0,1]$ is convex, so the projection $\Pi_{[0,1]}$ is well defined).

$$\forall n \in \mathbb{N} \qquad \forall k = (r,t) \in 1:q \quad \theta_k^{n+1} = \Pi_{[0,1]}[\theta_k^n + \alpha_n(\zeta_k - \bar{y_k}(\theta_k^n))] \tag{5.25}$$

It is clear that two parameters are important in the recursion of Equation 5.25: $\theta^0$ and $\alpha_n$. A specific section will discuss the choices of those two parameters in the chapter dedicated to the application of this algorithm on the European power system model. The algorithm stops when the multi-regional $LOLE$ convergence criterion is satisfied. It can be defined as the iteration at which, the modeler is satisfied with the solution with an $\epsilon$-quality : $LOLE \in [\zeta - \underline{\epsilon}, \zeta + \bar{\epsilon}]$, where $\underline{\epsilon}$ and $\bar{\epsilon}$ are the upper bound and lower bound of the solution quality confidence interval. A detailed description of the convergence criterion will also be discussed in the next chapter.

## 5.7 Conclusion

In this chapter, we have developed a multi-scale model designed to bridge the long-term scale of investments and the short-term scale required for the secure operation of the power system. Our approach consists of several key steps. Firstly, we introduced the concept of multi-scale modeling and delineated the essential stages involved in the development of such an approach. Secondly, we presented the theoretical framework underpinning the multi-scale model. This framework commences with the presentation of a scale separation map, serving to represent the distinct temporal scales under consideration. Subsequently, we introduced the optimization problems inherent to the constituent models. Recognizing the commonality of optimization paradigms in both models, we proposed a unified representation based on a matrix representation for both. This unified representation facilitated a straightforward mathematical formulation of the bridging scale algorithms. To simplify our introduction, we divided the overall multi-scale model into two primary components: a uni-directional component and a bi-directional component.

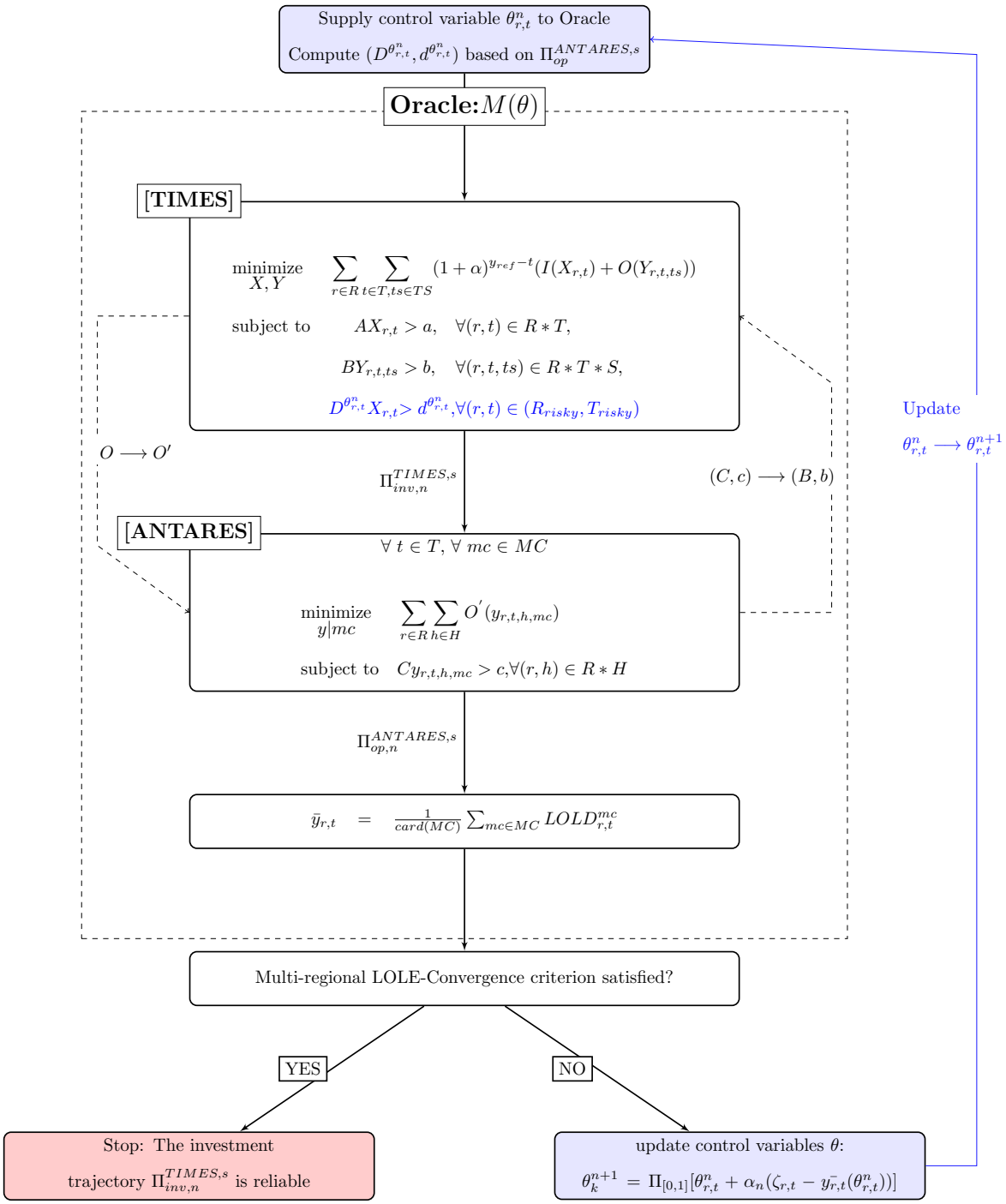


Figure 5.7: The overall multi-scale model based on LOLE-SRFP algorithm to build adequate investment trajectories for power system in transition

The primary objectives of the uni-directional part are twofold. Firstly, it aims to en-

sure the consistency of input data between both models. Secondly, it serves as the conduit for feeding the investment trajectory determined by the long-term energy planning model TIMES into the operational power system model ANTARES. The assessment of power generation adequacy is carried out between these two components. If the assessment reveals that the power generation mix decided by TIMES does not meet the required standards, the bi-directional part is activated.

The bi-directional part comprises two main elements: the design of adequacy constraint proxies and the algorithm that facilitates the feedback loop between both models. In this chapter, we have introduced a novel capacity constraint. The decision variables involved in the equation are the investment decision variables (in terms of installed capacities), while the parameters are derived from the dispatch of the model reflecting the effective participation of each investment into the supply/demand balance. To align the solution with the requisite adequacy levels, we have applied the approximation stochastic algorithm. To do so, we construct an object on which the stochastic approximation algorithm will operate. This object is called the new Residual Load Duration Curve, which rank all the hours of the year in a decreasing order in the sens of the operation. The hour number one is the most constrained from an operational point of view while the last hour is the hour with less constraint on the operation. Based on this object the stochastic approximation algorithm will try to find the hour that will trigger the desired $LOLE$ level.

# Chapter 6

# Application of the multi-scale model to the European interconnected power system

## Contents

In this chapter we apply the multi-scale model developed in the previous chapter to a large scale and multi-area interconnected power system, which is the European power system. The European Union's electricity grid is the most interconnected continental power network in the world [1]. We first introduce shortly the eTIMES-EU: a European long-term planning model developed using the TIMES model generator. Its key modeling assumptions and input data are given. This is important to understand the structure of the model and its related data. Then we introduce the main common data used in common with ANTARES model, the Monte Carlo Scenarios setting and the simulation strategy adopted. Two long-term scenarios are designed at the TIMES level: "scenario A" and "scenario B". "Scenario A" draws a future power system with high renewable installed capacities. "Scenario B" add a neutrality carbon constraint by 2050 to the constraint core of "scenario A". In the Results section, we provide detailed results for "Scenario A". First, the main outcomes of the uni-directional multi-scale model and its validity metrics are provided. Based on the power generation adequacy assessment, the stochastic approximation algorithm was applied to ensure adequacy with two distinct learning rate: decreasing and constant. The performance and convergence of both schemes are studied using two perspectives: a score perspective and a dynamical system perspective. The "score perspective" offers a metric for evaluating the convergence of iterative schemes, whereas the "dynamical system point of view" provides insights into the evolution of the solution trajectory. This is achieved through the concept of a phase diagram, which represents a system of ordinary differentiable equations. The obtained final adequate solution is then analyzed in terms of: power generation mix structures, related costs and $CO2$ emissions. Same analysis is carried out for "Scenario B".

**Résumé en français :**

Dans ce chapitre, nous appliquons le modèle multi-échelle développé dans le chapitre précédent à un système électrique interconnecté à grande échelle et multi-zone, qui est le système électrique européen. Le réseau électrique de l'Union européenne est le réseau continental le plus interconnecté au monde [2]. Nous introduisons d'abord brièvement l'eTIMES-EU : le modèle de planification à long terme européen utilisé. Ses principales hypothèses de modélisation et ses données d'entrée sont données. Cela est important pour comprendre la structure du modèle et ses données connexes. Ensuite, nous introduisons les principales données communes utilisées avec le modèle ANTARES, le cadre des scénarios de Monte-Carlo et la stratégie de simulation adoptée. Deux scénarios à long terme sont conçus au niveau de TIMES : "scénario A" et "scénario B". Le "scénario A" représente un système électrique futur avec une forte part d'EnR. Le "scénario B" ajoute une contrainte de neutralité carbone d'ici 2050 à l'ensemble de contrainte du "scénario A". Dans la section Résultats, nous four-

[1] The synchronous grid within continental Europe, globally recognized as the largest of its kind, functions as a unified system, maintaining a frequency of 50 Hz. This grid is supported by flexible HVDC links, providing electrical power to more than 500 million customers across 27 countries.

[2] Le réseau synchrone au sein de l'Europe continentale, mondialement reconnu comme le plus grand de son genre, fonctionne comme un système unifié, maintenant une fréquence de 50 Hz. Ce réseau est soutenu par des liens HVDC flexibles, fournissant de l'énergie électrique à plus de 500 millions de clients dans 27 pays.

nissons des résultats détaillés pour le "scénario A". Tout d'abord, les principaux résultats du modèle multi-échelle unidirectionnel et ses métriques de validité sont fournis. Sur la base de l'évaluation de l'adéquation de la production électrique, l'algorithme d'approximation stochastique a été appliqué pour garantir l'adéquation avec deux taux d'apprentissage distincts : décroissant et constant. Les performances et la convergence des deux schémas sont étudiées selon deux perspectives : une perspective de score et une perspective de système dynamique. La "perspective de score" offre une métrique pour évaluer la convergence des schémas itératifs, tandis que le "point de vue du système dynamique" offre une anlyse sur l'évolution de la trajectoire de solution. Cela est réalisé à travers le concept de diagramme de phase, qui représente un système d'équations différentielles ordinaires. La solution finale adéquate obtenue est ensuite analysée en termes de : structures de mix énergétique, coûts associés et émissions de $CO2$. La même analyse est réalisée pour le "scénario B".

## 6.1 Introduction to the key internal eTIMES-EU assumptions

In its thesis work Gildas SIGGINI developed eTIMES-EU, a European long-term power system planning model [3] [37]. We synthesis in this paragraph the main characteristics used in this model.

### 6.1.1 General Model overview

#### Overview of major inputs

The eTIMES-EU is supported by a large set of databases, with the following main exogenous inputs:

- End-use energy services: such as electricity demand. At this level the data used is coming from OSMOSE project [190].
- Main characteristics of the existing and future energy related technologies: such as efficiency, emissions, stock, availability, investment costs, operational and maintenance costs and discount rate. For the base year, data is provided by ENTSO-E on the transparency website page. The energy supply beyond the base year are compiled in a an extensive database with detailed technical and economic characteristics of new energy technologies. This compilation is based on the data provided by the Energy Technology Database and with their costs updated with International Renewable Energy Agency (IRENA) and International Energy Agency (IEA) costs projections.
- Present and futures sources of primary energy supply and their potentials. Potentials and cost for different primary resources correspond to data from ENergy Systems

[3] The system coverage of eTIMES-EU is only restricted to the power system

Potential Renewable Energy SOurces (ENSPRESO) for solar, wind and biomass potentials. The potential for geothermal and marine resources are based on the JRC-EU-TIMES model, while costs projection are based on IEA Energy Outlook projections.

- Policy constraints and assumptions. The policy constraints such as CO2 emission caps, taxes, subsidies and deployment trajectories are user-defined and can be tailored for each particular policy orientation. However, default policy constraints include acted complete coal and nuclear phase-out plans in the committed countries.

### Temporal and spatial resolution

The eTIMES-EU model uses a time-frame for analyzing the European electric system from 2016 to 2050. Investment and operational decisions are initially calibrated for the years 2016 and 2017, and subsequently computed by the model every five years from 2020 to 2050. To handle computational complexity efficiently and focus on specific sub-annual dynamics, each year is divided into time-slices, representing distinct periods. The eTIMES-EU model operates with 64 time-slices per year, with each time-slice corresponding to a segment of time within a typical season (4) and week, including both weekdays and weekends. These time-slices are further divided into eight sequential day periods, resulting in a total of 8 time-sequential day periods for each time-slice (refer to Figure 6.1). This consistent temporal resolution is uniformly applied across all regions within the model. The name of each time slice is composed of the three letter of each season ($DJF, MAM, JJA, SON$), the type of week ($B, E$) and the daily time-segment ($P1...P8$).

The eTIMES-EU model has a spatial coverage that includes 29 interconnected countries. Each individual country is represented as a distinct region within the model. It include all EU 27 countries except Cyprus and Malta. In addition to these EU countries, there are non-EU countries considered, namely Switzerland, Iceland, Norway, and the United Kingdom.

### Emissions considered in eTIMES-EU

The different emissions commodities related to processes activity tracked in the model are: CO2, sulphur dioxide (SO2), methane (CH4), nitrogen oxides (NOx), fluor carbons (CxFy), nitrogen dioxide (NO2), carbon monoxide (CO), volatile organic compounds (VOC), particulate PM 2.5 (PMA), particulate PM 10 (PMB) and sulphur hexafluoride (SF6). CO2 emissions levels are estimated through coefficients associated with the combustible fuels defined in the model. The emissions coefficients matrix is presented in table 54. However in the scope of our thesis, we focus only on the emissions associated with $CO_2$.

### Primary energy import prices and discount rate

Fuel prices considered in the eTIMES-EU are based on the IEA World Energy Outlook 2016 projections. Fossil commodities data are summarized in table 6.1 bellow. For Biomass resources, four main commodities are considered: biogas, municipal waste, industrial waste-sludge and wood products. The model consider that all this commodities are available in each

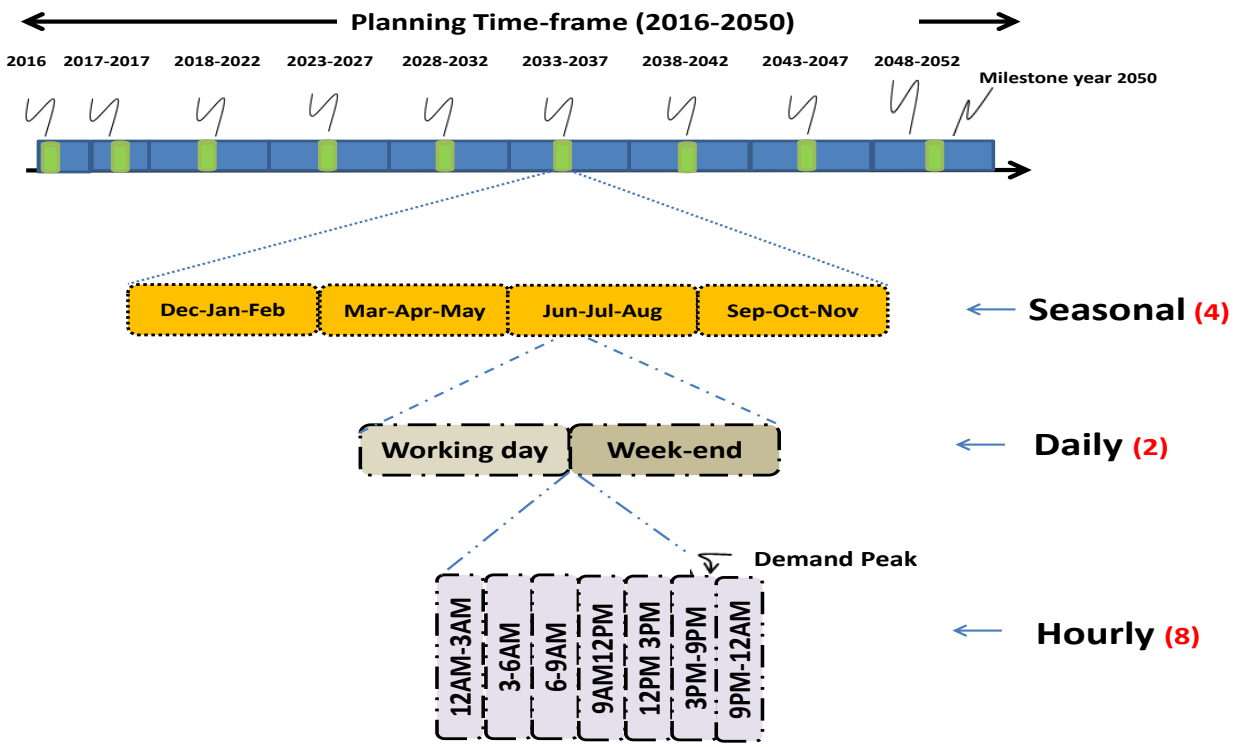


Figure 6.1: Time-slices temporal scale construction for the eTIMES-EU

region and a similar cost is applied. The biogas costs decrease linearly from 20.99 E/MWh in 2016 to 7.99 in 2050. Municipal waste and Industrial waste-sludge have a constant cost of 0.04 euro/MWh while Wood product have a constant value of 19.98 Euro/MWh.

| (Commodity,Year) | 2020 | 2030 | 2040 | 2050 |
|---|---|---|---|---|
| Hard Coal | 10.1 | 10.5 | 10.7 | 10.9 |
| Coke | 12.9 | 13.3 | 13.6 | 13.9 |
| Oil from feedstocks | 54.0 | 57.8 | 63.1 | 67.8 |
| Other petroleum products | 54.0 | 57.8 | 63.1 | 67.8 |
| Natural gas | 62.8 | 64.9 | 68.1 | 70.9 |
| Heavy fuel oil | 87.0 | 93.2 | 101.6 | 109.3 |
| Crude oil | 107.4 | 115.0 | 125.5 | 135.0 |
| Liquefied petroleum gas | 118.2 | 126.5 | 138.0 | 148.5 |
| Kerosene | 139.7 | 149.5 | 163.1 | 175.5 |
| Motor spirit | 139.7 | 149.5 | 163.1 | 175.5 |
| Diesel | 148.5 | 159.1 | 173.5 | 186.7 |

Table 6.1: Fossil fuel import prices (Euro/MWh) considered in the model

The eTIMES-EU considers the mining and the import of different primary energy sources.

Renewable resources -wind, solar, marine and geothermal- are also considered as locally mined with a supply cost of 0,036 Euro/MWh

Within the TIMES model, two distinct discount rates can be defined: a social discount rate and technology specific financial discount rate. The social discount rate reflects how future expenses and well-being should be valued in comparison to the present, and it is a matter of concern for social planners and governments, taking into account social, environmental, and economic considerations. On the other hand, the technology-specific financial discount rates are applicable to individual agents and involve factors such as project profitability, cost of capital, and risk aversion. In the eTIMES-EU only the social discount rate is taken into account with a rate of 8%.

### 6.1.2 Energy resources and technologies

Before detailing the related data of Energy technologies, it is important to note that the eTIMES-EU model take into account annual extraction limits from different fossil resources. For the technical potential for renewable electricity, eTIMES-EU considers the JRC ENSPRESO database to compute the overall potentials for solar and wind and the data from another European long-term energy planning model JRC-EU-TIMES model for hydro, geothermal and marine energy potentials [237]. Table 6.2 bellow depicts the maximal installed capacities considered in the eTIMES-EU model for hydro, solar and wind sources from 2020 to 2050.

| Region | Hydro potential (GW) | Solar potential (GW) | Wind offshore (GW) | Wind onshore potential (GW) |
|---|---|---|---|---|
| AT | 13.3 | 73 | 0 | 11 |
| BE | 0.9 | 52 | 2 | 8 |
| BG | 6.4 | 149 | 0 | 53 |
| CH | 18 | 20 | 0 | 0.075 |
| CZ | 1.4 | 112 | 0 | 76 |
| DE | 4.8 | 494 | 28 | 107 |
| DK | 0.01 | 76 | 27 | 55 |
| EE | 0.01 | 28 | 1 | 27 |
| ES | 34.2 | 658 | 1 | 704 |
| FI | 4.1 | 36 | 21 | 31 |
| FR | 28.1 | 822 | 16 | 813 |
| GR | 10 | 157 | 0 | 168 |
| HR | 2.2 | 50 | 5 | 24 |
| HU | 0.1 | 161 | 0 | 53 |
| IE | 0.4 | 113 | 1 | 147 |
| IS | 6.2 | 0 | 0 | 0.303 |
| IT | 18.3 | 443 | 5 | 178 |
| LT | 0.2 | 93 | 3 | 128 |
| LU | 0.2 | 3 | 0 | 1 |
| LV | 1.8 | 48 | 15 | 79 |
| NL | 0.04 | 42 | 48 | 49 |
| NO | 31.85 | 12 | 7.3 | 0.836 |
| PL | 0.95 | 447 | 12 | 102 |
| PT | 7.44 | 92 | 3.38 | 39 |
| RO | 16.3 | 381 | 9 | 169 |
| SE | 19.5 | 71 | 31 | 134 |
| SI | 1.9 | 18 | 0 | 2 |
| SK | 2.5 | 60 | 0 | 29 |
| UK | 4.5 | 347 | 104 | 230 |

Table 6.2: Maximal installed capacities considered in the eTIMES-EU model for hydro, solar and wind sources from 2020 to 2050

The eTIMES-EU model consider existing generation technologies and potential future technologies. Figure 6.2 bellow presents the supply sector that consider a branch of Mined resources or imported resources. Each technology have a set of technical, economical and environmental data (available in the thesis of Gildas Siggini [37]).

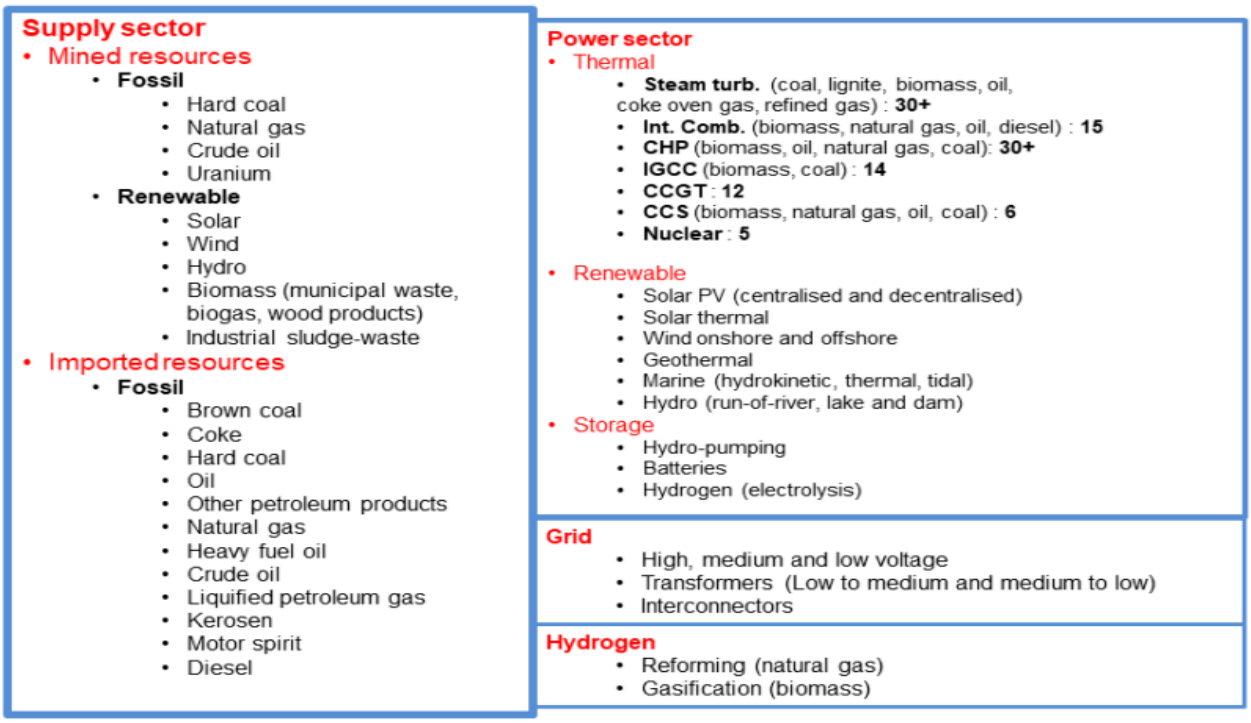


Figure 6.2: Technologies considered in the eTIMES-EU

Some key assumptions are incorporated for each technology to reflect as realistic as possible the transition targets. According to the European Commission's long-term strategy, actual projections call for a doubling of renewable energy deployment from 2020 to 2030 compared to the period of 2010-2019 [238]. Some of the assumptions incorporated in the eTIMES-EU model surpass these levels. We provide below a detailed account of the considerations for each production technology. It is important to note that unless explicitly stated, the statistics on maximum yearly installed capacity refer to the period from 2000 to 2018.

For **Solar PV**, the definition of maximum installed capacity per region in the eTIMES-EU is based on the data of the maximum yearly installed capacity over the period 2000-2018. As the investment within eTIMES-EU are deployed each 5 years, the maximum cumulative capacity over 5 years is calculated. The assumption that in the future, each country could realize two times the maximum yearly installed capacity is used to define the deployment constraints of the eTIMES-EU model. Each value represent the maximum capacity installed in 5 years. Table A.1 in the Appendix depicts the maximum allowed installed capacity for solar PV.

**The nuclear option** is subject of various considerations at European level (the data presented here is derived from the information provided in the thesis [37] and has not been updated to reflect recent policies or developments.). Countries that do not have this source of production at present wish to refrain from using this means of production in the future. Thus Austria (AT), Denmark (DK), Greece (GR) and Italy (IT) (mainly for seismic reasons),

Croatia (HR), Ireland (IE), Iceland (IS), Ireland (IE), Luxembourg (LU), Latvia (LV), Norway (NO) and Portugal (PT) do not plan to use nuclear power for energy production in the short or medium term. Lithuania (LT): Lithuania closed its last nuclear power plant in 2009, and plans for the construction of new plants are uncertain. Estonia is considering the nuclear option due to environmental pressure and in preparation for the post-shale era. Plans call for the construction of a 0.3 GW plant by 2030. Poland is considering the nuclear option from 2033 onwards to reduce its energy dependency. Plans include the construction of a total of 6 GW, with 3GW in 2033 and an additional 3 GW in 2039. Belgium intends to shut down its nuclear power plants by 2025, despite concerns about the consequences on prices and security of supply. Bulgaria plans to expand its nuclear fleet with at least one new nuclear power plant, but commissioning dates are uncertain. Switzerland has decided not to build new nuclear power plants but allows for the extension of existing plants, subject to safety evaluations. The Czech Republic plans to increase its production capacity by 2036, with additional plans for 2.4GW after 2040. Germany has decided to phase out nuclear power by 2022, following the Fukushima accident. Spain currently has no plans to build new nuclear power plants. Finland is constructing a new nuclear power plant, expected to be completed in 2021. Another project is also planned with a planned commissioning in 2028. France plans to reduce the share of nuclear power supply from 75% to 50%. The Flamanville power plant's operation has been delayed, and no other construction is currently planned before 2025. Hungary is scheduled to start the construction of a new nuclear power plant in 2020, with a commissioning in 2026. Another plant is planned to start in 2027. Netherlands (NL): There are currently no plans for nuclear reactors in the Netherlands. Sweden (SE): There are currently no plans for nuclear reactors in Sweden nor in Netherlands. Romania (RO): The commissioning of two nuclear units planned for 2021 and 2022 in Romania is likely to be delayed due to construction problems. Slovenia (SI): Slovenia is considering expansion plans for nuclear power, but details regarding the site and commissioning date are not available. Slovakia (SK): Slovakia operates two nuclear plants and plans to construct a third one in 2025. United Kingdom (UK): The UK expects to benefit from additional capacity provided by Hinkley Point C by 2025, with further capacity planned for 2027. A total of 7.8GW is proposed and awaiting approval. It's important to note that this information may not reflect the latest updates or changes in each country's nuclear power plans. Table A.5 in the Appendix depicts the maximum nuclear capacity extended for the existing stock per period, while Table A.6 in the Appendix depicts the maximum new nuclear installed capacity.

**Hydro energy**, it is widely recognized that the potential for large-scale infrastructure water projects in Europe, except for the Balkan region, has reached a global saturation point. New projects predominantly prioritize the development of small run-of-river plants or pumped storage hydropower (PSP). The eTIMES-EU model aligns with the hydroelectric potential expressed in the JRC-EU-TIMES model. However, it is important to note that this potential does not include pumped storage hydropower (PSP). A maximum hydro installed capacity is incorporated per period following the data of Table A.7.

**Fossil capacity:** The deployment constraint defined for fossil fuel capacities (natural gas, coal, petroleum products) reflects a rhythm allowing to install over the period 2020-2050,

at least 1.5 times the capacity in 2016.

**Grid Representation within eTIMES-EU**

The eTIMES-EU model does not explicitly incorporate the formal representation of energy commodities trade. Regions within the model can either produce energy resources internally or import them from unspecified external regions referred to as Rest of World (ROW).

In contrast, electricity trade is more comprehensively depicted in the model. All interconnections between the considered regions are represented, facilitating bilateral trade. Cross-border interconnections capacities are expressed as the maximum Net Transfer Capacities (NTC) in both directions of trade. Planned expansions of line capacities occur until 2030 in accordance with the TYNDP2016 report [239]. Beyond 2030, new investments in interconnections can be made, incurring a cost of $9999 Euro/kW$. No further investments are permitted in national grids.

### 6.1.3 Current and planned energy policies

Default policies considered in the eTIMES-EU model are acted coal policies listed in [240] and confirmed nuclear phase-out policies. The Table 6.3 below list the different assumptions for the countries.

| Region | Coal policy assumption | Nuclear policy assumption |
|---|---|---|
| AT | Coal free by 2020 | No nuclear plant |
| BE | Coal free since 2016, no new coal plant | Nuclear phase out in 2025 |
| BG | No particular policy | Added possible 2GW from 2045 to 2050 |
| CH | No coal in the mix | No new nuclear plant |
| CZ | No particular policy | Added possible 4.8GW from 2040 to 2050 |
| DE | Coal phase out in 2040 | Nuclear phase out in 2022 |
| DK | Coal phase out in 2030 | No nuclear plant |
| EE | No coal in the mix | Added possible 0.3GW in 2030 |
| ES | No particular policy | No new nuclear plant |
| FI | Coal phase out in 2030 | Added 1.7GW in 2020 and possible 1.2GW in 2030 |
| FR | Coal phase out by 2022 | Added 1.6GW in 2025 and possible 40GW from 2030 to 2050 |
| GR | Coal phase out in 2030 | No nuclear plant |
| HR | No particular policy | No nuclear plant |
| HU | Coal phase out by 2030 | Added possible 2.4GW in 2030 |
| IE | Coal phase out by 2025 | No nuclear plant |
| IS | No coal in the mix | No nuclear plant |
| IT | Coal phase out by 2025 | No nuclear plant |
| LU | No coal in the mix | No nuclear plant |
| LT | No coal in the mix | No nuclear plant |
| LV | No coal in the mix | No nuclear plant |
| NL | Coal phase out by 2029 | No new nuclear plant |
| NO | No coal in the mix | No nuclear plant |
| PL | No particular policy | Added possible 3GW in 2035 and 2040 |
| PT | Coal phase out by 2023 | No nuclear plant |
| RO | No particular policy | Added possible 1.44GW in 2030 |
| SE | Coal phase out by 2020 | No new nuclear plant |
| SI | No particular policy | Added possible 1.2GW in 2045 |
| SK | Coal phase out by 2023 | Added 0.47GW in 2020 and 2021 |
| UK | Coal phase out by 2024 | Added 1.7GW in 2020 and possible 12.8GW from 2030 to 2040 |

Table 6.3: Coal and nuclear policies in the eTIMES-EU model

## 6.2 Data, Monte Carlo and scenarios assumptions

The data presented here focuses only on the common data that both models must share for building the multi-scale model. Readers who want to have explanation on the bridging scale algorithm can refer to the previous Chapter. The data used in the following paragraph are based on the European OSMOSE project [241] [4]. The principal aim of this project is to investigate the need for flexibility and how it can be fulfilled by future energy systems with advanced stages of VRE integration. In the following paragraphs we present the data used especially electricity demand, capacity factors and the simulation strategy.

[4]The three scenarios were defined before the announcement of the Fit for 55 package by the European Union (July 2021)

### 6.2.1 Annual electricity demand projections

Within OSMOSE project three contrasted European long-term scenarios regarding emissions were selected. This three scenarios aim to cover the range of conceivable developments in the European energy sector. The main important driver of the development of this scenarios is the total carbon emissions:

- Current Goals Achieved (CGA): based on the current efforts to comply with the 2°C target. It translates in emission reduction of 40% by 2030, and 80% by 2050.
- Accelerated Transformation (AT): Ambitious pathway expecting to reduce emission by 50% in 2030 and 98% in 2050.
- Neglected Climate Action (NCA): current goals are not achieved and missed by 5% in 2030 and by 10% in 2050.

Another important driver of the development of the above scenarios is the final energy demand. Final energy demand refers to energy services demanded by consumers which differ from primary energy which includes loses from conversion and transmissions [5]. Three main final energy demand are considered. 1) original electricity 2) final demand for heat 3) final demand for passengers transport and freight. Original electricity demand only includes electricity that is not used within the heat or mobility sector. Original electricity uses that are traditionally supplied by electricity. It is assumed to be constant until 2050 in Current Goals Achieved and until 2030 in neglected Climate Action and Accelerated Transformation. In these scenarios demand is assumed to increase and decrease respectively by 5%. Final demand for heat is subdivided into low temperature (under 100 °C) heat and high temperature heat (mostly industrial process over 100°C). Values for heat, both low and high temperature, in the CGA scenario are based on data from the Heat Roadmap Europe project. Neglected Climate Action reflects a scenario where only 50% of insulation efforts are realized compared to CGA Baseline scenario. Assumptions regarding heat demand for the AT scenario follow the same trend until 2030 as the CGA scenario and decrease by 5% in 2050. Mobility demand assumptions are kept the same for all scenarios and based on PRIMES scenarios.

Based on a multi-model methodology assuming the assumption of the two drivers, the electricity demand was computed. The total demand for electricity is steered in different pathways depending on the two drivers: emissions and final energy demand level. Figure 6.3 depicts the breakdown of the total electricity demand across scenarios. It can be seen that in a general manner the demand rises steeply as emission limits become smaller towards 2050. Two effects are also observed. Smaller emission limits are found to increase the electricity demand, because more electricity is used for mobility and heating. Reduction in the final energy demand on the other hand decreases the overall electricity demand. It can be seen from the Figure that in 2050, total demand in CGA scenario is bellow demand in NCA, although emissions are smaller in CGA. This is because the demand for low temperature

[5] The EU efficiency target of 27% for example refers to the primary energy

heat in NCA is higher and as a result, more electricity is being needed to achieve the same degree of electrification in the heat sector.

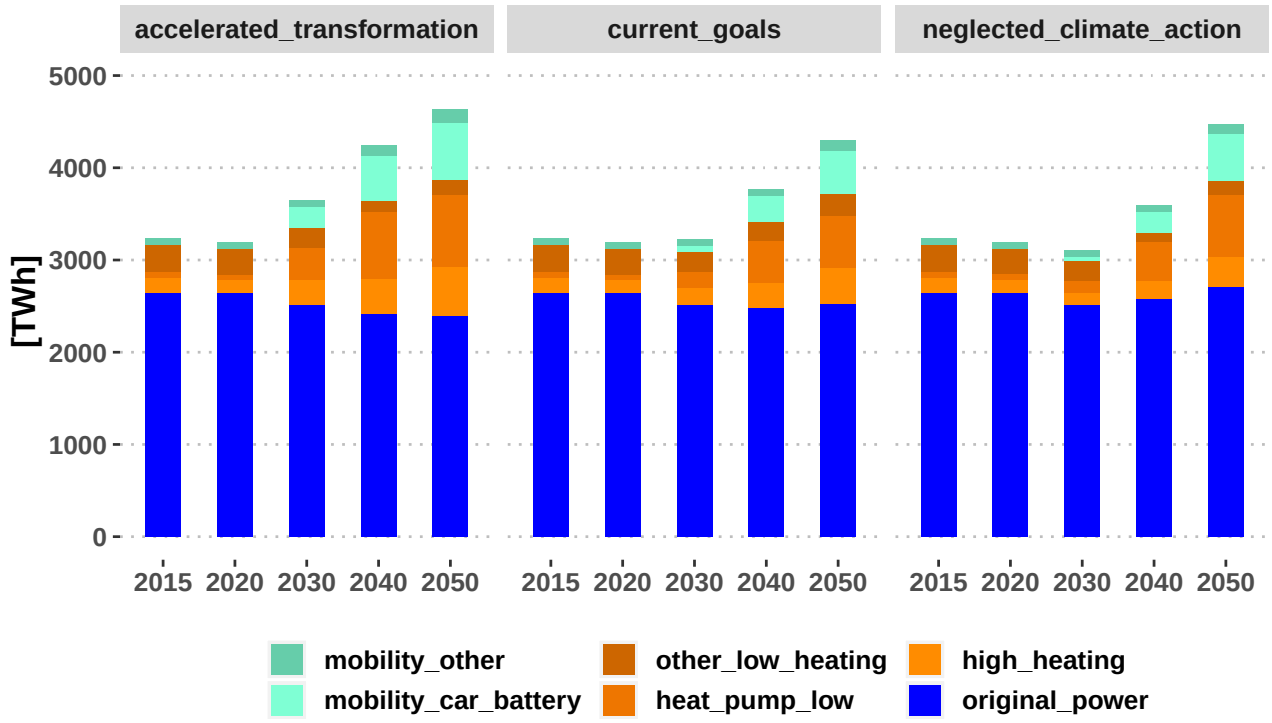


Figure 6.3: Final Energy demand across the three contrasted European long-term scenarios

Based on this data, the annual electricity demand within the long-term energy planning model eTIMES-EU was aggregated into two main components: electricity demand and vehicle electric demand. This aggregation follow the demand sectoral coverage within eTIMES-EU.

### 6.2.2 Monte Carlo Modeling

The data source used in this work follows the first OSMOSE simulation run (which have been taken from the e-Highway 2050 EU-project). This dataset only contained 1 time-series of load and hydro data and 11 time-series of renewable hourly capacity factors. There was therefore no suitable correlation between the load and the meteorological conditions driving VRES generation. This data set was used as a starting point, but a new action plan was put in place to elaborate more robust data. Each Monte Carlo Scenario is a combination of the load time-serie, the hydro inflows time-serie, 1 of the eleven time-series of wind and 1 of the eleven time-series of solar. In the following we detailed the data used for each stochastic parameter: (For reconciliation algorithm please refer to the Chapter 5).

### Load profiles

For each country a normalized hourly load profile is used (based on 2012 data). Figure 6.4 bellow shows a duration load curve for each country for total electricity demand and for vehicle electric.

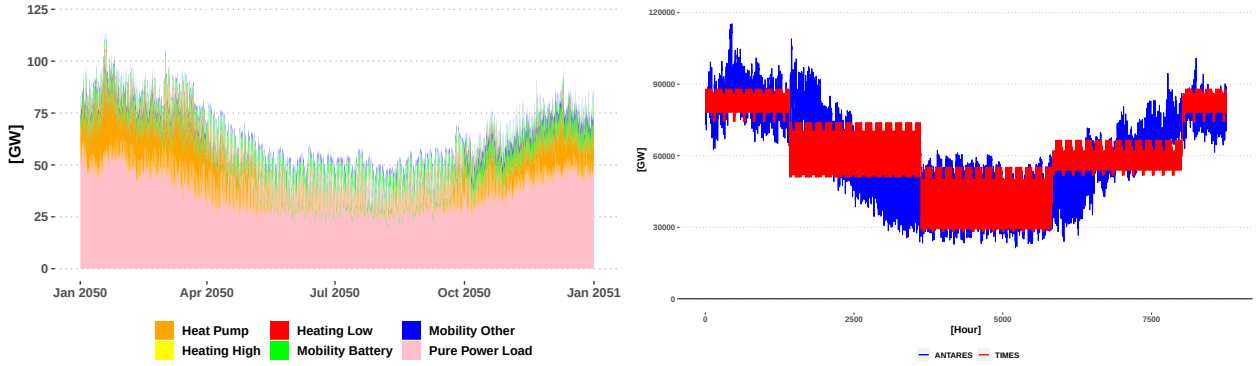


(a) (b)

Figure 6.4: Power load curve of the median climatic scenario: (a) represents the 2030 load curve breakdown by sector of activity and (b) the temperature sensitivity.

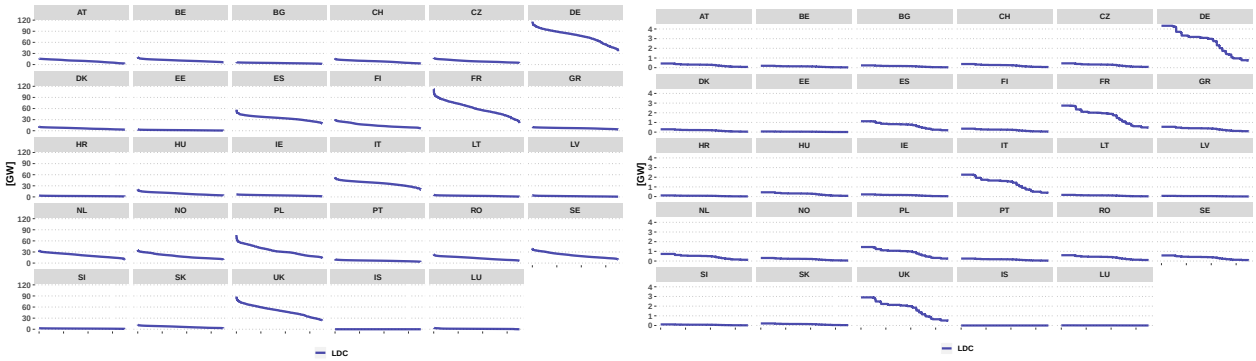


(a) (b)

Figure 6.5: Power load duration curves for European countries: (a) depict the electricity load curve, while (b) illustrate the electric vehicle load duration curve.

Within ANTARES, for the electric vehicle load, a percentage of the overall daily load corresponding to the charging of the electrical vehicles can be optimally positioned within a day by the optimization process.

### Wind and solar capacity factors

Figure 6.6 bellow depicts the capacity factors of wind and solar for the 11 time-series used.

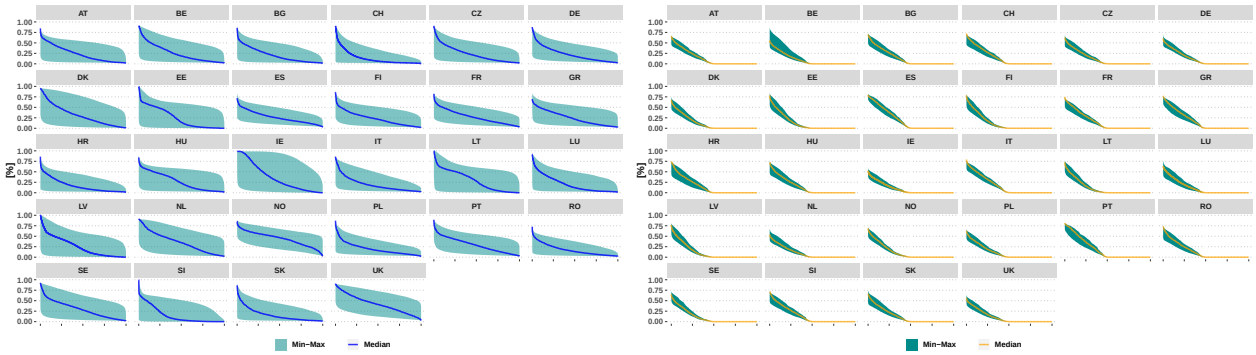


(a) Wind capacity factors duration curves for the 11 Monte Carlo Years,

(b) Solar capacity factors duration curves for the 11 Monte Carlo Years.

Figure 6.6: Wind and Solar load duration curves used in the Monte Carlo simulation.

### Hydro generation

For each country, one single year of hydrological data is used. Hydro-reservoir generation uses the inflow time-series. For RoR (Run of River) time-series, an equivalent capacity factor is estimated based on historical generation.

### Thermal availability

In contrary to the modeling used in the case of France, we don't include the planed and fortuitous unavailability. As a consequence, the thermal availability of each thermal unit is equal to its installed capacity for each hour in the year. Hence, for each Monte Carlo Year modeling, only one time-serie of thermal units available capacity is used (instead of 66 times-series in the French case application).

### 6.2.3 The simulation strategy and numerical considerations

The simulation strategy consists of two main components. The first one involves the configuration of the uni-directional multi-scale model, while the second one is related to the configuration of the stochastic approximation algorithm. We will now discuss the main characteristics of each component.

1. At the **multi-scale model level**, two long-term scenarios, "$s$=Scenario A" and "$s$=Scenario B," were developed. In "Scenario A, an objective of CO2 emissions reduction was introduced by means of a CO2 tax of up to 35 Euro/tCO2. In "Scenario B" the tax level was sharply increased to follow the trajectory developed in the work of "The value for climate action: a shadow price of carbon for valuation of investments and public actions" by Alain Quinet [242]. This report define a trajectory of values to achieve the goal of net zero GHG emissions by 2050. The report outlined specific time-bound targets for carbon prices: 54 Euro/tCO2eq in 2018, 87 Euro/tCO2e in 2020, 250 Euro/tCO2e in 2030, 500 Euro/tCO2e in 2040, and 775 Euro/tCO2e in 2050.

   The trajectory depicted in the black line in Figure 6.7 below represents the value of the $CO_2$ for France. For simplicity in our modeling, this trajectory was applied for all the European countries [6]. In addition to the CO2 tax, "Scenario B" sets a constraint on the $CO_2$ emissions in 2050 at the neutrality level, aiming for zero emissions at the European level, without establishing any constraint at intermediate periods within the planning time-frame nor at country levels. The model is free to find the optimal investment trajectory to reach neutrality by 2050. However, "Scenario B" faced numerical difficulties in finding a solution without relaxing a constraint on the deployment rates, as the constraints used in this scenario bind investments on different capacities. To study the impact of the $CO_2$ constraint on the multi-scale model, the constraint on the deployment of "other" technologies was relaxed. This decision was motivated by the fact that the deployment rate used in "Scenario A" did not allow finding a feasible solution when the stochastic approximation algorithm was applied, depleting all potentials.

[6] The Quinet Report deals only with France

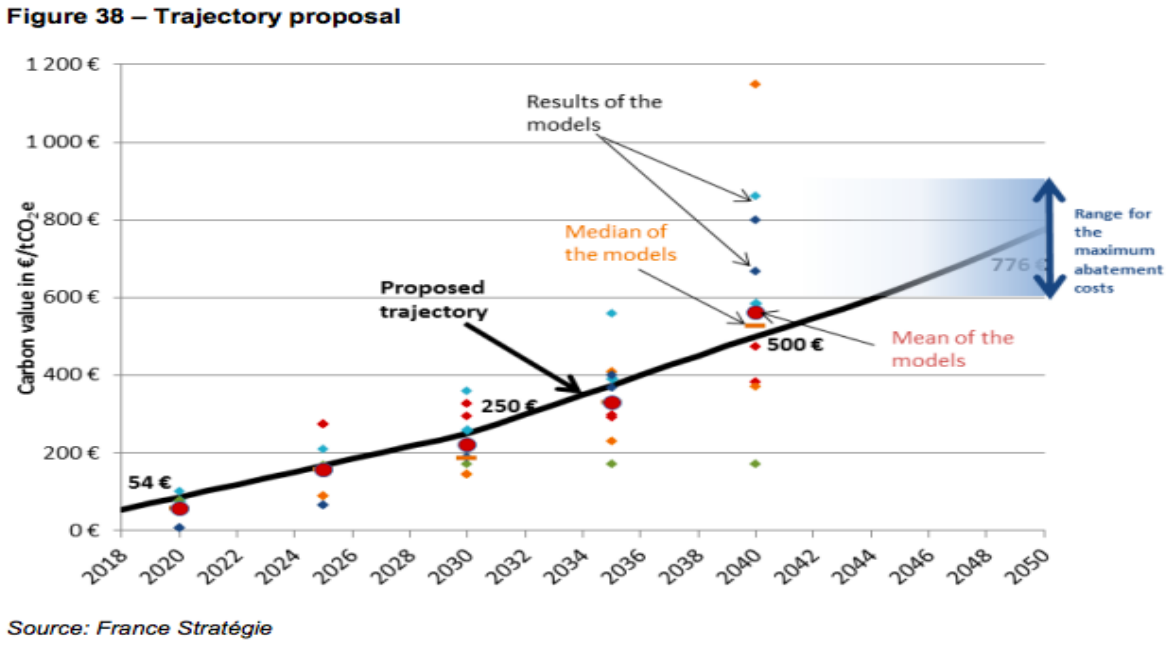


Figure 6.7: The trajectory assumed for the $CO_2$ tax for the scenario $B$ (source [242])

The main constraints used in the modeling of the two long-term scenarios are summarized in the Table 6.4 bellow.

| Scenario A | Scenario B |
|---|---|
| Demand trajectory following scenario "Current Goals" | Demand trajectory following scenario "Current Goals" |
| Wind, Solar and RoR capacity factor following the first time-serie (1/11) | Wind, Solar and RoR capacity factor following the first time-serie (1/11) |
| Hydro inflow following the the first time-serie (1/11) | Hydro inflow following the the first time-serie (1/11) |
| Lifetime of CO2 storage sites | Lifetime of CO2 storage sites |
| Annual CO2 storage capacity by country | Annual CO2 storage capacity by country |
| Lignite extraction costs by country | Lignite extraction costs by country Breakdown of heat demand |
| Activity and operating costs of lignite power plants | Activity and operating costs of lignite power plants |
| Installed transformer capacity (all types) | Installed transformer capacity (all types) |
| Transformer capacity factor | Transformer capacity factor |
| Maximum capacity of intra-EU interconnections | Maximum capacity of intra-EU interconnections |
| Residual interconnection capacity | Residual interconnection capacity |
| Annual interconnection capacity factor | Annual interconnection capacity factor |
| Interconnection efficiency | Interconnection efficiency |
| Interconnector lifetime | Interconnector lifetime |
| Cost of new interconnection capacity | Cost of new interconnection capacity |
| Other interconnection parameters | Other interconnection parameters |
| Investment cost of biomass power plants | Investment cost of biomass power plants |
| Year of availability of new technologies | Year of availability of new technologies |
| Process efficiency | Process efficiency |
| Residual capacities of existing technologies | Residual capacities of existing technologies |
| Annual capacity factor of existing plants | Annual capacity factor of existing plants |
| Cost of importing nuclear resources | Cost of importing nuclear resources |
| Nuclear fixed operated cost | Nuclear fixed operated cost |
| 3rd and 4th generation nuclear investment costs | 3rd and 4th generation nuclear investment costs |
| Investment costs for new fossil-fired capacity | Investment costs for new fossil-fired capacity |
| Investment cost of new alternative fossil-fired capacity | Investment cost of new alternative fossil-fired capacity |
| Investment cost of new renewable capacities | Investment cost of new renewable capacities |
| Investment cost of new alternative renewable capacities | Investment cost of new alternative renewable capacities |
| Tax $CO_2$ at 35 $Euro/tCO2$ | Tax on $CO_2$ emissions following Quinet Report |
| | Zero emissions in 2050 without intermediate bounds |

Table 6.4: The set of constraints corresponding to each modeled long-term scenario within eTIMES-EU

2. At the **Stochastic approximation** algorithm level, the simulation strategy consists of the design of two iterative schemes. The goal is to test the performance of the developed methodology under different configurations of the stochastic approximation algorithm. As seen in Chapter 5, two main important parameters are needed to be chosen by the modeler. The initial values of the control variable $\theta$ and the learning rate $\alpha$. In our work we chose two commonly used variants of stochastic approximation with different learning rate strategies: constant learning rate and decreasing learning rate.

   (a) **Decreasing Learning Rate:** in the decreasing learning rate strategy, the learning rate decreases as the iterative process progresses. This allows the algorithm to take larger steps in the beginning to quickly converge to a region close to the optimal solution and gradually reduce the step size to fine-tune the estimate. One common approach for decreasing the learning rate is to use a schedule that reduces the learning rate at each iteration. The update rule for the SA algorithm with a decreasing learning rate can be represented as: $\theta_{r,t}^{n+1} = \Pi_{[0,1]}[\theta_{r,t}^{n} + \alpha_n(\zeta_{r,t} - \bar{y_{r,t}}(\theta_{r,t}^{n}))]$, where $\alpha_n$ is the learning rate at iteration $n$, which decreases over time according to a predefined formula. In the literature of the SA, we found that a decreasing learning rate of $\frac{C}{n^\gamma}$ with $\gamma \in [0, 0.5]$ converge faster than a basic $\frac{1}{n}$. We chose then

to use a decreasing learning rate of $\alpha_n = 5.18 * 10^{-4}/n^(0.5)$ [7].

(b) **Constant Learning Rate:** for the constant learning rate strategy, the learning rate remains fixed throughout the iterations. This means that the step size remains the same, irrespective of the progress made in the iterative process. Mathematically, the update rule for the stochastic approximation algorithm with a constant learning rate can be represented as: $\theta_{r,t}^{n+1} = \Pi_{[0,1]}[\theta_{r,t}^{n} + \alpha(\zeta_{r,t} - \bar{y_{r,t}}(\theta_{r,t}^{n}))]$ where $\theta_{r,t}^{n}$ is the control variable at iteration $n$, $\alpha$ is the constant learning rate, and $\zeta_{r,t} - \bar{y_{r,t}}(\theta_{r,t}^{n}))$ the update direction at iteration $n$. It is important to note that $\theta_{r,t}^{n} \in [0,1]$, $\theta_{r,t} = 0$ is the first observation in the $nRLDC$ (peak hour: number 1) while $\theta_{r,t} = 1$ is the last observation (hour number $8786 * 11$). For this configuration, we chose $\alpha = 0.0001141$. This value corresponds to the number of Monte Carlo years simulated. With 11 Monte Carlo Years, a $LOLE$ equal to 3 hours/year is equivalent of 33 hours of shortage in the $nRLDC$. If we choose $\theta_0 = 0$, we expect to have a $LOLE$ of 0, to obtain 33 hours of shortage in the next iterations the $\alpha$ need to satisfy $33 = 0 + \alpha(3 - 0) \leftrightarrow \alpha = 11$.

The computational framework of the developed multi-scale model is supported by an autonomous workflow of scripts developed using R language. The numerical considerations to take into account are as follows (detailed numerical performance results for all scenarios will be presented in the results section).

- At TIMES level: in order to solve the optimization problem, the interior-point algorithm is used. Once the stochastic approximation algorithm is activated, the dual-simplex algorithm is used in order to trigger a warm start when the iterative process starts. This lead to a huge reduction (70%) in the computational time within the long-term power system planning model. In other words, for each iteration $n+1$, the TIMES solver commences from the solution obtained at iteration $n$.
- At ANTARES level: a parallelism of the solver is used to reduce the computational time. For each period, the 11 Monte Carlo years dispatch are solved in a parallel fashion.

To summarize the simulation strategy adopted for the application of the multi-scale model, the matrix bellow represent the four simulations carried out. All simulations were carried out in a server with 16 cores, using Windows.

| Learning rate/Scenario | Scenario A | Scenario B |
|---|---|---|
| Decreasing: 1 | A.1 | B.1 |
| Constant: 2 | A.2 | B.2 |

Table 6.5: The different simulations carried out with the multi-scale model developed

[7] $5.18 * 10^{-4} \in [0,1]$ is the equivalent of 50 (hours) $\in [1, 8760 * 11]$ (the interval of all dispatch hours simulated by ANTARES)

## 6.3 Results

In this section, we will present the results obtained from the utilization of the developed multi-scale model. The application of this model involves two distinct scenarios, each depicting a different future evolution of the power system. The steps of the Results follow the rational of the development of the multi-scale model developed in the previous Chapter. To begin, we present the results of the unidirectional part by providing detailed information on the two major components: the investment trajectory determined by TIMES and the operational trajectory determined by ANTARES. Once these two components are clearly defined, we proceed to illustrate the outcomes of various metrics presented in the theoretical part to validate the multi-scale model. The validation assessment is based on a comparison of dispatch, CO2 emissions, and electricity prices. By evaluating these results, we establish the validation of the unidirectional part of the multi-scale model, allowing us to proceed to the generation adequacy assessment.

Subsequently, we explicitly elaborate on the bi-directional part by employing graphical representations to illustrate the concept of the new Residual Load Duration Curve (introduced in section 5.5.3) and the functioning of the SA algorithm. The integrated multi-scale model's results are then detailed by analyzing the evolution of the $LOLE$ metric throughout the iterative process. The convergence assessment is evaluated using the score metric, and a dynamic perspective of the convergence is also provided for further analysis.

### 6.3.1 Main results of the unidirectional multi-scale model

#### $\Pi_{inv}$: TIMES's Investment trajectory

Once the data consistency and bridging scale algorithms are applied, TIMES model is run using the set of constraints defining the "Scenario A". The most important outcome of the optimization is the investment trajectory denoted by $\Pi_{inv}^{TIMES}$.

At the European level, Figure 6.8a depicts the total installed capacities for each period of the planning time-frame 2016-2050. In this scenario, where the CO2 tax stabilizes at Euro 35 per tonne from 2030 onwards, the evolution of the energy mix between 2016 and 2050 is characterized by contrasting dynamics for fossil fuels and renewables. The various announcements of coal phase-out lead to a near-abandonment of the resource by the end of the horizon. Nuclear energy also occupies a less significant role in the electricity mix by 2050. The overall share of fossil resources decreases from 38% in the base year to 19% in 2050. Solar and wind power substantially increase their share in the production mix, rising from 3% and 9% in 2016 to 23% and 32% in 2050, respectively. Hydropower and bioenergy maintain relatively constant shares by the end of the horizon compared to 2016. In 2030 and 2040, the share of renewables in the electricity mix is 48% and 64%, respectively. By 2050, this share reaches 76%. Also, following this scenario, interconnections capacities is also increased.

For the utilization of the multi-scale model, the investment trajectory provided to ANTARES as an input is specific to each region. Figure 6.8b illustrates the power generation mix in

each region across all the time periods. As observed in the figure, the power generation mix varies from one country to another. Natural gas and coal constitute the primary additional investments in fossil-based thermal technologies.

In Poland and the Czech Republic, wind energy plays a significant role in the production mix, reaching 46% and 39%, respectively, by the end of the horizon. Wind power plants also contribute a significant portion of total electricity production in the United Kingdom (56%), Denmark (83%), and Sweden (55%) by 2050. Countries with ample sunlight (Portugal, Spain, Greece) are incorporating increasing amounts of solar production over the studied period. Between 2016 and 2050, the total solar production in these three countries is multiplied by 12.

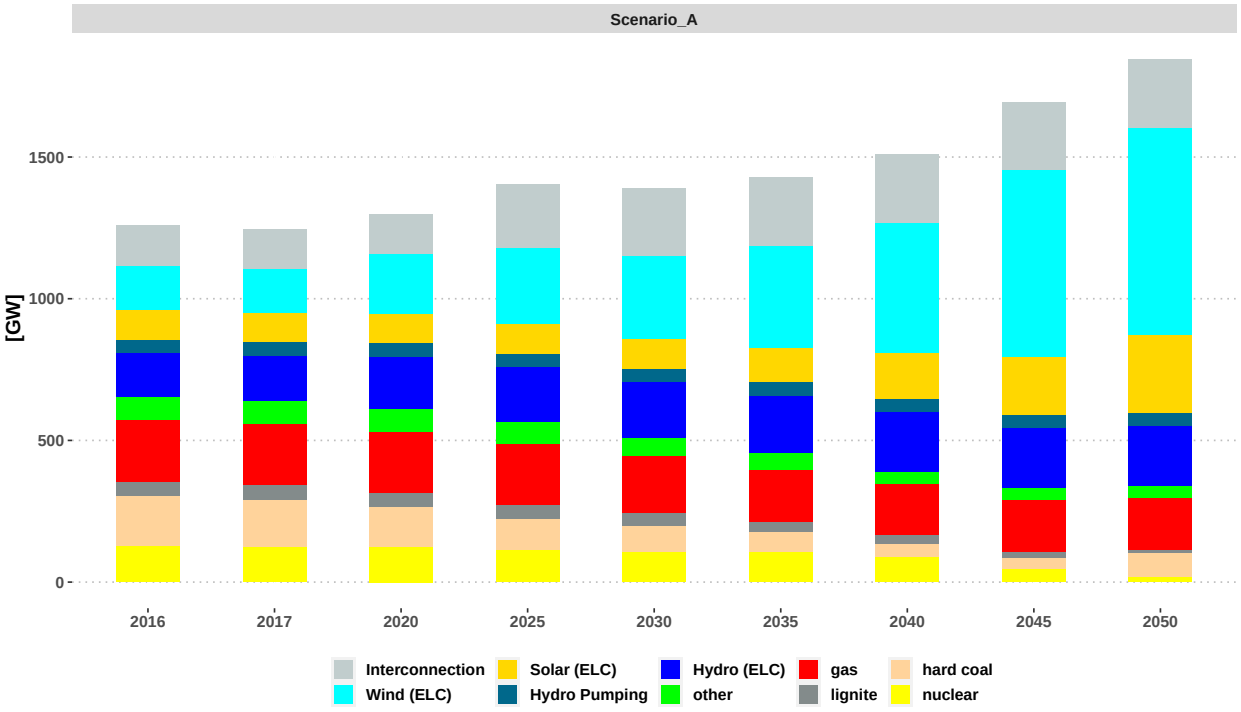


(a) The total installed capacities at the European level for the planning time-frame 2016-2050

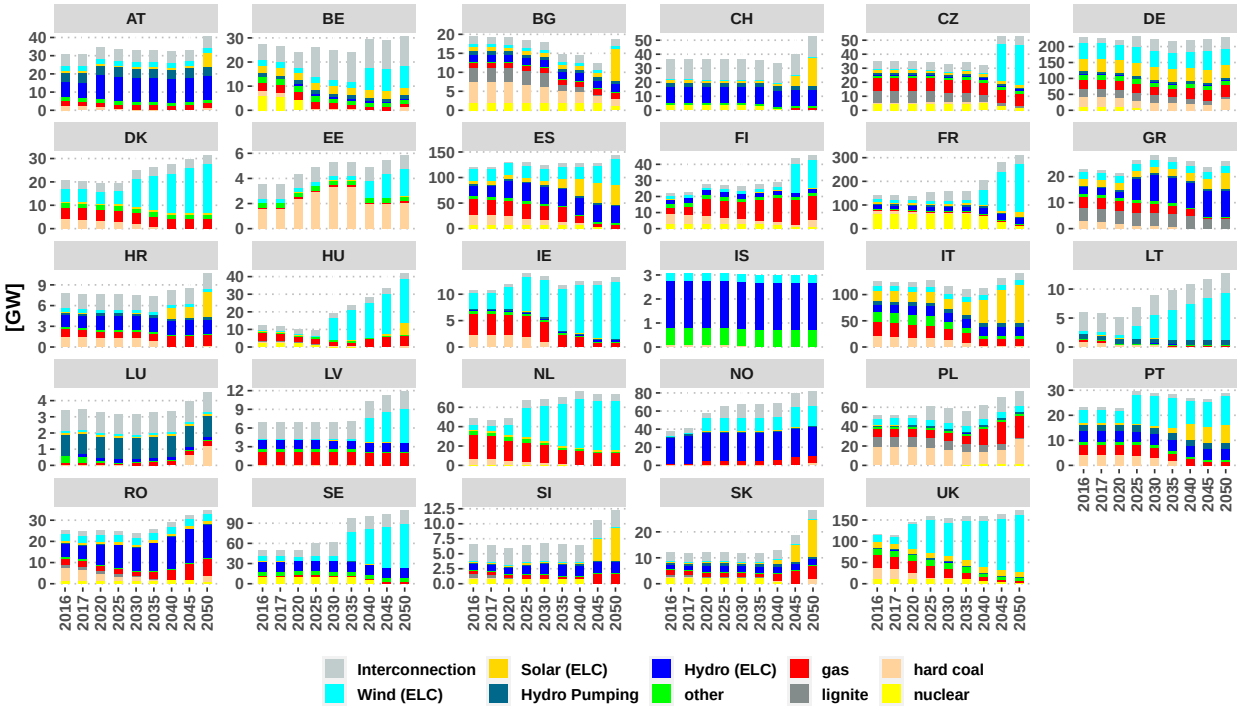


(b) The total installed capacities at the country level for the planning time-frame 2016-2050

Figure 6.8: The investment trajectory $\Pi_{inv}^{TIMES}$ for the planning time-frame 2016-2050 supplied to ANTARES for "Scenario A"

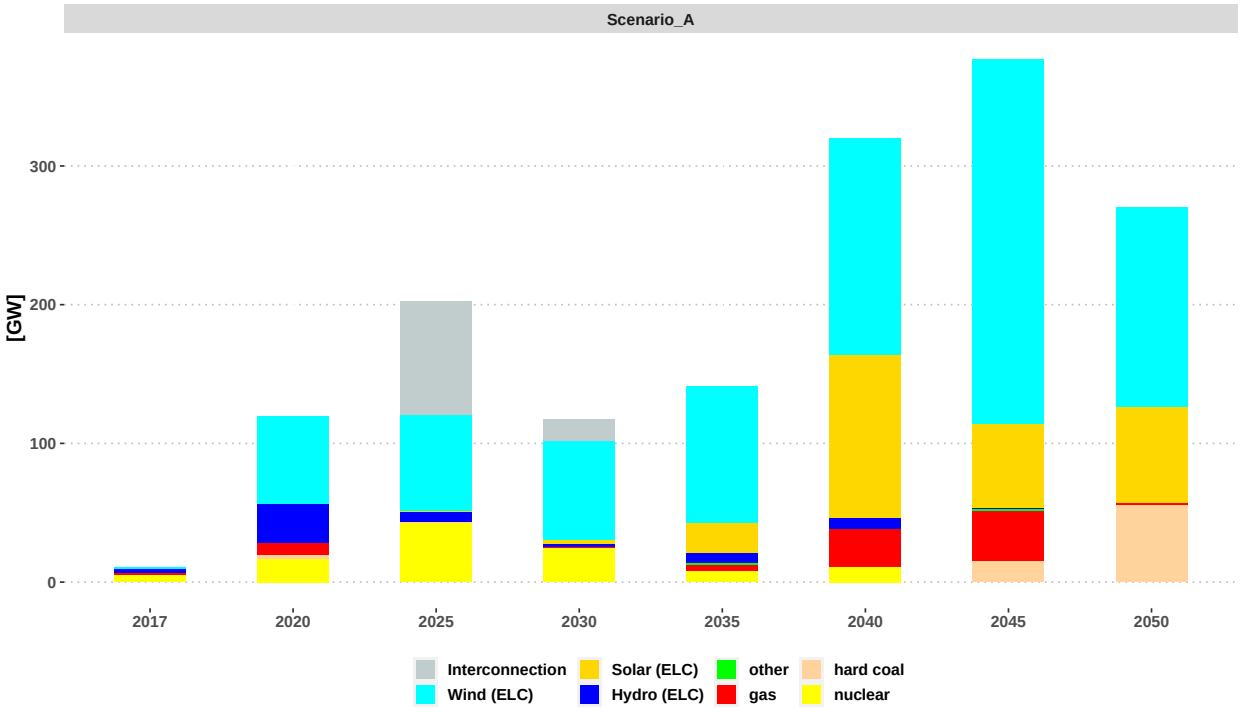


(a) The new installed capacities at the European level for the planning time-frame 2016-2050


(b) The new installed capacities at the country level for the planning time-frame 2016-2050

Figure 6.9: Evolution of the new installed capacities following "scenario A"

### $\Pi_{op}$: ANTARES's Operational trajectory

In the multi-scale model, TIMES is primarily utilized to determine the investment trajectory, while ANTARES is employed to compute the operational trajectory. The operational trajectory represents the hourly dispatch determined by ANTARES for each period within the planning period (Note that ANTARES provides the dispatch for each Monte Carlo Year). It should be noted that the power generation mix determined by TIMES is transferred to ANTARES only for the periods 2020, 2030, 2040, and 2050. Therefore, intermediate periods are not considered in the multi-scale model.

An example of the operational trajectory is illustrated in Figure 6.10. This figure illustrates that for each hour of the year, ANTARES provides a power dispatch stack for all available technologies. Nuclear power has the highest share until 2040, after which wind power takes over. This leads to a distinct operational structure, including spillage and exchanges.

It is important to keep in mind, that TIMES also provide an energy dispatch for each time-slice. Based on this energy dispatch, an average power dispatch is computed. This average power dispatch extracted from TIMES mimic the hourly dispatch provided by ANTARES. For each hour belonging to a given time-slice, TIMES sees the same power dispatch. Figure 6.11 depicts the equivalent hourly dispatch provided by TIMES. It can be seen from the figure, that TIMES ignore the hourly variability in the demand and then provide only 64 segment of the dispatch rather than 8760. This can lead to differences in terms of the use of each technologies and can create over or under estimation in the generation. This illustrate, why we ignore the dispatch provided by TIMES, and focus only on the dispatch of ANTARES as it is more accurate for the analysis of the power system operation.

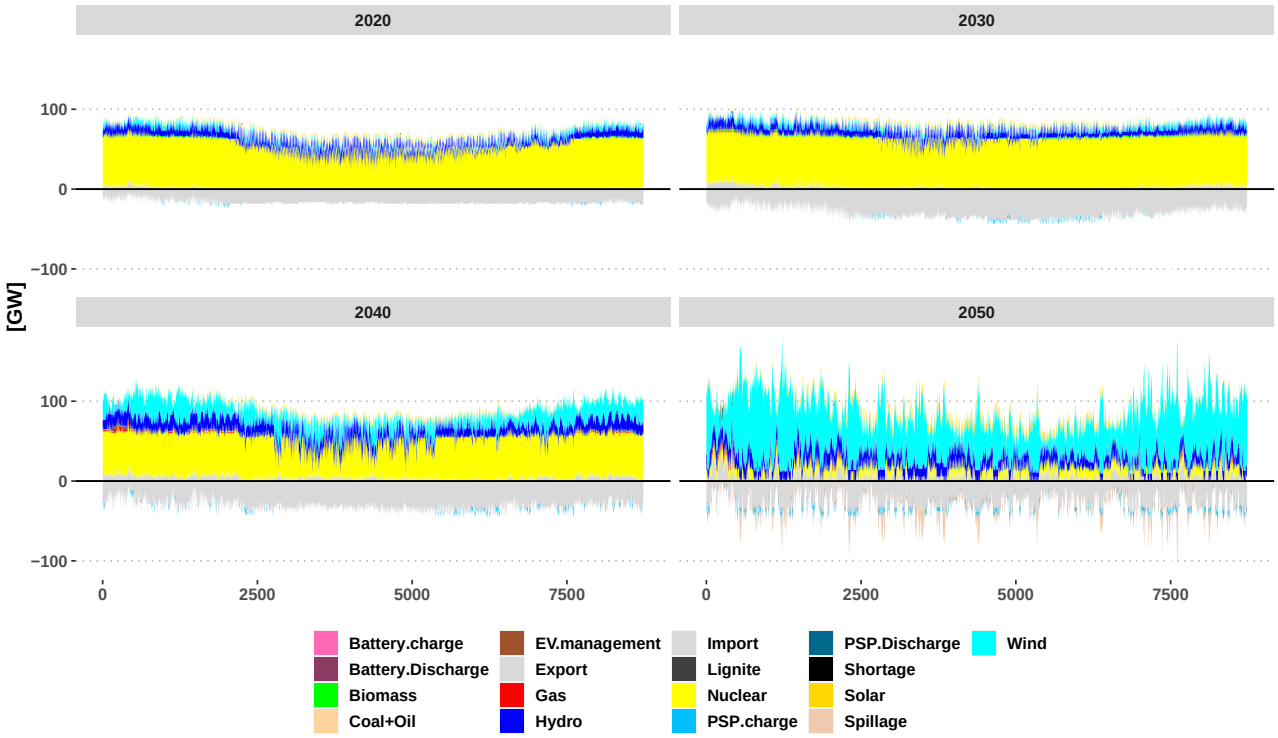


Figure 6.10: Illustration of the operational trajectory for France. Note that we illustrate here only the Monte Carlo year that served as a common input for both models. However the overall operational trajectory is constituted for each target period, by the resulted hourly power dispatch for each Monte Carlo year

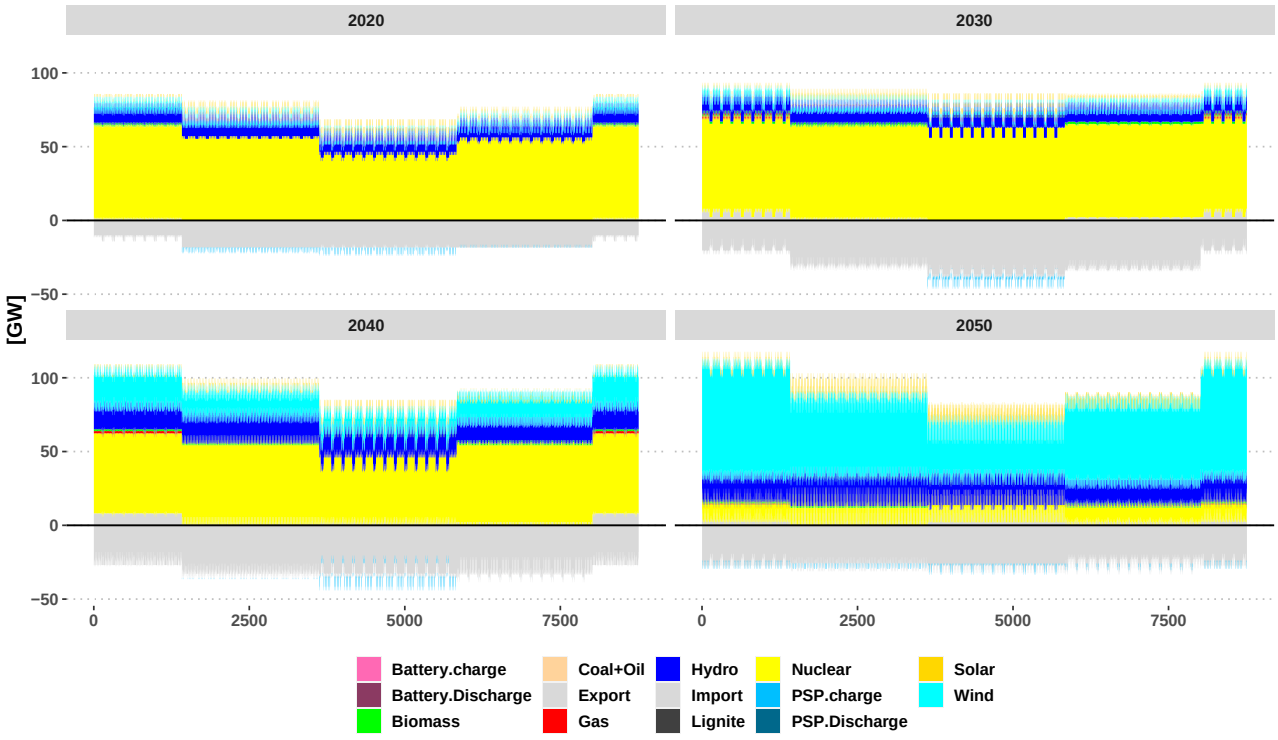


Figure 6.11: The power dispatch equivalent derived from energy dispatch resulted for TIMES operation. For each time-slice, TIMES operate the balance between supply and demand in term of energy, based on the length of each time-slice an average power dispatch is computed

In the following paragraph we compare the outcomes of the models at different measuring points. The main goal of this assessment is to validate the multi-scale model and to detect potential inaccuracies in the modeling framework. This comparison assumes ANTARES outcomes as a reference in the comparison, as it is the model dedicated for the operation of the power system.

### Dispatch comparisons

For each period, the annual power generation is derived from the dispatch outcomes provided by TIMES and ANTARES. The Figure 6.12 below illustrates the annual power generation by technology for each period in both models. The red point represents the annual demand shared by both models. It can be observed that globally, both models provide a similar mix of annual power generation to meet the electricity demand.

Spillage and shortage are treated in different way in both models. From the operational perspective of TIMES, there is a balance between energy supply and demand for each period, with no shortages or spillage occurring. However, it is important to note that in the modeling of renewables, TIMES does not explicitly consider VRE curtailment. The capacity factors of renewables are included as upper bound constraints. Therefore, if TIMES determines that it is feasible and beneficial to generate less than the capacity factor suggests, it will adjust

the generation accordingly. In contrast, ANTARES provides an hourly power dispatch, and since renewable are treated as fatal production, both spillage and shortage become decision variables in the optimization problem.

At the European level, the maximum difference between TIMES and ANTARES amounts to 200 TWh, which represents only 4% of the total electricity demand. This discrepancy is mainly due to the greater use of natural gas in ANTARES than in TIMES, offset by the greater use of coal and nuclear power in TIMES than in ANTARES. Two key factors contribute to this disparity:

- ANTARES, capturing greater variability in the demand, calls the use of natural gas as a peaking technology to meet the fluctuating electricity demand. In contrast, TIMES, with a reduced representation of demand variability, tends to rely more on base technologies.

- The modeling of thermal and hydro in both models is different. Therefore, their dispatch follows different decisions, which impact the variations between the two models.

The increasing penetration of renewables in the generation mix leads to a rise in spillage from 2040 to 2050. Additionally, the amount of energy not supplied also increases during this period, reaching a significant level by 2050. From an overall European perspective, a 4% difference in dispatch between TIMES and ANTARES is deemed acceptable (see Figure 6.12). However, the aggregation at the European level conceals the variations that occur in the dispatch at the country level. To capture these differences, we utilized a second metric that compares the discrepancies between both models normalized by the demand in each country. Figure 6.13 illustrates the technological differences for each technology over the planning time-frame. Each data point represents the normalized difference for a specific country, while the red points represent the median values for each technology and period across all countries. This figure includes some technologies that were omitted in the previous comparison, such as import and export, and PSP (Pumped Storage Plant) charging and discharging.

From this comparison, the following observations can be made:

- Marginal differences are observed for non-dispatchable power generation technologies, namely wind, solar, and Run of River. This can be attributed to the use of the same time-series of capacity factors in both models. The maximum difference observed is 2% for wind, which can be linked to the bridging scale methodology used for the capacity factor, where an average value affected for each time-slice may lead to slight discrepancies in production. Nevertheless, the median value over all countries remains centered around zero.

- For Hydro Reservoir, all countries show a null difference. The slight differences observed in some countries (around 10%) can be explained by the fact that the bridging methodology used for hydro in TIMES acts as an upper bound constraint, allowing TIMES not to utilize the entire allocated reservoir capacity.

- Regarding thermal power generation: as nuclear comes first in the merit order, the differences are lower. However, for the other technologies, differences can reach higher values, especially for natural gas due to its use as a peak technology.

- The use of import and export differs significantly between both models, mainly due to the different dispatch (and therefore the electricity marginal prices). The amount of electricity imported can reach high levels, with a maximum difference of 50%.

These findings highlight the importance of considering country-level variations when analyzing the differences between TIMES and ANTARES dispatch results. We consider that those difference are inherent to the modeling of the operation of the power system which is different in the two models. The levels observed for the technologies are then acceptable.

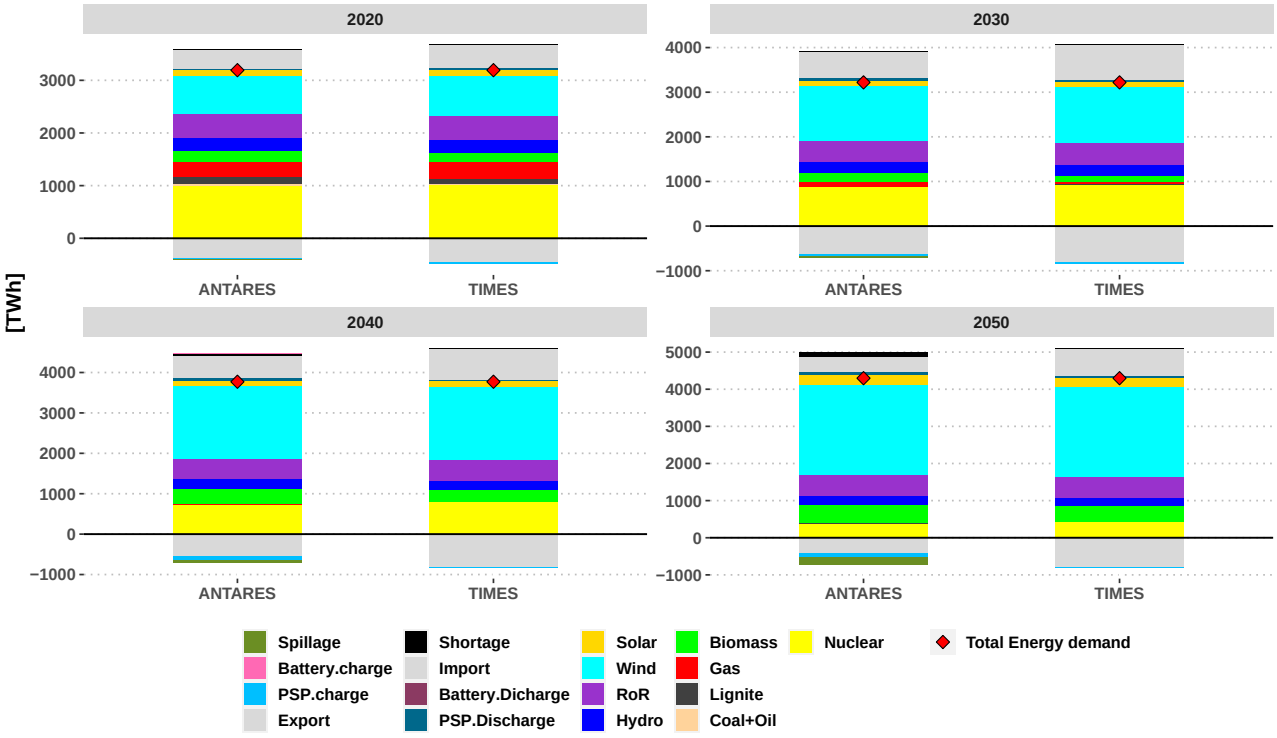


Figure 6.12: The comparison between the power generation mix in [TWh] at the European level between TIMES and ANTARES

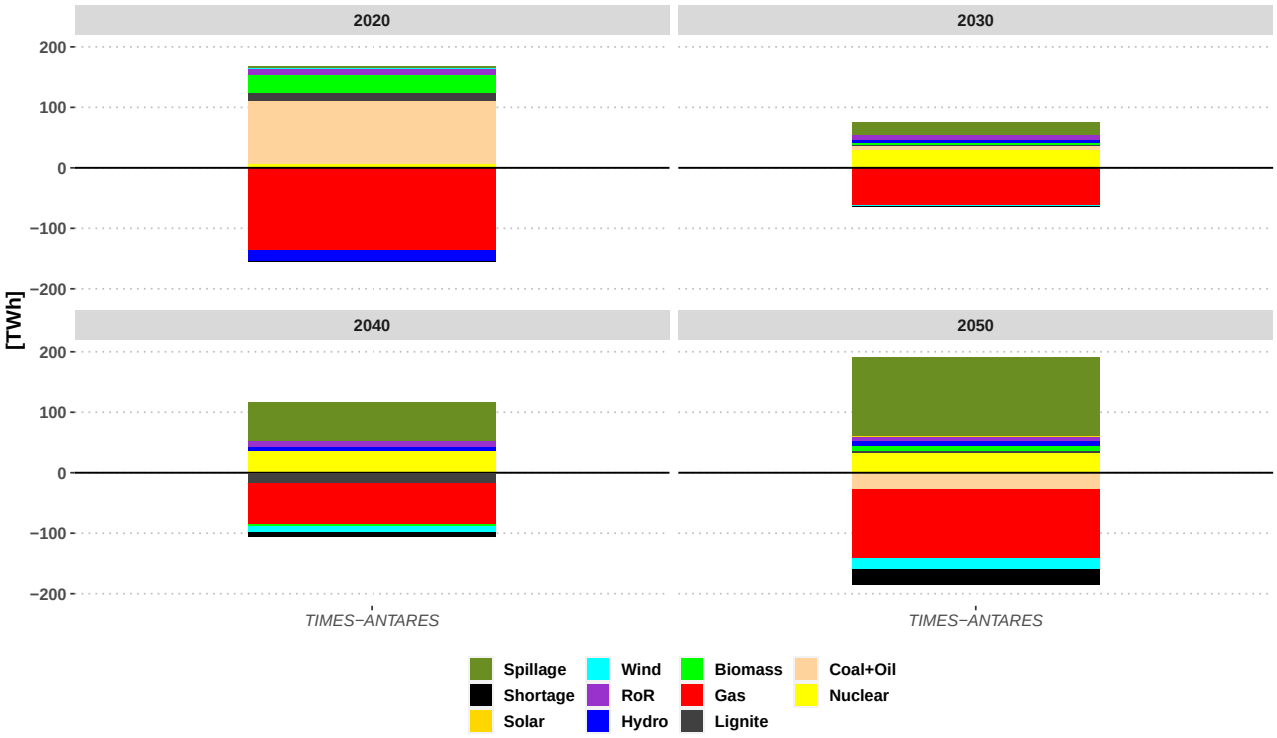


Figure 6.13: The difference in terms of power generation between TIMES and ANTARES. Negative values indicates that ANTARES produce more than TIMES and vice-versa

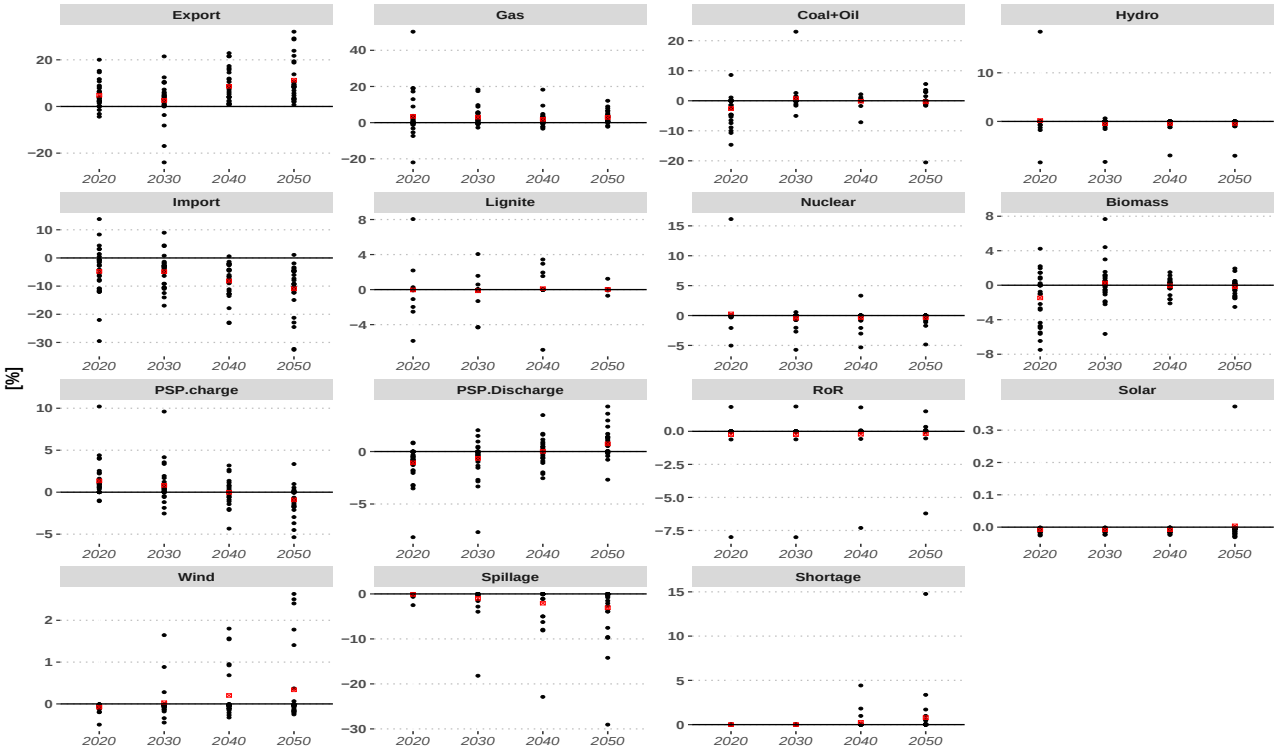


Figure 6.14: Annual generation differences normalized by the country demand technology by technology through the planning period

### Economical comparisons

The electricity price is selected as an economical measuring point for validation. In TIMES, this price corresponds to the dual value of the commodity balance constraint, while in ANTARES, it corresponds to the dual value of the supply/demand balance. The determination of the electricity marginal price within TIMES is performed with time-slices, while in ANTARES, it is resolved with hourly resolution. Figure 6.15 illustrates the evolution of the marginal price for different studied years and various countries. Hours on the left side of the Figure correspond to periods with lower electricity prices, while hours on the right side indicate periods with higher prices. Periods with zero marginal electricity prices correspond to hours when only technologies biding at 0 euro/MWh (renewables and Hydro) are satisfying the demand. The figure shows that both models capture different evolutions of prices through the year. In general, for the countries presented in the graph, both models have approximately the same evolution within the times-interval $[25, 75]$, but different or even significantly different evolution within the interval $[0, 25]$ and $[75, 100]$. The green line represents the median value over the year. It is evident that the disparities between the models stem from differences in the dispatch decisions they make. Upon analyzing the figure, two distinct cases become apparent:

- Certain periods and specific countries manifest a close alignment in the price evolu-

tion captured by both models. This is evident, for instance, in Belgium, Germany, and France. Higher prices during certain hours is due to shortage of supply when ANTARES is unable to meet the aggregate demand.

- There are periods and specific countries where the long-term model fails to replicate the precise price dynamics observed in the operational power system. Notably, in the case of the United Kingdom, TIMES inaccurately captures hours with zero marginal prices.

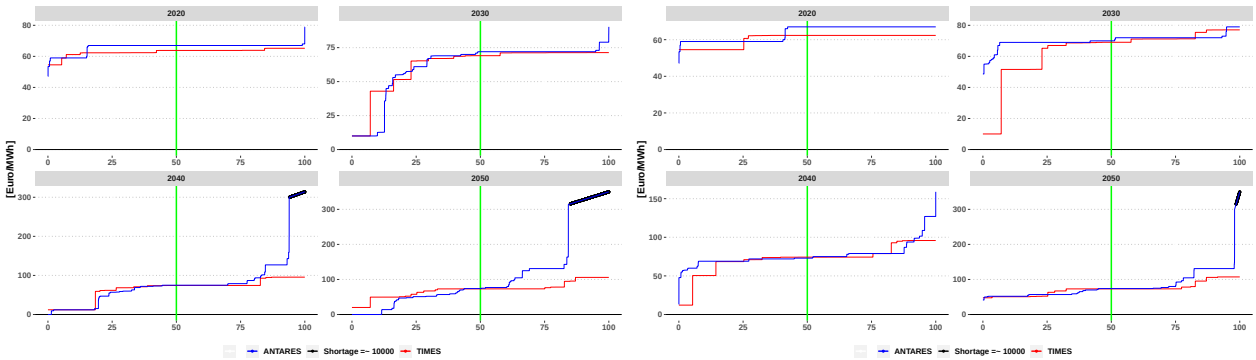


(a) BE




(b) DE

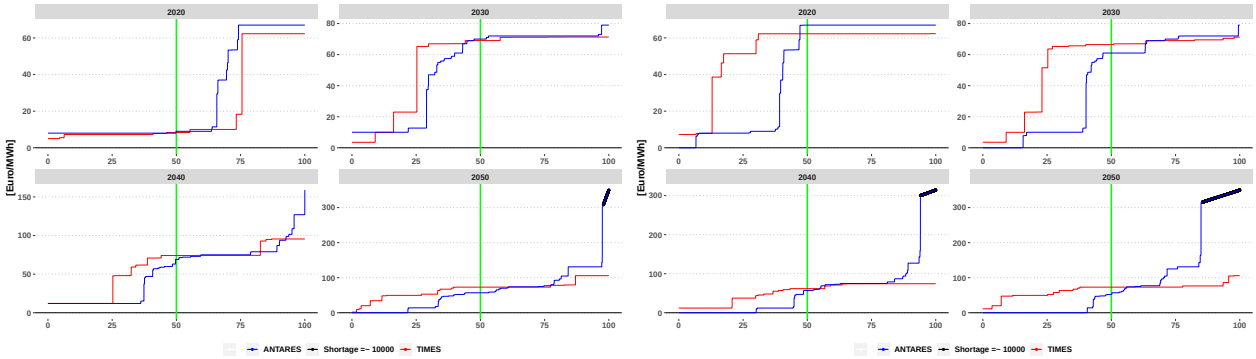


(c) FR




(d) UK

Figure 6.15: The marginal price duration curve comparison between TIMES (red) and ANTARES (blue) for different regions and periods. The green line corresponds to the median value, the black points represent the shortage hours with a price equal to the $VoLL = 10.000 Euro/MWh$

An important point to highlight at this stage is that while the price dynamics are "poorly" captured level within the long-term energy planning model, this price distribution cannot be employed to accurately estimate the revenues of various technologies. Because the gap between the accurate electricity price (seen by ANTARES) and the price computed by TIMES can lead to colossal differences in terms of revenues. Consequently a long-term energy planning model can't be used to estimate the profitability of a given technology. In other words

assessing the so-called "missing money" problem using long-term energy planning models can lead to an over or miss-estimation of its true value. Thus, the necessity of the short-term operational model to accurately assess the operational economics of the resulting power system from long-term energy planning models."

### Environmental comparisons

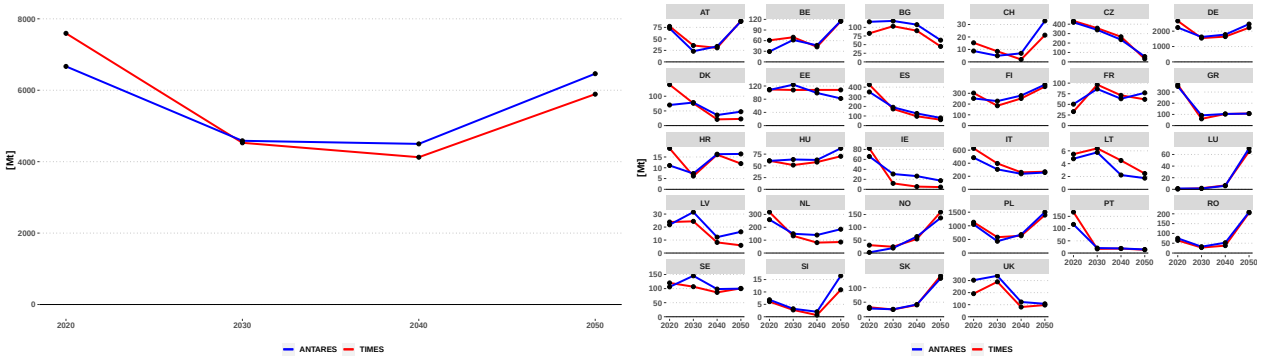


(a) $CO_2$ emissions over the planning time-frame at the European level. Red line is TIMES while blue line in ANTARES

(b) $CO_2$ emissions over the planning time-frame for each country. Red line is TIMES while blue line in ANTARES

Figure 6.16: $CO_2$ emission trajectory

The evolution of $CO_2$ emissions over the planning time-frame is illustrated at the European level in Figure 6.16a, and for each country in Figure 6.16b. The figures demonstrate that both models showcases comparable emission trajectories, with marginal differences. ANTARES follows a similar trend as TIMES, with only slight deviations.

In 2020, a difference of 12% is observed, primarily driven by higher emissions in TIMES due to its over-reliance on coal, a base load technology. In 2030 and 2040, the differences are minimal as the annual dispatch in both models displays little variation. However, from 2040 (+5%) to 2050 (+10%), ANTARES emits more $CO_2$ than TIMES. This is attributed to a reduction in the share of coal in the generation mix, with ANTARES compensating for the variability of hourly demand by relying more on natural gas. It is important to emphasize that a power generation mix with a high share of VRE installed capacity does not necessarily guarantee a reduction in emissions. Despite significant investments in solar and wind, the need for dispatchable thermal power plants, primarily fueled by natural gas and coal in 2050, results in $CO_2$ emissions reaching the same level as in 2020. At the country level, Figure 6.16b shows that both models follow the same trends in terms of $CO_2$ emissions.

### 6.3.2 Adequacy assessment through the trajectory

In the previous sections, our analysis was based on the outcomes of the Monte Carlo Scenario in ANTARES, which served as input for TIMES. In this section, the adequacy assessments rely on all simulated Monte Carlo scenarios to compute the $LOLE$ adequacy metric. The $LOLE$ metric is calculated over 11 Monte Carlo years. Figure 6.17 illustrates the evolution of the $LOLE$ metric for each country over the planning time-frame. A key assumption in our study is that a power generation mix is considered adequate for a given country if and only if $LOLE \leq 3$ hours/year.

Figure 6.17 shows that, starting from 2030, the power generation adequacy levels manifest insufficient supply. As more renewable are deployed, adequacy levels deteriorate. Specifically:

- In 2030, two countries have inadequate adequacy levels: Luxembourg (3.72 hours/year) and Hungary (18.45 hours/year).
- In 2040, twelve countries experience inadequate adequacy levels: Belgium (191.36 hours/year), Denmark (3.27 hours/year), Estonia (23.27 hours/year), Hungary (741.18 hours/year), Ireland (1506.45 hours/year), Lithuania (7.36 hours/year), Luxembourg (11.09 hours/year), Latvia (48.55 hours/year), Netherlands (92.36 hours/year), Romania (104.73 hours/year), Sweden (3.36 hours/year), and the United Kingdom (448.09 hours/year).
- In 2050, nineteen countries face inadequate adequacy levels: Belgium (456.27 hours/year), Germany (9 hours/year), Denmark (27.55 hours/year), Estonia (163.18 hours/year), Spain (17.27 hours/year), Finland (49.82 hours/year), France (39.09 hours/year), Hungary (695.18 hours/year), Ireland (3200 hours/year), Italy (47.73 hours/year), Lithuania (151.91 hours/year), Luxembourg (27.45 hours/year), Latvia (408.36 hours/year), Netherlands (551.91 hours/year), Poland (23.36 hours/year), Portugal (16 hours/year), Romania (7.36 hours/year), Sweden (33.73 hours/year), and the United Kingdom (1039 hours/year).

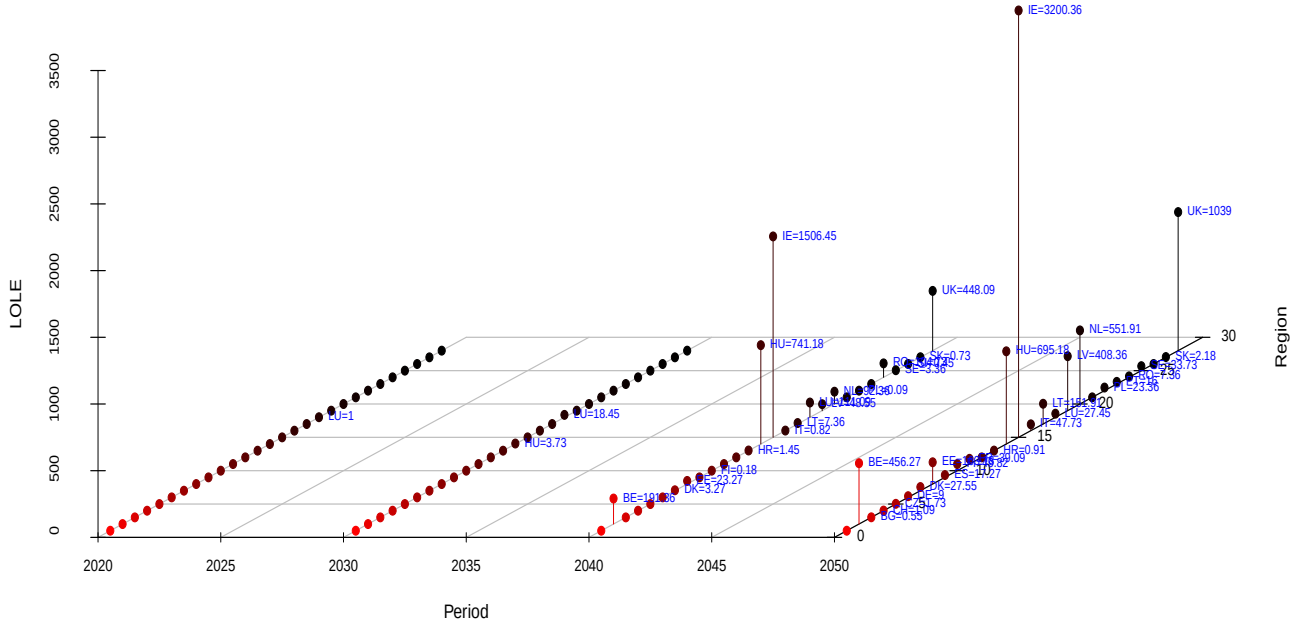


Figure 6.17: Solution A, the *LOLE* trajectory of the initial TIMES solution

It can be concluded that the power generation mixes determined by TIMES (based on the first Monte Carlo year) do not meet the power generation adequacy requirements for multiple countries. Additionally, it is important to emphasize that countries with high *LOLE* levels experience shortage hours **spread across the entire year**, rather than being limited to critical seasons with a high risk of shortage (For instance, during the winter in countries with thermally sensitive demand). Figure 6.18 displays the average shortage hours (averaged over the 11 simulated Monte Carlo years for each period) for Belgium and Ireland for two periods: 2040 and 2050. The last figure illustrates that the power generation mix determined by TIMES carries a high level of risk during critical seasons, with instances of 6 hours of shortage in Belgium (2050) and days with 18 hours of shortage in Ireland.

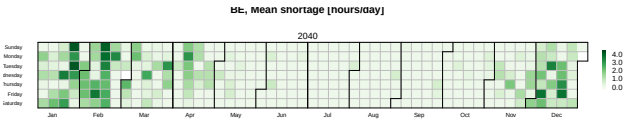


(a) Shortage hours temporal distribution for Belgium in 2040

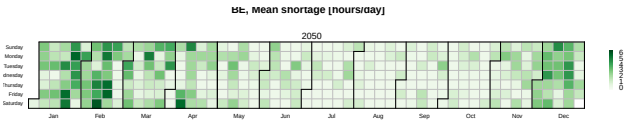


(b) Shortage hours temporal distribution for Belgium in 2050

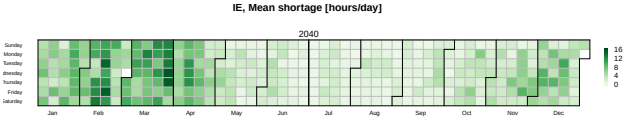


(c) Shortage hours temporal distribution for Ireland in 2040

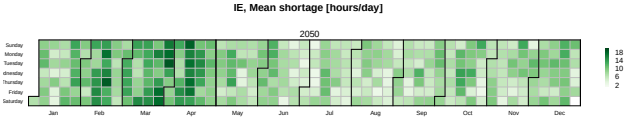


(d) Shortage hours temporal distribution for Ireland in 2050

Figure 6.18: Average daily shortage hours distribution over a complete year for Belgium and Ireland in 2040 and 2050

### 6.3.3 Simple Illustration of how the stochastic approximation algorithm works

In this paragraph, we aim to illustrate in simple way how the stochastic approximation algorithm works. The primary objective of the algorithm is to enhance the solution provided by TIMES by incorporating additional constraints to achieve a $LOLE$ of 3 hours per year.

Ideally, if we could mathematically formulate a constraint that accurately expresses $LOLE \leq 3 hours/day$ hours per year, solving the problem would be straightforward. However, given the complexities involved in incorporating this constraint into both the long-term planning model and the operational power system model, we have introduced a sizing constraint in terms of installed capacities. This constraint aims to establish a balance between supply and demand and can be considered as a proxy for the $LOLE$ constraint. Nevertheless, determining the coefficient of the sizing equation to trigger the desired $LOLE$ is challenging. To address this, we leverage the power generation dispatch outcomes from ANTARES to generate equations. Since we are dealing with a probabilistic metric, all Monte Carlo years used to compute the $LOLE$ are crucial. The research space is based on the new $nRLDC$, which arrange all possible operational scenarios in a decreasing order of constraint levels, starting from the most constrained situation to the hour with the highest spillage.

Based on the dispatch of the operational power system encompassed in $\Pi_{op} ANTARES$, the $nRLDC$ is constructed (see algorithm of the Chapter 4). Bellow we illustrate the $nRLDC$ of the Irish power system as it depicts higher levels of shortages. $X$ axis depicts the number of hours simulated in each year which represent the interval $[1 : 8760 * 11]$. $Y$ axis represent the new net load in $GW$. As it can be seen from the Figure 6.19 that only dispatchable thermal technologies are used to satisfy the "new" net load, as all other technologies was subtracted from the total load. The $nRLDC$ arrange the hours of the year in a decreasing manner. The first hours corresponds to the hours with high net load. The space filled by

the black color corresponds to the hours with insufficient supply with negative margins while hours with negative new net load corresponds to hours with spillage.

To illustrate the iterative process at a given iteration $n$, only three moves are to be considered. The $LOLE$ is estimated by $y^{-}_{r,t}$.

1. If $LOLE_{r,t} < \zeta_{r,t}$, the $\theta^{n+1}_{r,t}$ moves in the right direction of the $\theta^{n}_{r,t}$ with a negative drift equal to $\alpha_n(\zeta_{r,t} - y^{-}_{r,t}(\theta^{n}_{r,t}))$.

2. If $LOLE_{r,t} > \zeta_{r,t}$, the $\theta^{n+1}_{r,t}$ moves in the left direction of the $\theta^{n}_{r,t}$ with a positive drift equal to $\alpha_n(\zeta_{r,t} - y^{-}_{r,t}(\theta^{n}_{r,t}))$.

3. If $LOLE_{r,t} = \zeta_{r,t}$, the $\theta^{n+1}_{r,t}$ is stacked as the drift $\alpha_n(\zeta_{r,t} - y^{-}_{r,t}(\theta^{n}_{r,t}))$ is null.

To speed-up the algorithm when two consecutive $\theta_{r,t}$ at $n$ and $n+1$ are trapped in a plateau, a new condition on the $\theta_{r,t}$ variable is added to bring it out of the plateau. This is done due to the following rule: as long as the $nRLDC(\theta^{n+1}_{r,t}) = nRLDC(\theta^{n}_{r,t}))$, the $\theta^{n+1}_{r,t}$ continues to be updated until $nRLDC(\theta^{n+1}_{r,t})! = nRLDC(\theta^{n}_{r,t}))$.

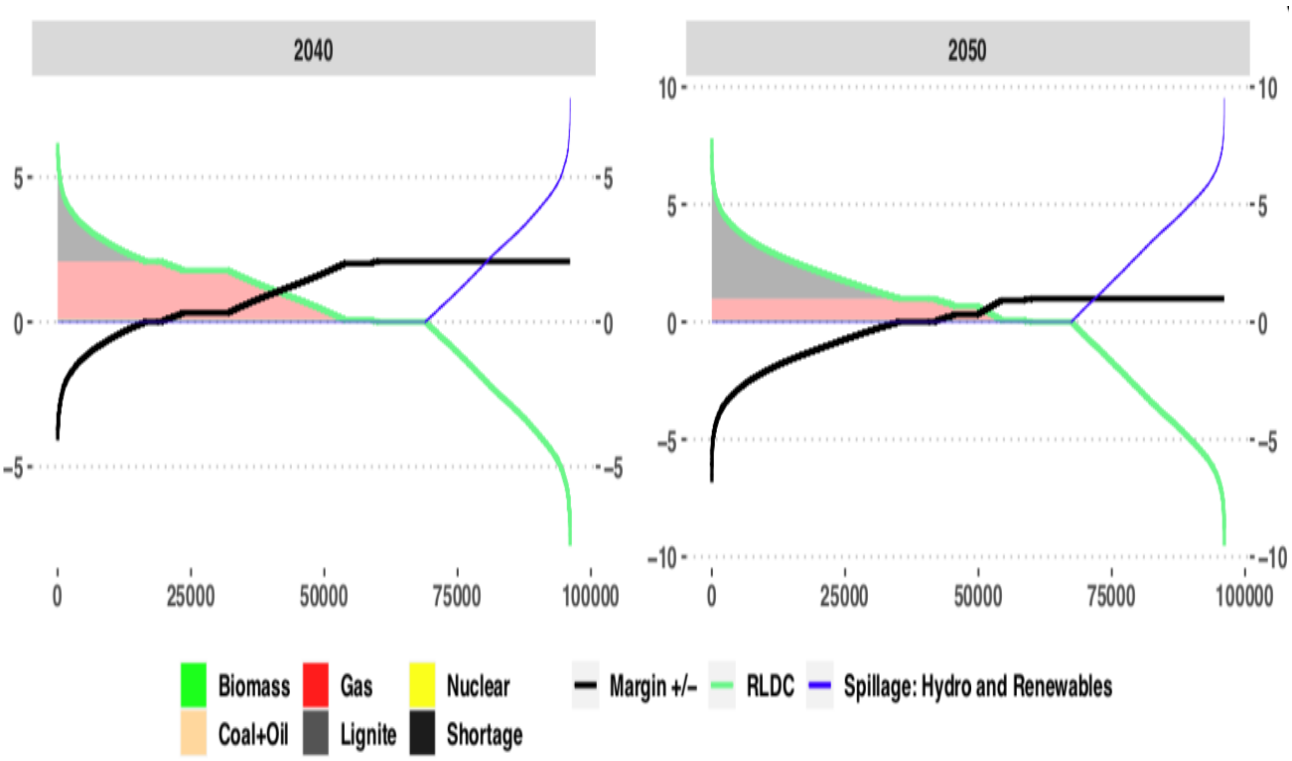


Figure 6.19: The "$nRLDC$" curve for Ireland in 2040 and 2050 is depicted in the graph. In the graph, the green curve represents the new net load, and the area below it is filled by thermal power generation and shortages. The black line indicates the margins, where a positive margin signifies adequacy, while a negative margin corresponds to the power not supplied. The blue line represents spillage.

### 6.3.4 Application of the Stochastic Approximation Algorithm to "Scenario A"

**Evolution of the $LOLE$ through iterations**

**Initialization of $\theta_{r,t}$ sequence**

The algorithm starts with the initialization of the $\theta_{r,t}$ sequence for each region $r$ and period $t$ $(r,t) \in (R_{risky}, T_{risky})$ [8]. Three initial positions corresponding to the maximum, mean, and minimum in the shortage space are evaluated to determine the initial values $\theta^0_{r,t}$. The position that yields a $LOLE$ value closest to 3 hours per year is selected. Once $\theta^0_{r,t}$ values are determined, the set of reinforcement constraints $D^{\theta^0_{r,t}} X_{r,t} > d^{\theta^0_{r,t}}, \forall (r,t) \in (R_{risky}, T_{risky})$ is generated and added to the first core of constraints of the initial TIMES model. Then the multi-scale Oracle is ran to estimate $\bar{y}_{r,t}$ (the $LOLE$ estimator). The recursion is then implemented for 500 iterations as $\theta^{n+1}_{r,t} = \Pi_{[0,1]}[\theta^n_{r,t} + \alpha_n(\zeta_{r,t} - \bar{y_{r,t}}(\theta^n_{r,t}))]$ [9].

Figures 6.20 and 6.21 below illustrate the evolution of the generation adequacy metric $LOLE$ for the 500 iterations, along with the corresponding changes in the control variable $\theta_{r,t}$. For countries with inadequate $LOLE$ levels, the SA algorithm aims to find the root vector $\theta_{r,t} * \forall (r,t) \in (R_{risky}, T_{risky})$ of $LOLE_{r,t}(\theta^*_{r,t}) = 3hours/year$ (represented by the red line in the figures). However, we relaxed the target solution with the interval $LOLE_{r,t}(\theta^*_{r,t}) \in [2.5, 3]$. From the figures, it can be observed that as the $\theta$ values vary within the solution space, the $LOLE_{r,t}$ values for each region also fluctuate. It is important to note that if the $LOLE_{r,t}$ for a specific region $r$ and period $t$ falls within the equilibrium zone, the iteration for the corresponding $\theta_{r,t}$ stops. We can distinguish three types of $LOLE$ performance:

1. Smooth evolution: The evolution of $\theta$ leads to a smooth transition of $LOLE$ values, ultimately reaching the equilibrium zone (e.g., $(BE, 2040)$ and $(DK, 2040)$).

2. Volatile evolution: The evolution of $\theta$ introduces significant volatility in the $LOLE$ values, resulting in fluctuations over the iterations (e.g., $(FI, 2050)$ and $(IT, 2050)$).

3. Resistant evolution: Despite changes in $\theta$, it is challenging to bring the $LOLE$ values within the equilibrium zone (e.g., $(LT, 2050)$, $(RO, 2050)$, and $(LU, 2050)$).

Two important factors that influence the performance of the multi-scale model in meeting generation adequacy requirements are the temporality of investments and the interconnection between power systems. These factors can have a combined effect on the algorithm's outcomes. The first factor relates to the temporal aspect of investments, where investments

[8] $(R_{risky}, T_{risky})$ for "Scenario A" includes the following pairs: $(LU, 2030), (HU, 2030), (BE, 2040)$, $(DK, 2040), (EE, 2040), (HU, 2040), (IE, 2040), (LT, 2040), (LU, 2040)$, $(LV, 2040), (NL, 2040), (RO, 2040), (SE, 2040), (UK, 2040), (BE, 2050), (DE, 2050)$, $(DK, 2050), (EE, 2050), (ES, 2050), (FI, 2050), (FR, 2050), (HU, 2050), (IE, 2050)$, $(IT, 2050), (LT, 2050), (LU, 2050), (LV, 2050), (NL, 2050)$, $(PL, 2050), (PT, 2050), (RO, 2050), (SE, 2050), (UK, 2050)$

[9] Note that $\zeta_{r,t} = 3hours/year$

made in a particular period $t$ have implications not only for the generation adequacy requirements in that period but also for the subsequent period $t + 1$, and so on, during life span of the new investment. An illustrative example is Romania, which has a $LOLE$ of 104 hours/year in 2040 and a relatively low $LOLE$ of 7 hours/year in 2050. By reinforcing the initial TIMES model with additional constraints in 2040, we are able to achieve convergence to the desired $LOLE$ target. However, this convergence in 2040 is accompanied by new investments that will have an impact not only in 2045 but also in 2050. Consequently, the reinforcement applied in 2050 alone will not be effective in bringing the $LOLE$ of Romania within the desired convergence zone, as the investments made in 2040 will already ensure a $LOLE$ of 0 hours/year in 2050. The second factor is the influence of interconnection between countries. When one country's power generation mix is reinforced, it directly affects the generation adequacy of other interconnected power generation mixes. Changes made to one country's reinforcement strategy can propagate through the interconnected systems, impacting their adequacy levels as well. Considering these underlying features of generation adequacy requirements, it is crucial to account for investment temporality and the interconnection between power systems when analyzing the performance of the algorithm to achieve desired adequacy targets.

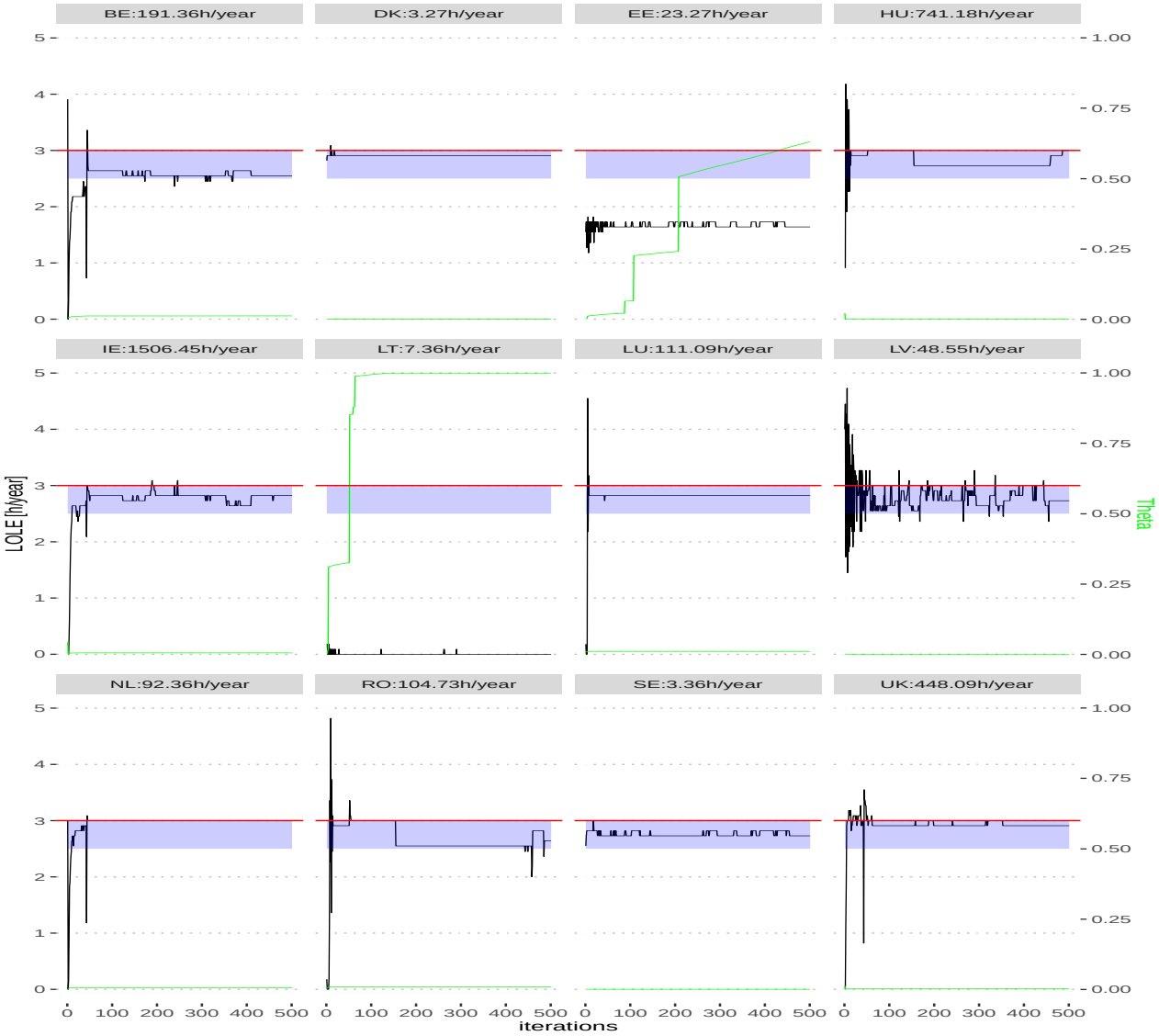


Figure 6.20: The evolution of $LOLE_{r,t}$ (black line) and $\theta_{r,t}$ (green line) through the iterative process for 500 iterations, for the period 2040. The blue space is the satisfactory solution space $[3 - 0.5, 3]$

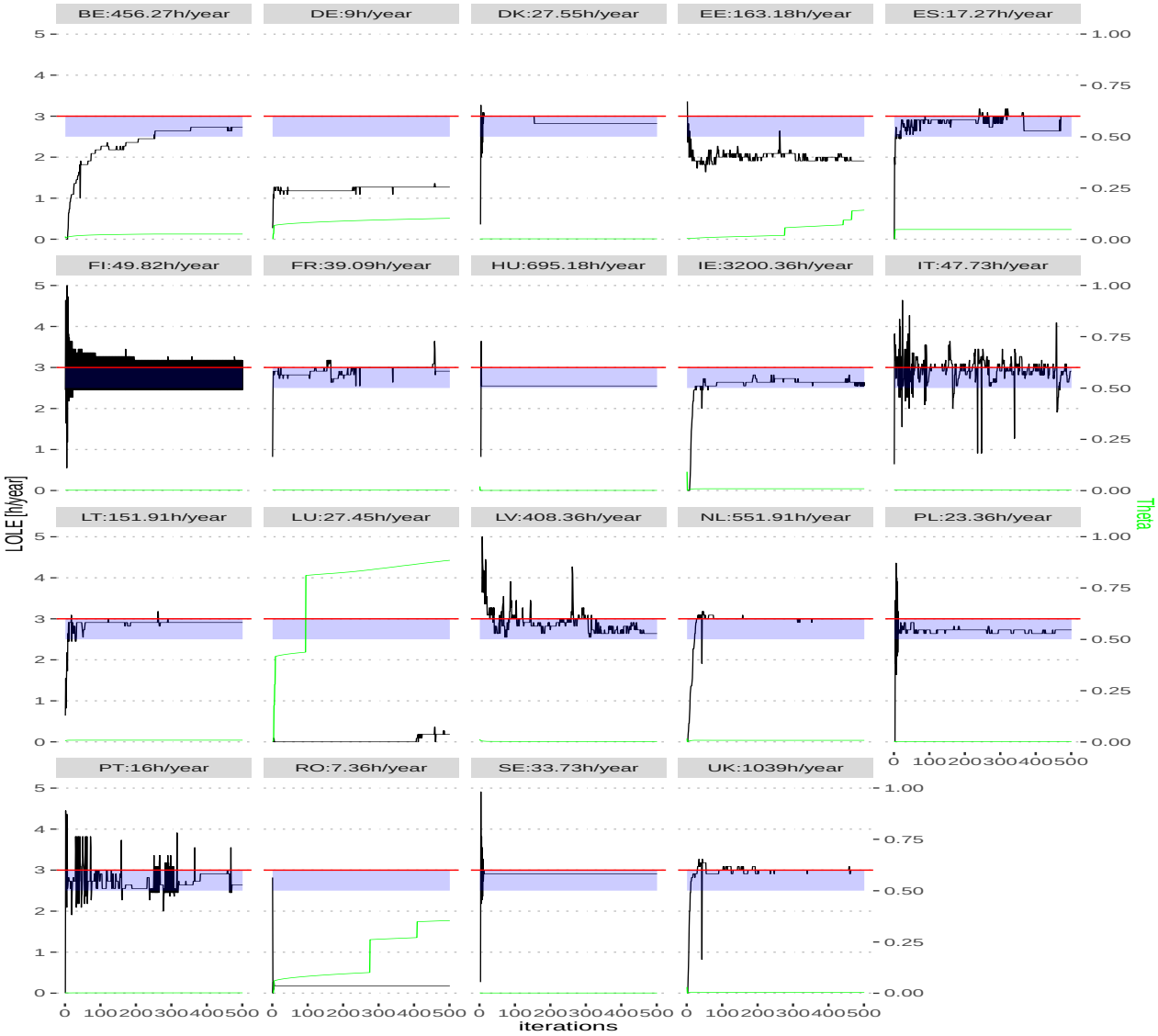


Figure 6.21: The evolution of $LOLE_{r,t}$ (black line) and $\theta_{r,t}$ (green line) through the iterative process for 500 iterations, for the period 2050. The blue space is the satisfactory solution space $[3 - 0.5, 3]$

**Assessment of the convergence**

The analysis carried out before on the evolution of the $LOLE$ metric focuses only on each country and period and do not provide information on convergence for the overall trajectory nor at the European level. In order to assess the overall convergence of the multi-scale, we developed a score metric that permits to estimate its performance.

Let $s_{r,t}$ be the function score of the region $r$ and period $t$. For each iteration $n$, this function gives a null score to a solution providing a $LOLE$ within the equilibrium zone, penalize marginally a solution providing a $LOLE$ within $[0, 2.5]$ with an affine function ($s_{r,t} = 1$ if $LOLE = 0$) and penalizing strongly a solution providing a $LOLE$ within $]3, 8780]$ ($s_{r,t} = 10$ if $LOLE = 8760$).

$$s_{r,t} = \begin{cases} 0 & LOLE \in [2.5, 3] \\ aLOLE + b & LOLE \in [0, 2.5[ \\ cLOLE + d & LOLE \in ]3, 8760] \end{cases} \tag{6.1}$$

To assess the convergence at the European level, we compute the sum of the scores across all risky regions within the period $t$: $S_t = \sum_{r \in R_{risky}} s_{r,t}$. To assess the convergence over the trajectory, we compute the sum over all the periods $S = \sum_{t \in T_{risky}} \sum_{r \in R_{risky}} s_{r,t}$. Another metric can be computed by weighting the simple score with the demand of each country. The weighted score is a score giving high weight to countries with significant demand while penalizing countries with reduced level of electricity demand.

Figure 6.22 depicts the periodic score for the two tested learning rates (1: $\alpha_n = 5.18 * 10^{-4}/n^{0.5}$, 2: $\alpha_n = 1.14 * 10^{-4}$). The first learning rate is a decreasing one, while the second learning rate is constant. The difference between the red line and the black line in the figure represents the disparity between the optimal solution (all risky solutions have a null score) and the obtained solution. The following remarks can be drawn :

- The initial TIMES solution have a high score which is increasing through the trajectory: the red point represent the score $S_t$ of the initial TIMES solution at each period $t$. The amplitude of the score doubled between 2040 and 2050.

- Two states of convergence can be seen in the graphs: a transient state and a steady state phase. The power generation adequacy levels is said to be in a transient state when the control variable $\theta_{r,t}$ changed and the $LOLE$ metric has not yet reached a stable level. Whereas the steady state is characterized by small changes in the score function. Some fluctuations are observed within the steady state phase, but the stability is quickly caught up. This fluctuations were to be expected, as in each iteration the optimization problem at the planning stage changes and that can create some numerical change in the solution, but the iterative process is capable to restore the stability to the adequacy levels by adjusting the $\theta$ position in the next iterations.

- The constant learning have the potential to reach solution close to the desired solution as it is faster, while the decreasing rate find itself trapped in an area and harder to move quickly. The constant learning rate involves keeping the step size fixed throughout

the iterations. On the other hand, the decreasing learning rate strategy adapts the step size over time, gradually reducing it as the optimization process progresses. This approach allows the algorithm to take larger steps in the early iterations, enabling rapid convergence to a region close to the optimal solution (30 iterations for the decreasing rate vs 80 iterations for the constant step-size). As the iterations proceed, the learning rate diminishes, allowing the algorithm to fine-tune the estimate and converge more robustly.

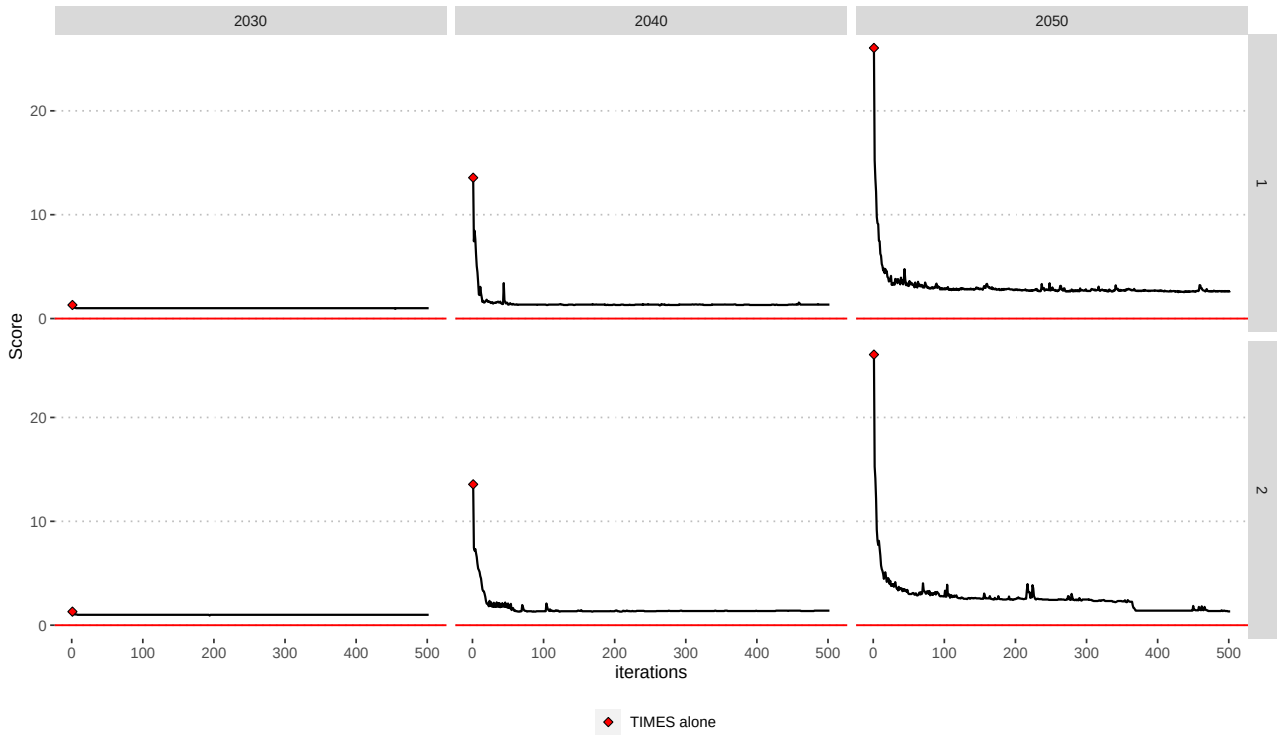


Figure 6.22: The evolution of the periodic score $S_t$, for the scheme 1 and the scheme 2

The overall convergence, as expressed by the score $S$, is presented in Figure 6.23. Both schemes start from the same initial point with a score of approximately 50. From the figure, it is evident that the overall convergence trajectory follows a similar pattern as the convergence of $S_t$. The transient state is rapidly reached, around iteration 100, with a decreasing learning rate in the first scheme. This slower movement of $\theta_{r,t}$ results in weak oscillations and a stable level of convergence.

In contrast, the constant learning rate scheme exhibits more pronounced oscillations but ultimately achieves a higher level of convergence at around iteration 360. The iteration that minimizes the overall score is considered as the final solution. In our analysis, we find that the decreasing scheme achieves the first minimal score at iteration $n_1 = 121$ with a score of $S = 4.876$, while the constant scheme achieves the minimal score at iteration $n_2 = 469$ with a score equal to $S = 3.728$.

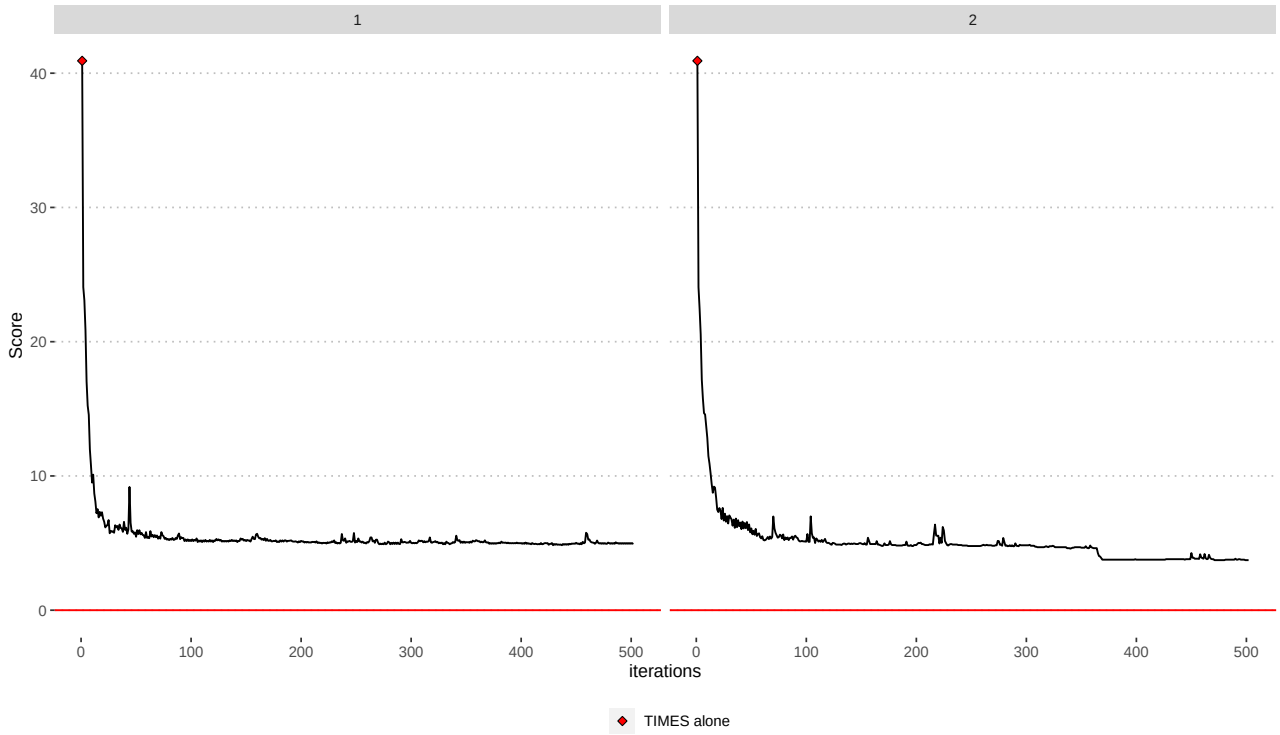


Figure 6.23: The overall trajectory of the approximation stochastic algorithm

**The application of dynamics to study the convergence of the stochastic approximation algorithm**

The problem at hand can be interpreted through the lens of non-linear dynamical systems. The equilibrium of this system corresponds to a point $\theta_{r,t}$ where power generation adequacy requirements are meet for each risky region. The recursive scheme employed in our multi-scale model, given by $\forall(r,t) \in (R_{risky}, T_{risky})\theta_{r,t}^{n+1} = \Pi_{[0,1]}[\theta_{r,t}^{n} + \alpha_n(\zeta_{r,t} - y_{r,t}^{-}(\theta_{r,t}^{n}))]$, can be reformulated as a system of ordinary differential equations (ODEs):

$$\frac{\theta_{r,t}^{n+1} - \theta_{r,t}^{n}}{a_n} = [\zeta_{r,t} - y_{r,t}^{-}(\theta_{r,t}^{n}))] \longleftrightarrow \dot{\theta}_{r,t} = F(\theta_{r,t}) \tag{6.2}$$

Equation 6.2 represents the dynamics of the system as a set of ODEs, with $F$ serving as the gap function between the $LOLE$ metric and the target value of power generation adequacy. This system of ODEs describes the behavior of a multi-region and multi-period dynamical system in search of an equilibrium that satisfies the desired power generation adequacy targets. The equilibrium point occurs when $\dot{\theta}_{r,t} = 0$. Assuming an equilibrium zone for the $LOLE$ of $[2.5, 3]$, the equilibrium state of the system of ODEs lies within the range $[0, 0.5]$.

To capture the dynamics associated with the developed algorithm, we construct a phase diagram for each component of the ODEs system. Since the function $F$ is not analytically

known and can only be accessed through simulation, we are unable to evaluate it at every point ($\theta$,$\dot{\theta}$) to draw a complete phase diagram. However, its values over the 500 iterations are well-defined, enabling us to plot the trajectory of the solution in a phase diagram represented by $(\theta_{r,t}, \dot{\theta}_{r,t})$. With the use of two learning rates (decreasing and constant) we can plot two field lines.

Figure 6.24,6.25,6.26 depicts the solution trajectory in the phase space ($\theta$,$\dot{\theta}$). The analysis of the figures yields several key observations:

- Each country exhibits its own unique dynamics in bringing the control variable $\theta_{r,t}$ to the equilibrium zone. Multiple and distinct trajectories are observed.
- We can identify three distinct types of dynamical behavior. Most countries demonstrate an attractor that guides $\theta$ towards the equilibrium zone of $[0, 0.5]$ (2040: HU, UK, NL, IE). Periodic behavior is observed in countries characterized by cyclic movement (2050: PT, FI, PL). Conversely, there are countries that lack an attractor altogether and struggle to enter the equilibrium zone.
- The convergence speed varies depending on the choice of learning rate scheme. The decreasing learning rate initially progresses rapidly but slows down as the iterations progress.
- In both schemes, the final points (at iteration 500) are close to each other, indicating that the solutions are in proximity to their respective equilibrium points.

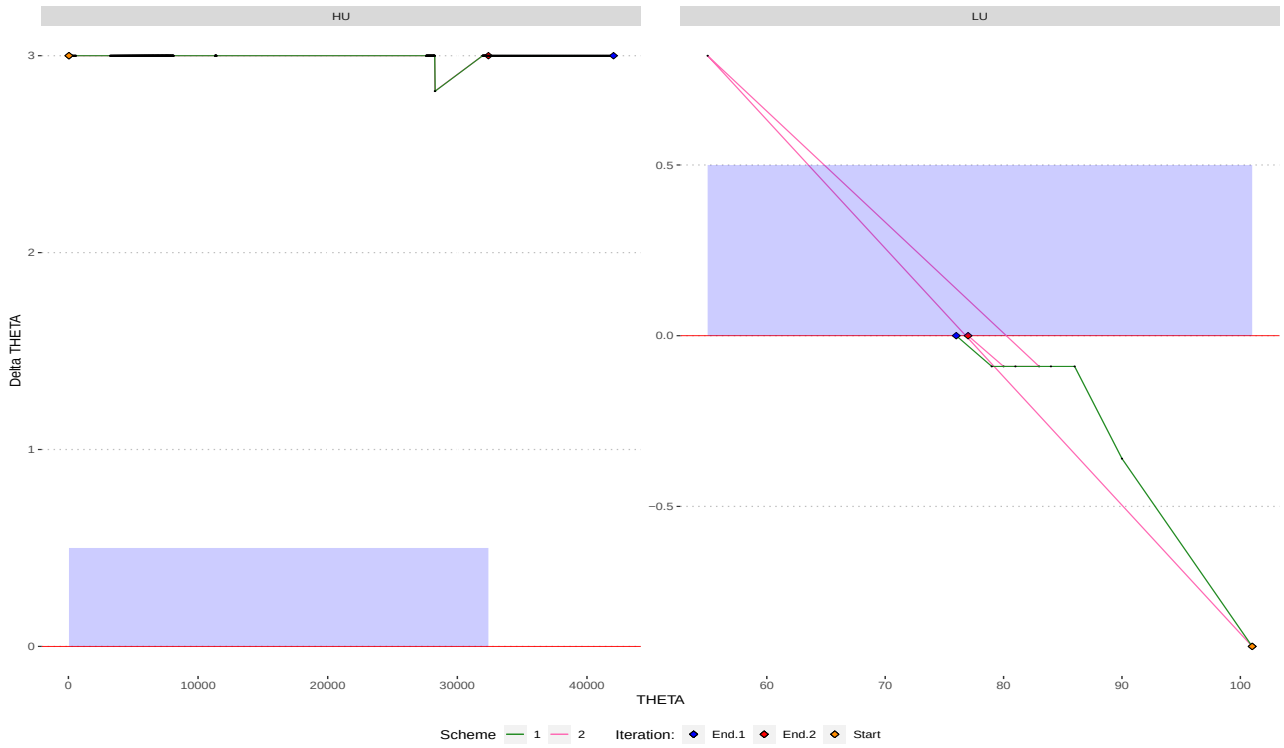


Figure 6.24: Phase diagram for the solution trajectory in 2030. The orange point represent the initial point, the scheme 1 and 2 are respectively the red line and pink line, while the solution are presented in the red and blue point

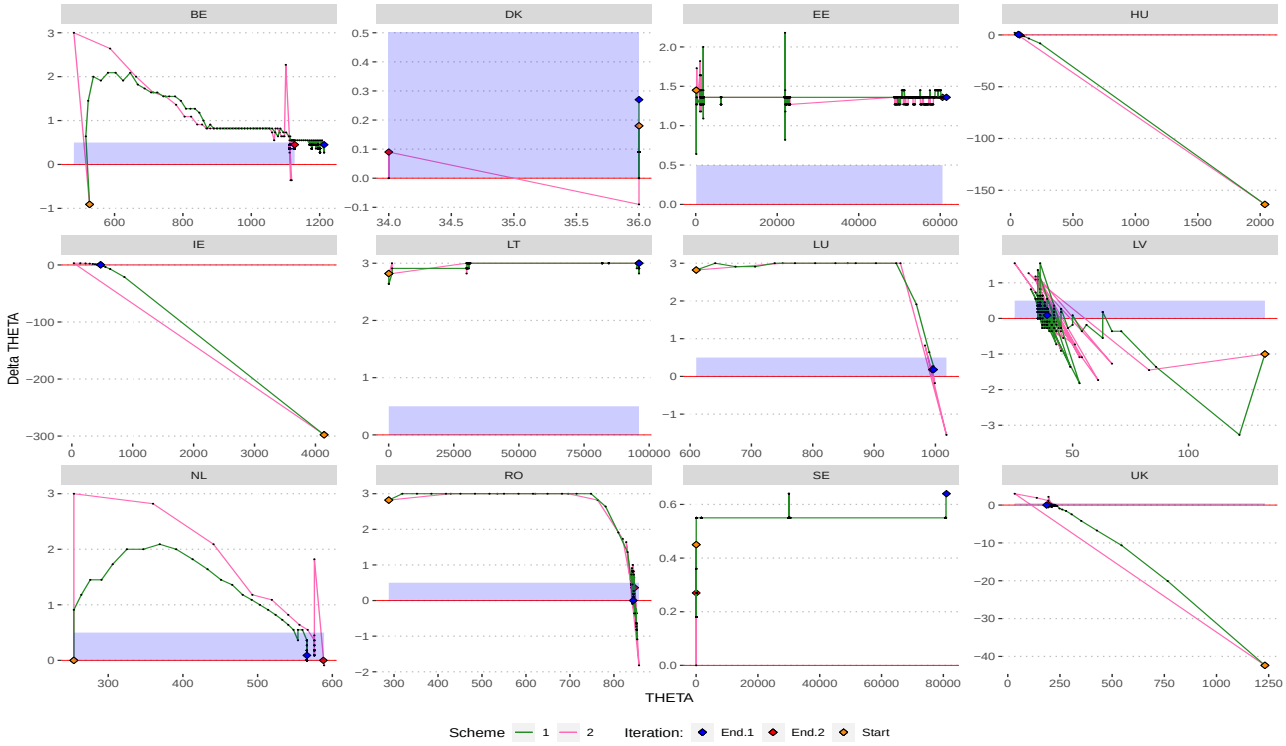


Figure 6.25: Phase diagram for the solution trajectory in 2040. The orange point represent the initial point, the scheme 1 and 2 are respectively the red line and pink line, while the solution are presented in the red and blue point

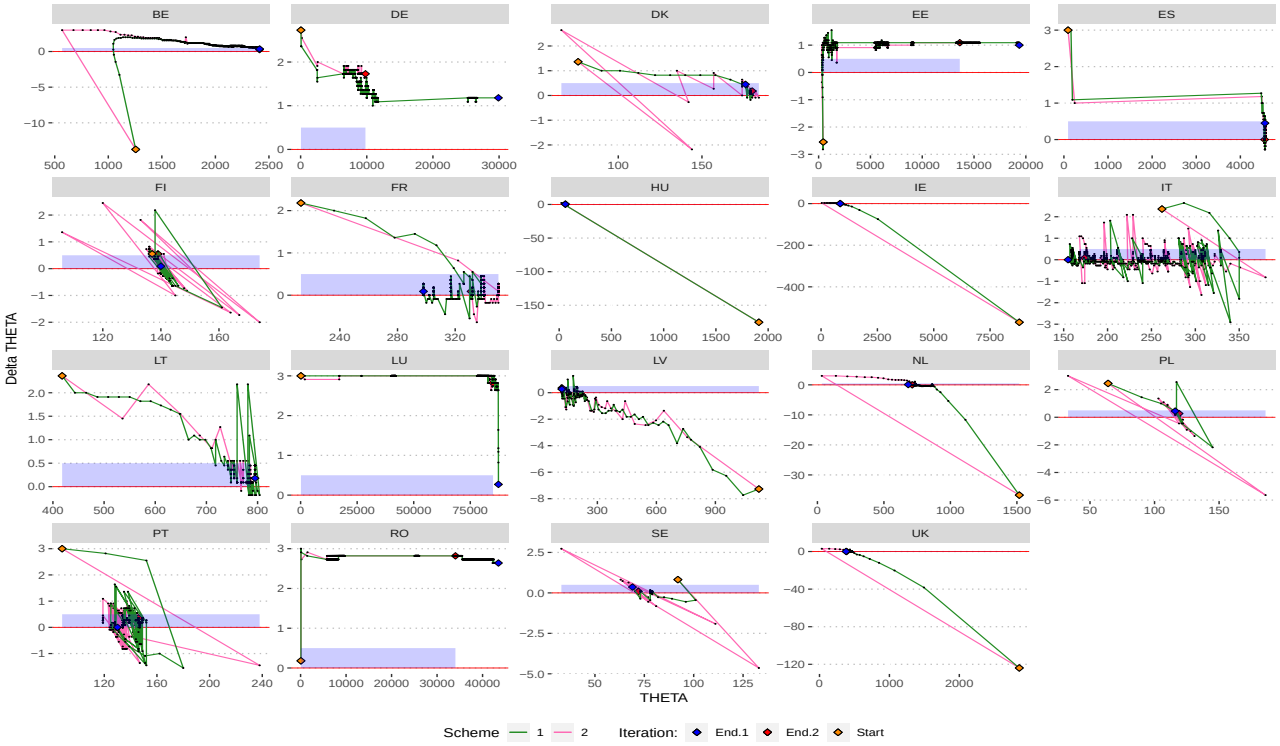


Figure 6.26: Phase diagram for the solution trajectory in 2050. The orange point represent the initial point, the scheme 1 and 2 are respectively the red line and pink line, while the solution are presented in the red and blue point

To have an indicator of the convergence at the European level, we can draw upon the concept of the barycenter, commonly used in physics to determine the equilibrium point of a finite set of point masses. The European barycenter can be calculated with equal weighting assigned to all countries (the adequacy of one country, X, carries the same weight as the adequacy of another country, Y). Alternatively, we can consider weighting by the level of demand (the adequacy of a country, X, with high electricity consumption is favored over the adequacy of a country, Y, with lower consumption). The results with equal weighting of 1 for all countries are represented in Figure 6.27 bellow.

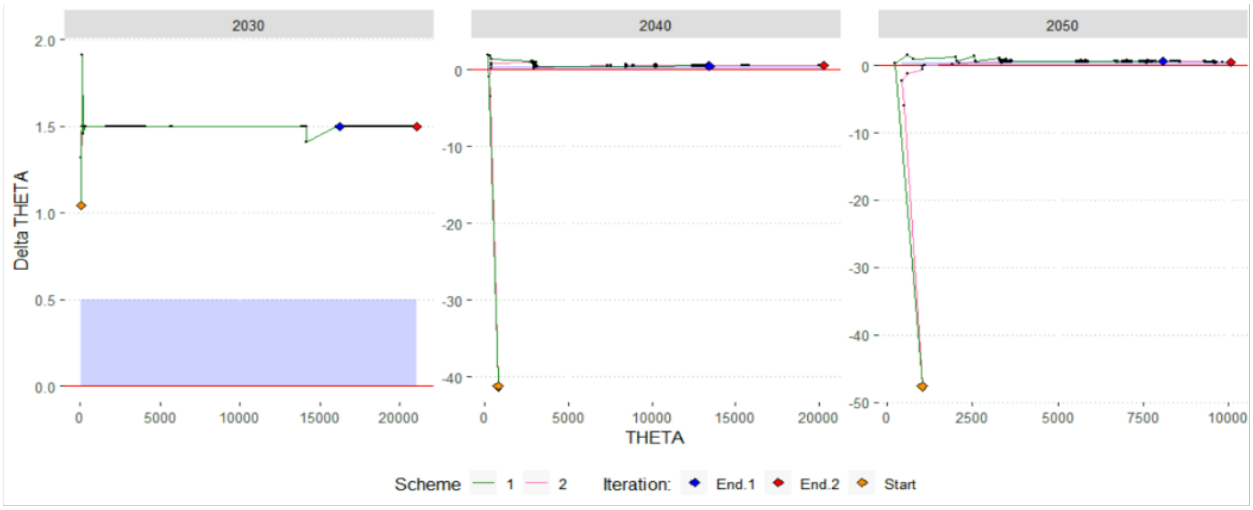


(a) Phase diagram for the solution trajectory for the european barycenter over all risky countries.

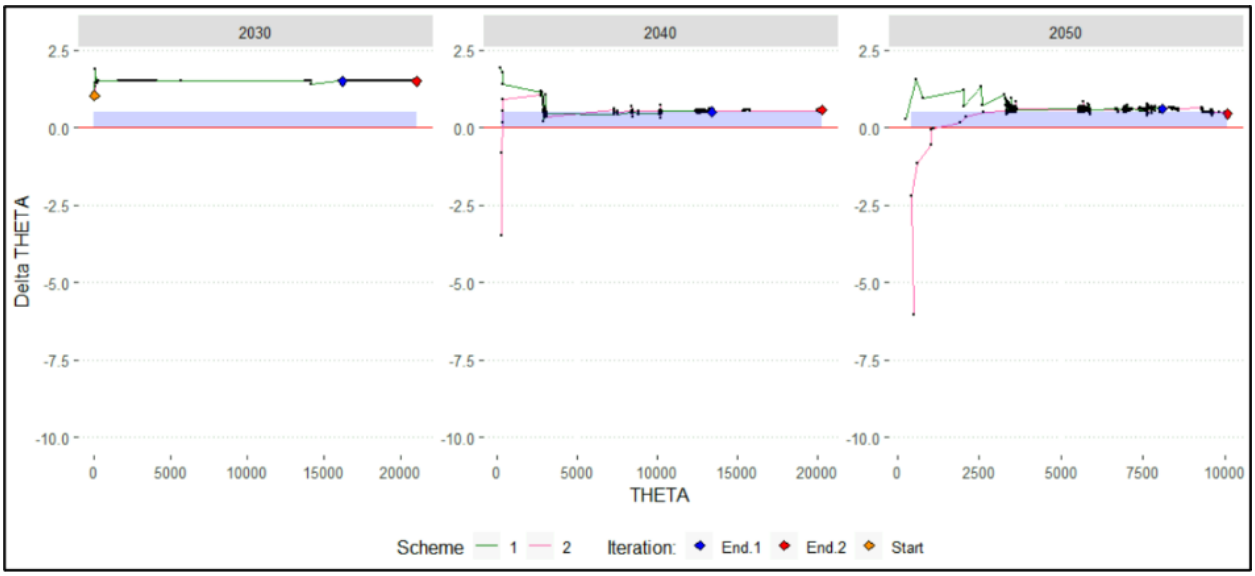


(b) A closer examination for the phase diagram for the solution trajectory for the european barycenter over all risky countries.

Figure 6.27: The phase diagram for the solution trajectory for the european barycenter over all risky countries.

In Figure 6.27, the barycenter's evolution demonstrates that in 2040 and 2050, the barycenter enters the solution area. However, in 2030, the barycenter, of the two inadequate countries (Luxembourg and Hungary), remains positively (in the sens that the LOLE is less to 2.5 hours/year) distant from the solution area as the algorithm wasn't able to bring the LOLE to [2.5,3] area. Despite both trajectories having distinct learning rates, the barycenter's evolution in both schemes closely parallels each other. The final two iterations are denoted by the red point for the constant learning rate and the blue point for the de-

creasing learning rate. Notably, the red point consistently reaches higher values in the $\theta$ space.

### Resulted power generation mix trajectory: structure and related costs

#### Power system structure

The evolution of new investments in each technology throughout the planning time-frame over the 500 iterations is illustrated in Figure 6.28. The figures show that following the deployment constraints of Scenario A, hydro, nuclear, other, and interconnections progress steadily and with minimal changes compared to the initial iteration. This is due to the fact that the initial solution are near to the maximal allowed installed capacities. On the other hand, natural gas, wind, solar, and hard coal exhibit significant changes across the iterations. Here are the observations for each period:

- In 2020: There are no significant changes in new investments for all technologies as no reinforcement constraints were generated for this period. The evolution of new investments remains stable throughout the iterations.

- In 2030: The changes in new investments are minimal. Natural gas increases by approximately 200 MW and stabilizes at 10.8 GW, while wind decreases by 200 MW and stabilizes at 204.8 GW. Nuclear power increases by approximately 500 MW and stabilizes at 89.7 GW, while Run of River decreases by 200 MW and stabilizes at 39.9 GW.

- In 2040: Two major technologies drive the changes in the power generation mix structure. Natural gas adds nearly 40 GW, reaching a plateau and subsequently increasing to 80 GW. The need for natural gas to ensure power generation adequacy requirements in 2040 and beyond doubles. Conversely, wind removes nearly 10 GW initially and gradually increases to reach 450 GW by the end.

- In 2050: The same trend is observed in 2050. Natural gas increases its new installed capacity to 150 GW, representing an additional 75 GW compared to the initial solution. Wind decreases its new investments by 20 GW. Hard coal adds approximately 10 GW and stabilizes at 81 GW.

It is also important to highlight that the reinforcement of the initial long-term energy planning model with adequacy proxy constraints have a substantial impact on the structure of the power generation mix. In fact, the adequacy proxy constraint not only add additional new investments to improve its adequacy but adjust investments of all other technologies with respect to deployment dynamics expressed in other constraints. As it can be seen from the Figure, countries that are (AT, BG, CH, CZ, GR,NO) not initially adequate are adjusting (principally retiring) their investments as neighboring countries are investing in new installed capacities to reach the power generation adequacy requirements. For example,

Austria retrieve 5 GW of solar power in 2050 which represent 60% of new investments in 2050.

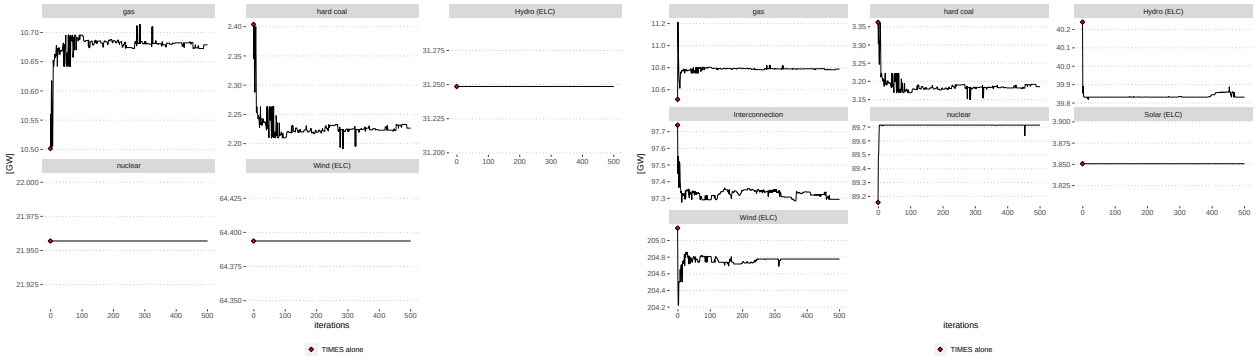


(a) 2020




(b) 2030

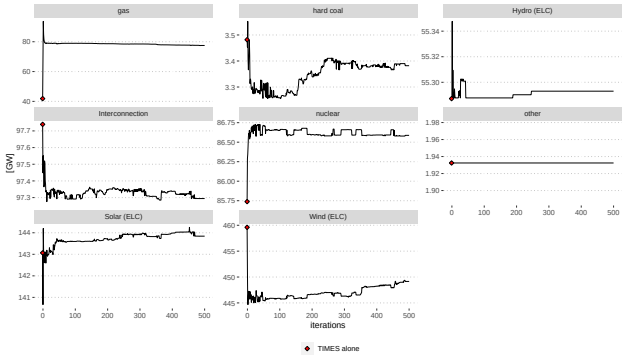


(c) 2040

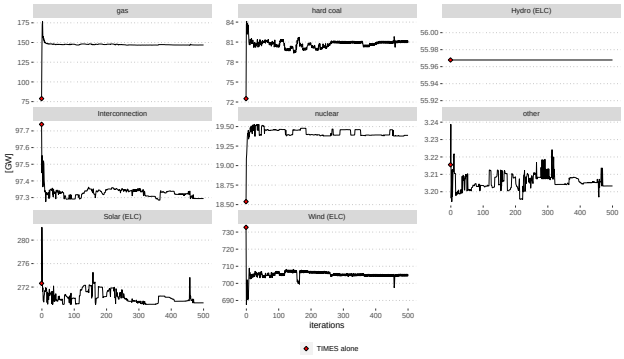


(d) 2050

Figure 6.28: The evolution of net new investments capacities (at the European level) throughout the iterative process for each period of the planning time-frame. It is important to remark that the scales for each technology is different, and that the oscillations are relative to the scale (some big visual oscillations are in fact minimal with only few Megawatts)

The power generation mix obtained from the multi-scale model corresponds to the iteration that achieves the lowest score. Figure 6.29, represents the difference in term of installed capacities between the final solution and the initial solution at the European level and country level country level. At the European level, an addition of nearly 40 GW of natural gas capacity is observed for 2040 and 2050, reaching approximately 80 GW by 2050. This represents a significant portion of the total installed capacity. On the other hand, investments in wind power are progressively reduced, reaching a reduction of approximately 30 GW by 2050. The addition of coal as an end-of-horizon effect is also noted, with a relatively low $CO_2$ tax of only 35 EUto and no constraint on $CO_2$ emissions.

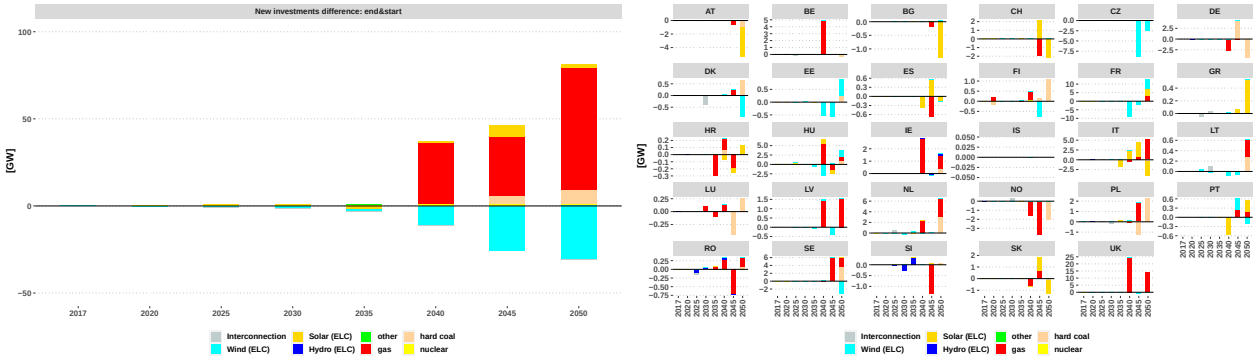


(a) The cumulative new investments differences between the initial European power generation mix and the final solution

(b) New investments differences between the initial solution and the final solution for each country

Figure 6.29: The difference in term of installed capacities between the final solution and the initial solution of "Sceanrio A" at the European level and country level country

The trajectory of power generation adequacy for each country can be observed in Figure 6.30. The algorithm successfully reduces the $LOLE$ levels to below 3 hours/year for the majority of countries, with a significant portion falling within the optimal range of $[2.5, 3]$. Since our framework only reinforces the initial TIMES solution, countries that do not exhibit generation adequacy risks are expected to maintain the same $LOLE$ levels. Hence, the final solution is deemed secure and complies with the requirements for power generation adequacy.

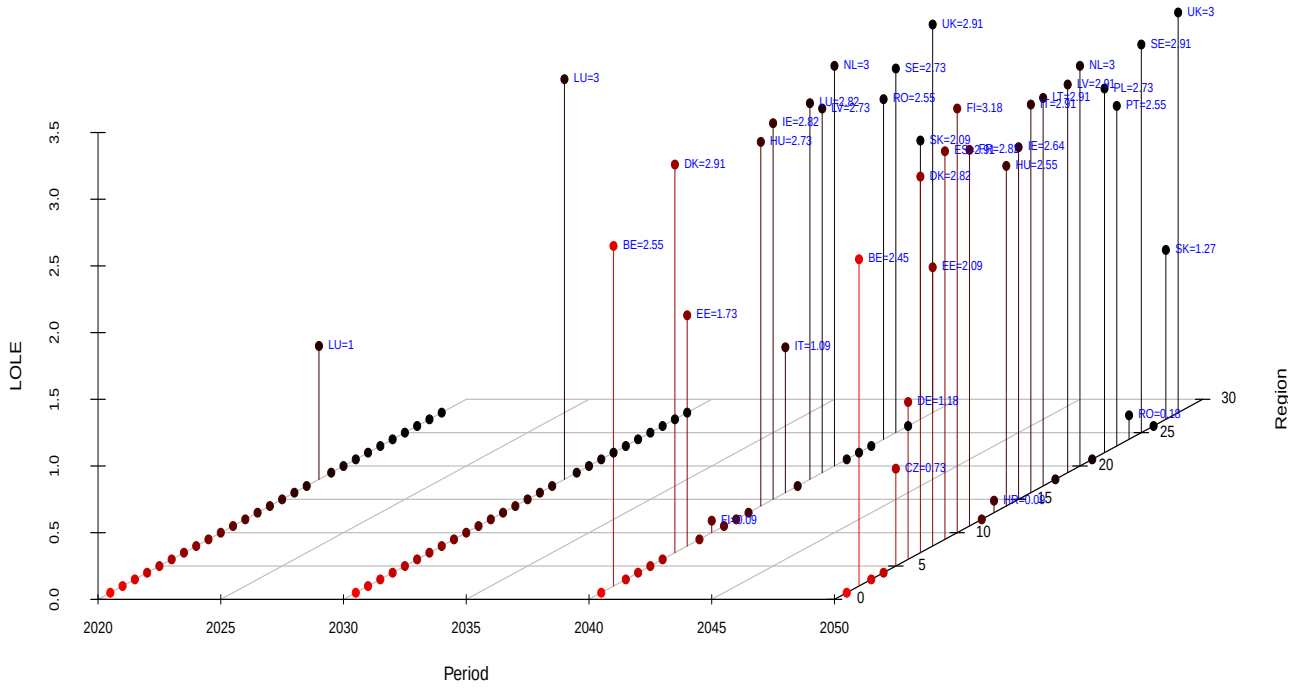


Figure 6.30: The *LOLE* trajectory of the final solution of "Scenario A" using the constant learning rate scheme

**Economics of reaching a secure power system**

The convergence to a solution satisfying power generation adequacy requirements has an economical cost. One important indicator is the total actualized system cost across the planning time-frame. This cost is derived from the objective function of the long-term energy system model TIMES and its evolution through the iterative feedback will highlight how the process is stable. Figure 6.31 bellow depicts the evolution of the total system cost for the two modeled schemes. It can be seen from the figure that the total system cost reach a stable levels after few iterations. While the difference in cost between both schemes is very marginal, the constant scheme have a higher cost than the decreasing scheme as it reach solution with lower scores than the decreasing learning rate. The first peak observed in the first scheme is due to the fact that the first iterations is a decreasing configuration moves the the positions very rapidly. However, after some iterations the amplitude of the learning rate diminishes so as theta. We can conclude that the total system cost is an economical indicator of the convergence of the process to the solution obtained. The difference between the initial solution represents in the red line and the final solution is in the order of Billion Euros for the first scheme abs for the second scheme.

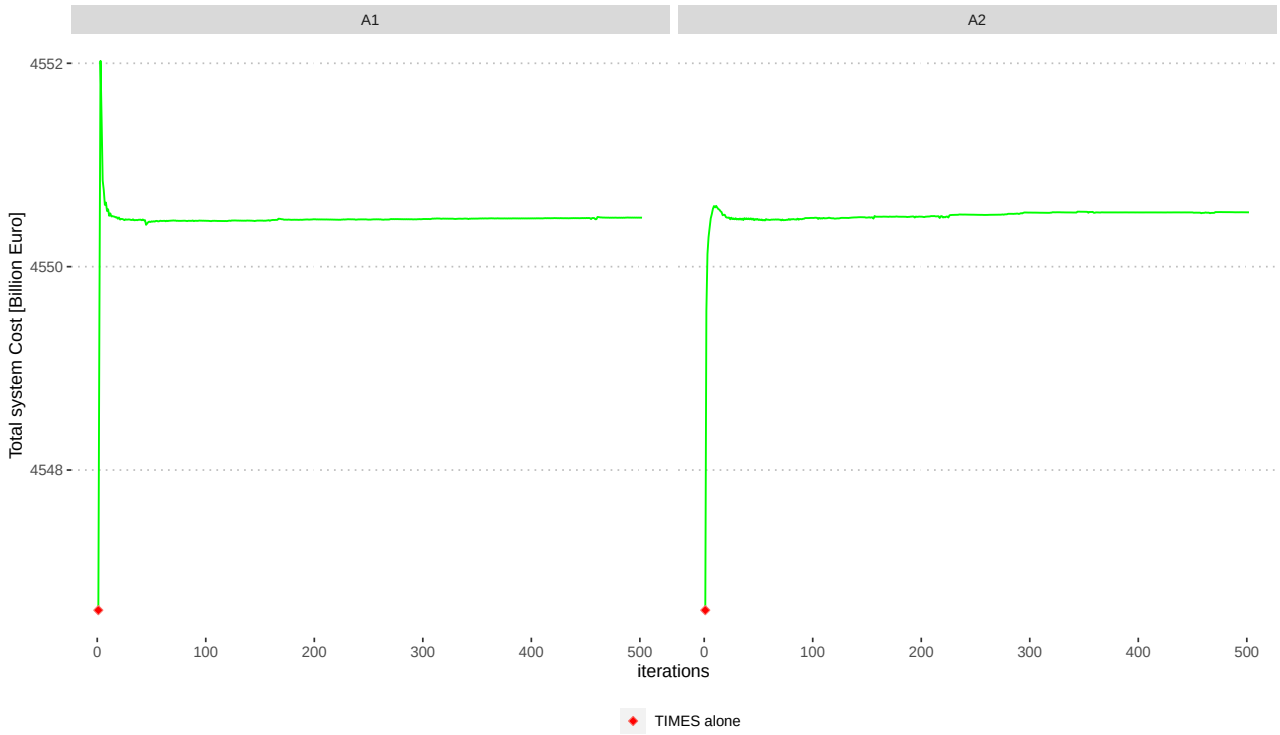


Figure 6.31: The evolution of the total actualized system cost over iterations for the two simulated schemes

Due to the discount rate term in the objective function, the total actualized cost gives minor weight to future investments cost compared to present investment cost. As the shortage is more severe in 2040 and 2050, the analysis of annualized costs provides valuable insights into the evolution of annual cash flows throughout the planning time-frame. The figure below illustrates the annualized total system cost at the European level, which encompasses investment costs, variable operational costs, fixed costs, subsidies and taxes costs, as well as trade costs. To meet the increasing electricity demand and satisfy the constraints of the modeled scenario, investments in new installed capacity progressively increase over the planning time-frame, nearly doubling between 2020 and 2050. Operational and fixed costs also exhibit an upward trend.

The difference between the initial and final solutions is represented in the Figure 6.32. It can be observed that until 2025, no significant differences exist between the two solutions. However, from 2025 onward, new investments are made to address anticipated shortages in 2030, 2040, and 2050. The under-investment observed in 2045 is mainly attributed to the fact that no adequacy assessment, and consequently no reinforcement, is conducted for that particular year. The planning model recognizes the necessity of the additional investments made in earlier periods to ensure power generation adequacy in subsequent years, as the optimization is carried out in a perfect foresight mode.


(a) The European annualized system cost over the planning time-frame for the initial and the final solution

(b) The annualized system cost difference between the final solution and the initial solution

Figure 6.32: The annualized system cost over the planing time-frame for the initial and final solution (left) and its difference (right)

### 6.3.5 Marginal analysis

The marginal analysis is crucial for understanding how the reinforcement of the initial long-term energy planning model shapes the solution. In the scatter plot of the Figure 6.33a, each data point represents the slack between the right-hand side (sum of decision variables weighted by effective participations) and left-hand side (constant value) of the adequacy proxy constraint for a specific country and period. The binding constraints have a slack value of 0, indicating high constraints (located on the right side of the $nRLDC$). Conversely, lower slack values represent less constrained equations (located on the left side of the $nRLDC$). Several observations can be made from this graph:

- The design of the reinforcement module within the long-term energy planning model demonstrates **its utilization flexibility**. Firstly, the adequacy proxy constraints are generated only for periods and countries that fail to meet power generation adequacy requirements. This flexibility was lacking in our earlier contributions that used reserve equations, where all periods were activated once the reserve equation was triggered. Secondly, as the control variable $\theta_{r,t}$ evolves during the search process, the number of generated constraints can be reduced. For example, in 2050, Luxembourg has only one constraint generated as $\theta_{r,t}$ reaches a value of 1. Figure 6.33a depicts the slack values for the different countries and periods with inadequate $LOLE$ levels.

- The dual value represents the shadow price associated with a specific constraint in a linear programming problem. The reinforcement constraints (or adequacy proxy constraints) can be seen as an equivalent to the demand-supply balance constraint. The difference lies in the decision variables: the first constraint is based on investment decisions, while the demand-supply balance constraint is based on operational/dispatch decision variables. The dual value of the demand-supply balance constraint provides the marginal cost of electricity. Similarly, the marginal value of the reinforcement constraints provides the **marginal value of investment for each period**. In other words, for each binding constraint, the dual value represents the amount by which the objective function (total actualized system cost) would decrease if the right-hand side of the constraint were relaxed by 1 GW while keeping all other variables fixed. From a consumer perspective, this can be interpreted as a premium on investments to reach adequacy. From a producer perspective, it can be viewed as a premium paid to producers for providing adequate capacity. This premium helps cover a portion of the investment costs associated with technologies that provide secure capacity. Figure 6.33b show the dual values. We limit our analysis in two observations:

  - This Figure illustrates that the investment premium required to attain adequacy differs from one country to another, spanning a wide range. For instance, some countries achieve a $LOLE$ of 0 hours/year by making investments in 2040, such as Romania, where the premium is nearly 0 Million Euro/GW. Conversely, Luxembourg in 2030 needs to rely on its internal investments to reduce its initial $LOLE$ from 3.72 to just 3 hours/year, incurring a premium of nearly 90 Million

Euro/GW. These variations in premium values can be attributed to a combination of factors, including differences in power system structures (each country favoring different technologies with distinct investment costs), inter-temporal interdependence of investments (adequacy in one period influencing others), and the level of demand (e.g., an additional 1 GW for Luxembourg is significant given its peak demand of only 800 MW).

– Additionally, the results reveal non-uniqueness in sizing hours. Different countries have multiple binding constraints at different hours, indicating that there isn't a single operational situation (hour) that triggers the desired LOLE level.

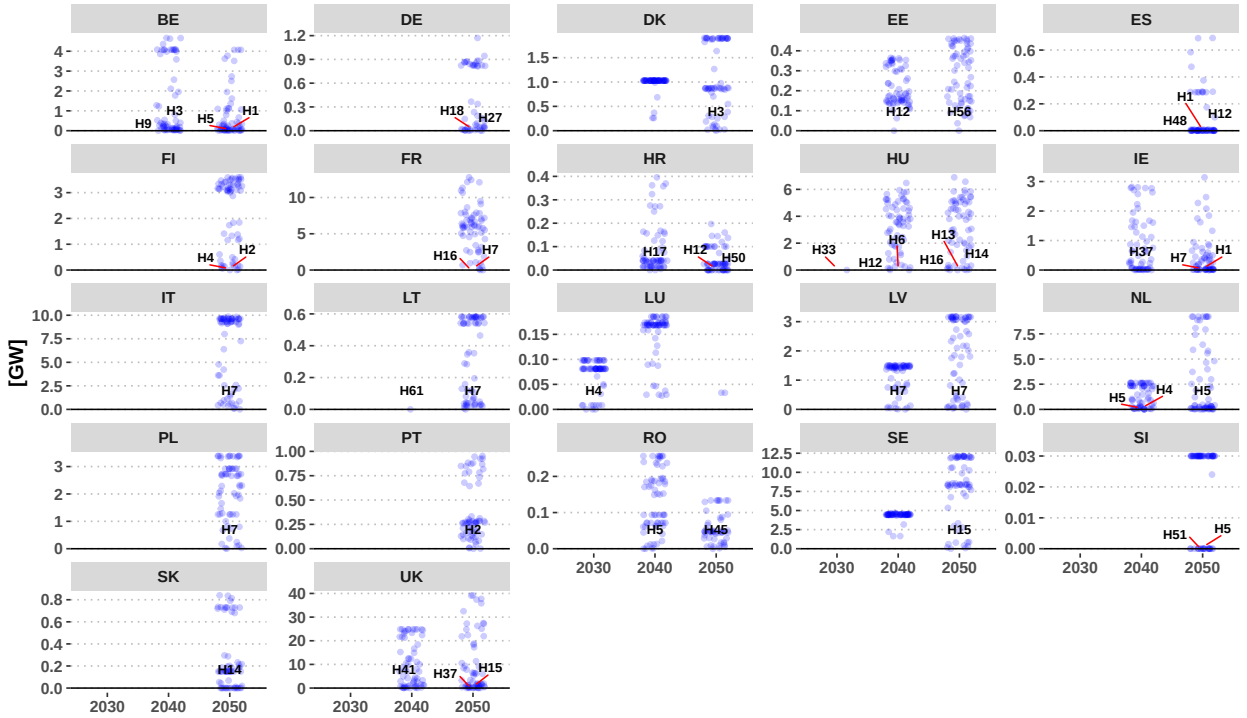


(a) Gap level of the proxy adequacy constraints

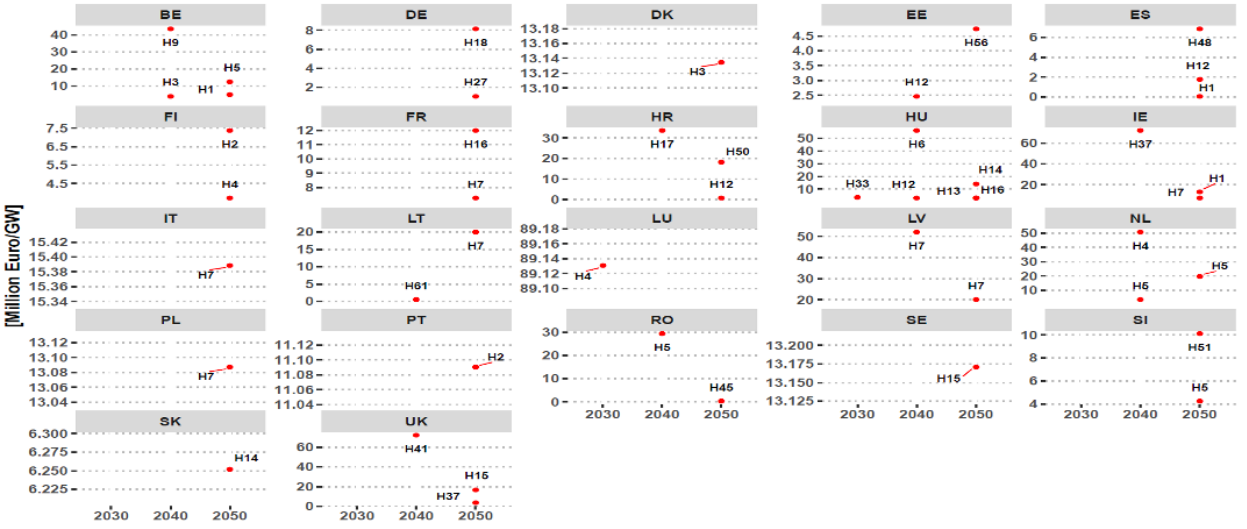


(b) Dual value of the adequacy constraint for all countries and periods with inadequate intiial power geration mix

Figure 6.33: The marginal analysis of power generation adequacy equations involves two key components:(a) The slack value of each equation at the optimal solution. (b) The dual values. Here, the index $\{H_n\}_{n\in 1:64}$ corresponds to the time-scale index of the adequacy temporal scale. In each region, a maximum of 64 equations can be generated for the reinforcement.

### 6.3.6 Results of the scenario B

In this section, we present the results obtained using "Scenario B". Since ANTARES does not inherently incorporate constraints on CO2 emissions, implementing "Scenario B" necessitates the introduction of an additional constraint, specifically addressing the reconciliation of CO2 emission limits. It is indispensable as ANTARES doesn't directly incorporate in its modeling a specific constraint related to $CO_2$ emissions limitation. Without this reconciliation, both models will follow different operational trajectories, making it challenging to achieve a reliable solution. The reinforcement of the planning model would be based on an operational trajectory that diverges from the planning model. For instance, if the planning model imposes a neutrality emission of $CO2$ for a certain period $t$, but no reconciliation of this constraint occurs within the operational power model, the overall power generation mix determined by the planning model will be transferred to the operational model. However, the operational model might utilize thermal power generation mix, which was not intended to be in operation by the planning model. This discrepancy leads to two significant consequences: 1) The adequacy assessment will be "optimistic" as the operational power system could potentially use additional capacities like thermal power generation plants, 2) The generation adequacy proxy constraints based on the operational trajectory of the operational power system might create a misleading signal to use thermal power generation in the sizing of the mix.

To reconcile the $CO_2$ emission constraint between the planning model and the operational model, we adopt the following rule: For a given region $r$ and period $t$," if the planning model does not utilize a particular technology in its operation, the installed capacities of the processes related to that technology are not transferred to the operational power system model. This rule allows us to mimic the $CO2$ emission constraint within the operational power system since the power system's operation significantly influences $CO2$ emissions. Consequently, the group of technologies decided to be used in the operation by the planning model will be the same technologies employed in the operation of the operational model. As a result, both models will share the same power generation mix for operation [10].

In the following paragraphs, we first present the power generation mix resulting from the set of constraints in "Scenario B" and the impact of the newly introduced reconciliation rule on the dispatch and emission trajectory within the operational power system model. Next, we conduct a power generation adequacy assessment for "Scenario B" to evaluate the initial solution's compliance with the power generation adequacy requirements. Finally, we present and compare the results of the stochastic approximation algorithm applied to this scenario with the results of "Scenario A."

[10]It is important to note, that this rule has no impact on the results of "Scenario A" as no technology complies with it in this scenario (each technology in the mix participated in the operation).

**Technical-economical analysis of the power generation mix structure and $CO_2$ emissions**

The power generation mix resulting from "Scenario B" is presented in the Figure 6.34 below. Notably, no investments in fossil-based power plants are made. It is crucial to emphasize that the installed capacity of fossil-based thermal technologies in 2050 mainly arises from the residual installed capacity of the base year. The power generation mix structure for each area is also depicted to illustrate the evolution at the countries levels. The Figure 6.35 displays the newly installed capacity at the European level, as well as for each country. From this analysis, the following observations can be made:

1. Investments in natural gas come to a halt from 2020, while investments in nuclear power follow a similar trend as observed in "Scenario A," due to the constraints on the implemented policies for nuclear.

2. Wind power exhibits the largest installed capacities and reaches a peak in 2025. This phenomenon can be explained by using a perfect foresight configuration with the neutrality constraint, which provides an optimal solution leading to significant initial investments (as also evident in the emission figure).

3. Solar capacities also experience investments in 2040 and 2050, predominantly in the southern regions of Europe where sunlight is abundant (e.g., Italy, Spain) or technically and economically viable (e.g., Germany).

4. From 2030 onwards, the new investments in dispatchable technologies are primarily restricted to biomass and geothermal sources. The high presence of geothermal capacities may be deemed "technically unfeasible" as the constraints on biomass and geothermal are relaxed. Nevertheless, since our focus is solely on applying the methodology to a scenario with the neutrality constraint, we consider this to be acceptable from a methodological standpoint.

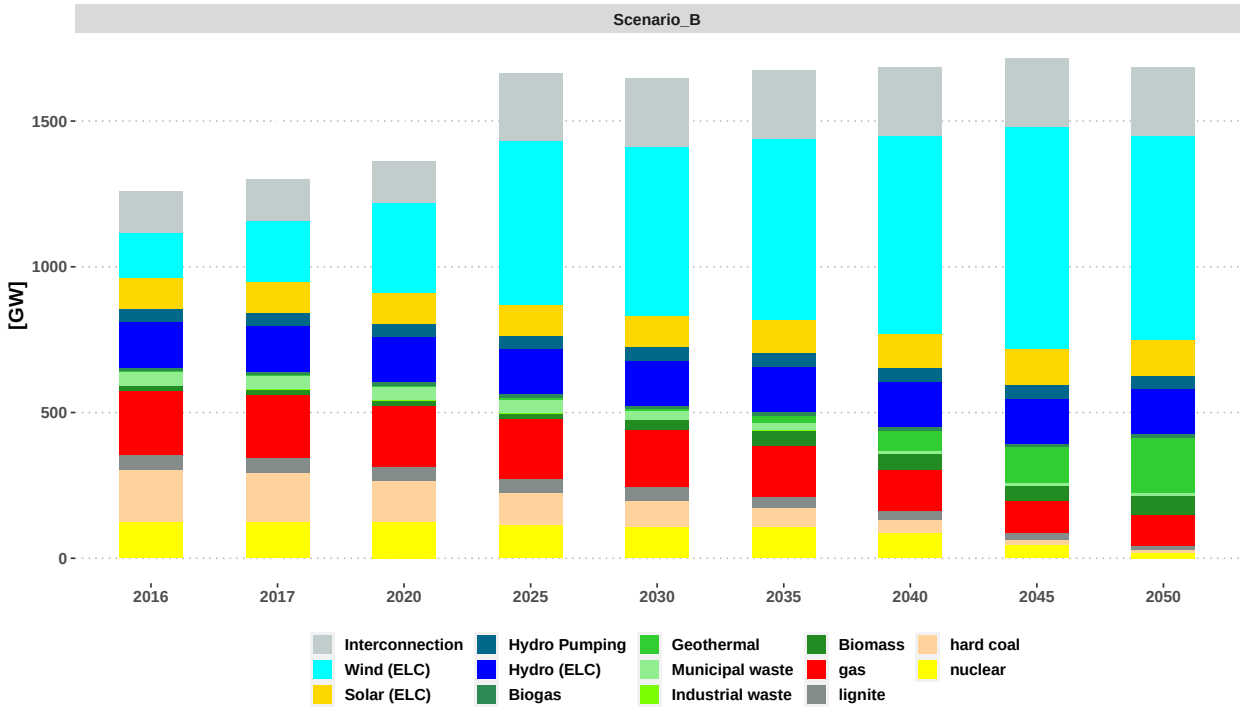


(a) The investment trajectory $\Pi_{inv}^{TIMES}$ at the European level for the planning time-frame 2016-2050

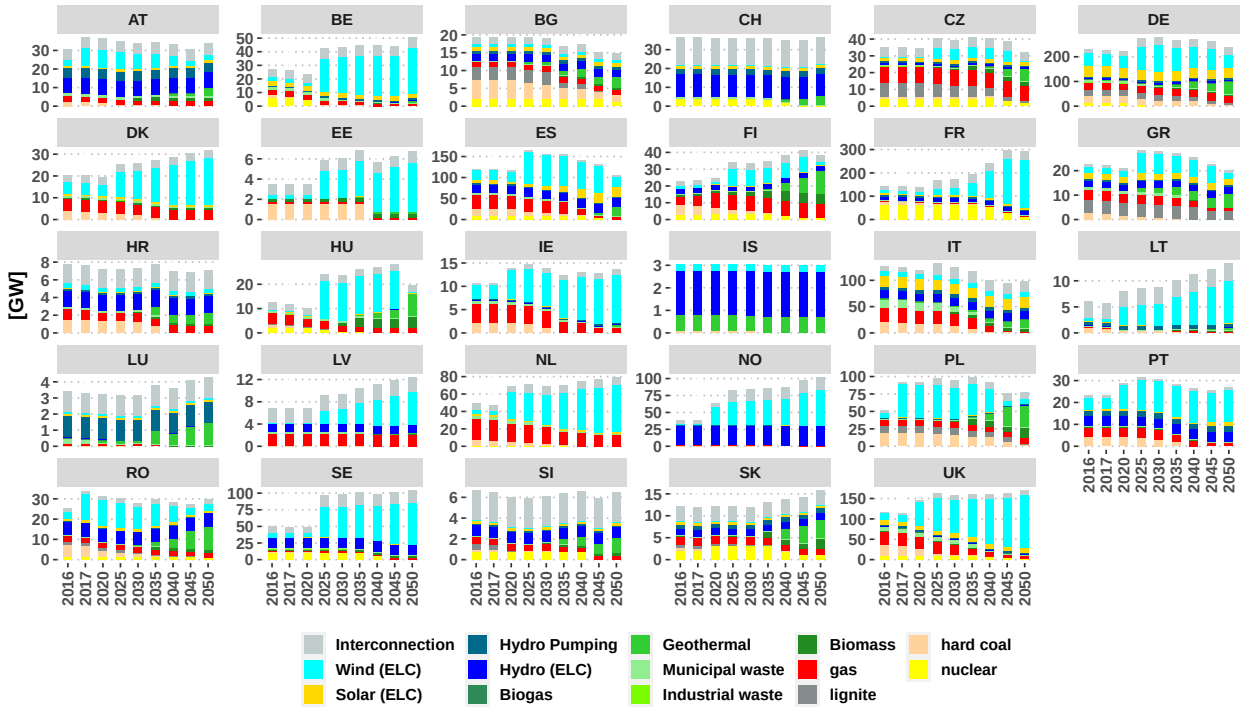


(b) The investment trajectory $\Pi_{inv}^{TIMES}$ at country by country for the planning time-frame 2016-2050

Figure 6.34: Scenario B, the investment trajectory $\Pi_{inv}^{TIMES}$ at the European level (a) and country by country level (b) for the planning time-frame 2016-2050

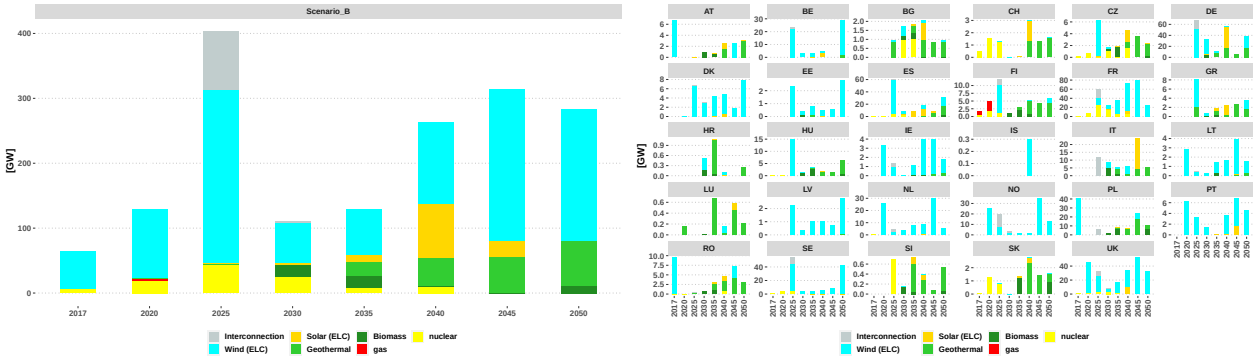


(a) The new installed capacities at the European level for the planning time-frame 2016-2050

(b) The new installed capacities at the country by country for the planning time-frame 2016-2050

Figure 6.35: The new installed capacities at the European level (a) and at the country by country level (b) for the planning time-frame 2016-2050

Based on the power generation mix obtained, the annual dispatch required to meet the electricity demand at each period is presented in the Figure 6.36 below. Several important remarks can be drawn from this figure:

1. The share of wind generation is steadily increasing, indicating the successful integration and utilization of wind energy in the power generation mix.

2. The share of nuclear power decreases over time and reaches marginal levels in 2050. Additionally, natural gas disappears from 2030 onward. Its presence in 2040 is attributed to the reconciliation rule employed in the ANTARES model. In fact, in 2030 and 2040 the $CO_2$ emissions within TIMES are marginal but not null which leads to the transfer of some natural gas capacities to ANTARES.

3. The difference between the dispatch results obtained from TIMES and ANTARES models does not exceed 4%. This small discrepancy is an important indicator that the reconciliation rule established to address the $CO_2$ constraint yields consistent and accurate results.

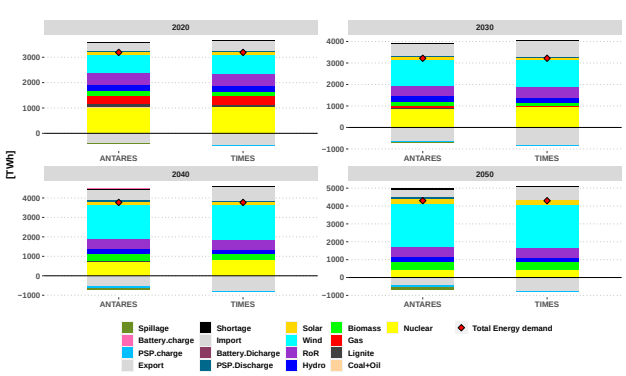


(a) Scenario B, the comparison between the power generation mix in [TWh] at the European level between TIMES and ANTARES

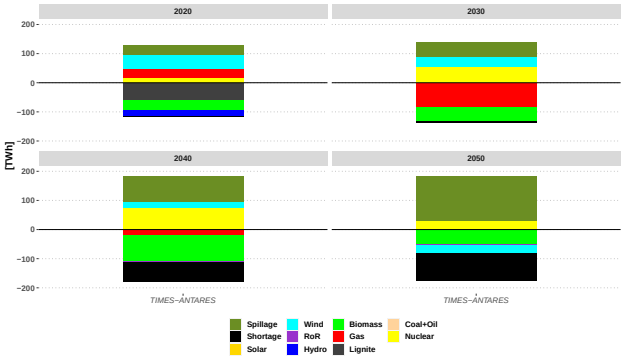


(b) Scenario B, the difference in terms of power generation between TIMES and ANTARES. Negative values indicates that ANTARES produce more than TIMES and vice-versa

Figure 6.36: Power generation dispatch trajectory for each constituent model and their related differences

Figure 6.37 depicts the $CO2$ emissions trajectory resulted form TIMES and ANTARES for "Scenario B". The trajectory of $CO_2$ emissions shows a significant decrease in total emissions at the European level, commencing from 2030. This rapid decline can be attributed to two crucial factors. Firstly, the absence of any intermediate constraints within the planning time-frame allows the model to determine the optimal path for emissions reduction freely. Secondly, the perfect-foresight configuration of the optimization problem in the long-term planning model enables the inclusion of the 2050 zero-emission constraint within its set of constraints (an anticipation of the increasing prices of $CO_2$ taxes). This emission reduction pathway is consistent with the substantial investments made in wind power in 2025, which significantly contribute to the overall reduction in $CO_2$ emissions.

In periods with marginal or null emissions (from 2030 to 2050), the differences between the models can be explained by the reconciliation rule operating at the technology level rather than the process level. The thermal dispatchable "other" group within ANTARES comprises various technologies such as biomass, industrial waste, municipal waste, geothermal, and biogas. To satisfy the neutrality constraint, TIMES does not use industrial waste and municipal waste, but it utilizes biomass, making the use of the "other" group non-null. Consequently, there is a transfer of installed capacities of waste technologies to ANTARES, which then has the possibility to utilize them. The difference is more pronounced in 2030, as natural gas is still marginally used in some countries (leading to the transfer of its related capacities to ANTARES).

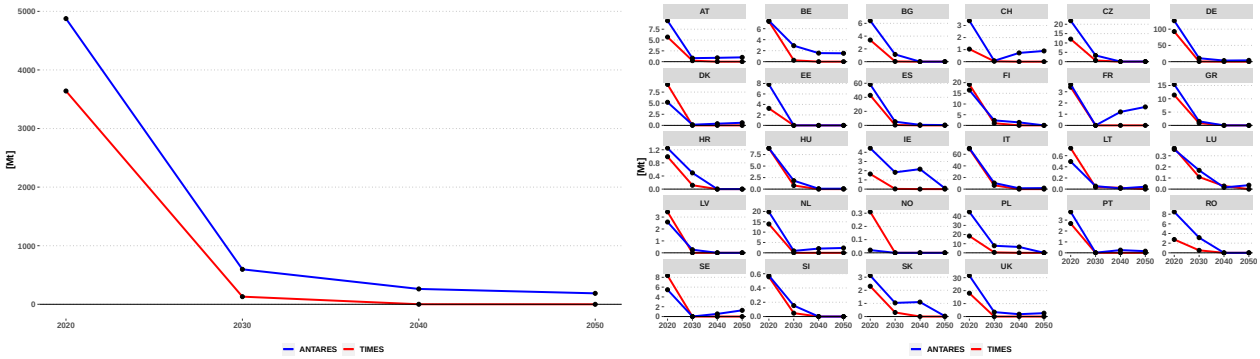


(a) $CO_2$ emissions over the planning time-frame at the European level. red line is TIMES while blue line in ANTARES

(b) $CO_2$ emissions over the planning time-frame for each country. red line is TIMES while blue line in ANTARES

Figure 6.37: $CO_2$ emission trajectory resulted from "Scenario B"

The power generation adequacy assessment for scenario B reveals that from 2030 onwards, almost all European countries have $LOLE$ levels above the 3h/year limit. Comparing to scenario A, the power generation mix decided by the initial solution shows high levels of insufficient supply. The figure below depicts the $LOLE$ trajectory for all the simulated countries.

- In 2020, only one country has inadequate adequacy with a $LOLE$ value of 9.82 hours/year.
- In 2030, the following countries have insufficient supply: Belgium (221.09 hours/year), Denmark (118 hours/year), Estonia (353.64 hours/year), Lithuania (20.73 hours/year), Luxembourg (98.45 hours/year), Latvia (439.82 hours/year), Netherlands (923.55 hours/year), Poland (57.09 hours/year), Portugal (22.91 hours/year), and United Kingdom (129.91 hours/year).
- In 2040, 26 countries have insufficient supply: Austria (121.09 hours/year), Belgium (1319.82 hours/year), Bulgaria (1040.36 hours/year), Switzerland (146.45 hours/year), Czech Republic (216.09 hours/year), Germany (547.82 hours/year), Denmark (730.27 hours/year), Estonia (1203.45 hours/year), Spain (1238.91 hours/year), France (157.09 hours/year), Greece (390.64 hours/year), Croatia (204.91 hours/year), Hungary (638.09 hours/year), Ireland (1050.73 hours/year), Italy (321.36 hours/year), Lithuania (307.09 hours/year), Luxembourg (594.18 hours/year), Latvia (1463.27 hours/year), Netherlands (2105.55 hours/year), Poland (225.09 hours/year), Portugal (850.18 hours/year), Romania (1686.64 hours/year), Sweden (48.18 hours/year), Slovenia (43.73 hours/year), Slovakia (42.45 hours/year), and United Kingdom (1138.45 hours/year).
- In 2050, 27 countries are not compliant with adequacy requirements: Austria (108 hours/year), Belgium (1131.64 hours/year), Bulgaria (716.36 hours/year), Switzerland

(193.91 hours/year), Czech Republic (417.18 hours/year), Germany (473.73 hours/year), Denmark (1119.64 hours/year), Estonia (1689.36 hours/year), Spain (421.18 hours/year), Finland (549.09 hours/year), France (477.09 hours/year), Greece (228.18 hours/year), Croatia (106.09 hours/year), Hungary (264.27 hours/year), Ireland (3300.73 hours/year), Italy (422.91 hours/year), Lithuania (449.64 hours/year), Luxembourg (391.82 hours/year), Latvia (1722.73 hours/year), Netherlands (2483.82 hours/year), Poland (239.45 hours/year), Portugal (431.73 hours/year), Romania (792.45 hours/year), Sweden (251.64 hours/year), Slovenia (59.45 hours/year), Slovakia (142.64 hours/year), and United Kingdom (1711.82 hours/year).

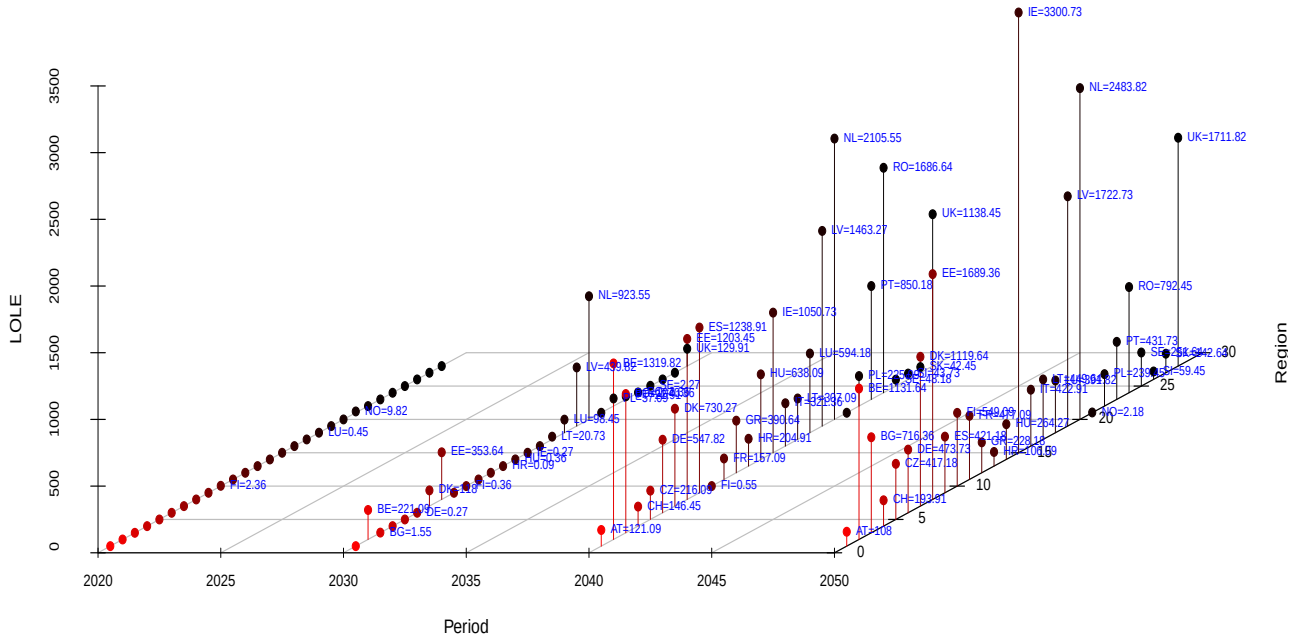


Figure 6.38: Scenario B, the *LOLE* trajectory of the initial TIMES solution

### Performance of the stochastic approximation algorithm

The same two schemes, decreasing and constant learning rates, were applied to assess the convergence of the stochastic approximation algorithm when applied to another long-term scenario. The focus was on two main aspects: the score at each period $t$ and the trajectory score analysis. The Figure 6.39 below shows the evolution of the score at each period $t$ for the two simulated schemes.

It can be observed from the Figure 6.39 that the initial solution score is higher in "Scenario B" compared to "Scenario A." For example, in 2050, "Scenario A" has a score of 25, while

"Scenario B" has a score of 50. The two regimes, transient phase, and steady-state phase, are also observed in both scenarios. However, four important points are to be noted:

- The gap between the target solution and the solution obtained is higher in "Scenario B." For the periods 2040 and 2050, "Scenario A" has a smaller gap to the target solution compared to "Scenario B." After 500 iterations, the algorithm is not able to reach a solution close to the target solution with a null score. Instead, it stabilizes at levels far away from the targeted solution.

- The steady-state phase shows regular oscillations. While "Scenario A" depicts a reduced number of oscillations, the score signal in "Scenario B" is noisy. This highlights the difficulty of finding a multi-regional equilibrium around a $LOLE$ adequacy target of 3 hours/year for a scenario with a neutrality $CO_2$ constraint.

- The constant learning rate scheme reaches a solution space closer to the optimal compared to the decreasing learning rate, which gets trapped. This behavior was also observed in "Scenario A".

- Intuitively, the decreasing learning rate should reduce the oscillations of the score function as the $\theta_{r,t}$ positions move slowly. However, the frequency and amplitude of the oscillations are the same for both learning rates.

The application of the stochastic approximation algorithm to "Scenario B" reveals challenges in achieving convergence to an optimal solution with high periodic-scores levels and regular oscillations in the steady-state phase. The constant learning rate scheme shows better performance in reaching solutions near the optimal, compared to the decreasing learning rate scheme.

The score trajectory is represented in the Figure 6.39 bellow. It can be seen form this figure, that the algorithm permits to drastically lower the level power generation adequacy but fail to find a solution near to the targeted optimal solution.

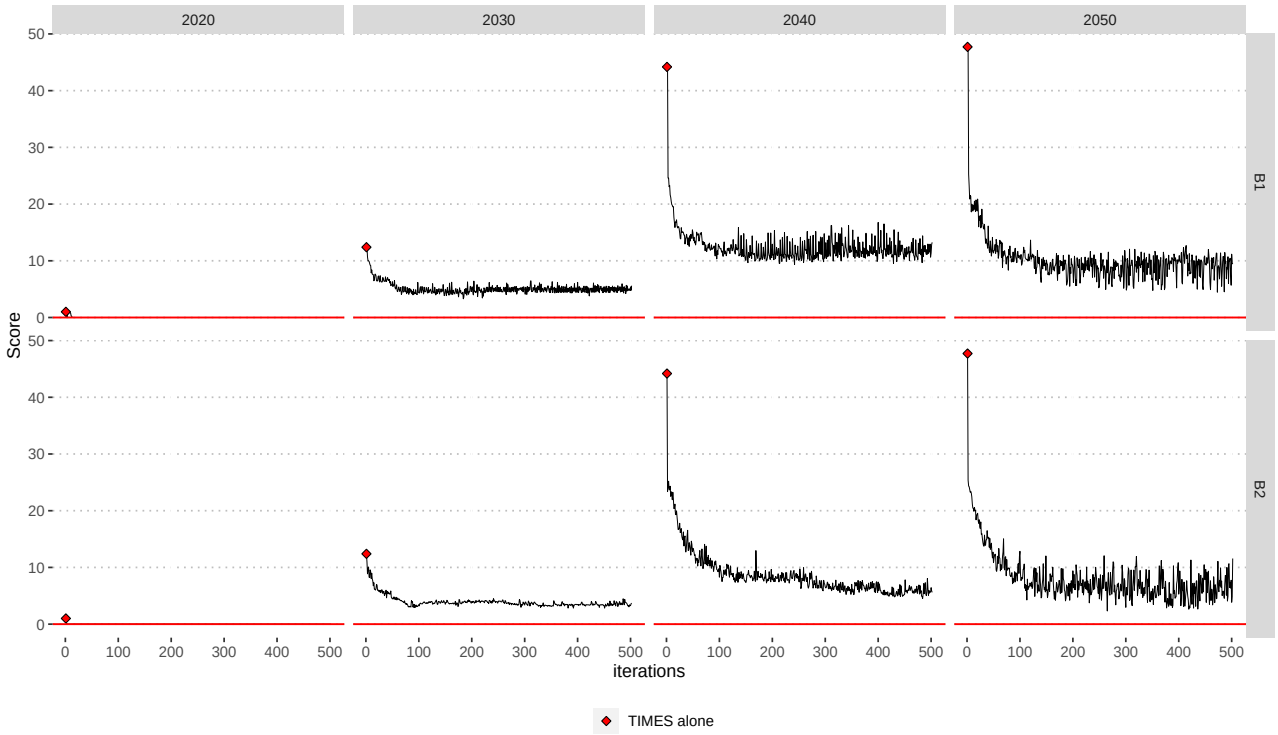


Figure 6.39: The evolution of the periodic score $S_t$, for the scheme 1 and the scheme 2

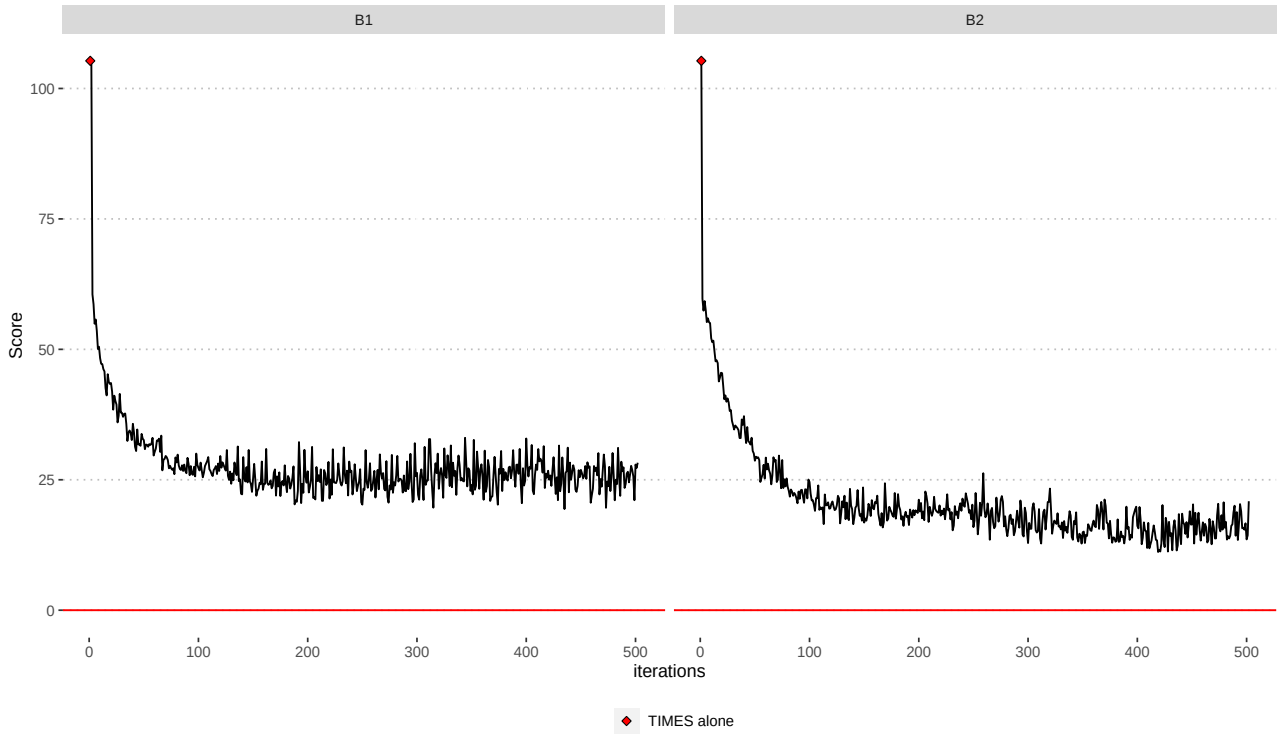


Figure 6.40: The evolution of the trajectory score $S$, for the scheme 1 and the scheme 2

The oscillations observed for the score metric are directly linked to the oscillations related to the new investments. Figure 6.41 bellow depicts the evolution of new investments by technology for each year over the 500 iterations. It can be seen from the figure that (once again the reader must pay attention to the y-scale):

1. For 2020 and 2030, the investments on new installed capacities are stable with reduced variability between iterations.

2. For 2040 and 2050, new investments on all technologies except wind and solar are stable. Wind and solar variability through iterations can be significant and can reach 15 GW for solar and 100 GW for wind.

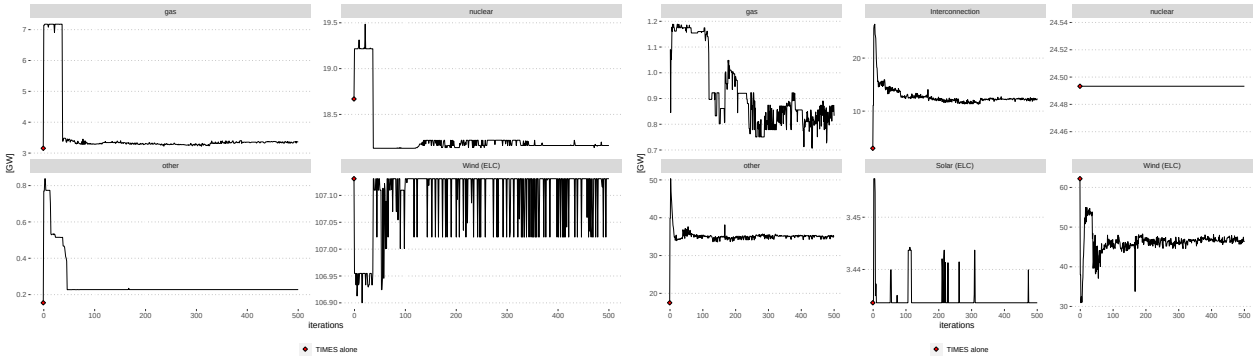


(a) 2020




(b) 2030

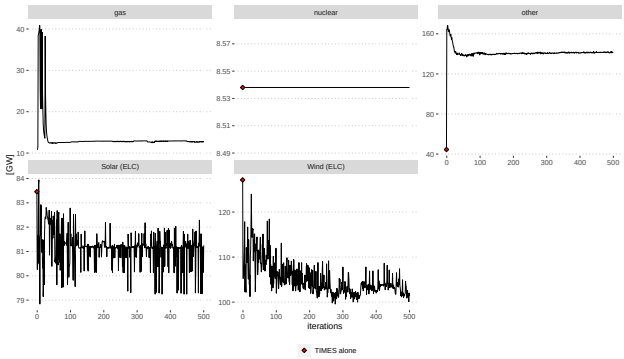


(c) 2040

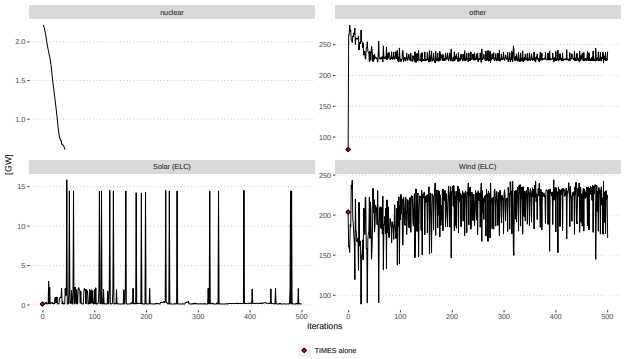


(d) 2050

Figure 6.41: The evolution of new investments capacities (at the European level) throughout the iterative process for each period of the planning time-frame. It is important to remark that the scales for each technology is different, and that the oscillations are relative to the scale (some big visual oscillations are in fact minimal with only few Megawatts)

While the score metrics shows regular oscillations with high amplitude, the total system cost seems to maintain very lower variability between iterations. In addition, both schemes have the approximately the same level of the total actualized cost.

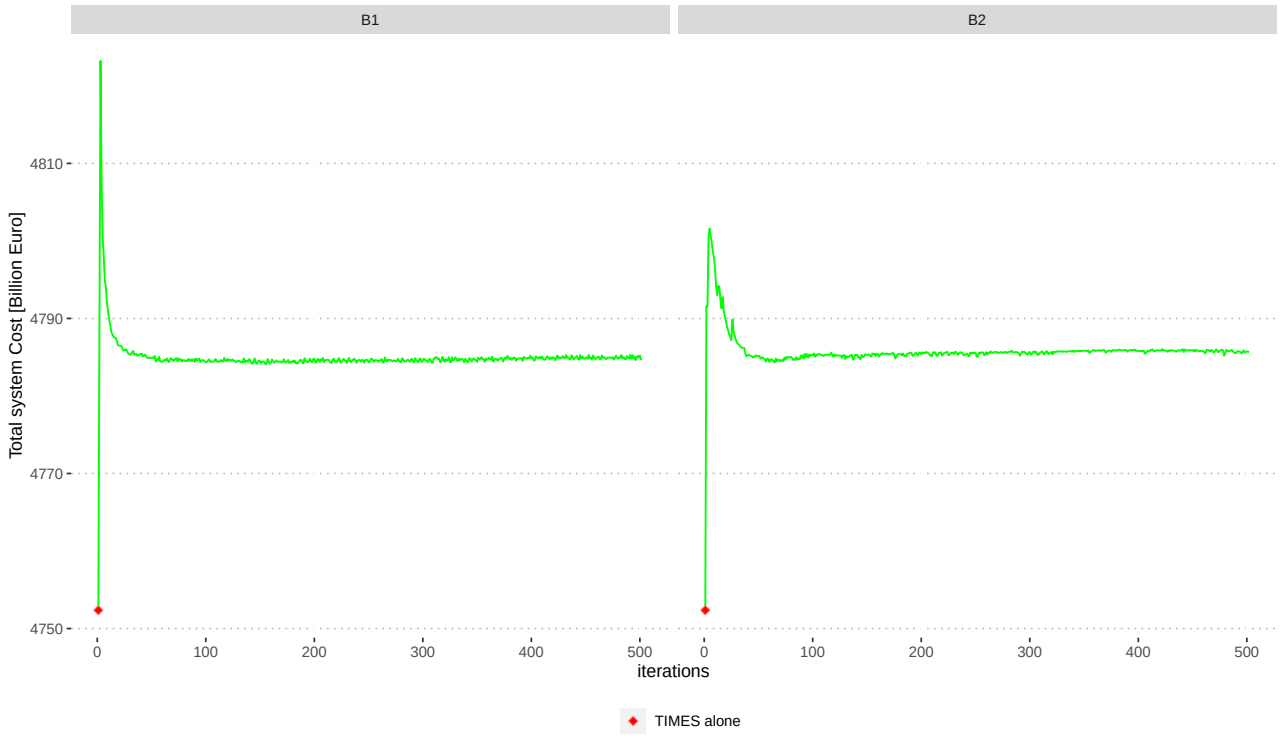


Figure 6.42: The evolution of the total actualised system cost over iterations for the two simulated schemes

The annualized costs for each period within the planning time-frame for the initial solution and the final solution representing the first minimal trajectory score is represented in Figure 6.43a, while its difference is represented in Figure 6.43b. First, it can be seen that additional investments are triggered from 2030 (the year where $LOLE$ metrics are not compliant with adequacy requirements). While only 3 Billion Euro (in 2050) was needed to obtain an adequate solution for "scenario A", additional 27 Billion Euro (in 2050) is needed for "scenario B". As generation adequacy levels are declining over the planning time-frame, additional investments are increasing to bring the resulted power generation mix to adequate generation levels. As no constraints were generated for 2035 and 2045, the model doesn't invest on it. This the case for 2035 when only the variable cost are increased as a result in the change of the power generation mix structure. In addition, as new investments are made before 2045 (to achieve adequacy in precedent periods), the model dis-invest in 2045 because the energy supply-demand balance was already achieved in the initial solution.

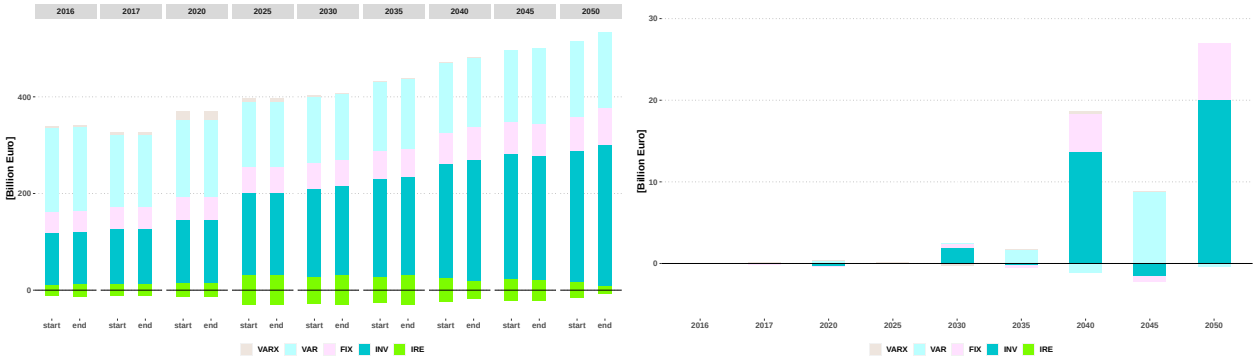


(a) The European annualized system cost difference between the initial solution ans the final solution for "Scenario B"

(b) The diference between the initial and final solution in terms of annualized cost for "Scenario B"

Figure 6.43: The evolution of the annualized total cost per period over the planning timeframe for "Scenario B" for the initial and final solution (left) and its related differences (right).

The final solution obtained for the two simulated schemes are: $n_1 = 433$ and $n_2 = 417$ with a corresponding scores of $S_1 = 19.38814$ $S_2 = 11.164$.

## 6.4 Discussion

The developed multi-scale model in the previous chapter was applied to the interconnected European power system, consisting of two scenarios referred to as "Scenario A" and "Scenario B." "Scenario A" represents a long-term scenario with a high share of renewables and constraints embodying enacted and planned policies regarding the evolution of coal and nuclear. In contrast, "Scenario B" introduces an additional constraint on CO2 emissions, aiming for zero emissions at the European level by 2050.

Key findings from this research include:

For "Scenario A":

1. The validity of the developed uni-directional multi-scale model is demonstrated through different measuring points, with a 7% difference in dispatch at the European level. However, differences are more pronounced at the country level, particularly for specific technologies. Environmental measuring points, differences do not exceed 15%. For the economical aspect represented by marginal electricity prices, the long-term energy planning model struggles to capture operational power system dynamics.

2. The power generation mix resulting from the long-term model does not meet adequacy limits for multiple countries in 2040 and 2050. The stochastic approximation algorithm is then employed, with a 500-iterations limit.

3. Both schemes of the stochastic approximation algorithm successfully improve the initial solution to meet adequacy requirements with a $LOLE$ of 3 hours/year.

4. The constant learning rate shows potential for reaching a solution space close to the optimum.

5. The convergence dynamics reveal two phases: a rapid transient phase, reached after approximately 100 iterations, characterized by a significant decrease in the score function, followed by a stable steady-state phase with minor fluctuations.

6. The power generation mix structure and the total annualized cost show stable convergence.

7. Both schemes provide equivalent solutions with marginal differences in cost and power generation mix structure.

8. Ensuring adequacy requires additional capacity investments of approximately 50 GW, alongside disinvestment in wind capacity by nearly -30 GW in 2050. This reflects the structural changes in the mix structure.

9. 3.5 Billion Euro additional annualized cost (nearly 3% of the total annualized cost in 2050) are needed to achieve the "best" obtained adequacy levels, but despite this huge effort, the mix is still not adequate.

For "Scenario B":

1. The additional reconciliation rule of the $CO_2$ emission constraint achieves similar emission trajectories in both models with acceptable differences, ensuring the validity of the uni-directional multi-scale model.

2. The long-term energy planning model's solution results in lower $CO_2$ emissions, approaching zero emissions by 2030.

3. Convergence dynamics for "Scenario B" exhibit higher oscillations compared to "Scenario A." Installed capacities evolve with significant gaps between iterations.

4. After 500 iterations, the algorithm cannot find a solution to bring all countries to $LOLE$ security levels within $[2.5, 3]$ hours/year.

5. The final solution includes countries unable to achieve $LOLE \leq 3 hours/year$, with the maximum $LOLE$ reaching 8 hours/year.

6. 30 Billion Euro additional annualized cost (nearly 3% of the total annualized cost in 2050) are needed to achieve the "best" obtained adequacy levels, but despite this huge effort, the mix is still not adequate.

In summary, the proposed multi-scale model, supported by the stochastic approximation algorithm, highlights the value of combining long-term energy planning with operational power systems to develop power generation mixes that meet adequacy requirements. This coupling approach enhances confidence in power generation mix outcomes derived from long-term planning models.

In the following paragraph we aim to discuss the results, some choices in the modeling and how it can affect the results.

**Discussion on the multi-scale model** The multi-scale model operates under a set of assumptions that can exert a significant impact on the outcomes. At this level, we can discern two primary facets: the bridging scale algorithm and the sensitivity analysis pertaining to specific input data. Concerning the bridging scale algorithms, a critical aspect revolves around the manner in which aggregation is executed. In our particular case, the mean statistic was chosen as the aggregation operator, applicable to metrics like capacity factors. Various methodologies have been proposed in the literature to derive values for each time slice. For instance, the process of selecting representative slices necessitates a delicate balance, with the objective of effectively capturing the load duration curve while also acknowledging potential correlations between load and VRE output, as discussed by de Sisternes and Webster [243].

On the input data front, the choice of the Monte Carlo year serving as input for the TIMES model holds paramount importance. The data employed in this case study encompass 1 load time series, 11 capacity factor time series, and 3 hydro generation time series. We opted for scenario number 1 for both VRE capacity factors and hydro generation, and this

selection was made arbitrarily, in contrast to the median scenario used for the case of France. This arbitrary selection was necessitated by our aim to develop a bi-directional strategy that remains independent of the choice of the Monte Carlo Year. However, it's crucial to note that the results obtained at the planning stage, particularly the power generation mix and power generation adequacy levels, are inevitably influenced by the chosen scenario. Feeding the model with a Monte Carlo Year characterized by lower capacity factors and a reduced hydro generation profile will lead to more shortages compared to a configuration employing a Monte Carlo Year with higher capacity factors and a more abundant hydro generation profile. Consequently, conducting a sensitivity analysis across various Monte Carlo Years to assess the impact on power generation, generation adequacy, and the performance of the stochastic approximation algorithm can provide valuable additional insights into our comprehension of the functioning of the multi-scale model.

Another significant aspect to consider is related to the modeling of the thermal power generation fleet. In our particular application, we didn't factor in the technical constraints that are associated with thermal power plants. It is of paramount importance to integrate these technical constraints of power plants into the modeling framework. Additionally, when evaluating power generation adequacy requirements, it's crucial to account for both unforeseen and planned unavailabilities of power plants.

**Why are we searching solutions with a $LOLE$ near to the target value?** An important question arises concerning why we seek solutions within the interval $[2.5, 3]$ hours/year for the $LOLE$ metric. This can be explained by three interconnected arguments: doctrinal, numerical, and economic.

- **Doctrinal Argument**: The power generation expansion problem we are addressing follows the paradigm of social welfare. It corresponds to an integrated criterion that takes into account the interests of all stakeholders. A society that accepts a $LOLE$ level of $\zeta = 3$ hours/year expresses its willingness to tolerate occasional electricity supply interruptions at that reliability level.

- **Numerical Argument**: Relaxing the $\zeta = 3$ level by 0.5 hours/year is motivated by the goal of finding a solution in which all initially inadequate countries achieve a $LOLE$ of 3 hours/year. From a numerical perspective, a solution is considered of good quality if the $LOLE$ criterion falls within the interval $[2.5, 3]$. Notably, the solution is only relaxed in the lower bound, as the upper bound is determined by legal regulations.

- **Economic Argument**: We evaluate the difference between a plan that considers a $LOLE$ of 0 hours/year and the solution we obtained using the iterative stochastic approximation algorithm. The solution that results in a $LOLE$ of zero is the initial solution strengthened with adequacy constraints, where $\theta_{r,t} = 0$ (considering the hours with higher shortage power). We find that its total system cost is higher. The figure 6.44 below illustrates the annualized cost for a solution with zero $LOLE$ level. It can be seen form the Figure that the annualized cost is five times greater than that of

the final solution obtained. In terms of installed capacities, we observe that a power generation mix with no zero adequacy risk requires additional investments amounting to nearly twice the needs of the obtained solution. Consequently, a solution close to 3 hours/year is more cost-effective than a solution with 0 hours/year.

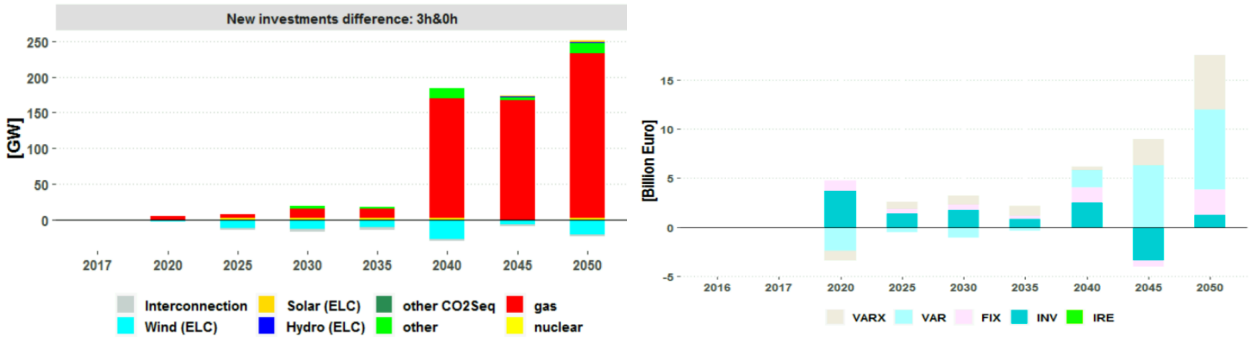


(a) The difference in newly installed capacities between a solution with a zero $LOLE$ level for all countries and the solution obtained through the SA algorithm.

(b) The difference between the initial (inadequate) and final solution with a zero $LOLE$ level in terms of annualized cost.

Figure 6.44: The difference between a solution with a zero $LOLE$ level with the solution obtained using the SA algorithm. (a) new installed capacities difference (b) annualized cost difference

**Discussion on the stochastic approximation algorithm principle and design:** Stochastic approximation schemes, widely used in diverse fields such as signal processing, optimization, machine learning, and economics/game theory [11], have gained popularity for several reasons.

- **Efficient Memory Usage:** Firstly, these algorithms demonstrate efficient memory utilization due to their Markovian updates. They rely solely on the current value and the observation at that moment, resulting in minimal memory requirements during implementation. In our application, the only data needed for the updates were the previous positions for the control variable $\theta_{r,t}$ and its related $LOLE$ value. However, for the analysis of the mix and other aspects, the outcomes of the planning model were stored.

- **Robustness to Noise:** Secondly, stochastic approximation algorithms exhibit robustness in handling noise, making them well-suited for "on-line" optimization tasks where system output may contain noise. The convergence analysis of these schemes

[11] In the prototypical setup of online learning in games, players make decisions in stages, selecting actions. They receive rewards determined by their chosen actions and their unique payoff functions, which are initially unknown. Using these payoffs and any observed information, players adjust their actions, and the process continues.

involves studying a deterministic Ordinary Differential Equation (ODE), simplifying the analysis and making it insensitive to noise statistics. In our case, the noise in the $LOLE$ function is attributed to the fact that we used only 11 Monte Carlo Years for its assessment. However, as we have seen previously, an accurate estimation of the LOLE metric requires 400-1000 Monte Carlo Years. Our assumption is that the 11 Monte Carlo Years we used provide a reasonable estimation of the $LOLE$ metric.

- **Suitability for Iterative Updates:** Additionally, SA schemes are highly suitable for iterative updates. Their Markovian nature lends itself well to modeling collective learning scenarios, where a group of agents iteratively interact and adjust their behavior based on recent observations. This characteristic facilitates effective modeling of collective learning phenomena. In the case of an interconnected system, the multi-functional version of the algorithm used in our work permits finding a solution where, for each period and each area, it learns from its own power generation adequacy (and, therefore, from other countries as the system is interconnected) to bring its power generation mix to adequate operation.

Overall, the combination of low memory requirements, noise robustness, and iterative update capabilities makes SA schemes suitable for addressing the problem of finding a multi-period multi-area power generation mix respecting power generation adequacy requirements.

The evaluation of the SA algorithm for the $LOLE$ problem could be carried out using five useful criteria.

- **Numerical Stability**: This criterion provides a qualitative evaluation of the algorithm's effectiveness when implemented on a computer. In all four simulations conducted, no instances of numerical instabilities were encountered. The only numerical instability observed was the occasional occurrence of a system anomaly within the R programming language, which supports the multi-scale model. This anomaly did not lead to any system shutdowns. Nevertheless, Scenario B encountered this situation on four occasions, potentially resulting in increased computational time, particularly when the simulations are not continuously monitored by the modeler.

- **Robustness**: Another qualitative measure, robustness, assesses the algorithm's sensitivity to initial parameter values (such as initial positions, denoted as $\theta_0$, and learning rates, denoted as $\alpha_n$). Modelers often employ heuristics to compute starting positions to expedite parameter tuning. In our application, the sensitivity of the initial $\theta$ positions was not assessed. It would be valuable to assess the sensitivity of this parameter on the outcomes of the model.

- **Convergence**: Convergence of the SA algorithms refers to asymptotic convergence within a probability measure. While it may not directly reflect finite-time performance, an algorithm guaranteeing asymptotic convergence is more favorable than one that doesn't. We were unable to verify the hypothesis of the convergence of the multi-dimensional version of the SA Theorem when applied to our problem. The only stop-

ping criteria for the algorithm is the number of iterations, which is set to 500 in all runs.

- **Computational Time Efficiency**: It is as a trade-off function linking solution quality to the time required to obtain it. Smaller values indicate superior computational efficiency. For the two schemes applied we show that.

- **Solution Quality**: This criterion quantitatively measures the algorithm's performance, with specific metrics to be defined as applicable. In our case, the solution quality can be quantified as the gap between the final solution score and zero. Generally, Scenario A has a solution with better quality than Scenario B. Also, for both scenarios, the configuration with a constant learning rate has better solution quality than the decreasing learning rate.

These measures are also important a priori to the design of numerically stable, robust, and computationally efficient algorithms.

## 6.5 Conclusion

In this chapter, we applied the developed multi-scale framework to the European power system, utilizing the eTIMES-EU long-term power system planning model developed by Gildas Sigguini. After introducing the fundamental assumptions underpinning this model's development, we elucidated the simulation strategy. This strategy encompasses the modeling of two primary long-term scenarios, namely "Scenario A" and "Scenario B." "Scenario A" portrays a scenario characterized by a substantial share of VRE installed capacities, alongside a carbon tax of 35 Euro/tCO2. In contrast, "Scenario B" retains the core constraints of "Scenario A" but incorporates a carbon tax that escalates to 750 Euro/tCO2 by 2050, coupled with a carbon neutrality constraint for the same year. Within the SA algorithm, two main schemes were employed: one featuring a constant learning rate and another with a decreasing learning rate. This simulation strategy resulted in four primary simulation runs, each comprising 500 iterations. The analytical approach for the results encompassed:

- Examination of unidirectional outcomes through comparisons of both models at various measurement points. Three principal measurement points were scrutinized: technical, represented by dispatch outcomes; economic, as reflected in marginal electricity prices; and environmental, assessed by $CO_2$ emissions.

- Adequacy assessment of the resulting power generation mix trajectories for each area over the planning time-frame.

- In instances where power generation adequacy requirements failed to meet $LOLE$ (Loss of Load Expectation) limit levels, the bi-directional aspect of the multi-scale model, supported by the stochastic approximation algorithm, was triggered.

- Evaluation of the performance of the SA algorithm, gauged by adequacy scores by period and trajectory. Additionally, a dynamical system analysis based on phase diagrams was conducted.

- Lastly, a detailed analysis and comparison were carried out between the final solution obtained by the multi-scale model and the initial solution.

The findings of the multi-scale model applied to the European power system model can be summarized at two distinct levels: the uni-directional part and the bi-directional part. For **the uni-directional** component, results shows that the multi-scale model performed well in terms of the disparity in dispatch outcomes between both models at the European level. Specifically, for "Scenario A," a difference of 4% concerning the total electricity demand was observed at the European level. However, these disparities were more pronounced when examined at the country level. A closer analysis of these variances on a technology-by-technology basis revealed that the differences between the models were substantial and, in certain countries, reached elevated levels. Regarding the economic measurement point, the discrepancies in marginal electricity prices between the two models indicated that TIMES struggled to capture the price dynamics throughout the year. In terms of the environmental measurement point, the differences in emissions at the European level did not exceed 15%, primarily stemming from disparities in dispatch between the two models. These findings held true for both "Scenario A" and "Scenario B."

For the power generation adequacy assessments, it was shown that for both scenarios, the power generation adequacy levels are not compliant with a $LOLE$ limit of 3 hours/year and this for a great number of countries. The distribution of shortage hours shows that the power generation mix decided by TIMES for specific countries is distributed at the entire year and not only the critical seasons such as winter.

**At the bi-directional** stage, the performance of the stochastic approximation algorithm to both models reveals common features between scenarios and distinct one. The common features can be summarized as: All the four runs reveals that the algorithm shows two main phases when iteration begin: a transient phase and a steady-state phase. The transient phase can be reached after 100 iterations, and then the steady-state phase begin. The constant learning rate performs well compared to the decreasing learning rate, as the constant learning rate can reach rapidly areas near to the optimum solution. The final adequate solution obtained need additional investments. Approximately, 1% of additional annualized cost is needed for "Scenario A", while 3% are needed for "Scenario B". The differences in the performance between scenarios can be summarized as: The score evolution for Scenario B shows more volatility than "Scenario A". The stabilization of the score metric for "Scenario B" is harder than "Scenario A". For "Scenario B" it is hard to find a solution near to the optimum.

# Chapter 7

# Conclusion

## 7.1 Summary and PhD contribution

This PhD work was initiated by a challenging question posed by the French Transmission System Operator (TSO) concerning the suitability of long-term energy planning models in addressing power generation adequacy requirements. It merges the modeling capabilities of RTE, focusing on power system operation via ANTARES, with the modeling expertise of Mines Paris in prospective planning using the TIMES framework. From a modeling perspective, the strategy was to adopt a multi-model approach that reconciles both methodologies, rather than embarking on the development of entirely new model from scratch. This approach has been previously utilized within the energy system modeling community, yielding promising results. The primary and exclusive objective of developing this multi-model approach is to ensure that the power generation mix derived from TIMES aligns with the power generation adequacy requirements assessed by ANTARES. Our initial application adheres to this established trend in the research community and aimed to create a bi-directional linking approach tailored to the French power system in a standalone basis (no interconnection with neighboring countries). Initially, we focused on a single target year within the planning time frame, followed by an expansion to encompass all periods within the planning time frame. This application holds substantial methodological significance, shedding light on the intricacies of the multi-model approach and elucidating how both models can interact to achieve the specified objective. However, power generation adequacy assessments cannot be confined solely to only a single-area level, given the interconnected nature of the French power system. Hence, we mathematically formulated a multi-scale model to construct multi-area investment trajectories that respect power generation adequacy requirements. Subsequently, this model was applied to the European Interconnected power system, encompassing 29 countries.

In **Chapter 2**, the context of the evolving power system landscape is outlined, providing necessary definitions of various facets of electricity security of supply. The chapter also defines different stages of the technico-economic assessment of the power system transition, including generation expansion planning, transmission planning, dispatch planning, and technical studies. Emphasis is placed on the need for an integrated approach that combines

these stages to ensure the development of operationally feasible transition trajectories.

This sets the stage for **Chapter 3**, which focuses into the modeling aspects of the thesis. Here, various energy system models are introduced, and a classification based on the existing literature is provided. The chapter addresses four primary challenges faced by long-term energy system models: temporal and spatial scales, generation adequacy awareness, uncertainty, and societal considerations. The thesis focuses on resolving challenges related to temporal scale, generation adequacy awareness, and short-term uncertainties. The proposed solution involves a multi-model linking approach. The literature review in this chapter identifies gaps in the current body of knowledge, leading to the formulation of the thesis's specific research focus. The four identified gaps include the need for a comprehensive and well-defined multi-model linking framework with a bi-directional approach and a clearly defined convergence criterion (first gap). The second gap pertains to incorporating long-term generation adequacy requirements using a probabilistic approach in the planning process. The third gap is concerned with considering the overall temporal investment trajectory when assessing long-term generation adequacy. Lastly, the fourth gap involves examining long-term generation adequacy requirements beyond national borders, accounting for interconnections. The thesis's focus is elaborated based on these four identified gaps, and the following paragraph highlights the contributions of each research axis.

In **Chapter 4**, we developed a bi-directional soft-linking methodology based on the estimation of capacity credit coefficients in the peaking-reserve equation. The algorithm performed effectively for the target year 2030 when applied to a scenario featuring a 60% VRE uptake in 2050, with a 40% share in 2030. Two simulation runs were conducted to assess the power generation adequacy requirements based on the resulting power generation mix from TIMES. The first simulation used 200 Monte Carlo years, and the second one employed 1,000 Monte Carlo years to simulate the dispatch. The results revealed the following key findings:

- Dispatch results from both models exhibit significant differences, primarily attributed to the underestimation of VRE and load variability, resulting in an overestimation of the residual load duration curve observed by TIMES.
- In both simulation sets, the power generation mix derived from TIMES for 2030 failed to meet the power generation adequacy requirements significantly.
- The simulation set with 200 Monte Carlo Years required 2 iterations to ensure compliance with the power generation adequacy requirements for 2030, while the simulation set with 1,000 Monte Carlo Years needed 7 iterations to achieve adequacy.
- To attain adequacy, an additional 28% of investments (in the total system cost of TIMES) were necessary.

The methodology developed to incorporate the entire trajectory in generation adequacy using the Rolling Horizon combined with the capacity-credit-based feedback proved its robustness when applied to different long-term scenarios and when parameters of the Rolling

Horizon changed. For a scenario with a 60% VRE uptake, a 15-year look-ahead period, and a 5-year overlap, the methodology was able to find an adequate solution over the entire trajectory. Various configurations for the 60% VRE uptake scenario yielded suitable solutions. Sensitivity analysis, particularly concerning the look-ahead period, revealed different investment dynamics across configurations, with 5-year and 10-year look-ahead periods showing plateaus lasting 10 and 15 years, respectively, with no investments made. Economically, disclosing data for the next 15 years was found to be equivalent to perfect foresight for the total actualized cost. Transitioning from a 60% VRE scenario to an 80% VRE scenario in 2050 revealed distinct phenomena in the Residual Load Duration Curve including modified dispatch profiles, reduced capacity credit for renewables, and an increase in the number of negative residual load hours. In a scenario with 100% VRE uptake, a substantial residual fossil thermal power fleet exists, allowing the power generation mix to remain adequate, resulting in a $LOLE$ of 1 hour/year. However, when this fleet is excluded from operation, the $LOLE$ increases to 1,000 hours/year. Consequently, the scenario with 100% VRE uptake necessitates additional constraint reconciliation between the long-term energy planning model and the operational power system model.

However, after considering Thomas Heggarty's discussion on our capacity credit estimation and a report that scrutinized the methodologies used for capacity credit parameter estimation, it became evident that the methodology was not suitable for application to a multi-area interconnected power system. In light of this limitation, the forthcoming chapter seeks to mathematically formulate a multi-scale model capable of bridging the gap between long-term investment planning and the short-term requirements for a secure operation. The objective is to establish a framework that can identify investment trajectories determined by long-term energy planning models while complying to generation adequacy requirements assessed by an operational power system model.

In **Chapter 5**, the multi-scale model bridging the long-term scale with the short-term scale was developed. Firstly, after a brief introduction to multi-scale modeling and steps to build multi-scale models a separation scale map was created to illustrate the scales under study. Both constituent optimization models were then formulated in matrix form, allowing for the description of all bridging scale algorithms and ensuring data input consistency. A new adequacy proxy constraint was introduced into the TIMES model. This equation is generated based on the dispatch operated by ANTARES for each investment asset, allowing TIMES to include shortage hours identified by ANTARES in its optimization and reinforce its initial optimization problem. The multi-scale model developed is supported by the Stochastic Approximation algorithm, enabling the determination of roots for the equation $LOLE(\theta) = \zeta$, where $\zeta$ represents the adequacy level requirements target and $\theta$ denotes the control variable. The control variable consists of a sizing hour searched within the space of all hours. This sizing hour is sought within all the simulated hours of the Monte Carlo Years, with an order established in this space by sorting all hours of the year in a decreasing order of the new net load time-series.

In **Chapter 6**, the multi-scale model was applied to the European power system consisting of 28 interconnected countries. The long-term energy planning model utilized in this

application is eTIMES-EU. Two long-term scenarios were designed: Sceanrio A and Scenario B. Scenario A depicts a future with high share of VRE, while Scenario B depicts the same future of Scenario A in addition to a constraint on $CO2$ emissions representing a neutrality in 2050. The validation of **the uni-directional model** at various measuring points shows that both models yield different dispatch decisions, but the disparity between them is not substantial. For instance, the difference in the total dispatch energy reaches 200 TWh which represent nearly 4% of the total electricity demand. For the environmental measuring point, the $CO_2$ emissions between both models have similar trajectories with a maximum difference of 15%. For the economical measuring point, the price dynamics seen by the operational model are not fully captured by TIMES model. Those differences are inherent to the modeling hypothesis and formulation of both models, and the validity of the uni-directional is proved [1].

The power generation adequacy assessment reveals that, for both scenarios, the power generation mix determined by TIMES does not meet the adequacy requirements from 2030 to 2050, impacting numerous countries. To address this issue, we employed two schemes for the SA algorithm to find power generation mixes that respect the adequacy requirements: one with a constant learning rate and the other with a decreasing learning rate. In each simulation set, we conducted 500 iterations. The research enabled to come to the following results:

1. Both schemes display a deceasing score curve over the 500 iterations that shows a two-phase pattern: **a transient phase** and a **steady-state phase**. The transient phase significantly reduces the score within approximately 100 iterations, while the steady-state phase yields minimal score reduction.

2. The score evolution for "Scenario A" features a stable steady-state phase, facilitating the stabilization of the $LOLE$. Conversely, the steady-state phase of Scenario B shows multiple oscillations, failing to stabilize the $LOLE$ within the $[2.5, 3]$ interval.

3. Explaining the oscillations in Scenario B is challenging, but we propose at least two plausible explanations. It may be impossible to find a solution where all European countries maintain a $LOLE$ of 3 hours per year in a scenario with zero emissions by 2050. Alternatively, the new Residual Load Duration Curve ($nRLDC$) of Scenario B may show more variability (due to the high uptake of VRE) than that of "Scenario A." Our analysis, which relies on only 11 Monte Carlo years, may not allow us to pinpoint the specific hour triggering the desired adequacy level.

4. In both scenarios, solutions with a constant learning rate tend to converge closer to the optimal solution compared to those with a decreasing learning rate.

5. To achieve the desired adequacy level, the long-term energy planning model adjust its power generation mix by investing in new dispatchable generation; principally natural

[1] The aim of the uni-directional linking is not to achieve perfect alignment of the dispatch outcomes between both models with zero difference, but rather to represent a similar operation of the power system in an acceptable manner.

gas for Scenario A and non-fossil based thermal for Scenario B. This new investments is accompanied by a dis-investment on wind power.

6. From an economical point of view, Scenario A need an additional annualized cost of 3 Billion Euro to achieve the best adequate solution, while Scenario B need an additional annualized cost of 27 Billion Euro in 2050.

## 7.2 Further work

In the field of multi-model and multi-scale modeling for power system planning and operation, this thesis has uncovered critical aspects into the interaction between long-term energy planning models (TIMES) and operational power system models (ANTARES). However, numerous avenues for further exploration emerge. In the following paragraph we propose several perspectives for future work.

**At the long-term planning model level** At the long-term planning model several improvements can be added:

- **Multi-sectorial Modeling as a "One System View"**: Future investment planning for the power system requires a holistic, multi-sectorial approach that takes into account not only the electricity sector but also considers natural gas, transportation, heating systems, and hydrogen. Developing multi-energy long-term planning models will allow for a comprehensive analysis of interactions and potential synergies between these different sectors.

- **Stochastic Optimization to Incorporate Uncertainties:** Given the substantial uncertainties associated with long-term factors such as fossil fuel prices, technological advancements, and policy frameworks, a promising avenue for future research involves the integration of these uncertainties into the analysis to formulate robust policy recommendations. The models used in this thesis employed the deterministic version of the TIMES model, assuming known and deterministic long-term factors. However, TIMES also offers a stochastic version that allows for the inclusion of both long-term and short-term uncertainties in the optimization problem. Long-term uncertainties may encompass demand projections, mitigation levels, and cost evolution, while short-term uncertainties can pertain to operational parameters like renewable capacity factors and load variability. Although ANTARES, representing the operational power system, incorporates some short-term uncertainties, extending the stochastic approach to TIMES could prove beneficial. A notable example is the work by Seljom, which developed a stochastic TIMES model that accounts for the intermittent nature of wind power and stochastic modeling of future electricity prices in countries with transmission capacity to Denmark [244].

- **Activating the dispatching and unit-commitment features:** The modeling of the operational characteristics of thermal power plants is a critical aspect of power system operation. This extension within the TIMES framework enables the integration of energy policy objectives, such as reducing CO2 emissions and increasing the use of renewable energy, while addressing daily unit-commitment and dispatch. While the existing literature extensively covers the standard MIP unit commitment problem, this particular formulation was found to be computationally challenging within the TIMES modeling framework. As a result, several alternative formulations were developed, leading to the implementation of three options:

  - Basic Unit-Commitment: This approach employs a linearized formulation for dispatching and is most effective when each technology can represent multiple units. While it may sacrifice some accuracy in modeling short-term operational constraints, it offers the advantage of solving a Linear Programming problem, resulting in the least impact on the model's size and solution times. This option encompasses the following features:

    (a) Start-up and shut-down capacities
    (b) Start-up and shut-down costs per unit of capacity started
    (c) Minimum stable operation level
    (d) Ramping rates and ramping costs during the dispatching phase per unit of capacity started
    (e) Minimum online and offline durations
    (f) Partial load efficiency losses during the dispatching phase.
    (g) Limits on the number of start-up cycles within each full process time slice.

  - Advanced Unit-Commitment: In addition to the basic formulation, this advanced option provides the flexibility to incorporate different start-up types based on the non-operational time following the shutdown of a power plant. It also allows for the identification of individual power plant units within the TIMES optimization problem.

  - Discrete Unit-Commitment: This option encompasses all the elements present in the advanced unit commitment approach. Furthermore, it introduces the capability to model individual process vintages, which can either consist of a single unit for each process vintage or incorporate multiple "virtual units" for each vintage.

These alternative formulations offer enhanced flexibility and computational efficiency in addressing the operational characteristics of thermal power plants within the TIMES framework. For more details in the modeling of this three options and their related cost/benefit in terms of the accuracy in the modeling and the computational time please refer to the report [245].

**At the operational power system model level**

- **Multi-sectorial Modeling as a "One System View"**: As for the long-term energy planning model, modeling the multi-energy system within ANTARES is possible. Transitioning from the exclusive modeling of the power system within ANTARES to a more comprehensive multi-energy system determined by TIMES can offer valuable contributions.

- **Increasing the number of Monte Carlo years:** In the specific context of modeling the French power system, the use of 1,000 Monte Carlo Years has proven to be sufficient for conducting a comprehensive power generation adequacy assessment. However, when extending this approach to model the European power system, it becomes evident that utilizing only 11 Monte Carlo years comes with certain limitations. There are two primary concerns:

    1. Accuracy of $LOLE$ Estimation: To accurately estimate the LOLE for the European power system, a considerably larger number of Monte Carlo years, typically ranging between 400 and 1,000, is required. This is due to the higher complexity and diversity of the European power system, which demands a more extensive set of scenarios to robustly assess generation adequacy.
    2. Resolution Challenges with $nRLDC$: Another issue arising from employing only 11 Monte Carlo years in the European context pertains to the resolution of the new Residual Load Duration Curve (nRLDC). The algorithm for stochastic approximation, when triggered, may encounter difficulties in finding the roots of the $LOLE$, particularly when a limited number of scenarios is used. To mitigate this, it is essential to increase the number of Monte Carlo years to ensure that different operational situations are presented. Analyzing the distribution of the variances between two successive hours with the $nRLDC$ for both scenarios can unveil certain characteristics of both scenarios.

**At the multi-scale model level:**

- **Bridging scale algorithms impact:** The development of the multi-scale model is based on a set of assumptions. Evaluating the sensitivity of those bridging scale algorithms to this assumption can bring important insights. Among others, the sensitivity of the bridging scale algorithm to the choice of the statistic allowing to pass from time-slices to hours and vice-versa and the choice of the Monte Carlo Year for input data consistency. Also, adding additional measuring points permitting to validate the uni-directional part of the multi-scale model can be beneficial.

- **The mathematical properties of the $LOLE$ stochastic root-finding problem:** The application of the stochastic approximation algorithm to the $LOLE$ problem was conducted without formally verifying the assumptions for convergence. Two key factors contributed to this approach. Firstly, our limited time-frame was primarily focused on

testing our methodology within practical constraints. Secondly, the level of mathematical rigor required for theoretical proof exceeded our current expertise. It's worth noting that the multi-functional theorem, which we could potentially employ for convergence proof, primarily addresses infinite convergence, whereas our goal was to assess convergence within a finite timeframe. Exploring the mathematical proprieties of the application of the root-finding stochastic problem to our multi-scale model enabling the estimation of the $LOLE$ can bring valuable insights.

- **Design of the stochastic approximation algorithm:**

  The design of the stochastic approximation algorithm is a critical aspect of our research, and several important perspectives can be considered for its enhancement:

  - **Optimal Initial Position Heuristics:** Developing heuristics to identify optimal initial positions for $\theta_{r,t}$ can significantly expedite convergence to solutions. These heuristics aim to minimize the number of iterations required for convergence.
  - **Exploration of Learning Rates:** Testing different learning rates during the iterative process is essential. Two main classes of learning rates should be investigated. For constant learning rates, various constants can be evaluated. For decreasing learning rates, a range of values for $\alpha \in [0, 1]$ $\frac{C}{n^\alpha}$, can be explored to determine their impact on convergence. Also, in using different learning rate for each country can be important as the structure of the $nRLDC$ are not the same and the convergence dynamics are not the same.
  - **Averaging of Control Variables:** Averaging the control variable positions can improve convergence. Iterations can benefit from averaging the current $\theta$ positions based on previous positions, as represented by $\bar{\theta_n} = \frac{1}{n}\sum_{i=1:n}\theta_i$. Averaged SA algorithms have been shown to handle a broader range of noise sequences than standalone stochastic approximation algorithms.

**Towards a practical use for Prospective exercises: Who knows?** The overarching principle guiding this thesis is fundamentally methodological, and it has been consistently underscored that the "scenarios" were developed exclusively as case studies. It is imperative to make clear that no recommendations concerning the future trajectory of the power system are to be derived from this work. This choice is entirely warranted, given the complex nature of prospective exercises that extend beyond the capacity of a single PhD candidate to conduct. In France, the extensive endeavors undertaken by RTE in numerous prospective exercises serve as a testament to the meticulous process of envisioning potential futures for the power system. For example, the methodology employed in the *Futurs énergétiques 2050* report embodies an innovative and participative approach to consultation. Scenarios are crafted transparently, with all study parameters subjected to discussion, delineation, and extensive deliberation within various working groups. This comprehensive process involved a total of 40 meetings, during which experts from approximately a hundred different organizations, including energy sector firms, non-governmental organizations, associations, think tanks, regulatory authorities, government bodies, and more, actively participated.

For the technical modeling phase, I believe that the multi-scale framework developed can find valuable applications in prospective studies. Below, I outline two potential ways in which the multi-scale model can be utilized in prospective exercises.

- Generating multiple long-term scenarios for power system evolution and assessing their power generation adequacy. One approach involves utilizing the scenarios outlined in the *Futurs Energétiques 2050* study as inputs for the long-term energy planning model. Six distinct scenarios have been formulated, each featuring unique characteristics and dynamics that depict the evolution of the French power system by the year 2050 [246]. The narratives of each scenario are presented in Appendix A.2.

- Another valuable perspective is to examine various evolutions of the adequacy criterion, defining multiple reliability standards, and extracting both technical and economic insights. In our analysis, we exclusively employ the probabilistic metric of Loss of Load Expectation (LOLE) along with a uniform adequacy level of $\zeta = 3 hours/year$ for all European countries. Exploring alternative risk metrics, such as the Expected Energy Not Supplied (EENS), represents a promising avenue for further research. Additionally, investigating different adequacy thresholds beyond the standard 3 hours/year would provide valuable insights.

## 7.3 The thesis in two sentences

From the inception of this thesis, drawing inspiration from research in the field of human sciences, I have held a steadfast belief that the essence of a thesis goes beyond its technical contributions. The "true" significance lies in the ability to encapsulate the entirety of the work in one or two concise sentences. If I were to distill the essence of my thesis, it would be as follows: "In the context of power system planning for the transition, placing sole reliance on the outcomes of long-term energy planning models is insufficient to furnish feasible operational pathways. Leveraging the potential of our developed multi-scale model, using operational power system models is instrumental in constructing adequate long-term trajectories, thereby instilling confidence in the pathways, especially when they serve as a foundation for policy decisions."

# Appendix A

# Appendix

## A.1 eTIMES-EU model

| (Region,Year) | 2020 | 2025 | 2030 | 2035 | 2040 | 2045 | 2050 |
|---|---|---|---|---|---|---|---|
| AT | 0.65 | 5.00 | 5.00 | 5.00 | 5.00 | 5.00 | 5.00 |
| BE | 1.66 | 9.72 | 9.72 | 9.72 | 9.72 | 9.72 | 9.72 |
| BG | 0.05 | 8.59 | 8.59 | 8.59 | 8.59 | 8.59 | 8.59 |
| CH | 1.36 | 5.00 | 5.00 | 5.00 | 5.00 | 5.00 | 5.00 |
| CZ | 0.03 | 12.62 | 12.62 | 12.62 | 12.62 | 12.62 | 12.62 |
| DE | 14.37 | 81.61 | 81.61 | 81.61 | 81.61 | 81.61 | 81.61 |
| DK | 0.37 | 5.00 | 5.00 | 5.00 | 5.00 | 5.00 | 5.00 |
| EE | 0.02 | 5.00 | 5.00 | 5.00 | 5.00 | 5.00 | 5.00 |
| ES | 0.08 | 28.90 | 28.90 | 28.90 | 28.90 | 28.90 | 28.90 |
| FI | 0.16 | 5.00 | 5.00 | 5.00 | 5.00 | 5.00 | 5.00 |
| FR | 3.49 | 19.60 | 19.60 | 19.60 | 19.60 | 19.60 | 19.60 |
| GR | 0.18 | 10.43 | 10.43 | 10.43 | 10.43 | 10.43 | 10.43 |
| HR | 0.00 | 5.00 | 5.00 | 5.00 | 5.00 | 5.00 | 5.00 |
| HU | 1.28 | 5.00 | 5.00 | 5.00 | 5.00 | 5.00 | 5.00 |
| IE | 0.05 | 5.00 | 5.00 | 5.00 | 5.00 | 5.00 | 5.00 |
| IS | 0.00 | 5.00 | 5.00 | 5.00 | 5.00 | 5.00 | 5.00 |
| IT | 1.75 | 95.39 | 95.39 | 95.39 | 95.39 | 95.39 | 95.39 |
| LT | 0.04 | 5.00 | 5.00 | 5.00 | 5.00 | 5.00 | 5.00 |
| LU | 0.02 | 5.00 | 5.00 | 5.00 | 5.00 | 5.00 | 5.00 |
| LV | 0.00 | 5.00 | 5.00 | 5.00 | 5.00 | 5.00 | 5.00 |
| NL | 4.99 | 16.19 | 16.19 | 16.19 | 16.19 | 16.19 | 16.19 |
| NO | 0.09 | 5.00 | 5.00 | 5.00 | 5.00 | 5.00 | 5.00 |
| PL | 0.80 | 5.00 | 5.00 | 5.00 | 5.00 | 5.00 | 5.00 |
| PT | 0.76 | 5.00 | 5.00 | 5.00 | 5.00 | 5.00 | 5.00 |
| RO | 0.01 | 7.20 | 7.20 | 7.20 | 7.20 | 7.20 | 7.20 |
| SE | 0.48 | 5.00 | 5.00 | 5.00 | 5.00 | 5.00 | 5.00 |
| SI | 0.04 | 5.00 | 5.00 | 5.00 | 5.00 | 5.00 | 5.00 |
| SK | 0.01 | 5.00 | 5.00 | 5.00 | 5.00 | 5.00 | 5.00 |
| UK | 1.33 | 40.73 | 40.73 | 40.73 | 40.73 | 40.73 | 40.73 |

Table A.1: Maximum solar capacity installed (GW) per region in the eTIMES-EU model

| (Region,Year) | 2020 | 2025 | 2030 | 2035 | 2040 | 2045 | 2050 |
|---|---|---|---|---|---|---|---|
| AT | 0.88 | 5.00 | 5.00 | 5.00 | 5.00 | 5.00 | 5.00 |
| BE | 1.03 | 5.00 | 5.00 | 5.00 | 5.00 | 5.00 | 5.00 |
| BG | 0.10 | 5.00 | 5.00 | 5.00 | 5.00 | 5.00 | 5.00 |
| CH | 0.06 | 5.00 | 5.00 | 5.00 | 5.00 | 5.00 | 5.00 |
| CZ | 0.09 | 5.00 | 5.00 | 5.00 | 5.00 | 5.00 | 5.00 |
| DE | 8.70 | 48.71 | 48.71 | 48.71 | 48.71 | 48.71 | 48.71 |
| DK | 0.62 | 5.00 | 5.00 | 5.00 | 5.00 | 5.00 | 5.00 |
| EE | 0.03 | 5.00 | 5.00 | 5.00 | 5.00 | 5.00 | 5.00 |
| ES | 6.78 | 30.98 | 30.98 | 30.98 | 30.98 | 30.98 | 30.98 |
| FI | 0.61 | 5.60 | 5.60 | 5.60 | 5.60 | 5.60 | 5.60 |
| FR | 7.25 | 19.31 | 19.31 | 19.31 | 19.31 | 19.31 | 19.31 |
| GR | 2.34 | 5.00 | 5.00 | 5.00 | 5.00 | 5.00 | 5.00 |
| HR | 0.17 | 5.00 | 5.00 | 5.00 | 5.00 | 5.00 | 5.00 |
| HU | 0.10 | 5.00 | 5.00 | 5.00 | 5.00 | 5.00 | 5.00 |
| IE | 1.64 | 5.32 | 5.32 | 5.32 | 5.32 | 5.32 | 5.32 |
| IS | 0.00 | 5.00 | 5.00 | 5.00 | 5.00 | 5.00 | 5.00 |
| IT | 2.27 | 13.54 | 13.54 | 13.54 | 13.54 | 13.54 | 13.54 |
| LT | 0.05 | 5.00 | 5.00 | 5.00 | 5.00 | 5.00 | 5.00 |
| LU | 0.04 | 5.00 | 5.00 | 5.00 | 5.00 | 5.00 | 5.00 |
| LV | 0.04 | 5.00 | 5.00 | 5.00 | 5.00 | 5.00 | 5.00 |
| NL | 0.66 | 5.00 | 5.00 | 5.00 | 5.00 | 5.00 | 5.00 |
| NO | 3.15 | 5.03 | 5.03 | 5.03 | 5.03 | 5.03 | 5.03 |
| PL | 0.17 | 10.50 | 10.50 | 10.50 | 10.50 | 10.50 | 10.50 |
| PT | 0.32 | 6.56 | 6.56 | 6.56 | 6.56 | 6.56 | 6.56 |
| RO | 0.50 | 9.51 | 9.51 | 9.51 | 9.51 | 9.51 | 9.51 |
| SE | 5.76 | 8.93 | 8.93 | 8.93 | 8.93 | 8.93 | 8.93 |
| SI | 0.08 | 5.00 | 5.00 | 5.00 | 5.00 | 5.00 | 5.00 |
| SK | 0.08 | 5.00 | 5.00 | 5.00 | 5.00 | 5.00 | 5.00 |
| UK | 3.05 | 17.65 | 17.65 | 17.65 | 17.65 | 17.65 | 17.65 |

Table A.2: Maximum onshore wind capacity installed (GW) per region in the eTIMES-EU model

| (Region,Year) | 2020 | 2025 | 2030 | 2035 | 2040 | 2045 | 2050 |
|---|---|---|---|---|---|---|---|
| AT | 0.00 | 0.00 | 0.00 | 0.00 | 0.00 | 0.00 | 0.00 |
| BE | 1.70 | 3.27 | 3.27 | 3.27 | 3.27 | 3.27 | 3.27 |
| BG | 0.00 | 0.00 | 0.00 | 0.00 | 0.00 | 0.00 | 0.00 |
| CH | 0.00 | 0.00 | 0.00 | 0.00 | 0.00 | 0.00 | 0.00 |
| CZ | 0.00 | 0.00 | 0.00 | 0.00 | 0.00 | 0.00 | 0.00 |
| DE | 5.20 | 22.89 | 22.89 | 22.89 | 22.89 | 22.89 | 22.89 |
| DK | 1.09 | 4.37 | 4.37 | 4.37 | 4.37 | 4.37 | 4.37 |
| EE | 0.00 | 1.00 | 1.00 | 1.00 | 1.00 | 1.00 | 1.00 |
| ES | 0.01 | 1.00 | 1.00 | 1.00 | 1.00 | 1.00 | 1.00 |
| FI | 0.00 | 1.00 | 1.00 | 1.00 | 1.00 | 1.00 | 1.00 |
| FR | 0.01 | 1.00 | 1.00 | 1.00 | 1.00 | 1.00 | 1.00 |
| GR | 0.00 | 0.00 | 0.00 | 0.00 | 0.00 | 0.00 | 0.00 |
| HR | 0.00 | 1.00 | 1.00 | 1.00 | 1.00 | 1.00 | 1.00 |
| HU | 0.00 | 0.00 | 0.00 | 0.00 | 0.00 | 0.00 | 0.00 |
| IE | 0.00 | 1.00 | 1.00 | 1.00 | 1.00 | 1.00 | 1.00 |
| IS | 0.00 | 0.00 | 0.00 | 0.00 | 0.00 | 0.00 | 0.00 |
| IT | 0.00 | 1.00 | 1.00 | 1.00 | 1.00 | 1.00 | 1.00 |
| LT | 0.00 | 1.00 | 1.00 | 1.00 | 1.00 | 1.00 | 1.00 |
| LU | 0.00 | 0.00 | 0.00 | 0.00 | 0.00 | 0.00 | 0.00 |
| LV | 0.00 | 1.00 | 1.00 | 1.00 | 1.00 | 1.00 | 1.00 |
| NL | 0.00 | 6.00 | 6.00 | 6.00 | 6.00 | 6.00 | 6.00 |
| NO | 0.00 | 1.00 | 1.00 | 1.00 | 1.00 | 1.00 | 1.00 |
| PL | 0.00 | 1.00 | 1.00 | 1.00 | 1.00 | 1.00 | 1.00 |
| PT | 0.02 | 1.00 | 1.00 | 1.00 | 1.00 | 1.00 | 1.00 |
| RO | 0.00 | 1.00 | 1.00 | 1.00 | 1.00 | 1.00 | 1.00 |
| SE | 0.01 | 1.09 | 1.09 | 1.09 | 1.09 | 1.09 | 1.09 |
| SI | 0.00 | 0.00 | 0.00 | 0.00 | 0.00 | 0.00 | 0.00 |
| SK | 0.00 | 0.00 | 0.00 | 0.00 | 0.00 | 0.00 | 0.00 |
| UK | 7.69 | 16.95 | 16.95 | 16.95 | 16.95 | 16.95 | 16.95 |

Table A.3: Maximum wind offshore capacity installed (GW) per region in the eTIMES-EU model

| (Region,Year) | 2020 | 2025 | 2030 | 2035 | 2040 | 2045 | 2050 |
|---|---|---|---|---|---|---|---|
| AT | 2.94 | 9.8 | 9.8 | 9.8 | 9.8 | 9.8 | 9.8 |
| BE | 1.32 | 4.4 | 4.4 | 4.4 | 4.4 | 4.4 | 4.4 |
| BG | 0.84 | 2.8 | 2.8 | 2.8 | 2.8 | 2.8 | 2.8 |
| CH | 0.15 | 0.5 | 0.5 | 0.5 | 0.5 | 0.5 | 0.5 |
| CZ | 0.51 | 1.7 | 1.7 | 1.7 | 1.7 | 1.7 | 1.7 |
| DE | 4.38 | 14.6 | 14.6 | 14.6 | 14.6 | 14.6 | 14.6 |
| DK | 2.91 | 9.7 | 9.7 | 9.7 | 9.7 | 9.7 | 9.7 |
| EE | 0.57 | 1.9 | 1.9 | 1.9 | 1.9 | 1.9 | 1.9 |
| ES | 0.84 | 2.8 | 2.8 | 2.8 | 2.8 | 2.8 | 2.8 |
| FI | 1.32 | 4.4 | 4.4 | 4.4 | 4.4 | 4.4 | 4.4 |
| FR | 1.26 | 4.2 | 4.2 | 4.2 | 4.2 | 4.2 | 4.2 |
| GR | 0.09 | 0.3 | 0.3 | 0.3 | 0.3 | 0.3 | 0.3 |
| HR | 0.15 | 0.5 | 0.5 | 0.5 | 0.5 | 0.5 | 0.5 |
| HU | 1.32 | 4.4 | 4.4 | 4.4 | 4.4 | 4.4 | 4.4 |
| IE | 0.18 | 0.6 | 0.6 | 0.6 | 0.6 | 0.6 | 0.6 |
| IS | 0 | 0 | 0 | 0 | 0 | 0 | 0 |
| IT | 3.12 | 10.4 | 10.4 | 10.4 | 10.4 | 10.4 | 10.4 |
| LT | 0.12 | 0.4 | 0.4 | 0.4 | 0.4 | 0.4 | 0.4 |
| LU | 0.06 | 0.2 | 0.2 | 0.2 | 0.2 | 0.2 | 0.2 |
| LV | 0.21 | 0.7 | 0.7 | 0.7 | 0.7 | 0.7 | 0.7 |
| NL | 0.69 | 2.3 | 2.3 | 2.3 | 2.3 | 2.3 | 2.3 |
| NO | 0.36 | 1.2 | 1.2 | 1.2 | 1.2 | 1.2 | 1.2 |
| PL | 1.77 | 5.9 | 5.9 | 5.9 | 5.9 | 5.9 | 5.9 |
| PT | 0.87 | 2.9 | 2.9 | 2.9 | 2.9 | 2.9 | 2.9 |
| RO | 0.27 | 0.9 | 0.9 | 0.9 | 0.9 | 0.9 | 0.9 |
| SE | 5.28 | 17.6 | 17.6 | 17.6 | 17.6 | 17.6 | 17.6 |
| SI | 0.21 | 0.7 | 0.7 | 0.7 | 0.7 | 0.7 | 0.7 |
| SK | 0.39 | 1.3 | 1.3 | 1.3 | 1.3 | 1.3 | 1.3 |
| UK | 8.88 | 29.6 | 29.6 | 29.6 | 29.6 | 29.6 | 29.6 |

Table A.4: Maximum bioenergy capacity installed (GW) per period in the eTIMES-EU model

| (Region,Year) | 2017 | 2020 | 2025 | 2030 | 2035 | 2040 | 2045 | 2050 |
|---|---|---|---|---|---|---|---|---|
| AT | 0.0 | 0.0 | 0.0 | 0.0 | 0.0 | 0.0 | 0.0 | 0.0 |
| BE | 0.0 | 0.0 | 0.0 | 0.0 | 0.0 | 0.0 | 0.0 | 0.0 |
| BG | 0.0 | 0.0 | 0.0 | 1.0 | 2.0 | 0.0 | 0.0 | 0.0 |
| CH | 0.5 | 1.6 | 1.3 | 0.0 | 0.0 | 0.0 | 0.0 | 0.0 |
| CZ | 0.3 | 0.8 | 0.2 | 1.1 | 0.1 | 1.9 | 0.0 | 0.0 |
| DE | 0.0 | 0.0 | 0.0 | 0.0 | 0.0 | 0.0 | 0.0 | 0.0 |
| DK | 0.0 | 0.0 | 0.0 | 0.0 | 0.0 | 0.0 | 0.0 | 0.0 |
| EE | 0.0 | 0.0 | 0.0 | 0.0 | 0.0 | 0.0 | 0.0 | 0.0 |
| ES | 0.0 | 0.0 | 4.1 | 3.3 | 0.0 | 0.0 | 0.0 | 0.0 |
| FI | 0.4 | 1.0 | 1.4 | 0.0 | 0.0 | 0.0 | 0.0 | 0.0 |
| FR | 2.0 | 7.5 | 26.2 | 17.0 | 5.5 | 6.3 | 0.0 | 0.0 |
| GR | 0.0 | 0.0 | 0.0 | 0.0 | 0.0 | 0.0 | 0.0 | 0.0 |
| HR | 0.0 | 0.0 | 0.0 | 0.0 | 0.0 | 0.0 | 0.0 | 0.0 |
| HU | 0.0 | 0.1 | 0.0 | 0.0 | 0.0 | 0.0 | 0.0 | 0.0 |
| IE | 0.0 | 0.0 | 0.0 | 0.0 | 0.0 | 0.0 | 0.0 | 0.0 |
| IS | 0.0 | 0.0 | 0.0 | 0.0 | 0.0 | 0.0 | 0.0 | 0.0 |
| IT | 0.0 | 0.0 | 0.0 | 0.0 | 0.0 | 0.0 | 0.0 | 0.0 |
| LT | 0.0 | 0.0 | 0.0 | 0.0 | 0.0 | 0.0 | 0.0 | 0.0 |
| LU | 0.0 | 0.0 | 0.0 | 0.0 | 0.0 | 0.0 | 0.0 | 0.0 |
| LV | 0.0 | 0.0 | 0.0 | 0.0 | 0.0 | 0.0 | 0.0 | 0.0 |
| NL | 0.1 | 0.4 | 0.0 | 0.0 | 0.0 | 0.0 | 0.0 | 0.0 |
| NO | 0.0 | 0.0 | 0.0 | 0.0 | 0.0 | 0.0 | 0.0 | 0.0 |
| PL | 0.0 | 0.0 | 0.0 | 0.0 | 0.0 | 0.0 | 0.0 | 0.0 |
| PT | 0.0 | 0.0 | 0.0 | 0.0 | 0.0 | 0.0 | 0.0 | 0.0 |
| RO | 0.0 | 0.0 | 0.0 | 0.0 | 0.0 | 0.7 | 0.0 | 0.0 |
| SE | 1.1 | 3.4 | 5.3 | 0.0 | 0.0 | 0.0 | 0.0 | 0.0 |
| SI | 0.0 | 0.0 | 0.7 | 0.0 | 0.0 | 0.0 | 0.0 | 0.0 |
| SK | 0.0 | 0.2 | 0.8 | 0.0 | 0.0 | 0.0 | 0.0 | 0.0 |
| UK | 0.7 | 2.1 | 2.8 | 2.9 | 1.1 | 0.0 | 0.0 | 0.0 |

Table A.5: Maximum nuclear capacity extended (GW) per period in the eTIMES-EU model

| (Region,Year) | 2020 | 2025 | 2030 | 2035 | 2040 | 2045 | 2050 |
|---|---|---|---|---|---|---|---|
| AT | 0.00 | 0.00 | 0.00 | 0.00 | 0.00 | 0.00 | 0.00 |
| BE | 0.00 | 0.00 | 0.00 | 0.00 | 0.00 | 0.00 | 0.00 |
| BG | 0.00 | 0.00 | 0.00 | 0.00 | 0.00 | 1.00 | 1.00 |
| CH | 0.00 | 0.00 | 0.00 | 0.00 | 0.00 | 0.00 | 0.00 |
| CZ | 0.00 | 0.00 | 0.00 | 0.00 | 2.40 | 1.20 | 1.20 |
| DE | 0.00 | 0.00 | 0.00 | 0.00 | 0.00 | 0.00 | 0.00 |
| DK | 0.00 | 0.00 | 0.00 | 0.00 | 0.00 | 0.00 | 0.00 |
| EE | 0.00 | 0.00 | 0.30 | 0.00 | 0.00 | 0.00 | 0.00 |
| ES | 0.00 | 0.00 | 0.00 | 0.00 | 0.00 | 0.00 | 0.00 |
| FI | 1.60 | 0.00 | 1.20 | 0.00 | 0.00 | 0.00 | 0.00 |
| FR | 0.00 | 1.60 | 8.00 | 8.00 | 8.00 | 8.00 | 8.00 |
| GR | 0.00 | 0.00 | 0.00 | 0.00 | 0.00 | 0.00 | 0.00 |
| HR | 0.00 | 0.00 | 0.00 | 0.00 | 0.00 | 0.00 | 0.00 |
| HU | 0.00 | 0.00 | 2.40 | 0.00 | 0.00 | 0.00 | 0.00 |
| IE | 0.00 | 0.00 | 0.00 | 0.00 | 0.00 | 0.00 | 0.00 |
| IS | 0.00 | 0.00 | 0.00 | 0.00 | 0.00 | 0.00 | 0.00 |
| IT | 0.00 | 0.00 | 0.00 | 0.00 | 0.00 | 0.00 | 0.00 |
| LT | 0.00 | 0.00 | 0.00 | 0.00 | 0.00 | 0.00 | 0.00 |
| LU | 0.00 | 0.00 | 0.00 | 0.00 | 0.00 | 0.00 | 0.00 |
| LV | 0.00 | 0.00 | 0.00 | 0.00 | 0.00 | 0.00 | 0.00 |
| NL | 0.00 | 0.00 | 0.00 | 0.00 | 0.00 | 0.00 | 0.00 |
| NO | 0.00 | 0.00 | 0.00 | 0.00 | 0.00 | 0.00 | 0.00 |
| PL | 0.00 | 0.00 | 0.00 | 3.00 | 3.00 | 0.00 | 0.00 |
| PT | 0.00 | 0.00 | 0.00 | 0.00 | 0.00 | 0.00 | 0.00 |
| RO | 0.00 | 0.00 | 1.44 | 0.00 | 0.00 | 0.00 | 0.00 |
| SE | 0.00 | 0.00 | 0.00 | 0.00 | 0.00 | 0.00 | 0.00 |
| SI | 0.00 | 0.00 | 0.00 | 0.00 | 0.00 | 1.20 | 0.00 |
| SK | 0.47 | 0.47 | 0.00 | 0.00 | 0.00 | 0.00 | 0.00 |
| UK | 0.00 | 1.72 | 0.00 | 5.00 | 3.90 | 3.90 | 0.00 |

Table A.6: Maximum nuclear capacity extended (GW) per period in the eTIMES-EU model

| (Region,Year) | 2020 | 2025 | 2030 | 2035 | 2040 | 2045 | 2050 |
|---|---|---|---|---|---|---|---|
| AT | 0.31 | 0.31 | 0.31 | 0.31 | 0.31 | 0.31 | 0.31 |
| BE | 0.00 | 0.00 | 0.00 | 0.00 | 0.00 | 0.00 | 0.00 |
| BG | 0.30 | 0.30 | 0.30 | 0.30 | 0.30 | 0.30 | 0.30 |
| CH | 0.19 | 0.19 | 0.19 | 0.19 | 0.19 | 0.19 | 0.19 |
| CZ | 0.02 | 0.02 | 0.02 | 0.02 | 0.02 | 0.02 | 0.02 |
| DE | 0.02 | 0.02 | 0.02 | 0.02 | 0.02 | 0.02 | 0.02 |
| DK | 0.00 | 0.00 | 0.00 | 0.00 | 0.00 | 0.00 | 0.00 |
| EE | 0.00 | 0.00 | 0.00 | 0.00 | 0.00 | 0.00 | 0.00 |
| ES | 1.23 | 1.23 | 1.23 | 1.23 | 1.23 | 1.23 | 1.23 |
| FI | 0.06 | 0.06 | 0.06 | 0.06 | 0.06 | 0.06 | 0.06 |
| FR | 0.68 | 0.68 | 0.68 | 0.68 | 0.68 | 0.68 | 0.68 |
| GR | 0.52 | 0.52 | 0.52 | 0.52 | 0.52 | 0.52 | 0.52 |
| HR | 0.03 | 0.03 | 0.03 | 0.03 | 0.03 | 0.03 | 0.03 |
| HU | 0.00 | 0.00 | 0.00 | 0.00 | 0.00 | 0.00 | 0.00 |
| IE | 0.01 | 0.01 | 0.01 | 0.01 | 0.01 | 0.01 | 0.01 |
| IS | 0.30 | 0.30 | 0.30 | 0.30 | 0.30 | 0.30 | 0.30 |
| IT | 0.28 | 0.28 | 0.28 | 0.28 | 0.28 | 0.28 | 0.28 |
| LT | 0.01 | 0.01 | 0.01 | 0.01 | 0.01 | 0.01 | 0.01 |
| LU | 0.00 | 0.00 | 0.00 | 0.00 | 0.00 | 0.00 | 0.00 |
| LV | 0.02 | 0.02 | 0.02 | 0.02 | 0.02 | 0.02 | 0.02 |
| NL | 0.00 | 0.00 | 0.00 | 0.00 | 0.00 | 0.00 | 0.00 |
| NO | 1.07 | 1.07 | 1.07 | 1.07 | 1.07 | 1.07 | 1.07 |
| PL | 0.23 | 0.23 | 0.23 | 0.23 | 0.23 | 0.23 | 0.23 |
| PT | 0.55 | 0.55 | 0.55 | 0.55 | 0.55 | 0.55 | 0.55 |
| RO | 0.69 | 0.69 | 0.69 | 0.69 | 0.69 | 0.69 | 0.69 |
| SE | 1.15 | 1.15 | 1.15 | 1.15 | 1.15 | 1.15 | 1.15 |
| SI | 0.04 | 0.04 | 0.04 | 0.04 | 0.04 | 0.04 | 0.04 |
| SK | 0.06 | 0.06 | 0.06 | 0.06 | 0.06 | 0.06 | 0.06 |
| UK | 0.01 | 0.01 | 0.01 | 0.01 | 0.01 | 0.01 | 0.01 |

Table A.7: Maximum hydro capacity installed (GW) per period in the eTIMES-EU model

## A.2 Narratives of "Futures Énergétiques 2050"

1. **M0 or A 100% Renewable Electricity Mix by 2050:** This scenario is characterized by an accelerated phase-out of nuclear power compared to the trajectory defined in the Multi-Year Energy Program (PPE). Its objective is to achieve a power mix entirely based on renewable energies by 2050. The development rates for photovoltaic, wind, and marine energies are pushed to their maximum to reach this goal, surpassing the best European performances in this regard. This scenario also involves mobilizing a substantial flexibility portfolio and demands a more rapid mastery of decarbonized gas production compared to other scenarios.

2. **M1 or Distributed Renewable Energies across the Territory:** This scenario, which does not include the renewal of the nuclear fleet and foresees the complete cessation of nuclear production by 2060, is characterized by a significant development of renewable energies distributed across the national territory. This development heavily relies on the photovoltaic sector, with a strategy of widespread ground-based and rooftop solar panel installations, even in less sunny regions. It also emphasizes the growth of self-consumption for households, businesses, and small enterprises. Onshore wind power also experiences expansion. The growth of distributed energy production entails strong involvement from local stakeholders and local authorities. The power mix in this scenario is accompanied by the development of flexibility solutions such as storage and demand-side flexibility.

3. **M23 or Centralized Development of Renewable Energies around Large Facilities:** This scenario, which does not involve the renewal of the nuclear fleet and foresees the complete cessation of nuclear production by 2060, is characterized by a substantial development of all renewable energy sectors, driven by the installation of large production facilities. Its rationale is based on economic optimization (cost minimization), targeting technologies and areas with the best performance and economies of scale. This principle leads to significant development of large wind farms on both land and sea. The growth of the photovoltaic sector is also rapid, organized primarily around extensive "solar farms." The development of flexibility is substantial, almost equivalent to that in scenario M1.

4. **N1 or Revitalizing the Nuclear Sector – Low Industrial Trajectory:** Scenario N1 is characterized by the initiation of a program for the construction of new nuclear reactors of the EPR2 type. Focused on the commissioning of a pair of reactors every approximately five years, in line with the New Nuclear France (NNF) program, it aims to have eight reactors in operation by 2050. To compensate for the closure of existing nuclear reactors, it also relies on significant development of renewable energies, following the guidelines of the Multiannual Energy Plan (PPE) with a particular emphasis on offshore wind. As a result, a substantial level of flexibility is required to maintain the supply-demand balance, though it is lower compared to the scenarios labeled as M.

5. **N2 or A Bold Revival of the Nuclear Sector – High Industrial Trajectory**: Scenario N2 is structured around the rapid launch of a program for the construction of new EPR2-type nuclear reactors, following a schedule corresponding to the maximum capacity communicated to date by the nuclear industry (a pair of reactors every four years starting in 2035, followed by a progressive acceleration). The development of new EPR reactors is complemented by continued robust growth in renewable energies, although at a slightly less accelerated pace compared to scenarios M and N1. Similarly, the level of flexibilities required to maintain the supply-demand balance is also more limited than in these scenarios.

6. **N03: A Mix Comprising 50% Nuclear and 50% Renewable Energy by 2050** Scenario N03 is designed around a proactive and diversified development of new nuclear energy. It includes the rapid launch of a construction program for new EPR2-type nuclear reactors, following a schedule corresponding to the maximum capacity communicated to date by the nuclear industry (a pair of reactors every four years starting in 2035, with a progressive acceleration), as well as the development of small modular reactors (SMRs). Additionally, the operation of existing nuclear facilities is extended for as long as possible. Renewable energy development continues at a more moderate pace than in other scenarios, and this scenario demands the least development of flexibilities. It is characterized by a production mix evenly divided between renewable and nuclear energy by 2050.

# Bibliography


1. *World Energy Outlook 2019* IEA Webstore. https://webstore.iea.org/world-energy-outlook-2019 (2020).
2. *Decision-making for High Renewable Electricity Futures in the United States — Request PDF* https://www.researchgate.net/publication/259171441_Decision-making_for_High_Renewable_Electricity_Futures_in_the_United_States (2020).
3. IEA. *Harnessing Variable Renewables - A Guide to the Balancing Challenge* https://www.oecd.org/publications/harnessing-variable-renewables-9789264111394-en.htm (2020).
4. Mai, T. *et al.* Renewable Electricity Futures for the United States. *IEEE Transactions on Sustainable Energy* **5,** 372–378. ISSN: 1949-3029 (2014).
5. Miketa, A. & Ueckerdt, F. *PLANNING FOR THE RENEWABLE FUTURE LONG-TERM MODELLING AND TOOLS TO EXPAND VARIABLE RENEWABLE POWER IN EMERGING ECONOMIES* (Jan. 17, 2017).
6. *Advancing climate services for the European renewable energy sector through capacity building and user engagement — Elsevier Enhanced Reader* https://reader.elsevier.com/reader/sd/pii/S2405880719300809?token=4AA24CB9B564F0A9A9E2B2DB92F5499C (2019).
7. Institute, M. E. *Power System Security Assessment of the future National Electricity Market* https://www.energy.gov.au/publications/power-system-security-assessment-future-national-electricity-market (2020).
8. *Final Report Summary - MILESECURE-2050 (Multidimensional Impact of the Low-carbon European Strategy on Energy Security, and Socio-Economic Dimension up to 2050 perspective) — FP7* CORDIS — European Commission. https://cordis.europa.eu/project/id/320169/reporting (2023).
9. Gracceva, F. & Zeniewski, P. A systemic approach to assessing energy security in a low-carbon EU energy system. *Applied Energy* **123,** 335–348. ISSN: 0306-2619. http://www.sciencedirect.com/science/article/pii/S0306261913010179 (2020) (June 15, 2014).

10. International Energy Agency. *Secure and Efficient Electricity Supply: During the Transition to Low Carbon Power Systems* ISBN: 978-92-64-20763-9. https://www.oecd-ilibrary.org/energy/secure-and-efficient-electricity-supply_9789264207639-en (2023) (OECD, Apr. 28, 2014).

11. IRENA. *Planning for the renewable future: Long-term modelling and tools to expand variable renewable power in emerging economies* en. 2017. /publications/2017/Jan/Planning-for-the-renewable-future-Long-term-modelling-and-tools-to-expand-variable-renewable-power (2018).

12. Pfenninger, S. Energy scientists must show their workings. en. *Nature News* **542,** 393. http://www.nature.com/news/energy-scientists-must-show-their-workings-1.21517 (2018) (Feb. 2017).

13. Pfenninger, S., DeCarolis, J., Hirth, L., Quoilin, S. & Staffell, I. The importance of open data and software: Is energy research lagging behind? *Energy Policy* **101,** 211–215. ISSN: 0301-4215. http://www.sciencedirect.com/science/article/pii/S0301421516306516 (2018) (Feb. 2017).

14. Helistö, N., Kiviluoma, J., Holttinen, H., Lara, J. D. & Hodge, B.-M. Including operational aspects in the planning of power systems with large amounts of variable generation: A review of modeling approaches. en. *Wiley Interdisciplinary Reviews: Energy and Environment* **0,** e341. ISSN: 2041-840X. https://onlinelibrary.wiley.com/doi/abs/10.1002/wene.341 (2019) (2019).

15. Nweke, C. I., Leanez, F., Drayton, G. R. & Kolhe, M. *Benefits of chronological optimization in capacity planning for electricity markets* in *2012 IEEE International Conference on Power System Technology (POWERCON)* (Oct. 2012), 1–6.

16. Drouineau, M., Assoumou, E., Mazauric, V. & Maïzi, N. Increasing shares of intermittent sources in Reunion Island: Impacts on the future reliability of power supply. *Renewable and Sustainable Energy Reviews* **46,** 120–128. ISSN: 1364-0321. http://www.sciencedirect.com/science/article/pii/S1364032115001124 (2019) (June 2015).

17. Drouineau, M., Maïzi, N. & Mazauric, V. Impacts of intermittent sources on the quality of power supply: The key role of reliability indicators. *Applied Energy* **116,** 333–343. ISSN: 0306-2619. http://www.sciencedirect.com/science/article/pii/S030626191300977X (2019) (Mar. 2014).

18. Maïzi, N. *et al.* Maximizing intermittency in 100% renewable and reliable power systems: A holistic approach applied to Reunion Island in 2030. *Applied Energy. Transformative Innovations for a Sustainable Future – Part III* **227,** 332–341. ISSN: 0306-2619. http://www.sciencedirect.com/science/article/pii/S0306261917310747 (2019) (Oct. 2018).

19. Spiecker, S. & Weber, C. The future of the European electricity system and the impact of fluctuating renewable energy – A scenario analysis. *Energy Policy* **65,** 185–197. ISSN: 0301-4215. http://www.sciencedirect.com/science/article/pii/S0301421513010549 (2019) (Feb. 2014).

20. Ludig, S., Schmid, E., Haller, M. & Bauer, N. Assessment of transformation strategies for the German power sector under the uncertainty of demand development and technology availability. *Renewable and Sustainable Energy Reviews* **46,** 143–156. ISSN: 1364-0321. http://www.sciencedirect.com/science/article/pii/S136403211500132X (2018) (June 2015).

21. Merrick, J. H. On representation of temporal variability in electricity capacity planning models. *Energy Economics* **59,** 261–274. ISSN: 0140-9883. http://www.sciencedirect.com/science/article/pii/S0140988316302018 (2018) (Sept. 2016).

22. Nahmmacher, P., Schmid, E., Hirth, L. & Knopf, B. *Carpe Diem: A Novel Approach to Select Representative Days for Long-Term Power System Models with High Shares of Renewable Energy Sources* en. SSRN Scholarly Paper ID 2537072 (Social Science Research Network, Rochester, NY, Dec. 2014). https://papers.ssrn.com/abstract=2537072 (2018).

23. Nelson, J. *et al.* High-resolution modeling of the western North American power system demonstrates low-cost and low-carbon futures. *Energy Policy* **43,** 436–447. ISSN: 0301-4215. http://www.sciencedirect.com/science/article/pii/S0301421512000365 (2018) (Apr. 2012).

24. Nicolosi, M. The Importance of High Temporal Resolution in Modeling Renewable Energy Penetration Scenarios. en. https://escholarship.org/uc/item/9rh9v9t4 (2018) (Oct. 2010).

25. Park, S. Y., Yun, B.-Y., Yun, C. Y., Lee, D. H. & Choi, D. G. An analysis of the optimum renewable energy portfolio using the bottom–up model: Focusing on the electricity generation sector in South Korea. *Renewable and Sustainable Energy Reviews* **53,** 319–329. ISSN: 1364-0321. http://www.sciencedirect.com/science/article/pii/S1364032115008758 (2018) (Jan. 2016).

26. Pina, A., Silva, C. & Ferrão, P. Modeling hourly electricity dynamics for policy making in long-term scenarios. *Energy Policy* **39,** 4692–4702. ISSN: 0301-4215. http://www.sciencedirect.com/science/article/pii/S0301421511005180 (2019) (Sept. 2011).

27. Poncelet, K., Delarue, E., Six, D., Duerinck, J. & D'haeseleer, W. Impact of the level of temporal and operational detail in energy-system planning models. *Applied Energy* **162,** 631–643. ISSN: 0306-2619. http://www.sciencedirect.com/science/article/pii/S0306261915013276 (2018) (Jan. 2016).

28. Kannan, R. & Turton, H. A Long-Term Electricity Dispatch Model with the TIMES Framework. en. *Environmental Modeling & Assessment* **18,** 325–343. ISSN: 1573-2967. https://doi.org/10.1007/s10666-012-9346-y (2018) (June 2013).

29. Wene, C. .-O. Energy-economy analysis: Linking the macroeconomic and systems engineering approaches. *Energy* **21,** 809–824. ISSN: 0360-5442. http://www.sciencedirect.com/science/article/pii/0360544296000175 (2018) (Sept. 1996).

30. Deane, J. P., Chiodi, A., Gargiulo, M. & Ó Gallachóir, B. P. Soft-linking of a power systems model to an energy systems model. *Energy. 8th World Energy System Conference, WESC 2010* **42,** 303–312. ISSN: 0360-5442. http://www.sciencedirect.com/science/article/pii/S0360544212002551 (2018) (June 2012).

31. Deane, J. P., Gracceva, F., Chiodi, A., Gargiulo, M. & Gallachóir, B. P. Ó. Assessing power system security. A framework and a multi model approach. *International Journal of Electrical Power & Energy Systems* **73,** 283–297. ISSN: 0142-0615. http://www.sciencedirect.com/science/article/pii/S0142061515002021 (2018) (Dec. 2015).

32. Partelow, S. What is a framework? Understanding their purpose, value, development and use. *Journal of Environmental Studies and Sciences* **13** (Apr. 2023).

33. De Transport d'Electricité, R. *Forecast assessment of electricity supply-demand balance (Bilan prévisionnel de l'équilibre offre-demande d'électricité en France - édition 2018)* en. Direction de l'économie, de la prospective et de la transparence, RTE, La Défense, France. 2018. https://www.rte-france.com/en/article/forecast-assessment-electricity-supply-demand-balance (2019).

34. Krakowski, V., Assoumou, E., Mazauric, V. & Maïzi, N. Feasible path toward 40–100% renewable energy shares for power supply in France by 2050: A prospective analysis. *Applied Energy* **171,** 501–522. ISSN: 0306-2619. http://www.sciencedirect.com/science/article/pii/S0306261916304251 (2018) (June 2016).

35. Maïzi, N. & Assoumou, E. Future prospects for nuclear power in France. *Applied Energy* **136,** 849–859. ISSN: 0306-2619. http://www.sciencedirect.com/science/article/pii/S0306261914002967 (2018) (Dec. 31, 2014).

36. Seck, G. S., Krakowski, V., Assoumou, E., Maïzi, N. & Mazauric, V. Reliability-constrained scenarios with increasing shares of renewables for the French power sector in 2050. *Energy Procedia. Proceedings of the 9th International Conference on Applied Energy* **142,** 3041–3048. ISSN: 1876-6102. http://www.sciencedirect.com/science/article/pii/S1876610217361970 (2018) (Dec. 2017).

37. Siggini, G. *Approche intégrée pour l'analyse prospective de la décarbonisation profonde du système électrique européen à l'horizon 2050 face à la variabilité climatique* PhD thesis (Université Paris sciences et lettres, Mar. 25, 2021). https://pastel.hal.science/tel-03274729 (2023).

38. Agency, I. E. *World Energy Outlook 2022* https://www.oecd-ilibrary.org/content/publication/3a469970-en (2022).

39. Agency, I. E. *Renewables 2022: Analysis and forecast to 2027* https://www.oecd.org/publications/market-report-series-renewables-25202774.htm (2023).

40. IRENA. *Renewable Power Generation Costs in 2020* June 22, 2021. https://www.irena.org/publications/2021/Jun/Renewable-Power-Costs-in-2020 (2023).

41. IEA. *Hydropower Special Market Report – Analysis* IEA. https://www.iea.org/reports/hydropower-special-market-report (2023).

42. Agency, I. E. *World Energy Outlook 2022 Free Dataset - Data product* IEA. https://www.iea.org/data-and-statistics/data-product/world-energy-outlook-2022-free-dataset (2023).

43. INTERNATIONAL ENERGY & AGENCY. World Energy Outlook 2022.

44. Nuclear Energy Agency. *The Costs of Decarbonisation: System Costs with High Shares of Nuclear and Renewables* ISBN: 978-92-64-31218-0. https://www.oecd-ilibrary.org/nuclear-energy/the-costs-of-decarbonisation_9789264312180-en (2019) (OECD, Jan. 29, 2019).

45. IEA. *Nuclear Power in a Clean Energy System – Analysis* IEA. https://www.iea.org/reports/nuclear-power-in-a-clean-energy-system (2023).

46. *Coal in Net Zero Transitions – Analysis* IEA. https://www.iea.org/reports/coal-in-net-zero-transitions (2023).

47. IEA. *System Integration of Renewables: An update on Best Practice* 2018. https://iea.blob.core.windows.net/assets/3b21ebb1-2e4c-4528-aa95-98b56314028e/System_Integration_of_Renewables.pdf.

48. Heggarty, T. *Techno-economic optimisation of the mix of power system flexibility solutions* PhD thesis (Université Paris sciences et lettres, Sept. 7, 2021). https://pastel.archives-ouvertes.fr/tel-03461279 (2023).

49. Cany, C., Mansilla, C., Mathonnière, G. & da Costa, P. Nuclear power supply: Going against the misconceptions. Evidence of nuclear flexibility from the French experience. *Energy* **151,** 289–296. ISSN: 0360-5442. https://www.sciencedirect.com/science/article/pii/S0360544218304729 (2023) (May 15, 2018).

50. Agency, I. E. *Status of Power System Transformation 2019* 32. https://www.oecd-ilibrary.org/content/publication/7c49400a-en (2019).

51. International Energy Agency & Réseau de Transport d'Electricité. *Conditions and Requirements for the Technical Feasibility of a Power System with a High Share of Renewables in France Towards 2050* ISBN: 978-92-64-74764-7. https://www.oecd-ilibrary.org/energy/conditions-and-requirements-for-the-technical-feasibility-of-a-power-system-with-a-high-share-of-renewables-in-france-towards-2050_6be9f3ac-en (2023) (OECD, Mar. 16, 2021).

52. IEA. *Electricity Networks: Infrastructure and Operations* 2013. https://iea.blob.core.windows.net/assets/55442f80-71b9-4026-8d13-01134f51e2f2/ElectricityNetworks20
FINAL.pdf.

53. World Energy Investment 2022. https://iea.blob.core.windows.net/assets/b0beda65-8a1d-46ae-87a2-f95947ec2714/WorldEnergyInvestment2022.pdf (2022).

54. IEA. Status of Power System Transformation 2019.

55. Agency, I. E. Secure Energy Transitions in the Power Sector (2021).

56. Boiteux, M. *Coûts marginaux à court et à long terme* Mar. 15, 1949. https://www.larevuedelenergie.com/wp-content/uploads/2020/04/Boiteux-1956-La-vente-au-cout-marginal-revue-energie.pdf.

57. Profumo, F., Bompard, E. & Fulli, I. G. ELECTRICITY SECURITY: MODELS AND METHODS FOR SUPPORTING THE POLICY DECISION MAKING IN THE EUROPEAN UNION.

58. Committee, T. I. *Final Report on the Major Blackout caused by the 2018 Hokkaido Eastern Iburi Earthquake* 2018. https://www.occto.or.jp/iinkai/hokkaido_kensho/files/Final_report_hokkaido_blackout_summarized.pdf.

59. Regulator, A. E. *Investigation report into South Australia's 2016 state-wide blackout* Australian Energy Regulator. https://www.aer.gov.au/wholesale-markets/compliance-reporting/investigation-report-into-south-australias-2016-state-wide-blackout (2023).

60. International Energy Agency. *Analytical Frameworks for Electricity Security* ISBN: 978-92-64-67656-5. https://www.oecd-ilibrary.org/energy/analytical-frameworks-for-electricity-security_899a38f9-en (2023) (OECD, Apr. 29, 2021).

61. International Energy Agency. *Power systems in transition: Challenges and opportunities ahead for electricity security* ISBN: 978-92-64-72595-9. https://www.oecd-ilibrary.org/energy/power-systems-in-transition_4ad57c0e-en (2023) (OECD, Nov. 6, 2020).

62. Weg, G. Definition and monitoring of security of supply on the European electricity markets, MD. https://www.bmwk.de/Redaktion/EN/Publikationen/Studien/definition-and-monitoring-of-security-of-supply-on-the-european-electricity-markets-from-2017-to-2019.html (2019).

63. AESO. *Resource Adequacy Criteria Overview and Alberta Historical Performance* 2017. https://www.aeso.ca/assets/Uploads/Resource-Adequacy-Criterion-toWorkgroup.pdf.

64. 1972: Miners' strike turns off the lights. http://news.bbc.co.uk/onthisday/hi/dates/stories/february/16/newsid_2757000/2757099.stm (2023) (Feb. 16, 1972).

65. *The 1974 Three Day Week & Electricity Rationing — the Blackout report* https://www.theblackoutreport.co.uk/2021/01/06/three-day-week-1974/ (2023).

66. Almeida, D. N. *et al.* A crise no fornecimento e distribuição de energia elétrica no Brasil em 2001: uma análise panorâmica com foco em na prevenção de eventos análogos futuros. *Revista de Gestão Ambiental e Sustentabilidade* **11.** Number: 1, 20080. ISSN: 2316-9834. https://periodicos.uninove.br/geas/article/view/20080 (2023) (Mar. 14, 2022).

67. Kimura, O. & Nishio, K.-i. Saving Electricity in a Hurry: A Japanese Experience after the Great East Japan Earthquake in 2011. https://www.researchgate.net/publication/259827282_Saving_Electricity_in_a_Hurry_a_Japanese_Experience_After_the_Great_East_Japan_Earthquake_in_2011.

68. Kimura, O. & Nishio, K.-I. *Saving Electricity in a Hurry: a Japanese Experience After the Great East Japan Earthquake in 2011* (July 23, 2013).

69. Sarhan, A., Ramachandaramurthy, V. K., Kiong, T. S. & Ekanayake, J. Definitions and dimensions for electricity security assessment: A Review. *Sustainable Energy Technologies and Assessments* **48,** 101626. ISSN: 2213-1388. https://www.sciencedirect.com/science/article/pii/S2213138821006408 (2023) (Dec. 1, 2021).

70. Westphal, K., Pastukhova, M. & Pepe, J. M. Geopolitics of electricity: grids, space and (political) power. Publisher: Stiftung Wissenschaft und Politik (SWP), German Institute for International and Security Affairs. https://www.swp-berlin.org/10.18449/2022RP06/ (2023) (2022).

71. ENTSOE. *Risk Preparedness Regulation: Proposal for Methodology for identifying regional electricity crisis scenarios - European Network of Transmission System Operators for Electricity - Citizen Space* https://consultations.entsoe.eu/system-operations/risk-preparedness-regulation-methodology-for-ident/ (2023).

72. Zinaman, O. & Miller, M. The Evolving Role of the Power Sector Regulator: A Clean Energy Regulators Initiative Report. *Technical Report* (2014).

73. Wen, C. *et al.* Household willingness to pay for improving electricity services in Sumba Island, Indonesia: A choice experiment under a multi-tier framework. *Energy Research & Social Science* **88,** 102503. ISSN: 2214-6296. https://www.sciencedirect.com/science/article/pii/S2214629622000111 (2023) (June 1, 2022).

74. Gorman, W. The quest to quantify the value of lost load: A critical review of the economics of power outages. *The Electricity Journal* **35,** 107187. ISSN: 1040-6190. https://www.sciencedirect.com/science/article/pii/S1040619022001130 (2022).

75. Security of EU electricity supply in 2021: Report on Member States approaches to assess and ensure adequacy. https://acer.europa.eu/Publications/ACER_Security_of_EU_Electricity_Supply_2021.pdf (2022).

76. Debnath, K. & Goel, L. Power system planning : a reliability perspective. *Electric Power Systems Research* **34,** 179–185. ISSN: 0378-7796. https://www.sciencedirect.com/science/article/pii/037877969500976X (1995).

77. M, P. B., A, S., G, F. & N, H. *Generation Adequacy Methodologies Review* Other LD-1A-27944-EN-C (print),LD-1A-27944-EN-N (online) (Luxembourg (Luxembourg), 2016).

78. Shiwen, Y., Hui, H., Chengzhi, W., Hao, G. & Hao, F. Review on Risk Assessment of Power System. *Procedia Computer Science* **109.** 8th International Conference on Ambient Systems, Networks and Technologies, ANT-2017 and the 7th International Conference on Sustainable Energy Information Technology, SEIT 2017, 16-19 May 2017, Madeira, Portugal, 1200–1205. ISSN: 1877-0509. https://www.sciencedirect.com/science/article/pii/S1877050917310748 (2017).

79. Haringa, G., Jordan, G. & Garver, L. Application of Monte Carlo simulation to multi-area reliability evaluations. *IEEE Computer Applications in Power* **4,** 21–25 (1991).

80. Doquet, M., Fourment, C. & Roudergues, J.-M. *Generation and transmission adequacy of large interconnected power systems: A contribution to the renewal of Monte-Carlo approaches* (2011), 1–6.

81. Mantysaari, P. *EU Electricity Trade Law: The Legal Tools of Electricity Producers in the Internal Electricity Market* 1–614. ISBN: 978-3-319-16512-7 (Jan. 2015).

82. Hofmann, H. & Turk, A. *Legal Challenges in EU Administrative Law: Towards an Integrated Administration* 1–397. ISBN: 9781847207883 (June 2009).

83. De Transport d'Electricité, R. *Forecast assessment of electricity supply-demand balance (Bilan prévisionnel de l'équilibre offre-demande d'électricité en France - édition 2017)* en. Direction de l'économie, de la prospective et de la transparence, RTE, La Défense, France. 2018. https://assets.rte-france.com/prod/public/2020-06/bp2017_complet_vf_compressed.pdf (2019).

84. CRE. *Délibération de la Commission de régulation de l'énergie du 25 mai 2022 portant proposition d'une valeur du critère de sécurité d'approvisionnement électrique pour la France métropolitaine continentale prévu à l'article L. 141-7 du code de l'énergie* (2022). www.cre.fr/content/download/25572/file/220525_2022-152-Prop-critere-securite_approvisionnement.pdf.

85. ACER/CEER. *Annual Report on the Results of Monitoring the Internal Electricity and Natural Gas Markets in 2017 - Electricity Wholesale Markets Volume* 2018. https://acer.europa.eu/Official_documents/Acts_of_the_Agency/Publication/MMR%202017%20-%20ELECTRICITY.pdf.

86. Project, R. A. *Realising the benefits of European market integration* Regulatory Assistance Project. https://www.raponline.org/knowledge-center/realising-the-benefits-of-european-market-integration/ (2023).

87. Koltsaklis, N. E. & Dagoumas, A. S. State-of-the-art generation expansion planning: A review. *Applied Energy* **230,** 563–589. ISSN: 0306-2619. https://www.sciencedirect.com/science/article/pii/S0306261918312583 (2023) (Nov. 15, 2018).

88. Ryan, S. M., McCalley, J. D. & Woodruff, D. L. Long Term Resource Planning for Electric Power Systems Under Uncertainty.

89. Diakov, V., Cole, W., Sullivan, P., Brinkman, G. & Margolis, R. *Improving Power System Modeling. A Tool to Link Capacity Expansion and Production Cost Models* NREL/TP-6A20-64905 (National Renewable Energy Lab. (NREL), Golden, CO (United States), Nov. 1, 2015). https://www.osti.gov/biblio/1233204 (2023).

90. Gonen, T. *Electrical Power Transmission System Engineering: Analysis and Design, Third Edition* Google-Books-ID: 6KbNBQAAQBAJ. 1082 pp. ISBN: 978-1-4822-3223-3 (CRC Press, Aug. 18, 2015).

91. Stoll, H. G. *Least-Cost Electric Utility Planning* Google-Books-ID: 1QB6DsxdeFMC. 824 pp. ISBN: 978-0-471-63614-4 (Wiley, June 26, 1989).

92. Madrigal, M. & Stoft, S. *Transmission Expansion for Renewable Energy Scale-Up : Emerging Lessons and Recommendations* ISBN: 978-0-8213-9598-1. http://hdl.handle.net/10986/9375 (2023) (Washington, DC: World Bank, 2012).

93. Holttinen, H. *et al. Recommended Practices for Wind Integration Studies, RP16 issued by IEA Implementing Agreement on Wind RD&D, Oct 2013. [Online]. Available: www.ieawind.org.* (Oct. 15, 2013).

94. irena. *POWER SYSTEM FLEXIBILITY FOR THE ENERGY TRANSITION*

95. Kies, A., Schyska, B. U. & Von Bremen, L. Curtailment in a Highly Renewable Power System and Its Effect on Capacity Factors. *Energies* **9.** Number: 7 Publisher: Multidisciplinary Digital Publishing Institute, 510. ISSN: 1996-1073. https://www.mdpi.com/1996-1073/9/7/510 (2023) (July 2016).

96. Lacerda, J. S. & van den Bergh, J. C. J. M. Mismatch of wind power capacity and generation: causing factors, GHG emissions and potential policy responses. *Journal of Cleaner Production. New approaches for transitions to low fossil carbon societies: promoting opportunities for effective development, diffusion andimplementation of technologies, policies and strategies* **128,** 178–189. ISSN: 0959-6526. https://www.sciencedirect.com/science/article/pii/S095965261501094X (2023) (Aug. 1, 2016).

97. Allwood, J. M. *et al.* in *Climate Change 2014: Mitigation of Climate Change. Contribution of Working Group III to the Fifth Assessment Report of the Intergovernmental Panel on Climate Change* 1247–1279 (Cambridge University Press, 2014). https://www.ipcc.ch/site/assets/uploads/2018/02/ipcc_wg3_ar5_annex-i.pdf (2023).

98. Starfield, A. M., Smith, K. A. & Bleloch, A. L. *How to Model it: Problem Solving for the Computer Age* Google-Books-ID: qIJlQ6BDXd4C. 224 pp. ISBN: 978-0-07-005897-2 (McGraw-Hill, 1990).

99. Hourcade, J. C., Richels, R., Robinson, J. R. & Schrattenholzer, L. in (eds Bruce, J. P., Lee, H. & Haites, E. F.) (Cambridge University Press, Cambridge, 1996). ISBN: 978-0-521-56431-1. https://iiasa.dev.local/ (2023).

100. Lemke, P. *et al.* in *IPCC.* Journal Abbreviation: IPCC. (Jan. 1, 2007).

101. Durance, P. & Godet, M. Scenario building: Uses and abuses. *Technological Forecasting and Social Change. Strategic Foresight* **77,** 1488–1492. ISSN: 0040-1625. https://www.sciencedirect.com/science/article/pii/S0040162510001289 (2023) (Nov. 1, 2010).

102. Wiebe, K. *et al.* Scenario Development and Foresight Analysis: Exploring Options to Inform Choices. *Annual Review of Environment and Resources* **43.** _eprint: https://doi.org/10.1146/annurev-environ-102017-030109, 545–570. https://doi.org/10.1146/annurev-environ-102017-030109 (2023) (2018).

103. Quist, J. & Vergragt, P. Past and future of backcasting: The shift to stakeholder participation and a proposal for a methodological framework. *Futures* **38,** 1027–1045. ISSN: 0016-3287. https://www.sciencedirect.com/science/article/pii/S0016328706000541 (2023) (Nov. 1, 2006).

104. Robinson, J. Futures Under Glass: A Recipe for People Who Hate to Predict. *Futures* **22,** 820–842 (Oct. 1, 1990).

105. Herrmann, N. *Regional Energy 2050: A sustainability-oriented strategic backcasting methodology for local utilities* (Jan. 1, 2011).

106. Höjer, M. *et al.* Scenarios in selected tools for environmental systems analysis. *Journal of Cleaner Production* **16,** 1958–1970. ISSN: 0959-6526. https://www.sciencedirect.com/science/article/pii/S0959652608000188 (2023) (Dec. 1, 2008).

107. Anderson, K. L. Reconciling the electricity industry with sustainable development: backcasting — a strategic alternative. *Futures* **33,** 607–623. ISSN: 0016-3287. https://www.sciencedirect.com/science/article/pii/S0016328701000040 (2023) (Sept. 1, 2001).

108. Cook, D. *The Natural Step: Towards a Sustainable Society* Google-Books-ID: khAKAQAAMAAJ. 100 pp. ISBN: 978-1-903998-47-2 (Green Books for the Schumacher Society, 2004).

109. Mander, S. L. *et al.* The Tyndall decarbonisation scenarios—Part I: Development of a backcasting methodology with stakeholder participation. *Energy Policy* **36,** 3754–3763. ISSN: 0301-4215. https://www.sciencedirect.com/science/article/pii/S0301421508002851 (2023) (Oct. 1, 2008).

110. Cao, K.-K., Cebulla, F., Gómez Vilchez, J. J., Mousavi, B. & Prehofer, S. Raising awareness in model-based energy scenario studies—a transparency checklist. *Energy, Sustainability and Society* **6,** 28. ISSN: 2192-0567. https://doi.org/10.1186/s13705-016-0090-z (2023) (Sept. 28, 2016).

111. Grubb, M., Edmonds, J., ten Brink, P. & Morrison, M. The Costs of Limiting Fossil-Fuel CO2 Emissions: A Survey and Analysis. *Annual Review of Energy and the Environment* **18.** _eprint: https://doi.org/10.1146/annurev.eg.18.110193.002145, 397–478. https://doi.org/10.1146/annurev.eg.18.110193.002145 (2023) (1993).

112. Kannan, R. *Integrated top-down and bottom-up approaches in power generation planning using life cycle based evaluation* Accepted: 2008-09-17T11:11:30Z. Thesis (2005). https://dr.ntu.edu.sg/handle/10356/6299 (2023).

113. Hourcade, J.-C., Jaccard, M., Bataille, C. & Ghersi, F. *Hybrid Modeling: New Answers to Old Challenges Introduction to the Special Issue of The Energy Journal* INIS-FR–21-1569 INIS Reference Number: 53004749 (France, 2006), 17.

114. Van Beeck, N. Classification of Energy Models.

115. Schinko, T., Bachner, G., Schleicher, S. P. & Steininger, K. W. Modeling for insights not numbers: The long-term low-carbon transformation. *Atmósfera* **30.** Publisher: Elsevier, 137–161. ISSN: 0187-6236. https://www.elsevier.es/en-revista-atmosfera-76-articulo-modeling-for-insights-not-numbers-S0187623617300474 (2023) (Apr. 1, 2017).

116. Nakata, T., Silva Herran, D. & Rodionov, M. Application of energy system models for designing a low-carbon society. *Progress in Energy and Combustion Science* **37,** 462–502 (Aug. 1, 2011).

117. Hall, L. M. H. & Buckley, A. R. A review of energy systems models in the UK: Prevalent usage and categorisation. *Applied Energy* **169,** 607–628. ISSN: 0306-2619. https://www.sciencedirect.com/science/article/pii/S0306261916301672 (2023) (May 1, 2016).

118. Tomaschek, J. *Long-term optimization of the transport sector to address greenhouse gas reduction targets under rapid growth : application of an energy system model for Gauteng province, South Africa* Accepted: 2014-04-09 Journal Abbreviation: Langfristige Optimierung des Verkehrssektors zur Erreichung von Treibhausgasreduktionszielen unter schnellem Wachstum : Anwendung eines Energiesystemmodells für die Provinz Gauteng, Südafrika. doctoralThesis (2013). http://elib.uni-stuttgart.de/handle/11682/2330 (2023).

119. Hedenus, F., Johansson, D. & Lindgren, K. A Critical Assessment of Energy-economy-climate Models for Policy Analysis (2013).

120. Alain, G. & Gaël, G. *Comparaison des modèles météorologiques, climatiques et économiques* Section: Alain Grandjean. 2017. http://www.chair-energy-prosperity.org/publications/comparaison-modeles-meteorologiques-climatiques-economiques/ (2023).

121. Hoffman, K. C. & Wood, D. O. Energy System Modeling and Forecasting. *Annual Review of Energy* **1.** _eprint: https://doi.org/10.1146/annurev.eg.01.110176.002231, 423–453. https://doi.org/10.1146/annurev.eg.01.110176.002231 (2023) (1976).

122. Kydes, A. S. *Brookhaven Energy System Optimization Model: its variants and uses. [BESOM; TESOM; MARKAL]* in. Report Number: BNL–50873, 6146529 (May 1, 1978), BNL–50873, 6146529. http://www.osti.gov/servlets/purl/6146529/ (2023).

123. Covarrubias, A. J. Expansion Planning for Electric Power Systems. *IAEA BULLETIN.*

124. Després, J., Hadjsaid, N., Criqui, P. & Noirot, I. Modelling the impacts of variable renewable sources on the power sector: Reconsidering the typology of energy modelling tools. *Energy* **80,** 486–495. ISSN: 0360-5442. http://www.sciencedirect.com/science/article/pii/S0360544214013620 (2019) (Feb. 1, 2015).

125. Kannan, R. The development and application of a temporal MARKAL energy system model using flexible time slicing. *Applied Energy* **88,** 2261–2272. ISSN: 0306-2619. https://www.sciencedirect.com/science/article/pii/S0306261910005866 (2023) (June 1, 2011).

126. Fodstad, M. *et al.* Next frontiers in energy system modelling: A review on challenges and the state of the art. *Renewable and Sustainable Energy Reviews* **160,** 112246. ISSN: 1364-0321. https://www.sciencedirect.com/science/article/pii/S136403212200168X (2023) (May 1, 2022).

127. Haydt, G., Leal, V., Pina, A. & Silva, C. A. The relevance of the energy resource dynamics in the mid/long-term energy planning models. *Renewable Energy* **36,** 3068–3074. ISSN: 0960-1481. http://www.sciencedirect.com/science/article/pii/S096014811100142X (2020) (Nov. 1, 2011).

128. Prina, M., Manzolini, G., Moser, D., Nastasi, B. & Sparber, W. Classification and challenges of bottom-up energy system models - A review. *Renewable and Sustainable Energy Reviews* **129,** 109917 (Sept. 1, 2020).

129. Nijkamp, P. Regional Dimensions of Energy Scarcity. *Environment and Planning C: Government and Policy* **1.** Publisher: SAGE Publications Ltd STM, 179–192. ISSN: 0263-774X. https://doi.org/10.1068/c010179 (2023) (June 1, 1983).

130. Krishnan, V. & Cole, W. *Evaluating the value of high spatial resolution in national capacity expansion models using ReEDS* in *2016 IEEE Power and Energy Society General Meeting (PESGM)* 2016 IEEE Power and Energy Society General Meeting (PESGM). ISSN: 1944-9933 (July 2016), 1–5.

131. Poncelet, K., Delarue, E. & D'haeseleer, W. Unit commitment constraints in long-term planning models: Relevance, pitfalls and the role of assumptions on flexibility. *Applied Energy* **258,** 113843. ISSN: 0306-2619. https://www.sciencedirect.com/science/article/pii/S0306261919315302 (2023) (Jan. 15, 2020).

132. Loulou, R., Goldstein, G. & Noble, K. Documentation for the MARKAL Family of Models. *Energy Technology Systems Analysis Programme,* 65–73 (2004).

133. Short, W. *et al.* Regional Energy Deployment System (ReEDS). **303** (Jan. 2011).

134. Bialasiewicz, J. & Muljadi, E. Analysis of renewable-energy systems using RPM-SIM simulator. *Industrial Electronics, IEEE Transactions on* **53,** 1137–1143 (July 2006).

135. Reimers, A., Cole, W. & Frew, B. The impact of planning reserve margins in long-term planning models of the electricity sector. *Energy Policy* **125,** 1–8. ISSN: 0301-4215. https://www.sciencedirect.com/science/article/pii/S0301421518306797 (2019).

136. Mertens, T., Bruninx, K., Duerinck, J. & Delarue, E. Adequacy aware long-term energy-system optimization models considering stochastic peak demand. *Advances in Applied Energy* **4,** 100072. ISSN: 2666-7924. https://www.sciencedirect.com/science/article/pii/S2666792421000640 (2021).

137. Pfenninger, S., Hawkes, A. & Keirstead, J. Energy systems modeling for twenty-first century energy challenges. *RENEWABLE AND SUSTAINABLE ENERGY REVIEWS* **33,** 74–86. ISSN: 1364-0321 (2014).

138. Kiureghian, A. D. & Ditlevsen, O. Aleatory or epistemic? Does it matter? *Structural Safety* **31.** Risk Acceptance and Risk Communication, 105–112. ISSN: 0167-4730. https://www.sciencedirect.com/science/article/pii/S0167473008000556 (2009).

139. Usher, W. & Strachan, N. Critical mid-term uncertainties in long-term decarbonisation pathways. *Energy Policy* **41,** 433–444. https://EconPapers.repec.org/RePEc:eee:enepol:v:41:y:2012:i:c:p:433-444 (2012).

140. Trutnevyte, E., McDowall, W., Tomei, J. & Keppo, I. Energy scenario choices: Insights from a retrospective review of UK energy futures. *Renewable and Sustainable Energy Reviews* **55,** 326–337. ISSN: 1364-0321. https://www.sciencedirect.com/science/article/pii/S1364032115011466 (2016).

141. Morgan, M. & Keith, D. Improving the way we think about projecting future energy use and emissions of carbon dioxide. *Climatic Change* **90,** 189–215 (Oct. 2008).

142. Yue, X. *et al.* A review of approaches to uncertainty assessment in energy system optimization models. *Energy Strategy Reviews* **21,** 204–217. ISSN: 2211-467X. https://www.sciencedirect.com/science/article/pii/S2211467X18300543 (2018).

143. Kanudia, A. & Loulou, R. Robust responses to climate change via stochastic MARKAL: The case of Quebec. *European Journal of Operational Research* **106,** 15–30. ISSN: 0377-2217. https://www.sciencedirect.com/science/article/pii/S0377221798003567 (1998).

144. Messner, S., Golodnikov, A. & Gritsevskii, A. A stochastic version of the dynamic linear programming model MESSAGE III. *Energy* **21,** 775–784. ISSN: 0360-5442. https://www.sciencedirect.com/science/article/pii/0360544296000254 (1996).

145. Loulou, R. & Lehtila, A. Stochastic programming and tradeoff analysis in TIMES. *TIMES Version 3.3 User Note* (2012).

146. Labriet, M., Kanudia, A. & Loulou, R. Climate mitigation under an uncertain technology future: A TIAM-World analysis. *Energy Economics* **34.** The Asia Modeling Exercise: Exploring the Role of Asia in Mitigating Climate Change, S366–S377. ISSN: 0140-9883. https://www.sciencedirect.com/science/article/pii/S0140988312000461 (2012).

147. Keppo, I. & Zwaan, B. The Impact of Uncertainty in Climate Targets and CO2 Storage Availability on Long-Term Emissions Abatement. *Environmental Modeling and Assessment* **17,** 177–191 (Apr. 2011).

148. Labriet, M., Loulou, R., Kanudia, A., *et al. Is A 2 degrees celsius warming achievable under high uncertainty?: analysis with the TIMES integrated assessment model* (Groupe d'études et de recherche en analyse des décisions, 2008).

149. Usher, W. & Strachan, N. Critical mid-term uncertainties in long-term decarbonisation pathways. *Energy Policy* **41.** Modeling Transport (Energy) Demand and Policies, 433–444. ISSN: 0301-4215. https://www.sciencedirect.com/science/article/pii/S0301421511008810 (2012).

150. Hu, M.-C. & Hobbs, B. F. Analysis of multi-pollutant policies for the U.S. power sector under technology and policy uncertainty using MARKAL. *Energy* **35.** The 3rd International Conference on Sustainable Energy and Environmental Protection, SEEP 2009, 5430–5442. ISSN: 0360-5442. https://www.sciencedirect.com/science/article/pii/S0360544210003658 (2010).

151. Hunter, K., Sreepathi, S. & DeCarolis, J. F. Modeling for insight using Tools for Energy Model Optimization and Analysis (Temoa). *Energy Economics* **40,** 339–349. ISSN: 0140-9883. https://www.sciencedirect.com/science/article/pii/S014098831300159X (2013).

152. DeCarolis, J. F. Using modeling to generate alternatives (MGA) to expand our thinking on energy futures. *Energy Economics* **33,** 145–152. ISSN: 0140-9883. https://www.sciencedirect.com/science/article/pii/S0140988310000721 (2011).

153. Biresselioglu, M. E., Demir, M. H., Demirbag Kaplan, M. & Solak, B. Individuals, collectives, and energy transition: Analysing the motivators and barriers of European decarbonisation. *Energy Research and Social Science* **66,** 101493. ISSN: 2214-6296. https://www.sciencedirect.com/science/article/pii/S2214629620300700 (2020).

154. Cashmore, M., Rudolph, D., Larsen, S. & Nielsen, H. International experiences with opposition to wind energy siting decisions: Lessons for environmental and social appraisal. *Journal of Environmental Planning and Management* **Forthcoming** (May 2018).

155. Trutnevyte, E. Does cost optimization approximate the real-world energy transition? *Energy* **106,** 182–193 (Mar. 2016).

156. Turnheim, B. *et al.* Evaluating sustainability transitions pathways: Bridging analytical approaches to address governance challenges. *Global Environmental Change* **35,** 239–253 (Nov. 2015).

157. Upham, P., Oltra, C. & Boso, A. Towards a cross-paradigmatic framework of the social acceptance of energy systems. *Energy Research and Social Science* **8,** 100–112. ISSN: 2214-6296. https://www.sciencedirect.com/science/article/pii/S221462961500064X (2015).

158. Chang, M. *et al.* Trends in tools and approaches for modelling the energy transition. *Applied Energy* **290,** 116731. ISSN: 0306-2619. https://www.sciencedirect.com/science/article/pii/S0306261921002476 (2023) (May 15, 2021).

159. Helgesen, P. I. & Tomasgard, A. From linking to integration of energy system models and computational general equilibrium models – Effects on equilibria and convergence. *Energy* **159,** 1218–1233. ISSN: 0360-5442. https://www.sciencedirect.com/science/article/pii/S0360544218312118 (2023) (Sept. 15, 2018).

160. Blanco, H. *et al.* Life cycle assessment integration into energy system models: An application for Power-to-Methane in the EU. *Applied Energy* **259,** 114160. ISSN: 0306-2619. https://www.sciencedirect.com/science/article/pii/S0306261919318471 (2023) (Feb. 1, 2020).

161. Blanco, H., Gómez Vilchez, J. J., Nijs, W., Thiel, C. & Faaij, A. Soft-linking of a behavioral model for transport with energy system cost optimization applied to hydrogen in EU. *Renewable and Sustainable Energy Reviews* **115,** 109349. ISSN: 1364-0321. https://www.sciencedirect.com/science/article/pii/S136403211930557X (2023) (Nov. 1, 2019).

162. Riva, F., Gardumi, F., Tognollo, A. & Colombo, E. Soft-linking energy demand and optimisation models for local long-term electricity planning: An application to rural India. *Energy* **166,** 32–46. ISSN: 0360-5442. https://www.sciencedirect.com/science/article/pii/S0360544218320577 (2023) (Jan. 1, 2019).

163. Krook-Riekkola, A., Berg, C., Ahlgren, E. O. & Söderholm, P. Challenges in top-down and bottom-up soft-linking: Lessons from linking a Swedish energy system model with a CGE model. *Energy* **141,** 803–817. ISSN: 0360-5442. https://www.sciencedirect.com/science/article/pii/S0360544217316274 (2023) (Dec. 15, 2017).

164. Soria, R. *et al.* Modelling concentrated solar power (CSP) in the Brazilian energy system: A soft-linked model coupling approach. *Energy* **116,** 265–280. ISSN: 0360-5442. https://www.sciencedirect.com/science/article/pii/S0360544216313214 (2023) (Dec. 1, 2016).

165. Pina, A., Silva, C. A. & Ferrão, P. High-resolution modeling framework for planning electricity systems with high penetration of renewables. *Applied Energy* **112,** 215–223. ISSN: 0306-2619. https://www.sciencedirect.com/science/article/pii/S030626191300487X (2023) (Dec. 1, 2013).

166. Pavičević, M. *et al.* The potential of sector coupling in future European energy systems: Soft linking between the Dispa-SET and JRC-EU-TIMES models. *Applied Energy* **267,** 115100. ISSN: 0306-2619. https://www.sciencedirect.com/science/article/pii/S0306261920306127 (2023) (June 1, 2020).

167. Chang, M., Lund, H., Thellufsen, J. Z. & Østergaard, P. Perspectives on purpose-driven coupling of energy system models. *Energy* **265,** 126335 (Dec. 1, 2022).

168. Lund, H. *et al.* Simulation versus Optimisation: Theoretical Positions in Energy System Modelling. *Energies* **10.** Number: 7 Publisher: Multidisciplinary Digital Publishing Institute, 840. ISSN: 1996-1073. https://www.mdpi.com/1996-1073/10/7/840 (2023) (July 2017).

169. Collins, S. *et al.* Integrating short term variations of the power system into integrated energy system models: A methodological review. *Renewable and Sustainable Energy Reviews* **76,** 839–856. ISSN: 1364-0321. http://www.sciencedirect.com/science/article/pii/S1364032117304264 (2018) (Sept. 2017).

170. Seljom, P., Rosenberg, E., Schäffer, L. E. & Fodstad, M. Bidirectional linkage between a long-term energy system and a short-term power market model. *Energy* **198,** 117311. ISSN: 0360-5442. http://www.sciencedirect.com/science/article/pii/S0360544220304187 (2020) (May 1, 2020).

171. Welsch, M. *et al.* Incorporating flexibility requirements into long-term energy system models – A case study on high levels of renewable electricity penetration in Ireland. *Applied Energy* **135,** 600–615. ISSN: 0306-2619. http://www.sciencedirect.com/science/article/pii/S0306261914008836 (2018) (Dec. 2014).

172. Brouwer, A. S., van den Broek, M., Seebregts, A. & Faaij, A. Operational flexibility and economics of power plants in future low-carbon power systems. *Applied Energy* **156,** 107–128. ISSN: 0306-2619. http://www.sciencedirect.com/science/article/pii/S0306261915008235 (2020) (Oct. 15, 2015).

173. Collins, S., Deane, J. P. & Ó Gallachóir, B. Adding value to EU energy policy analysis using a multi-model approach with an EU-28 electricity dispatch model. *Energy* **130,** 433–447. ISSN: 0360-5442. https://www.sciencedirect.com/science/article/pii/S036054421730748X (2023) (July 1, 2017).

174. Deane, J. P., Drayton, G. & Ó Gallachóir, B. P. The impact of sub-hourly modelling in power systems with significant levels of renewable generation. *Applied Energy* **113,** 152–158. ISSN: 0306-2619. http://www.sciencedirect.com/science/article/pii/S030626191300593X (2019) (Jan. 1, 2014).

175. Quoilin, S., Nijs, W., Gonzalez, I. H., Zucker, A. & Thiel, C. *Evaluation of simplified flexibility evaluation tools using a unit commitment model* in *2015 12th International Conference on the European Energy Market (EEM)* 2015 12th International Conference on the European Energy Market (EEM). ISSN: 2165-4093 (May 2015), 1–5.

176. Rosen, J., Tietze-Stöckinger, I. & Rentz, O. Model-based analysis of effects from large-scale wind power production. *Energy. ECOS 05. 18th International Conference on Efficiency, Cost, Optimization, Simulation, and Environmental Impact of Energy Systems* **32,** 575–583. ISSN: 0360-5442. https://www.sciencedirect.com/science/article/pii/S0360544206001605 (2023) (Apr. 1, 2007).

177. Brinkerink, M. *et al.* Assessing global climate change mitigation scenarios from a power system perspective using a novel multi-model framework. *Environmental Modelling & Software* **150,** 105336. ISSN: 1364-8152. https://www.sciencedirect.com/science/article/pii/S1364815222000421 (2023) (Apr. 1, 2022).

178. Gong, C. C. *et al.* Bidirectional coupling of a long-term integrated assessment model REMIND v3.0.0 with an hourly power sector model DIETER v1.0.2. *EGUsphere.* Publisher: Copernicus GmbH, 1–68. https://egusphere.copernicus.org/preprints/2022/egusphere-2022-885/ (2023) (Oct. 7, 2022).

179. Heggarty, T. *Techno-economic optimisation of the mix of power system flexibility solutions* Theses (Université Paris sciences et lettres, 2021). https://pastel.hal.science/tel-03461279.

180. Seljom, P. & Tomasgard, A. Short-term uncertainty in long-term energy system models — A case study of wind power in Denmark. *Energy Economics* **49,** 157–167. ISSN: 0140-9883. http://www.sciencedirect.com/science/article/pii/S0140988315000419 (2019) (May 1, 2015).

181. Giarola, S. *et al.* Challenges in the harmonisation of global integrated assessment models: A comprehensive methodology to reduce model response heterogeneity. *Science of The Total Environment* **783,** 146861. ISSN: 0048-9697. https://www.sciencedirect.com/science/article/pii/S0048969721019318 (2023) (Aug. 20, 2021).

182. Alimou, Y., Maïzi, N., Bourmaud, J.-Y. & Li, M. Assessing the security of electricity supply through multi-scale modeling: The TIMES-ANTARES linking approach. *Applied Energy* **279,** 115717. ISSN: 0306-2619. http://www.sciencedirect.com/science/article/pii/S0306261920312101 (2021) (Dec. 1, 2020).

183. Loulou, R. & Kanudia, A. en. in *Decision & Control in Management Science: Essays in Honor of Alain Haurie* (ed Zaccour, G.) 153–175 (Springer US, Boston, MA, 2002). ISBN: 978-1-4757-3561-1. https://doi.org/10.1007/978-1-4757-3561-1_9 (2018).

184. Connolly, D., Lund, H., Mathiesen, B. V. & Leahy, M. A review of computer tools for analysing the integration of renewable energy into various energy systems. *Applied Energy* **87,** 1059–1082. ISSN: 0306-2619. http://www.sciencedirect.com/science/article/pii/S0306261909004188 (2018) (Apr. 2010).

185. Loulou, R., Remme, U., Kanudia, A., Lehtila, A. & Goldstein, G. Documentation for the TIMES Model Part II. *Energy technology systems analysis programme (ETSAP)* (2005).

186. *e-Highway 2050: Objectives* http://www.e-highway2050.eu/objectives/ (2018).

187. *TWENTIES project* Oct. 2013. https://windeurope.org/about-wind/reports/twenties-project/ (2018).

188. ENTSO-E. *Mid-term Adequacy Forecast 2018: Methodology and details results* en-us. 2018. https://www.entsoe.eu/outlooks/midterm/ (2018).

189. *TYNDP 2018* en-us. https://tyndp.entsoe.eu/tyndp2018/ (2018).

190. Lhuillier, N. *et al. Optimal System-Mix Of Flexibility Solutions For European Electricity: Optimal Mix of Flexibility* (2022). https://www.osmose-h2020.eu/wp-content/uploads/2022/05/OSMOSE_D1.3-Optimal-Mix-of-Flexibility_20220430_V1.pdf.

191. ENTSOE. *European Resource Adequacy Assessment* (). https://www.entsoe.eu/outlooks/eraa/.

192. Doquet, M., Gonzalez, R., Lepy, S., Momot, E. & Verrier, F. A new tool for adequacy reporting of electric systems: ANTARES. *42nd International Conference on Large High Voltage Electric Systems 2008, CIGRE 2008* (Jan. 2008).

193. RTE. *ANTARES optimization problemes formulation* 2017. https://antares.rte-france.com/?page_id=19&lang=en.

194. Doquet, M. *Use of a stochastic process to sample wind power curves in planning studies* in *2007 IEEE Lausanne Power Tech* (July 2007), 663–670.

195. Doquet, M., Fourment, C. & Roudergues, J. *Generation&transmission adequacy of large interconnected power systems: A contribution to the renewal of Monte-Carlo approaches* in *2011 IEEE Trondheim PowerTech* (June 2011), 1–6.

196. Riekkola, A. K., Charlotte Berg, Erik O. Ahlgren & Söderholm, P. *Challenges in Soft-Linking: The Case of EMEC and TIMES-Sweden - Konjunkturinstitutet* en. text (2013). https://www.konj.se/english/publications/working-papers/working-paper/2013-12-20-challenges-in-soft-linking-the-case-of-emec-and-times-sweden.html (2019).

197. CEER. *Assessment of Electricity Generation Adequacy in European Countries* 2014. https://cleanenergysolutions.org/es/resources/assessment-electricity-generation-adequacy-european-countries (2018).

198. D. Mills, A., Wiser, R. & Orlando Lawrence, E. Changes in the Economic Value of Variable Generation at High Penetration Levels: A Pilot Case Study of California (June 2012).

199. Madaeni, S. H., Sioshansi, R. & Denholm, P. Comparing Capacity Value Estimation Techniques for Photovoltaic Solar Power. *IEEE Journal of Photovoltaics* **3,** 407–415. ISSN: 2156-3381 (Jan. 2013).

200. Madaeni, S. H., Sioshansi, R. & Denholm, P. *Comparison of Capacity Value Methods for Photovoltaics in the Western United States* English. Tech. rep. NREL/TP-6A20-54704 (National Renewable Energy Lab. (NREL), Golden, CO (United States), July 2012). https://www.osti.gov/biblio/1046871 (2018).

201. Mills, A. & Wiser, R. *An Evaluation of Solar Valuation Methods Used in Utility Planning and Procurement Processes* 2012.

202. IEA. *World Energy Model Documentation.* Organisation for Economic Co-operation and Development (OECD), International Energy Agency (IEA), Paris, France. 2015. https://www.iea.org/weo/weomodel/ (2018).

203. Poncelet, K., Delarue, E., Duerinck, J., Six, D. & D'haeseleer, W. The importance of integrating the variability of renewables in long-term energy planning models. *Rome, Italy* (2014).

204. Le, K. D. & Day, J. T. Rolling Horizon Method: A New Optimization Technique for Generation Expansion Studies. *IEEE Transactions on Power Apparatus and Systems* **PAS-101.** Conference Name: IEEE Transactions on Power Apparatus and Systems, 3112–3116. ISSN: 0018-9510 (Sept. 1982).

205. Powell, W. B. *Approximate Dynamic Programming: Solving the Curses of Dimensionality* Google-Books-ID: WWWDkd65TdYC. 488 pp. ISBN: 978-0-470-18295-6 (John Wiley & Sons, Oct. 5, 2007).

206. Perez, R., Ross, J., Hoff, T. & Taylor, M. Photovoltaic Capacity Valuation Methods (May 2008).

207. Tadmor, E. B. & Miller, R. E. *Modeling Materials: Continuum, Atomistic and Multiscale Techniques* ISBN: 978-0-521-85698-0. https://www.cambridge.org/core/books/modeling-materials/7CC4027C34755637D8F641A0C8C26835 (2023) (Cambridge University Press, Cambridge, 2011).

208. Hoekstra, A., Chopard, B. & Coveney, P. Multiscale modelling and simulation: a position paper. *Philosophical Transactions of the Royal Society A: Mathematical, Physical and Engineering Sciences* **372.** Publisher: Royal Society, 20130377. https://royalsocietypublishing.org/doi/10.1098/rsta.2013.0377 (2023) (Aug. 6, 2014).

209. Radhakrishnan, R. A survey of multiscale modeling: Foundations, historical milestones, current status, and future prospects. *Aiche Journal. American Institute of Chemical Engineers* **67,** e17026. ISSN: 0001-1541. https://www.ncbi.nlm.nih.gov/pmc/articles/PMC7988612/ (2023) (Mar. 2021).

210. Walpole, J., Papin, J. A. & Peirce, S. M. Multiscale Computational Models of Complex Biological Systems. *Annual review of biomedical engineering* **15,** 137–154. ISSN: 1523-9829. https://www.ncbi.nlm.nih.gov/pmc/articles/PMC3970111/ (2023) (2013).

211. Hoekstra, A. G., Chopard, B., Coster, D., Portegies Zwart, S. & Coveney, P. V. Multiscale computing for science and engineering in the era of exascale performance. *Philosophical Transactions of the Royal Society A: Mathematical, Physical and Engineering Sciences* **377.** Publisher: Royal Society, 20180144. https://royalsocietypublishing.org/doi/10.1098/rsta.2018.0144 (2023) (Feb. 18, 2019).

212. Groen, D., Zasada, S. J. & Coveney, P. V. Survey of Multiscale and Multiphysics Applications and Communities. *Computing in Science & Engineering* **16.** Conference Name: Computing in Science & Engineering, 34–43. ISSN: 1558-366X (Mar. 2014).

213. Baeurle, S. Multiscale modeling of polymer materials using field-theoretic methodologies: A survey about recent developments. *Journal of Mathematical Chemistry* **46,** 363–426 (Aug. 1, 2009).

214. Li, Q. & Van Roekel, L. Towards multiscale modeling of ocean surface turbulent mixing using coupled MPAS-Ocean v6.3 and PALM v5.0. *Geoscientific Model Development* **14.** Publisher: Copernicus GmbH, 2011–2028. ISSN: 1991-959X. https://gmd.copernicus.org/articles/14/2011/2021/ (2022) (Apr. 15, 2021).

215. Mohr, K. *NASA Multi-scale Modeling Framework (MMF) — Earth* Publisher: 610 Web Dev. https://earth.gsfc.nasa.gov/meso/models/mmf (2023).

216. Gibson, C., Ostrom, E. & Ahn, T. The Concept of Scale and the Human Dimensions of Global Change: A Survey. *Ecological Economics* **32,** 217–239 (Feb. 1, 2000).

217. Fish, J. Multiscale Methods: Bridging the Scales in Science and Engineering. ISSN: 9780199233854 (Oct. 1, 2009).

218. Site, L. D. What is a Multiscale Problem in Molecular Dynamics? *Entropy* **16.** Number: 1 Publisher: Multidisciplinary Digital Publishing Institute, 23–40. ISSN: 1099-4300. https://www.mdpi.com/1099-4300/16/1/23 (2023) (Jan. 2014).

219. Groen, D. *et al.* Mastering the scales: a survey on the benefits of multiscale computing software. *Philosophical Transactions of the Royal Society A: Mathematical, Physical and Engineering Sciences* **377.** Publisher: Royal Society, 20180147. https://royalsocietypublishing.org/doi/10.1098/rsta.2018.0147 (2023) (Feb. 18, 2019).

220. Vervoort, J. M. *et al.* Exploring Dimensions, Scales, and Cross-scale Dynamics from the Perspectives of Change Agents in Social–ecological Systems. *Ecology and Society* **17.** Publisher: Resilience Alliance Inc. ISSN: 1708-3087. https://www.jstor.org/stable/26269212 (2023) (2012).

221. Bishara, D., Xie, Y., Liu, W. & Li, S. A State-of-the-Art Review on Machine Learning-Based Multiscale Modeling, Simulation, Homogenization and Design of Materials. *Archives of Computational Methods in Engineering* **30** (Aug. 5, 2022).

222. Peng, G. C. Y. *et al.* Multiscale Modeling Meets Machine Learning: What Can We Learn? *Archives of Computational Methods in Engineering* **28,** 1017–1037. ISSN: 1886-1784. https://doi.org/10.1007/s11831-020-09405-5 (2023) (May 1, 2021).

223. Elizar, E., Zulkifley, M. A., Muharar, R., Zaman, M. H. M. & Mustaza, S. M. A Review on Multiscale-Deep-Learning Applications. *Sensors* **22.** Number: 19 Publisher: Multidisciplinary Digital Publishing Institute, 7384. ISSN: 1424-8220. https://www.mdpi.com/1424-8220/22/19/7384 (2023) (Jan. 2022).

224. Alber, M. *et al.* Integrating machine learning and multiscale modeling—perspectives, challenges, and opportunities in the biological, biomedical, and behavioral sciences. *npj Digital Medicine* **2.** Number: 1 Publisher: Nature Publishing Group, 1–11. ISSN: 2398-6352. https://www.nature.com/articles/s41746-019-0193-y (2022) (Nov. 25, 2019).

225. Yang, A. & Marquardt, W. An ontological conceptualization of multiscale models. *Computers & Chemical Engineering* **33,** 822–837. ISSN: 0098-1354. https://www.sciencedirect.com/science/article/pii/S0098135408002524 (2023) (Apr. 21, 2009).

226. Chopard, B., Borgdorff, J. & Hoekstra, A. G. A framework for multi-scale modelling. *Philosophical Transactions of the Royal Society A: Mathematical, Physical and Engineering Sciences* **372,** 20130378. https://royalsocietypublishing.org/doi/10.1098/rsta.2013.0378 (2020) (Aug. 6, 2014).

227. *Multiscale Applications on European e-Infrastructures — MAPPER Project — Fact Sheet — FP7 — CORDIS — European Commission* https://cordis.europa.eu/project/id/261507/fr (2023).

228. Karabasov, S., Nerukh, D., Hoekstra, A., Chopard, B. & Coveney, P. V. Multiscale modelling: approaches and challenges. *Philosophical transactions. Series A, Mathematical, physical, and engineering sciences* **372,** 20130390. ISSN: 1364-503X. https://www.ncbi.nlm.nih.gov/pmc/articles/PMC4084530/ (2023) (Aug. 6, 2014).

229. Zaitchik, B. F. *et al.* in *Connecting the Sustainable Development Goals: The WEF Nexus: Understanding the Role of the WEF Nexus in the 2030 Agenda* (eds Cavalli, L. & Vergalli, S.) 71–88 (Springer International Publishing, Cham, 2022). ISBN: 978-3-031-01336-2. https://doi.org/10.1007/978-3-031-01336-2_7 (2023).

230. Loulou, R. Documentation for the TIMES Model PART II. *Energy Technology Systems Analysis Programme.* https://iea-etsap.org/docs/Documentation_for_the_TIMES_Model-Part-II_July-2016.pdf (2016).

231. Evangelos, P. & Antti, L. *Dispatching and unit commitment features in TIMES* (2016). https://iea-etsap.org/docs/TIMES_Dispatching_Documentation.pdf.

232. Lhuillier, N. & Bourmaud, J.-Y. *Optimal Mix of Flexibility-Appendixes D1.3* (). https://www.osmose-h2020.eu/wp-content/uploads/2022/05/OSMOSE_D1.3-Appendix-A-Model-B-Dataset-and-C-Environmental-Impact_20220429_V1.pdf.

233. Robbins, H. & Monro, S. A Stochastic Approximation Method. *The Annals of Mathematical Statistics* **22.** Publisher: Institute of Mathematical Statistics, 400–407. ISSN: 0003-4851, 2168-8990. https://projecteuclid.org/journals/annals-of-mathematical-statistics/volume-22/issue-3/A-Stochastic-Approximation-Method/10.1214/aoms/1177729586.full (2023) (Sept. 1951).

234. Chen, H. & Schmeiser, B. *Retrospective approximation algorithms for stochastic root finding* in *Proceedings of Winter Simulation Conference* Proceedings of Winter Simulation Conference (Dec. 1994), 255–261.

235. Pasupathy, R. & Kim, S. The stochastic root-finding problem: Overview, solutions, and open questions. *ACM Transactions on Modeling and Computer Simulation* **21,** 19:1–19:23. ISSN: 1049-3301. https://doi.org/10.1145/1921598.1921603 (2023) (2011).

236. Blum, J. R. Multidimensional Stochastic Approximation Methods. *The Annals of Mathematical Statistics* **25.** Publisher: Institute of Mathematical Statistics, 737–744. ISSN: 0003-4851, 2168-8990. https://projecteuclid.org/journals/annals-of-mathematical-statistics/volume-25/issue-4/Multidimensional-Stochastic-Approximation-Methods/10.1214/aoms/1177728659.full (2023) (Dec. 1954).

237. S, G. D. C. S. *et al. The JRC-EU-TIMES model - Assessing the long-term role of the SET Plan Energy technologies* Scientific analysis or review LD-NA-26292-EN-C (print), LD-NA-26292-EN-N (online) (Luxembourg (Luxembourg), 2013).

238. Fabian Hein & Matthias Buck. *The European Power Sector in 2019: Up-to-Date Analysis on the Electricity Transition* 2020. https://www.agora-energiewende.de/fileadmin/Projekte/2019/Jahresauswertung_EU_2019/Agora_Sandbag_Slides_Webinar_European_Power_Sector_in_2019_20022020.pdf.

239. ENTSO-E. *Project list TYNDP2016 assessments. 2016.* (). https://www.entsoe.eu/publications/tyndp/tyndp-2016/.

240. Europe Beyond Coal. *Overview: National coal phase-out announcements in Europe* Mar. 2019. :%20https://beyond-coal.eu/wp-content/uploads/2019/02/Overview-ofnational-coal-phase-out-announcements-Europe-Beyond-Coal-March-2019.pdf..

241. BOURMAUD, J.-Y. *et al. OSMOSE WP1 dataset* (). https://zenodo.org/record/6375020.

242. Alain, Q. *et al. LA VALEUR DE L'ACTION POUR LE CLIMAT UNE VALEUR TUTÉLAIRE DU CARBONE POUR ÉVALUER LES INVESTISSEMENTS ET LES POLITIQUES PUBLIQUES* (2019).

243. Jiménez, F. & Webster, M. D. *Optimal Selection of Sample Weeks for Approximating the Net Load in Generation Planning Problems* in (2013). https://api.semanticscholar.org/CorpusID:14654767.

244. Seljom, P. & Tomasgard, A. Short-term uncertainty in long-term energy system models: A case study of wind power in Denmark. *Energy Economics* **49,** 157–167. ISSN: 0140-9883. https://www.sciencedirect.com/science/article/pii/S0140988315000419 (2015).

245. Evangelos, P. & Antti, L. Dispatching and unit commitment features in TIMES. https://iea-etsap.org/docs/TIMES_Dispatching_Documentation.pdf (Aug. 2016).

246. RTE. *Futurs énergétiques 2050* https://rte-futursenergetiques2050.com/.

## RÉSUMÉ

Les exercices de prospective long-terme et les simulations de l'équilibre offre-demande sont deux éléments clefs de la planification/opération à moindre coût du système électrique. Le premier vise à déterminer une trajectoire d'investissements à partir de scénarios exogènes d'évolution du contexte énergétique global. En revanche, le second a pour but principal de diagnostiquer les risques de défaillance possibles, à parc de production donné. Malgré leur évidente proximité, ces exercices sont souvent portés et mis en œuvre de façon complètement indépendante. Cette approche totalement découplée conduit les prospectivistes à proposer des plans long-terme sans aucune analyse pertinente du risque de défaillance. Symétriquement, les études d'équilibre offre-demande à moyen-terme (cinq à dix ans) sont confrontées aux plus grandes difficultés lorsqu'il s'agit de valider la rentabilité des investissements nécessaires pour "passer la pointe". Il s'agit dans cette thèse de questionner dans une démarche prospective les exigences de robustesse du futur système électrique conformément au critère de défaillance réglementaire. Cela passe par le développement d'une approche multi-échelle qui concilie l'échelle temporelle à long terme, caractéristique de la planification optimale, avec l'échelle à court terme propre à l'opération du système électrique. Cette approche permettra ainsi de trouver, pour un scénario de transition donné, une trajectoire d'investissement fiable respectant le critère de défaillance réglementaire. Ce travail vise à combiner pleinement les forces des outils de modélisation du Centre des Mathématiques Appliquée des Mines de Paris (l'outil de planification optimale d'investissements : TIMES) et de RTE (l'outil de placement optimale de production : ANTARES), afin de relever le défi de la planification adéquate de la transition du système électrique. Techniquement, cette thèse proposera la construction d'un modèle multi-échelle basé sur un couplage bidirectionnel des deux outils, appliqué ensuite au système électrique interconnecté européen pour la trajectoire 2020-2050.



## MOTS CLÉS

Systèmes électriques, Europe, Transitions, Prospective, Sécurité d'Approvisionnement.



## ABSTRACT

Long-term energy scenario modeling and dispatch simulations are two key stages in the methodology for a cost-effective transition to a low-carbon power system. Although these stages are equally important, they are often performed independently. This decoupled approach can lead to future investment trajectories decided by long-term energy models with no guarantee of a reliable electricity supply. To tackle this problem, the aim of this PhD is to develop a multi-scale framework using a multi-model approach to address European power system adequacy requirements in the long term.



## KEYWORDS

Power systems, Europe, Transitions, Prospective, Security of Supply.